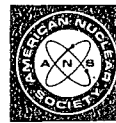


KfK 3880/1  
December 1984

# Fifth International Meeting on Thermal Nuclear Reactor Safety

Held at Karlsruhe Sept. 9-13, 1984

Proceedings Vol 1



Nuclear Research Center  
Karlsruhe



KfK 3880/1 B

**FIFTH INTERNATIONAL MEETING  
ON THERMAL NUCLEAR REACTOR SAFETY**

held at KARLSRUHE, September 9 - 13, 1984

**VOLUME 1**

- Chapter 1: Opening Addresses and Invited Papers
- Chapter 2: Safety Related Operation Experience
- Chapter 3: System and Component Behavior
- Chapter 4: Safety Systems and Function Optimization

Compiled by G. Bork and H. Rininsland  
Karlsruhe Nuclear Research Center  
Project Nuclear Safety

© Copyright 1984 by  
Kerntechnische Gesellschaft e. V., Bonn  
All rights reserved

Available from  
Kernforschungszentrum Karlsruhe GmbH  
Literaturabteilung  
Postfach 3640 · D-7500 Karlsruhe 1  
Printed in the Federal Republic of Germany

ISSN 0303-4003



Foreword

The 5th International Meeting on Thermal Nuclear Reactor Safety was held in Karlsruhe on September 9-13, 1984; it was attended by some 500 scientists and engineers from 25 countries. The conference was jointly sponsored by the European Nuclear Society (ENS), the American Nuclear Society (ANS), the Canadian Nuclear Society (CNS) and the Japan Atomic Energy Society (JAES). The meeting was further endorsed by, and organized in cooperation with, the Nuclear Energy Agency (NEA) of the Organization for Economic Cooperation and Development, the International Atomic Energy Agency (IAEA), and the Commission of the European Communities (CEC). Host organizations were the Kerntechnische Gesellschaft (KTG) and the Kernforschungszentrum Karlsruhe (KfK). The meeting was the fifth in a series of international meetings in the same subject areas with ANS and ENS as primary sponsors.

The Karlsruhe reactor safety meeting was held to reflect on the present status of engineered safety systems in nuclear power plants and to represent the findings of international safety research.

Seven invited experts of international reputation outlined the present state of the art in survey lectures. Moreover, more than 200 technical and scientific papers selected from 280 submitted papers, dealt with recent findings in reactor safety technology and research in the following areas: safety systems and functions optimization; man machine interface and emergency response; code development and verification; system and component behavior; fuel behavior during severe accidents; core debris and core concrete interaction; fission product behavior; containment response; probabilistic risk assessment. We wish to thank all speakers for their valuable contributions.

The meeting was concluded by a panel discussion on "Progress and Trends in Reactor Safety Technology and Research - What Has Been Achieved to Date? - What Remains to Be Done?"

It is not possible to acknowledge individually all persons who contributed to the meeting. We are greatly indebted to H.H. Hennies, President of the German Kerntechnische Gesellschaft (KTG), and J.M. Hendrie, President of the American Nuclear Society (ANS) who served as General Chairmen, and to A. Birkhofer as Chairman of the Technical Program Committee. Many thanks are due to the members of the Steering Committee, the Technical Program Committee, the Review Committee and the Organizing Committee.

The 6th International Meeting on Thermal Nuclear Reactor Safety was announced to take place in February 1986 at San Diego, California.

Volume 1Chapter 1

## Opening Addresses and Invited Papers (Plenary Sessions)

Opening Addresses:	pages
1.1 H.H. Hennies, General Chairman	3 - 8
1.2 G. Weiser, Baden-Württemberg State Minister	9 - 19
1.3 K.H. Narjes, Member of the Commission of the European Communities	21 - 34
Invited Papers (Plenary Sessions):	
1.4 A. Gauvenet: Nuclear Reactor Operation Across the World	35 - 54
1.5 W. Dircks, G. Naschi: Regulatory Trends in OECD Member Countries	55 - 72
1.6 D.O. Pickman, A. Fiege: Fuel Behavior Under DBA Conditions	73 - 94
1.7 W.R. Stratton: Review of Recent Source Term Investigations	95 - 110
1.8 W.G. Morison, W.J. Penn: Containment Systems Capability	111 - 138
1.9 H.W. Lewis: Probabilistic Risk Assessment - Merits and Limitations	139 - 148
1.10 J.H. Gittus, F.R. Allen: Safety Goals Approaches	149 - 164
1.11 A. Birkhofer: Advances and Trends in Reactor Safety Research and Technology	165 - 178

Chapter 2  
Safety Related Operation Experience

	pages
2.1 K.J. Laakso: Systematic Analysis of Plant Disturbances with a View to Reducing Scram Frequency	181 - 190
2.2 R. Japavaire, B. Fourest: An Example of Operating Experience in France: The Tricastin 1 Incident on August 3, 1982	191 - 198
2.3 G. Gros, D. Perrault: Control Rod Guide Tube Support Pin Cracking at French Plants	199 - 209
2.4 P.J. Amico: Fault Tree Analysis of Westinghouse Solid State Protection System Scram Reliability	210 - 219
2.5 T. Meslin, A. Carnino, B. Payen, A. Cahuzac: Station Blackout: A Test on a Plant at Power Lessons Learned for Safety Studies	220 - 229
2.6 P. Cassette, G. Giroux, H. Roche, J.J. Seveon: Evaluation of Primary Coolant Leaks and Assessment of Detection Methods	230 - 238
2.7 G. Dredemis, B. Fourest: Systematic Safety Evaluation of Old Nuclear Power Plants	239 - 247
2.8 J. Magdalinski, R. Ivars: Hydrogen Water Chemistry - A Proven Method to Inhibit Intergranular Stress Corrosion Cracking in Boiling Water Reactors	248 - 257

	pages
2.9 R. Schraewer, B. Wintermann: The Fine Motion Control Rod Drive and Reactor Scram System of KWU; Design, Long Term Operational Behaviour and Experiences	258 - 267
2.10 E. Legath: Power Uprates in ASEA-ATOM Boiling Water Reactors	268 - 272
2.11 K. Fischer, H. Kastl, M. Kurzawe: Dose Reduction by Application of Advanced Methods for Testing and Repairing of Steam Generator Tubes	273 - 282
2.12 R.G. Sauvé, W.W. Teper Investigation of A Liquid Zone Control Assembly Failure at a Nuclear Generating Station	283 - 294

### Chapter 3

#### System and Component Behavior

3.1 F.J. Erbacher: Interaction Between Fuel Clad Ballooning and Thermal- Hydraulics in a LOCA	299 - 310
3.2 M.A. Bolander, C.D. Fletcher, C.B. Davis, C.M. Kullberg, B.D. Stitt, M.E. Waterman, J.D. Burt: RELAP5 Thermal-Hydraulic Analyses of Overcooling Sequences in a Pressurized Water Reactor	311 - 319
3.3 J.E. Koenig, R.C. Smith: TRAP-PF1 Analyses of Potential Pressurized-Thermal-Shock Transients at a Combustion-Engineering PWR	320 - 329
3.4 W. Häfner, L. Wolf: Review and Assessment of American Experiments and Theoretical Models for Thermal Mixing PTS-Phenomena as Basis for Designing HDR-Experiments TEMB	330 - 347

	pages
3.5 J.Q. Howieson, L.J. Watt, S.D. Grant, P.G. Hawley, S. Girgis: CANDU LOCA Analysis with Loss of Offsite Power to Meet LWR Acceptance Criteria as Applied in Japan	348 - 356
3.6 U.S. Rohatgi, C. Yuelys-Miksis, P. Saha: An Assessment of Appendix K Conservatism for Large Break LOCA in a Westinghouse PWR	357 - 365
3.7 P. Gulshani, M.Z. Caplan, N.J. Spinks: THERMOSS: A Thermohydraulic Model of Flow Stagnation in a Horizontal Fuel Channel	366 - 375
3.8 N.J. Spinks, A.C.D. Wright, M.Z. Caplan, S. Prawirosoehardjo, P. Gulshani: Thermosyphoning in the CANDU Reactor	376 - 384
3.9 K.H. Ardron, V.S. Krishnan, J.P. Mallory, D.A. Scarth: Studies of Hot-Wall Delay Effects Pertinent to CANDU LOCA Analysis	385 - 396
3.10 J.T. Rogers: A Study of the Failure of the Moderator Cooling System in a Severe Accident Sequence in a CANDU Reactor	397 - 408
3.11 S.E. Meier: Fluid-Structure Interaction in Pressure Water Reactors	409 - 415
3.12 J.A. Kobussen, R. Mylonas, W.X. Zheng: RETRAN Predictions for Pressure Transients Following a Feedwater Line Break and Consequent Check Valve Closing	416 - 425
3.13 J.A. Desoisa, C.P. Greef: Reactor Fault Simulation at the Closure of the Windscale Advanced Gas-Cooled Reactor: Analysis of Transient Tests	426 - 435

	pages
3.14 G. Herbold, E.J. Kersting: Analysis of a Total Loss of AC-Power in a German PWR	436 - 447
3.15 C.A. Dobbe, R. Chambers, P.D. Bayless: Thermal-Hydraulic and Core Damage Analysis of the Station Blackout Transient in Pressurized Water Reactors	448 - 456
3.16 R. Bisanz, B. Burger, U. Lang, M. Schindler, F. Schmidt, H. Unger: Analysis of Severe LOCA Problems Using RELAP5 and TRAC	457 - 466
3.17 R.R. Schultz, Y. Kukita, Y. Koizumi, K. Tasaka: A LSTF Simulation of the TMI-2 Scenario in a Westinghouse Type Four Loop PWR	467 - 476
3.18 E.F. Hicken: Results from the OECD-LOFT Consortium Tests	477
3.19 P.J. Fehrenbach, I.J. Hastings, J.A. Walsworth, R.C. Spencer, J.J. Lipsett, C.E.L. Hunt, R.D. Delaney: Zircaloy-Sheathed UO <sub>2</sub> Fuel Performance During In-Reactor LOCA Transients	478 - 487
3.20 V.I. Nath, E. Kohn: High Temperature Oxidation of CANDU Fuel During LOCA	488 - 497
3.21 R.M. Mandl, B. Brand, H. Schmidt: The Importance of End-of-Blowdown Phase on Refill/ Reflood for the Case of Combined ECC Injection. Results from PKL Tests	498 - 507
3.22 M. Spiga: Heat Transfer in PWR U-Tube Steam Generators	508 - 515
3.23 F.J. Erbacher, P. Ihle, K. Rust, K. Wiehr: Temperature and Quenching Behavior of Undeformed, Ballooned and Burst Fuel Rods in a LOCA	516 - 524

	pages
3.24 D.G. Reddy, C.F. Fighetti: A Study of Rod Bowing Effect on Critical Heat Flux in PWR Rod Bundles	525 - 534
3.25 H. Kianjah, V.K. Dhir, A. Singh: Enhancement of Heat Transfer in Disperse Flow and Downstream of Blockages in Rod Bundles	535 - 545
3.26 D. Saphier, J. Rodnizky, G. Meister: Transient Analysis of an HTGR Plant With the DSNP Simulation System	546 - 555

#### Chapter 4

#### Safety Systems and Function Optimization

4.1 R. Martin, H. Guesnon: Safeguard Pumps Qualification for French Nuclear Plants The EPEC Test Loop	559 - 573
4.2 P. Wietstock: Hydrodynamical Tests with an Original PWR Heat Removal Pump	574 - 580
4.3 G. Depond, H. Sureau: Steam Generator Tube Rupture Risk Impact on Design and Operation of French PWR Plants	581 - 587
4.4 L. Cave, W.E. Kastenberg, K.Y. Lin: A Value/Impact Assessment for Alternative Decay Heat Removal Systems	588 - 596
4.5 H.A. Maurer: Cost Benefit Analysis of Reactor Safety Systems	597 - 606



	pages
4.6 A. Renard, R. Holzer, J. Basselier, K. Hnilica, Cl. Vandenberg: Safety Assessment from Studies of LWR's Burning Plutonium Fuel	607 - 616
4.7 J.L. Platten: Periodic (Inservice) Inspection of Nuclear Station Piping Welds, for the Minimum Overall Radiation Risk	617 - 625
4.8 P. Grimm, J.M. Paratte, K. Foskolos, C. Maeder: Parametric Studies on the Reactivity of Spent Fuel Storage Pools	626 - 633
4.9 W. Geiger: The CEC Shared Cost Action Research Programme on the Safety of Thermal Water Reactors: Results in the Sub-Area "Protection of Nuclear Power Plants Against External Gas Cloud Explosions"	634 - 642
4.10 G.P. Celata, M. Cumo, G.E. Farelllo, P.C. Incalcaterra: Physical Insight in the Evaluation of Jet Forces in Loss of Coolant Accidents	643 - 654
4.11 A. Singh, D. Abdollahian: Critical Flow Thru Safety Valves	655 - 665
4.12 A. Aust, H.-R. Niemann, H.D. Fürst, G.F. Schultheiss: Chugging-Related Load Reduction for Pressure Suppression Systems	666 - 674
4.13 S.A. Andersson, S. Helmersson, L.-E. Johansson: Improved Fuel Cycle Flexibility and Economy: Verification Tests with BWR Coolant Flow Range Extension	675 - 682

	pages
4.14 M. Bielmeier, M. Schindler, H. Unger, H. Gasteiger, H. Stepan, H. Körber: Investigation of the ECC-Efficiency in the Case of Small Leaks in a 1300 MW <sub>e1</sub> Boiling Water Reactor	683 - 692
4.15 H. Fabian, K. Frischengruber: Safety Concept and Evaluation of the 745 MW KWU- Pressurized Heavy Water Reactor (PHWR)	693 - 711
4.16 P. Antony-Spies, D.Göbel, M. Becker: Survey of KWU's Safety Related Containment Work for American Boiling Water Reactors	712 - 719

## Volume 2

### Chapter 5

#### Man Machine Interface and Emergency Response

5.1 W. Aleite, K.H. Geyer: Safety Parameter Display System Functions are Integrated Parts of the KWU KONVOI Process Information System (SPDS Functions are parts of the KWU-PRINS)	723 - 732
5.2 R. Marcille: Man-Machine Interface Enhancement Undertaken by EDF to Minimize Human Errors	733 - 739
5.3 B. Wahlström, G. Mancini: International Research and Information Dissemination in the Field of Human Factors of Nuclear Power	740 - 751
5.4 K. Hartel: Simulator Modelling of the PWR	752 - 761
5.5 J.D. Lewins: Simulation for Nuclear Reactor Technology	762 - 765

	pages
5.6 T. Eckered, W. Essler: Emergency Planning and Preparedness in EC Countries	766 - 775
5.7 S. Hassanien: Bruce Nuclear Generating Station 'A' Operational Review for Loss of Coolant Accident with Fuel Failure Scenario	776 - 785
5.8 E. Hussein, J.C. Luxat: Heat Transport Inventory Monitoring for CANDU-PHW Reactors	786 - 795
5.9 S. Guarro, D. Okrent: Logic Flowgraph Model for Disturbance Analysis of a PWR Pressurizer System	796 - 803
5.10 R.C. Knobel: A Symptom Based Decision Tree Approach to Boiling Water Reactor Emergency Operating Procedures	804 - 813
5.11 R.T. Curtis, B.B. Agrawal: Recent Results from the U.S. Severe Accident Sequence Analysis (SASA) Program	814 - 823
5.12 T.S. Margulies, J.A. Martin, Jr.: Precalculated Doses for Emergency Response	824 - 832
5.13 H. Sureau, J. Mesnage: Physical State Approach to PWR Emergency Operating Procedures: Recent Developments in France	833 - 841
5.14 A. Brunet, T. Meslin: Validation of Event Oriented Procedures	842 - 846

## Chapter 6

## Fuel Behavior during Severe Accidents

	pages
6.1 R.W. Wright, M. Silberberg, G.P. Marino: Status of the Joint Program of Severe Fuel Damage Research of the USNRC and Foreign Partners	851 - 857
6.2 J.N. Lillington: Assessment of SCDAP by Analysis of In-Pile Experiments; Power Burst Facility - Severe Fuel Damage Scoping Test	858 - 875
6.3 P.E. MacDonald, C.L. Nalezny, R.K. McCardell: Severe Fuel Damage Test 1-1 Results	876 - 887
6.4 L.J. Siefken: SCDAP Code Analysis of the Power Burst Facility Severe Fuel Damage Test 1-1	888 - 896
6.5 C.M. Allison, D.L. Hagrman, G.A. Berna: The Influence of Zircaloy Oxidation and Melting Behavior on Core Behavior during a Severe Accident	897 - 907
6.6 R. Bisanz, F. Schmidt: Analysis of the PBF Severe Fuel Damage Experiments with EXMEL-B	908 - 916
6.7 A.C. Marshall, P.S. Pickard, K.O. Reil, J.B. Rivard, K.T. Stalker: DF-1: An ACRR Separate Effects Experiment on Severe Fuel Damage	917 - 927
6.8 G. Schanz, H. Uetsuka, S. Leistikow: Investigations of Zircaloy-4 Cladding Oxidation under Steam Starvation and Hydrogen Blanketing Conditions	928 - 937
6.9 S. Saito, S. Shiozawa: Severe Fuel Damage in Steam and Helium Environments Observed in In-Reactor Experiments	938 - 947

	pages
6.10 U. Lang, F. Schmidt, R. Bisanz: Analysis of the Fuel Heatup and Melting Experiments NIELS- CORA with the Code System SSYST-4	948 - 957
6.11 S.H. Kim, R.P. Taleyarkhan, M.Z. Podowski, R.T. Lahey, Jr.: An Analysis of Core Meltdown Accidents for BWRs	958 - 967
6.12 P. Cybulskis: In-Vessel Hydrogen Generation Analyses with MARCH 2	968 - 977
6.13 C. Blahnik, W.J. Dick, D.W. McKean: Post Accident Hydrogen Production and Control in Ontario Hydro CANDU Reactors	978 - 987
6.14 G.I. Hadaller, R. Sawala, E. Kohn, G.H. Archinoff, S.L. Wadsworth: Experiments Investigating the Thermal-Mechanical Behaviour of CANDU Fuel under Severely Degraded Cooling	988 - 998
6.15 M.S. El-Genk, S.-H. Kim, D. Erickson: Post-Accident Heat Removal Analysis: An Assessment of the Composition of Core Debris Beds	999 - 1014
6.16 P. Hofmann, H.J. Neitzel: External and Internal Reaction of Zircaloy Tubing with Oxygen and UO <sub>2</sub> and its Modeling	1015 - 1025
6.17 A. Denis, E.A. Garcia: Simulation of the Interaction Between Uranium Dioxide and Zircaloy	1026 - 1034
6.18 A. Skokan: High Temperature Phase Relations in the U-Zr-O System	1035 - 1042
6.19 H.E. Rosinger, K. Demoline, R.K. Rondeau: The Dissolution of UO <sub>2</sub> by Molten Zircaloy-4 Cladding	1043 - 1056

	pages
6.20 W. Eifler: Thermal Hydraulic Severe Accident Phenomena in Small Fuel Rod Bundles during Simulation Experiments	1057 - 1066
6.21 A.W.P. Newbigging, A.I. Russell, E. Turner: Post-Irradiation Examination of Fuel Subjected to Pressurized High Temperature Transients in WAGR	1067 - 1075
<u>Chapter 7</u>	
Core Debris Behavior and Core Concrete Interaction	
7.1 B.W. Spencer, L.M. McUmbur, J.J. Sienicki: Results and Analysis of Reactor-Material Experiments on Ex-Vessel Corium Quench and Dispersal	1079 - 1089
7.2 T. Schulenberg, U. Müller: A Refined Model for the Coolability of Core Debris with Flow Entry from the Bottom	1090 - 1097
7.3 B.J. Kim, M.L. Corradini: Recent Film Boiling Calculations: Implication on Fuel-Coolant Interactions	1098 - 1107
7.4 T. Ginsberg, J.C. Chen: Quench Cooling of Superheated Debris Beds in Containment during LWR Core Meltdown Accidents	1108 - 1117
7.5 B.D. Turland, N.J. Brealey: Improvements to Core-Concrete Interaction Models	1118 - 1127
7.6 S.B. Burson: Contributions to Containment Threat from High-Temperature Core-Debris Cavity Interactions	1128 - 1137
7.7 P.G. Kroeger, Y. Shiina: Transient Moisture Migration in Concrete During Severe Reactor Accidents	1138 - 1147

Staedtke, H.	Vol. 3, P. 1656	Wolf, L.	Vol. 3, P. 1867
Stalker, K.T.	Vol. 2, P. 917	Worth, B.	Vol. 3, P. 1656
Stepan, H.	Vol. 1, P. 683	Wright, A.C.D.	Vol. 1, P. 376
Stitt, B.D.	Vol. 1, P. 311	Wright, W.R.	Vol. 2, P. 851
Stora, J.P.	Vol. 3, P. 1398	Young, M.F.	Vol. 2, P. 1196
Stratton, W.R.	Vol. 1, P. 95	Yuelys-Miksis, C.	Vol. 1, P. 357
Sureau, H.	Vol. 1, P. 581	Zheng, W.X.	Vol. 1, P. 416
Sureau, H.	Vol. 2, P. 833		
Svensson, H.	Vol. 3, P. 1791		
Szabados, L.	Vol. 3, P. 1689		
Taleyarkhan, R.P.	Vol. 2, P. 958		
Tamm, H.	Vol. 2, P. 1327		
Tasaka, K.	Vol. 3, P. 1811		
Tattegrain, A.	Vol. 3, P. 1645		
Teper, W.W.	Vol. 1, P. 283		
Thadani, A.	Vol. 3, P. 1881		
Thomauske, K.	Vol. 2, P. 1216		
Thurgood, M.J.	Vol. 3, P. 1867		
Togo, Y.	Vol. 3, P. 1554		
Tomkins, J.L.	Vol. 2, P. 1196		
Toth, I.	Vol. 3, P. 1689		
Traiforos, S.A.	Vol. 2, P. 1301		
Trotabas, M.	Vol. 3, P. 1645		
Turland, B.D.	Vol. 2, P. 1118		
Turner, E.	Vol. 2, P. 1067		
Tweedy, J.N.	Vol. 3, P. 1898		
Uetsuka, H.	Vol. 2, P. 928		
Unger, H.	Vol. 1, P. 457		
Unger, H.	Vol. 1, P. 683		
Unger, H.	Vol. 2, P. 1167		
Unger, H.	Vol. 3, P. 1564		
Vandenberg, Cl.	Vol. 1, P. 607		
Villeroux, G.	Vol. 3, P. 1967		
Vinjamuri, K.	Vol. 3, P. 1583		
Vogt, S.	Vol. 3, P. 2016		
Waraanperä, Y.	Vol. 3, P. 1791		
Wadsworth, S.L.	Vol. 2, P. 988		
Wagner, K.C.	Vol. 3, P. 1801		
Wagner, K.C.	Vol. 3, P. 1840		
Wahlström, B.	Vol. 2, P. 740		
Walsworth, J.A.	Vol. 1, P. 478		
Warlop, R.	Vol. 3, P. 1398		
Warman, E.A.	Vol. 3, P. 1478		
Waterman, M.E.	Vol. 1, P. 311		
Watt, L.J.	Vol. 1, P. 348		
Weiser, G.	Vol. 1, P. 9		
Wells, A.C.	Vol. 3, P. 1423		
Wells, J.E.	Vol. 3, P. 1947		
Werle, H.	Vol. 2, P. 1216		
Wheatley, P.D.	Vol. 3, P. 1840		
Wiehr, K.	Vol. 1, P. 516		
Wietstock, P.	Vol. 1, P. 574		
Wilhelm, J.G.	Vol. 3, P. 1514		
Wilhelm, J.G.	Vol. 3, P. 1572		
Wintermann, B.	Vol. 1, P. 258		
Wittek, P.	Vol. 3, P. 2016		
Wolf, L.	Vol. 1, P. 330		





## LIST OF PARTICIPANTS

ABBEY, FRANK	UKAEA	GB-	WARRINGTON WA3 4NE
ACHE, PROF.DR. H.J.	KFK GMBH	D -7500	KARLSRUHE
ADAM, PROF.DR. ERNST	TU DRESDEN	DDR -	8027 DRESDEN
ADAMS, R.E.	OAK RIDGE N.L.	USA -	37831 OAK RIDGE, TENN.
ADELHELM, DR. CHRISTEL	KFK GMBH	D -7500	KARLSRUHE
ADRIAN, DR. H.W.W.	NUCOR	D -5300	BONN 2
AFSHAR, DR. ALI	AEOI	IR -	TEHERAN
AL OMAR, DR.	ATOMIC EN.C.B.	CDN-	OTTAWA ONTARIO KIP 5S9
AL-ARAJI, DR. SAMI R.	IAEC	IRQ -	BAGHDAD
ALBRECHT, DR. HELMUT	KFK GMBH	D -7500	KARLSRUHE
ALEITE, WERNER	KWU ERLANGEN	D -8521	SPARDORF
ALLISON, C.M.	EG&G IDAHO INC	USA -	IDAHO FALLS, 83415
ALMENAS, KAZYS	UNIV. MARYLAND	USA -	TRAIFOROS, MD. 20740
ALSMEYER, DR. HANS	KFK GMBH	D -7500	KARLSRUHE
ALTER, DR. JOSEPH	ISR. ATOMIC EC	IL -	TEL-AVIV, 61070
ALY, A.M. MORTADA	ATOMIC EN.C.B.	CDN -	OTTAWA, ONT. KIP 5S9
AMICO, PAUL J.	APP.RISK TECH.	USA -	21045 COLUMBIA, MARYL.
ANALYTIS, GERASSIMOS	EIR	CH-5303	WÜRENKLINGEN
ANDERKO, KURT	KFK GMBH	D -7500	KARLSRUHE
ANDERSON, DR. G.S.	BNFL	GB -	PRESTON PR4 ODB
ANDREANI, MICHELE	UNIV. PISA	I -	PISA
ANDREWS, W. BILL	BATTELLE NW	USA -	RICHLAND, WA
ANNUNZIATO, ALESSANDRO	ENEA	I-00198	ROMA
ANTONY-SPIES, DR. PETER	KWU OFFENBACH	D -6050	OFFENBACH
ARDRON, K.H.	AECL	CDN -	PINAWA MANITOBA ROEILLO
ARNAUD, A.M.	CEA	F-13115	SAINT-PAUL-LEZ-DURANCE
ARO, ILARI	SÄTTELYTUR.	SF -	00101 HELSINKI
ASCHEUER, H.	GRS	D -5000	KÖLN 1
AUST, ECKHARD	GKSS	D -2054	GEESTHACHT
BACHOFNER, EMIL	OKG AB	S-11187	STOCKHOLM
BARBE, BERNARD	CEA	F-92260	FONTENAY-AUX-ROSES
BARI, ROBERT A.	BROOKHAVEN N.L.	USA -	UPTON NY, 11973
BARLEON, LEOPOLD	KFK GMBH	D -7500	KARLSRUHE
BARTSCH, HANS	SWED. ST.POWER	S-16287	VÄLLINGBY
BAUMANN, DR. WALTER	KFK GMBH	D -7500	KARLSRUHE
BECKER, DR. MANFRED	KWU OFFENBACH	D -6050	OFFENBACH
BECKER, KURT	ROY.INST.TECH.	S-10044	STOCKHOLM
BECKER, PROF.DR. KLAUS	DIN NORMEN	D -1000	BERLIN 30
BENJAMIN, ALLAN S.	SANDIA N.L.	USA -	ALBUQUERQUE, NM 87111
BERG, DR. KARL-HEINZ	BMI	D -5300	BONN 7
BERGSTRÖM, STIG O.W.	STUDSVIK	S-61182	NYKÖPING
BESI, ANDREA	CEC ISPRA	I-21020	ISPRA (VARESE)
BIELMEIER, MICHEAL	UNIV. STUTTG.	D -7000	STUTTGART 80
BISANZ, REINHOLD	UNIV. STUTTG.	D -7000	STUTTGART 80
BLAHNIK, C.	ONTARIO HYDRO	CDN -	TORONTO, ONT. M5G IX6
BLANK, DR. H.	KFK GMBH	D -7500	KARLSRUHE
BLEJWAS, THOMAS E.	SANDIA N.L.	USA -	ALBUQUERQUE, NM 87112
BLOMQUIST, ROLAND	STUDSVIK	S-61182	NYKÖPING
BOEHM, FRANZ	UNIV. STUTTG.	D -7000	STUTTGART 80
BOLANDER, MARK	EG&G IDAHO INC	USA -	IDAHO FALLS ID, 83415
BOLDT, KENNETH R.	SANDIA N.L.	USA -	ALBUQUERQUE NM, 87185
BORGWALDT, DR. HORST	KFK GMBH	D -7500	KARLSRUHE 1
BORK, GERHARD	KFK GMBH	D -7500	KARLSRUHE
BOZZOLA, S.	ANSALDO IMP.	I -	
BRESTRICH, DR. INGO	TÜV BADEN	D -6800	MANNHEIM 1
BRISBOIS, JACQUES	CEA	F-92260	FONTENAY-AUX-ROSES
BRITAN, IAN	AEE WINFRITH	GB -	DORSET DT2 8DH
BROCKMANN,	TÜV RHEINLAND	D -5000	KÖLN 90
BROWN, R.A.	ONTARIO HYDRO	CDN -	TORONTO, ONT. M5G IX6
BRÜCKNER, DR. A.	KFK GMBH	D -7500	KARLSRUHE
BUCLIN, JEAN-PAUL	SA ENERGIE	CH-1001	LAUSANNE
BUESCHER, DR. B.J.	EG&G IDAHO INC	D -7513	STUTENSEE 5

BURGER, BERND	UNIV. STUTTG.	D -7000	STUTTGART 80
BURKE, RICHARD P.	SANDIA N.L.	USA -	ALBUQUERQUE NM, 87185
BURSON, DR. S. BRADLEY	US NRC	USA -	20555 WASHINGTON D.C.
BÜNEMANN, DIETRICH	GKSS	D -2054	GEESTHACHT-TESPERHUDE
BÜRGER, MANFRED	UNIV. STUTTG.	D -7000	STUTTGART 80
BÜTTNER, WOLF-E.	GRS	D -8046	GARCHING
CACCIABUE, CARLO PIETRO	CEC ISPRA	I-21020	ISPRA (VARESE)
CAHUZAC, ANTOINE	ELECTR. FRANCE	F-75006	PARIS
CAMBIEN, ISABELL	KFK GMBH	D -7513	STUTENSEE 1
CARACHALIOS, CONSTANTIN	UNIV. STUTTG.	D -7000	STUTTGART 80
CARDEIRA, F.	PORT.NUCL.SOC.	P -	LISSABON
CARNINO, ANNICK	ELECTR. FRANCE	F-75008	PARIS
CARTER, JAMES C.	T.E.C.	USA -	KNOXVILLE, TENNESSEE
CASSETTE, PHILIPPE	CEA	F-92260	FONTENAY-AUX-ROSES
CAVE, L.	RISK ASSESSMT.	GB -	TUNBRIDGE WELLS, KENT
CENERINO, GERARD	CEA	F-92260	FONTENAY-AUX-ROSES
CHADHA, J.A.	ONTARIO HYDRO	CDN -	TORONTO, ONT. M8Z 5S4
CIGARINI, MARCO	KFK GMBH	D -7500	KARLSRUHE
CLARK, J.M.	SCOTL.EL.BOARD	GB -	GLASGOW, G44 4BE
CLOUGH, DR. P.N.	UKAEA	GB -	WARRINGTON, WA3 4NE
COLE, RANDALL K.	SANDIA N.L.	D -7500	KARLSRUHE 1
CONTE, DR. MADELEINE	CEA	F-92260	FONTENAY-AUX-ROSES
COSTAZ, JEAN-LOUIS	EDF (SEPTEN)	F-69628	VILLEURBANNE
CURCA-TIVIG, FLORIN	UNIV. STUTTG.	D -7000	STUTTGART 80
CURTIS, ROBERT	US NRC	USA -	GAITHERSBURG MD 20878
DALLE DONNE, PROF. M.	KFK GMBH	D -7500	KARLSRUHE
DE BOECK, BENOIT	ASS. VINCOTTE	B -1180	BRUSSELS
DELJA, ALEKSANDAR	FAC. MECH.ENG.	YU -	BEOGRAD
DENNING, DR. RICHARD S.	BATTELLE	USA -	COLUMBUS, OHIO 43201
DEUBER, DR. H.	KFK GMBH	D -7500	KARLSRUHE
DIENST, DR. WOLFGANG	KFK GMBH	D -7500	KARLSRUHE
DILLMANN, HANS-GEORG	KFK GMBH	D -7500	KARLSRUHE
DOBBE, CHARLES	EG&G IDAHO INC	USA -	IDAHO FALLS ID, 83415
DREDEMIS, GEOFFROY	CEA	F-92260	FONTENAY-AUX-ROSES
DROLSHAMMER, O.	KFK GMBH	D -7500	KARLSRUHE
DROUIN, M.T.	SCIENCE APPL.	USA -	87102 ALBUQUERQUE N.MEX
DUCO, JEAN	CEA	F-92260	FONTENAY-AUX-ROSES
DUNCKER, PETER	KWU KARLSTEIN	D -8757	KARLSTEIN
ECKERED, THOMAS	RAADET F. KKA	S-10248	STOCKHOLM
EDWARDS, A.R.	UKAEA	GB -	WARRINGTON WA3 5QU
EGLIN, WOLFGANG	BADENWERK	D -7500	KARLSRUHE 1
EHRHARDT, DR. JOACHIM	KFK GMBH	D -7500	KARLSRUHE
EIFLER, WALTER	CEC ISPRA	I-21020	ISPRA (VARESE)
EL-GENK, MOHAMED S.	UNIV. N.MEXICO	USA -	ALBUQUERQUE, NM 87131
EL-SHANAWANY, DR. M.	NNC	GB -	LEICESTER, LE8 3LH
ENERHOLM, ANDERS	ROY.INST.TECH.	S-10044	STOCKHOLM
ERBACHER, F.J.	KFK GMBH	D -7500	KARLSRUHE
ERVEN, ULRICH	GRS	D -5100	AACHEN
ESPEFÄLT, RALF	SWED.ST.POWER	S-16287	VÄLLINGBY
FABIAN, DR. HERMANN	KWU ERLANGEN	D -8520	ERLANGEN
FABREGA,	CEA	F-13115	SAINT-PAUL-LEZ-DURANCE
FAIRCLOTH, REGINALD L.	UKAEA	GB -	OXON
FARELLO, ELVIO	ENEA	I -	ROMA
FASOLI-STELLA, PAOLA	CEC ISPRA	I-21020	ISPRA (VARESE)
FEHRENBACH, DR. P.J.	AECL	CDN -	CHALK RIVER, ONTARIO
FERMANDJIAN, JEAN	CEA	F-92260	FONTENAY-AUX-ROSES
FERRELL, W.L.	SCIENCE APPL.	USA -	87102 ALBUQUERQUE N.MEX
FERRERO, CLAUDIO	KFK GMBH	D -7500	KARLSRUHE
FEUERSTEIN, DR. H.	KFK GMBH	D -7500	KARLSRUHE
FIEGE, A.	KFK GMBH	D -7500	KARLSRUHE
FINZI, S.	CEC BRUSSELS	B -	BRUSSELS
FIORENZA, JOSEF	KWU ERLANGEN	D -8520	ERLANGEN

FISCHER, DR. KARSTEN	BATTELLE	D -6000	FRANKFURT 90
FISCHER, DR. P.-M.	KFK GMBH	D -7500	KARLSRUHE
FOUREST, BERNARD	CEA	F-92260	FONTENAY-AUX-ROSES
FRESCURA, G.M.	ONTARIO HYDRO	CDN -	TORONTO ONT. M5G IX6
FRISCHENGROBER, KURT	KWU ERLANGEN	D -8520	ERLANGEN
FROMENTIN,	EIR	CH-5303	WÜRENLINGEN
FRÖHLICH, DR. REIMAR	KFK GMBH	D -7500	KARLSRUHE
FUCHS, HANS	MOTOR-COLUMBUS	CH-5401	BADEN
FURRER, DR. MAX	EIR	CH-5303	WÜRENLINGEN
FYNBO, PETER B.	RISO NAT.LAB.	DK-4000	ROSKILDE
GABALLAH, DR. IBRAHIM	HRB GMBH	D -6800	MANNHEIM 1
GARDNER, RICHMOND	STONE& WEBSTER	USA -	BOSTON, 02107
GARLAND, J.A.	AERE HARWELL	GB -	OXFORDSHIRE OXII ORA
GAUDENZIO, MARIOTTI	ENEL-CRTN	I-56100	PISA
GAUVENET, ANDRE	ELECTR. FRANCE	F-75008	PARIS
GEIGER, DR. WERNER	BATTELLE	D -6000	FRANKFURT
GIESEKE, DR. JAMES	BATTELLE	USA -	COLUMBUS OHIO 43201
GILBY, ERNEST V.	GILBY ASS.	GB -	KNUTSFORD, CHE. WA169DZ
GILL, RALPH	GRS	D -8046	GARCHING
GINSBERG, DR. THEODORE	BROOKHAVEN N.L	USA -	UPTON, NY 11973
GIROUX, CHRISTIAN	CEA	F-92260	FONTENAY-AUX-ROSES
GITTUS, DR. J.H.	UKAEA	GB -	CULCHETH, WARR. WA3 4NE
GOUFFON, ALAIN	CEA	F-92260	FONTENAY-AUX-ROSES
GOVAERTS, PAUL	S.C.K./C.E.N.	B -2400	MOL
GOVAERTS, PIERRE	ASS. VINCOTTE	B -1180	BRUSSELS
GREEF, DR. C.P.	C.E.E.B.	GB -	GLOUCESTERSHIRE GLB 9PB
GREMM, DR. OTTO	KWU ERLANGEN	D -8520	ERLANGEN
GRIFFITH, JERRY D.	US ENERGY DEP.	USA -	WASHINGTON DC, 20545
GRIMM, PETER	EIR	CH-5303	WÜRENLINGEN
GROOS, DR. EKKEHARD	KFA JÜLICH	D -5170	JÜLICH
GROS, G.	CEA	F-92260	FONTENAY-AUX-ROSES
GRÄSLUND, CHRISTIAN	SWEDISH NPI	S-10252	STOCKHOLM
GUARRO, SERGIO	LLNL	USA -	LIVERMORE, CA 94550
GUESNON, HENRI	FRAMATOME	F-92084	PARIS LA DEFENSE
GULDEN, DR. WERNER	KFK GMBH	D -7500	KARLSRUHE
HADALLER, G.I.	WESTINGHOUSE	CDN -	HAMILTON ONT. L8N 3K2
HAGEN, DR. S.	KFK GMBH	D -7500	KARLSRUHE
HALL, PETER	CEGB	GB -	GLOUCESTER
HARPER, FREDERICK T.	SANDIA N.L.	USA -	ALBUQUERQUE, NM 87185
HASCHKE, DR. DIETER	EIR	CH-5303	WÜRENLINGEN
HASSANIEN, DR. S.	ONTARIO HYDRO	CDN -	TIVERTON ONT. NOG 2TO
HAUSSERMANN,	NUCL.EN.AGENCY	F-75016	PARIS
HEDGRAN, ARNE	ROY.INST.TECH.	S-10044	STOCKHOLM
HELLSTRAND, ERIC	STUDSVIK	S-61182	NYKÖPING
HENDRIE, DR. JOSEPH M.	AMERICAN NUCL.	USA -	UPTON NY, 11973
HENNIES, DR. H.H.	KFK GMBH	D -7500	KARLSRUHE
HENNINGS, DR. WILFRIED	KFA JÜLICH	D -5170	JÜLICH
HERBOLD, G.	GRS	D -8046	GARCHING
HERTRICH, DR. MICHAEL	BMI	D -5300	BONN 1
HEUSER, DR. F.W.	GRS	D -5000	KÖLN 1
HICKEN, PROF.DR. E.	GRS	D -8046	GARCHING
HILL, DR. T.F.	ATOMIC EN.CORP	ZA-0001	PRETORIA, SOUTH AFRICA
HINDLE, EDWARD D.	UKAEA	GB -	PRESTON, PR4 ORR
HIRMER, FRANZ	KWU ERLANGEN	D -8520	ERLANGEN
HIRSCHBERG, STEFAN	AB ASEA-ATOM	S-72104	VÄSTERAS
HOCKE, KLAUS-DIETER	UNIV. STUTTG.	D -7000	STUTTGART 80
HOERTNER, DR. HELMUT	GRS	D -8046	GARCHING
HOFMANN, DR. PETER	KFK GMBH	D -7500	KARLSRUHE
HOFMANN, G.	KFK GMBH	D -7500	KARLSRUHE
HOFMANN, WOLFHARD	KWU OFFENBACH	D -6050	OFFENBACH
HOHMANN, HERMANN	CEC ISPRA	I-21020	ISPRA (VARESE)
HOLTBECKER, HELMUT	CEC ISPRA	I-21020	ISPRA (VARESE)

HOLZER, ROBERT	NIS	D -6450	HANAU 1
HOSEMANN, DR. J.P.	KFK GMBH	D -7500	KARLSRUHE
HOWIESON, J.Q.	AECL	CDN -	MISSISSAUGA ONT L5K 1B2
HÖGBERG, LARS	NUCL.P. INSP.	S-10252	STOCKHOLM
HÄFNER, H.	KFK GMBH	D -7500	KARLSRUHE
HÄFNER, WOLFGANG	BATTELLE	D -6000	FRANKFURT 90
IHLE, P.	KFK GMBH	D -7500	KARLSRUHE
ILBERG, DR. DAN	BROOKHAVEN N.L	USA -	UPTON NY, 11973
ISRAEL, MATHIEU	ELECTR. FRANCE	F-92141	CLAMART CEDEX
JACOBS, GÜNTER	KFK GMBH	D -7500	KARLSRUHE
JAHNS, ARMIN	GRS	D -5000	KÖLN 1
JAPAVAIRE, ROBERT	CEA	F-92260	FONTENAY-AUX-ROSES
JASSIM, MOHAMED WIDAD	IAEC	IRQ -	BAGHDAD
JESCHKI, WOLFGANG	HSK	CH-5303	WÜRENLINGEN
JOHANSSON, KJELL O.	STUDSVIK	S-61182	NYKÖPING
KALLENBACH, ULRICH	UNIV. STUTTG.	D -7000	STUTTGART 80
KALLI, HAIKLEI	UNIV. LAPPEEN.	SF -	53851 LAPPEENRANTA 85
KALVERBOER, C.	N.V. PZEM	NL-4430	AA MIDDELBURG
KANZLEITER, T.F.	BATTELLE	D -6000	FRANKFURT 90
KAPULLA, DR. H.	KFK GMBH	D -7500	KARLSRUHE
KARB, E.	KFK GMBH	D -7500	KARLSRUHE
KARWAT, PROF.DR. HELMUT	TU MÜNCHEN	D -8046	GARCHING
KASTENBERG, WILLIAM	UCLA	USA -	LOS ANGELES CA, 90024
KATO, MASAMI	NIPPON ATOMIC	J -	KAWASAKI-CITY
KATZENMEIER, GUSTAV	KFK GMBH	D -7500	KARLSRUHE 1
KELLY, JOHN E.	SANDIA N.L.	USA -	ALBUQUERQUE NM, 87185
KERSTING, E.	GRS	D -8046	GARCHING
KESSLER, PROF. G.	KFK GMBH	D -7500	KARLSRUHE 1
KIM, BYONG-JOO	UNIV. WISCONS.	USA -	MADISON WI, 53705
KINSMAN, DR. PETER R.	UKAEA	GB -	WARRINGTON
KISSEL, HELMUT	KFK GMBH	D -7500	KARLSRUHE
KLEWE-NEBENIUS, DR. H.	KFK GMBH	D -7500	KARLSRUHE
KNOBEL, RONALD C.	KNOBEL & ASS.	USA -	LYONS GA, 30436
KOBUSSEN, J.	EIR	CH-5303	WÜRENLINGEN
KODAIRA, HIDEKI	UNIV. TOKYO	J - 113	TOKYO
KOENIG, JAN	LOS ALAMOS N.L	USA -	LOS ALAMOS, NM
KOHLI, RAJIV	BATTELLE	USA -	COLUMBUS OHIO 43201
KOHN, DR. E.	AECL	CDN -	MISSISSAUGA ONT L5K 1B2
KOLEV, DR.-ING. NIKOLAY	KFK GMBH	D -7500	KARLSRUHE
KOLLAS, JOHN G.	GREEK AEC	GR -	ACHIA PARASKEVI
KOLLATH, DR. KLAUS	GRS MBH	D -5000	KÖLN
KOMORIYA, DR. H.	ARGONNE N.L.	USA -	ARGONNE IL, 60540
KOMSI, MATTI	IMATRAN VOIMA	SF -	00101 HELSINKI 10
KOSTER, A.	NUCOR	ZA-0001	PRETORIA, SOUTH AFRICA
KOTAKE, SHOJI	MITSUBISHI RES	J - 100	TOKYO, CHIYODA-KU
KOUTSOVELIS, G.	KFK GMBH	D -7500	KARLSRUHE
KRAFT, ROLF	KFK GMBH	D -7500	KARLSRUHE
KRESS, DR. TOM S.	OAK RIDGE N.L.	USA -	37831 OAK RIDGE, TENN.
KREWER, KARL HEINZ	BMFT	D -5300	BONN
KRIEG, R.	KFK GMBH	D -7500	KARLSRUHE
KROEGER, P.G.	BROOKHAVEN N.L	USA -	UPTON, NY 11973
KRUGER, DR. P.J.	NUCOR	D -5300	BONN 2
KRÖSING, GERD	BVV-SV	D -8000	MÜNCHEN 70
KUCZERA, DR. B.	KFK GMBH	D -7500	KARLSRUHE
KUHLMANN, DR. MICHAEL	BATTELLE	USA -	COLUMBUS OHIO 43201
KUMMERER, PROF. K.	KFK GMBH	D -7500	KARLSRUHE
KURZAWA, MICHAEL	KWU KARLSTEIN	D -8757	KARLSTEIN
KUTTRUF, HELMUT	DR. LEDERMANN	D -6834	KETSCH
KÜSTERS, DR. HEINZ	KFK GMBH	D -7500	KARLSRUHE
KÖBERLEIN, DR. KLAUS	GRS	D -8046	GARCHING
KÖNIG, DR. L.	KFK GMBH	D -7500	KARLSRUHE
KÜRBER, DR H.	AP (ANG.PHYS.)	D -7261	GECHINGEN

L'HERITEAU, JEAN-PIERRE	CEA	F-92260	FONTENAY-AUX-ROSES
LAMROTH, HARRY	IMATRAN VOIMA	SF -	00101 HELSINKI 10
LANG, ULRICH	UNIV. STUTTG.	D -7000	STUTTGART 80
LANORE, JEANNE-MARIE	CEA	F-92260	FONTENAY-AUX-ROSES
LAPPA, DAVID ALLAN	LLNL	USA -	LIVERMORE, CA 94550
LARKINS, DR. JOHN T.	US NRC	USA -	WASHINGTON DC, 20555
LAURIDSEN, KURT	RISO NAT.LAB.	DK-4000	ROSKILDE
LEE, W.	ONTARIO HYDRO	CDN -	TORONTO ONT. M5G IX6
LEIMEISTER, HANS-R.	GRS	D -5000	KÖLN 1
LEISTIKOW, DR. S.	KFK GMBH	D -7500	KARLSRUHE 1
LEMANSKA, MIRIAM	SOREG NRC	IL -	70600 YERNE
LEUSCHNER, DR. A.H.	NUCOR	ZA-0001	PRETORIA, SOUTH AFRICA
LEUTHROTH, CLAUDE	CEA	F-13115	SAINT-PAUL-LEZ-DURANCE
LEVEN, DR. DIETRICH	GRS MBH	D -5000	KÖLN
LEVINE, SAUL	US NRC	USA -	GAITHERSBURG MD, 20878
LEWINS, DR. JEFFERY	UNIV. CAMBRIDG	GB -	CAMBRIDGE
LEWIS, PROF.H.W.	UNIV. CALIF.	USA -	SANTA BARBARA CA, 93106
LIEBER, KARL	EIR	CH-5303	WÜRENLINGEN
LIENART, P.	EDF/SPT	F-75384	PARIS CEDEX 08
LILLINGTON, J.N.	UKAEA	GB -	DORCHESTER, DOR.DT2 8DH
LITAI, DR. DAN	ISR. ATOMIC EC	IL -	TEL-AVIV 61070
LOEWENSTEIN, WALTER	EPRI	USA -	PALO ALTO, CA.
LOMAZZI, FRANCO	NIRA	I-16100	GENOVA
LONG, STEWART W.	COMBUSTION ENG	USA -	SPRINGFIELD VA, 22152
LONGWORTH, J.P.	CEGB	GB -	BERKELEY, GLOS.
LOOMIS, GUY G.	EG&G IDAHO INC	USA -	IDAHO FALLS, ID. 93401
LUMMERZHEIM, DR. DIETHARD	GRS MBH	D -5000	KÖLN
LUXAT, J.C.	ONTARIO HYDRO	CDN -	TORONTO ONT. M5G IX6
MAGDALINSKI, JAN	AB ASEA-ATOM	S-72104	VÄSTERAS
MAILLAT, A.	CEA	F-13115	SAINT-PAUL-LEZ-DURANCE
MALAUSSCHEK, HANS	KFK GMBH	D -7500	KARLSRUHE
MALCOLM, ERNST L.	US NRC	USA -	20555 WASHINGTON D.C.
MALHERBE, J.	C.E.N.	F-91191	GIF-SUR-YVETTE
MANDL, RAFAEL	KWU ERLANGEN	D -8520	ERLANGEN
MANIORI, DAVIDE	ENEA-DISP	I -	ROMA
MANSOOR, SYED HASAN	KFK GMBH	D -7500	KARLSRUHE
MARCILLE, R.	EDF/SPT	F-75384	PARIS CEDEX 08
MARTIN, IVAN C.	AECL	CDN -	CHALK RIVER ONT, KOJIJO
MARTIN, ROGER	EDF (SEPTEN)	F-69626	VILLEURBANNE CEDEX
MARTILA, JOUKO	SÄTELLYTUR.	SF -	00101 HELSINKI
MATSUMOTO, MASAKI	HITACHI LTD	J -	IBARAKI-KEN
MAURER, H.A.	CEC BRUSSELS	B -1049	BRUSSELS
MAYR, PETER	UNIV. STUTTG.	D -7000	STUTTGART 80
MAZZINI, M.	UNIV. PISA	I-56100	PISA
MC CAULEY, EDWARD W.	LLNL	USA -	LIVERMORE CA, 94550
MEIER, DR. SIGURD	GRS	D -5000	KÖLN 1
MERCIER, DR. OLIVER	EIR	CH-5303	WÜRENLINGEN
MERCIER, PIERRE	HYDRO-QUEBEC	CDN -	GENTILLY, QUEBEC
MERKLEIN, WALTER	KWU ERLANGEN	D -8520	ERLANGEN
MESLIN,	EDF/SPT	F-75384	PARIS CEDEX 08
MESNAGE, JOSETTE	FRAMATOME	F-92084	PARIS LA DEFENSE
METZIG, DR. GUNTARD	KFK GMBH	D -7500	KARLSRUHE
METZINGER, DR. J.	MPI	D -6900	HEIDELBERG
MEYER, DR. LEONHARD	KFK GMBH	D -7500	KARLSRUHE
MICHAEL, HORST	STONE& WEBSTER	USA -	BOSTON MA
MICHELSSEN, B.	RISO NAT.LAB.	DK-4000	ROSKILDE
MIETTINEN, JAAKKO	TECH.RES.CENTR	SF -	HELSINKI
MILHELM, JEAN-LUC	CEA	F-92260	FONTENAY-AUX-ROSES
MITCHELL, KEITH	NNC	GB -	LEICESTER, LE8 3LH
MOBERG, LARS	SCANDPOWER	N -2007	KJELLER
MORELL, DR. WILFRED	KWU ERLANGEN	D -8520	ERLANGEN
MORISON, W.G.	ONTARIO HYDRO	CDN -	TORONTO ONTARIO

MORLOCK, GÜNTER	GRS	D -5000	KÖLN 1
MUNZ, PROF.DR. D.	KFK GMBH	D -7500	KARLSRUHE
MURATA, KENNETH K.	SANDIA N.L.	USA -	ALBUQUERQUE N.M. 87185
MÜLLER, KLAUS	KFK GMBH	D -7500	KARLSRUHE
MÜLLER, PROF.DR. U.	KFK GMBH	D -7500	KARLSRUHE
MÜLLER-DIETSCH, W.	KFK GMBH	D -7500	KARLSRUHE
N.N.	UMWELT-MIN.	D -7000	STUTTGART 1
NAGEL, DR. KLAUS	KFK GMBH	D -7500	KARLSRUHE
NASCHI, GIOVANNI	ENEA-DISP	I -	ROMA
NEITZEL, H.J.	KFK GMBH	D -7500	KARLSRUHE
NEWBIGGING, A.	UKAEA	GB -	SELLAFIELD, CUMBRIA
NICHOLS, ALAN L.	UKAEA	GB -	DORCHESTER, DORSET
NISHIO, MASAHIDE	TOSHIBA	J -	YOKOHAMA-SHI
NISSEN, KLAUS L.	KFK GMBH	D -7500	KARLSRUHE
NORWOOD, KEITH S.	UKAEA	GB -	DIDCOT OXON, OX11 0RA
O'DONNELL, E.P.	EBASCO SERVICE	USA	NEW YORK, NY 10048
OBATA, HIDEO	CENTURY RES.C.	J - 103	TOKYO, CHUO-KU
OHLMEYER, HERMANN	HEW	D -2000	HAMBURG 60
OKAZAKI, MOTOAKI	JINS	J - 108	MINATOKU, TOKYO
OLLIKKALA, HANNU	SÄTELLYTUR.	SF -	00101 HELSINKI
ORTH, KARLHEINZ	KWU ERLANGEN	D -8520	ERLANGEN
OSBORNE, M.F.	OAK RIDGE N.L.	USA -	OAK RIDGE, TN 37831
OSETEK, DANIEL J.	EG&G IDAHO INC	USA -	IDAHO FALLS, ID 83401
PANITZ, DR. HANS-JÜRGEN	KFK GMBH	D -7500	KARLSRUHE
PASLER, HORST	KFK GMBH	D -7500	KARLSRUHE
PEEHS, DR. MARTIN	KWU ERLANGEN	D -8520	ERLANGEN
PELCE,	CEA	F-92260	FONTENAY-AUX-ROSES
PENN, W.J.	ONTARIO HYDRO	CDN -	TORONTO ONTARIO
PERINIC, D.	KFK GMBH	D -7500	KARLSRUHE
PERNECZKY, DR. LASZLO	INST.F.PHYSICS	H -1525	BUDAPEST
PERRAULT, D.	CEA	F-92260	FONTENAY-AUX-ROSES
PERSSON, AKE H.	SYDKRAFT AB	S-21701	MALMÖ
PERSSON, LEIF	SYDKRAFT AB	S-21701	MALMÖ
PETERSEN, DR. C.	KFK GMBH	D -7500	KARLSRUHE
PETIT, GERARD	EDF (SEPTEN)	F-69626	VILLEURBANNE CEDEX
PETRANGELI, GIANNI	ENEA-DISP	I -	ROMA
PFRANG, W.	KFK GMBH	D -7500	KARLSRUHE
PFÖRTNER, DR. HERMANN	ICT-BERGHAUSEN	D -7507	PFINTZAL 1
PICKARD, PAUL S.	SANDIA N.L.	USA -	ALBUQUERQUE NM, 87185
PICKMAN, D.O.	UKAEA	GB -	ST.ANNES-ON-SEA FY8 IHP
PLATTEN, JAMES L.	AECL	CDN -	MISSISSAUGA ONTARIO
PODOWSKI, DR. MICHAEL Z.	RENSSEL.POLYT.	USA -	TROY, NY 12180-3590
POINTER, W.	GRS	D -8046	GARCHING
PON, DR. G.A.	AECL	CDN -	MISSISSAUGA ONT L5K 1B2
PREISCHL, WOLFGANG	GRS	D -8046	GARCHING
PROHASKA, DR. GÜNTER	HSK	CH-5303	WÜRENLINGEN
RASMUSSEN, INGVAR	RISO NAT.LAB.	DK-4000	ROSKILDE
RASTAS, AMI	INDUSTR. POWER	SF -	27160 OLKILUOTO
REDDY, DR. DEVUNI GANESH	UNIV. COLUMBIA	USA -	NEW YORK NY, 10027
REHME, PROF.DR.-ING KLAUS	KFK GMBH	D -7500	KARLSRUHE
REIMANN, DR. M.	KFK GMBH	D -7500	KARLSRUHE
REISER, H.	KFK GMBH	D -7500	KARLSRUHE
RENARD, ALFRED	BELGONUCLEAIRE	B -1050	BRÜSSEL
REOCREUX, DR. MICHEL	CEA	F-92260	FONTENAY-AUX-ROSES
RHODES, N.	CHAM LTD	GB -	WIMBLEDON, SW19 5AU
RICKETTS, CRAIG	KFK GMBH	D -7500	KARLSRUHE
RIEBOLD, W.L.	CEC ISPRA	I-21020	ISPRA (VARESE)
RININSLAND, DR. H.	KFK GMBH	D -7500	KARLSRUHE
RIVIERE, JOEL	CEA	F-92260	FONTENAY-AUX-ROSES
ROCHE, HENRI	CEA	F-92260	FONTENAY-AUX-ROSES
ROGERS, J.T.	UNIV. CARLETON	CDN -	OTTAWA, ONT. K1S 5B6
ROHAIGI, U.S.	BROOKHAVEN N.L	USA -	UPTON, NY 11973

ROHDE, J.	GRS	D -8046	GARCHING
ROLLINGER, FRANCOIS	CEA	F-92260	FONTENAY-AUX-ROSES
ROOTLEDGE, KEVIN	NNC	GB -	LEICESTER, LE8 3LH
ROSINGER, DR. HERBERT E.	AECL	CDN -	PINAWA, MAN. ROE ILO
ROSS, DENWOOD	US NRC	USA -	WASHINGTON DC, 20555
ROUSSEAU, JEAN CLAUDE	CEA	F-38041	GRENOBLE CEDEX
ROYEN, JACQUES	OECD	F-75016	PARIS
RUBIN, MARK	US NRC	USA -	SILVER SPRING, MD 20906
RÜDINGER, DR. V.	KFK GMBH	D -7500	KARLSRUHE
SAHA, PRADIP	BROOKHAVEN N.L	USA -	UPTON, NY 11973
SAITO, SHINZO	JAERI	J - 319	11 IBARAKI-KEN
SALM, R.	BBR	D -6800	MANNHEIM 1
SANFORD, ISRAEL	US NRC	USA -	ROCKVILLE MD, 20852
SAUAR, TOR	SCANDPOWER	N -2007	KJELLER
SAVOLAINEN, DR. ILKKA	TECH.RES.CENTR	SF -	00181 HELSINKI 18
SCHANZ, GERHARD	KFK GMBH	D -7500	KARLSRUHE 1
SCHAUER, DR. DALE A.	LLNL	USA -	LIVERMORE CA, 94550
SCHAUER, DR. VACLAN	KFK GMBH	D -7500	KARLSRUHE
SCHENK, DR. HERBERT	KKW OBRIGHEIM	D -6951	OBRIGHEIM
SCHEUERMANN, WALTER	UNIV. STUTTG.	D -7000	STUTTGART 80
SCHIKARSKI, PROF.DR. W.	KFK GMBH	D -7500	KARLSRUHE
SCHIKORR, MICHEAL DR.	KFK GMBH	D -7500	KARLSRUHE
SCHIVO, ANGEL MIGUEL	KWU ERLANGEN	D -8520	ERLANGEN
SCHLENKER, DR. HANS-V.	RWE AG	D -4300	ESSEN 1
SCHMIDT, FRITZ	UNIV. STUTTG.	D -7000	STUTTGART 80
SCHMIDT, HANS E.	INST.F.TRANSU.	D -7500	KARLSRUHE
SCHMIDT, TH.	KFK GMBH	D -7500	KARLSRUHE
SCHMIDT, WERNER PAUL	KFK GMBH	D -7500	KARLSRUHE
SCHMITT, ANDRE	CEA	F-92260	FONTENAY-AUX-ROSES
SCHNEIDER, AMIRAM	NRCN	IL -	BEER SHEVA
SCHNEIDER, R.O.	KFK GMBH	D -7500	KARLSRUHE
SCHOLL, KARL-HEINZ	KFK GMBH	D -7500	KARLSRUHE 1
SCHOLZ, DR. DIETER	TÜV BADEN	D -6800	MANNHEIM 1
SCHRAEWER, DR. ROLF	KWU OFFENBACH	D -6050	OFFENBACH
SCHULENBERG, DR. THOMAS	DORNIER	D -7990	FRIEDRICHSHAFEN 1
SCHULTHEISS, PROF.DR. G.	GKSS	D -2054	GEESTHACHT
SCHULTZ, RICHARD R.	US NRC	USA -	IDAHO FALLS ID, 83401
SCHWAGER, DR. JÖRG	TÜV RHEINLAND	D -5000	KÖLN 1
SCHÖCK, DR. WERNER	KFK GMBH	D -7500	KARLSRUHE
SEGEV, GYORA	ISR. ATOMIC EC	IL -	61070 TEL-AVIV
SEHGAL, BAL RAJ	EPRI	USA -	PALO ALTO, CA 94303
SEIPEL, HEINZ	BMFT	D -5300	BONN
SENGPIEL, WOLFGANG	KFK GMBH	D -7500	KARLSRUHE
SEVEON, JEAN-JACQUES	CEA	F-92260	FONTENAY-AUX-ROSES
SHIGEHIRO NUKATSUKA,	MITSUBISHI API	J -	TOKYO
SHINAISHIN, DR. MERVAT	ÄGYPT.NUCL.SOC	ET -	TALA MONOFIA
SILBERBERG, MEL	US NRC	USA -	WASHINGTON, DC 20555
SKOKAN, DR. ALFRED	KFK GMBH	D -7500	KARLSRUHE
SKUPINSKI, DR. E.	CEC BRUSSELS	B -1040	BRUSSELS
SNAREY, V.L.	MOD	GB -	BATH. BAI 7EG
SNYDER, A.WM.	SANDIA N.L.	USA -	ALBUQUERQUE NM 87185
SOBRERO, ENRICO	UNIV. BOLOGNA	I-40136	BOLOGNA
SPASOJEVIC, PROF.DR. D.	INST. B-KIDRIC	YU -	11001 BEOGRAD
SPIGA, MARCO	UNIV. BOLOGNA	I-40136	BOLOGNA
SPINKS, N.J.	AECL	CDN -	MISSISSAUGA ONT L5K 1B2
STADIE, KLAUS B.	OECD	F-75016	PARIS
STAMBOLICH, J.Y.	ONTARIO HYDRO	CDN -	TORONTO ONTARIO
STAMM, DR. H.H.	KFK GMBH	D -7500	KARLSRUHE
STARR, MARKHAM	NNC	GB -	LEICESTER, LE8 3LH
STENGÅRDE, LARS	AB ASEA-ATOM	S-72104	VÄSTERAS
STERN, DR. ELI	ISR. ATOMIC EC	IL -	61070 TEL-AVIV
STOLZ, JEAN	ELECTR. FRANCE	F-75008	PARIS

STRATTON, WILLIAM R.	STRATTON & ASS	USA -	LOS ALAMOS, NM 87544
STRUWE, DR.-ING. DANKWARD	KFK GMBH	D -7500	KARLSRUHE
STUHRMANN, DR. HORST-B.	RW-TÜV	D -4300	ESSEN 1
STÄDTKE, HERBERT	EURATOM	I-21020	ISPRA
SUN, YUFA	SWR ERI	TJ -	CHENGDU, SICHUAN
TAKAHASHI, RYOICHI	INST.OF TECHN.	J - 152	TOKYO
TAMM, DR. HEIKI	AECL	CDN -	OTTAWA ONT, K1A 1E5
TANI, DR. AKIRA	NAIG NRL	J - 210	KAWASAKI (-KU)
TEAGUE, H.J	SAFETY&RELIAB.	GB -	WARRINGTON WA3 4NE CHE.
TEPER, W.	ONTARIO HYDRO	CDN -	TORONTO ONT.
THADANI, ASHOK	US NRC	USA -	BETHESDA, MD. 20814
TIBERINI, DR. ANTONIO	KKW LEIBSTADT	CH-4353	LEIBSTADT
TOGO, YASUMASA	UNIV. TOKYO	J -	TOKYO
TOIVOLA, AHTI	TEOLLISUUDEN	SF -	27160 OLKILUOTO
TORGERSON, D.F.	AECL	CDN -	PINAWA MANITOBA ROE ILO
TRAUBOTH, PROF.DR. H.	KFK GMBH	D -7500	KARLSRUHE
TURLAND, DR. B.D.	UKAEA	GB -	ABINGDON, OXON OX14 3DB
TVETEN, ULF	ENERGY TECHN.	N -2007	KJELLER
TZE YAO CHU,	SANDIA N.L.	USA -	ALBUQUERQUE NM, 87185
UETSUKA, HIROSHI	KFK GMBH	D -7500	KARLSRUHE 1
UNGER, PROF.DR. H.	UNIV. STUTT.G.	D -7000	STUTT.GART 80
VAN DER EECKEN, DIRK	SCK-CEN	B -2400	MOL
VIGNESOULT, NICOLE	CEA	F-92260	FONTENAY-AUX-ROSES
VINCK, W.	CEC BRUSSELS	B-1049	BRUSSELS
VOGEL, RICHARD	EPRI	USA -	PALO ALTO CA.
VOGES, DIPL.-MATH. UDO	KFK GMBH	D -7500	KARLSRUHE
VOGT, SIEGFRIED	KFK GMBH	D -7500	KARLSRUHE
VRIESEMA, J.	ECN	NL-1755	ZG PETTEN
WAARANPERÄ, YNGVE	AB ASEA-ATOM	S-72104	VÄSTERAS
WADLE, MATTHIAS	KFK GMBH	D -7500	KARLSRUHE
WAGNER, K.	KFK GMBH	D -7500	KARLSRUHE
WAHBA, DR. A.	GRS	D -8046	GARCHING
WAHLSTRÖM, BJÖRN	TECH.RES.CENTR	SF -	02150 ESPOO 15
WAIBEL, E.	BBR	D -6800	MANNHEIM 1
WARMAN, EDWARD	STONE& WEBSTER	USA -	BOSTON MA
WATZINGER, HEINRICH	KWU ERLANGEN	D -8520	ERLANGEN
WEGENER, H.	KFK GMBH	D -7500	KARLSRUHE
WEIL, DR. LEOPOLD	BMI	D -5300	BONN 1
WEISER, G. MINISTER	UMWELT-MIN.	D -7000	STUTT.GART 1
WEITZE, HARTMUT	KKW GÖSGEN	CH-4658	DÄNIKEN
WELLS, JAMES E.	LLNL	USA -	LIVERMORE, CA. 94550
WERLE, DR. HEINRICH	KFK GMBH	D -7500	KARLSRUHE
WHEAT, LARRY	INPO	USA -	ATLANTA, GEORGIA 30339
WIEHR, K.	KFK GMBH	D -7500	KARLSRUHE
WIETSTOCK, PETER	GKSS	D -2054	GEESTHACHT
WIGGER, BERNHARD	BADENWERK	D -7500	KARLSRUHE
WILD, H.	KFK GMBH	D -7500	KARLSRUHE
WILHELM, JÜRGEN	KFK GMBH	D -7500	KARLSRUHE
WINKLER, W.	GRS	D -8046	GARCHING
WIRTZ, P.	BBR	D -6800	MANNHEIM 1
WIRTZ, PROF.DR. K.	KFK GMBH	D -7500	KARLSRUHE
WITTEK, PETER	KFK GMBH	D -7500	KARLSRUHE
WOLF, DR. LOTHAR	BATTELLE	D -6000	FRANKFURT 90
WOLTERS, DR. JOHANNES	KFA JÜLICH	D -5170	JÜLICH
WRIGHT, R.W.	US NRC	USA -	WASHINGTON DC, 20555
YADIGAROGLU, PROF.DR. G.	ETH	CH -	ZÜRICH
YE SHURONG,	SWR ERI	TJ -	CHENGDU, SICHUAN
YIFTAH, PROF. SH.	SOREQ NRC	IL -	YAVNE
YIZAK, GUREVITZ	NRCN	IL -	BEER - SHEVA
ZAMMITE, R.	CEA	F-92260	FONTENAY-AUX-ROSES
ZILLIOX, CLAUDE	EDF (SEPTEN)	F-69626	VILLEURBANNE CEDEX
ZURITA-CENTELLES, A.	UNIV. HANNOVER	D -3000	HANNOVER 21



Chapter 1

## Opening Addresses and Invited Papers (Plenary Sessions)

Opening Addresses:	pages
1.1 H.H. Hennies, General Chairman	3 - 8
1.2 G. Weiser, Baden-Württemberg State Minister	9 - 19
1.3 K.H. Narjes, Member of the Commission of the European Communities	21 - 34
Invited Papers (Plenary Sessions):	
1.4 A. Gauvenet: Nuclear Reactor Operation Across the World	35 - 54
1.5 W. Dircks, G. Naschi: Regulatory Trends in OECD Member Countries	55 - 72
1.6 D.O. Pickman, A. Fiege: Fuel Behavior Under DBA Conditions	73 - 94
1.7 W.R. Stratton: Review of Recent Source Term Investigations	95 - 110
1.8 W.G. Morison, W.J. Penn: Containment Systems Capability	111 - 138
1.9 H.W. Lewis: Probabilistic Risk Assessment - Merits and Limitations	139 - 148
1.10 J.H. Gittus, F.R. Allen: Safety Goals Approaches	149 - 164
1.11 A. Birkhofer: Advances and Trends in Reactor Safety Research and Technology	165 - 178



Opening Address by Dr. H. H. Hennies

Ladies and gentlemen:

At this opening of the 5th International Conference on Thermal Reactor Safety I would like to welcome you all in Karlsruhe. I am particularly happy to see so many friends and guests from all over the world and I hope that we will be able to continue successfully the tradition of this series of meetings. A special word of welcome goes to Minister Weiser of the State Government of this State of Baden-Württemberg and to Dr. Narjes of the Commission of the European Communities, who will be here in a couple of minutes. I also have pleasure in welcoming the Rector of the University of Karlsruhe, Prof. Kuhnle, who will attend this morning's session, and among our foreign guests I would like to welcome in particular the President of the American Nuclear Society, Dr. Joe Hendrie.

The German Kerntechnische Gesellschaft as the sponsor and the Karlsruhe Nuclear Research Center as the organizer of this conference have been, and are, grateful for the support they have received from many sides. I would like to mention especially the European Nuclear Society, the American Nuclear Society, the Canadian Nuclear Society, the Japan Atomic Energy Society, the Nuclear Energy Agency of OECD, the International Atomic Energy Agency, the Commission of the European Communities, and the Badenwerk utility.

This meeting will deal with findings of research into the safety of reactors, and most of the contributions will be devoted to the safety of light water reactors, which is the reactor line supplying most of the nuclear electricity today. This very mature reactor system makes an increasing contri-

bution to our electricity supply. Especially in Europe, nuclear power in many countries has already reached a level of 40 to 50% of the electricity supply.

This applies to Finland, Sweden, Belgium, France, and Switzerland. In the Federal Republic of Germany, at present about 25% of the public electricity supply comes from nuclear reactors. This percentage is likely to increase very soon, as a number of large nuclear power plants will be going on stream.

Several hundred large power reactors in all parts of the world are proof of the fact that nuclear power has now outgrown its development years and has become an established technology. The reliability of reactors has improved continuously and the accident record is still extremely positive in the sense that neither the persons working in these facilities nor the public in their environments have suffered damage due to radioactivity.

The hazard potential undoubtedly associated with handling radioactive materials is the reason for the intensive worldwide research in the field of reactor safety. Especially after the accident which occurred some five years ago at the Three Mile Island plant in the United States, many theoretical and experimental studies have been conducted on the accident behavior of light water reactors. Although their results have not led to any major changes in reactor facilities, they have improved some details of the systems in specific cases. Especially our knowledge about the possible production of hydrogen has been enhanced and measures have been initiated to prevent ignition or explosions. This process has now largely been completed and I think it is safe to say that we now understand well enough the behavior of reactors in normal operation and under all kinds of credible accident conditions and that the existing

safety systems in accidents react in such a way that there will be no detriment to the public.

Of course, this question can never be answered for good; it is therefore only natural in research and development to inquire again and again whether our assertions continue to be valid also in the light of more recent findings. We will try to do so over the next few days and, on Thursday at the panel discussion, will attempt to strike a balance by asking what remains to be done in the field of reactor safety research.

The sixties and seventies were mainly devoted to investigating the sequences and the consequences of the so-called design basis accidents; especially the loss-of-coolant accident and the behavior of the emergency core cooling systems were given much attention. In recent years, more effort has been concentrated on the highly improbable but, as far as consequences are concerned, much more dangerous core disruptive accidents. These accidents, including the core meltdown accident, are so improbable, to the best of our knowledge, that formally they are not even taken into account in the licensing procedure on the construction and operation of nuclear power plants. Yet, they do play a considerable role in the public debate about the risks of nuclear energy. For this reason, reactor safety research has been trying for years to find an answer to the question of the extent of damage likely to be associated with these accidents. These studies have been conducted in many places all over the world. In the Federal Republic of Germany, where some initial work was started more than ten years ago, they have been intensified recently, the Karlsruhe Nuclear Research Center having made a major contribution. The results of these activities are

very important and should have a considerable impact on the future assessment of the risks of nuclear power, for it is seen that all former statements on the consequences of core disruptive accidents were wrong, inasmuch as most of the consequences indicated were much too severe.

This was due to the conservative treatment in the absence of detailed theoretical and experimental studies. Today, we are on much more solid ground in this sector. Even in case of a total core meltdown there would be no national disaster. The so-called China syndrome, i.e., the core melting through the building foundations, will not occur and the reactor containment can be expected to fail at such a late point in time that the release potential for radioactive particles by then will have decreased by many orders of magnitude.

We feel that these studies can be concluded very soon and that the results will then be available in a quantitative format. In the Federal Republic of Germany, the consequence will certainly be that the new version of the German Risk Study, which is to be available by late 1985, will show much slighter consequences for these types of accident. At our Karlsruhe Nuclear Research Center, tests are at present going on about the interaction between metal melts and concrete, which are quite impressive. I would like to encourage you to have a look at this facility; we call it BETA. This can be arranged within our program of tours today and tomorrow.

Of course, the general statement I just made holds true world-wide; it also applies to all variants of light water reactors. However, since these facilities do differ from type to type, even from plant to plant, one must be careful in comparing specific, individual results and must not conclude from the differences in findings to the bandwidth of error inherent in these statements.

I hope that this meeting will bring us a step closer to our goal: to understand better the behavior of reactors in normal operation and, especially, under accident conditions.

When defining the work still to be done we should also examine very carefully what degree of accuracy is needed. It is neither possible nor necessary, for an accident as improbable as the melting of the whole reactor core, to calculate within a factor of 2 or 3 the consequences of activity releases. One order of magnitude or perhaps more is certainly sufficient.

At the Karlsruhe Nuclear Research Center we feel that, for German light water reactors, this goal will have been reached in two years' time at the latest; we will then considerably cut down on research expenditures in this field.

Ladies and gentlemen, I would not want to conclude without expressing my sincere gratitude to all those who, for more than one year, have been instrumental in preparing this conference: the members of the Steering Committee, the members of the Program Committee headed by Prof. Birkhofer, and the members of the Selection Committee. My special thanks go to the staff members of the Karlsruhe Nuclear Research Center who actively participated in the preparation: Dr. Rininsland

together with Mr. Bork, Mrs. Schröder and Mrs. Pleli have worked very hard to make this conference, hopefully, a success.

Nuclear technology, especially problems of reactor safety, are part and parcel of the political environment, and for this reason it is my special pleasure to welcome Minister Weiser and Dr. Narjes, who has arrived in the meantime. They will present the views of the Baden-Württemberg State Government and of the Commission of the European Communities on the problems we are addressing. Minister Weiser, the floor is yours.



Address by the Baden-Württemberg State Minister  
of the Interior, G. Weiser

Ladies and gentlemen:

It is a pleasure and also a great honor for me to be able to welcome at this 5th International Meeting on Reactor Safety such a large number of experts in the field of nuclear technology who have come to Karlsruhe from so many countries. I would like to convey to you the best wishes of the State Government of Baden-Württemberg, particularly of the Minister President, Mr. Späth, and again I would like to welcome you very cordially in this State.

The State Government of Baden-Württemberg, and in particular myself as the Minister responsible for the safety of nuclear technology in this State, appreciate very much that this conference is being held in Karlsruhe, the city where, more than 27 years ago, the Kernreaktor Bau- und Betriebsgesellschaft mbH was founded by the Federal Republic of Germany and the State of Baden-Württemberg to build the FR2 research reactor and some additional institutes, which then developed into the Karlsruhe Nuclear Research Center, one of the major research establishments in the field of nuclear technology.

The openness to new technological developments and to international exchanges of experience has since the beginning of the use of nuclear energy in this country been a natural prerequisite to successful scientific work. Many events with international participation at the Karlsruhe Nuclear Research Center in the past have been evidence of that important function.

Today's meeting is in line with this tradition, which has been cultivated at the Karlsruhe Nuclear Research Center for almost as long as the State of Baden-Württemberg has existed. When the Nuclear Research Center was founded, the State of Baden-Württemberg was just four years old.

I hope you will bear with me if, as a representative of the State Government, I mention with a certain amount of pride a number of examples to indicate that, here in Baden-Württemberg, major contributions are being made or have been made towards the development of nuclear technology and towards the solution of related safety questions.

In addition to the FR2 research reactor, which I have mentioned before, the first German designed and built reactor after 1945, I would like to mention as a further example in the Federal Republic of Germany a reactor developed in this country, the multipurpose research reactor at Karlsruhe, which in its eighteen years of operation proved the technical maturity of the underlying concept of a heavy water moderated and heavy water cooled pressurized water reactor.

In the field of advanced reactor technology, the compact sodium cooled nuclear reactor at Karlsruhe should be mentioned, whose operation for many years has contributed important know-how in the field of the technology of fast breeders and which, within the framework of the fast breeder research project, will continue to play an important role in the future.

Also one of the larger nuclear power plants in West Germany was built in Baden-Württemberg, i.e., the Obrigheim Nuclear Power Station, which is a demonstration plant of the PWR type that has been in successful operation for more than 110,000 hours and which, like the plant at Neckarwestheim commissioned eight years later, holds a good position in terms of availability worldwide. Three other major nuclear power plants in Baden-Württemberg are being commissioned or under construction. In WAK, a small pilot reprocessing plant in Karlsruhe, which has been in operation since 1971, a major contribution is made towards research and technological testing of reprocessing spent nuclear fuels.

In addition to the many practical experiences the operation of these plants has yielded, thorough research in the field of nuclear technology is being undertaken also at the universities of this State and at the Karlsruhe Nuclear Research Center. Some of that research specifically deals with questions of reactor safety.

One prominent example in that context is the comprehensive Nuclear Safety Project of the Kernforschungszentrum Karlsruhe, whose extensive line of research, e.g., on the behavior of fuel elements and other reactor components during accidents, tests on the developments of hypothetical core meltdown accidents, and activities to improve fission product retention and reduce

radiation exposure, has found recognition and acceptance internationally.

Another important research project of the Karlsruhe Nuclear Research Center in the field of reactor safety are the large scale tests carried out under realistic conditions on full scale reactor components of the decommissioned Superheated Steam Reactor of Großwelzheim in Bavaria. I would like to mention, by way of example, particularly the thermal shock tests of the reactor pressure vessel, experiments on the effects of loss-of-coolant accidents on pressure vessel internals and on safety valves as well as the seismic experiments carried out there.

In addition, the Center also runs a number of major projects with safety and environmental implications in the field of fast breeders, uranium enrichment, reprocessing of spent fuel elements and treatment of radioactive wastes, nuclear fusion and, recently, also in the field of environmental research within the framework of the "European Research Center for Air Pollution Control" Project.

Another major center of reactor safety research in Baden-Württemberg is the Materials Testing Institute (MPA) of the University of Stuttgart headed by Prof. Kußmaul, which works on questions of materials and strength of materials. Although this is not the main topic of this meeting, the important contributions to reactor safety

coming from that Institute, which will celebrate its 100th anniversary this year, should be emphasized. MPA's work on the safety of pressurized components and systems has contributed greatly and has won international acclaim. Broad research and development programs have been carried out with the most modern, sometimes unique, testing equipment to assess materials and component behavior under extreme conditions. The so-called basic safety concept for pressurized components has been established theoretically and backed experimentally to exclude reliably the occurrence of large breaks. This "leak-before-break" principle is now being applied not only in this country, but also abroad.

Another research activity conducted in the State of Baden-Württemberg, which I would like to mention, is the comprehensive emergency core cooling project, UPTF, which is being prepared on behalf of the Federal Ministry for Research and Technology as part of an international large scale research project involving the United States and Japan. The test rig which, apart from the absence of nuclear heating, simulates the primary system of a large PWR on a 1:1 scale, was built at the Mannheim power plant headed by Dr. Schoch. Another major project of reactor safety research is thus being supported by the technical facilities of that power plant. The tests, which are to be started in the second half of 1985, will supplement many earlier emergency core cooling

tests carried out elsewhere.

Ladies and gentlemen, the topic of this meeting, reactor safety, has always been one of the most vital and most widely discussed subjects in the public with respect to the peaceful use of nuclear energy. Nuclear power plants contain large amounts of radioactive substances whose handling must be managed safely and which must be kept from the environment reliably by a system of multiple barriers. It is not for nothing that licensing and supervisory procedures for nuclear power plants include stringent safety requirements to guarantee the protection of the workforce and the population in the vicinity of these plants, some of which requirements go far beyond the standard in other technical fields. The Government of the State of Baden-Württemberg has never left any doubt about the fact that it assigns the greatest importance to the safety of nuclear power plants and thus the protection of people.

The strictness of the licensing procedures and the thorough control exercised by the regulatory authority, as well as the efforts made by vendors and operators of nuclear power plants, have been successful. The operating experience accumulated with the technical safety systems of nuclear power plants in this country has been very positive. Major incidents with radiological consequences to the environment have been avoided so far.

Monitoring the emissions of radioactive substances from nuclear power plants and additional pollution control in the environment of plants, the results of which exercises are published annually, show that the exposure levels to persons arising from nuclear power plants in this country, including the incidents that have occurred so far, are not only within the framework of the dose limits for normal operation under the German Radiation Protection Ordinance, but as a rule have been underrun by a sizable margin.

My Ministry will ensure that conditions remain like this by its safety related cooperation in the licensing procedures and its intensive supervisory activities. This supervision is further intensified by the startup, in the near future, of the Nuclear Reactor Remote Surveillance System in Baden-Württemberg. The operation of this automatic system is also an expression of the State Government's dedication to the justified safety requirements of our public.

In comparing nuclear power plants and conventional thermal power plants we should not overlook that also coal fired power plants emit radioactive substances due to the natural radioactive components contained in the fuel. The resultant environmental radiation exposure, as you know, is quite comparable to that resulting from normal operation of nuclear

power plants. However, coal fired power plants produce other types of emissions in addition. Even if the required 85% desulfurization is achieved down to 270 milligrams of sulfur dioxide per cubic meter of offgas, and even if nitrogen oxides are reduced to 200 milligrams per cubic meter of offgas, electricity generation in coal fired power plants, equivalent to 1300 MWe nuclear power plants, is still associated with emissions annually of some 8000 tonnes of sulfur dioxide and 6000 tonnes of nitrogen oxides. In addition, the problem of waste disposal in connection with desulfurization and reduction of nitrogen oxides must also be solved.

Being responsible in this State for the solution of these problems, I often say that I do not hope that one day the same innocents who carry those fliers saying that one should stop talking and instead do something for desulfurization, when they find that there is no more sulfur and no more fly ash in power plant emissions, will come along and demand that there should be no sulfur and no fly ash on our waste disposal sites. We have to solve these problems in a holistic approach. It is still easier to describe problems than to find appropriate solutions.

In addition, ladies and gentlemen, I think that environmental problems should not be discussed by people who are not very knowledgeable in



the field, use only slogans and thus add to the doubts in the minds of the public. If I look at some of those rallies, the people attending them and the people who deal with these problems in a very emotional way, and others who make very emotional speeches and thus increase their uncertainty, I sometimes wonder whether those who use slogans and think this will solve problems will at all realize whether they can shoulder this responsibility.

I think that so far we have jointly ensured that safety is guaranteed, and this is something to which the public has a vested right. We will continue to make efforts in this field. I am very grateful to everybody who makes his contribution in his particular sector in the scientific field.

Ladies and gentlemen, in coal fired power plants, the total amount of carbon burnt is released into the atmosphere as carbon dioxide.

According to the operating experience accumulated so far, nuclear power plants have been found to be acceptable not only with respect to their risk, compared to other risks of life, but they justifiably can be regarded as a particularly non-polluting technology of electricity generation. It is therefore regrettable that the resistance of concerned environmentalists in the past has been, and still is, directed especially against nuclear power plants. Let

me only remind you of the thesis argued particularly in this state, and coming always from the same source, about the connection between the emissions of radioactive substances from nuclear power plants or, more generally, ionizing radiation, and the widespread diseases of our forests. I think that those who were against building the Wyhl Nuclear Power Plant in the Black Forest and at the same time wanted to build a new coal fired power plant in the same region should take a look at their own positions with respect to environmental protection. They should seek further education before voicing theses in the public which cannot be supported.

In the State of Baden-Württemberg, we have a great interest in reducing the resistance against nuclear power plants, for electricity from nuclear power will be particularly important in this State with its high population density. The use of nuclear power, to my mind, will be indispensable also in the future, not only because of the less polluting electricity generation compared with the emissions from fossil fired power plants. The State Government therefore, both for environmental and economic reasons, in the long run wants to cover a major portion of the base load requirement of electricity from nuclear power plants.

Ladies and gentlemen, although nuclear power plants have already achieved a very high safety standard, further improvements in the safety

and reliability of these plants will remain our constant concern. We are all called upon to contribute to the best of our knowledge and ability. Particularly, in the field of nuclear energy, the evaluation of operating experience, the results of safety research, and the exchange of knowledge and experience are of particular importance.

Let me therefore wish you a very fruitful exchange of experiences and views and the best of success for this conference and, last but not least, a very pleasant stay in this State, which is still beautiful despite the many environmental problems we have.



Address by Mr. Narjes, Member of the Commission of the European Communities

Chairmen, Mr. Minister, Mr. Rector, Ladies and Gentlemen:

On behalf of the Commission of European Communities which, besides IAEA and NEA, is one of the international organizations sponsoring this meeting, I would like to welcome you very cordially at the 5th International Conference on the Safety of Light Water Reactors, a meeting which is being attended by a large number of leading experts from all parts of the world as members of the nuclear community.

The joint organizers of this meeting are the European Nuclear Energy Society, the American Nuclear Society, the Canadian Nuclear Society and also, last but not least, the Japan Atomic Energy Society.

The international character of the event is not only proof of the importance attached to the problems of nuclear safety worldwide, but is also a good example of the present effective international cooperation and successful joint actions in the field of nuclear safety extending also to international projects in safety research.

Irrespective of a number of continuing problems, nuclear power in many European countries is contributing more and more to the generation of electricity. Unfortunately, this is not true of all European countries. I would like to draw your attention especially to the situation in France and Belgium, two countries in which the use of nuclear power is far advanced and the share of nuclear power in electricity generation is above 50%.

As a consequence of the oil crisis in the seventies, France decided on its ambitious, far reaching program of nuclear power plant construction and continues it, irrespective of the decline in the energy requirement in recent years. France thus has an excess now of nuclear generating capacity, can make more economic use of energy and export electricity to almost all European countries, such as Italy, the Netherlands, Germany, especially to Baden-Württemberg, the host state of this meeting.

Baden-Württemberg can benefit directly from the French nuclear power program, I hope at satisfactory prices, and can align its own nuclear power plant program with these services.

I am very much in favor of exchanging goods of all kinds and also services across the European frontiers, including the transmission of energy, for this is an excellent instrument of cooperation.

Irrespective of the many efforts taken in public information programs and other public relations activities, the public acceptance of nuclear power is still a major problem in some European countries; this is also true of the Federal Republic of Germany.

The debate about nuclear power is almost a classical example of the problems of guidance and orientation arising in legitimate democratic disputes in a highly industrialized environment. We cannot solve these problems without the assistance of the media. They play a key role. We cannot simply stand by and accuse the media of having opened their pages to a tide of irrationalism. Also the media participate

in the gradual learning processes about technical and scientific subjects and can arrive at definitive solutions only step by step.

I think we all should try to seek an unbiased discussion of the pros and cons. We should clearly separate opinion and information and we should also refrain from agitation. We should not suppress or promote fears and apprehensions. We should also point out what the risks are with which we must live and can live, and it is under this aspect that the successful work in the field of reactor safety and its representation to the public plays such an important role.

Not every procedure trying to convince the public of the need for nuclear power will work equally well in all member countries of the Community; each country will have to seek its own solutions.

In some countries of the Community, e.g., many programs are restricted to an outline of facts and data in order to convince the public in the hope that this provides an adequate amount of information to the public. In other member countries, arguments are used which are more emotional, thus causing psychological barriers to be built up against the acceptance of unbiased information.

At this conference, safety problems will be discussed at a high technical level, but I hope that this meeting will also contribute to informing the public about the present state of safety of nuclear installations.

Nuclear power is a feasible solution helping us to solve our energy supply problems through sufficient ways and means of safety utilizing this source of energy. In the nuclear power plants all over the world we have accumulated a record of safe and economic operation for 3000 reactor years. With respect to their availability, nuclear power plants compared to conventional power plants show an excellent record, availability, after all, being one of the main criteria by which to assess plants of this type. In view of the high capital costs of nuclear power plants, availability indeed is a factor of great importance, for unforeseen outages can be very expensive. An unplanned outage of a 1000 MWe nuclear power plant may cost more than DM 1 million a day, and this sum does not include the costs of the replacement electricity to be purchased. Reports about power failures and plant outages and plants to be decommissioned should also be regarded as sufficient proof of the absolute priority of reactor safety.

Data published at the 1983 World Energy Conference, covering a number of years, incidentally show that the reliability of nuclear power plants is equivalent to the reliability of conventional facilities. Some member countries of the European Communities in recent years have been able to demonstrate in a striking way what competent management can do to improve reliability and output.

In this connection, I would like to mention the 1300 MWe pressurized water reactor of Grafenrheinfeld in Germany, which started commercial operation in mid-1982 and which, according to information from the plant vendor, has supplied more electricity in 1983 than any other reactor in the



world. That plant has a load factor of 87.6% and produced some 10,000 GWh, which is a record for a single reactor. Even higher load factors of about 92% were reported from some smaller plants, and the older facility of Stade was operated at a load factor of more than 86% as recently as in 1983. These are recent data documenting the high availability and the excellent performance of nuclear power plants in Europe.

After these rather general remarks I would like to enter into the details of the subject of this conference, which is reactor safety, especially the contribution the European Communities can make to the solution of at least some of the problems still open.

The Commission has always stressed very much the harmonization of criteria, rules and guidelines within the Community. In a number of working parties it promotes opportunities for discussions and dialogs and for mutual exchanges of information about safety methods, legal provisions, standards, and specific safety programs. The Commission feels that the harmonization of existing national rules and guidelines in nuclear safety should emerge naturally from a series of continuing discussions throughout the Community and should not be the result of some policy handed down from somewhere in the Community.

In these activities, the Commission is based on a Council decision of July 22, 1975 about the technological problems of safety in nuclear power in which the Council of Ministers agreed "that in stepwise harmonization of safety requirements

and criteria a step-by-step procedure is adopted in order to ensure uniform and sufficient protection of the public and the environment against radiation hazards from nuclear activities and, at the same time, the development of commercial interaction is promoted. However, this harmonization should not result in a safety level lower than what has already been achieved."

Some modest progress has so far been made in this field, on the basis of which the Commission has planned to continue this effort, also in the interest of industrial policy.

In another field, radiation protection, there is more progress. The duty of the Community to set up uniform safety standards for the protection of the health of the public and the workforce and to ensure that these rules are implemented, is laid down in the Euratom Agreement.

In Article 33 of the Euratom Agreement, the duties of the member countries, on the one hand, and the rights of the Commission, on the other hand, have created more positive conditions for a high degree of harmonization within the European framework. This also implies international cooperation in the broad field of labor hygiene and health protection.

A relatively complete catalog of legislation has now been drafted in the Community countries, which takes into account obligations within Euratom.

As radiation protection is a permanent duty, this radiation protection policy must now be expanded and updated. Whenever

an amendment is made, all recent findings in the fields of radiobiology, medicine and physics should be taken into account and the experience made in applying the basic standards in the past should be considered.

These attempts to adapt safety criteria and standards are supported by a number of research efforts, to which also the Community contributes.

Within the framework of reactor safety research, we have also learned more about the origins, the sequences and the consequences of potential accidents and broadened our bases for the definition of safety related requirements and criteria. Moreover, new possibilities have been created to ensure safe reactor operation.

The development of nuclear power, from the early days, has been accompanied by extensive safety research programs. Although the power plants now existing are being operated with a sufficient degree of safety, there are several reasons to advocate the continuation of reactor safety research programs:

1. Designers and power plant operators need the findings of this research in order to improve the protection of their workforce, the public and the environment and the plants themselves. The research programs, through better knowledge of potential accident sequences, are to allow the safety margins to be quantified in the designs of commercial nuclear power plants.
2. The results of safety research are indispensable to the improvement of licensing procedures, for in the light

of those research findings, acceptable design bases and the limits of plant operation can be cast into more definitive frameworks and the measures to be taken in incidents can be defined more effectively.

3. Much attention must be devoted also to continuous feedback of information from licensing authorities and supervisory institutions to research institutions so that research efforts can be reconsidered regularly and can be better aligned to technical requirements, for these authorities and institutions in their day-to-day work must apply rules and guidelines and also test and inspection procedures.

Joint research and development work has contributed importantly to the safety concepts. The following areas should be mentioned in particular: the safety of pressure vessels and pipes, non-destructive tests, studies of thermal stresses and mechanical stresses acting on the reactor core under major accident conditions, and the stresses acting on the containment as a result of internal accidents, and the loads to which nuclear power plants may be exposed as a result of external impacts.

Nuclear technology is one of our modern high technologies, to use a journalese term. We should therefore try, in the safety assessment of all advanced technical facilities, to apply uniform technical rules to ensure that the operation of these plants will not entail major hazards to the public and to the workforce employed in those plants.

In the present political and social context, as I said, the research conducted about safety also makes an important and

indispensable contribution towards promoting the acceptance of nuclear power in the public. Potential hazards associated with nuclear power generation are now assessed in a more realistic way and are compared with those risks, which must exist in a highly developed society as a result of industrialized technical processes. Research and development work in the field of risk analysis has developed new instruments for a systematic assessment of safety problems. Comprehensive analyses of the risks of power reactors have helped to establish an important framework within which to assess safety related criteria.

The present research programs of the Community and the industrialized countries continuing to advance light water power reactors, especially the United States, have grown considerably in recent years. The accident in Three Mile Island in 1979 has shown the importance of the role and the behavior of the operator under accident conditions and also for the consequences of accidents. In the case of TMI, serious fuel damage occurred.

We have learned more about the problems associated with typical incidents to be borne in mind in designing reactors; we therefore now study anomalous events which, even if they occur on a very small scale, can negatively affect the normal operation of a plant, and we are also studying much more severe accidents, even though their occurrence may be very improbable indeed.

For many years, most of the research activities of the Community in the field of technical problems of nuclear safety have been carried out within the framework of

programs of the Community Research Center. Since 1973, reactor safety has been the main topic of those programs.

They comprise theoretical and experimental activities on accident analysis and the analysis of accident consequences and on the improvement of methods and instruments of accident prevention. Special efforts are made with respect to the development and application of new, advanced methods in order to minimize the uncertainties inherent in probabilistic risk assessment.

Major analytical and experimental topics are the investigation of physics phenomena, which play a decisive role in loss-of-coolant accidents, and also of the transients associated with serious damage to the reactor core. These studies are being conducted to improve or validate the safety codes and, if possible, generate new information to allow more efficient procedures to be set up for operation and for emergency conditions.

One example of research devoted to hypothetical major accidents with very low probability of occurrence was the SUPER-SARA Project which, within the framework of an in-pile experiment, was to study the behavior of light water reactor fuel in case of a loss-of-coolant accident. However, in the very planning stage of the ambitious project it was found that the expected benefit to reactor development and accident research would not justify the tremendous costs of these series of tests. Financial considerations caused the project to be abandoned.

A more positive example to be mentioned is research conducted at the Ispra Community Research Center, which has meanwhile

been widely accepted in the nuclear community; I am referring to the LOBI Project, which simulates a loss-of-coolant accident in a four-loop pressurized water reactor of 1300 MWe. The experiments were also supported by the German Federal Ministry for Research and Technology and the findings are being discussed in an ad hoc working group in cooperation with national experts and are exploited for the benefit of all those involved.

One example of cooperation in the field of safety research throughout the countries of the Community and beyond is the PISC Program devoted to the Inspection of Steel Components. It was initiated by a joint working group of OECD and the Commission for Safety Problems of Reactor Components Made of Steel. The program serves to test the methods and techniques presently applied in non-destructive testing and, if possible, improve them. The LOBI and PISC programs are also major parts of the 1984-1987 program of the Ispra Community Research Center about the technological problems of nuclear safety.

Besides the work conducted in the laboratories of the Community Research Center, the Commission in order to maintain its key role in nuclear safety, has also created the possibility to run research in the laboratories of the member countries by bearing part of the costs.

As far as this type of research projects is concerned, the Commission has proposed another four-year program between 1984 and 1987, which will continue the research started within the first program, but will cover a broader range of technical subjects.

This program will either supplement or support the research conducted at Ispra and will be integrated into the national programs.

In the form proposed at present, research efforts break down into three categories: research on accident prevention, improvement of our knowledge about accident phenomena so that accident consequences can be limited and, finally, research about probabilistic assessment techniques. These three categories are closely interrelated. It should be added that some of the topics mentioned are not restricted to the narrow field of light water reactor power plants and include also human factors and man-machine interaction.

The high costs of the programs of safety research, which use test facilities of a very large scale, need result in international research efforts. Within the proposal presented about cost sharing, participation in international research projects or programs carried out outside the Community countries has been envisaged.

It is regrettable, therefore, that the European Council of Ministers so far, for budgetary reasons, has not been able to adopt this program. The continuation of our cooperation within the Community in this important field of reactor safety right now is being jeopardized, which is even more regrettable, as the efforts of the Commission have had, and still have, the support of most of the members of the European Parliament. Several resolutions in the European Parliament have pointed to the urgency of this work. The Commission nevertheless will do everything within its powers in the future to support reactor safety and reactor safety research



and to remove obstacles to exchange of knowledge and services.  
Nuclear nationalism is not a solution for the future, let  
alone for safety engineering and radiation protection.

This conference, too, will help to communicate the right  
solutions.

I wish you a very successful meeting.



NUCLEAR-REACTOR OPERATION  
ACROSS THE WORLD

---

André Gauvenet

Electricité de France  
Paris, France

---

Abstract

---

For a number of years, and especially since the accident to TMI-2, a great deal of world attention has been given to the problems of operating nuclear power stations.

With the help of numerous data banks, both national and international, it has been possible to exchange information on results and to pass on to all interested parties the reports on incidents and their analysis. These exchanges have certainly been very beneficial.

In view of the wide diversity of presentation, it is difficult to pick out the most significant parameters, apart from overall results. However in what follows an attempt is made to do this, in an essentially qualitative form.

1 - INTRODUCTION

1.1 The accident at Three Mile Island (with regard to which it should be remembered that despite its apparent gravity it caused no human injury) marked an important stage in the development of safety concepts and devices in nuclear power stations. The findings concern in particular the amount of radioactivity released in the Reactor Building during the accident at TMI, and the appearance of a hydrogen bubble caused a great deal of rethinking internationally. Certain conclusions on these problems, which will be very important for the future, will no doubt come to the surface in the next two or three years.

1.2 Since 1979, there has been no serious accident to a nuclear reactor. None has been shut down for a very long period (except the TMI reactors). These good results are probably partly due to the renewed attention that has been given since 1979 to a number of essential problems. The old reactors have been modified where possible. In the design of the units at present under construction, the changes have been even more considerable.

I shall mention here the operational factors, such as the greater attention paid to the human element (and consequently to training and the internal organization of power plants), and in this context to the relationship between man and machines, to automation (how far should it go?), and to the new arrangements in control rooms, including the safety boards.

I also note the considerable effort made, often of an original nature, in the area of the planning and drafting of procedures (especially for accident situations), as well as the introduction of specialists (Shift Technical Advisors in the United States, Ingénieurs de Sécurité et Radio-protection in France) who can make a progressive analysis of incidents and consequently give invaluable advice in the event of a serious accident, as this analysis method offers diversified redundancy compared with the conventional codified method used by operators.

Lastly, I shall mention the development of measures taken in the event of an accident, which have once more been partially inspired by the shortcomings found at the time of the TMI accident.

1.3 In practice, the results of the operation of nuclear power stations are given in the reports and statistics in the form of an evaluation of the load or availability factors, to whose definition I shall come back later. It is relatively easy to publish these statistics on a monthly or annual basis, and to establish a classification featuring "successes" and "failures".

I would not go as far as to say that these presentations, which sometimes remind one of a championship league, have no meaning; but I would like to try to pick out the parameters that seem to me particularly significant in the trends in power-plant load (or availability) factors, assessing these trends not only at short, but above all at medium or long term. The ideal for the future will be to draw up an evaluation of a large part of the working life of each plant, and finally of its whole life.

Certain questions come up immediately; we shall complete them later.

For example:

- 1.3.1 - Do plants in which fuel is renewed during operation have a better load factor than those in which fuel is renewed during shutdown?
- 1.3.2 - Does the load factor change more or less systematically with the increasing age of the plant? (Number of fuel cycles for water-cooled power plants.)
- 1.3.3 - Considerable change can follow the initial period of a plant's working life. If, in a given country, the shutdown periods are deliberately extended for systematic inspections and tests, does this have a measurable effect?

- on availability during operational periods?
- on availability during the mature period, when outage durations can be reduced?

This shows, amongst other things, that one must assess both overall availability (including shutdowns) and availability outside shutdown periods.

1.3.4 - Plants are of different types; they are built differently and have different ratings; they operate in countries with different technological habits, probably linked to what may be called national cultures. What is the influence of these various parameters?

1.3.5 - In studying the parameters, account must be taken of special cases, some of which will not be the same in the future:

- the influence of series construction, which facilitates commissioning and operation, but which may cause problems, sometimes difficult ones, in exploiting experience, since when a modification is decided on it has to be applied to all the reactors in the series, in operation or under construction. Even in the absence of series construction, some important components may be standardized, and this may already pose generic problems.
- for countries in which the share of nuclear energy in total energy production is becoming large (above 30-50% perhaps) it is essential to plan and apply a "load following" procedure.

This naturally affect the significance (and the representative nature) of the load and availability factors.

- Studies are in progress for the use of new fuels in water-cooled reactors. It is obviously premature to discuss these today. These new fuels should, when they are ready, enable availability to be increased systematically, provided they do not cause incidents in themselves, and above all, perhaps, provided extended operating periods do not have an incidence on the general problems of maintenance and tests.

1.4 Although, as I have already said, nuclear power plants are at present working satisfactorily in terms of safety and availability (these are partially linked), incidents occur, as in any industrial installation; some are of small importance, and only affect individual components, but others have complex effects. The action taken prevents these incidents from degenerating, but they are considered as possible precursors of more serious ones. Lastly, some may be considered as particularly important.

In all countries, incidents are classified in fairly similar ways, and when they exceed a certain degree of seriousness must be reported to the safety authorities. Data banks have appeared for plant safety and/or reliability, and here again the thinking that followed the TMI accident has given new impetus to a trend that would probably have occurred anyway, but which was strongly encouraged by it.

Certain data banks are international. They enable valuable exchanges of information to take place - for example, the lessons of experience from serious incidents on certain power plants can be used preventively on others.

These are some of the international data banks existing now:

- The International Atomic Energy Agency (PRIS)
- OECD - NEA (IRS)
- Euratom (JRC-ISPRA)
- INPO
- UNIPÉDE (in project).

These systems are additional and adapted to the national systems, some of which are now highly developed.

I have made wide use of the results and comments of the IAEA, NEA and INPO, as well as certain data from Euratom. I am very grateful to these organizations.

## 2 - PLANT AVAILABILITY - SIGNIFICANT PARAMETERS

I shall first give a few statistics, mostly from IAEA, which cover a large proportion (80%) of the world's nuclear power stations.

2.1 Let us recall a few definitions:

- The load factor (LF) is given by the relation (in French : CP) :

$$LF = \frac{E}{P_n \times H}$$

in which E is the net energy produced (MWhe)  
 P<sub>n</sub> is net maximum capacity (MWe)  
 H is the number of hours in the period in question.

- The availability factor (or coefficient) AF is (in French : CD)

$$AF = \frac{E_n}{P_n \times H}$$

in which E<sub>n</sub> is the net energy corresponding to the net power available and P<sub>n</sub> and H are as defined above.

The load factor (or production coefficient) is used universally. The availability factor is useful when the unit in question is being operated below the energy available (load following).

Here, for example, are the load and availability factors for French power plants in 1983:

LF (Load Factor) : 64.5%

AF (Availability Factor) : 67.8%

Cumulative results since each plant was first coupled up:

LF (Load Factor) : 58.6%

AF (Availability Factor) : 61.7%

1.2.2 Figures 1, 2 and 3 give some overall results for nuclear-power-plant operation throughout the world.

Comments:

The curves for PWR reactors (below 600 MWe and 600 MWe and above) are traced on each graph for reference.

- Broadly speaking, it can be said that plants that are recharged while operating (GCR and PHWR) have a slightly higher load factor on average than that of the reference PWRs.

- For each type of reactor, there appears to be a characteristic pattern for the first years of service (varying for different parameters, and in particular in length when it has been possible to use experience with the first reactors for subsequent similar or identical ones). The load factor then rises, falling again when the plant is 10 to 15 years old.

It would therefore seem that after an optimum adult age (5 to 10 years), most nuclear units follow a more or less general aging pattern.

In my opinion this is only partly true. It is certain that systematic faults appear on plants of different types after a number of years. This is the case for example for:

- faults due to structural corrosion or deformation of the graphite in GCRs,
- faults due to corrosion of the steam circuits in BWRs,
- faults leading through corrosion to the breakage of pins in the structures carrying the control rods of PWRs,
- faults in steam generators for most types of reactor except BWRs.

On this subject it should be noted:

- that some of these faults may appear quite early (5 to 7 years), as for example for the pins,
- and that many of them lead to shutdowns for varying periods, and in any case of significant duration,
- and that some of these faults are fairly generic, even when the reactors have not been constructed as a series,

- and that it is possible that, with some of these faults corrected, the plants can start off again on another period of maturity. (But this remains to be proved in the next few years.) We are apparently in a transition zone for different types of reactor.

Note finally that the number of reactors that have reached an age of more than 10 years (or 15 years, depending on the case) is very small. Only one has reached the maximum age.

Consequently, while it is true that for this small number of reactors there is a tendency to age and to outages, sometimes prolonged, for maintenance, repairs or even just for detailed inspections, the load-factor values are hardly significant as the numbers they cover are too small.

2.3 Another way to look at the trend in load factors against time is to make overall averages from one year to the next for each country.

The IAEA has calculated general averages for the whole lives of the plants in a given country. It looks as if these averages mean something. One can also calculate sliding averages over certain years, and averages for the period after the time of teething troubles (for the countries with significant programmes, this does not differ from the previous case).

The results for all the operating times of different types of reactor (up to and including 1983) are given in table 1.

The averages for the whole period of each nuclear programme vary very little if we except the teething years, whose effect incidentally is different in the different countries.

These averages range from 59% to 81.5% for the PWRs of 600 MWe and above that have been taken as examples.

The spreads around the averages vary little; their sizes are as follows:

PWR	600 MWe	10 to 12%	
PWR	600 MWe	10 to 14%	(20% for the 8th year)
BWR	600 MWe	13 to 18%	(19% for the 9th year)
BWR	60 MWe	5 to 12%	

These tables show a fairly high degree of diversity. Too many factors are involved for lessons to be learned, especially in cases where the load factor is growing compared with the general average.

We should note, for example:

- the effect of the teething years, when the programme is not growing rapidly.
- the temporary influence of TMI since:



. in that year, some reactors were shut down temporarily,  
 . special inspections and maintenance were ordered.

- the "bad years", generally few in number, correspond to a more or less generic fault, which when found was corrected fairly quickly.

The trend in annual outages is also interesting (see table 2).

This table gives, as an example, the statistics for annual outages in 1982.

If we except the special case of the heavy-water reactors (recharged during operation), all the other types, including AGR and GCR, had in 1982 annual outages of around 2,500 hours (i.e. 28% of total time in the year). In fact, these times range between 2,100 and 2,860 hours, i.e. within 16% of 2,500. Secondly, the proportion of planned and unplanned outages is not very different for these reactors (75 and 25% respectively).

### 3 - THE MOST IMPORTANT INCIDENTS

I have so far been concerned with what may be called fundamental faults, such as those caused by physico-chemical phenomena, sometimes aggravated by mechanical phenomena, which are among the essential causes of aging.

These are not, properly speaking, occasional faults, even though technological progress may enable them to be overcome. They are often faults that existed in classical energy technologies, where they were tolerated because they were relatively easy and cheap to repair, while in nuclear reactors this type of repair has to be done under radiation: it is sometimes impossible, short of replacing a large proportion of the equipment (e.g. steam generators).

I would now like to consider, in more general terms, the most important incidents that occur in power plants, whose analysis leads in principle to improvements for the present (in plants in service), and even more for the future (plants at the design or construction stages).

These incidents are examined very closely, and more and more on an international basis.

#### 3.1 What can be called a significant incident?

To a large extent, the definition varies between countries, as it is the safety authorities who decide. There are of course contacts and exchanges between these authorities, and they tend towards homogeneity in the definitions. The international bodies, and especially IAEA (PRIS system) have created a standard procedure for incident reporting which is tending to become general; we however have here definitions and comments that concern both safety and reliability, and their scope is wider than that of the official government definitions.

OECD-NEA, though it does not collect complete statistics, gives a detailed analysis of incidents.

In what follows I shall comment on the most important incidents, without confining myself to "significant" incidents in the strict sense.

### 3.2 How many important incidents are there per unit, and what is the trend?

The number of incidents varies from one country to another, and also with the type and age of the plant. It is well known, for example, that the number of emergency shutdowns varies widely from one country to another: for example, among those for which I have the most information, the U.S.A., Sweden, France and Japan for water-cooled reactors.

But I am talking here about the most important incidents, which only include certain emergency shutdowns; their number appears more consistent.

I have noted, depending on the country and with the reservations mentioned above, between 0.5 and 4 important incidents per unit per year, the term "important" meaning that such incidents can be considered as possible precursors, or that at least they require lessons to be learned from them in technical and/or human terms.

If we consider emergency shutdowns (rarely considered important), we find that their number varies considerably, between 0.4 and 15 per unit per year, and this variation is very interesting. But the very definition of emergency shutdowns varies between countries: (whether they are automatic or not; classification varying with the length of the shutdown).

The trend in the annual number of incidents is slow. In general, there are more in the first year of operation; the number then falls at varying rates, usually rather irregularly. The same applies to emergency shutdowns.

### 3.3 How can these incidents be classified?

Their importance depends more on their consequences than their causes. Causes and consequences are however two essential elements in their analysis.

The different countries concerned, the IAEA and OECD-NEA have developed such classifications. It can also be said that the consequences, if we go beyond considerations strictly confined to safety, can be examined from a practical point of view:

- the length of the resulting shutdown,
- whether or not electricity production is interrupted,
- the amount of energy production lost.

OECD-NEA, with its IRS system, goes much further, examining the conclusions to be drawn from incidents.

The shutdown resulting from the incident may be either immediate and due to the incident itself, or later for additional maintenance or replacement of a component. In the latter case, the shutdown may be at the time of the annual outage, and its duration more or less masked; it may be classified as planned or unplanned, depending on the case.

This type of classification is interesting, but it is difficult to interpret all its aspects. One can however deduce from it a certain priority in the analysis of cases.

Taking into account this first classification, it is interesting to examine the causes of incidents on a triple reference system:

- What type of component has failed (valvegear, pumps, water or electricity supply, etc.)?
- What system (in the widest sense) has been affected by the incident? For example, the primary or secondary cooling system, the control rod system, the reactor vessel, turbine, etc.
- What "technology", in the widest sense, is concerned? For example, mechanical, electrical, electronic, or human factors.

Here are a few results of these analyses. I shall only mention those I consider the main ones, since detailed technical presentations in this conference will surely give more detailed results. (Figures 4 and 5, table 3)

Just as I dwelt above on generic (or one might say supergeneric) problems arising from corrosion, I shall note here the importance of certain components among others, which break down often. For example:

- valvegear: 11 to 14% of incidents
- pumps: 9 to 11%
- certain circuits: 9 to 11%

In general, component failures are responsible for 20 to 25% of unavailability, or 50 to 70% of the hours of unplanned outage.

Curiously enough, the unavailability percentages arising from equipment failures are fairly constant for the different types of water-cooled reactor.

With regard to systems, the following come up particularly often:

- incidents on turbines and generators : 20 to 25% of cases
- incidents in the reactor proper : 8 to 12%
- the primary cooling circuit : 13 to 27%
- the monitoring system : 18 to 22%
- water supply : 10 to 13%

These are rough figures, which show the importance of the secondary circuit and the non-nuclear part in incidents (up to 70% of cases).

For the third reference system, the results of the analyses, expressed as percentages, vary widely from one electricity company to another, especially for the share of human error in incidents.

This percentage varies not only for the reason indicated, but also because the human environment can vary considerably (in the training of people and teams, of course, but also more directly in the drafting of

procedures, references to equipment elements and places, possible ambiguities, different degrees of automation, the way data and results are presented, etc.). This point is so important that I will come back to it. The reports on human factors are incidentally still few and far between, except for specific analyses.

In any case, I shall mention here, rather than result averages which do not mean much, varied or even extreme situations that give percentages of 20 to 33% of human failure (as a percentage of causes of incidents).

3.4 How do these factors vary from case to case? What are the significant parameters?

Since the measuring yardsticks for incidents vary enormously and are difficult to compare, one can therefore only conjecture.

As I said above, the first years of operation are of particular importance, with multiple incidents (and extended annual outages).

It is certain that this is less noticeable some time after the very first power plants were brought into service, especially for the later plants built as a series or those for which there has just been some standardization (for example in their essential components).

It would seem that at present we are more or less everywhere in a phase of improvement and maturity, much more than in one of aging. To explain this very qualitative conclusion, I tend to eliminate certain statistical aberrations and not to take too much account of the "important but curable faults", which though they have a considerable influence on the load factor in terms of outage time are only transitory, as correction takes place relatively quickly. These are complaints of maturity, after those of youth, but they precede those of age which have yet to appear.

Other explanatory parameters may be the "personality" of the constructor, of the operating company and the country in question.

The constructor may include the licensor, but at the present advanced stage of nuclear technology construction quality (in varying degrees by local contractors), and that of materials and components, and above all the quality insurance methods used in the construction and operation, are probably more important.

Our different countries and electricity companies have their own traditions of technique and human relations which situate them to varying extents in these fields.

3.5 I would like to add a few words on two particularly important problems, which are linked to operation.

- What are the consequences, for the present and future, of the analyses of incidents that are carried out systematically in our different countries at INPO, OECD-NEA, etc.?

They are no doubt beneficial, but the fall-out of these analyses is not

perceived immediately. Their exploitation in operation and a fortiori in the design of various parts of a nuclear plant demands a great deal of time and care, especially if the constructor is itself involved in it.

I would add that, except in cases of force majeure for which immediate action is necessary, it is often desirable to wait and reflect before making the modifications that seem appropriate. A modification that seemed obviously right has sometimes proved to create many disadvantages for reliability and operation. Reviews of consistency are particularly important here.

Preliminary tests, sometimes of long duration, and good liaison between the constructor and operator are essential conditions for the technical improvements that result in particular from the lessons of experience.

- It is well known that while many systematic tests are essential, some may prove risky at long term:

- either because the reliability of a component (a Diesel engine for instance) may diminish for its planned operational use if it is tested too often,

- or because too frequent application of a complicated test, especially when it is manual, may create a risk of systematic incidents.

There is no doubt a balance has to be struck here.

#### 4. HUMAN AND TECHNICAL PROBLEMS

While human problems (the so-called human factor) were not discovered for the first time with the TMI accident, it must be admitted that with some exceptions they had not been given enough attention previously.

We ought to have drawn inspiration earlier, as we do today, from aeronautical technologies, in which human problems have for long had priority attention: it is recognized that with very advanced techniques human failure is a leading cause of incidents.

Since 1979, much has been done. I will classify it in 5 categories:

1. Training
2. Explanation and information
3. Presentation and aids to operators
4. Taking incident situations into account
5. A proper balance in man-machine relations.

The first two points have been discussed at length. Training has improved, in particular with the use of simulators that take more and more complicated and realistic accident situations into account, and also by additional means such as Computer-Assisted Teaching, which provides operator training for accident cases, and function simulators.

Information and explanation still require much effort to arrive at total understanding of procedures, signs and symbols. Some new developments

(colour codes, for example) are not easy to apply in operating power plants.

Adequate presentation of data and results is also being achieved more or less everywhere.

It often involves complete redesign of control rooms to simplify the amount of information and how it is read; once more, this is often difficult in completed power plants. These problems will be covered at length during our meetings.

I shall link together the efforts made to take account of incident situations and proper use of machines, i.e. in this case computers.

New safety boards that display the results of calculations and sometimes new procedures for special situations, and lastly the redundant use of an engineer (STA, ISR) to analyze difficult situations, will lead us in the future to give very close attention to a whole series of problems that are both technical and human, complex and promising. These new developments are already appearing.

It is lastly obvious that the best operators are those who have been chosen well, trained well and kept up to date; but they are also those who are particularly motivated. This is a difficult element to define, which varies from country to country.

#### 5. OTHER PROBLEMS

Many other problems could be discussed here; some have already been mentioned. I have by no means dealt with all the important problems and I have concentrated on water-cooled reactors, in view of their numerical importance.

I will raise a few special points that were deliberately omitted above.

##### 5.1 The reduction of workers' exposure doses:

Very great efforts have been made and are in progress to follow the recommendations of ICRP. These concern:

- workforce training,
- physical protection of fixed or mobile irradiators,
- water chemistry and the choice of alloys used in circuits.

5.2 Establishing measures to be taken in the case of an accident, both inside and outside power plants.

##### 5.3 Environmental problems:

The object is to minimize and standardize radioactive (and technical) waste, and to keep the public informed on routine problems and incidents. On this last point, each country has its customs, and no rules.

can be laid down. Here again, the situation has changed much since TMI.

5.4 Lastly, I would like to mention certain advantages of fast-neutron plants, which are as yet not very numerous and hardly appear in the statistics. However, they deserve mention:

- they are easy to operate, both in normal and accident conditions; this is essentially because the cooling circuits are not pressurized, and there is therefore no risk of a double-phase (liquid, vapour) accident system.
- workforce exposure doses are low; collective doses are substantially reduced.

## 6. CONCLUSION

### General comments:

I would like to draw some essentially qualitative conclusions from power-plant operation in recent years, and in so doing reply, if possible, to the questions raised in the introduction.

1. We should note the great efforts made everywhere in nuclear power-plant operation. This effort did not begin in 1979, at the time of the TMI 2 accident, but it has developed a great deal since then. The new awareness is however not yet general. It has not always filtered down to the operating teams, or at least not enough. Too often, we have heard talk of "craftsman" technical habits, which are those of the conventional plants, whereas nuclear operation demands more rigorous methods and discipline that was not necessary before.

This progress in operation has been accelerated by the collective action that has been taken to assemble and analyze accident information and to learn from it; this action is often international, either because the data banks and analyses are themselves international, or because publications and meetings permit very fruitful confrontation of information and points of view.

2. While these efforts are visible, especially to managements, their results are not always apparent, especially when the quality criterion taken is the load factor in the different plants. Some people may think that the effectiveness of these efforts is reduced, partially at least, by the effect of power-plant aging. I do not really think this is so. I will come back to it in a moment.

I believe above all that when it is necessary to modify components and techniques or it is desired to change human individual or collective behaviour, no results are seen immediately.

Some techniques can only really be modified when the time comes to replace the equipment. Some changes can only be made on new units, whose design and construction can only be renovated then.

I would add that while the time required for action can sometimes be a fatal constraint, it can be useful: some technical modifications, if they are made too early, can create new defects: this means that numerous tests, sometimes at full scale, are necessary.

3. Results sometimes appear contradictory. Some load factors may increase and others diminish.

In the period immediately after TMI, load factors dropped in many countries, because the safety authorities often demanded inquiries that required certain reactors to be shut down, or detailed inspections. To this must be added the appearance of certain faults, some of which were generic, which should be called complaints of maturity rather than of old age.

There is nothing to tell us at present whether a given preventive measure is or not, taking into account its disadvantages now, a productive investment for the future. This is the case of numerous tests carried out either during shutdown or operation. They may prove very beneficial for the future (knowledge of the equipment, prevention of certain incidents, etc.). But their very number may in itself be a cause of aging!

The progress we may expect from present efforts will probably only appear some time in the future, and the visible fluctuations in the apparent quality of power plants are dominated by the technical habits of each country rather than by the modifications that are taking place. These technical habits often relate more to construction quality than to operating quality.

4. On certain points, the results appear to show the influence of certain precise parameters. I say "appear", as it is extremely difficult to establish true correlations here, in view of the complexity of the systems and also the variety of the methods of presentation and analysis used in the different companies. Present conclusions are very qualitative.

Among the correlations that seem to me significant I would mention:

4.1 The influence of the fuel-loading method, during operation or not. In the case of the heavy-water reactors, it seems indeed that charging during operation gives them an advantage. This is not clear at present for the graphite-gas reactors, for which other factors apply the other way around (and in particular the problem of the deterioration of certain structures, which requires intervention and which could come under what I call maturity since this problem appears soluble).

4.2 The influence of aging, on the other hand, seems to me to have to be kept for later, as I have already said.

4.3 The rate of development of the nuclear programmes in each country plays a role that works a priori in contrary directions. If this rate is fast, it brings up teething problems each year that are not always eliminated by repetitive experience, especially when the models are evolving, sometimes rapidly.



The rate of construction also affects personnel recruitment and training. Despite the efforts made everywhere, problems of selection and training time may arise if emergencies occur. In the light of experience, I do not however think that this factor is significant at present.

4.4 The advantages and disadvantages of series construction have often been discussed. Its effect is certainly favourable on safety analyses, on construction methods and times and consequently on costs, and also on ease of operation (interchangeability of staff and of some equipment).

Against this it is often opposed that there are risks of generic incidents and possible difficulties in exploiting experience, when substantial technical modifications, as is sometimes the case, become necessary (modification time and costs).

In fact many reactors that are apparently different nevertheless have generic characters, due to the standardization of components. This incidentally partly explains the interest of each operator in what the others are experiencing, and why it is sought to internationalize some problems.

4.5 The effect of unit ratings is also difficult to interpret. In the case of PWRs and BWRs, it seems that the crossing of the (incidentally artificial) frontier of 600 MW has led to reduced reliability. This is not true of the other types of reactor.

Here again, many factors may apply. For instance:

- sometimes, the still unabsorbed youth effect of a new system (especially when it has been necessary to renovate conventional components completely);
- the effect of innovation in itself, which while promising for later may initially have an unfavourable effect: the changes may not take account of or aggravate hidden faults.
- the search for the lowest establishment cost, which is sometimes more conspicuous when one moves from prototypes to industrial routine.

4.6 One factor that seems to me very important, though it is a priori scarcely quantifiable, is construction quality, and in particular quality control and consequently the methods used for it.

Quality in component manufacture, even more than in its assembly, seems to me an essential problem; and this quality, together with the methods used to check it, seems to me to vary considerably from one country to another, despite appearances. In this field, traditions and "technical culture" still vary a great deal in the different countries.

4.7 It is possible that certain methods used to improve quality can have disadvantages in operation, for example with regard to worker exposure doses. This is for instance the case when certain inspections are frequently repeated, or when "commandos" with special training (always the same team) are used in delicate work exposed to radiation. These problems are being examined by the Nuclear Energy Agency.

On the subject of doses, with which I shall not deal further, the choice of basic materials and water chemistry play essential roles. There is intense international cooperation on this.

5. I have mentioned incidents of varying importance, both concerned with safety and not.

It is extremely difficult to draw conclusions other than very general ones from this, while detailed analysis of each incident is of the closest interest to every operator and should also interest every manufacturer. On this subject, playback of incidents to manufacturers and the incorporation of their lessons in new construction are still, in my opinion, far from satisfactory, and yet they are essential. INPO is at present conducting an interesting experiment on this.

Statistics of incidents and their interpretation are still very individual in character, despite the growing effort (which looks like succeeding) made by the international bodies, IAEA (PRIS system) and NEA (IRS). The international standards are beginning to be used generally.

I have emphasized the by no means negligible importance of incidents in the conventional part of power plants (turbine, driers, superheaters, etc.), and of those concerning basic components like valvegear and pumps, as well as the capital importance of the numerous incidents that occur in the cooling circuit, especially the secondary one. Reliability of the steam generators plays an essential role.

Some repetitive incidents such as emergency shutdowns have an undisputed influence at present on load factors, and for the future on component aging.

Human problems, which have received much attention since the TMI accident, are analyzed in a way that makes international comparison very difficult.

In particular, some design or manufacture defects, which have numerous consequences for operation, can be due to human error (for example in manufacture, and then in quality control). These consequences may be difficult to pinpoint, but they deserve mention.

6. To conclude, I would like to mention some problems for the future, which though well known seem to me particularly important: they also concern the different types of error and incident I have mentioned.

6.1 Firstly, there is the policy for maintenance and trials during operation (either at the time of annual outage or when the reactor is functioning).

The policies adopted by the different companies, either on their own initiative or prompted by the safety authorities, are without doubt exceedingly diverse, and I am not sure that analysis of these policies, the lessons to be drawn from them, and the adaptation of these lessons to the different national cultures have been conducted in a sufficiently systematic manner.

6.2 A proper balance between human action and automation has not been attained - far from it. It is certain that when they were first introduced, and still now, reactors using ordinary water were often less automated than some of their predecessors, like the gas reactors.

Automation is progressing slowly, for example, in the new control rooms, for diagnosis of incidents. It is desirable that it should be taken further, especially in the field of testing and of various current procedures in which the risk of error is not negligible. Big changes are going on at present in all this.

What is the final conclusion?

The record of nuclear-power-plant operation throughout the world is clearly very positive. No really serious incident has occurred for 5 years, even though the number of operating hours in plants has become considerable.

Redundancies and "in-depth defence" systems have shown much progress.

However, all the lessons of TMI have still not become current practice yet. My impression, and probably that of my listeners, is that we are in a transition period from three points of view:

- The age of the earliest reactors; the real problems of aging may appear in the next few years;
- We are resolving the most obvious problems of "maturity";
- We are taking more complete account of the lessons of TMI (and of other incidents too), and in particular in respect of human factors and the man-machine balance (automation).

The most important development in recent years is certainly the establishment of data banks on incidents at national or world level, and the growing and ever more effective intervention of the big international bodies, such as IAEA, OECD-NEA and the European Community.

Their joint efforts clearly augur well for the future.

Table 1:

**Reactors PWR ≥ 600 MW(e)** 21

Country Number	% of electricity generated from nuclear		Total reactors %		Global mean %
	in 1982	in 1983	in 1982	in 1983	
1	30,9	46,6	82	77,6	77,9
2	28,8	30,6	75,7	70,6	75,4
3	10,6	10,0	96,8	89,3	80,2
4	43	42,4	83,4	86,4	79,4
5	28	29,3	84,4	86,0	81,5
6	30,3	33,4	89,6	80,7	70,2
7	17,7	17,3	69,1	72,1	66,3
8	39,2	40,1	66	64,7	65,3
9	39,3	51,6	67,7	66,6	61,8
10	12,1	11,8	59,3	57,4	61
11	19,5	17,1	68	69,0	59

Table 2:

**AVERAGE FULL OUTAGE STATISTICS  
FOR REACTORS DURING 1982** 7

Reactor Type	Number of Units	Average Outage Hours (per Unit)	Planned Outages %	Unplanned Outages %
PHWR < 600 MW(e)	9	3315	27,2	72,8
PHWR ≥ 600 MW(e)	4	1079	11,7	88,3
AGR	4	2208	70,6	21,5
GCR < 600 MW(e)	26	2609	70,6	29,4
PWR < 600 MW(e)	48	2212	81,3	18,7
PWR ≥ 600 MW(e)	72	2860	69,7	33,3
BWR < 600 MW(e)	16	2089	79,7	20,3
BWR ≥ 600 MW(e)	38	2795	70,9	29,1

Source: IAEA

Table 3:

**CAUSES OF UNAVAILABILITY 1971 TO 1982** 9 bis

Outage Cause	Planned Full Outages Time Lost %	Unplanned Full Outages Time Lost %
EQUIPMENT FAILURE		70.21
OPERATION ERROR		1.81
REFUELLING (INCLUDING MAINTENANCE)	66.88	2.90
MAINTENANCE AND REPAIR	29.32	13.38
TESTING OF PLANT SYSTEMS/ COMPONENTS	0.06	0.04
TRAINING AND LICENSING	0.04	0.01
REGULATORY LIMITATION	1.09	4.03
OTHER CAUSES	1.12	7.02

Source: IAEA

Figure 1:

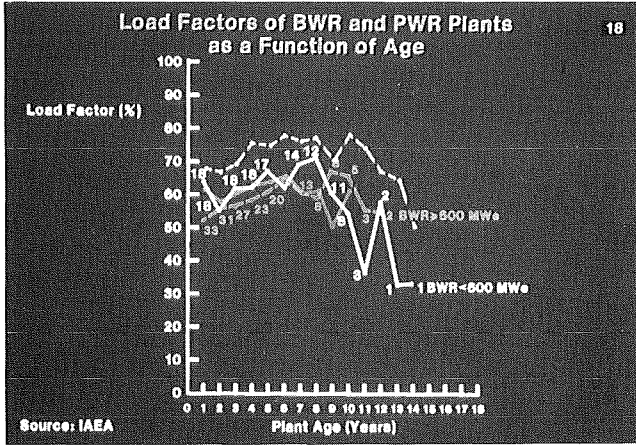


Figure 2:

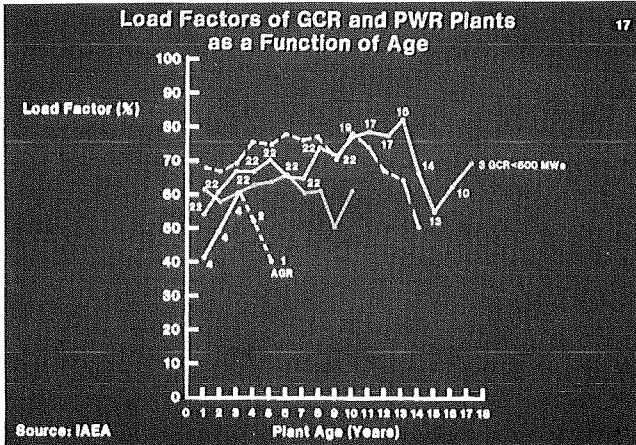


Figure 3:

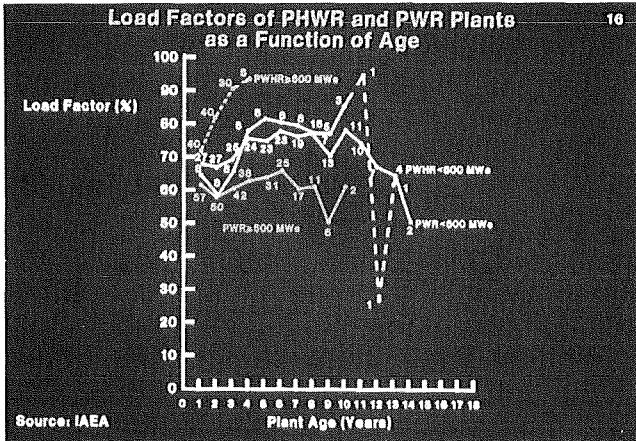


Figure 4:

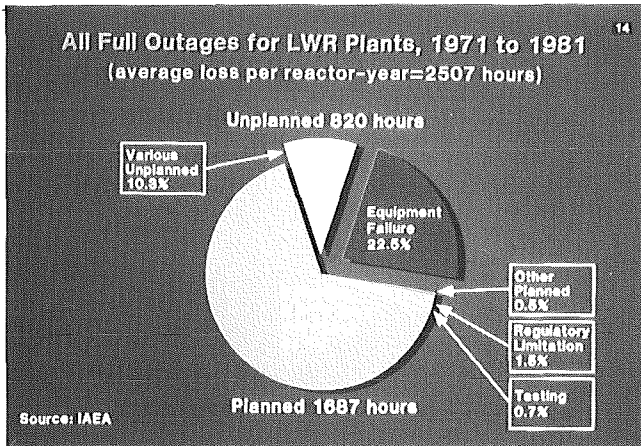
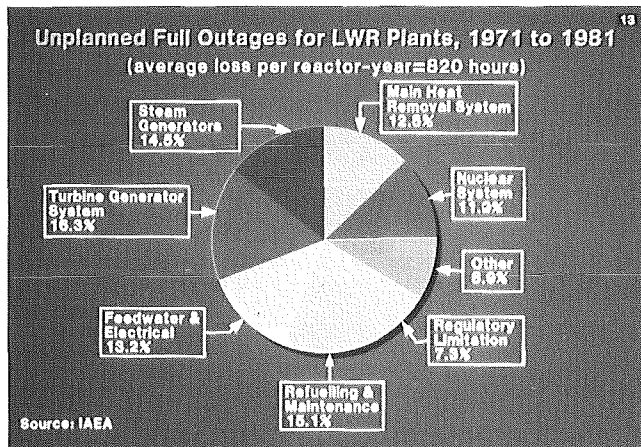


Figure 5:



6th July 1984

Regulatory Trends in OECD Member Countries

Presented by W. Dircks (USNRC)

and G. Naschi (ENEA)

on behalf of the OECD-NEA

Committee on the Safety of Nuclear Installations

## ABSTRACT

At the beginnings of commercial nuclear power, national approaches to safety regulation tended to follow the strong U.S. lead. With the subsequent development and spread of nuclear technology, countries have since established regulatory practices specific to their own situation and no country now dominates the development of regulatory positions.

Even so, several recent common developments can be discerned, including: a natural transition in regulatory effort away from licensing of new plants to ensuring the safety of operating plants; greater emphasis on learning from operational experience; moves towards standardising plant designs and refining general safety criteria; redirection of safety research and development of new regulatory approaches to the severe accident question

following the TMI accident; more attention to the human element in plant safety; use of the knowledge coming from large research programmes to develop new regulatory requirements; increased application of probabilistic assessment techniques to a broad range of regulatory problems.

The introduction of probabilistic approaches into safety analyses, and the program of international information exchange and joint assessment conducted under CSNI are both contributing to a better understanding of the common basis of nuclear safety regulation.

The future is likely to see more attention being paid to the problems associated with plant ageing, and a further convergence of approaches as safety research advances, operational experience accumulates and assessment techniques are further refined.

### Introduction

1. Commercial nuclear power based on the light water reactor (LWR) was first developed in the United States. Accordingly, it was natural that for quite some time the United States had an unmatched influence on the development of the related regulatory safety philosophy. Other countries adopting the LWR often tended to follow the U.S. lead, by either modelling their own regulatory processes directly on the U.S. approach, or by at least attempting to develop schemes compatible with U.S. regulatory practice.



However, these early regulatory requirements were developed when reactor technology was rapidly evolving, and when both reactors and the potential consequences of accidents in them were relatively small. Furthermore the first regulations had to be developed on the basis of a limited understanding of reactor behaviour in abnormal situations. Safety-related technical information was sparse since safety research was at an embryonic stage and little operating experience was available. What experience there was related to the first prototype reactors, and needed to be extrapolated greatly in order to predict the behaviour of the first generation of commercial plants which were five to ten times larger. As a result a pragmatic approach had to be adopted in devising early regulations. The need for caution made it necessary to incorporate conservative assumptions due to the gaps in knowledge. (The resulting conservatism in reactor design were vividly demonstrated by the TMI accident, where weak points in certain areas were compensated for by the intentional over-design in others.) The size of industrial power reactors has since doubled again, and increasing technical understanding from research and operating experience has led to new and deeper technical insights into safety questions.

2. In recent years, rising expectations of individuals in industrial countries have led to continuing demands that large-scale industrial activities be conducted with no risk to the public. Nuclear power has borne the brunt of this mood, in large part because of the intangible nature of radioactivity and because of the military uses by which nuclear fission first came to public attention. This has contributed to increasing pressure for more stringent safety requirements, criteria and standards.

3. Several countries have now developed an independent capability in nuclear technology. Reactor vendors in different countries have produced various commercial LWR designs, which have been adopted by many utilities. Along with this spreading of nuclear technology, recent public debates subsequent to the publication of the U.S. Reactor Safety Study (WASH-1400) and the TMI accident have obliged each country to establish national regulations as a function of their individual situations.

4. All of these developments have combined to produce the current situation where no country clearly dominates the development of regulatory positions. When countries need to formulate new safety policies or practices, they are faced with a multitude of technical arguments and options as well as differing practices in other countries.

#### Recent Common Trends in LWR Regulation

Development of Advanced LWR Designs and Refinements in General Safety Criteria  
-----

5. Notwithstanding this situation where diverse regulatory approaches exist, one can identify several recent trends common to most countries. From the very beginnings of commercial nuclear power, it was clear that the rate that new capacity came on line would eventually slow down as the industry matured. In consequence, regulatory authorities would have to shift their efforts steadily from the task of licensing new plants to ensuring that plants on-line were operated safely.

The TMI accident has underlined a need now for greater regulatory surveillance of operating plants. Ever-increasing efforts are being made to feed lessons from the rapidly accumulating operating experience back to operational practice and regulatory activities. In several countries regulatory authorities supervise a systematic programme of periodic re-evaluations of plants throughout their operating life.

6. There is also a move towards evolving standardised advanced reactor designs, which should be both cheaper to build and more straightforward to regulate. This approach is now being followed up in several countries with major nuclear programmes, including France (the N4 1400 MWe PWR), the Federal Republic of Germany (the KONVOI scheme), Italy (PUN) and the United States (GESSAR 2, CESSAR System 80, RESAR SP/90 designs). Parallel to these schemes are regulatory efforts to refine general safety criteria, taking full advantage of the lessons learned from operating experience, the insights gained from safety research and the new analytical tools provided by probabilistic approaches to safety assessment. The new criteria include, for instance, revised requirements on the design, materials and inspection of primary circuit components, pressure vessels and steam generators, which are all aimed at reducing failure probabilities.

#### Long Term Regulatory Consequences of the TMI Accident

-----

7. During the TMI accident the reactor core experienced transient conditions much more severe than foreseen in the design basis calculations. Even so there were no demonstrable offsite health consequences. The U.S.

regulations in force when TMI was licensed were based on defining a "maximum credible accident" and demonstrating that its consequences could be contained. Any worse situation that one might conceive was considered to be so unlikely that it was classed as "incredible". This in turn meant that there was no need to take precautions against such events or their consequences. This whole approach had first been challenged publically by Reg. Farmer in 1967. Since no technology was free of risk, he pointed out, the mere fact of using nuclear reactors implied acceptance of some degree of risk. There was no logical way of differentiating between "credible" and "incredible" accidents. The 1975 U.S. Reactor Safety Study took this argument further and made the first quantitative estimates of the probability and consequences of the complete spectrum of conceivable LWR accidents. The lengthy debate following the 1979 TMI accident on whether or not the design basis had been passed led to reconsideration of the regulatory philosophy to adopt regarding "severe" accidents, i.e. those involving loss of key systems and eventual damage to the core. Although the TMI accident had the effect of concentrating the minds of the assessors on this issue, the result was limited to some changes in emphasis. The consensus now seems to be that resources should be devoted more to preventing severe accidents than to mitigating their effects.

8. The accident at TMI also showed that inadequate attention had previously been given to the role of the human element in avoiding and countering accidents. It pointed up a need to clarify management responsibilities, especially in relation to those of regulatory authorities, for assuring safety during both routine operation and emergencies. Also identified was a need to ensure that technical advice was available during an

emergency, either by upgrading certain shift personnel or by engaging experts who were not directly involved in operating the plant. Regulatory authorities in different countries have since reviewed the role of management, the availability of technical expertise, and emergency planning for reactor accidents. Concentrated efforts are being made to see that provisions are improved where necessary.

9. The accident also brought to the fore the question of how reasonable it was to expect operators to act effectively following a serious perturbation to reactor operation, considering the stress imposed on them and the often inadequate and even contradictory information available to them. Many countries have since devoted substantial work on various aspects of the human factors question: redesign of control rooms in order to support operators in responding to an accident, design of emergency procedures in terms of the plant state to supplement those for each specific event sequence, provision of control room simulators for training staff to handle abnormal situations, and identifying extra equipment and making provision in advance to permit unusual system configurations that could enable operators to keep control of a situation involving core degradation.

#### Introduction of Probabilistic Techniques in Safety Analysis

-----

10. In most technologies, safety requirements have been defined through an empirical trial-and-error method, often in the wake of accidents which have resulted in major loss of life. This approach was never considered acceptable in the nuclear industry. As noted above, extreme prudence in setting the

first regulations led to substantial conservatism in early plant designs, in order to compensate for the limited knowledge of reactor behaviour in unusual operating conditions. Regulatory organisations have recently devoted great efforts to develop and evaluate probabilistic methods of analysis suitable for making safety assessments. These new tools provide an additional means for assessing the level of safety in various parts of each plant and in the plant as a whole. It is becoming possible to demonstrate that balanced safety coverage is being maintained over the entire plant. In consequence, certain current safety requirements may turn out to be superfluous, while other measures may warrant reinforcement to remedy weak points. Even with the uncertainty inherent to global risk assessments, the risk-equalisation approach can provide useful indications of the safety value of various changes to reactor design or in its operation, and on how to set priorities on regulatory issues requiring attention or additional research.

11. The most comprehensive potential regulatory use of probabilistic methods is in the process of granting construction and operating licenses. Although the use of PRA is growing, it seems likely for the present that in most countries such studies will not be a required component of an application for a plant license. (In some countries a preliminary probabilistic safety assessment is required at the early design stage.) Some countries have gone so far as to develop "safety goals" in terms of accident probability and consequences. Safety goal efforts can at best serve as sources of guidance to decision-makers for their evaluation of accidents beyond the design basis and the relative risk of nuclear and other sources of power.

12. Following WASH-1400 and TMI there has been a more systematic use of probabilistic techniques like fault trees and event trees, not only to evaluate and improve safety levels within a given plant, but also to compare the levels attained by different plants in the country, and even by plants abroad. Event tree analyses are making it possible to balance deterministically-based decisions with probabilistic insights. For instance, system reliability analyses are now being used to develop optimum programmes of quality assurance and preventative maintenance schedules.

13. The increasing use of probabilistic techniques is also helping to improve the common technical basis for regulation among OECD Member countries. For example, by the very nature of event trees they cannot incorporate the concept of inviolable barriers (nor of "incredible" sequences of events). As a result, it is generally agreed that the severe accident issue will not be resolved without the assistance of probabilistic techniques of analysis.

#### Contributions of Safety Research

-----

14. Several large scale nuclear safety research programmes were begun in the 1960's and 1970's. These are now producing the answers to many of the long-standing technical questions about the safety of modern nuclear plants. The results of these studies and the introduction of the probabilistic approach to assessing safety are allowing regulatory authorities to fix their policies and requirements on the basis of measured physical phenomena and best-estimate calculations, rather than conservative bounding arguments. This should contribute towards a refinement of licensing approaches into a coherent streamlined whole from a series of positions taken on individual issues.

15. On the severe accident question, for example, as noted above, many experts agree that emphasis should be placed on prevention rather than mitigation. Recent research indicates further that radioactive releases from severe accidents may be lower than predicted in the predominantly conservative assessments used in previous risk studies. Preliminary indications from this work indicate that this could have a substantial influence on the understanding of the consequences of severe accidents, hence emergency planning for them. Some countries are now applying the probabilistic approach to investigate the value of deliberate controlled venting of the containment atmosphere in certain accidents. By affecting the timing of the radioactive release, it is suggested, it should be possible to reduce both its size and the eventual consequences. However containments differ widely, and their detailed behaviour plays a key role in an accident sequence. Further work will be needed before the value of venting can be firmly established.

16. In parallel, following extensive experimental and theoretical studies there is less concern today that large steam explosions after a core melt present a realistic threat to containment integrity. A number of countries are continuing to carry out research into the behaviour of hydrogen generated from the zircaloy-water reaction, corium reactions and the behaviour of fission products inside the containment.

#### Evolution and Influence of CSNI Activities

-----

17. The international co-operation on safety matters organised through the NEA Committee on the Safety of Nuclear Installations (CSNI) constitutes another means for limiting the current tendency to regulatory divergence. The



evolution of CSNI's programme over the years has also reflected the trends in the preoccupations of national regulatory authorities. When the Committee was established in the early 1970's, its activities were concentrated on identifying safety research needed to improve understanding of reactor behaviour in accident conditions, the performance of safety systems and interactions between plant systems. CSNI has since been steadily shifting its efforts towards the comparison and joint assessment of research results and operating experience. This helps ensure that regulators in all countries have a common data base, as wide as possible, available to them. This fosters the development of technically coherent safety requirements in all countries (even if detailed designs will always vary somewhat for a variety of reasons). Following are several illustrative examples of recent developments in the CSNI programme.

18. In order to profit from the lessons of operating experience, all regulatory authorities have long-running programmes to collect and evaluate reports of safety-related occurrences. To maximise the benefits from these national schemes, CSNI established in 1981 an international Incident Reporting System (IRS) covering all OECD countries with operating power reactors (which represent about 80% of the world's nuclear capacity). Hundreds of incidents of particular safety interest have since been circulated through the IRS. As well as broadening the background information available to safety analysts for assessing incidents in their own country, the IRS gives regulatory authorities advance warning of potential safety problems and of the approaches being taken elsewhere to solve them.

19. Because of the strong influence that different countries' policies can have on one another, it is increasingly important for regulatory authorities to have regular opportunities to exchange views with their counterparts in other countries on important basic technical issues and regulatory practices. The CSNI sub-Committee on Licensing has held special meetings in recent years on several regulatory topics, including the backfitting of safety equipment, advance planning for nuclear emergencies, and the selection of sites for nuclear power plants.

20. The emergency planning case illustrates well how different practices can develop unrecognised. This area was the subject of a topical meeting of the sub-Committee in June 1981. The fundamental principles underlying emergency planning were reviewed, as were the practical measures that had been adopted or proposed in the different countries. Whilst all countries currently carry out emergency planning around nuclear plants, there were different views about its relationship with the licensing process. Considerable differences in actual practices were found, for example, in the scale and organisation of emergency planning, basic attitudes thereto, reference levels, the demands of the licensing process, the extent of public involvement, and so on. While some of these variations arose from countries' different traditions and administrative structures and were thus to be expected, others were technical in nature and primarily a result of current uncertainties in the source term.

21. In June 1983 the Nuclear Energy Agency convened an informal meeting of the Heads of the regulatory authorities from those countries having the broadest experience of industrial nuclear power development. The aim was to improve, at the highest level, mutual understanding of current trends in nuclear safety. The Heads of nuclear regulatory authorities acknowledged that in recent years there had been a growing tendency for OECD regulatory policies to diverge, and they undertook to work towards greater harmony, primarily through CSNI. As a practical step, they agreed to consult together in this framework as new major regulatory positions were being developed so that, first, some warning of impending changes could be given and, second, other countries could contribute to the process. These consultations have been implemented in the form of special meetings, two of which have been held so far.

22. The first was a special meeting convened early in 1984 to consider the regulatory basis for actions taken with regard to the problem of pipe cracking in boiling water reactors. After reviewing countries' experience with this phenomenon, the meeting went on to examine various technical aspects of detection and analysis of crack behaviour and how to mitigate the problem. It concluded with a general discussion of regulatory positions. The special meeting reached a number of conclusions: the phenomenon of inter-granular stress corrosion cracking (IGSCC) was well understood, low carbon material was preferable where stainless steels were used, and precise sizing of cracks during in-service inspection was a key safety factor in plants containing susceptible piping. Indeed the point was made strongly that the main reason for countries adopting conservative safety margins with regard to pipe failure

was lack of confidence in methods of predicting crack growth and in the precision of ultrasonic sizing methods. The meeting went a long way towards clarifying the position regarding pipe cracking in BWRs, provided a great deal of information about what countries were doing and why, and reached consensus about the merits of the various interim solutions. As a result of the meeting there will be a fundamental technical compatibility between the different approaches that the various national authorities come to adopt.

23. The second meeting, held in May 1984, took up the question of general safety criteria for advanced LWR designs. In some countries, most plants are of unique design, which means that regulatory authorities must review each of them in detail. The results are both high construction costs and a high level of regulatory effort required to license them. With the recent development of probabilistic techniques for safety analysis, a steady stream of results coming from safety research, and rapidly accumulating operating experience, regulatory bodies are now in a position to devise a new generation of general safety criteria that are more balanced and internally coherent. Such a development will contribute to more uniform plant designs, which will cost less to build and be easier to regulate. Consistent with this idea, the purpose of this meeting was to promote more coherent regulatory approaches among Member countries.

24. The meeting first reviewed the current programmes in France, the Federal Republic of Germany, Italy and the United States to develop standardised advanced PWR designs, along with related efforts in these and several other countries to revise existing general safety criteria. Several

specific issues related to safety criteria were then singled out for further discussion. For example, it was noted that the United States was the only country to have formulated quantitative safety goals, and even there, these were being implemented on a limited trial basis. Most other countries were waiting for the results of the U.S. trial before proceeding much further in this area. Discussion of the degree to which operators are allowed to intervene during emergency situations revealed that the underlying philosophies in each country were not as dissimilar as the differences in the formal criteria would imply. Significant differences were found in the single-failure criteria in use in various countries. It was noted that whereas a single-failure criteria could be stated in rather general terms, its application was often quite complex. Even though probabilistic analyses of the current practices might show that there were no significant differences between them as regards risk, there was no clear picture of the philosophies on which the different practices were based. Concerning the question of anticipated transients without scram (ATWS), the meeting found that many countries were in the process of formulating or finalising new criteria. Approaches under consideration included efforts to reduce scram frequency and improve the reliability of existing scram systems, or a requirement for diverse actuation - or even complete - scram systems.

25. The meeting was very useful for identifying the fundamental philosophies of countries on a broad range of current interrelated questions. Future meetings will delve deeper into the reasons underlying the observed differences in several specific areas, and it will be valuable to take into account industry views in these discussions.

Future Outlook

26. The rules and regulations governing nuclear power programmes are necessarily complex. As illustrated above, the original U.S. lead in LWR regulation has given way to the current regulatory situation in which each country conducts largely independent activities reflecting its own particular situation. The natural tendency for these parallel efforts to diverge is being limited by the widespread introduction of probabilistic approaches to safety assessment - a trend given added impetus by WASH-1400 and TMI, and by the international collaboration organised through CSNI.

27. Nuclear regulation has come a long way from the initial attempts which had to incorporate substantial conservatisms to compensate for limited basic technical knowledge of the time. Regulation is becoming more coherent and balanced as a result of ever-increasing understanding from research and operating experience and the availability of more powerful assessment tools. Regulators are using the most modern analytical techniques and research results available in order to improve understanding of reactor behaviour and to make safety assessments as efficient and definitive as possible. Along with the development of standardised advanced LWR designs, work towards the development of general safety criteria should also encourage further convergence of different countries' approaches.

28. As stated earlier in the paper, there is a clear trend whereby regulatory authorities are applying the lessons from operating experience to improve regulatory processes. New questions will certainly arise in connection with plant ageing, and the regulation will need increased flexibility in order to devise plant-specific interim remedies to enable continued operation with adequate safety margins, quite apart from long-term solutions which may need several years to develop and implement.

29. It should always be kept in mind that by the very nature of the regulation function, the responsible authorities cannot take the lead in nuclear power development. Regulatory bodies can only strive to be responsive to advances (such as standardised plants), novelties (such as controlled venting), and proposed technological changes (such as improved instrumentation). It is up to industry to identify ways to improve plants and to see to it that they are operated in a safe manner. The nuclear industry must always remember that dedication and will on the part of all involved is indispensable to keeping nuclear power safe.





## FUEL BEHAVIOUR UNDER DBA CONDITIONS

- (1) D O Pickman
- (2) A Fiege

- (1) United Kingdom Atomic Energy Authority  
Springfields Works, Salwick, Preston, PR4 ORR, UK
- (2) Kernforschungszentrum Karlsruhe GmbH,  
Postfach 3640, D-7500 Karlsruhe 1, West Germany

## ABSTRACT

In a Design Basis Accident the fuel cladding experiences a temperature transient which is terminated when the core is reflooded by the ECCS. Depending on the severity of the transient, in terms of the peak temperature attained and the duration, cladding may be embrittled or may undergo substantial deformation. Both these processes have potential for affecting subsequent coolability during reflood. The embrittlement of cladding is caused by oxidation and oxygen pick-up by the metal. During this oxidation hydrogen is generated and may accumulate in the pressure vessel or primary containment. This paper reviews the status of fuel behaviour with particular emphasis on embrittlement and deformation.

## INTRODUCTION

To ensure that fuel elements remain intact and retain a coolable geometry after a Design Basis loss-of-coolant accident (DBA) is an important requirement in all LWRs and various criteria have been established and specified by licensing authorities to this end.

CSNI/NEA, through the medium of its Emergency Core Cooling Working Group and later its Principal Working Group No. 2 (PWG 2), have promoted studies in the thermal-hydraulic and fuel behaviour areas and reviewed the evidence, concluding in general terms that the necessary criteria will be met by present designs. PWG 2 has also sponsored the preparation of a State-of-the-Art Report (SOAR) to be published shortly. Contributions from all OECD countries have been sought in the preparation of this SOAR which will be submitted to PWG 2 for approval.

The DBA is the worst conceivable LOCA, a guillotine break of a cold leg, but there are a range of smaller breaks more likely in practice than the DBA. Depending on the size, the rate of vessel depressurisation may be slow, but the core will not uncover, even partially, with ECCS in operation. This review does not deal with the severe consequences that could arise from a LOCA if the ECCS failed. It is, in the main, specific to PWRs, but much of the data reviewed is equally applicable to BWRs.

## TEMPERATURE TRANSIENTS

The temperature transient experienced by the fuel elements in a DBA is of crucial importance in determining what, if any, damage will occur. For a large breach of the primary circuit the blowdown time is very short, of the order of 20 s, and the stored heat in the fuel is largely removed during this period. The temperature then starts to rise because the fission products generate decay heat. The rate of temperature rise and the peak temperature reached depend on the magnitude of the decay heat, and the internal and external heat transfer from fuel to cladding and cladding to the external environment. The external heat transfer depends on the type of ECCS adopted, cold leg injection or combined hot and cold

leg. During refill steam is generated by residual heat in the system, but the temperature will continue to ramp. During reflood, ie once the coolant starts to cover the core, the heat transfer improves and a mixture of steam and water droplets arrests and reverses the ramp, ultimately quenching the fuel.

The duration of the period that the cladding spends above about 925K is critical, because only above this temperature does significant oxidation and deformation occur. A typical time above this temperature is in the range 100-150 s. Because the rate of temperature rise during the ramp and the peak temperature attained are dependent on the prior rating and burn-up of the fuel, there are a range of temperature transients for different fuel rods, illustrated schematically in Fig. 1.

#### POTENTIAL DAMAGE MECHANISMS

Concern about fuel behaviour in the short-term transients typical of large break LOCAS is centred on the two phenomena of clad embrittlement and deformation. A subsidiary concern would arise should the oxidation of the Zircaloy cladding result in the generation of a large volume of hydrogen.

Embrittlement arises from pick-up of  $O_2$  in the metal underlying the oxide layer and a sufficient thickness of unembrittled material is required to resist the thermal shock when the cladding is eventually quenched. If a lot of clad rupture should occur, the resulting geometry may inhibit coolant flow through the region and cause a hot spot, apart from which a major spill of  $UO_2$  would cause major clean-up problems.

It is well known that Zircaloy can deform to very high strains in the high  $\alpha$ -phase region (975-1125K) under certain conditions and the concern over clad deformation is whether such large strains can arise in practice and whether they will result in such a degree of blockage that cooling during the reflood stage and subsequently is impaired.

In the remaining parts of this paper the evidence available from many sources on these phenomena is reviewed and general conclusions are drawn.

#### OXIDATION

##### Oxidation Kinetics

The oxidation of the Zircaloy alloys in steam has been very extensively studied by many investigators<sup>1,2,3,4,5,6</sup>. These alloys are oxidised by steam over a wide range of temperature, but the effects on the underlying cladding only become significant in the DBA context above 1050K.

The rate of reaction is temperature dependent and with unlimited availability of steam is generally believed to be controlled by the rate of diffusion of oxygen anions in the anion deficient oxide layer at temperatures above 1200K. Over a wide temperature range Zircaloy oxidation has been shown to obey a parabolic rate law,  $w^2 = K_p t$ , where  $w$  is the weight gain,  $t$  the time and  $K_p$  is the parabolic rate constant which is dependent on temperature according to an Arrhenius expression. At temperatures below the  $\alpha/\beta$  transus some workers<sup>2</sup> report a change in oxidation kinetics to a cubic growth rate, and over longer times (up to 25 hours) at temperatures below 1300K Leistikow<sup>4</sup> found accelerated oxidation with linear kinetics probably caused by oxide cracking and which may be associated with the tetragonal to monoclinic phase change in the zirconia.

Most of the data on Zircaloy oxidation has been obtained in isothermal tests, but parabolic rate constants derived from transient heating tests performed by Sagat et al at Chalk River are in good agreement with those determined in isothermal tests.

#### Effects of Irradiation

During a LOCA  $\gamma$ -irradiation will deposit energy in the Zircaloy and steam. From work on the effects of irradiation on the oxidation of Zr alloys in steam at lower temperatures no enhancement of oxidation is expected, which is in agreement with theoretical predictions.

#### Effect of Specimen Geometry

The initial parabolic oxidation kinetics will change when the oxygen content of the substrate metal increases, which occurs in practice with thin specimens, such as fuel cladding, at temperatures above about 1145K where the flux of  $O_2$  into the  $\beta$ -phase is substantial.

#### Effect of Pre-Oxidation

Fuel cladding rapidly develops an oxide layer in-reactor, which can vary in thickness from a few microns to 50-100  $\mu m$  depending on the reactor system and the water chemistry control. In any subsequent high temperature excursion it has been shown that these pre-formed oxides are generally protective and behave similarly to oxides formed at higher temperatures, although at temperatures below about 1400K there may be some memory effect while oxygen gradients adjust by diffusion.

#### Effect of Impurities in Steam

Impurities most likely to be present in steam during the refill and reflood processes are air and hydrogen, the latter from oxidation of the clad by steam. In pure oxygen or air, Leistikow showed that oxidation rates were similar to, but slightly higher than, those in steam, the rate in air being the highest.

Cathcart<sup>10</sup> and Furuta<sup>11</sup> have studied the effect of  $H_2$  in steam on oxidation rate. While small additions had no effect for  $H_2/H_2O$  ratios above 0.3 there was a marked reduction in oxidation rate at 1275K and above, reaching a maximum of a factor 3 at a volume ratio of 2.

#### Effects of Deformation and Rupture

During a typical LOCA temperature transient the cladding may be deforming and may indeed rupture during the time period when most of the oxidation is occurring. The effects of deformation and rupture are therefore amongst the most important. Several investigators have studied oxidation and simultaneous deformation in creep or tensile tests<sup>12,13</sup> and have observed enhanced oxidation (thickness increase) with factors varying between 1.2 and 2. The temperature range covered was 975K to 1275K. There is, of course, some enhanced oxidation (weight gain) because of the creation of new surface, but the increased oxide thickness is a result of increased access of steam to the underlying metal when cracks form in the oxide. Regions of increased penetration of  $\alpha$ -Zr[O] beneath cracks in the oxide film are observed. The thinning of the underlying metal, especially close to a rupture, would also be expected to enhance oxidation because of the earlier saturation of the  $\beta$ -phase layer. At and close to a rupture the thinning effect of deformation and the enhanced oxidation rate are compounded by double sided oxidation, operative from the time of rupture although internal oxidation is more influenced by steam starvation by  $H_2$  generated by the oxidation reaction.

### Stress and Dimensional Change Effects

The molar volume of  $ZrO_2$  is appreciably greater than that of Zr (Pilling-Bedworth ratio about 1.5) and significant compressive stresses are generated in the zirconia layer which are balanced by tensile stresses in the underlying metal. The Zircaloy is also subject to dilation as a result of the oxygen in solution, and at increasing temperature and time the oxidation dilation effect dominates. The nett result of these stresses generated in the clad and oxide layer is that tensile strains of the order of 1% are generated within a few hours at temperatures above 1075K.

### Structural Changes

Oxidation at temperatures within the  $\alpha$ -phase range, up to 1145K, results in little structural change in Zircaloy, apart from some grain growth. At temperatures above the  $\alpha/\beta$  transus the flux of  $O_2$  from the oxide/metal interface increases and the increasing  $O_2$  content close to the interface results in a layer of retained  $\alpha$ -phase,  $O_2$  being an  $\alpha$ -stabilising element. With increasing temperature and time the thickness of this so-called 'retained  $\alpha$ -phase' layer ( $\alpha$ -Zr[O]) increases at the expense of the prior  $\beta$ -phase layer. The distinction between these two regions is very clear on subsequent metallography (Fig. 2).

### Internal Oxidation

During a DBA the external pressure on the cladding reduces rapidly to near atmospheric and the cladding initially expands away from the fuel. There is therefore no hard contact between  $UO_2$  and cladding and internal oxidation from this source during a typical LOCA transient is minimal.

### EMBRITTLMENT

The importance of oxidation during typical LOCA transients is that if the  $\alpha/\beta$  transus temperature is exceeded then the inherently brittle phases, zirconia and  $\alpha$ -Zr[O] are formed and oxygen diffuses into the underlying  $\beta$ -phase. The fracture toughness of the  $\beta$ -phase is reduced by  $O_2$  and the tube may be completely embrittled unless a sufficient thickness of unembrittled  $\beta$ -phase remains.

The fragmentation of embrittled cladding could in principle occur over a range of temperatures below the peak temperature obtained in the LOCA, by seismic forces, hydraulic forces during refill and reflood, thermal shock during re-wetting, or mechanical forces associated with fuel handling and transportation. Most attention has been devoted to fragmentation by thermal shock on re-wetting which takes place at the Leidenfrost point in the temperature range 750-875K<sup>14</sup>. Fragmentation during fuel handling or transportation would occur at ambient temperature.

As a result of experimental studies of fragmentation behaviour and correlation with cladding condition, structure and extent of oxidation, various criteria for avoiding fragmentation have been proposed.

Criteria related specifically to fragmentation by thermal shock were adopted by the US AEC in 1973<sup>15</sup>, and similar criteria have now been adopted by most other countries involved with LWRs. These criteria are:

1. The calculated maximum fuel element cladding temperature shall not exceed 1477K.
2. The calculated total oxidation of the cladding shall nowhere exceed 0.17 times the total cladding thickness before oxidation.

The widely used 17% criterion was based on quenching experiments and has been reviewed and extended by Parsons<sup>18</sup> and Chung and Kassner<sup>14</sup>. The extent of oxidation in these experiments was expressed as the fractional wall thickness of Zircaloy which would be converted to stoichiometric zirconia if all the oxygen taken up were converted to  $ZrO_2$ . It is therefore a measure of the total Zr reacted or the total  $O_2$  uptake<sup>2</sup> without regard to the detailed reactions or oxygen distribution in the clad wall. This equivalent metal reacted concept, although not accurately describing the condition of the cladding, was found to correlate well with survival or failure of the cladding under the thermal shock of re-wetting.

Other work has confirmed that the fracture toughness of Zircaloy is not uniquely dependent on total oxidation, but is particularly influenced by the profile of diffused  $O_2$  in the  $\beta$ -phase. The resultant mechanical properties of the cladding will depend on the details of a particular LOCA transient including heating and cooling rates as well as time at maximum temperature, in that they determine the eventual location of the oxide and  $\alpha$ -Zr[O] phase boundaries as well as the amount and distribution of  $O_2$  in the  $\beta$ -phase.

The 1477K maximum temperature criterion<sup>17</sup> (the '2200F' limit) was applied on the basis of work by Hobson and Rittenhouse<sup>17</sup> who found that the growth of the oxide and  $\alpha$ -Zr[O] phases accelerated above this temperature. In relation to embrittlement of cladding it has little validity as a criterion, but the concept of a maximum acceptable temperature may be desirable for other reasons such as compatibility between cladding and structural components.

#### Relationship between Embrittlement and Distribution of Oxygen

Diffusion calculations based on ideal models were used by Pawel<sup>18</sup> to predict  $O_2$  concentration profiles within the cladding wall and for comparison with the results of Hobson<sup>19</sup> on deformation of ring specimens cut from oxidised tubes. Sawatzky<sup>20</sup> measured the tensile properties of oxidised Zircaloy 4 as a function of temperature and oxygen concentration and as a result proposed an alternative embrittlement criterion, that the  $O_2$  content should not exceed 0.7 w/o over at least half the cladding thickness.

Chung and Kassner<sup>14</sup> carried out a comprehensive study of the fracture behaviour of Zircaloy which they related to various parameters for expressing the extent of oxidation. Parameters used were: equivalent cladding reacted (ECR); fractional saturation of  $\beta$ -phase ( $F_\beta$ ); fractional thickness of  $\beta$ -phase ( $F_w$ ); and thickness of  $\beta$ -phase layer containing less than a specified amount of  $O_2$  ( $L_{C\alpha}$ ). A number of these criteria were found to depend on the rate at which cladding was cooled through the  $\alpha/\beta$  transformation temperature and Chung and Kassner concluded that the best correlation was with the minimum thickness of  $\beta$ -phase layer containing less than a specified concentration of  $O_2$  ( $L_{C\alpha}$ ). The failure map for this criterion is shown in Fig. 3 and the chosen values were 0.1 mm and 0.9 w/o  $O_2$  for fast cooled and 1.0 w/o  $O_2$  for slow cooled cladding, ie cladding with a thickness of prior  $\beta$ -phase containing less than 0.9 w/o  $O_2$  of 0.1 mm or more would not fail by fragmentation. This criterion is obeyed irrespective of wall thickness, overall oxidation or maximum temperature of oxidation exposure. Thus in a LOCA, regardless of clad thinning, rupture and internal oxidation, this criterion is valid, whereas the ECR criterion is very conservative.

There being little or no accurate data on the magnitude of post-LOCA low temperature clad loadings representing seismic or handling loads, Chang and Kassner<sup>14</sup> chose a 0.3J impact as a best estimate and performed such tests at 300K. This led them to propose an embrittlement criterion for such events of a minimum 0.3 mm thickness of  $\beta$ -phase layer with less than 0.7 w/o  $O_2$ .

Limited data on fragmentation is available from experiments performed in PBF as part of the IE and PCM series. Failures occurred both on quenching and on subsequent handling. Haggag<sup>21</sup> reviewed these results and found poor agreement with the ECR and  $F_w$  criteria for both types of failure, but that the Chung and Kassner criterion predicted the thermal shock failures. No criterion predicted the handling failures, but the problem may lie in the difficulty in calculation of the  $\beta$ -phase oxygen concentration gradient for a specimen experiencing a non-isothermal film boiling transient.

#### CALCULATION OF TRANSIENT OXIDATION, HYDROGEN GENERATION AND EMBRITTLEMENT

Having established criteria for oxidation and embrittlement of Zircaloy in a DBA, it is necessary for any postulated transient to be able to calculate whether these criteria would be breached, or not. Oxidation, and hence equivalent metal reacted, can be calculated using the isothermal parabolic rate constants by approximating the transient to a series of small isothermal steps, the sum of the isothermal oxidations representing the total oxidation in the transient. However, in order to be able to apply the more complex criteria, depending on the detailed distribution of  $O_2$  in the  $\beta$ -phase, it is necessary to use more sophisticated techniques and fundamental oxygen transport data.

Calculational techniques such as BILD 5 and COBILD are available for semi-infinite parabolic growth conditions and more complex codes such as SIMTRAN/MULTRAN<sup>22</sup>, ZORO<sup>25</sup> and PRECIP-II<sup>24</sup> which take account of changes in the parabolic rates due to approach to saturation. Values of diffusion coefficients<sup>19,25</sup> and interface solubilities<sup>26,27</sup> have been determined and published. These codes do not, however, account for certain aspects of complex transients, for example, the anomalous oxidation in transients with two temperature peaks. Suzuki and Kawasaki<sup>4</sup> improved and extended the SIMTRAN code for predicting oxidation in LOCA conditions and the resulting PRECIP-II code predicts weight gain, oxide and  $\alpha$ -Zr[O] phase thickness to within 10% of measured data from LOCA transients.

It can be concluded that computer codes such as SIMTRAN/MULTRAN and PRECIP-II are accurate enough for calculation of oxidation under typical LOCA conditions.

#### Calculation of Hydrogen Generation

The hydrogen generated from the Zircaloy-steam reaction in a large break LOCA is the most significant quantity of  $H_2$  generated during the first few hours after such an accident, although in the longer term  $H_2$  production by radiolysis or other metal corrosion reactions is likely to dominate. The USNRC have laid down a maximum hydrogen generation criterion for licensing purposes. This criterion states that the calculated total amount of  $H_2$  generated from the chemical reaction of the cladding with water or steam shall not exceed 0.01 times the hypothetical amount that would be generated if all the metal in the cladding cylinders surrounding the fuel, excluding the cladding surrounding the plenum volume, were to react.

The  $H_2$  released during oxidation of Zircaloy by steam is directly proportional to the  $O_2$  consumed or Zircaloy reacted. For each kilogram of Zr reacted 0.491 m<sup>3</sup> (STP) hydrogen are produced.

Ocken<sup>28</sup> has suggested that internal and external heating of specimens results in parabolic rate constants with different pre-exponential factors and activation energies due to the different temperature gradients across the cladding wall, but the uncertainty in temperature measurement in such work is greater and data from isothermal tests is generally used to calculate  $H_2$  generation.

In conditions of steam limitation (steam-hydrogen mixtures), most likely in beyond DBA situations, lower oxidation rates have been measured and  $H_2$  generation would also be reduced. The rate limiting process is not steam starvation, but probably a surface reaction limitation.

#### PLASTIC DEFORMATION OF CLADDING

The driving force for cladding deformation in a LOCA is the internal gas pressure, pre-pressurisation plus released fission gas, which coupled with the temperature increase can lead to high strain rates. The creep strength of Zircaloy falls rapidly with temperature and the ductility is high, particularly in the high  $\alpha$ -phase region even under oxidising conditions. Strains of 100% or more have been measured, compared with the 30% or so needed to cause neighbouring rods to interact in a typical PWR assembly. The key questions to be answered are what magnitude of strains will occur in practice; how much blockage of coolant flow channels will occur and whether the blocked region will be coolable.

#### Factors Controlling Deformation and Rupture

The basic factors controlling deformation of Zircaloy cladding are stress, temperature, time and creep strength, the latter being influenced by material composition (within specification), grain size, anisotropy and oxidation state. When the temperature of a stressed tube is uniform, unstable deformation sets in at a particular axial location at a low strain value and rapidly leads to rupture. The location of such a rupture will be influenced by local factors such as variations in material properties or dimensions and the probability of rupture occurring on a neighbouring rod at the same axial location is small. In a cooled environment, however, such as one with unidirectional steam flow, once a local diameter increase occurs its temperature will be reduced and deformation will proceed towards one end of the original deformed region depending on the direction of any axial temperature gradient. For example, in upflowing steam, if the decay heat gradient is flat, deformation will continue in an upwards direction because of the increasing degree of superheat of the steam. This, in turn, will lead to larger strains and to 'carrot' shaped overall deformation, as well as to similar deformation in a similar location on neighbouring rods.

The internal gas pressure can be calculated by one of the well established steady state fuel performance codes, allowance being made for stored gas<sup>29</sup> temperature variations in the LOCA. What experimental evidence there is shows that additional fission product gas release does not occur in a typical LOCA transient. This evidence is supported by post-irradiation heating data and by code predictions, which indicate negligible additional fission gas release apart from the small quantity expected if new cracks form in the  $UO_2$

Despite the high inherent ductility of Zircaloy, local exhaustion of ductility can occur at low overall strain values if there is a circumferential temperature variation around the cladding. This is particularly marked because of the high temperature sensitivity of Zircaloy, and the magnitude of the effect is illustrated in Fig. 4.

Non-uniformity of either external or internal heat transfer is the most likely cause of circumferential temperature gradients, but the anisotropic behaviour of Zircaloy tubing (preponderance of radial or near radial basal poles) can accentuate temperature gradients once formed. This is because this particular texture is very resistant to wall thinning and the deformation tends to be accommodated by an axial flow of material and shortening, causing the tube to bow away from the hot side and the hot side to remain straight. This strain anisotropy effect has been directly observed and is at a maximum in the range 1000K to 1050K.

Mechanical interaction will occur if the combined radial strains of neighbouring rods exceed about 65%. After touching, the radii of curvature of the arcs of cladding not in contact decrease, so reducing the hoop stresses and deformation is more likely to continue above and below the contacting region. Time to rupture generally increases if mechanical interaction occurs.

Fuel cladding under normal service conditions is most commonly in the cold-worked and stress-relieved condition, the structure consisting of distorted lenticular grains. This structure, which also contains irradiation induced defects, recrystallises rapidly above about 975K (ca 10s) and the defects are annihilated by the advancing boundaries of the recrystallising structure, leading to the possibility of high circumferential strains in the range 975-1075K. Above about 1075-1095K the transformation to the  $\beta$ -phase begins. The presence of  $\beta$ -phase in the  $\alpha$ -phase matrix reduces the strength considerably. This, combined with the temperature dependence of the amount of  $\beta$ -phase present, means that in this mixed phase region, although ductility remains high, the sensitivity to circumferential temperature gradients is increased and large strains do not usually occur.

A large body of experimental data is available on the deformation of Zircaloy, including materials property tests, tests on simulated fuel rods heated by various techniques out-of-reactor, single and multi-rod irradiation experiments. Some of the key results of these experiments and programmes are summarised in the following sections.

#### Single Rod In-Reactor Tests

Three series of in-reactor single rod LOCA tests have been reported. KfK<sup>29</sup> tested short (50 cm active length) PWR type rods in the FR2 reactor. The behaviour of irradiated rods (2500-35,000 MWd/tU) was compared with that of unirradiated rods and rods with electrically heated simulators. Various rod internal pressures were used. Transients with a peak temperature of about 1200K and heat-up rates in the range 6-20 K/S resulted in all pressurised rods rupturing during the heat-up phase. Rods strained circumferentially over their entire heated lengths, the axial strain profile corresponding to the power profile with the maximum strain and rupture occurring near the peak power position. Burst strains of irradiated, unirradiated and electrically heated rods are shown in Fig. 5. There was no noticeable effect of irradiation damage or fission products on deformation or rupture, although it is known that such effects could be expected at lower temperatures. A further observation was that fuel fragments slumped into the ballooned region of the cladding at the time of burst, but that no additional fragmentation occurred as a result of the LOCA transient.



A series of tests (LOC) performed in the PBF reactor at INEL<sup>31</sup> had 0.91 m long rods of a 15 x 15 PWR type. Peak temperature and internal pressure were varied in these tests which included irradiated and unirradiated rods. Nine rods in this series ballooned and ruptured in the centre third of the fuelled length over which the power distribution was flat. Maximum clad strain varied from 19% to 74%, but there was such a big variation in heating rate, 0-100 K/s, and burst temperature, 1066-1350K, that no clear conclusion on the effect of irradiation could be established. The data from this test series are included in Fig. 5 and fit well into the scatter band of other data.

#### Multi-Rod In-Reactor Tests

Multi-rod tests in-reactor, provided the rods are of an adequate length and sufficient in number to reveal interaction effects, are the most relevant of all tests in demonstrating behaviour in a LOCA. Such tests are, however, the most difficult and expensive to carry out. There are problems in the design of such tests, bearing in mind that the number of rods is necessarily limited, that they are closely confined in a reactor loop, and that the loop integrity must be protected from contact by deforming fuel rods. Correct representation of the resistance to outwards movement by swelling rods after they start to interact and of flow by-pass around a swelling region are problems not fully solved in the experiments that have been performed so far.

Four multi-rod tests have been performed by the US NRC and UKAEA in a test loop in the NRU reactor at Chalk River. Bundles tested were of full length PWR fuel rods of a 17 x 17 design. The rods were in fact some 600 mm longer than the reactor core. A maximum of 12 rods (4 x 4 less corner rods) could be pressurised and these were surrounded by a row of unpressurised guard rods at standard pitch. The rods were not pre-irradiated, except they were taken briefly to full power three times to pre-crack the UO<sub>2</sub> pellets. The decay heat was simulated by running the reactor at low power with steam cooling and the transient started by shutting off the steam flow, so that the rods heated up adiabatically at about 8 K/s. The transients were terminated either by tripping the reactor or by bottom reflooding with water at a controlled rate. In three of the tests, MT1, 2 and 4, run by US NRC, the deformation occurred during the ramp, but in the other test, MT3, run by UKAEA, the major part of the deformation occurred during the flat topped part of the transient. The deformations produced in these experiments are shown in Fig. 6. It is evident that the deformation in all cases was substantially co-planar and in MT3<sup>2</sup> the grids had a significant effect on the axial shape of the balloons, a consequence of de-superheating of the steam in the steam/water droplet mixture as it passes through the upstream spacer grid. The swollen section of the MT3 bundle, with guard rods removed, is shown in Fig. 7. Post-irradiation examination of rods from the MT series showed that except for the actual burst positions, or where rods were dented by adjacent bursts, the bulges remained circular. This indicated that the mechanical restraint from rod to rod interaction seen in some tests with a larger number of rods was not present. Haste<sup>33</sup> has modelled the effect of the presence of more pressurised rods and concluded that the measured flow blockage in MT3 of 55% would have increased to 70%.

A multi-rod test (215P) was performed by CEA France in the PHEBUS loop on a 5 x 5 pressurised rod bundle of 17 x 17 PWR type rods with an 800 mm active length. Twenty-one of the rods burst within 14 s of one another at the top of the ramp, about 1110K, just prior to the start of re-flooding. Rods in a central 3 x 2 array, showed typical 'carrot' shaped co-planar deformation with peak clad strains of 43-53% and strains in excess of 33% over about 80 mm length. Four external tie rods provided mechanical restraint to two central cross bundle rows of rods at right angles. This restraint was sufficient to cause mechanical interaction and the central rod deformed into a shape close to the theoretical

square. The average flow restriction in the central 3 x 3 array, including 3 rods with low strains, was 56%<sup>34</sup> and the greatest individual sub-channel flow reduction 80%.

#### Out-Reactor Tests

Several important series of out-reactor tests, single and multi-rod, have been conducted, notably in the FRG, USA, Japan and UK. It is on the basis of data obtained from these many experiments that the safety of PWR fuel assemblies under DBA conditions has been established. The role of the in-reactor experiments has been to demonstrate the validity of the more extensive out-reactor experiments and to endorse the data base that they represent for validation of the predictive codes required for licensing calculations.

To review all the out-reactor tests in detail would be a task beyond the compass of this paper. It is proposed to review firstly the key aspects of some of the single rod tests, to describe the results obtained in the REBEKA series of tests conducted as part of the PNS programme by KfK and to comment briefly on supporting or contradictory findings from the other multi-rod programmes.

Provided comparable and realistic test conditions are adopted, remarkably similar single rod behaviour has been found in most experiments. To provide the best simulation the following requirements should be satisfied:

- (a) internal heating with pellet/clad gap simulation
- (b) simulator length should exceed one inter-grid span
- (c) external radiative heat loss should be prevented
- (d) coolant flow should be simulated
- (e) bending should be restrained

Much of the early reported work was done using direct resistance heating of the cladding with large radiative heat losses or external radiant heating with little or no external convective cooling. Early observations of large diametral strains (up to more than 100%) over long lengths were unrealistic of anything other than an improbable flow starvation situation. Work with realistic steam flow, typical of the refill and reflood stages of a DBA, resulted in a swelling of very different morphology, with the position of maximum swelling displaced in the direction of steam flow, the length much reduced and with a tendency for the swollen portion to have a carrot shape. Large swelling strains were found in the high  $\alpha$ ,  $\alpha+\beta$  and  $\beta$ -phase fields, except that in oxidising conditions, such as in steam, there was a dramatic reduction in ductility above about 1150K. The very elongated balloons found in early UK work<sup>35</sup> were a result of largely radiative cooling, which increased with strain, and the high temperature dependence of creep. As one axial region strained and cooled, it stabilised and creep started in neighbouring regions. Under significant convective flows the superheating of the flowing steam produces a temperature gradient, positive in the downstream direction, and maximum strains appear close to the downstream end of the heated length. There is still some thermal stabilisation involved, but in practice further extension in the downstream direction is inhibited by the end of the heated length, or, in a long multi-rod bundle by the restraint of the spacer grid and the de-superheating of steam in the grid region. Since when clad straining occurs there is simultaneous wall thinning and diameter increase, both leading to higher local stresses, it follows that to avoid instability the reduction in creep rate due to the temperature drop must override the increase due to the higher

stress. At very high ramp rates ( $> 20$  K/s) the thermal stabilisation mechanism can be overridden and local instability occur. In such cases the balloons are generally short and not co-planar.

In the REBEKA multi-rod test programme at Karlsruhe<sup>36</sup> 6 tests have been conducted, R1 to R4 with 3 x 3 bundles of pressurised rods and an external row of guard rods at standard pitch, R5 and R6 with 7 x 7 bundles of pressurised rods and a restraint shroud half a rod pitch from the centres of the outer rods. Although most of the tests were designed to investigate the behaviour of fuel in a PWR (17 x 17 design) with combined upper and lower plenum injection, typical of KWU designs, one test, R6, represented a cold leg injection only design. The rods used in the REBEKA tests were all full length having a heated length of 3900 mm and were ramped at 7K/s. The test loop was able to circulate steam from the top or bottom and reflooding water from the bottom. The axial strain distributions obtained are shown in Fig. 8. In particular the results of tests R5 and R6 illustrate the big difference between tests simulating the combined injection and cold leg injection systems. The results of R6 are very similar in general terms to the results of the MT3 in-reactor experiment<sup>32</sup> and go a long way towards confirming the view that properly conducted out-reactor experiments are a valid representation of in-reactor behaviour. An explanation for the behaviour in R5 has been given by Erbacher et al<sup>37</sup>. At the onset of reflooding, the downflow of steam has established a temperature gradient in the rods with peak temperature near the bottom ends. This temperature profile reverses over a time period following the start of re-flood, but because of various inhomogeneities in the rod bundle caused by locally different rod power and coolant flow, the individual rods have different temperature histories and burst at different times. Because of the time variation of axial temperature profile this leads to different burst locations.

Tests have been reported by JAERI<sup>38</sup> on 7 x 7 bundles of 15 x 15 PWR type. Many of the tests were performed with a very low steam flow and an unheated shroud. Rods near the centre deformed more and the presence of unheated rods, simulating control rods, did not reduce the strain in neighbouring rods<sup>39</sup>. In later tests the unheated shroud was replaced by a guard ring of heated rods which resulted in greater and more co-planar deformation. A final test series to investigate the maximum flow blockage had the shroud reintroduced between the test bundle and the guard rods. Tests were performed at ramp rates of 1 K/s and 7 K/s and 4 control rod guide tubes were introduced in some tests. Flow restrictions in the range 80-90% were produced, with slightly higher values in the slow ramp tests and a greater axial extent of the high blockage region in the tests with control rod guide tubes<sup>40</sup>.

Tests at ORNL on 4 x 4, 6 x 6 and 8 x 8 bundles of 17 x 17 type PWR rods have been reported. Many of the tests were performed with high ramp rates (28 K/s) and low downward steam flows. Heated or unheated shrouds were used, the latter at half a rod pitch from the outer rod surfaces to examine the effect of test array size on deformation and rod-to-rod interaction. In the 8 x 8 test B.3<sup>41</sup> all the rods (except one that failed to retain pressure) burst within a few seconds at about 1050K. Peak strains varied from 25-75% and interaction resulted in some deformed rods having a 'square' section. The ORNL conclusion was that flow area restriction may be underestimated by the use of small unrestrained arrays and that 2 rows of deforming guard rods are necessary to simulate the radial temperature and mechanical boundary conditions of a large array of rods such as a whole fuel assembly. It should be noted that this conclusion is based on single phase coolant tests and that the bundle size effect found in tests with 2-phase cooling is not so pronounced. Test B.6<sup>42</sup>, the last of the ORNL series was designed to fail at 1200K, well into the  $\alpha + \beta$  phase region to check whether the smaller

strains found in single rod tests would also apply in a multi-rod test. The results confirmed this expectation with burst strains ranging from 22-56% and maximum blockage over a 4 x 4 region of 46%.

A large programme of single rod testing has been conducted by the UKAEA<sup>43</sup> using resistance heating of the cladding under various external heat transfer conditions. The dramatic effect of oxidation above about 1150K was observed and in later work the strain-cooling effect leading to axially extended deformation, under either mainly radiative or convective cooling conditions, was demonstrated, together with the effect of steam flow in modifying the typical strain morphology. Some 4 x 4 multi-rod tests have been conducted to examine rod-to-rod interaction for code development purposes, and a major facility, MERLIN, capable of testing 72 rod bundles, is being commissioned. Work using irradiated fuel rods heated by external radiant heating, showed that the deformation was comparable to that obtained in the unirradiated cladding tests. Behaviour of the fuel pellet stack was a prime interest in this work. In tests at 975-1075K, deformation was stopped at about 40% strain; the fuel was fixed by resin in-filling and the spatial distribution examined by X-radiography, gamma scanning and sectioning. Less than 5% of fuel axial relocation was found in the ballooned regions.

#### BLOCKAGE MEASUREMENT

One of the most important outputs from a multi-rod LOCA experiment is an assessment of the blockage caused within the bundle of rods and its axial variation. Because in so many experiments the external restraint has not been correctly represented, rods have pushed apart when interaction started and little sub-channel blockage has resulted. However, because many investigators have used a total area method of assessing blockage, the measured blockage may appear to be much larger than it actually is. Using this method, blockage values in excess of 100% can be calculated, when substantial coolant sub-channels remain. If the blockage is defined in terms of the change in cross-sectional area within the original coolant channel area, then values in excess of 100% are not possible. This method can be applied by using a transparent mask over sections of the bundle. There can still be large differences between blockage values derived by this 'mask' method over a number of rods and maximum sub-channel blockage. A mathematical description of sub-channel blockage has been derived for use in the MABEL code in the UK.

#### COOLABILITY

The importance of all the work on clad swelling in DBA simulation tests is to enable an assessment to be made of the effect of local blockages on coolability. This information does not readily come out of the many multi-rod experiments that have been conducted, because they are eventually reflooded under forced cooling conditions without a representative flow by-pass path.

The effect of a blockage on coolability is determined by the extent of local sub-channel blockage in terms of area reduction, length over which the area reduction extends and number of neighbouring sub-channels affected. A reduction in sub-channel area does not necessarily result in reduced cooling, the situation being influenced by many factors. Firstly, the clad lift-off causes at least a temporary decoupling from the decay heat source and is accompanied by a drop in temperature and more rapid rewetting, secondly, up to a certain area reduction the coolant flow velocity may be accelerated, causing improved cooling and, thirdly, entrained water droplets may be broken up causing local de-superheating of the steam phase. The overall effect is, of course, very much influenced by the increase in pressure drop in the blocked region and the ready availability of

alternative flow paths. An interesting feature of some of the REBEKA tests was the formation of a second rewetting front in the region of a clad rupture which persisted and advanced until the primary rewetting front caught up.

Numerous experiments have been carried out to measure the effect of blockages on coolability. The FLECHT series of tests sponsored by Westinghouse, EPRI and NRC have been criticised on grounds of the unrepresentative simulation of deformation and because they were performed under forced cooling conditions without by-pass.

Reflood tests conducted by KfK in the FEBA facility on 5 x 5 arrays, having a 3 x 3 grouping with attached double tapered sleeves (180 mm in total length), showed that with a 90% blockage there was only a small temperature increase downstream of the blockage as compared with rods in the unblocked region<sup>45</sup>. These tests were done under forced reflood conditions with by-pass and taken in conjunction with results from the FLECHT series and the JAERI SLABCORE test facility on larger arrays are considered to represent a convincing demonstration of coolability of severely deformed bundles.

Experiments were performed by the UKAEA in the THETIS facility<sup>46</sup>. Arrays of 7 x 7 full length fuel rod simulators had idealised ballooned regions attached as sleeves to a 4 x 4 group of rods representing a 90% flow blockage over a 200 mm length. During reflood the rewetting front velocity reduced in the region of the peak cosine heat flux, but time to rewet in the blocked and unblocked regions was very similar, except at the highest bundle power (200 KW) when it was late by about 10 s in the blocked region. The surface heat flux reduced away from the rewetting front because of steam superheating and spacer grids only reduced the superheat if they were wet. The blocked region was cooled successfully providing the reflood rate was not less than 30 mm/s. Cooling was very dependent on water droplets penetrating the blocked region, which was a function of droplet velocity, greater some distance ahead of the rewetting front.

It appears from these test results that concern about lack of coolability does not arise if local blockages do not exceed 90%.

#### PREDICTIVE COMPUTER CODES

The ability to predict fuel clad deformation in any postulated LOCA is important in the licensing context. Workers in several countries have developed codes for this purpose which attempt to predict deformation, its distribution and termination by rupture, maximum clad temperature and, in some cases, the extent and effects of interaction between neighbouring rods.

Such codes typically take input information on coolant conditions from a thermal-hydraulic code and data on fuel condition from a steady state fuel performance code. A range of sub-codes calculate clad stresses, temperatures and deformation. The modelling of cladding behaviour requires good creep data, representative of the cladding used, or to be used. Even within specification creep properties of Zircaloy can vary quite widely because of small variations in composition, texture and structure.

The version FRAP-T5<sup>47</sup> of the well known US code developed at INEL calculates the transient response of a single fuel rod under a range of accidents including LOCAs. Fuel temperature, internal gas pressure and deformation are calculated iteratively using various sub codes, with input data from FRAP-S or FRAPCON and RELAP. A sub-code FRAIL predicts failure of the cladding and sub-channel blockage. There is a later version FRAP-T6 which has an improved swelling sub-code BALON-2 and a better fission gas release model FASTGRASS.

The SSYST code has been developed in the FRG, the latest version being SSYST-3<sup>48</sup>. This code takes input on the fuel state from COMETHE and on thermalhydraulics from RELAP 4/MOD 6. Sub-modules calculate heat transport, gap conductance, rod internal pressure, Zircaloy oxidation and clad deformation. The code has been used to model FR2 and REBEKA experiments and is used to predict core behaviour in a LOCA, including a probabilistic analysis.

MABEL is an interactive thermalhydraulic-deformation code developed in the UK<sup>49</sup>. The code takes input from one of the fuel performance codes SLEUTH-78, MINIPAT or HOTROD and from either RELAP 4/MOD 6 or TRAC. Starting from the steady state MABEL-2 performs a series of transient calculations at variable timesteps, including sub-channel heat transfer, fuel to clad gap, fuel and cladding temperatures, fuel rod internal pressure and clad deformation. The code also calculates clad deformation after interaction with 8 swelling neighbouring rods.

Other available codes include: CUPIDON<sup>50</sup>, developed by CEA, which uses the RESTA or DEMETER fuel performance codes and RELAP; CARATE<sup>51</sup> developed by KWU; and ACCREL-2<sup>52</sup>, developed by VTT Finland, which is a fast running modular code suitable for core-wide fission product release studies.

Validation of LOCA codes is an ongoing process. The clad deformation codes are generally accurate and well validated, but the problem with the combined codes is the relative inaccuracy of temperature prediction (up to 150K) which, combined with the high temperature sensitivity of deformation, leads to inaccurate predictions for particular cases. The problem basically is that the blowdown, refill and reflood processes in an intricate mechanical core are very complex. A further problem is to input the factors which lead to circumferential temperature gradients in the cladding. Some codes attempt this by introducing an arbitrary pellet eccentricity distribution factor during the ballooning process. Recognising that progress in the development of LOCA fuel behaviour codes might be advanced by such exercises, CSNI has initiated an International Standard Problem, ISP 14 based on a test performed in REBEKA in 1983.

#### DISCUSSION AND CONCLUSIONS

The state of knowledge on fuel behaviour in a DBA has advanced enormously in recent years as a result of the intensive world-wide R&D effort that has been deployed. Progress has been accelerated by excellent collaboration and free exchange of information, and by the various specialist meetings on the subject organised by CSNI, IAEA and other bodies.

#### Oxidation and Embrittlement

As with other phenomena, the effects of oxidation in leading to embrittlement are strongly dependent on the duration and peak temperature of a particular transient. If the upper bound temperature is not above about 1150K and the time before quench does not exceed about 300 s, then the risk of embrittlement either on quenching or during subsequent post-quench operations is negligible.

For transients exceeding these limits of temperature and time data is available to predict the extent of oxidation, and the criteria of Chung and Kassner<sup>14</sup> are recommended as appropriate to assess the risk of fragmentation during quench or subsequently. Calculation methods to assess the state of cladding in relation to these criteria are available.

The risk of fragmentation is not one which should be accepted, because the indeterminate geometry which will result is not amenable to coolability calculations or experiments.

## Hydrogen Generation

The hydrogen released as Zircaloy is oxidised in steam is directly proportional to the oxygen consumed by oxidation and oxygen pick-up of the Zircaloy. The calculation of hydrogen generation can be made using the available parabolic rates of reaction over the temperature range from 975K-1475K, or higher. It is unlikely that steam starvation will limit oxidation or H<sub>2</sub> generation under DBA conditions.

## Clad Deformation

Clad deformation is primarily influenced by stress, temperature and time in a transient. Because of the influence of oxidation and O<sub>2</sub> pick-up on creep and ductility, the most extensive deformation will not occur in the highest temperature transient experienced by peak rated fuel. Such fuel is likely to rupture with high, but very local, strain during or soon after the ramp up to peak temperature. Maximum strains, with an axial extension of the strained region of about 200 mm will occur in fuel cladding which reaches temperatures in the range 975-1125K. The location of peak strain (and rupture) regions on rods is very dependent on the nature of the ECCS used. For combined injection systems a random distribution within one spacer grid span can be expected, but in systems with cold-leg injection only deformation is expected to be substantially co-planar on all rods and displaced towards the upper end of the critical spacer grid span. Some more limited deformation can be expected in a neighbouring inter grid span.

The maximum clad swelling that will occur on rods whose cladding reaches the high  $\alpha$ -phase temperature range is expected to be about 80%. The resultant degree of coolant flow blockage, assuming swelling of several rows of neighbouring rods to beyond the 30% strain required to interact, and assuming a distribution of strains below the peak value, is about 70%. However, since much of the data was determined on limited size bundles of unirradiated rods, out-reactor, it is probably safer to conclude that the maximum flow blockage in a local area of some tens of rods could reach 80%.

The available experimental data on coolability gives no reason to believe that such an area, with an 80% flow blockage, should not be coolable both in the short and long term. Test results on 90% flow blockages, in which there was very little effect on coolability, represent a sufficient margin to give confidence in the 80% case.

The development of computer modelling codes to predict oxidation and hydrogen generation is well advanced, provided parabolic kinetics obtain, and codes for the prediction of clad deformation are satisfactory, but temperature uncertainties arising from the thermal-hydraulic codes restrict the accuracy of prediction for particular experiments. The representation of factors causing circumferential temperature gradients, and so limited deformation, has not been satisfactorily solved in any of these codes and seems likely to be based on arbitrary assumptions for some time to come.

If there is any area in which more data would be welcome, it is to confirm understanding on larger bundles and pre-irradiated fuel, since both factors appear to promote somewhat larger strains, but some of the large bundle factors have already been taken into account in arriving at a best estimate flow blockage of 70%, so it would appear very safe to assume a worst case of 80% for coolability assessment purposes.

## ACKNOWLEDGEMENT

The authors would like to thank their many colleagues in the UKAEA and KfK, as well as workers in many other organisations, on whose data and test results this review is based. Particular thanks go to those people who have made contributions to the CSNI State-of-the-Art Report, on which the authors have drawn heavily, and to the UKAEA authors, Mr C A Mann, Mr E D Hindle and Dr P D Parsons, who have written the Report.



## REFERENCES

1. BAKER L and JUST L C. Report No. ANL 6548, May 1962.
2. PAWEL R E et al. J Electrochem. Soc. 1979 126 (7) 1105-1111.
3. PAWEL R E and CAMPBELL J J. J. Electrochem. Soc. 1980 127 (10) October 2188-2194.
4. LEISTIKOW S et al. CSNI/IAEA Specialists' Meeting Riso, 1983.
5. KAWASAKI S et al. J. Nucl. Sci. Technol. 1978 15 (8) August 589-596.
6. PARSONS P D and MILLER W N. UKAEA report ND-R-7(S), 1977.
7. SAGAT S. AECL Unpublished work.
8. ASHER R C. UKAEA Report AERE-R-7454, 1973.
9. LEISTIKOW S et al. KfK Report 3587, 1978.
10. CATHCART J V et al. ORNL/NUREG-17, 85-93 1977.
11. FURUTA T et al. J. Nucl. Sci. and Technol. 1982 105 1119-1131.
12. LEISTIKOW S and KRAFT R. Proc. Sixth European Congress on Metallic Corrosion, London, Sept. 1977.
13. FURUTA T and KAWASAKI S. J. Nuc. Sci. Technol. 1980 17 (3) 243-45.
14. CHUNG H M and KASSNER T F. NUREG/CR-1344, Jan. 1980.
15. DOCKET-RM-50-1 (Vol. 1). USAEC, Washington, 1973.
16. PARSONS P D. Paper presented at the 6th Water Reactor Safety Information Meeting. Gaithersburg, 1978.
17. HOBSON D O and RITTENHOUSE P L. ORNL Report 4758, 1972.
18. PAWEL R E. J. Nuc. Materials, 1974 50 247-258.
19. HOBSON D O. Proc. ANS Top. Meeting on Water Reactor Safety, Salt Lake City, 1973. CONF-730304.
20. SAWATZKY H. Proc. 4th Int. Conf. on Zr in the Nuclear Industry, 1978 ASTM STP 681.
21. HAGGAG F M. NUREG/CR-2757 1982.
22. MALANG S. ORNL Report 5083, Nov. 1975.
23. DOBSON W G and BIEDERMAN R R. EPRI Report NP-347, 1976.
24. SUZUKI M and KAWASAKI S. J. Nucl. Sci. Technol. 1980 17 (4) 291-300.

25. PARSONS P D. UKAEA Report TRG Report 2882(S). 1977.
26. GEBHARDT E et al. J. Nucl. Materials 1961 4 255-268.
27. CHUNG H M et al. Quarterly Progress Report, ANL 75-72, 1975.
28. OCKEN H. Nucl. Technology 1980 47 343.
29. KARB E H et al. KfK Report 3346, 1983.
30. HOFMANN P and SPINO J. ANS/ENS Topical Meeting, Sun Valley, 1981.
31. BROUGHTON J H et al. ANS/ENS Topical Meeting, Sun Valley, 1981.
32. MOHR C L et al. NUREG/CR-2528, PNL 4166, 1983.
33. HASTE T J. UKAEA Report ND-R-988(S).
34. ADROGUER B et al. Paper to CSNI/IAEA Specialist's Meeting, Riso, 1983.
35. HINDLE E D. UKAEA Report ND-R-6(S), 1977.
36. ERBACHER F J et al. Paper to 9th Water Reactor Safety Information Meeting, Gaithersburg, 1981.
37. ERBACHER F J et al. Paper to CSNI/IAEA Specialist's Meeting, Riso, 1983.
38. KAWASAKI S. Private communication.
39. KAWASAKI S et al. Paper to ANS/ENS Topical Meeting, Sun Valley, 1981.
40. KAWASAKI S et al. Paper to CSNI/IAEA Specialist's Meeting, Riso, 1983.
41. CHAPMAN R H. Paper to 8th Water Reactor Safety Information Meeting, Gaithersburg, 1980.
42. CHAPMAN R H. NUREG/CR-2911 (ORNL/TM-8485), 1982.
43. HINDLE E D and MANN C A. UKAEA Report ND-R-364(S), 1980.
44. GARLICK A and HINDMARCH P. UKAEA Report ND-R-628(W), 1983.
45. FIEGE A. KfK Report 3442B, 1983.
46. PEARSON K G et al. UKAEA Report AEEW-R1591, 1983.
47. SIEFKEN L J et al. NUREG/CR-0840, 1979.
48. BORGWALDT H and GULDEN W. KfK Report 3359, 1982.
49. BOWRING R W et al. UKAEA Report (4 parts) AEEW-R-1529, 1530, 1531 and 1532.
50. HOUDAILLE B et al. Paper to CSNI/IAEA Specialist's Meeting, Riso, 1983.
51. EBERLE R et al. Paper to CSNI Specialist's Meeting, Espoo, 1980.
52. KELPPE S. Private communication.

- Fig. 1 'Typical fuel clad temperature and system pressure transients following a cold leg break LOCA.'<sup>45</sup>
- Fig. 2 'Zircaloy-2 oxidised in steam at 1675K for 200 s'.
- Fig. 3 'Thermal shock failure map for Zircaloy-4 cladding. Cooling rate 100 K/s.'<sup>14</sup>
- Fig. 4 'Dependence of burst strain of Zircaloy-4 cladding on azimuthal temperature variation from REBEKA tests'.
- Fig. 5 'Burst strain of Zircaloy cladding as a function of temperature.'<sup>45</sup>
- Fig. 6 'Axial distribution of clad strain in cladding of rods from NRU MT3 test'.
- Fig. 7 'Clad deformation of pressurised rods from NRU MT3 test'.
- Fig. 8 'Influence of flow direction on axial distribution of clad ballooning.'<sup>36</sup>

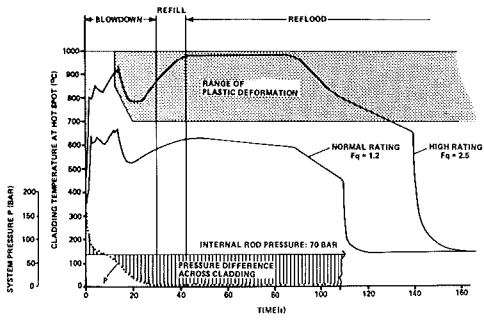


Fig. 1.

Typical fuel clad temperature and system pressure transients following a cold leg break LOCA.

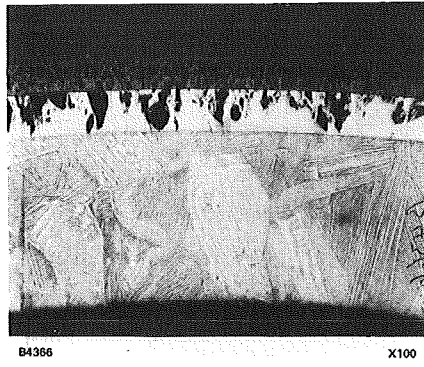


Fig 2.

Zircaloy-2 oxidised in steam at 1675K for 200 s.

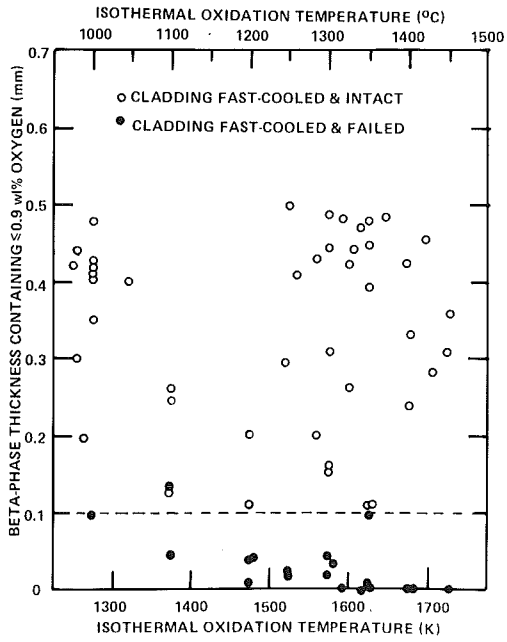


Fig. 3.

Thermal shock failure map for Zircaloy-4 cladding. Cooling rate 100 K/s.

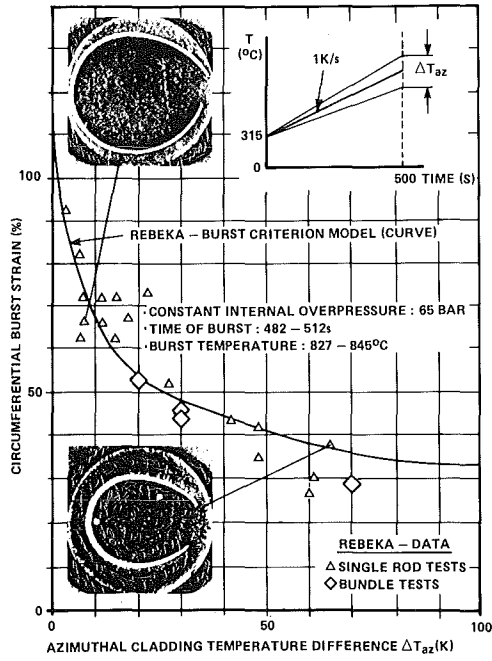


Fig. 4.

Dependence of burst strain of Zircaloy-4 cladding on azimuthal temperature variation from REBEKA tests.

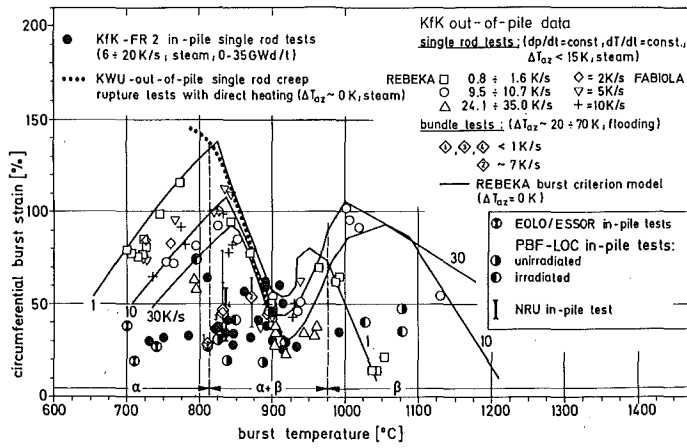


Fig. 5.

Burst strain of Zircaloy cladding as a function of temperature.

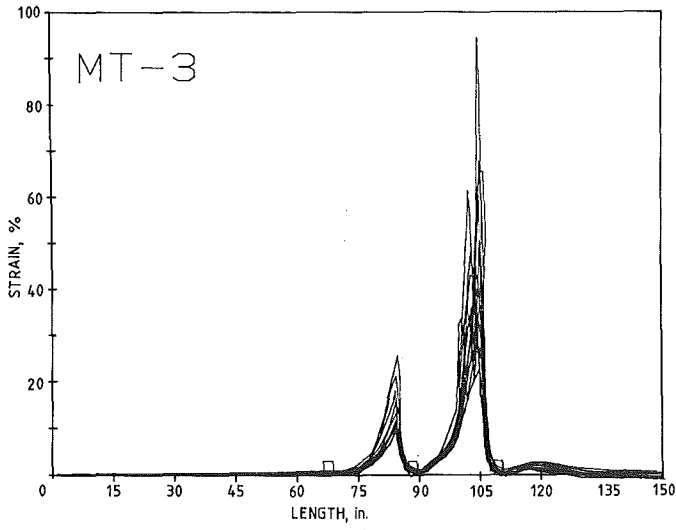


Fig. 6.

Axial distribution of clad strain in cladding of rods from NRU MT3 test.

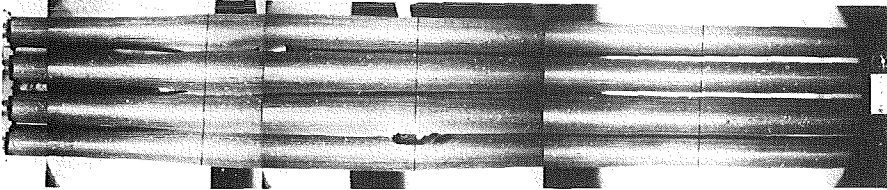


Fig. 7.

Clad deformation of pressurised rods from NRU MT3 test.

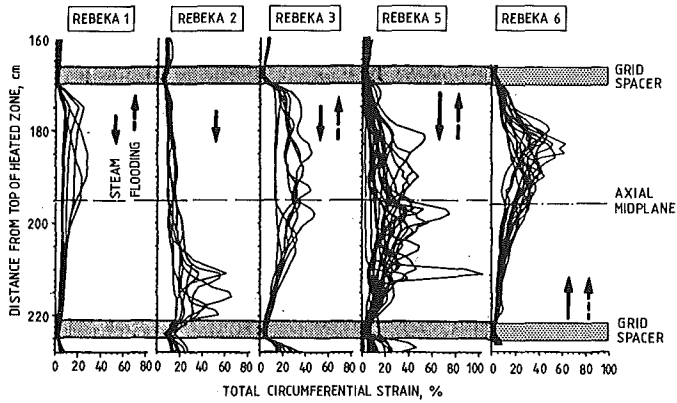


Fig. 8.

Influence of flow direction on axial distribution of clad ballooning.

## REVIEW OF RECENT SOURCE TERM INVESTIGATIONS

Presented by William R. Stratton\*

2 Acoma Lane, Los Alamos, N.M. 87544, U.S.A.

\*This review is based largely on the study recently completed by the American Nuclear Society's Special Committee on Source Terms. Committee members are: M. Christian Devillers, France; M. Sergio Finzi, CEC (alternates, M. William Vinck, M. Anesto Della Loggia, M. Brian Tolley); Dr. Mario Fontana, U.S.A.; Mr. Michael Hayns, United Kingdom; Dr. Hans H. Hennies, F.R.G. (alternate, Mr. Peter Hoseman); Dr. Herbert J. C. Kouts, U.S.A.; Mr. Saul Levine, U.S.A.; Dr. A. P. Malinauskas, U.S.A.; Mr. James F. Mallay, U.S.A.; Mr. Andrew Millunzi, U.S.A.; Mr. Masao Nozawa, Japan (alternate, Dr. Ryohei Kiyose); Dr. Walter Pasedag, U.S.A.; Mr. A. Schuerenkaemper, JRC-Euratom; Dr. Robert L. Seale, U.S.A. (Vice Chairman); Dr. William R. Stratton, U.S.A. (Chairman); Dr. Richard C. Vogel, U.S.A.; Mr. Edward A. Warman, U.S.A. Individuals who contributed significantly to the report are: Mr. Andrew Pressesky, U.S.A.; Dr. Walton Rodger, U.S.A.; Dr. Thomas Kress, U.S.A.; Dr. Robert Burns, U.S.A.

## ABSTRACT

The state of knowledge relative to the evaluation of source terms subsequent to a severe reactor accident is examined. The following matters are assessed: the methods and assumptions used to describe fission product behavior and retention associated with various phenomena, response of plant systems and structures, and a summary of source term results obtained by various investigators. These are compared to results quoted in WASH-1400.

## INTRODUCTION

The source term means that amount and type of radioactive materials which would be available for escape to the environment from a reactor which has undergone a severe accident. This is an accident in which fuel is damaged by overheating to the point of allowing substantial escape of fission products to the containment from the fuel and the containment may not have functioned adequately to prevent the escape of significant amounts of radioactivity to the environment.

Source terms have been recognized from the early days of nuclear energy development as the important factor of risk. Because the technology for making accurate and valid estimates of the source term was not available at that time, the conservative, non-mechanistic assumption was made that essentially all of the fission products could be released from a severely damaged reactor. This conservative assumption was later slightly modified and incorporated into regulations which are still in force at this time.

This early assumption and the subsequent regulations focussed on radioiodine as the principal substance of concern. This was because of its relative abundance, its high biological activity (iodine is known to concentrate in the thyroid), and its assumed elemental gaseous form, which provided ready transportability.

During the Three Mile Island accident in 1979, a surprisingly small amount of iodine escaped to the environment, contrary to expectations based on regulatory prescriptions. It was then theorized that the iodine, escaping from the fuel into a chemically reducing atmosphere (due to the presence of water and hydrogen) became an iodide, was readily dissolved in the water, and so became unavailable for escape. Thus, chemistry, which previously had been largely neglected, was seen to play an important role in severe accidents. Other aspects of severe accident considerations were identified at that time. As a result, large programs to investigate source terms, with the objective of providing a more realistic and accurate estimate, were undertaken by government agencies and industry, both in the U.S. and abroad.

The principal focus of this work was the analysis of severe accident sequences chosen because they represented the upper range of consequences and/or exemplified phenomena believed to be important in understanding the chemical and physical processes that determine fission product behavior in severe accidents. This work is an extension of the methodology brought to a considerable stage of maturity by WASH-1400 (The Reactor Safety Study, 1975), an earlier effort to quantify the risk from nuclear energy.

The American Nuclear Society chartered the Special Committee on Source Terms to examine the state of knowledge relative to the source term, and the methods and assumptions used to describe fission product behavior and retention associated with various phenomena, plant systems, and structures in a severe reactor accident. The Committee was also to provide a summary of source term results obtained by various investigators, and to compare these data to those presented in WASH-1400.

The Committee recognized that both probability and consequences are intrinsic elements of risk; however, the Committee's charge included only an examination of consequences as predicted by analyses, and these only up to the point of potential escape of radioactivity to the environment. The probability of occurrence was examined in a general way to show that severe accidents are predicted to be exceedingly rare.

#### CONSIDERATION OF SEVERE ACCIDENT SEQUENCES

The accidents upon which analysts are focussing their attention comprise four families of sequences, namely: the large and small break loss of coolant accidents, the transient initiated accident, and the containment bypass sequence.

The details of the scenario that a specific accident sequence follows depends on the assumptions made about the operations of engineered safety features (ESFs). If a fraction of the capacity of ESFs is assumed to function, the sequence may be terminated or its consequences greatly ameliorated. Also, later phases of a given sequence depend strongly on what is postulated to happen in earlier phases. For example, if only a fraction of the fuel degrades sufficiently to form a debris bed at the bottom of the reactor pressure vessel, reactor vessel penetration and, subsequently, core-concrete reaction would not be expected to occur. Reactor design also strongly influences accident progression.



A large number of scenarios have been derived from the four families of sequences listed above and examined by the numerous investigators in this field. The ones previously believed to have high potential consequences have been studied in sufficient detail to make source term estimates. Because of the large number of sequences that have been so examined, and since no additional sequences have been revealed which could lead to high consequences, the Committee is persuaded that the analytical field as represented by the four families of sequences is, for all practical purposes, complete.

Some sequences are predicted to be very protracted in time, so that important additional considerations may include, for instance, restoration of interrupted electrical power or operator action to place a disabled ESF back into operation. Such sequences may be terminated or greatly ameliorated by these events and actions. Operator actions generally are not taken into account in the analyses.

Significant advances in technology that have taken place since the completion of the Reactor Safety Study (WASH-1400) include: serious consideration of the chemistry of fission products; careful treatment of aerosols, evaluation of containment integrity; elimination of concerns related to steam explosions and short term overpressures as modes of containment failure; more realistic approaches to fuel degradation in severe accidents; and the recognition that base mat penetration by hot core debris is a much slower process than previously postulated and results in very little, if any, escape of radioactivity to the environment.

#### IMPORTANT RADIONUCLIDES

Typically, a large number of fission product species exist in the fuel in a nuclear reactor. Radionuclides escaping into the environment in the unlikely event of a severe reactor accident vary in their importance as to potential consequences. The factors determining the importance of a radionuclide in this regard are: 1) its total inventory in the reactor; 2) its physical and chemical properties which determine its behavior in the plant and the environment; and 3) its biological characteristics. Some of these factors are inherent, and others depend on features of the accident and plant design; thus, the importance of a radionuclide depends to a significant extent on specific aspects of the hypothetical accident sequence being considered.

Radioiodine has long been and still is considered to be a very important radionuclide. However, it is clear that its treatment has been significantly over-conservative, and even historically incorrect. Other important radionuclides include cesium, tellurium, and, of much lesser importance, some of the alkaline earths and noble metals. Like iodine, the importance of cesium also has been previously overstated.

The noble gases, though very volatile, are chemically inert, and thus have a low importance in severe accidents.

## CHEMICAL AND PHYSICAL PROCESSES AND THEIR APPLICATION TO THE SOURCE TERM

A number of fundamental chemical and physical processes are importantly involved in severe accident sequences. These phenomena control the escape of fission products from overheated fuel, and the transport and behavior of fission products in the reactor coolant system (RCS), containment, and contiguous structures. The chemical environment and applicable aerosol processes play an important role. The natural processes and their application to accident sequences, and the operation of engineered safety features and containment systems in the amelioration of the source term are summarized below.

## Chemical Forms and Interactions

The fission products that are released from severely damaged fuel are subsequently transported through the RCS either in elemental form or as a corresponding oxide. The important exceptions, however, are the halogens (I, Br), the alkali metals (Cs, Rb), the chalcogens (Te, Se), and the alkaline earths (Sr, Ba).

Because cesium is present in ten-fold excess over iodine, and water is available, the predominant form of fission product cesium in the RCS will be cesium hydroxide. In contrast, the predominant form of fission product iodine will be cesium iodide, because of the reducing environment. Cesium hydroxide can react with metal oxide surfaces or with boron control rod or reactor shim materials, and this may result indirectly in the decomposition of CsI and the formation of other iodide compounds. However, the dominant processes will be the dissolution of these highly soluble chemical forms in any water that is present, and their proclivity for the formation of aerosols.

Tellurium, which is an iodine precursor in the decay scheme, will behave differently from cesium during the course of an accident; this could result in the formation of small amounts of radioactive iodine in regions devoid of cesium. This addition to the source term is not expected to be significant.

A hydrogen burn or radiation effects may increase the production of volatile organic iodides in the containment building, but the concentrations that might be produced are expected to be small.

## Aerosols

In a severe accident, energy from the decay of fission products, from the exothermic reaction of overheated fuel cladding with steam, and, in some accidents, from continued fission can cause the fuel and core material to heat up and result in the vaporization of the more volatile fission products, components of control rods, and structural material. These vapors can nucleate to form aerosols or can condense on cooler RCS surfaces or on other aerosol particles present. An analysis of the physical and chemical processes which can occur is necessary to determine the amount of these materials escaping to containment or contiguous buildings.

The transport and deposition of fission products and aerosols within the RCS is a transient convection problem of a multicomponent, multiphase mixture with simultaneous heat and mass transfer, chemical reactions, and aerosol kinetics. The flows may be laminar or turbulent, and conditions are

typically dominated by natural convection during much of the time in many of the accident sequences. A number of transport phenomena are modeled in the analyses to represent these processes. Some very similar considerations are required in the containment; however, transport mechanisms for fission product vapors do not appear to be important there because of the lower temperatures. There are a number of computer codes available for treating most of these phenomena. Presently, only Trap-Melt, Retain, and RAFT are formulated for direct application to the RCS.

#### Escape of Materials from a Degraded Core

The escape of fission products and other materials from the reactor core in which the fuel has undergone substantial degradation in an accident occurs during fuel overheating, fragmentation, liquefaction, debris bed formation, and from core debris-concrete reaction. Chemical forms of materials escaping from a degraded core can be predicted from thermodynamic calculations.

A number of models have been developed to predict the escape of fission products from fuel during heat-up. However, since a large fraction of the volatile fission products is expected to escape before fuel degradation, the choice of models for these species is not very important. Also, comparative calculations using the different models provide escape rates that are substantially similar.

Non-fission product material escapes from the core during heat-up in far larger quantities than fission products. These releases are important because the resultant aerosols strongly influence the transport and attenuation of air-borne fission products in the reactor coolant system and in the containment.

If the hot core debris causes penetration of the reactor vessel and comes into contact with the base-mat, the concrete could be eroded by the debris, possibly resulting in the generation of combustible gases ( $H_2$  and CO) and substantial quantities of aerosols. These aerosols would be made up mostly of non-radioactive material, but would be expected to carry some quantities of fission products. It is postulated that the escape would be caused principally by sparging of the gases created during concrete erosion.

Models for predicting escape of fission products during this phase of an accident have been formulated recently. These models are far more mechanistic than the model used in WASH-1400, which was based on simple volatility calculations.

Recent code developments (such as the code, MELPROG) indicate that limits can be placed on the extent of severe core damage and the amount of fuel reaching containment in a severe accident. Former assessments had been little better than conservative postulates.

#### Reactor Coolant System and Containment Transport and Retention Characteristics

Fission product retention in the RCS was not taken into account in WASH-1400 because of uncertainties in the technology and the need for conservative evaluation. Current analyses, however, indicate that a significant fraction of the vaporized fission products would be retained in the reactor vessel upper internals and, in some accident sequences, in other parts of the RCS. Revaporization of the deposited materials could occur due to continued decay heating, with fission product compounds moving to a cooler surface.

Materials not retained in the RCS leak to containment or other structures as aerosols borne with the escaping mixture of hydrogen and steam. There, the aerosols undergo physical attenuation processes, principally agglomeration and settling. Current capability to model such processes in containment is substantially improved over WASH-1400.

Additional aerosols containing fission products could be generated if the accident proceeds to the reactor vessel penetration stage. This would result from such mechanisms as forcible ejection of degraded core material from a pressurized reactor vessel, energetic interaction of hot core debris with a water pool below the vessel, or from degradation of the concrete base mat by hot core debris.

Containment protection engineered safety features could reduce the airborne concentration in a matter of minutes, while natural aerosol processes would achieve similar reduction in a matter of hours. Therefore, release of radio-nuclides to the environment in significant quantities would occur only if breaching of the containment is postulated to occur in the first several hours following the onset of severe fuel damage.

#### Containment

Containment is a key factor in determining if a severe accident results in a significant source term. If containment is not breached, the leakage of radioactivity would be inconsequential. If containment breaching is delayed for more than a few hours subsequent to core degradation, there would be a very large reduction in the source term due to the performance of containment engineered safety features and the effects of natural aerosol depletion processes.

Containments are required by regulation to be able to accommodate design basis accident pressure and temperature conditions. Higher challenges can be imposed by severe accidents. These could include steam explosions, steam pressure pulses, hydrogen burns, and long term over-pressure conditions caused by steam production by decay heat or the buildup of non-condensable gases such as hydrogen or carbon dioxide.

Because the methodology is extremely complex, conservative simplified analytical methods generally are used to assess the capability of containments to meet these challenges. The loadings represented above are slow from a mechanical response aspect; thus, static analysis usually suffices for determining expected containment response.

As noted previously, steam production by decay heat is an important loading mechanism. Containment integrity is protected by engineered safety features such as containment sprays or atmosphere coolers. These systems are designed to extract the heat load; therefore, it is necessary to postulate their failure to pose a significant long term pressure challenge to containment. Passive heat transfer through the walls is insufficient to prevent long term pressure buildup by decay heat effects.

Excessively high temperatures, combined with elevated pressure, can cause breaching to develop in containment seals and penetrations. These are thought to be likely sources of containment openings in severe accidents. Another possible source is a procedural failure to close valves or other openings which penetrate containment.

An important consideration is that containments generally are partially or entirely surrounded by auxiliary structures, such as the service building or turbine hall in the case of PWRs, or the reactor building for BWRs. Leakage occurring from containment breaching is likely to be into such structures, with their large volumes and surface areas providing opportunities for additional natural depletion processes to reduce significantly any leakage to the environment.

The Committee concluded that containment breaching by a missile generated by a steam explosion within the reactor vessel, breaching by hydrogen deflagration, or breaching directly by a pressure pulse from a steam explosion are not credible events. The Committee observed that margins against overpressure breaching were in the range of factors of two to four, because of conservatism in design methods and the use of materials in construction with better properties than the design values. Also, the Committee observed that breaching is most likely to occur as the opening of small pressure sensitive leakage paths which would also serve to mitigate the rise of internal pressure.

#### COMPUTER PROGRAMS FOR ACCIDENT ANALYSIS

A variety of computer programs (codes) have been developed to predict radionuclide release, transport, and attenuation in the analysis of severe reactor accidents. The codes are arranged in suites, with each element in the suite addressing some part of the sequence. Output from one code often serves as input for the code covering the succeeding part of the sequence.

The codes are based on established physical and chemical laws and principles, and the computations are performed on computers. Approximations and limitations on applicability are used to simplify the codes so that computations are not excessively time-consuming. Experiments are used to provide information of use to the developer, and to check how well a given code or group of codes represent reality.

Standardized problems can be calculated to compare the performances of codes which purportedly are used to predict the same part of a sequence. Limited experience with standardized problems for some computer codes and pre-prediction of experiments appear to indicate that there is a basis for substantial confidence in severe accident analyses performed by knowledgeable analysts using current computer codes.

#### PARAMETRIC STUDY OF FISSION PRODUCT RETENTION

A parametric study of fission product retention in PWR containment structures and contiguous structures due to physical retention processes was conducted on the Committee's behalf. No active engineered safety features (e.g., containment sprays) were assumed to function; thus, only naturally occurring retention processes were considered in the study.

The study represents a careful appraisal of a number of parameters which affect fission product retention in PWRs which had been neglected or oversimplified in some analyses. Due to the paucity of data and the state of technology at the time of the Reactor Safety Study (WASH-1400), most of the parameters addressed in the present study were not included at that time.

The study includes analyses of releases of fission products with a postulated pre-existing breach of the containment, and early (i.e., during the first several hours) and late (24 hrs.) breaches of the containment. The results indicate that fission product releases for postulated early breaches of containment are comparable to those for pre-existing openings. However, without a pre-existing opening, containment breach is not expected to occur for days, if at all. The releases associated with late containment openings are observed to be small in comparison with those for pre-existing openings. Thus, the study is focussed on the potential releases associated with pre-existing openings.

Inclusion of these effects results in a large overall reduction in releases of fission products to the environment when the effects are considered together, although the reduction from any single effect is not very large when considered alone.

In another phase of the study, it is shown that releases in the containment bypass accident (V sequence) could be small. This is because the postulated break in the low pressure emergency core cooling system piping would be submerged in water draining from the refueling water storage tank, based on a review of the Surry plant design. The V sequence is very plant specific, justifying additional review of the generic applicability of this finding to other plants.

The results of this study of fission product retention in containment and structures outside containment can be combined with the results of studies of retention in the core and RCS performed by other investigators. When the reductions reported in the study are combined appropriately with the reductions from studies of retention in the RCS, such as those reported in the recent NRC sponsored work at Battelle Columbus Laboratories (BMI-2104), very low predicted releases result. More recently, detailed studies of aerosol retention in structures exterior to containment have been completed by the IDCOR program investigators.

#### COMPARISON OF RESULTS

The results of a large number of computations of course terms for the four families of sequences previously listed have been tabulated and compared, to draw inferences from the data to the extent possible, recognizing the difficulties in the face of variations in assumptions and modeling between investigators. Tables I-VI are included here, with results arranged in accordance with the type of reactor, investigator, accident sequence, and the timing of containment opening. More detailed tables will be included in the report of the Special Committee. Data include that for the corresponding WASH-1400 release category.

TABLE I  
PRE-EXISTING OPENING  
COMPARISON WITH WASH-1400 CATEGORY PWR-2

Plant and Accident Sequence	Area of Pre-existing Opening (m <sup>2</sup> )	Calculations Done by	Fraction of Core Inventory Released to Environment		
			I	Cs	Te
PWR-2	--	WASH-1400	7.0E-01*	5.0E-01	3.0E-01
Surry-AB <sub>β</sub>	3.3E-02	BMI	8.7E-02	8.5E-02	7.0E-02
Surry-AB <sub>β</sub> (a)	3.3E-02	BMI	5.0E-02	4.9E-02	4.7E-02
Surry-AB <sub>β</sub> (b)	3.3E-02	SWEC	4.7E-02	4.6E-02	3.2E-02
Surry-AB <sub>β</sub> (b)	9.3E-03	SWEC	1.2E-02	1.2E-02	8.9E-03
France-900Mw-AB <sub>β</sub> (c)	5.0E-03	CEA	5.2E-02	5.2E-02	--
FRG-1300Mw-FK-2	7.1E-02	KfK	6.4E-03	6.9E-03	--
Surry-TMLB <sub>β</sub> (b)	9.3E-02	SWEC	1.5E-02	1.3E-02	6.4E-02
Surry-TMLB <sub>β</sub> (b)	9.3E-03	SWEC	2.1E-03	2.1E-03	2.3E-02
France-900Mw-TMLB <sub>β</sub>	5.0E-03	CEA	1.7E-02	1.5E-02	--
Zion-TMLB	5.1E-02	IDCOR	1.0E-02	1.0E-02	3.0E-04
Sequoyah S <sub>2</sub> HFP	5.1E-02	IDCOR	2.0E-02	2.0E-02	4.6E-03
Surry-V	1.9E-02	BMI	4.1E-01	4.0E-01	1.2E-01
Surry-V	1.9E-02	SWEC	1.0E-02	1.0E-02	6.5E-03
Zion-V	9.3E-03	IDCOR	8.0E-05	8.0E-05	8.0E-05
Sequoyah-V	9.3E-03	IDCOR	1.0E-04	1.0E-04	1.0E-04

\*7.0E-01 read as 7.0 x 10<sup>-1</sup>

- (a) Repeat of 1st reported calculation with four node model of containment.  
 (b) Retention in RCS taken from BMI-2104 Volume V.  
 (c) Retention in RCS taken from BMI-2104 Volume I, Retention outside containment neglected.

TABLE II  
EARLY CONTAINMENT BREACH  
COMPARISON WITH WASH-1400 CATEGORY PWR-2

Plant and Accident Sequence	Containment Breach		Calculation Done by	Fraction of Core Inventory Released to Environment		
	Area(m <sup>2</sup> )	Time(hr)		I	Cs	Te
PWR-2	--	2.5	WASH-1400	7.0E-01	5.0E-01	3.0E-01
Surry-AB- $\gamma$	6.5E-01	4.5	BMI	5.7E-02	5.9E-02	1.4E-01
Surry-AB- $\delta$ (a)	9.3E-02	0.5	SWEC	8.4E-02	8.4E-02	5.3E-02
Surry-AB- $\delta$ (a)	9.3E-03	0.5	SWEC	1.6E-02	1.6E-02	1.6E-02
Surry-AB- $\delta$ (a)	9.3E-02	3.0	SWEC	8.4E-03	8.4E-03	1.1E-02
Surry-TMLB- $\delta$	6.5E-01	2.5	BMI	4.4E-02	4.3E-02	1.1E-01
Surry-TMLB- $\zeta$ (a)	9.3E-02	3.0	SWEC	1.5E-02	1.3E-02	6.4E-02
Surry-TMLB- $\zeta$ (b)		12.0	BMI	2.6E-03	3.0E-04	7.9E-02
Sequoyah-TMLB	6.5E-01	2.5	BMI	1.7E-02	2.3E-02	1.4E-02
Sequoyah-TMLB	6.5E-01	9.0	BMI	3.9E-02	4.5E-04	2.3E-03

- (a) RCS retention based on BMI-2104 Volume V.  
 (b) Based on base mat penetration neglecting retention in earth, etc., outside containment, essentially a puff release.

TABLE III  
LATE CONTAINMENT BREACH  
COMPARISON WITH WASH-1400 CATEGORY PWR-2

Plant and Accident Sequence	Containment Breach		Calculation Done by	Fraction of Core Inventory Released to Environment		
	Area(m <sup>2</sup> )	Time(hr)		I	Cs	Te
PWR-2	--	25	WASH-1400	7.0E-01	5.0E-01	3.0E-01
Surry-AB <sub>z</sub> (a)	--	24	BMI	4.8E-05	4.7E-05	4.0E-05
Surry-AB <sub>z</sub> (b)	9.3E-02	24	SWEC	4.0E-04	4.0E-04	1.9E-03
Surry-AB <sub>z</sub> (b)	9.3E-03	24	SWEC	3.0E-04	3.0E-04	1.4E-03
Surry-TMLB <sub>z</sub> (b)	9.3E-02	27	SWEC	3.6E-05	3.5E-05	1.8E-03
Surry-TMLB <sub>z</sub> (b)	9.3E-03	27	SWEC	2.8E-05	7.7E-05	1.4E-03
Zion-TMLB <sub>z</sub> (d)	4.6E-02	32	IDCOR	2.0E-03	2.0E-03	2.0E-05
Zion-TMLB <sub>z</sub> (d)	4.6E-02	32	IDCOR	2.0E-03	2.0E-03	2.0E-05
Sequoyah-TMLB <sub>z</sub> (c)	9.3E-03	28	IDCOR	2.0E-04	2.0E-04	2.0E-04
Indian Pt. AB <sub>z</sub> (c)	--	24	NYPA	3.0E-06	8.6E-06	1.3E-06
Indian Pt. TMLB <sub>z</sub> (c)	--	24	NYPA	1.9E-05	1.7E-05	1.9E-05
Indian Pt. TMLB <sub>z</sub> (c,d)	--	24	NYPA	4.2E-06	2.2E-06	3.3E-09
FRG-1300Mw-FK-6	3.0E-02	120	KfK	1.0E-04	1.0E-06	--
FRG-1300Mw-FK-6(e)	3.0E-02	120	KfK	4.7E-07	5.6E-09	--
Sequoyah-S <sub>2</sub> HF	9.3E-03	24	IDCOR	6.0E-04	6.0E-04	2.0E-04

- (a) Based on base mat melt-through, neglecting retention in earth, etc, outside containment, essentially a puff release  
 (b) RCS retention taken from BMI-2104 Volume V  
 (c) Puff release at 24 hrs.  
 (d) Pump Seal LOCA  
 (e) Filtered

TABLE IV  
CONTAINMENT BREACH PRIOR TO CORE DEGRADATION  
COMPARISON WITH WASH-1400 CATEGORY BWR-2

Plant and Accident Sequence	Containment Opening		Calculation Done by	Fraction of Core Inventory Released to Environment		
	Area(m <sup>2</sup> )	Time(hr)		I	Cs	Te
BWR-2	--	30	WASH-1400	9.0E-01	5.0E-01	3.0E-01
Peach Bottom-TC <sub>z</sub> '	6.5E-01	0.97	BMI	3.4E-01	2.9E-01	3.2E-01
Peach Bottom-TC <sub>z</sub> '	6.5E-01	0.97	BMI	2.0E-01	1.6E-01	2.1E-01
Peach Bottom-TC	1.9E-02	13.0	IDCOR	3.0E-02	3.0E-02	7.0E-02
BWR-3000-TC	5.0E-01	--	ELSAM	7.0E-03	2.0E-04	2.0E-04
Shoreham-TC	--	0.5	SAI	7.3E-02	2.5E-02	< 5.0E-04
Grand Gulf-TC	9.3E-02	1.33	BMI	1.0E-01	3.5E-02	1.3E-01
Grand Gulf-TC	1.4E-01	1.0	IDCOR	8.0E-04	8.0E-04	8.0E-04
Peach Bottom-TW	6.5E-01	29.2	BMI	2.8E-01	2.7E-01	1.8E-01
Peach Bottom-TW(a)	9.3E-03	34	IDCOR	1.3E-01	1.3E-01	1.3E-01
Shoreham-TW	--	24	SAI	2.0E-04	2.5E-02	< 3.0E-03
BWR-3000	5.0E-01	33.6	ELSAM	7.0E-03	2.0E-04	2.0E-04
Browns Ferry-TW	--	--	ORNL	2.0E-03	5.8E-05	--
Grand Gulf-TQW	9.3E-03	40	IDCOR	3.0E-04	3.0E-04	2.0E-04
Grand Gulf-TPI	--	22.2	BMI	5.1E-02	3.4E-02	3.2E-02

- (a) If CRD flow or drywell sprays are reestablished after vessel failure or before hour 65, the releases for this sequence are reduced to 3.0E-02.



TABLE V  
CONTAINMENT BREACH DURING CORE DEGRADATION  
COMPARISON WITH WASH-1400 CATEGORY BWR-2

Plant and Accident Sequence	Containment Breach		Calculation Done by	Fraction of Core Inventory Released to Environment		
	Area(m <sup>2</sup> )	Time(hr)		I	Cs	Te
BWR-2	--	30	WASH-1400	9.0E-01	5.0E-01	3.0E-01
Peach Bottom-AE	6.5E-01	0.56	BMI	2.1E-01	2.1E-01	6.7E-01
Shoreham-AV	--	1.5	SAI	1.6E-01	2.8E-02	<2.5E-02
BWR-3000-AW	--	--	ELSAM	1.1E-01	1.0E-01	1.0E-01

TABLE VI  
CONTAINMENT BREACH SUBSTANTIALLY AFTER CORE DEGRADATION  
COMPARISON WITH WASH-1400 CATEGORY BWR-3

Plant and Accident Sequence	Containment Breach		Calculation Done by	Fraction of Core Inventory Released to Environment		
	Area(m <sup>2</sup> )	Time(hr)		I	Cs	Te
BWR-3	--	30	WASH-1400	1.0E-01	1.0E-01	3.0E-01
Peach Bottom-TQUV	9.3E-03	18	IDCOR	5.0E-02	5.0E-02	4.0E-02
Shoreham-TQUV	--	--	SAI	2.0E-04	9.0E-05	<4.0E-05
Browns Ferry-TQUV	--	4	ORNL	7.1E-03	--	--
Grand Gulf-TQUV	--	13.9	BMI	1.2E-03	7.1E-04	4.5E-03
Grand Gulf-TQUV	9.3E-03	47	IDCOR	7.0E-05	7.0E-05	3.0E-05
Grand Gulf-AE	9.3E-02	58	IDCOR	<1.0E-05	1.0E-05	1.0E-05
Peach Bottom-S <sub>1</sub> E	9.3E-03	23	IDCOR	1.0E-02	1.0E-02	1.0E-02

## PWR Observations

a) Late containment breach results show very low releases to the environment and good agreement among investigators.

b) Early containment breach results are somewhat higher than for late breaching and have a wider spread.

c) Pre-existing opening results show close agreement for similar cases and have releases in the mid-range.

d) The data indicate that lower releases are obtained when a more detailed (4-node) representation of containment is used rather than the usual single node representation. The importance of incorporating details of containment and auxiliary structures in an analysis is thus emphasized.

## BWR Observations

For early containment breach, and for breach occurring during core degradation, the results are from one to two orders of magnitude higher than the late opening case; however, the results in a given investigator's work are fairly self-consistent, and all cases (with one exception) are substantially lower than calculated in WASH-1400.

The higher results and the data spread are attributed to: (a) Differences in assumptions, e.g., containment opening size. (b) Whether aerosol attenuation in the reactor building was taken into account. (c) Assumption of excessive suppression pool bypass for large containment opening cases. (d) An error in one of the scrubbing models used for suppression pools. (e) Use of inappropriate thermal-hydraulic modeling.

The Committee is persuaded that, if these differences are properly accounted for, the BWR releases in general would not be greatly different from the PWR releases.

## FINDINGS, OBSERVATIONS, AND RECOMMENDATIONS OF THE COMMITTEE

## Major Finding

The Committee has concluded that the state of knowledge and the analytical methods and assumptions on which current calculations of the source term are based have progressed far beyond those on which WASH-1400 (The Reactor Safety Study, 1975) was based. In general, an ample foundation has been provided to warrant reductions of the source term estimates in WASH-1400 by more than an order of magnitude to as much as several orders of magnitude. This major conclusion is based on reviews of chemical and physical processes relevant to severe accident analysis; severe accident sequences which bound risk from nuclear power plants and represent the ranges of phenomena involved; the status of severe accident modeling and calculational codes; containment capability; and the results of a number of source term studies performed both here and abroad. In addition, the Committee has considered studies performed on its behalf of a number of important parameters and phenomena which had not previously been given adequate emphasis. The noble gases are exceptions because of their chemically inert character, and because they do not undergo the wide range of chemical and physical interactions which are the fundamental cause of the

reduced release of most fission products; however, the very fact that they are inert also leads to low radiological consequences.

#### Findings Supporting or Qualifying the Major Finding

a) Iodine will be released and transported predominantly as cesium iodide and cesium as cesium hydroxide. These species will form aerosols and be subject to aerosol depletion processes, are highly soluble in water, which will be present, and can be irreversibly adsorbed onto metal surfaces, resulting in greatly reduced releases compared to WASH-1400. This finding holds for all light water reactors and all accident sequences.

b) The more severe accident sequences developed in WASH-1400 and more recent Probabilistic Risk Assessment studies provide a sufficiently complete basis for in-depth analyses of source terms. These sequences cover the high end of the release spectrum and involve the phenomena and processes that are considered to affect the escape and transport of fission products.

c) Sequences and plant details are important in estimating plant-specific source terms.

d) If there is no breach of containment, there is essentially no release of fission products; if containment breach is delayed more than a few hours after core degradation, the source term is greatly reduced, independent of the final size of containment breach. Containment is less susceptible to early breaching than previously believed.

e) A substantial basis exists for knowledgeable analysts to calculate LWR source terms with a high degree of confidence in the results.

#### Specific Findings Relative to Containment

a) Three of the four causes of early containment breach are no longer considered credible. These are: steam explosion within the reactor vessel; hydrogen deflagration; and steam explosions in containment. The fourth potential cause of early containment breach, a pre-existing opening in containment, is important in severe accidents.

b) Because of previously underestimated containment strengths, times to containment breach have been unrealistically short. Longer times to breach allow a greater degree of aerosol depletion.

c) The development of distributed containment breaching (cracking) serves to limit pressure rise and is likely to prevent gross containment breaching, while allowing only small quantities of radioactivity to leak out.

d) The penetration of the base mat by hot core debris has a much lower potential than estimated in WASH-1400, and would lead to minor releases only if it were to occur. Therefore, this mechanism for fission product escape is unimportant.

e) Pressure suppression pools in BWRs are very effective in removing fission products, as shown experimentally.

f) The effectiveness of ice-condensers in removing fission products is predicted to be high, but has not been shown experimentally.

g) In some plants, containment bypass accidents will release fission products under water in flooded compartments; in these cases, the release will be very small. In other plants, the release will take place inside containment, as a containment protected small breach accident; in these plants, the release also will be low. In yet other plants, the release will take place in a large auxiliary building; in these cases, it will be necessary to consider the aerosol depletion and other processes, which can be quite effective. These considerations point up the importance of plant design differences in calculating source terms.

#### Thermal Hydraulics

The technology is sufficiently advanced and tested against experiments for accident analysis purposes.

#### Fission Product Transport and Deposition

a) The follow factors, which have significant release attenuating effects, have been inadequately treated or omitted in many analyses: size of containment opening; timing of containment opening; diffusio-phoresis; suspended liquid water in containment; compartments within containment; and adjacent buildings and structures surrounding containment.

b) Revaporization of deposited fission products in the RCS can occur, but is not yet well characterized. However, conservative formulations generally are used, and some retention in the RCS will be long term and will result in decreases in the source term.

#### Escape of Material from a Degraded Core

Differences in several available models in predictions of the escape of fission products from overheated fuel are not significant.

#### Computer Programs for Accident Analysis

Substantial development of computer programs has taken place since the publication of WASH-1400, including some useful diverse development, which provides a certain degree of testing. In addition, the data base supporting the computer programs is substantially larger and more complete than that which existed a decade ago. Finally, in the Committee's view, many of the difficulties attributed to computer programs are more closely related to differing assumptions and boundary conditions than to the algorithms used. Also, the Committee concludes that the existing codes are generally conservative representations of the processes involved in severe accidents.

#### Matters Where Additional Investigation Appears Warranted

These areas of additional investigation are suggested to confirm existing source term calculations and to assure that no important phenomenon has been neglected. They should be evaluated in-depth to ascertain whether further, and how much, work is necessary. The Committee believes that these will not cause a major impact on its assessment.

- a) Surface/fission product chemistry.
- b) Tellurium behavior.
- c) Role of boron in fission product chemistry.
- d) Rate and mode of core damage progression.
- e) Role of control rod material.
- f) Role of contiguous buildings and containment compartments.
- g) Effect of suspended water and diffusiophoresis.
- h) Revaporization of deposited fission products.
- i) The development of a de minimum criterion.
- j) Uncertainty estimates.



## CONTAINMENT SYSTEMS CAPABILITY

W.G. Morison, Ontario Hydro, Canada  
W.J. Penn, Ontario Hydro, Canada  
K. Hassmann, Kraftwerk Union, West Germany  
J.D. Stevenson, Stevenson and Associates, U.S.A.  
K. Elisson, ASEA-ATOM, Sweden

## ABSTRACT

This paper provides a summary of the designs and capabilities of principal containment systems associated with BWR, PWR and PHWR reactors in operation and under construction in the United States, Canada, West Germany and Sweden.

The many conceptual differences in design and modes of operation following accidents are briefly described, with commentary on their evolution and alternatives considered. Specific examples for each reactor system in operation in the four countries are detailed [1,2,3,4]. The containment design differences and requirements are mainly attributable to the fundamental arrangements of the reactor and secondary side systems, and their demonstrated behaviour during normal operation and following accident conditions. However, two other important considerations which strongly influence design are national regulatory requirements [5,6,7,8] and the number of generating units in a station. These broad issues, together with site conditions and proximity to population, dominate containment performance requirements for economic generation of electricity and public safety.

Emphasis is focused on the capability of the various systems to meet design basis accidents. However, the TMI-2 incident has caused plant owners and regulators to examine the ultimate capability of containments, far beyond maximum credible accident bases. Postulated severe degraded core accidents, with a predicted frequency several orders of magnitude lower than other recognized world-wide hazards for which protection is provided, are currently under intense scrutiny [9,10,11]. This paper describes the status of some of these studies.

## CONTAINMENT FUNCTIONAL AND DESIGN REQUIREMENTS

The universally accepted philosophy for providing assurance of nuclear safety in accidents is the adoption of the principle of "defense in depth", which prevents or limits the release of radioactive material for a wide range of circumstances. "Defense in depth" embodies a multiplicity of physical and chemical actions attributable to station process systems, but specifically includes three, often duplicated and diverse, safety systems to effect prompt reactor shut-down, ensure continuing and controlled heat

removal and automatically minimize/prevent radioactive release to the environment.

Containment systems are the ultimate line of defense and safety barrier for preventing the escape of radionuclides to the environment. The functional requirements of containment do not differ in principle for BWR, PWR and PHWR systems, but design requirements are significantly different. The design requirements are not only set by the overall arrangement of the primary reactor and secondary systems, but also (importantly) by national code and regulatory differences. A major additional influence which determines containment system designs is the extent, rate and duration of accident pressure and temperature transients.

During normal operation the function of all containments is to minimize the release of gaseous, liquid, and solid radioactive materials produced during electricity production and which are not retained in process systems. The objective is to ensure that emissions are as low as reasonably achievable; economic and social factors taken into account. Following an accident, the objectives are to retain radioactive materials released as a result of process equipment failure.

Thus, containment system designs have evolved from the basis that they should provide radiation shielding and retain all of the steam and water discharged following an internal reactor system piping failure. The primary element of containment systems is a practical engineered and economic "leak-tight" building which covers and encloses the reactor systems. Piping or ventilation systems which might convey radioactive material outside the containment boundary are isolated immediately after an abnormal condition is detected. Sub-systems to reduce pressure in the building also feature in the designs. In some designs these systems include venting to "gravel" beds or the atmosphere in a controlled manner to ensure safe regulatory releases are met.

In addition to the provision for internal containment loads, protection of containment and hence reactor systems against external loads (i.e., earthquakes, hurricanes, tornadoes, explosions, aircraft impacts and plant induced missiles), are also major design requirements.

#### PRESSURIZED HEAVY WATER REACTOR DESIGN REQUIREMENTS

In Canada, PHWR containment designs must adhere to the CSA N290.3 standard which differs only in detail from similar ASME codes. The CANDU containment design requirements are uniquely influenced by the adoption of multi-unit stations (eight units in the case of Pickering NGS, four units per station in other plants) and on-power refuelling, where a single integrated containment system employing negative pressures, dousing water pressure suppression and a vacuum building is deployed. Elsewhere in Canada and overseas, AECL designed 600 MWe single CANDU units include similar dousing water pressure suppression systems and filtered air discharge.

The fundamental difference in design of PHWR's and LWR's, namely the physical separation of the primary coolant and moderator systems within the PHW reactors, reduces the probability of core melt in postulated severe accidents by orders of magnitude. In essence, the large heat sink provided



by the moderator system gives high assurance of fuel channel integrity, and prevents gross fuel melting to the extent that meltdown sequences are not generally considered credible [12].

The design of CANDU containment features are influenced by the structure of the Canadian Atomic Energy Control Board (AECB) regulatory requirements. To provide understanding of this influence, the AECB Siting Guide [6] is briefly described. The logic of this Guide is based on a two-tier radiation dose limit applied separately to the most exposed individual and to the population. Process failures are judged against a "single failure" dose limit (e.g. 3 rem to the thyroid of the most exposed individual). In common with LWR systems, these single failures range up to a guillotine break of the largest-diameter heat transport system piping. The limiting frequency of serious process failures (those requiring intervention by a safety system in order to prevent fuel failures) is one per three years. It must be emphasized that "single failure" in this context is a different concept than that used in LWR licensing logic. In this case it means total failure of a system with no mitigating action by other process systems; only the safety systems can be credited.

The second part of the AECB Guide requires the analysis of "dual failures", involving serious process failures with simultaneous failure of one of the safety systems (either the emergency coolant systems, or a major containment subsystem) to perform its function. This particular requirement is unique, but not necessarily more demanding than those of other national regulatory jurisdictions. The thyroid dose limit to the most exposed individual from these "dual failures" is 250 rem. Containment design is strongly influenced by the requirement to meet this dose limit.

#### LIGHT WATER REACTOR DESIGN REQUIREMENTS

The majority of nuclear power reactors in operation and under construction in the world today are either Pressurized Water Reactors (PWR) or Boiling Water Reactors (BWR).

The design requirements of PWR and BWR Containment Systems must adhere to the national codes and regulatory licensing requirements in the country of plant siting. In the United States principles have been developed for steel and concrete structures by the American Society for Mechanical Engineers (ASME) and American Concrete Institute (ACI). These code requirements for containments and their subcomponents, have historically developed over the last thirty years culminating in an ASME and a joint ACI-ASME Code, which caters to the many different combinations of steel and concrete structures which constitute the containment of operating reactors and those under construction. The ACI-ASME code combines a factored load approach with allowable stress criteria for all internal and external load consequences.

The various national codes, in addition to consideration of the ASME (steel) and ACI-ASME (concrete) codes for containment design, performance and serviceability, reflect geographical, social, political and regulatory requirements in their own environment. Thus the "Kerntechnischer Ausschuss", Swedish and Canadian codes reflect differences from those in the United States, as well as alternative requirements for external loads such as historical seismicity, siting conditions, and threats of local explosion and aircraft crashes.

The accident internal service load is historically associated with any single component failure in the generating plant having a frequency typically greater than  $10^{-7}$  events/yr which causes a maximum energy, pressure, temperature, and radioactive release. In this regard, the design basis accident for which most containment systems are conservatively designed is the largest double-ended primary pipe rupture, (predicted frequency of  $10^{-4}$ /yr), recognizing that while continued operation of the core cooling system is likely, its full credit cannot be assured in all accident conditions.

Certain combinations of extreme internal/external loads are also typically used in design of containments. Perhaps the most famous one is the combination of LOCA with some level of earthquake. In this issue, there is no general agreement worldwide. In the United States, for example, the largest postulated LOCA has been combined with the largest Safe Shutdown Earthquake (SSE). In other countries, while the combination is considered, it is not necessarily assumed that the largest LOCA and the largest earthquake are coincident. The reasoning for this position is that the reactor coolant system is specifically designed to resist earthquakes, therefore earthquakes do not cause LOCA's, but such an independent event cannot be discounted immediately following. The impact of military aircraft, blast waves and a turbine wheel rupture impact are also considered in many designs.

The following categories of loads are not normally considered in the design process but have received increasing attention in determining containment performance capability.

The first category includes those loads with a negligible frequency ( $< 10^{-7}$  per yr). Such loads would typically include meteorites, large commercial aircraft impact, and volcanic eruption.

The second category involves extreme internal accidents. Most countries typically do not combine LOCA with a secondary system failure as a design basis, although analysis of this combination is often undertaken. Rotating equipment and pipe support failure within containment are also not typically considered. Also major component rupture, such as vessel, pump, steam generator and pressurizer are not typically a design basis.

The third category involves the question of the degraded core, the so-called "Class 9" accident. There are three particular types of containment loads that might be associated with such a situation. These loads include degraded cores possibly leading to some melting of containment, steam explosion, and hydrogen generation if it results in deflagration. As a result, containment overpressurization at elevated temperatures due to postulated failure of mitigation systems is under study.

#### CHANGING EMPHASIS ON PERFORMANCE REQUIREMENTS

Table I [10] summarizes the evolution of containment performance criteria. The order listed, relates to the growing emphasis that each have received over the last forty years, culminating with containment capability for degraded core accidents.

TABLE I: EVOLUTION OF PERFORMANCE CRITERIA

- 
1. Criteria for radiological releases
  2. Criteria for direct radiation doses
  3. Protection against external missiles
  4. Consideration of degraded cores
- 

The criteria for radiological releases were the first to be developed. For all but extremely remote sites, this led to the use of containment systems with acceptable leakage related to site specific characteristics. Most often these pressure retention containments were freestanding steel or steel-lined concrete structures which, for LWR designs, could be demonstrated to leak considerably less than 1 percent of the containment volume per day during accident conditions. For multi-unit CANDU systems, where accident source terms and energy release into containment are lower, and filtered venting to control long term releases is deployed, leakage rates of less than 1 percent per hour have been adopted.

These criteria provided protection against leakage but not from direct radiation due to radioactive material within the containment after accidents. It was initially assumed that people near the site could be evacuated to minimize their exposure from material inside containment if an accident occurred.

The next criterion added was the requirement of shielding from direct radiation at all but the most remote sites. This led to the widespread use of steel-lined, reinforced or prestressed concrete structures for containment which combined low leakage capability with shielding from possible radiation.

The next important criteria to be added were for protection against external phenomena, such as missiles resulting from tornadoes. Similar criteria were developed relating to aircraft crashes at sites depending on the frequency of air traffic. These additional criteria made the use of reinforced or prestressed concrete containments or the addition of a special concrete missile shield essential.

The fourth set of criteria associated with degraded cores, or more precisely the need for them, have been under intense scrutiny and debate since the Three Mile Island Unit 2 accident on March 28, 1979. There are two major investigations addressing these issues in the United States. One is a series of programs funded by the NRC on containment integrity. In these programs the behaviour of isolation features, structural capacity of containment, leakage characteristics of mechanical and electrical penetrations and behaviour of the base mat when subjected to a core melt are being investigated [13,14,15,16]. The other major investigation is the extensive U.S. IDCOR Program [9], which is currently under discussion with the USNRC. Also, intensive studies [2], concentrating on the sequences of core meltdowns and the accompanying accident consequences, have been conducted in the Federal Republic of Germany during

the past ten years to ascertain the ultimate capability of containment systems for their operating LWR's. In Canada, important fission product distribution studies concentrating on "Lessons learnt from Three Mile Island" have resulted in containment design modifications. Also, heavy emphasis on dual failure accidents (e.g.: a large LOCA resulting in stagnation cooling conditions plus assumed coincidental containment impairment) continues in that country.

#### CONTAINMENT SYSTEMS AND COMPONENT FUNCTION

The specific details of existing containment systems depend on the project commitment dates, but their generic nature are a function of reactor type, site location, utility preference, economic considerations, number of units per station and national regulatory influence. Thus, there is considerable design diversity in existing structures, although basic concepts have not radically changed in more than twenty years.

In the 1940's, the control of public exposure following a design basis accident was provided by the use of large exclusion areas, rather than a containment structure. For example, the Clinton pile at Oak Ridge was associated with a 60,000 acre site, the Hanford production reactors with a larger area and the U.S. National Reactor Testing Station was located in the Idaho desert. The need to locate nuclear power plants nearer the consumer resulted in containment systems. Early containments were static pressure envelopes with few penetrations. These were not practical for commercial electrical generating stations. Subsequently, active containment structures, with a multiplicity of penetrations designed to close on accident signals to form a leak-tight barrier, evolved. Later, systems were introduced to suppress pressure and temperature within containment following accidents, and also mitigate fission product transport to the environment either by chemical means, controlled filtered venting or returning leakage to containment by the addition of an outer barrier and pumping circuits.

Tables II and III, respectively, list the principal containment systems which are in general use, and those which have seen less use or just studied.

Figure 1 illustrates the many variations of PWR containments in operation or committed by 1972, worldwide. The variations on the three basic systems, (i.e.: the dry pressure retention containment, the ice condenser pressure suppression and subatmospheric pressure suppression) include single versus multiple barrier, the geometry of the steel or concrete structures and the nature of allowable structural stress. The dominant system is the medium pressure, dry containment with a single pre-stressed concrete cylinder. The majority of these containments are in the United States.

Today, the tendency for PWR containments is towards two dry barriers to fission product release, with provision to filter and vent the annular separation space.

All modern BWR containments are of the pressure suppression type (wet well and dry well) in order to reduce containment volume. This is because, in a design basis accident, BWR's would blow down by far the largest volume of high energy fluids of all water reactor systems. There are three variants (General Electric Company, Mark I, II and III) of this basic system, with

TABLE II: PRINCIPAL CONTAINMENT SYSTEMS

---

Confinement:	Reactor systems enclosed in a low leakage building, filtered discharge and negative pressure.
Low Pressure:	Large diameter hemispherical dome, 35 kPa.
Medium Pressure:	Low leakage PWR steel or steel lined concrete structure (0.2 to 0.5 MPa). Variants in France and U.S.
High Pressure:	Low leakage, PWR for pressures 0.5 MPa, steel vessel (FRG, U.S. and France).
Pressure Suppression:	BWR system within compact low leakage steel or steel lined concrete structure, water and drywell energy suppression.
Ice Condenser:	A PWR energy suppression system
CANDU Pressure Suppression:	Reactor and primary systems within steel lined prestressed concrete containment at negative pressure. Pressure suppression by dousing.
CANDU Shared Containment:	Large prestressed concrete containment at negative pressure surrounding multi-units connected to vacuum building. Pressure control via dousing and filtered venting.

---

TABLE III: OTHER SYSTEMS IN USE OR STUDIED

---

Multiple Containment:	Two pressure retaining low leakage barriers
Pressure Release:	Controlled filtered venting and scrubbing
Stronger Containment:	Increased wall thickness for 0.85 MPa
Shallow Underground:	Standard containment with 10 m overburden
Deep Underground:	Containment 30 m underground, turbine at grade
Increased Volume:	Double normal volume, 0.42 MPa pressure
Compartment Venting:	Vented to high pressure structure with douse
Thinned Base Mat:	Permit Core melt to inert gravel bed.
Evacuated Containment:	Operates at 35 kPa or less.

---

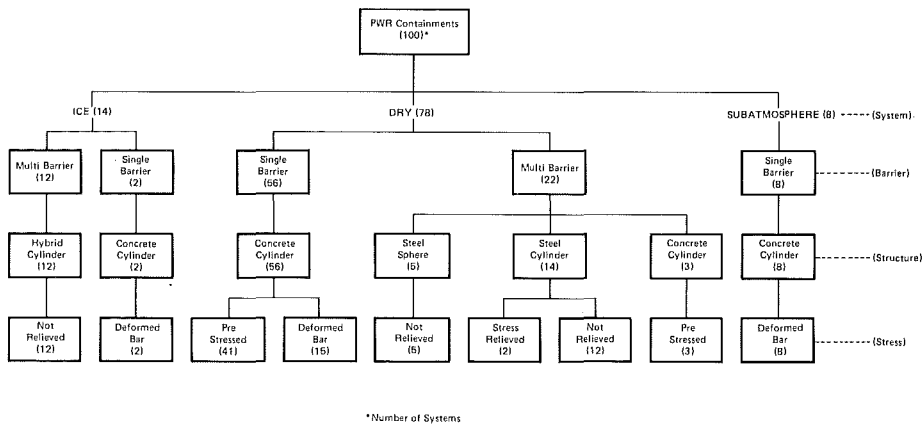


FIGURE 1  
PWR Containment Designs  
(Committed by 1972)

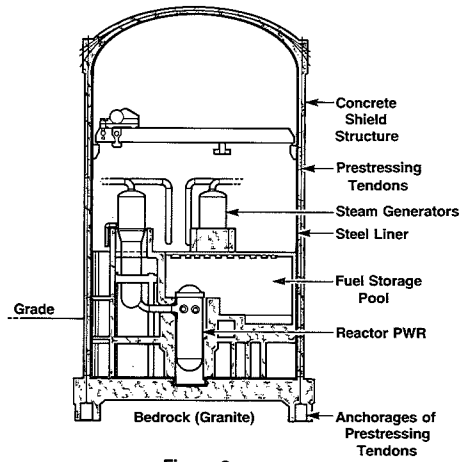
specific differences adopted in West Germany and Sweden. The Canadian PHWR System requires the lowest demand for design basis accident energy containment due to the physical separation of primary, secondary and moderator systems.

In more recent times there has been a trend towards standardization for PWR, BWR and PHWR containments with differences in detail only dependent on the country of siting. Selected designs for the United States, West Germany, Sweden and Canada follow.

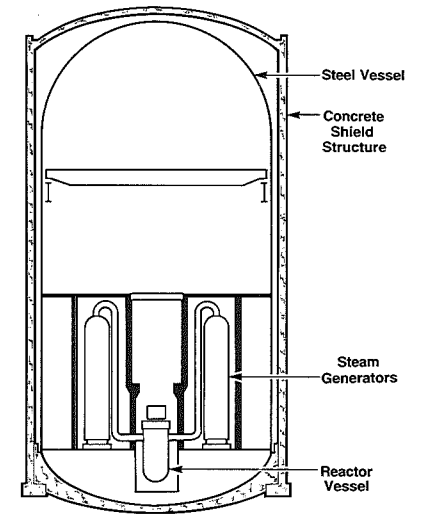
PRESSURIZED WATER REACTOR CONTAINMENTS

Figure 2 shows a low leakage, pressure retention design, consisting of a prestressed concrete cylinder with a steel liner. A vertical buttress system, together with a horizontal ring at the spring line, is used to anchor prestressing tendons. The dome and cylinder are separately prestressed. This design is widely used in the United States. More recent modifications to the design eliminates the dome ring, introduces partial buttresses in a hemispherical dome and anchors the wall and some dome tendons at the base mat. As noted in Figure 1, this type of single barrier containment is the most widely used in PWR stations operating today. Another version of this type of containment is the deformed bar-reinforced concrete cylinder and dome.

Steel containments, either cylindrical or spherical, are widely used in U.S., West Germany and Japan. In these double barrier designs a concrete biological shield, which also serves to protect against external loads, surrounds the steel containment. The cylindrical design shown schematically in Figure 3 has wide application in the United States and Japan.



**Figure 2**  
**Dry Containment: Steel Lined Prestressed Structure**



**Figure 3**  
**Dry Containment: Steel Vessel Within Concrete Shield Structure**

A common form of double barrier containment in the future is expected to be the steel sphere surrounded by a concrete shield building, as developed in West Germany, and also applied to some plants designed in the U.S. Figure 4 shows a sectional view of the German, 1300 MWe Biblis B plant [2]. The inner detached steel shell of the containment (wall thickness 29 mm) constitutes a passive pressure tight barrier. The containment sphere has a free volume of 70,000 m<sup>3</sup>. The concrete structures within the steel containment (about 15,000 m<sup>3</sup>) also reduce longterm pressurization by their heat storage capacity, and physically separate safety systems and the irradiated fuel storage pool.

The annulus between the steel containment and the outer concrete shielding (1.8 m thick), which is exhausted through a qualified filter system and stack, provides for additional deposition of radioactive products in the event of containment impairment. A subatmospheric pressure system is designed to direct flows from compartments having lower activity to those with higher activity following any accident.

Another double barrier annulus concept developed in France, includes a cylindrical concrete containment lined with steel and an outer concrete shield. Recently, France has developed a design for 1300 MWe plants which does not require the steel liner.

Two types of pressure control containments have been developed for PWR's, the subatmosphere containment (- 5.0 psig operating pressure), and the ice condenser.

A typical ice condenser containment is shown in Figure 5. Steam and air resulting from an accident is forced by the pressure from the lower compartment through the ice beds where the steam is condensed. The design pressure for this containment is one bar whereas a PWR dry containment for the same rating would range from three to five bar. However, current economic considerations have limited this design to 1000 MWe units and larger.

#### BOILING WATER REACTOR CONTAINMENTS

All modern BWR containments are of the pressure suppression type, incorporating drywells and wetwells as pressure suppression chambers. Following a LOCA, the steam/water flow causes a rapid increase of pressure and temperature in the drywell. The pressure difference between the dry and wet wells forces the contained water out of the blowdown pipes and high pressure steam then flows to the wetwell pool. Steam condensation occurs and non-condensable gases collect in the wetwell airspace or compression chamber. Given the relatively small containment volume of BWR's compared with other reactor systems, this condensation process is the key element in limiting maximum pressures to 3 bar or less.

During the last thirty years there have been progressive changes to the shape, geometry, size and location of the various suppression chambers relative to the reactor core within containment. The latest Mark III General Electric design is shown in Figure 6. The quenching pool has been moved to the side whereas in the previous Mark II design it was underneath



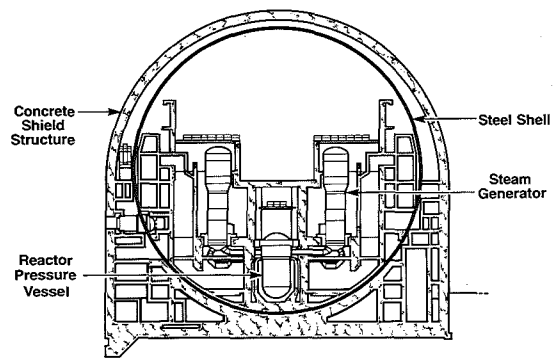


Figure 4  
 Dry Containment: Spherical Steel Vessel  
 Within Concrete Shield Structure

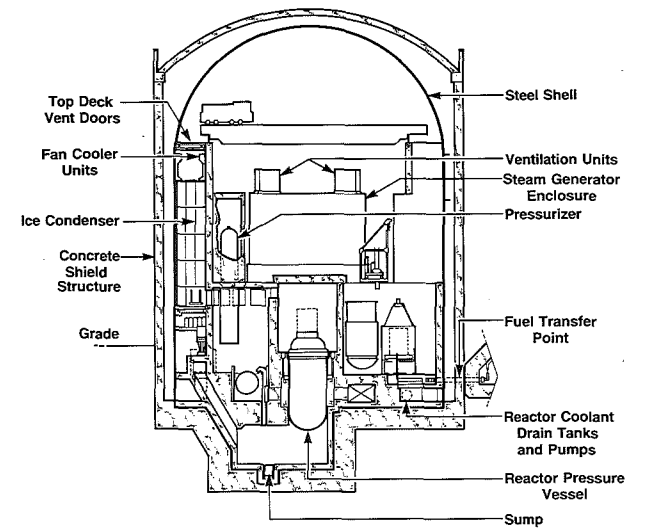


Figure 5  
 Ice Condenser: Steel Shell Within  
 Concrete Shield Structure

the reactor vessel. This made it possible to reduce the elevation of the reactor vessel, and created the best compromise with regard to the height of the vessel, its accessibility and construction of containment. The design shown in Figure 6 uses a steel containment within a concrete shield. However, because of localized dynamic loading from the wetwell during LOCA and Safety Relief Valve discharge, the steel containment was replaced by a hybrid shell in later designs. This hybrid employs a concrete base mat, a concrete shell in the pool region with a steel containment shell above the pool. In future applications of U.S. built BWR's, it is anticipated that a full height reinforced concrete shell would be the preferred arrangement, which is also the practice in other countries.

Modern large BWR's typified by the U.S. General Electric Mark III design, the Gundremmingen KRB-2 1300 MWe units in West Germany and the Swedish BWR-75 1000 MWe units, have steel liners and cylindrical pre-stressed concrete containment structures. The German and Swedish designs, however, have retained features of the Mark II concept where the drywell is both under and over the reactor vessel. The overall objective of these systems is to maintain low design pressure with relatively small containment volumes, and to provide for an emergency condenser during plant transients and accidents.

In West Germany, earlier BWR containments were a spherical steel shell. The current KRB-2 design is changed as shown in Figure 7. It consists of a cylindrical prestressed concrete structure with an embedded steel liner which is protected by additional concrete. The drywell space surrounds the reactor vessel and heat transport piping extending to the second isolation valve. Many large diameter vent pipes from the drywell extending into the pool provide the path to condense LOCA induced steam/water mixtures. A separate pressure relief system provides for coolant pressure control. The containment is protected from large wetwell overpressures relative to that in the drywell during LOCA, by vacuum breaker swing check valves which allow pressure equalization in the two chambers. The suppression system design pressure is typically 4 bar compared with maximum expected LOCA pressures of less than 3 bar. The wall of the reactor building serves as a secondary containment and the annular space between it and containment is subatmospheric to prevent leakage to the environment. German regulatory authorities require the reactor building walls to withstand an external blast wave of 0.45 bar, a site dependent earthquake and the crash impact of military aircraft. To provide further assurance of containment integrity from external events the reactor buildings are not rigidly joined, apart from the common foundation.

Figure 8 shows a sectional view of the Swedish BWR 75 containment [4] which is a reinforced, partly prestressed concrete cylinder provided with an embedded liner of carbon steel. The drywell, wetwell and blowdown pipes are similarly arranged to the German KRB design, and the entire containment is totally steel lined. A different labyrinth arrangement exists between the upper drywell and wetwell than in the West German design. The containment and reactor building basement structure is different, but each design has no structural tie (other than expansion joints) between containment and adjacent buildings. The steel liner embedment of between 20 to 30 cms within the concrete is deeper than the KRB containment. The upper drywell contains primary and secondary reactor process systems, including main steam, feed water and containment cooling systems. The

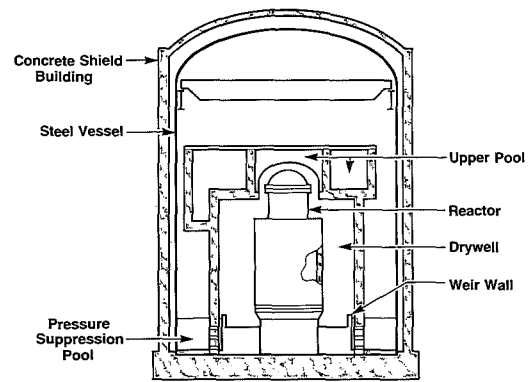


Figure 6  
 Pressure Suppression Containment: Steel Vessel  
 Within Concrete Shield Building  
 (BWR Mark III Containment)

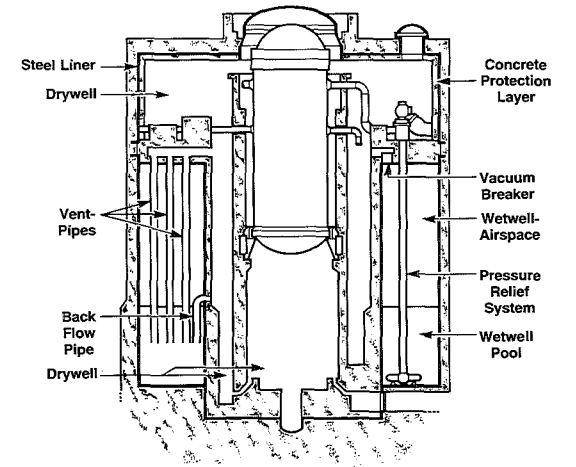


Figure 7  
 KRB-2 PRESSURE SUPPRESSION CONTAINMENT  
 (BWR CONCEPT)

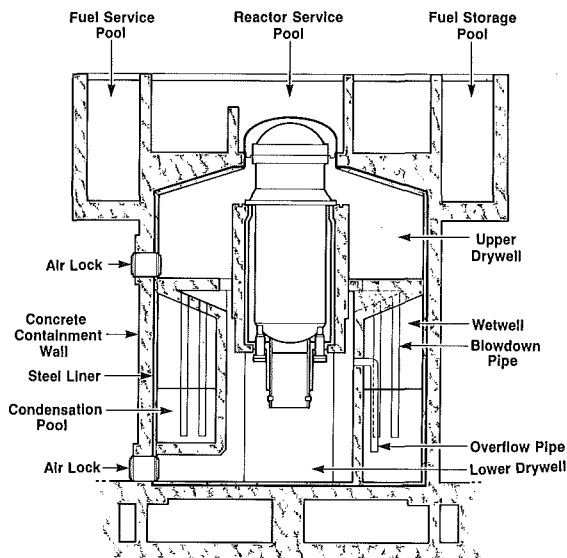


Figure 8  
Swedish BWR 75 Containment: Steel Lined  
Concrete Shield Structure

lower drywell contains systems such as the control rod drives and recirculation pump motors. The wetwell is an annular enclosure. Blow-out panels in the lower part of the reactor concrete shield provide a path to the lower drywell in the event of a LOCA within the reactor compartment.

#### PRESSURIZED HEAVY WATER REACTOR CONTAINMENTS

This section concentrates on the CANDU containment system associated with the multi-unit stations in Canada [3]. The single 600 MWe units designed by AECL, use similar negative pressure containment (NPC) systems with the omission of a vacuum building.

The NPC1 design concept, (where reactor units are isolated from one another), is used in the eight-unit Pickering NGS station, which came into service in the period 1971-1985. The second major type (NPC2), was used in the four-unit Bruce NGS A station, which came into service in 1977-1979, and in all subsequent four unit stations.

The prime difference between the NPC1 and NPC2 concepts is that the latter locates most of the supporting process equipment outside the primary containment envelope, although it follows that some equipment must be in secondary confinement areas. Another feature of NPC2 is that the four reactor vaults are interconnected during normal operation due to the choice of common on-power fuelling systems for all units.

The main reason for adoption of the NPC containment concept was increased effectiveness required to satisfy concerns for relative close population siting which existed at the time of the Pickering NGS A project commitment. The NPC2 design was developed primarily to improve maintenance access to process equipment during operation.

The basic operating principle of negative pressure containment is to maintain a negative pressure such that air leakage through the structure is inward. Any discharge required to maintain this negative pressure differential is along defined pathways which can be filtered, treated and monitored to control releases to the environment.

Figure 9 shows the NPC2 containment envelope which is normally at sub-atmospheric pressure. In the event of a LOCA, various systems act to provide for short and long term pressure and effluent control. The short term period extends from the LOCA, when very fast pressure transients are experienced with possible "puff" releases of radioactivity, to the re-establishment of sub-atmospheric pressure within containment. The long term period is associated with the initial activation of the Emergency Filtered Air Discharge System (EFADS) until cleanup operations are complete. EFADS is manually activated when containment pressure approaches atmospheric several days after the event. Figure 10 lists the systems which collectively perform the containment function in the two time frames.

The principles of pressure control used in the CANDU NPC2 containment in the short term are "pressure relief" followed by "steam suppression" as depicted in Figure 11. Following LOCA the reactor vaults and fuelling duct connecting the multi-unit station are pressurized by the resulting high enthalpy fluid flashing to steam. The extent of pressure rise is limited by the very large volume of the containment envelope. The increase in pressure, acting across the Pressure Relief Valve (PRV) pistons, automatically opens the valves and releases the air-steam mixture into the vacuum building (VB).

The steam suppression function is carried out by a dousing system located in the vacuum building. When the PRV's open and VB pressure rises, water is forced over a weir structure and into spray headers located under the dousing tank. The spray water falls through the steam-air mixture, reduces pressure, and provides for soluble fission product retention.

The principle of effluent control used in the short term is isolation by physical barriers. Containment operates at 98 kPa (-.5 psig) and the vacuum building at 7 kPa (-13.7 psig). Typical design pressures for containment are 170-200 kPa (10-14 psig) and 50 kPa (-7 psig) for the V.B.

#### CONTAINMENT CAPABILITY STUDIES

Over many years, there have been numerous containment studies [2,3,11,13] performed with the aim of establishing design parameters, proving that regulatory limits for design basis events are met and identifying ultimate capability to withstand severe postulated accidents. Given, that current research to provide "best estimate" source terms and fission product transport, is also important to demonstrating

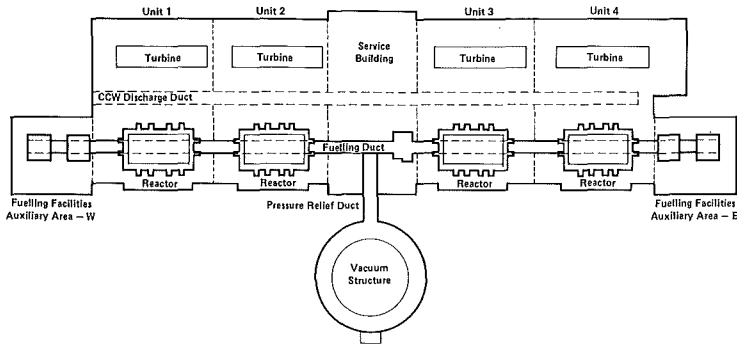


**Figure 9**  
Multi-Unit CANDU containment

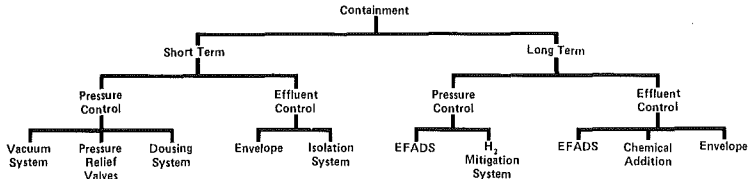


**Figure 10**  
CANDU Containment Systems

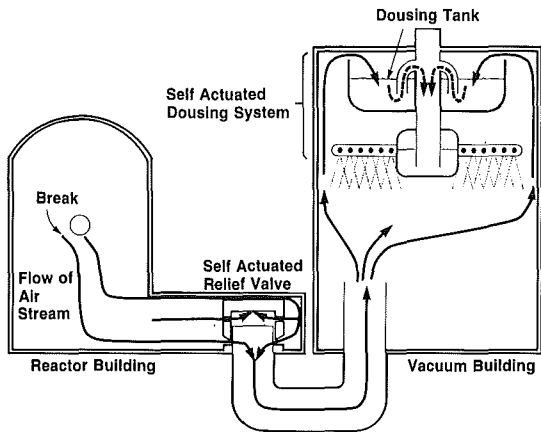


**Figure 11**  
Operation - Negative Pressure Containment

containment capability, there is no doubt that high emphasis of nuclear reactor safety R&D today, is on containment systems.

This section summarizes this containment R&D, and provides a few examples of the many studies performed in West Germany, Sweden, USA and Canada to demonstrate containment capability for LWR and PHWR nuclear stations. Present studies are largely associated with very low frequency ( $\leq 10^{-7}$  events per year), high consequence events, since it is generally recognized that all containment systems are adequately designed for likely accidents.

#### Containment Research

Tables IV and V provide a synopsis of typical integral containment tests for PWR's and BWR's to verify containment analysis codes, and assure adequate designs. Many experiments have been performed elsewhere, notably in Japan.

TABLE IV: INTEGRAL PWR CONTAINMENT EXPERIMENTS

Year	Facility	Measurement Purpose	Specific Information
1965	CSE, USA	Vessel blowdown	Fission product transport and removal.
1970	CVTR, INEL, USA	Peak pressure and temperature effects	Axial wall temperature distribution, heat transfer coefficients.
1975	Battelle, Frankfurt	Pressure and temperature measurements during blowdown	Pressure waves, wall temperatures, H/T coefficients, jet impingement and hydrogen distribution.
1981	Lucas Heights	Pressure/temperature response, small steel containment	Compartment pressure/temperature and heat transfer.
1982	HDR, Karlstein	Blowdown for different break sizes/locations	Wall temperatures, steam-air concentrations, jet impingement, strains, accelerations.
1983-6	Sandia Nat. Labs., N.M.	Failure conditions/modes beyond DBA	Structural failure mode, leakage paths, penetrations behaviour, base mat melt, bypass, margins.

In addition to these integral tests, there have also been numerous separate effects tests performed in all countries (often involving international collaboration eg: Marviken) to understand jet impingement loads, vent flows and condensation heat transfer. Experiments [17,18] to determine the effects of external missiles, (including large steel piping and segments of a turbine rotor), impacting on containment have been performed in the U.S. and elsewhere.

In Canada, as elsewhere, there have been a number of on-site containment tests during the period 1970-1983 conducted by AECL and Ontario Hydro to determine leakage rates and the thermal utilization of dousing flow in the Vacuum Buildings, and/or containment. In addition separate effects tests of all containments have been performed over the period 1960 to 1984 to understand transient compressible flow in interconnected volumes, jet loading, tee-junction losses, vessel-pipe fluid mixing and liquid-steam phase separation at tee junctions.

TABLE V: BWR CONTAINMENT EXPERIMENTS

Year	Facility	Measurement, Purpose
1960's	Humboldt Bay Bodega Bay	Drywell, Wetwell Pressure transients
1972/73	Marviken, Sweden	Full scale containment tests
1972,75	GKM 1, KKB	Vent Pipe Loads, Full scale
1975, 77	Karlstein Large Tank and concrete cells	Multivent pipe tests
1976/77	GKM 2S	Vent pipe and pool wall loads, condensation, transient and static tests
1978/80	Studsvik, Sweden	Pool swell in different geometries
1984	GKSS	Vent clearing, pool swell and fall back.
1983/86	Sandia Nat. Labs., N.M.	Large scale, Mk I, II, III overpressure tests, failure mode/ timing, and design margins.

The majority of current containment research is centred on the ultimate capability of LWR systems when subjected to severe accidents in the Class 9 category as typified by the IDCOR program. The Industry Degraded Core Rulemaking (IDCOR) Program in the U.S. is supported by sixty-two nuclear utilities, architect-engineers, LWR vendors in the United States, and by Japan and Sweden. The IDCOR mission was to develop a comprehensive, technically sound position on the issues related to potential severe accidents in light water power reactors.



IDCOR resulted from the USNRC's evaluation of the TMI-2 degraded core condition which was more severe than that previously assumed in a design basis accident. In October 1980, the NRC initiated a "long-term rulemaking to consider to what extent, if any, nuclear power plants should be designed to deal effectively with degraded core and core melt accidents". The NRC's rulemaking proposed to address the objectives and content of a degraded core-related regulation, the related design and operational improvements under consideration, their effects on other safety considerations, and the costs and benefits of design and operational improvements.

Subsequently, the NRC issued a proposed Commission Policy Statement [19], to implement the October 2, 1980, "Advance Notice of Rulemaking", and identify the severe accident decision process on specific standard plant designs and on other classes of existing plants which may or may not include rulemaking.

IDCOR identified key issues and phenomena; developed analytical methods; analyzed the severe accident behaviour of four representative plants; and extended the results as generically as possible. The methods used in the study were "best-estimate", rather than conservative engineering approaches in technical analysis, usually characteristic of licensing submissions. Existing methods and experimental data were thoroughly reviewed and new programs were undertaken where confident support of prior positions was uncertain. In general, IDCOR has demonstrated that consequences of dominant severe accident sequences are significantly less than previously anticipated. Most accident sequences require long times to progress, allowing time to achieve safe stable states.

Table VI lists the reactor safety phenomena considered in reaching these conclusions.

---

TABLE VI SEVERE ACCIDENT PHENOMENA ADDRESSED  
BY IDCOR TO ESTABLISH ULTIMATE  
CONTAINMENT CAPABILITY

---

1. Steam explosions causing pressure pulses, liquid slugs or missiles
  2. Overpressure due to rapid steam generation
  3. Overpressure due to hydrogen generation combustion
  4. Containment by-pass via interface systems to environment
  5. Overpressure due to noncondensable gases
  6. Melt through of containment base mat
  7. Overpressure due to loss of containment heat removal
  8. Containment failure modes
  9. Radionuclide release and transport
-

While studies continue, the most important results to date, are: containment overpressure capability is several times the pressure associated with the design basis accident; limited impairments of the containment envelope would likely occur on failure, thus stabilizing or gradually reducing pressures which would limit the rate of radioactive release; hydrogen related concerns can be mitigated or do not exist; and early failures of containment due to all causes are most unlikely, thus permitting sufficient time for interdictory actions.

Corium and Fissium experiments [20,21] are also on-going in the U.S., West Germany and Sweden. Concrete-Corium interaction tests to determine the extent of base-mat erosion are continuing in West Germany and U.S.A. Current experiments at Sandia National Laboratories [13,14,15,16] sponsored by USNRC, are addressing the issue of "when, where and how" will various steel and concrete containments fail and the resultant extent of radioactive release. Large scale models have or are being constructed to identify containment safety margins, and the integrity of containment pipe and electrical penetration assemblies when subject to overpressure loads. This large program is scheduled for completion by the end of 1986. In West Germany [2], studies suggest that the weak point of their PWR containment is associated with the sealing box which is part of the main airlock, in the event of overpressure accompanying a Class 9 accident. It is considered that the failure mode will be "leak instead of break", which will either result in a maximum stabilized containment pressure below ultimate capability, or reducing pressure. In other words, containment pressure relief will occur rather than gross containment failure. Experiments to prove this engineering assessment are now being planned [2].

Another area of research of importance to all nuclear power systems, and prompted by TMI-2, is that of ensuring control of hydrogen generation in severe accidents. This subject is the focus of attention of a current IAEA working group who are reviewing the issues identified in Table VII, using information from the major investigations already carried out by EPRI, Sandia Labs and WNRE.

TABLE VII: IAEA REVIEW OF HYDROGEN STUDIES

- 
1. Hydrogen distribution in containment
  2. Lower flammability limits
  3. Combustion limits of H<sub>2</sub>-air-steam-CO<sub>2</sub> mixtures
  4. Available hydrogen and oxygen detectors
  5. Pre-inerting as a mitigation scheme
  6. Effectiveness of various ignition sources
  7. Controlled burning and extinguishing systems
  8. Fog/spray suppression
  9. Minimum equipment to survive degraded-core accident.
-

These studies are confirming that hydrogen re-combiners or igniters for controlled burning, will prevent large containment overpressures. In many containments, the predicted volumetric concentration of hydrogen is far too low for combustion to occur.

#### Containment Response Analyses

The objectives of containment analysis are to establish design parameters and to verify that regulatory dose limits are not exceeded following any process system failure which leads to a release of radioactive material within the containment envelope. Design and regulatory processes require that containment response be analysed for a large number and variety of postulated system pipe failures ranging from a small leak up to a guillotine failure of the largest piping in the heat transport system.

##### A. PHWR Analyses

For CANDU reactors, accidents are characterized according to the postulated LOCA break discharge rate, since this parameter has the dominant effect on subsequent containment response. A coolant channel end-fitting failure is used to bound the radiological consequences of small breaks in the heat transport system piping. The accident sequence postulated is an instantaneous maximum opening break, with the resultant ejection of all 13 fuel bundles from the channel. Severance of an end fitting results in an initial coolant discharge rate up to 200 kg/s. The ejected fuel bundles will likely be damaged on impact with the reactor vault, and will release fission products into containment at a rate dependent on the extent of fuel cooling.

The containment pressure due to small breaks is strongly affected by containment heat sinks and, in particular, by the number of vault air cooling units assumed operational at the time of the break. Figure 12 shows containment pressure transients for various initial break discharge rates. For small breaks above 80 kg/s, the duration of the overpressure period is determined by the time for the pressure relief manifold to pressurize to the setpoint of the pressure relief valves (PRV's). Below this discharge rate, energy removal due to air coolers and condensation on cold surfaces is sufficient to offset the energy addition from the break, with the result that the containment pressure can remain slightly above atmospheric without initiating PRV opening. The containment overpressure period will then last until either the break energy discharge rate decreases sufficiently that the heat sinks are able to reduce the pressure to subatmospheric by steam condensation, or the operator manually intervenes by switching the PRV's to control mode.

In spite of the potentially extended containment overpressure period for certain small breaks, releases into the environment are very small since fuel damage is limited to a fraction of the core inventory.

Certain large breaks in the heat transport system, which could result in coolant stagnation within fuel channels, are capable of producing extensive fuel failures throughout the core. In addition, the initial pressure excursion presents a challenge to containment integrity. Figure 13 shows the estimated pressure transients in the accident vault and

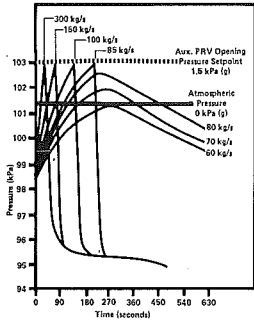


Figure 12  
Negative Pressure Containment Response  
(Small Break)

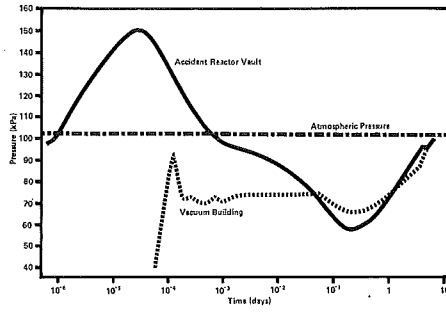


Figure 13  
Negative Pressure Containment Response  
(Large Break)

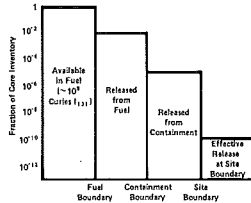


Figure 14  
Typical Attenuation CANDU  
(Large Break)

vacuum building following a postulated guillotine break in a pump suction line.

In this event, a peak pressure of 150 kPa occurs in the accident vault at less than 3 seconds. This is substantially below the containment design pressure. One minute after the break, the accident reactor vault becomes subatmospheric. From this time onward, the heat removal rate exceeds the steaming rate at the break. The containment atmosphere continues to cool down and depressurize, until in the long term it becomes repressurized by air in-leakage, instrument air, and any gas evolution within the containment envelope.

Even with the fuel cladding damaged, the fission product release from the fuel is initially limited to a gradual escape of the "free" inventory of volatiles. Only when the fuel heats up to high temperatures (well in excess of 1000°C) can a significant amount of volatiles start escaping from the "bound" inventory. Thus, the concentration of activity in containment takes some time to build up to appreciable levels. With the effective

pressure suppression provided by the NPC system, the amount of activity escaping to the environment by pressure-driven leakage is correspondingly small.

The bulk of activity enters the containment during the subatmospheric holdup period. These fission products then experience decay and undergo numerous interactions before a small portion is gradually released by (EFAD) filtered venting. With the exception of noble gases, the fission products become trapped in water within containment either by dissolution in liquid droplets or by becoming nucleation centers for liquid aerosols. Eventually, the airborne activity consists of only the noble gases and a small amount of volatile chemical compounds (e.g. organic iodides) in equilibrium with the solution on the floor.

Figure 14 illustrates the mitigating processes of CANDU containment systems in terms of  $I^{131}$  attenuation resulting from the largest LOCA. Assuming the most adverse weather conditions, the "effective release" is an equivalent amount of  $I^{131}$  that an individual could receive if present at the exclusion boundary for several months. The total attenuation for this severe accident is at least ten orders of magnitude, and the resultant dose, if individuals remained indefinitely at the site boundary, is within regulatory requirements.

In Canada, the current emphasis is on studies to delay or reduce the extent of containment venting even though regulatory limits are met. Regulatory requirements demand that dual failure dose limits not be exceeded for LOCA's coincident with various containment impairments including failure of isolation dampers, simultaneous deflation of four airlock seals on a double door system, failure of pressure relief valves and loss of reactor vault air cooling units.

#### B. PWR Analyses

As an example, the containment response analysis performed in West Germany [2] to establish DBA parameters, and capability in severely degraded core accidents for the standard 1300 MWe PWR is next described. While assumptions required by the German Advisory Committee on Reactor Safeguards (RSK) are not the same as those in the United States, the analysis results are generally typical of most PWR's. Also, while the extent and timing of BWR severe accidents is different from PWR's, the questions on ultimate containment capability are not dissimilar. The German containment design basis accident (DBA) is a double ended break in a main coolant pipe. For containment design purposes, RSK also requires a number of conservative assumptions which include:

- (a) Decay heat according to ANS Standard plus 20 percent.
- (b) Maximum LOCA pressure assuming a 2 percent decrease in containment volume, and a 2 percent increase in primary and secondary circuit volumes (blowdown mass and energy include one secondary steam generator content).
- (c) A 15 percent safety margin applied to calculated maximum LOCA pressure, and

- (d) The steel containment shell to be designed for maximum containment atmospheric temperature (145°C), rather than its expected temperature (60°C).

Figure 15 shows that the "best estimate" of the maximum LOCA pressure will be 4.2 bar. Also shown, are the design calculation results assuming (a) (b) and (d) above, for the pressure transients when the additional energy from the assumed secondary break is either excluded or included. The containment design pressure of 6.3 bar includes the additional assumption (c). The containment test pressure of 7.74 bar, prior to reactor criticality, is set by the difference in yield at the testing and LOCA temperatures. Thus, there is a substantial margin (up to 84 percent) between the expected LOCA pressure and the demonstrated test capability.

In the event of a core melt-down, there would be a substantial release of fission products and steam/water to containment. The extent of release to the environment is highly dependent on the containment isolation time, the extent and nature of any containment leakage, and the transport and driving force paths from the annular space between containment and the reactor building. A very important mitigating process in this regard, is the finding [22] that all radioactive substances, with the exception of the noble gases and airborne gaseous iodine, are bound to aerosol particles and subject to highly effective removal mechanisms. These removal mechanisms, involving plate-out and absorption on containment structures, reduce aerosol mass concentrations by five to six orders of magnitude within five days. Containment overpressure failure at the weakest point is not expected during this period.

Figure 16 shows the predicted pressure variation in containment for a core melt-down sequence. The maximum transient pressure during blowdown of 5.3 bar is reached at 17 seconds after LOCA. The transient LOCA pressure which is relieved by the containment volume and condensation reduces to 2.5 bar during the next  $10^3$  s. The core melt-down process due to the onset of evaporation of the moderator water and assumed complete absence of emergency forced cooling, commences at about 20 minutes.

Core degradation then proceeds accompanied by hydrogen production due to steam/zirconium reactions. Shortly after one hour, the core structure is predicted to fail allowing significant amounts of core material to drop into the water contained in the lower plenum of the reactor vessel, with the resultant violent evolution of steam.

Subsequently, at about 1.9 h after blowdown, reactor vessel failure is predicted to occur and core melt interaction with the concrete basemat begins. Given that 80 tonnes of metallic melt and 130 tonnes of oxide melt at a temperature of 2400°C are assumed available, it is predicted that the concrete shielding surrounding the reactor vessel will be eroded within 7 h causing the containment sump water to contact the melt. Violent evaporation of the sump water in the isolated containment, subsequently results in its pressurization to design pressure after three days and to 9 bar after five days, as shown in Figure 16. This sequence of events raises the question of ultimate containment overpressure capability, the mode and extent of containment failure, and subsequent extent of radioactive release from the annulus between containment and the reactor building, via filtration to the environment. These questions also highlight the "defense in depth" provided in LWR stations for public protection, and the extended time available for any necessary emergency evacuation.

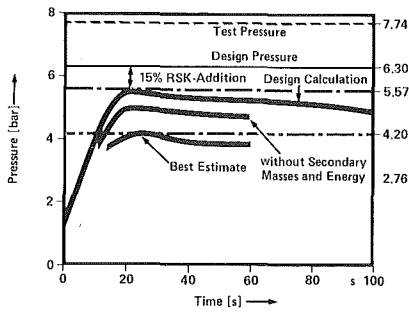


**Figure 15**  
DBA Pressure Transients For  
Standard 1300 MWE German PWR

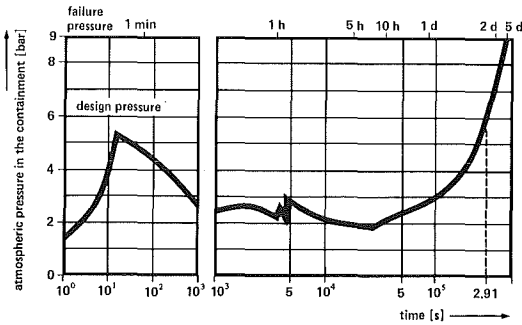


**Figure 16**  
German PWR Containment in Core Melt  
Accompanied by Failure of the Sump Cooling System

Recent studies in West Germany [2] and those of IDCOR [9] in the United States are showing that containment overpressure capability before failure is up to 2-3 times design pressure for the undisturbed steel shell. As an example, West German experts predict overpressure failure of the 1300 MWe standard PWR containment to be above 14 bar in this case, and that the mode of failure will be "leak instead of break".

It is considered that containment overpressure will result in a leak at weak points, such as in main airlock components or at electrical/pipe penetrations, and will either permit a stabilization or reduction of containment pressures. The net result is the maintenance of major containment integrity, and only gradual activity release (likely after filtration), to the environment. Also, recent West German studies and those in the United States have demonstrated that previously assessed source terms are too high by several orders of magnitude.

#### SUMMARY

This paper has discussed the functional requirements, the evolution of designs and the influence of national regulatory requirements on containments for PWR, BWR and PHWR reactors. Particular containment designs are not only a function of national siting requirements in the United States, West Germany, Sweden and Canada, but also relate to specific reactor system performance in perceived accident conditions, and the number of reactors constituting the generating station. In all cases, it is evident that the various containment systems easily meet their design basis accidents. Since the TMI-2 accident all jurisdictions have examined the need for design changes to meet post-accident scenarios.

In Canada, increasing attention has been placed on large stagnation LOCA's with assumed coincidental containment impairments. In this regard, methods to delay or reduce the extent of atmospheric venting of containment to relieve pressure are under active study, even though regulatory limits are met.

In West Germany, the United States and Sweden, emphasis is on the ultimate capability of PWR and BWR containments to withstand overpressures and evaluate environmental releases for class 9 core melt accidents, which are beyond or bordering on the range of credible frequency. Current information from the U.S. based IDCOR study and the independent West German and Swedish research work, indicate that LWR containment designs are capable of withstanding overpressures up to three and possibly four times their design pressure. In the event of containment failure, it is predicted that radioactive release will likely result from gradual leakage from weak points (rather than a gross containment break) to the reactor building, resulting in a slow and delayed discharge to the environment. Experiments and scaled tests of containments have been performed or are currently underway in many countries to determine ultimate containment ability and failure modes. These tests, together with allied fission product source term and transport tests, and comprehensive experiments on hydrogen generation and mitigation, are an important area of reactor safety research today.

In addition, research in the U.S. is directed at decoupling LOCA plus SSE as a design basis, and reducing postulated high energy system pipe breaks and loading phenomena.

If containment failure were to occur, in either the CANDU, PWR or BWR reactor systems, it is predicted to do so many days following the most severe postulated accident, permitting adequate time for assurance of public safety.

#### ACKNOWLEDGMENTS

The authors wish to thank the following for their helpful suggestions and information: W.A. von Rieseemann, Sandia National Laboratories, U.S., Dr. Byink, KWU, Erlangen, West Germany and R.E. Pauls, F.K. King, J. Skears, C. Gordon of Ontario Hydro, Canada.

#### REFERENCES

1. J.D. Stevenson, "Current Status of Containment Design", Proc., of the Workshop on Containment Integrity, NUREG/CP-0033, SAND 82-1659, October 1982.
2. W. Braun, K. Hassmann, H.H. Hennies, J.P. Hosemann. "The Reactor Containment of German Pressurized Water Reactors of Standard Design", Int. Conf. on Containment Design, Toronto, June 1984.
3. C. Blahnik, D.W. McKean, D.A. Meneley, J. Skears, N. Yousef. "Principles of Operation of CANDU Multi-Unit Containment Systems", Int. Conf. on Containment Design, Toronto, June 1984.
4. "Summary Description of the BWR Reactor Containment" BWR 300, 4/BU-A, ASEA-ATOM, August 1981.



5. J.D. Stevenson, "Containment Structures for Pressurized Water Reactor Systems: Past, Present and Future State of the Art". Proc. 2nd Int. Conf. on Structural Mechs. in Reactor Tech., Berlin, August 1973.
6. D.G. Hurst, F.C. Boyd, "Reactor Licensing and Safety Requirements" Proc. CNA 12th Annual Conference, Ottawa, June 1972.
7. RSK-Leitlinien fuer Druckwasserreaktoren, 3rd Ed., October 1981. Also, RSK-Leitlinien fuer Siedewasserreaktoren, E9.80.
8. Code of Federal Regulations, 10CFR 0.735-1, App A Criterion 16, 50 and 51, Revised January 1984.
9. A.R. Buhl, M.H. Fontana, "IDCOR - The Technical Foundation and Process for Severe Accident Decisions", Int. Conf. on Containment Design, Toronto, June 1984.
10. R.P. Schmitz, "Nuclear Reactor Containment" Int. Conf. on Containment Design, Toronto, June 1984.
11. Proceedings of the Second Workshop on Containment Integrity, Arlington, VA, June 1984 (to be published).
12. R.A. Brown, C. Blahnik, A.P. Muzumdar, "Degraded Cooling in a CANDU", Second Int. Topical Meeting on Nuclear Reactor Thermal Hydraulics, Santa Barbara, January 1983.
13. T.E. Blejwas, et al., "Background Study and Preliminary Plans for a Program on the Safety Margins of Containments", NUREG/CR-2549, SAND 82-0324, May 1982.
14. T.E. Blejwas, W.A. von Rieseemann and J.F. Costello, "The NRC Containment Integrity Program", Paper No. J1/1, 7th SMIRT Conf., August 1983.
15. W. Sebrell, "The Potential for Containment Leak Paths Through Electrical Penetration Assemblies Under Severe Accident Conditions", NUREG/CR-3234, SAND 83-0538, July 1983.
16. C.V. Subramanien, "Integrity of Containment Penetrations Under Severe Accident Conditions", See Ref. 11.
17. A.E. Stephenson, "Full Scale Tornado Missile Impact Tests", EPRI NP-440, July 1977.
18. R.L. Woodfin, "Full Scale Turbine Missile Concrete Impact Tests", EPRI NP-2745, January 1983.
19. "Proposed Commission Policy Statement on Severe Accidents and Related Views on Nuclear Reactor Regulation", SECY-82-1B, November 1982, 48FR16014, April 1983.
20. Albrecht, Wild, "Review of the Main Results of the SASCHA Program On Fission Product Release Under Core Melting Conditions". ANS Topical Meeting, July 1984, Utah, USA.

21. H. Rininsland, "BETA (Core-Concrete Interaction) and DEMONA (Demonstration of NAUA)". Proc Int Conf. LWR Severe Accident Evaluation, Cambridge Massachusetts, September 1983.
22. K. Hassmann, P. Hosemann, "Consequences of Degraded Core Accidents" NUC Eng and Design, Vol 81, 1984.

PROBABILISTIC RISK ASSESSMENT  
MERITS AND LIMITATIONS

H. W. Lewis

University of California, Department of Physics  
Santa Barbara, California 93106, U.S.A.

ABSTRACT

The merits and limitations of probabilistic risk assessment are discussed, with a special effort to distinguish between those limitations which are intrinsic to the method as practiced and those which are not. Emphasis is on the limitations, even though probabilistic risk assessment is the most rational and effective way to study the safety of reactors.

INTRODUCTION

Probabilistic risk assessment (PRA) is regarded with suspicion in some quarters, both for reasons which will emerge in the discussion of its limitations, and for less defensible reasons. There is a great deal of resistance to the use of probability, especially in the face of the great uncertainties that are inevitable accompaniments of current assessments. Licensing decisions, in particular, must be unequivocal, and there are great problems in laying a probabilistic base for binary decision-making. The uncertainties are of course also present in any other form of analysis -- they are not invented by PRA -- but there is no way to conceal them in a properly performed PRA, as there is in a deterministic process. Though much of what follows will focus on limitations, PRA (not necessarily as currently practiced) is the rational way to make safety assessments.

It is necessary to make one disclaimer. Though I have had, and now have, connections with the regulatory agencies in my country, nothing that follows reflects anything but my own personal views, as will be quite clear from the context. I wish it were not so.

PROBABILITY

The concept of probability requires a few words, particularly when one is dealing with extremely low probabilities of rare events -- often events that have never occurred, and may never occur. Such a probability can not be defined as the limit of a frequency, but is instead a measure of the odds of a fair bet on

whether or not the event will occur. These odds are inevitably derived from a combination of expert opinion and of operating experience, and are bound to change as our experience and our wisdom increase. They are also themselves uncertain, and it is perfectly reasonable to speak of a probability of a probability, as a measure of the uncertainty in estimating the odds of a fair bet. Bookmakers have this problem in everyday life, and seem not to be bothered by it as much as nuclear engineers. Such probabilities and probability distributions must be kept current, and must be responsive to the accumulation of operating experience. On the other hand, it is important to resist the temptation to overstate the predictive power of operating experience -- the fact that something has happened after 1000 hours of operation does not mean that it will happen every hundred hours. The fact that something that was estimated as having a very low probability actually happened does not necessarily mean that the original probability was wrong. A disciplined approach to the estimation of probability, and to the uncertainty in the estimated probability is essential to the proper use of PRA. In particular, it is *wrong* to describe the probability of (say) a core melt by a single number, without any reference to the uncertainty in that number. Indeed, it is not helpful to describe the uncertainty by a single number, though that is almost universal practice. The point of this section is that the concept of probability should be treated with respect.

#### MERITS

The merits of PRA are so clear that they hardly need mentioning. In the first place, performance of a PRA on a plant requires at the beginning that the structure of the plant be fully understood, along with the interactions, both intentional and inadvertent, among its constituent parts. The various possible accident sequences must be written down explicitly and understood, and finally reasonable probabilities of failure must be assigned to the elements of each accident chain. All of this requires such depth of analysis that it is almost inevitable that a greater understanding of the vulnerabilities of the plant is obtained in a disciplined and rational way. More often than not, the process itself leads to changes in design or procedures whose effect is to reduce the probabilities of the dominant accident sequences. Finally, PRA provides a correct procedure for the integration of operational data and expert opinion, which is essential for the analysis of the low probability events in which we are interested.

#### LIMITATIONS - INTRINSIC

The line between intrinsic and practical limitations is indistinct, but there are some limitations that are easier to fix than others. Nearly all of the limitations we will list in this section could be dealt with in a better world, but it seems to be extremely difficult at present. In the next section we will deal with the limitations which are simply matters of practice, and

which are bound to improve as understanding of the techniques becomes more widespread. Nonetheless, in my personal view, the limitations in the second group are far more damaging to the utility of PRA at the present time.

a) Completeness - It is a truism that not all possible accident sequences are contained in a PRA, and that will always be true. It is true at two levels. In the first place, it is obvious that, being mortal, we have not thought of everything, and it is always possible that one of the accident sequences we have not thought of is of transcendent importance. As time goes by without the revelation of important new sequences, this becomes less likely, but it is never out of the question. At a second level, no accident sequence in a PRA is intended to be unique -- there are far too many unique sequences, differing in only minor details. Each is meant as a surrogate for a class of related sequences, and the probability for the sequence is meant as an aggregate of all these probabilities. (This is particularly important to remember when people look back at something that has occurred, like Three Mile Island, and ask whether it was predicted by a PRA.) There is no cure for incompleteness, but concern about it is bound to decrease with time and with the accumulation of wisdom and experience.

b) Inadequate Data Base - The data base will always be inadequate, again at several levels. For items that fail frequently, like valves, information about the mean rate of failure may accumulate, but questions about the failure distribution are bound to remain. The population is not homogeneous, the failure rates are sensitive to maintenance practice, etc., and it is out of the question that the technology will stagnate to the point at which one will have a complete failure rate distribution for such items. It would be an indictment of the industry if it were to happen. For items that have never failed, like reactor pressure vessels, failure rate estimates will have to come from informed estimates of the effectiveness of inspections at both the manufacturing and maintenance levels, along with improving understanding of fracture mechanics and of radiation effects. These items are unlikely to close in the foreseeable future. There are intermediate cases between these two extremes, but it is clear that the data base will always be inadequate for those who would like a clean empirical approach to risk assessment. For mortals, this requires that PRAs be done with a judicious mixture of expertise, data, and judgment.

c) Fault Tree/Event Tree Analysis - There are some structural imperfections in the conventional format for a PRA, that can not be removed without fundamental change. Recall that these analyses are usually structured from the and- and or- gates borrowed from Boolean symbolic logic (and now familiar because of digital electronics), and that many relationships can not be expressed in these terms. For example, such logic symbols are used to describe whether or not a component fails, but provide no means of describing the gradual degradation of a component. Such logic is intrinsically sequential, and cannot easily describe unstable

loops or such things. Nor does it have provision for the measurement of time, except in terms of temporal priority, so that a component failure that takes place over six days is indistinguishable from one that takes six microseconds. That is not a description of the real world. Of course, one can make *ad hoc* procedures to deal with some of these extreme cases, but the basic limitation is intrinsic to the structure.

d) Human Performance - It need hardly be said that it is difficult to predict human performance, yet nearly all events in reactors so far have involved human intervention of some sort. In a PRA, human *error* is accounted for in some averaged way (though there is no way to predict the depths of human ingenuity in making mistakes), but there is little or no accounting for human *positive* input. Yet humans are capable of constructive input in accident situations, and it is surely biased to consider only the negative aspects. (This has implications also for the difficult question of the right degree of automation, on which whole nations disagree.) It would be very useful for someone to make a random search of events initiated by mechanical failure, just to find out how often innovative behavior by the operators, beyond their standard procedures, helped to control the incident. A higher level of automation will make it easier to do PRAs, by eliminating this human unpredictability, but may make reactors less safe.

e) Common Cause Failures - A common cause failure compromises the effectiveness of a fault tree/event tree analysis by producing concurrent failures in supposedly independent systems. The standard examples are external events -- earthquakes, tornadoes, floods, sabotage, etc. -- but manufacturing errors and maintenance errors are other examples. (In the U.S. an aircraft had failures in all three supposedly independent engines on one flight, because the same maintenance crew had made the same mistake on all three engines one night.) It is possible to protect against known causes of such failure, but it is difficult to incorporate them into a PRA. It is in fact done, but it is not done well.

#### LIMITATIONS - PRACTICAL

The limitations that follow are my personal list of things that we don't seem to be doing as well as we might -- others could well have a different list, or even differ about items in this one. One should rejoice at the fact that there are things to be improved, and that in fact most of them can be improved. There is no special order to this list, though some items are clearly more important than others.

a) Consistency - By now there have been dozens of PRAs performed, and it is impressive that, though they contain great uncertainties, the results for the final probability of core melt are not widely divergent. It is well to bear in mind that some of this consistency is illusory, since there is considerable communica-

tion within the community of purveyors of PRAs. We will discuss the meaning of uncertainty next.

b) Uncertainty - The large uncertainties in the final results of PRAs are well-known, and it is worth discussing what is meant by such large uncertainties. When we state that the computed estimate of (say) a core-melt probability is uncertain by a factor of plus or minus ten, that is an almost meaningless statement, just as it is almost meaningless to state the original probability without some description of the uncertainty. One is, in both cases, trying to describe an unknown distribution, the probability distribution for the probability of core melt, by one or two parameters, and that can simply not be done. Nor, on the other hand, is there ever enough information available to properly describe the entire distribution. This can lead one into considerable confusion about just what is meant by the numbers quoted as the end results of a PRA.

It is very popular, for lack of better information, to assume that all distributions involved in PRAs are lognormal, and there is indeed in the central limit theorem some basis for this approximation in some cases. Just as an example, suppose the probability distribution for the probability of core melt in a particular reactor is in fact described by a lognormal distribution, and suppose that the standard deviation is a factor of ten. In that hypothetical but not atypical case, the mean probability will be a factor of fourteen larger than the median, and it is clearly important to know just which one interests us most. One hears people speaking of the "best estimate" without clarifying what is meant. If indeed it is the median that is meant, then it is not at all clear which is most important to the protection of society, though it is more likely the mean than the median. This is not meant to argue for one or the other, but only to say that quoted probabilities without this much specificity have little meaning.

These comments are even more relevant to statements about the uncertainties in the estimates of probability, which are usually stated as plus or minus a factor of  $x$ , without any clarity in what is meant. Is it a standard deviation in a conjectured lognormal curve? Is it an absolute set of bounds? Is it a rough estimate (whatever that means) of the psychological indecision of the purveyor of the PRA? What is it? These may seem like academic questions, but they must be answered if the final result of the PRA is to be of use to society. There are large factors contained in the alternate definitions of these terms, and to handle them loosely is simply not responsible. It is, however, common.

As a final comment on uncertainty (though there is far more to be said), there is a natural human tendency to believe that the right answer is in the middle of the "uncertainty band". (Usually, with these broad distributions, people mean the logarithmic uncertainty band.) If this were so, of course, there wouldn't be as much uncertainty. It is important to keep emphasizing that a

genuine uncertainty in probability means that the "true" probability may very well be displaced from the center in either direction, by an amount comparable to the uncertainty. Uncertainties are real. In a PRA there is an opportunity to deal with them carefully, but they are equally present in a deterministic assessment, though well concealed.

c) Categorization - As mentioned earlier, each accident sequence in a PRA must really be regarded as a surrogate for a class or category of sequences of the same general type, and its probability as the sum of all the probabilities of its class members. It is therefore incorrect to observe a sequence in practice, and to then ask in retrospect whether it was contained in a particular PRA. (Of course, if *nothing* like it has been considered, that is another matter.) In particular, it is incorrect to infer that the probability of a sequence is high, just because it has been observed, and to then mistrust a PRA because it seems not to have given a high probability for that particular sequence. Remember all the sequences in the PRA that *haven't* yet been seen. This is a common misunderstanding of the meaning of probability among people unfamiliar with the concept, and we all have to deal with it in speaking to non-professional groups and individuals.

d) Human Positive Input - We have already said that analysts normally treat humans as just another component of the system, which either works normally or malfunctions. In fact, of course, though a valve or relay may not be able to rise above the occasion and perform innovatively, a human can. There are many cases, of which the first Browns Ferry fire is a good example. There a control rod drive pump was used innovatively to cool the core, though it would have been impossible to make allowance for such action in a PRA. My personal view is that such a human resource is an important defense, and its omission from PRAs is a major defect. This is a self-nourishing defect, in that failure to recognize the value of positive human intervention (as we do, for example, in aviation) lowers our sights in terms of the quality required of reactor operators. I do not like to fly with pilots whose upper bound of performance is the instruction book. It is, however, extremely difficult to see how to incorporate such a factor into a PRA.

e) Bottom-Lining - During the course of the performance of a PRA many intermediate results are obtained about the expected behavior and reliability of systems and subsystems, about failure modes and sequence morphologies and probabilities, etc. These results vary in reliability for many reasons, among them those mentioned above and below, and the insight they provide varies accordingly. When they are all combined to provide a "bottom line" estimate of the probability of damage to life and property, this is inevitably the weakest and least reliable result of the PRA. Nonetheless, social and regulatory pressures combine to provide emphasis on this small fraction of the PRA output, impairing the credibility of the entire process. One cannot deny that there is a great societal hunger for the bottom line, but it is the weakest use of PRA and emphasis on it detracts from the



many other benefits of the analysis. One should resist one-digit statements about safety.

f) Consequences - The previous statements are particularly relevant when one carries the result of the calculation to an estimate of the probability of a certain number of latent cancers in the population, because this calculation combines all previous uncertainties with the genuine uncertainty about the effects of extremely low levels of radiation on large numbers of people. These effects will never be understood empirically, because they are so small that there is no possibility, even if there were a large accident with radiation release, of an epidemiological determination of the level of damage. There is, after all, a fifteen percent probability that we each die of cancer anyway, and one man-rem contributes less than one thousandth of this. It may, so far as we know, contribute nothing. As the source term research comes to its conclusion, the number of predicted acute fatalities will probably also be greatly reduced. Short of a monumental breakthrough in our understanding of the mechanism of radiation-induced cancer, there will always be great uncertainty in these predictions.

g) Conservatism - Unfortunately, PRAs are done in a regulatory environment, which does not reward realistic estimates. In an ideal world, one would make an estimate of the safety of a reactor as realistically as possible, and then, and only then, apply a sufficient safety factor to satisfy the conservative needs of society. It is a sad fact that people who make PRAs always deal with uncertainty by erring in the conservative direction, thereby giving the entire enterprise an unknown, but substantial, bias. Even though an error in either direction is an error, one learns quickly that an error in the non-conservative direction produces a flood of abuse, while a conservative error produces hardly a murmur. One can cite many examples. This has three important consequences.

First, the magnitude of the error is normally unknown, since it is pervasive and unquantified, perhaps, in many cases, unquantifiable. This makes the meaning of the bottom-line estimates of risk even murkier than before, with the consequent disservice to all who look at them, for whatever purpose. To the extent that the numbers are taken seriously, they then deceive the regulators and mislead the public. That is bad.

Second, the excuse is often given that a calculation done conservatively at every point in doubt, must, in the end, lead to a conservative result. *That statement is false.* (It also confuses the duty of the practitioner of PRA, which is to honestly analyze the plant, with that of the regulator, which is to assure that degree of safety required by the public.) A conservatism is a misstatement, however honorably motivated, and there is a theorem in logic to the effect that if a collection of postulates has one which is false, it is then possible to prove any theorem. This theorem is not obvious, but it is true. There is *no reason to have confidence* that a calculation done conservatively at each

decision point will lead to a conservative result. It is easy to think of counterexamples.

Third, conservatism can lead to gross distortions of priorities. Consider two accident sequences, A and B, of which A has the lower median (or mean) probability, but much greater uncertainty. Conservative estimates of each will have a larger effect on A, and may very well invert their order. One will then find oneself giving greater regulatory and research attention to the sequence of lesser importance. (An example will be cited below.) This problem is so widespread in the regulatory apparatus, at least in my country, that it would not be unfair to say that our regulatory effort is directed mostly against uncertainty, rather than against risk.

Probably the single greatest defect in the use of PRA is the failure to understand and account for uncertainty.

h) External Events - External events can lead to common cause failures, and the difficulty in accounting for them in the context of a PRA leads to the assignment of particularly great uncertainty to the estimates. In the U.S.A. accidents induced by earthquakes are a good example. Because there are such great uncertainties, the difficulties mentioned at the end of the last section are present in force, with the consequence (in my view) that we greatly overestimate the seismic threat. This distortion of priorities leads to misplaced regulatory and research effort, with a consequent *reduction* in the level of safety. (Who can forget how the overemphasis on large LOCA, in the years before Three Mile Island, led to neglect of the problems associated with transients and small LOCA, and therefore directly to the accident?) We may yet learn, at Diablo Canyon (near my home), that the years of fighting about the overstated seismic threat have diverted us from any real problems afflicting the plant.

i) Safety Goals - No one knows "how safe is safe enough", so it is natural that regulatory agencies should grasp at any straw in seeking reasonable standards for a proper standard of regulation. Whether in the form of *de minimis* levels of exposure or in the form of quantitative criteria for licensing, these always depend upon some quantitative measure of the safety of a reactor, and that can only be given by a realistic PRA. But there are problems.

In the first place, PRAs will, for the foreseeable future, have built-in uncertainties of factors of ten or more, and there is no reasonable way to set standards which are so unclear. Even so, this is often done, and the USNRC has promulgated proposed quantitative safety goals which are precisely stated, even in the face of these great uncertainties, and in which it is not even clear whether it is the median or mean or something else that is meant. These exactly stated goals produce a false illusion of precision, and I have heard experts say that the calculated probability of core melt is .00015, and that it needs to be reduced to below .0001. That is simply wrong! It is easy to

lose track of the meaning of probability in the face of great uncertainty, as mentioned earlier, and, in particular, to ascribe greater accuracy to the calculations than is justified.

The second problem is to find some reasonable source for the goal as stated. In a rational world, the level of societal risk we are willing to accept from a technology bears some relation to the benefits we perceive from it, or at least to the drawbacks of the alternatives. For most (if not all) technologies these balancing estimates are made informally, through the normal process of social intercourse. In particular, they involve more than risk. We accept aviation -- most of us flew to Karlsruhe -- despite the known risk, because it is a relatively fast and comfortable form of transportation. We drive cars for the same reason. We eat strange foods at distant castles. We stand in front of strange audiences delivering speeches. In each of these cases we *could* reduce the risk, but there is more to life's judgments than the reduction of risk. On the other hand, there are some risks we don't take, and in each case there is some tacit balance struck which involves many considerations of risk and benefit. The point is that the evaluation of benefits is even more difficult than the evaluation of risk -- it is not just financial benefit that is involved -- and is the responsibility of the entire society, not just the regulatory apparatus. How does one match the impact of coal-burning on the German forests against reactor risk. What about the coal miners?

The USNRC has promulgated a set of quantitative safety goals, for evaluation, test, and comment, which ignores these considerations, and which is, in my personal view, wholly irrational. The criteria are based on bottom-line estimates of the effects of reactor accidents on human health (see above), are precisely stated without any mention of the uncertainty problems (see above), and are derived entirely from risk considerations (see above). Specifically, they seek to make the risk of reactor-induced cancer to the nearby population less than .001 of the risk of cancer from other causes, and less than .001 of that due to other alternative means of generating electricity. It is easy to see the fundamental flaw in such criteria. For the first, notice only that a substantial fraction of cancer in the U.S. is unambiguously due to cigarette smoking -- does this mean that a reduction in cigarette smoking requires an improvement in the safety of nuclear power plants? What is the connection? For the second, suppose I invent a hypothetical means of generating electricity which is absolutely safe, but which produces enough foul-smelling waste to cover the entire country to a depth of one meter. Must reactors be absolutely safe to compete? These are efforts by an agency which is responsible only for risk to find some risk-based goals, and such an effort is doomed to failure.

This is not to say that there is no merit in quantitative safety goals -- quite the contrary. It is extremely important to find a way out of the open-ended regulatory dilemma in which we find ourselves. Quantitative goals which are stated as ill-defined objectives for the regulatory agencies, provided as guidance for

the necessarily deterministic regulatory process, and which are derived from an arbitrary estimate of the level of safety desired by the public in view of the public benefits, would be very helpful. It is amusing that, in the U.S., the corresponding regulatory agency for aviation, the Federal Aviation Administration, has no defined quantitative goals, yet regulates an accepted technology. (This was not always so, and there are still many people afraid of flying.) When asked, officials of the FAA will normally say that they do everything in their power to continue to make flying safer, yet that is not true. There is room in the rational management of a society for social contracts which are not drawn up precisely by lawyers.

In addition, PRA-derived goals for the safety and reliability of subsystems can be very helpful in determining design tradeoffs, as long as they are not somehow translated into acceptance criteria by the regulatory agencies. One cannot help but sympathize with regulators who are required to decide how safe is safe enough in the everyday course of events, without much help.

j) The Use of PRA - Despite all that has been said above, the limitations on the performance of a PRA are small compared to the problems involved in integrating PRAs into the regulatory environment. Regulatory decisions are often made whimsically, and PRA provides a mechanism for assessing the impact of such decisions on the safety of nuclear power, even in the face of the problems listed above. Its use should be widespread and enthusiastic, rather than limited and grudging. Perhaps that will change, in time.

#### CONCLUSIONS

There is little to add here. Probabilistic Risk Assessment is a known (perhaps the only currently known) methodology for the quantitative assessment of reactor risk, and thereby the best known way to provide a rational base for reactor regulation. It also serves as a systematic means for the quantification of the performance of a plant under upset conditions, and thereby a means for the identification of weak points in design or operation. It is not used as effectively as it can be, nor have the regulatory agencies yet effectively integrated PRA, with its inevitable uncertainties, into their operations. There is more room for progress in that area than there is in the improved performance of PRAs. In that arena, the major need among those mentioned above is a systematic purging of the conservative influence on the conduct of a PRA, so that the results (including the uncertainties) are given generally understood meaning.

FIFTH INTERNATIONAL MEETING ON  
THERMAL NUCLEAR REACTOR SAFETY

## SAFETY GOALS APPROACHES

Invited Paper

Dr J H Gittus  
Dr F R Allen  
Safety and Reliability Directorate  
UKAEA

## INTRODUCTION

Absolute safety and zero risk are unattainable in any of man's endeavours. Any human activity has an element of risk attached to it, even the activity of physical inactivity, so prevalent in developed societies amongst the population of desk-bound office workers, has associated medical risks.

In the field of nuclear power, there is a well developed technology for identifying and quantifying the risks associated with the operation of power plant. Indeed, nuclear power safety assessment may be said to be at the forefront in this area, and techniques developed in the nuclear field are now being applied elsewhere. Given this capacity to quantify risks, even down to extremely low levels of probability for the case of very unlikely accidents with the potential for significant consequences, it is natural to look for corresponding statements on acceptable levels for such risks. An initial attempt to produce an acceptance criterion quantified in terms of frequency events was made by Farmer. This initial criterion was stated in terms of the frequencies of various levels of release of  $I^{131}$ . Subsequently many other proposals have been put forward suggesting acceptable frequencies for various events whose consequences were expressed in a variety of ways. A milestone was reached in 1982 when the USNRC published their proposed safety goals which incorporated an element of probabilistic assessment. Proposals such as that by AECB (Canada) make the distinction between a rigid acceptance criterion, which must be met, and a target or safety goal which should be aimed at.

The development of such approaches forms the subject of what follows.

## OBJECTIVES OF SAFETY GOALS AND CRITERIA

Safety goals and acceptance criteria may be proposed with a variety of objectives in view. The scope and detail of the criteria proposed will vary depending upon which objectives are addressed. Also, the objectives may have a bearing on the underlying philosophy and so on the approach adopted.

a. Public Demonstration of Safety Adequacy

Goals and Criteria aimed at this objective seek to draw comparisons between risks in the field under discussion and those elsewhere. As a result,

they are often fairly broadly drawn rather than relying on detailed plant-specific requirements. They will tend to lean towards comparison with other risks, either technological risks assumed to be already accepted by society, or natural hazards of recognised rarity such as lightning strikes, meteorites, etc.

b. Regulatory and Licensing Decisions

Where safety goals and criteria form part of the regulatory and licensing decision-making process, they need to be clear and unambiguous. Consequently, a considerable amount of detail may be necessary in order to specify the requirements with sufficient precision. The inclusion of this detail is necessary if the criteria are to be useful in a regulatory context; however it can result in requirements which are specific to a certain design of plant.

c. Aiding Siting Decisions

Criteria aimed at aiding siting decisions need to address the plant in the context of the proposed site and so must link the characteristics of the plant to the impact on the area surrounding the site. The plant characteristics might, for example, be expressed in terms of assessed frequencies of releases of various categories of activity, and the surroundings of the site in terms of the population distribution, meteorology, topography, and geology. Depending on the approach adopted, either the plant characteristics or the site surroundings might be assumed to be 'typical' or 'standardised' data.

d. Aiding Design Development

In order to aid design development, safety goals and criteria expressed in terms of targets for the plant characteristics are the most useful. In this way development of the design can be decoupled from site-specific aspects. However, such criteria must retain some link to the surroundings of the site either directly or by means of consequence analysis at a later stage. The use of quantified acceptability criteria in design development can have great benefits in producing a balanced or optimised design and also in efficiently allocating the resources used to produce such a design.

e. Aiding Research Priority Decisions

In addition to aiding design development, safety goals may be aimed at aiding research priority decisions. In this case it is particularly useful if the safety goal or criterion addresses the problem of uncertainties in the results of quantified safety assessments, since the areas which contribute to significant uncertainty in the risk estimates are those of relevance in prioritising research work.

f. Rationalisation of Resource Allocation

Safety goals and criteria may be set with the objective of rationalisation of resource allocation. Optimisation of a design or a research programme are examples of this which have been mentioned above. Other examples include optimisation of safeguards, or of maintenance and inspection periods.

As will be seen from the above, the objectives for setting safety goals and safety criteria cover a wide span and in some cases the different objectives result in very different requirements which seem sometimes to be mutually exclusive. To date, most safety goals and criteria have addressed primarily (a), (b) and (d) above. The proposals which have been made include a

wide variety of different approaches. These differences can be described in terms of the differing forms in which the goals or criteria are stated and in terms of the differing underlying philosophies.

#### FORMS OF SAFETY GOALS

Safety goals and safety criteria are usually formulated in terms of a constraint on some aspect of an activity. The form of the constraint depends to a certain extent on the objective or objectives being addressed. Safety goals and criteria already published have included constraints on the following:-

##### a. Plant Damage (Fig 1)

The constraint may be expressed in terms of frequency limits on specified states of the plant, for example the US ACRS criteria (1) include acceptable limits and targets for specific core damage states, such as core melt, as do the USNRC Safety Goals. (2) The constraint may be expressed in terms of more severe but less specific plant states, such as those of the UK CEBG Design Safety Guidelines (3) which require the sum of the frequencies of all sequences leading to large uncontrolled releases of activity to be less than  $10^{-6}$  per year, or of the ACRS criteria which have a constraint on the frequency of core melt with significant release (of  $5 \times 10^{-5}$  per year as an upper limit and  $10^{-8}$  per year as a goal). Such constraints are clearly not site specific.

##### b. Radioactivity Releases (Fig 2)

As an alternative to constraints on plant state frequencies, constraints may be quoted in terms of the frequencies of releases of activity. The earliest numerical safety criterion of all, proposed by Farmer, (4) was of this form. However, subsequent proposals have not taken this form.

##### c. Radiation Dose (Fig 3)

Several criteria are based on or include constraints on radiation dose to members of the public. In the UK both the NII safety assessment principles (5) and the CEBG Design Safety Guidelines (3) constrain the acceptable frequencies of releases of activity leading to various doses to members of the public. These doses are expressed in terms of the Emergency Reference Level of 10 rem, a dose specified by the UK Medical Research Council as being a level of dose at which countermeasures should be considered. (Recently the UK NRPB have made more detailed recommendations on this topic (6)). It is important to note that the CEBG DSG is for all accidents in each consequence decade whilst the NII assessment level is for discrete sequences. The Canadian AECEB criteria proposals (1) are expressed in terms of reference values for the sum of the frequencies of all accidents leading to specified dose levels covering the range from routine releases up to severe accidents.

##### d. Individual Risk (Fig 4)

Criteria expressed in terms of radiation dose may clearly be related to individual risk values. In addition, several published criteria or safety goals include constraints on individual risk. The US ACRS gives limits on the risk to the most highly exposed individuals. The Kinchin criterion (7) proposes

acceptable values for individual risk. The USNRC Safety Goals include limits for individual risk specified as a percentage (0.1%) of the 'background' risk. All these specify different values for the case of early death and delayed death, with some weighting factor between these.

e. Societal Risk (Fig 5)

In addition to constraints on individual risk, some criteria contain statements on societal risk, either as a single figure (for example the expected number of deaths per year of reactor operation) or more commonly in graphical form. In some cases (eg the Kinchin criterion) the constraint is an iso-risk line, that is, one where the frequency decreases in inverse proportion to the increasing severity of consequences, but in some cases an element of risk aversion is incorporated so that frequencies are constrained to fall more rapidly than this. The US ACRS proposals include a weighting in the formula for evaluating the number of 'equivalent early deaths' for this purpose. The USNRC Safety Goal relates acceptable risk to a proportion (0.1%) of the background risk. Such criteria are of interest in comparing risks in different fields such as other technologies or natural or background risks.

f. Cost-benefit Aspects (Table 1)

The ICRP in recommending that radiation exposure should be 'as low as reasonably achievable' allow for an optimisation in radiological protection by balancing benefits against costs. This concept is also incorporated into some published safety criteria, for example the USNRC safety goals give a figure in dollars per man-rem for the assessment of an incremental reduction of societal risks below the numerical guidelines, and the ACRS give figures for assessment of the cost-effectiveness of measures to reduce both early and delayed deaths.

PHILOSOPHICAL BASIS - Table 2

The philosophical basis underlying published safety criteria or safety goals may vary, indeed in some cases it may not be stated at all. Various reference points may be identified with which to compare the risk levels derived.

a. Comparison with Prevailing Risk Levels in Society

Several criteria and safety goals are based on comparing the risk level which they represent with that current in society. In the case of USNRC safety goals, the risk level is expressed as a percentage (0.1%) of that resulting from all causes. In other cases the link is less direct but for example both Farmer and Kinchin derived their criteria in the context of prevailing risks in society.

In a document recently submitted to the Public Inquiry into the building of the Sizewell 'B' PWR (8), Locke (a consultant to the UK Health and Safety Executive) considers the risks posed by a nuclear plant just meeting the NII Safety Assessment Principles. In relation to natural hazards he considers land contamination and large scale evacuation and re-location. The frequency of such an event in the borderline nuclear case considered is 1 in 300,000 per year. This is contrasted with the frequency of 1 in 1,000 per year which is the estimated frequency of a North Sea tide overtopping the newly-installed Thames Barrage and flooding London.

b. Comparison with other Technological Risks



Many criteria and goals are based on comparison with other, apparently acceptable, technological risks. The USNRC's safety goals require that the risk from nuclear power plant accidents should be comparable to or less than the risks from generating electricity by viable competing technologies. Others, for example, the Farmer criterion and the US ACRS, are also based on inter-comparison with other technological risks.

In the document by Locke (8), the risks from a nuclear plant just meeting the NII Safety Assessment Principles are compared also with risks from other industrial plant. He finds the risk of small scale accidents, such as might require local temporary evacuation, arising from the borderline nuclear plant to compare favourably with risks of similar events, for example, LPG storage or a chemical factory. More severe accidents, with lower frequencies, are compared with similar consequence accidents involving railway trains or aircraft, or large chemical complexes. Again the result is that the risk implied by the NII safety assessment principles is lower than those from 'conventional' sources.

c. Consideration of Low Probability Natural Hazards

Some criteria, for example those proposed by Farmer and Kinchin, refer to the risks posed by low probability events such as lightning strike and meteorites.

d. Consideration of Accepted Voluntary Risk Levels

The Kinchin criterion is derived in relation to accepted voluntary risks in society as a whole. Comparison is also made with other risks such as risks from illness and disease which are not accepted by society and which as a result are the subject of research programmes. From these, an indication of the boundary between acceptable and non-acceptable risk levels is inferred.

#### COMPARISON OF EXISTING SAFETY CRITERIA AND SAFETY GOALS

Published proposals for risk acceptability criteria and safety goals differ widely in their approach and structure, in their philosophical basis and the form of constraint adopted. In the preceding discussion, examples have been given of some of these. It is tempting to compare the relative stringency of the various criteria available. This is possible in some cases where equivalent figures are given, but in most cases the differences between the form of constraint do not permit direct comparison. Even when apparently equivalent figures are given, care must be exercised. For example the CEGB and NII lines in Fig 3 appear to be comparable but in fact are significantly different, the CEGB one is for all sequences whereas the NII one is for a single discrete sequence. However, where comparisons can be made then it is useful to do this, and an extensive comparison has been prepared in the Federal Republic of Germany. Amongst international organisations the NEA has provided the forum for useful discussions in this field through its Committee for the Safety of Nuclear Installations, whose Principal Working Group 5 covers Risk Assessment, and also through its Licensing Group. The CEC is also active in this area: it has a permanent working party on Safety Goals and Objectives whose recent report reviews the position in CEC member countries.

In practice, any criterion or safety goal must be assessed in a specific context of typical data on population, meteorology, atmospheric dispersion and

health physics, as well (possibly) as plant-specific data. As an example of what is involved, the NII have recently carried out an exercise relating their Safety Assessment Principles to levels of risk to the public (9). In order to do this, they have had to make assumptions on the spectrum of accident sequences for the plant concerned, the population distribution around the site and the meteorological data for the site, as well as detailed assumptions regarding the type of release. The result of this is that the Safety Assessment Principles are tentatively estimated to be equivalent in risk terms to an upper limit for individual risk of death from cancer of the order of  $10^{-6}$  per year for an individual at the site boundary. This is shown on Figure 4 as 'NII Inferred'. This value corresponds to accidental releases and a figure of similar magnitude is obtained for routine releases.

With regard to societal risk, the results are even more dependent upon the assumptions made and the NII have calculated a band of possible risks which reflect this difficulty. The results of the NII calculations are shown superimposed on Figure 5 where the band of possible risks for each of the two assumptions for the spectrum of plant risks (A and B) is shown. The wide range of results is obvious from this. The risk of 10 fatalities, for example, varies over 2½ decades, depending upon the assumptions made. Since the various published criteria and goals have evolved in different parts of the world, where population distributions and meteorology in particular may be very different, the choice of 'appropriate' or 'typical' data for such a comparison becomes very difficult. Therefore it is no simple matter to take a comparison of different criteria and goals beyond that presented already. The prevailing impression emerging from that comparison is the very wide span of approaches encompassed by these criteria.

#### THE PRACTICAL APPLICATIONS OF SAFETY CRITERIA AND SAFETY GOALS

The practical application of safety criteria and safety goals throws up many difficulties. Some of these may be peculiar to a particular way in which the constraints are framed, or to a particular design-specific aspect. However others are indicative of more fundamental problems underlying the application of many formulations. These can be seen as falling into two categories - those relating to information requirements for the application of a criterion, and those relating to choice of various options or alternatives in carrying out the assessment.

##### 1. Information Requirements

Some safety criteria or safety goals apply to the plant itself, in isolation from siting considerations. Examples of this are those criteria applying to plant damage states (ACRS, NRC, CEGB). A plant design can be assessed against these, to a greater or lesser extent, without the need to consider site-specific data such as population, meteorology etc. Other criteria or goals, however, relating to societal risk, for example, can only be considered in relation either to a specific site or to some 'typical' location. These are therefore more difficult to use at the stage of design development, since the site may not be specified at this stage. Criteria and goals relating to individual risk fall in between these two extremes. These may, for example, be applied at the site boundary, which is a less site-specific constraint than one which requires consideration of the distribution of the surrounding population.

## 2. Alternative Methods of Assessment

In many areas, the numerical result of a quantitative safety assessment can depend strongly upon the choices made during the assessment. These may be summarised in the following possible approaches which could be adopted in various areas:

### a. Degree of Pessimism

In many areas it is possible to choose either to carry out a 'conservative' or 'bounding' calculation, or to carry out a 'best estimate' calculation. It is usual in certain cases to choose a conservative calculation: this is usually the case for example in licensing areas particularly where design basis accidents are being considered. In other areas it is more usual to consider best estimate calculations, an example being in severe accidents beyond the design basis for which there may not be clearly defined conservative assumptions which can be made. The convention as to what assumptions and methods are 'usual' in particular cases may vary from country to country, from group to group, and also may change with time. It is clearly essential that calculations should involve the same degree of pessimism as that which those proposing the criteria or goals assumed would be used; it is clearly not sensible to compare 'conservative' calculations with criteria or goals intended for 'best estimate' calculations, or vice versa. Therefore it is necessary for those proposing criteria to indicate what degree of pessimism they intend should be employed.

### b. Population to be Considered

As a particular example of the need to specify the degree of pessimism, is the need to specify whether 'populations' and 'individuals' referred to in safety criteria or safety goals should be average in some sense, or those most highly exposed, or (hypothetical) persons located at the most exposed location accessible to the public. It is possible to frame constraints in terms of any of these alternatives, with valid reasons for the choice, but unless the choice is clearly specified wide disparities can seem to exist between different formulations because of this.

### c. Interpretation of Analysis Results including Areas of Uncertainty

In carrying out a complete safety analysis there are various areas which currently present technical problems in that the analysis methods or the data base or both are not sufficiently developed for quantification to the same degree of certainty as the rest of the analysis. Such areas are the subject of current research and of much debate: they include, for example, human factors, common cause effects, certain external events, etc. Inclusion of such aspects, and the method by which they are included, could have a marked effect on the results of the analysis. Further, these are areas where there is prospect of considerable evolution in techniques in the future, and so the effects on the analysis could well change with time. Therefore it is important that, where such changes might affect the interpretation of a safety criterion or goal, some guidance should be given as to how they should be interpreted for this purpose.

### d. Risk Cutoff

It is the nature of the risk from radioactive discharges that, as the material moves further from the point of discharge, although it becomes diluted

and dispersed, the number of people who might be exposed increases rapidly although the risk to the individual in the distant population may be infinitesimal. Because of this effect, which can cause unnecessary emphasis to be placed on those most distant and therefore least at risk, it is sometimes the case that societal risk criteria imply some cutoff point at which the infinitesimal risks to distant individuals cease to be added into the total. However, because the effects of this on the totals which result from the mathematical analysis can be significant, it is essential that in any criterion or goal which is intended for use with such a cutoff, this is made clear so that compatible calculations can be carried out.

e. Treatment of Multi-plant Sites

Many nuclear sites contain more than one reactor installation. Therefore it is essential in defining a safety goal or safety criterion to make clear whether the constraints in terms of frequencies etc apply to an individual reactor, to a particular installation, to the site as a whole, or even (in some cases) to a national programme involving several sites.

f. Treatment of Mitigation and Emergency Response

In many postulated accident scenarios it is possible to mitigate or even remove the consequences by some emergency response, either by the site personnel or by public authorities, at the time of the accident. In a realistic analysis, this would be taken into account, but in many safety criteria consideration of such actions is explicitly or implicitly excluded. It is obviously essential that the proposers of a criterion should state what their intentions are on this aspect.

#### KEY QUESTIONS

From the review of the various approaches to safety goals and safety criteria, several key problems emerge which any new or revised proposals should seek to address. These fall into the following three broad areas:

1. Problems in Defining Acceptability

Various problems remain in the area of definition of acceptable risks. These include:

- a. The concept of risk aversion - should it be incorporated into safety goals and if so, how?
- b. The weighting between early and late effects is seen by several bodies as a meaningful and useful approach but weighting factors have been proposed which cover a wide range.
- c. Optimisation between risks from routine operation and risks from accidents.

2. Specific Problems in Assessment Methods, Techniques and Data Bases

In many areas, items can be identified on which there is as yet no clear

consensus and which may require interpretation when applying safety goals or safety criteria to a particular plant. Where this is the case, the safety goals or criteria should include some guidance on the interpretation to be adopted. Some of these are mentioned below:

- a. The treatment of uncertainties.
- b. The treatment of mitigation and emergency response.
- c. The effect of in-service modifications.
- d. The effects of human factors and human reliability.
- e. The effects of common-cause failures.
- f. The application of a risk cutoff when calculating societal risk.
- g. The consideration of time-dependent populations.

### 3. General Problems Related to Application

Some general areas can be identified, as opposed to the fairly specific technical problems mentioned above, which relate to the applications of safety goals or safety criteria to an actual plant. These may be grouped as follows:

- a. Should the criteria or goals be specified in great detail to give clear but possibly very rigid design specific requirements, or should a broader 'in principle' approach be adopted with amplification where necessary by associated guidance notes?
- b. Should criteria or safety goals be intended as a rigid boundary to be adhered to, as a target to be aimed at, or should they include both an upper rigid limit and a lower target?
- c. Should safety criteria or safety goals be specified in terms of 'conservative' or 'best estimate' analyses? Is it possible to define a reasonable but clearly conservative route for calculating the outcome of severe (beyond design basis) accidents?
- d. What range of applicability should be aimed for? Should criteria or goals be plant-specific or applicable to a range of plant types or indeed to a variety of installations?
- e. Should safety goals or criteria be framed in relation to a specified or implied 'typical' site or population distribution, or should they always relate to actual populations?
- f. How should uncertainties or errors be addressed? Should the criteria or goals be essentially single-valued or should they specify the confidence associated with a constraint in some way?

### CONCLUSIONS - WHAT SHOULD WE BE AIMING FOR?

The overall aims and objectives for setting safety goals and safety criteria may vary, so also may the philosophical basis. As a result the formats adopted for safety goals and criteria cover a wide range, making inter-comparison difficult. This difficulty is compounded in many cases because the underlying assumptions are in many cases not fully specified - a fact which also makes application of particular goals or criteria to specific plant difficult in some cases. Key questions relating to the formulation of safety goals have been set out which seek to shed light on the way forward.

But the question remains, what should we be aiming for? In assessing the acceptability of a safety case three tests can be proposed:

The first is that of consistency. Our experience is often obtained from events in poorly characterised situations such as incidents or accidents. We cannot make predictions on this basis alone. Predictions are made based on data from well-characterised experiments and using an analytical capability. However these predictions must be consistent with our experience if they are to form a firm foundation for predicting the safety of nuclear plant.

The second test is the test of completeness. This is linked to the first, for without experience we do not have a sound basis on which to make a test of completeness. Therefore in some areas it may be necessary to 'generate' such experience by integral testing programmes in order to satisfy the test of completeness.

The third test is the test of importance. The greatest attention should be paid to the most important topics. To be able to address the question of importance, we must be able to satisfy the tests of consistency and completeness, at least to some extent. Having done this, even roughly, the test of importance may tell us that our present knowledge is adequate to decide on the importance or unimportance of a topic. The need for further work in this topic will thus be determined by this test.

In formulating safety goals and safety criteria, our aim is to set down the rules to be used in this last and vital test of importance; however we must not forget that this test rests upon the two other tests of consistency and completeness.

## REFERENCES

- (1) An Approach to Quantitative Safety Goals for Nuclear Power Plants  
NUREG-0739 (1980)
  - (2) Safety Goals for Nuclear Power Plants: A Discussion Paper  
NUREG-0880 (1982)
  - (3) Design Safety Criteria for CEGB Nuclear Power Stations  
HS/R 167/81 (CEGB) (1982)
- also
- Pressurised Water Reactor Design Safety Guidelines DSG-2 (CEGB)  
(1982)
- (4) Siting Criteria - A New Approach. F R Farmer Atom (128)  
pp 152 - 170 (UKAEA, 1967)
  - (5) Safety Assessment Principles for Nuclear Power Reactors,  
HMNII, (1979)
  - (6) ERL 2. Emergency Reference Levels: Criteria for limiting doses to  
the public in the event of accidental exposure to radiation  
HMSO, 1981
  - (7) Design Criteria, Concepts and Features Important to Safety and Licensing  
G H Kinchin, ANS/ENS Meeting on Fast Reactor Safety, Seattle 1979
  - (8) The Range of Risks from a PWR at Sizewell - an Overview. J Locke  
NII/S/92 (SAF) (1984). (Submitted to the Sizewell 'B' Power Station  
Public Inquiry)
  - (9) The Relationship between the NII's Assessment Principles and Levels  
of Risk. NII/S/83 (SAF) (1984) (Submitted to the Sizewell 'B' Power  
Station Public Inquiry)
  - (10) Cost Benefit Analysis in Optimising the Radiological Protection of  
the Public: a Provisional Framework NRPB ASP-4 (1981)
  - (11) Risk Criteria for Nuclear Power Plants: a Pragmatic Proposal.  
C Starr ANS/ENS Conference, Washington 1980.

TABLE 1  
Cost-Benefit Aspects

ACRS (1)	\$1m per delayed cancer death averted.	
	\$5m per early equivalent (weighted) death averted.	
USNRC(2)	\$1,000 per man-rem averted.	
UK NRPB (10)	Annual dose $5 \times 10^{-5}$ Sv ( $5 \times 10^{-3}$ rem)	£2000/man Sv (£20/man rem)
	Annual dose between $5 \times 10^{-5}$ and $5 \times 10^{-4}$ Sv ( $5 \times 10^{-3}$ and $5 \times 10^{-2}$ rem)	£10,000/man Sv (£100/man rem)
	Annual dose between $5 \times 10^{-4}$ and $5 \times 10^{-3}$ Sv ( $5 \times 10^{-2}$ and $5 \times 10^{-1}$ rem)	£50,000/man Sv (£500/man rem)

TABLE 2  
Philosophical Bases

	Farmer	Kinchin	USNRC	ACRS
Prevailing risk levels	I	I	D	
Technological risks	I		D	I
Natural hazards	I	D		I
Voluntary risks		I		

D Direct comparison  
 I Indirect comparison



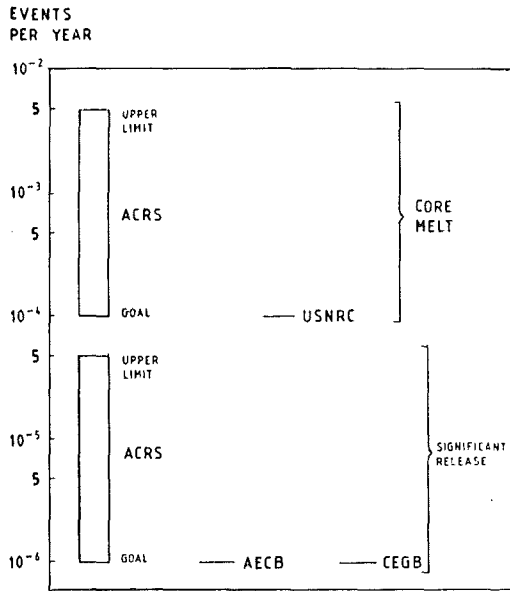


FIG. 1 CRITERIA RELATING TO PLANT DAMAGE STATES

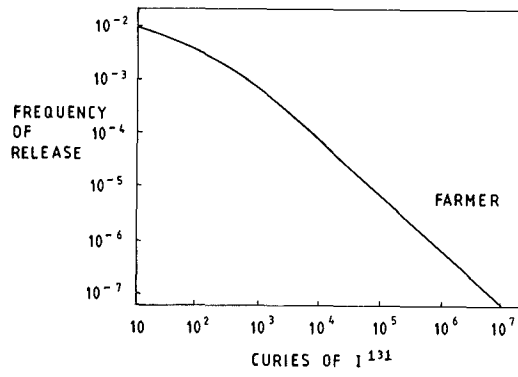


FIG. 2 CRITERIA RELATING TO RADIOACTIVITY RELEASES

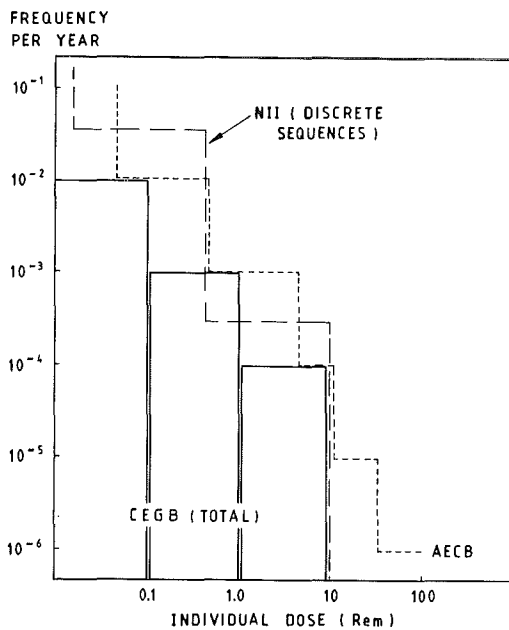


FIG. 3 CRITERIA RELATING TO RADIATION DOSE

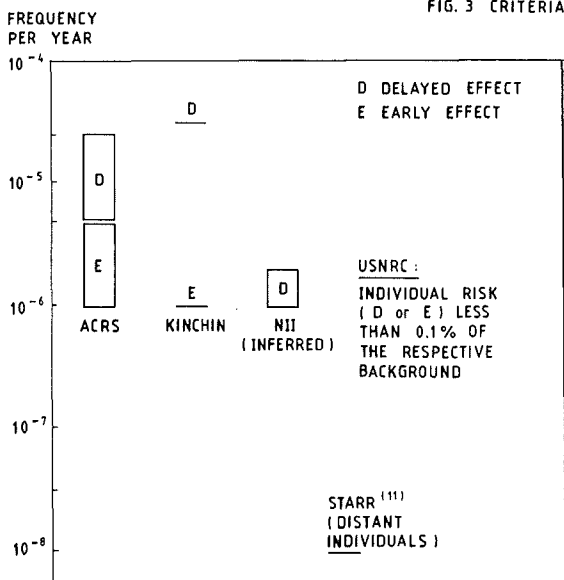
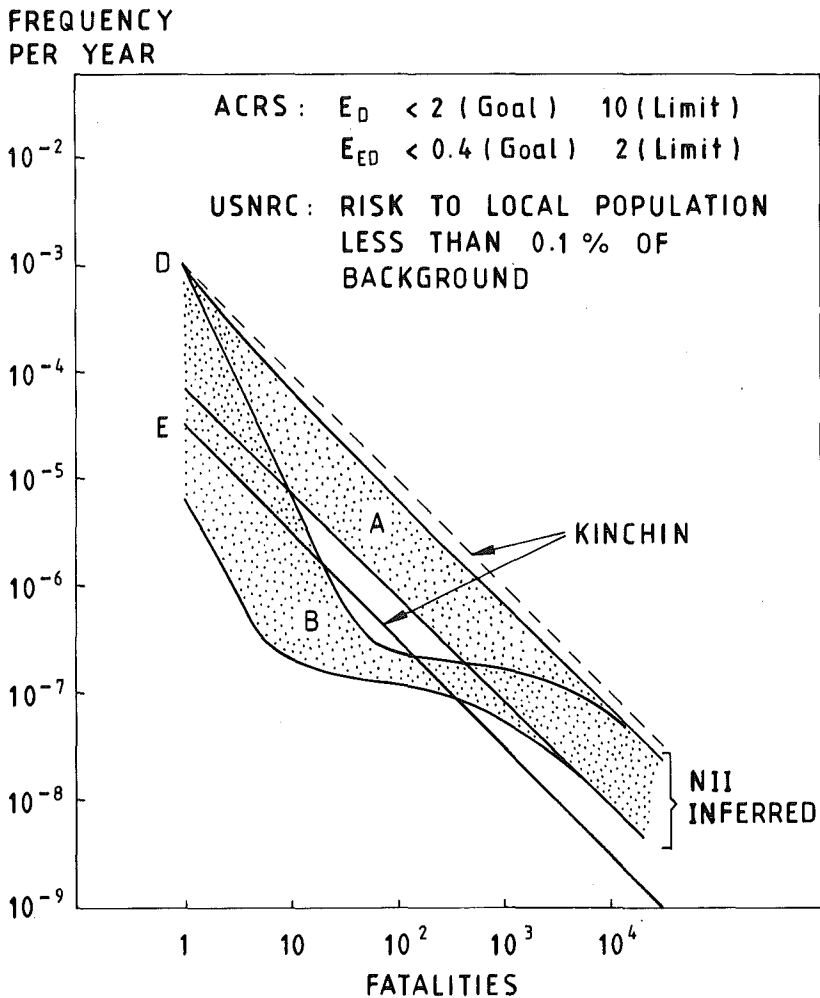


FIG. 4 CRITERIA RELATING TO INDIVIDUAL RISK



KEY:  
 D DELAYED EFFECTS  
 E EARLY EFFECTS  
 $E_D$  EXPECTED NUMBER OF CANCER DEATHS  
 $E_{ED}$  WEIGHTED EXPECTED NUMBER OF EARLY DEATHS

FIG. 5 CRITERIA RELATING TO SOCIETAL RISK



ADVANCES AND TRENDS IN REACTOR SAFETY RESEARCH AND  
TECHNOLOGY

Prof. Dr. A. Birkhofer

Gesellschaft für Reaktorsicherheit (GRS) mbH  
Forschungsgelände, 8046 Garching, FRG

"Safety has been an important consideration from the very beginning of the development of nuclear reactors". This is the opening sentence of the famous book on "The Technology of Nuclear Reactor Safety", published in 1964 by T.J. Thompson and J.G. Beckerly.

A number of fundamentals did remain unchanged over four decades of reactor development. So, reactor safety is still based to a high degree on the theoretical analysis of postulated accidents, in order to anticipate and thus to avoid bad experiences.

Also, like in the early years, safety of nuclear power plants in all countries is supervised by governmental agencies and is seen to a high degree as a public affair.

One consequence has been, that complex technical matters had to be explained and discussed in front of non-technical decision-making bodies and of a broader public. On this field nuclear energy played a pioneering role also for other technologies.

In spite of these and other conformities, a lot has changed from the safety design of early small scale reactors until that of modern commercial nuclear power plants.

For a number of years the problem of power excursions played a predominant role in accident analysis. Severe excursions in research reactors like SPERT and SL-1 gave an additional rise to analyse very carefully the dynamic behavior of reactor cores and to develop effective protection systems.

Due to the small size of the nuclear reactor plants safety of the public could be achieved either by geographic isolation or by containments, which like an "umbrella" protected the environment in any case.

The Ergen-Report in 1966 made clear that it is not sufficient to limit the radioactive releases after a Loss-of-coolant accident (LOCA) by means of a containment. It had been recognized that the integrity of containments could be jeopardized by a core melt down. Therefore, something had to be done to maintain core cooling in case of an accident. In the following years concentrated attention has been given to all aspects of emergency core cooling.

A specific experiment in the first "SEMISCALE"-test facility and a growing tendency to lower core damage in case of a complete failure of a main coolant pipe (MCA - maximum credible accident) resulted, in 1971, in the publication of the "Interim Acceptance Criteria for Emergency Core Cooling Systems" of the USNRC followed by extensive hearings and a large research program.

In the seventies research about the effectiveness of ECCS concentrated on large break LOCA's, because such breaks would produce the highest loads

on the reactor system. Some small break analysis had been done at that time and more significant research was planned after the major questions related to large break LOCA had been answered. However, the event of TMI-2 and results from risk studies changed the priorities. More emphasis has been put on operational transients and small break LOCA's.

Although some research to study core melt phenomena started at the end of the sixties and beginning of the seventies the major increase in funding and efforts was pushed by the TMI-2 accident.

In addition to thermohydraulic research, material issues have been considered and addressed. Material research started with the study of neutron irradiation, while other material behavior has been considered to be known. However, during manufacturing of big pressure vessels, underclad cracking and reheat cracking were found. At the beginning of the seventies an extensive (and expensive) research program on material issues was initiated. In addition, limitation of radiation dose to the reactor pressure vessel was required by new guidelines.

It has to be realized that reactor safety research requires time, funding and expertise. The time span between the realization of a "problem" and its solution can be more than 20 years as in the case of large break LOCA research. For severe accident research this period could be reduced to about 8-10 years. This acceleration is due to effective project management, trained experts and experienced laboratories.

By analysing the steps and progress in LOCA research it can be seen that this research was organized such that new projects were based on former results. This procedure was acceptable from a plant safety point of view because the design of ECCS was based on conservative assumptions.

In fig. 1 time-history of the budget for reactor safety research of two selected organizations is shown in relative units. Despite the fact that inflation has not been taken into account a major increase in the budgets between 1970 and 1980, the additional push by the TMI-2 accident and the decrease after the year 1982 can be recognized.

The question is, whether it is advisable to further decrease the budgets.

An advisory board to DOE has assessed the annual expenditures for LWR safety R+D within the free world to be about 800 million US\$. This number includes efforts by governmental agencies as well as industry. It can be compared with a produced electrical power of about 800-1000 TWh in 1983 with the expected increase as shown in fig. 2. Currently, industry and governmental agencies together are spending only a few percent of a sum, matching the costs of the produced electrical power, for nuclear safety research. This is about equal to the relative funding for safety research within the automobile industry.

Considering the great importance, reactor safety is given by the public for good reasons, we may ask ourselves whether is justified to continue the present trend of decreasing nuclear safety research expenditures.

Let me return to the technical questions. Many safety problems in nuclear engineering are not very different from those in nonnuclear fields. However, they are complex for a variety of reasons:

- In nonnuclear industries components can often be tested in advance or during operation. In nuclear technology, the component and system behavior cannot in all cases be directly studied and experimentally verified, especially for low probability events.
- For design or operational purposes component and system behavior has to be simulated by means of computer codes. Most problems are mathematically very complex and sometimes highly nonlinear.
- Due to the harsh environment - including radiation - material and design requirements are specific.
- Stringent licensing requirements lead to conservative assumptions resulting in complex designs.

The area of reactor safety research and technology is wide spread. Dr. Stratton has covered the present status on source term research and Mr. Gauvenet evaluated existing operating experience. To avoid duplication, I will not assess both topics in detail. My comments will concentrate on the following topics:

- Thermohydraulics and fuel behavior research for transients including loss-of-coolant-accidents
- Physical phenomena and system behavior during severe accidents
- Material issues of the pressure boundary and secondary circuit
- Probabilistic methods in reactor safety
- Optimization of instrumentation and control, including man-machine interaction
- Interaction between licensing and research.

#### THERMOHYDRAULICS AND FUEL BEHAVIOR RESEARCH FOR TRANSIENTS INCLUDING LOSS-OF-COOLANT ACCIDENTS

The objectives in thermohydraulics and fuel behavior research are to prove the effectiveness of reactor control and ECC-systems, during an accident. These objectives require a detailed description and simulation of physical phenomena and system behavior and, in addition, allow the assessment of safety margins remaining if design limits should be exceeded.

The physical phenomena during operational transients, small and large break LOCA's have been studied and simulated mostly with appropriate computer codes.

Three-dimensional effects need further study in certain areas, like large break LOCA, the mixing behavior related to the pressurized-thermal-shock (PTS) problem or stratification during small break LOCA.

System behavior in case of operational transients and small break LOCA's for large reactors has successfully been simulated in research facilities in spite of scaling problems. Most of the older test facilities, like LOFT and LOBI, have been designed primarily for large break LOCA research and were later modified to address small break LOCA and operational transients.

The ROSA-IV and BETHSY facilities now under construction or in the planning phase have been designed to study small break and transient system

behavior. Realising the capabilities of these facilities, between 150 and 200 experiments will be available at the end of this decade in addition to about 400 integral experiments which are available now.

Construction and operation of thermohydraulic test facilities is expensive. It should be envisaged that a group of interested countries could operate an existing facility to continue research and, especially, keep a group of experts trained. This would allow fast reactions to unforeseen events.

The OECD LOFT Project is an example of successful implementation of this concept. In fig. 3 the time schedule for existing or planned integral test facilities is shown.

Fuel behavior research has recently been assessed by a Principal Working Group of CSNI. It stated that the relevant research work has been done and an appropriate computer simulation has been achieved.

There are, however, some areas in which more or better data or codes are desirable, e. g. blockages in large rod bundles and high burn-up fuel, modelling of co-planarity and maximum swelling strain, high temperature oxidation, modelling of PCI in the presence of aggressive fission products and fission product release during transients. A status report is under preparation.

In summary, this area is well covered and international cooperation has been very successful.

Computer codes in thermohydraulics are a major factor in reactor safety assessment. Codes for detailed assessments, e.g. for design purposes or prediction of complex accident conditions, are needed in addition to fast running codes for parametric studies and for use in simulators or plant analysers.

To decrease the verification effort the same code should be used for both purposes with - perhaps - coarse nodalisation and large time steps for faster running applications.

To avoid misleading results codes should - as far as possible - calculate best-estimate behavior. Conservative assumptions - if any - should be included in the initial conditions (e.g. power level), boundary conditions (e.g. availability of systems) or design limits. Best-estimate assumptions are first of all necessary for codes to be used in simulators or plant analysers.

Past experience with experiments and calculations has shown that complex codes are not necessary in all cases and simpler codes are sufficient in many cases. A typical case is the simulation of fluid/structure interactions.

Major codes simulating system behavior like TRAC, RELAP, DRUFAN, CATHARE require developmental efforts of 100 man-years or more and are now nearly finalized. Maintenance may require 0.5 million dollars/year or more.

To increase confidence in code results, two efforts are underway.

1. Within CSNI a verification matrix is being prepared in order to allow comparisons between different codes and to demonstrate the capabilities of these codes. It might be possible to approve a code for licensing



calculations after successfully simulating the experiments of this matrix. In Fig. 4 an overview of the proposed verification matrix is given.

2. Experience shows that the user is sometimes the "most uncertain variable", and therefore it has been proposed to initiate users groups for the codes. This was one result of International Standard Problem Exercises, when different participants used the same code version.

Considerable research results, valuable code work and operating experience have been accumulated during the last three decades in the nuclear field. For the overall benefit efforts should be undertaken to use this know-how also in non-nuclear areas.

Based on the current state of knowledge systems can be optimized, e.g. by adjusting number, pressure level and injection location of ECC-systems. As an example, in the FRG high pressure injection has been relocated from the cold to the hot leg side to avoid pressurized thermal shock.

In summary:

What has been done?

The main objectives for thermohydraulics and fuel behavior research within the DBA frame have been achieved.

What remains to be done?

- System behavior assuming multiple failures should be simulated in computer codes and test facilities mainly to study the interaction between different components including instrumentation and control more realistic. This recommendation is supported by operating experience.
- Fast running codes are required for plant analysers and simulators.
- Three dimensional effects have to be studied and modelled in some areas.
- At all times at least one test facility should be maintained to allow fast reactions in case of unforeseen events.
- Improve confidence in computer code calculations by using verification matrices and install users groups.

#### PHYSICAL PHENOMENA AND SYSTEM BEHAVIOR DURING SEVERE ACCIDENTS

To further assess the overall safety of plants, analyses and experiments are currently underway using the assumption that ECC-systems are partly, temporarily or completely ineffective.

The objective is to study the physical phenomena and system behavior during severe accidents with the aim to identify and - if advisable - to further reduce potential risks.

Risk studies and the TMI-2 accident have increased the efforts in the severe accident area. Whether and which additional safety systems are appropriate to minimize technical risks has to be decided on the basis of sound analyses of the real system behavior in case of an accident.

For the analysis of the analysis of in-vessel behavior it is useful to define three categories of core degradation.

- Category I: Core temperatures and core damage stay within design limits but licensing requirements have been violated.
- Category II: Core is degraded to an extent that cooling can be restored by flooding.
- Category III: The coolability of the core cannot be restored, rapid energy transfer into the remaining fluid may happen.

Using this categorization, in contrast to a "melt no melt" approach the effectiveness of measures against core melt (accident management) can be assessed more adequately.

Experimental and analytical work on core behavior has been performed or is underway. The progression of accident investigations into substantial core degradation and finally core melt resulted in out-of-pile and in-pile experiments for oxidation behavior, hydrogen production,  $UO_2$ - $ZrO_2$ -interaction, debris bed formation and the beginning of core melt. Most experts agree that relatively simple codes should be linked to those experiments. This opinion is based on the lack of experiments studying the maximum permissible core degradation under which cooling can be restored ("point of no return").

Steam explosion phenomena have been subject to intensive research. Although detailed mechanisms are still imperfectly understood, it can be judged that in-vessel steam explosions capable of damaging the containment are very unlikely.

In fig. 5 the times for specific events, such as core uncover, are shown. For the most probable cases, transients and small breaks, generally hours are available before high core degradation would occur. The time span would allow for appropriate counter measures. For example, to increase the time to core uncover in case of high system pressure, the accumulator could be used. By opening the pressurizer valves, the system pressure could be sufficiently decreased to allow accumulator injection (fig. 6). This water reservoir of the accumulators alone would increase the time until core uncover by about 1 1/2 hour, so that other actions could be undertaken by plant personnel.

In summary, appropriate accident management actions have the potential to decrease core melt probability substantially.

Ex-vessel phenomena cover a wider range of events, e.g. rapid melt/water interaction, melt/concrete interaction including crust formation, hydrogen distribution and burn, temperature and pressure behavior. Excellent work is underway and will improve the understanding of those phenomena.

Containments are designed for DBA's with safety margins which would allow, in general, higher loads than design loads. Therefore, with most containments, no early failure would occur except in case of leakages.

Appropriate measures, using existing components, could further reduce the loads on the containment. It has to be analysed which measures should be taken after electrical power is restored. Studies performed and system behavior during the TMI-2 accident have shown that a flexible use of existing systems can effectively be used to restore coolability and to prevent core melt through.

Survivability of instruments and necessary components should be tested. The assessment of loads on containment, structural components and instruments should be based on realistic conditions in order to avoid an accumulation of conservatism. Uncertainty bands of the results should be estimated which is sometimes difficult due to the lack of experimental data.

The knowledge of the behavior of fission products during a hypothetical accident has been very much improved in the last few years and conservative assumptions could be reduced. With the better understanding of the relevant processes a reduction of estimated source terms could be achieved.

The amount of reduction of the source term, however, depends very much on both the reactor type and the special accident sequences. The source terms are greatly influenced for example by the deposition in the primary system for small LOCA, by the separation within the containment and by the retention in the annulus and auxiliary building in the case of containment leakages. An international consensus on fission product behavior in the case of an accident should be achievable within the next years.

In summary:

What has been done?

An extensive research program is underway or has been completed with many results already in hand. Further results will be available within the next years.

What remains to be done?

- Containment failure modes and possible leakages should be studied in more detail.
- A common understanding about the physical phenomena and their relevance has to be reached, e.g. through CSNI expert groups.
- Accident management should be further improved to allow appropriate measures using existing components.

#### MATERIAL ISSUES OF THE PRESSURE BOUNDARY AND SECONDARY CIRCUIT

The main safety objective is to avoid material failures which could initiate accidents. Therefore,

- possible failure mechanisms and the influencing variables must be understood
- the safety margins should be known at any time
- the quality of design and material must be high to minimize the potential for failures.

Material aspects related to components are - due to time limitation - not part of my presentation.

In the past, the causes responsible for the development of micro- and macro-cracks in heat-affected zones have been determined and the significance of these defects with respect to the safety of the components has been deeply investigated. In addition, optimized parameters to prevent cracks and degradation of material toughness for new components have been studied and approaches to determine the critical crack length and leak-before-break conditions have been developed. Remote control

manipulators and computerized data processing are used to improve non-destructive testing techniques.

Based on these improvements it has been decided in Germany and in the US (for some plants) that a guillotine-type break of a main coolant pipe has only to be considered for specific "umbrella-type" analyses. This approach results in a simpler layout of the system by eliminating pipe whip restraints, optimizing the supports and simplifying and making more effective inspection.

In the future, research in material issues has to be continued to further improve and validate knowledge and calculation methods.

#### PROBABILISTIC METHODS IN REACTOR SAFETY

The objective is to gain additional insights into safety aspects to improve the reliability of system and to develop a quantitative measure of safety.

Very high functional reliability of safety related systems has always been a major demand in reactor technology. Deterministic criteria have been and are being applied to assess reliability, e.g. the single-failure criterion, and the requirements of redundancy, diversity and fail-safe-design.

Soon, however, efforts have been made to arrive at quantitative measures of reliability. For that purpose probabilistic methods have been developed and are being used in growing extent. The use of probabilistic methods has been stimulated by various incentives.

- To arrive at highly reliable systems, it is helpful to compare different system designs and procedures. The most appropriate way is to quantify and to compare the respective reliabilities.
- It was felt that the application of deterministic criteria, although leading to a high level of overall safety, can not guarantee a balance between the different aspects of safety. A comprehensive probabilistic analysis of the plant, considering the interaction of the various safety and operational systems, can determine weak features in sensitive areas as well as excessive features in less important areas.
- Beyond the scope of system reliability assessment probabilistic methods are being extensively used in risk analyses. Some of these studies have been aimed at an estimation of the accident risk, which is posed to the public by nuclear power plants. Up to now, more than 30 Probabilistic Risk Analyses (PRA) have been performed in different countries.

Today, the probabilistic approach is considered mainly as an alternative, and in many respects powerful method to assess the technical safety. The use of PRAs in public discussion plays only a minor role for several reasons which will not be discussed here.

Probabilistic safety analyses have proven to be useful in many instances, for plant specific as well as for generic decisions. They provide information in which way core damage could occur and how it can be prevented and they allow a relative ranking of safety issues. In many cases, qualitative insights gained during the analysis are more important than quantitative bottom line results.

Probabilistic analyses and especially PRAs are an attempt to prognosticate the future behavior of systems. Like all prognoses they are unavoidably affected with uncertainties. Various sources of uncertainty can be identified, ranging from incomplete knowledge of accident behavior of the plant to the lack of component and human reliability data. Some of the problems are inherent to the method. So, it will always be necessary to include subjective judgment especially if very remote accident sequences have to be considered.

An intensive evaluation of operating experiences and a comparison with analytical results is most important for further improvements.

What has been done?

- Effective probabilistic methods have been developed and applied in many instances to gain better insights into safety issues.
- They are widely accepted as a useful addition to the approved deterministic approach.

What remains to be done?

- A broader basis for component reliability data has to be established. For this purpose detailed evaluation of operating experiences including maintenance and repair of components is required.
- The confidence in probabilistic analyses should be improved by comparisons between operating experience and analytical results on the level of systems. Appropriate analytical consideration of system interdependences has to be checked by evaluating abnormal occurrences.
- Methods have to be developed and data have to be collected which allow a more realistic consideration of human influence and common cause failures.

#### OPTIMIZATION OF INSTRUMENTATION AND CONTROL SYSTEMS, INCLUDING MAN-MACHINE INTERACTION

The objective is to improve the plant availability while maintaining the high safety standard by means of advanced I&C systems, by computerized aids to the operators and by early detection of incipient failures.

The availability (and safety) of nuclear power plants is considerably influenced by the effectiveness of I&C systems, by the degree and scope of automation, by the skill and knowledge of the operating crew and by the quality of maintenance.

Substantial research in the human factors area has been performed especially in the US during the last years following the TMI-accident. This has led to improvements of the control room design, of operating procedures and of the training of personnel.

Nevertheless, there is still a need for further research especially with respect to a better structuring of alarms, a greater transparency of complex systems, a better support in decision making. In addition, maintainability and testability of systems should be improved.

Extensive work has been performed in this area in the various countries, which can only be highlighted here.

The development of various Safety Parameter Display Systems (SPDS) the human factors field, research on modified I&C-concepts characterize the US-situation.

The work in France was concentrated to a great extent on the development of a symptom-oriented approach for unforeseen events. The introduction of the so-called U- and H-procedures and of the pertinent hardware features as well as research on the organizational aspects indicate the leading role in this field.

In Japan great research efforts are undertaken to develop advanced control rooms and computerized operator aids.

The situation in Germany is not directly comparable because of the early introduction of a high degree and scope of automation within the operational systems and also within the engineered safeguards. Especially the limitation systems have to be mentioned. They have demonstrated their effectiveness in limiting disturbances and avoiding unnecessary scrams, component stresses and containment isolation.

They allow for an early detection of disturbances and for appropriate countermeasures like limitation of reactor power and other process parameters. These systems allow to restrict the reactor protection system to such events when the reactor has to be shutdown together with containment isolation in most cases.

Another important aspect is the use of redundant control systems in order to reduce deviations from normal operation caused by control system malfunctions. This I&C-concept has proven to be effective. Further development of microprocessor technology will allow even more efficient limitation and control systems. Other areas of interest are the development of advanced control rooms with computer-based operator aids.

In order to detect incipient failures as early as possible, diagnostic methods like loose-parts monitoring and on-line vibration analysis are being developed. Up to now the long-term stability of monitored vibration functions (patterns) during the undisturbed power operation could be shown.

The main aim of further research is to study the influence of changed operational conditions (reactor power, pressure, temperature, number of main coolant pumps in operation) on the patterns. In a second step influence of changed mechanical parameters on these patterns will be investigated by analytical model calculations.

By comparing the two kinds of deviations in the monitored functions a bandwidth of "allowed changes" of the patterns in question can be defined and recommendations for performing vibration monitoring will be worked out.

In addition to training simulators more flexible plant analysers are under development in different countries using existing as well as newly developed safety analysis codes. The analysers should be capable to provide easy-to-use, cheap and reliable tools for fast analysis of transients and loss-of-coolant accidents.

What has been done?

- Advanced design of instrumentation and control systems, based on operating experience and pertinent research, has improved plant availability and safety.

- Human influence on plant safety, in spite of automation, has been realized. This resulted in initiation of relevant research projects.

What remains to be done?

- The general philosophy should be to detect disturbances as early as possible in order to avoid hard countermeasures.
- Systems should be designed to allow a flexible response to abnormal occurrences.

#### INTERACTION BETWEEN RESEARCH AND LICENSING

In most countries, responsibility for reactor safety research is maintained separate from licensing and supervision of operation. Research has to develop the knowledge needed, while licensing has to determine the necessary safety level.

In the licensing process, the results of research must be considered in order to achieve well balanced decisions. On the other hand research has to consider operational experience, but it must remain free from licensing pressure. Research is broad; licensing is somewhat more focused on actual needs.

In reactor safety research one has to adopt a realistic, best estimate philosophy, while in licensing a conservative approach which sometimes results in nonphysical assumptions and results, must be maintained.

Therefore, to improve confidence, the physical process should always be simulated using best estimate procedures and conservatism should be applied only to design limits (safety margins) and initial and boundary conditions (e.g. initial power level and system availabilities).

The licensing process is mainly based on rules and guidelines. These rules and guidelines must satisfy licensing requirements while maintaining enough flexibility to allow and encourage progress. In my view, too many regulations and overenforcement hinder rapid incorporation of new results, actual needs and potential improvements. Countries with significant operations and licensing experience should be encouraged to adjust rules and guidelines more often to actual needs than it is experienced now.

Finally, international cooperation in research areas has been significantly improving and common understanding is progressing e.g. through CSNI efforts.

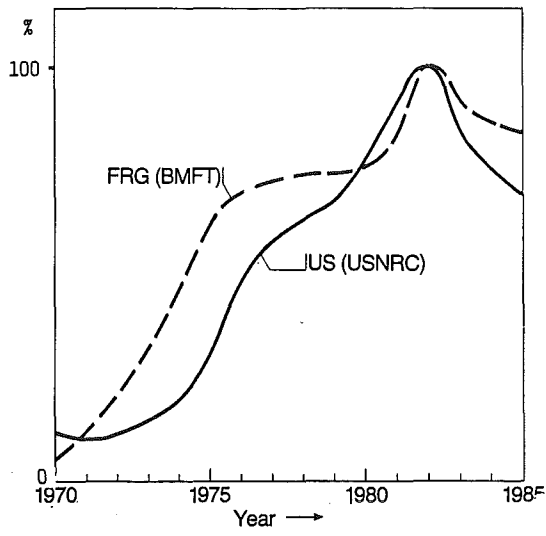


Fig. 1: Relative Budget Development in Selected Organisations

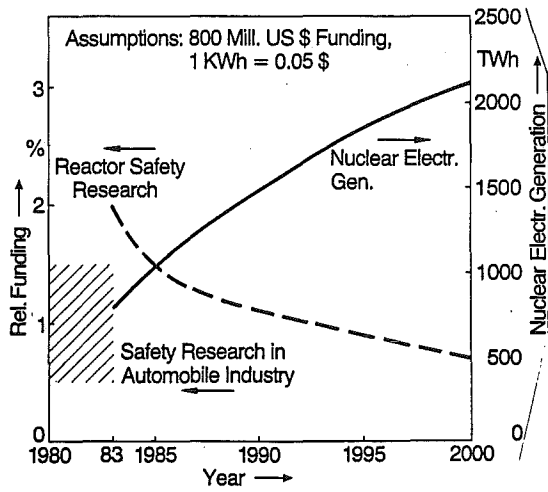


Fig. 2: Nuclear Electricity Generation (OECD Countries) and Relative Funding for Reactor Safety Research



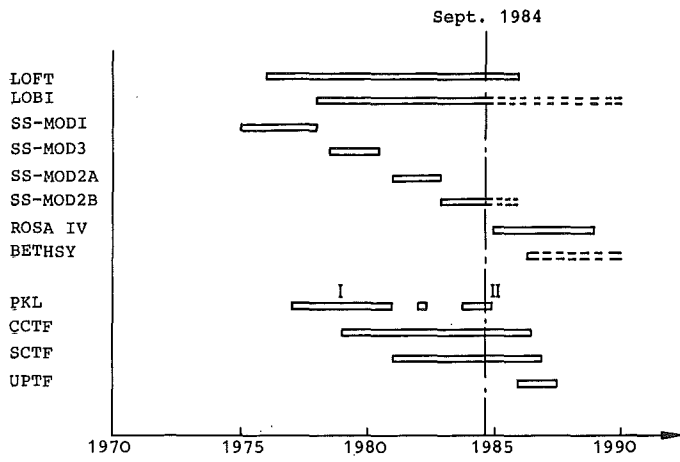


Fig. 3: Time Schedule of Integral Tests

		Transients	Small/ Intermediate Break LOCA	Large Break LOCA
Separate Effect Tests	no. of facilities	-	6	10
	no. of tests	-	13	20
System Behavior Tests (no. of tests)	LOFT (3)	LOFT (7)	LOFT (4)	
	ROSA-IV (open)	ROSA-IV (open)	CCTF (3)	
	LOBI-II (open)	PKL (4)	PKL (3)	
		LOBI-II (2)	LOBI-I (4)	
		SEMISCALE (2)	SEMISCALE (2)	
	BETHSY (open)	BETHSY (open)	(BETHSY, open)	
	SPES (open)	SPES (open)	(SPES open)	

Fig. 4: Proposal for an Assessment Matrix for PWR System Codes

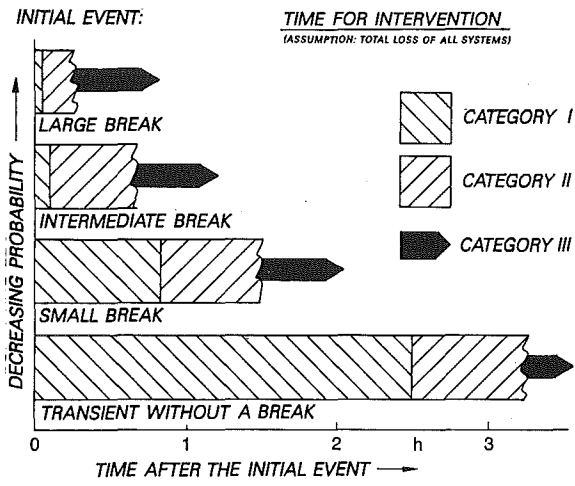


Fig. 5: Categories of Accidents

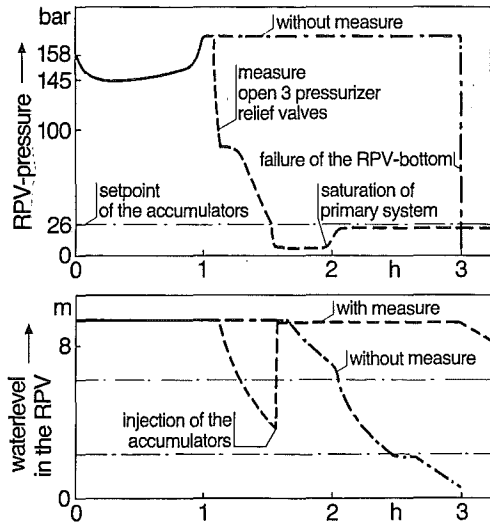


Fig. 6: Example for an Unspecified Action  
Event: Station black out  
Measure: Open 3 pressurizer relief valves

Chapter 2  
Safety Related Operation Experience

	pages
2.1 K.J. Laakso: Systematic Analysis of Plant Disturbances with a View to Reducing Scram Frequency	181 - 190
2.2 R. Japavaire, B. Fourest: An Example of Operating Experience in France: The Tricastin 1 Incident on August 3, 1982	191 - 198
2.3 G. Gros, D. Perrault: Control Rod Guide Tube Support Pin Cracking at French Plants	199 - 209
2.4 P.J. Amico: Fault Tree Analysis of Westinghouse Solid State Protection System Scram Reliability	210 - 219
2.5 T. Meslin, A. Carnino, B. Payen, A. Cahuzac: Station Blackout: A Test on a Plant at Power Lessons Learned for Safety Studies	220 - 229
2.6 P. Cassette, G. Giroux, H. Roche, J.J. Seveon: Evaluation of Primary Coolant Leaks and Assessment of Detection Methods	230 - 238
2.7 G. Dredemis, B. Fourest: Systematic Safety Evaluation of Old Nuclear Power Plants	239 - 247
2.8 J. Magdalinski, R. Ivars: Hydrogen Water Chemistry - A Proven Method to Inhibit Intergranular Stress Corrosion Cracking in Boiling Water Reactors	248 - 257

pages

- |      |  |           |
|------|--|-----------|
| 2.9  | R. Schraewer, B. Wintermann:<br>The Fine Motion Control Rod Drive and Reactor Scram<br>System of KWU; Design, Long Term Operational Behaviour<br>and Experiences | 258 - 267 |
| 2.10 | E. Legath:<br>Power Uprates in ASEA-ATOM Boiling Water Reactors  | 268 - 272 |
| 2.11 | K. Fischer, H. Kastl, M. Kurzawe:<br>Dose Reduction by Application of Advanced Methods<br>for Testing and Repairing of Steam Generator Tubes                     | 273 - 282 |
| 2.12 | R.G. Sauvé, W.W. Teper<br>Investigation of A Liquid Zone Control Assembly Failure<br>at a Nuclear Generating Station   | 283 - 294 |

## SYSTEMATIC ANALYSIS OF PLANT DISTURBANCES WITH A VIEW TO REDUCING SCRAM FREQUENCY

Kari J. Laakso

AB ASEA-ATOM  
S-721 04 Västerås, Sweden

### ABSTRACT

The goal of this project is to improve plant safety and reliability in Swedish BWRs by reducing the frequency of reactor scrams.

The history of plant disturbances leading to reactor scrams and turbine trips in five Swedish nuclear power units was reviewed and the contributing causes were carefully analyzed. A total of 625 plant disturbances was included in the search.

Improvements to be made in the units were identified and the merits of possible modifications were assessed using reliability engineering and PRA techniques. Emphasis was given to design improvements in the NSSS (Nuclear Steam Supply System) as well as in the electricity generation (turbine plant) area.

Examples of various types of recommended modifications will be given, including either their proven or expected efficiency in reducing scram frequency.

The project [1] was sponsored by the Swedish Nuclear Power Inspectorate.

### BACKGROUND

The background to this study is that the probability of deficient reactor core cooling, which may cause severe reactor core damage [2], being caused by transients is much higher than that caused by a postulated LOCA (Loss-of coolant accident). Sufficient reason exists therefore to aim at decreasing the reactor scram frequency even further. Such a reduction of transient frequency would also lead to a reduction of unanticipated electricity production losses and to a reduction of thermally and dynamically induced stresses that may contribute to damage and leakage in components and piping. Some transient events, for instance turbine trips, which do not lead to reactor scrams may, nevertheless, have an effect on nuclear safety. A reduction of such events also contributes to a lower probability of deficient core cooling.

Another background to this study is the principal recommendation - included in the U.S. Kemeny Commissions report [3] and in the Swedish State Public Investigation [4] after the nuclear accident in 1979 at Three Mile Island, U.S.A. - that the industry needs an improved feedback and learning from operating experience.

The present study is based on follow-up and analysis of Swedish BWR plant disturbance experience up to and including 1982. The units are of earlier ASEA-ATOM design and they are owned by Swedish utilities. Four of the five turbine plants analyzed are designed by and manufactured by ASEA STAL AB, three of them in license co-operation with Brown, Boveri & Cie. The first unit, Oskarshamn 1, was synchronized to the power grid in 1971. In this way the study covers an analysis and feedback of a total of 44 years operating experience.

In the case of the later BWRs, since 1980-1982 in commercial operation, a systematic approach was taken to reduce the transient frequency. Feedback of operating experience from the earlier units was implemented in the functional analysis and commissioning of the newer units and in the training of their personnel by the vendors and the owners. Suitable design modifications were introduced as a result of the analysis of commissioning tests and experienced operational disturbances, in these newer units TVO I and II (ASEA-ATOM turnkey deliveries in Finland) and Forsmark 1 and 2 in Sweden.

The resulting design improvements, the more mature BWR design implemented by the vendors (ASEA-ATOM and ASEA STAL) and the performance of the utility personnel have contributed to the fact that these newer units have exhibited a fairly low scram frequency from the start of operation. For example, the mean figure for TVO I and II is about 2 scrams per year and unit during the later period 1982-1983. It is therefore evident that this design and operating know-how can, in a systematic way, be used to support the owners in reducing the transient frequency in BWRs even further.

#### THE NUMBER OF THE EVENTS

The project "An analysis of steps to be taken in order to reduce the reactor scram frequency in Swedish BWRs" covers the history of all plant disturbances leading to automatic or manual reactor scrams, turbine trips and generator load rejections in five different units.

The annual distribution of the number of reactor scrams in the two oldest units, from the first synchronization with the grid up to and including 1982, is presented in Fig. 1.

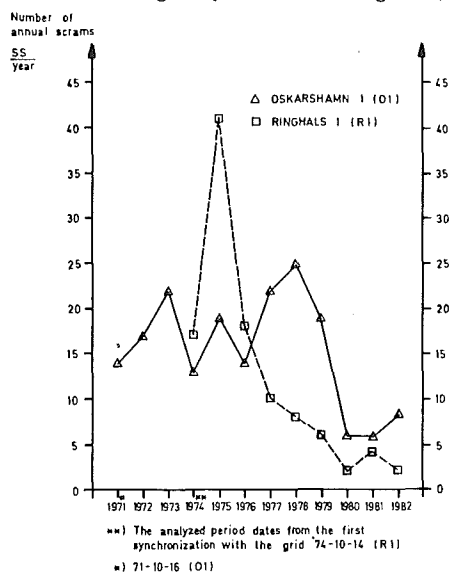


Fig. 1 Oskarshamn 1 and Ringhals 1 units.  
Comparison of the annual scram frequencies

The long-term trend for the number of these events has been decreasing. The mean figure for e.g. the 1st unit in Ringhals is about 12 scrams per year. The trend for the scram frequency in this unit has been, however, decreasing since 1976 and is now 3 scrams per year during the later period 1980-1982.

The study contains an analysis of a total of 625 events, of which 476 are reactor scrams and 240 turbine trips, some of which also gave rise to reactor scram. Reactor scrams occurring at all operational states (incl. trips during start-up or shut-down of the reactor when the reactor was critical) were included in the search.

A total of 1188 failure events has been identified as contributing causes to the analyzed plant disturbances in the five different units. The failure events which have contributed to the reactor scrams in the first unit of Oskarshamn have been broken down into plant parts and failure types in Fig. 2.

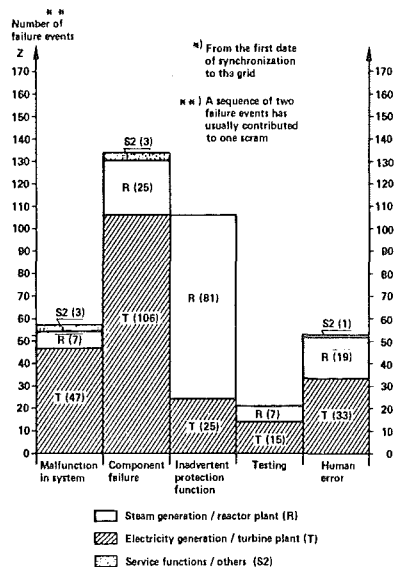


Fig. 2 Oskarshamn, unit 1  
Reactor scram analysis. Breakdown of the failure events (1971\* - 1982) into plant parts and failure types

As seen in Fig 2 a large number of failure events, which have contributed to reactor scrams, originate from the turbine plant systems and components and from the inadvertent protection functions of the reactor.

#### METHODS AND MODEL USED IN THE ANALYSIS

The sequence of the plant disturbances, and the failure functions contributing to reactor scrams, turbine trips and generator load rejections, has been analyzed by using the event reports or analyses, operation reports and maintenance reports from the power plants as source material. Additional information, concerning the disturbances and the corrective actions, has been collected through discussions at the units. Preliminary event analyses, prepared during this project, were used as source material for these discussions with the operation management and personnel.

To be able to systematically identify the contributing causes to the plant disturbances and to divide the contributing causes into failure types five different failure types were defined. The failure types are shown in Table I. The failure types are specified so that each one is matched with one type of corrective action required.

Table I Failure types

<p><u>1. System malfunction</u></p> <ul style="list-style-type: none"> <li>- Unsuitable design due to insufficient knowledge of behaviour of process variables</li> <li>- Poor redundancy</li> </ul>
<p><u>2. Component failure</u></p> <ul style="list-style-type: none"> <li>- Component unsuited to the environment</li> <li>- Unreliable component which can be a result of poor preventive maintenance</li> </ul>
<p><u>3. Inadvertent protection function</u></p> <ul style="list-style-type: none"> <li>- Protection function was tripped even though the event would not have caused any damage (if the trip had not occurred)</li> </ul>
<p><u>4. Testing</u></p> <ul style="list-style-type: none"> <li>- Intentional trip due to planned test</li> <li>- Unplanned trip initiated during testing</li> </ul>
<p><u>5. Human error</u></p> <ul style="list-style-type: none"> <li>- Incorrect, incomplete or unclear operating instructions (procedures)</li> <li>- Deviations from operating instructions</li> </ul>

In order to be able to systematically divide the contributing causes to the plant disturbances into the plant parts and equipment involved, a suitable functional group division was developed for this study.

These functional groups (FG) have been made similar for different units. Therefore these FGs can easily be used for transfer of operating experience concerning failure functions and corrective actions between different units at functional group level.

This functional group division is based on function, and not on the hardware, which makes a functional analysis of the plant disturbances easier than by using the traditional plant system and equipment classifications.



An example of an event analysis concerning the Ringhals 1 unit is shown in Fig. 3 as follows.

EVENT ANALYSIS - RINGHALS 1		
BLOCK R1	DATE 190623	TIME 15.53
	SKI NO	109
TRIPPING CONDITION	1: LS	GENERATOR LOAD REJECTION, TURBINE TRIP AND
	2: TS503*004	BYPASS BLOCKING OF ONE TURBINE
	3: S511	REACTOR SCRAM
	OPERATIONAL DATA BEFORE DISTURBANCE	OPERATIONAL DATA AFTER DISTURBANCE
OPERATIONAL STATE	A	
REACTOR POWER (MWT)	2100	
HC-FLOW (KG/S)		
CONTROL ROD CONFIGURATION		
GENERATOR POWER (MWE)	709 (+ 383 + 326)	000
FAILURE EVENTS	FUNCTIONAL GROUP	FAILURE TYPE
1. EARTH FAULT CURRENT IN THE 400 KV-TRANSMISSION LINE AND IN THE MAIN TRANSFORMERS FOR RINGHALS 1 CAUSED BY LIGHTNING. THE 400 KV-LINE STENKULLEN - STROMMA - HORRED TRIPPED OUT.	S2:07	2
2. BOTH THE BLOCK BREAKERS 621 T11/T12-400-S TRIPPED AND THE CONNECTED TURBO GENERATORS T611 AND T612 TRIED TO ESTABLISH AN IN-HOUSE TURBINE OPERATION. ONE OF THE STEAM THROTTLE VALVES FOR ONE OF THE HP-TURBINES, T611 PROBABLY CLOSED TOO SLOWLY. TURBINE T611 THEREFORE ACCELERATED, WHICH GAVE TURBINE OVERSPEED TRIP (TS503).	T1:01	1
3. THE SPEED OF THE TRIPPED TURBINE T611 DECREASED AND LED TO VOLTAGE DROP IN THE 6 KV AUXILIARY POWER SUPPLY, WHICH GAVE STOP OF THE CONNECTED CONDENSER COOLING WATER PUMPS ABOUT 1 MINUTE AFTER THE LIGHTNING. THIS GAVE RISE TO BY-PASS BLOCKING (004) INTO THE CONDENSER CONNECTED TO THE TURBINE T611.	T4:04	1
4. THE REACTOR POWER WAS AUTOMATICALLY REDUCED, BUT THE POWER STILL SLIGHTLY EXCEEDED THE DUMPING CAPACITY OF THE REMAINING (T612) CONDENSER. THE REACTOR WAS SCRAMMED BY THE TRIPPING CONDITION S511 (TURBINE TRIP AND BYPASS BLOCKING OF ONE TURBINE AND REACTOR POWER > 607).	R1:06	1
FUNCTIONAL GROUPS:(FUNCTION/EQUIPMENT)	FAILURE TYPES:	
R1 STEAM GENERATION/REACTOR	T1 GENERATION OF MECHANICAL WORK/ TURBINE	S1,S2 SERVICE FUNCTIONS/ OTHERS
R2 CONTAINMENT OF RADIO-ACTIVITY/SIPS	T2 GENERATION OF ELECTRICITY 20KV/ GENERATOR	1 SYSTEM MALFUNCTION
R3 REACTOR MAINTENANCE/HANLING AND STORAGE EQUIPMENT	T3 FEED WATER GENERATION 70 BAR,180 C/ CONDENSATE FEED WATER AND PRE-HEATERS	2 COMPONENT FAILURE
R4 EMERGENCY CORE COOLING/ SAFETY SYSTEMS	T4 GEN. EL 400 KV, 6 KV /TRANSFORMERS AND AUXILIARY POWER	3 INADVERTENT PROTECTION FUNCTION
R5 SERVICE FUNCTIONS/OTHERS	T5 SERVICE FUNCTIONS/OTHERS	4 TESTING
		5 HUMAN ERROR

Fig. 3 Event analysis. An example

It should be noticed that one reactor scram is usually caused by several interacting failure events and/or functional deficiencies in different plant parts and functional groups of the unit.

All 625 event analyses, worked out during this project, were systematically documented in the similar standardized forms, as shown in the example above. Thus storing of all event analyses in a transient analysis data base was facilitated.

A computer program has been used to store, sort and select the event analysis data accumulated during the study. This computer program has facilitated the statistical treatment of the many failure events and thus the identification of either the recurring event sequences or the recurring failure events and their long-term trends.

For the first unit in Ringhals a probabilistic risk assessment study [5] was available. According to this PRA study the offsite power disturbances have a significant effect as initiating transients on the probability of severe reactor core damage.

Consequently an event tree is prepared in Fig. 4, which is based on selection and a qualitative and a quantitative analysis of both the recurring scram sequences and the interacting failure events included in the scram sequences, occurred as a consequence of offsite power disturbances.

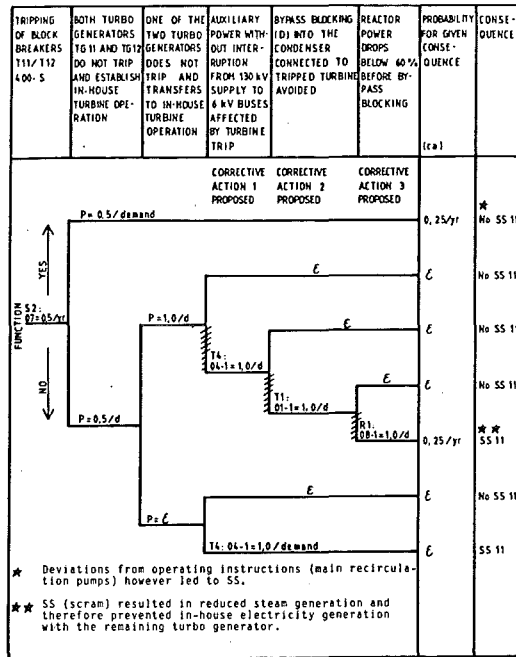


Fig. 4 An event tree showing generator full load rejections which always led to reactor scrams

When working out this event tree several selected event analyses, exhibiting similar event sequences to the analysis in Fig. 3, have been used as source material. In that way all offsite (400 kV) power disturbances, up to and including 1981, were included in the source material.

This prepared initiating event analysis data, in conjunction with identification of the dominant accident sequences that could follow according to the unit-specific PRA study, could then be applied in order to form a model, for ranking the nuclear safety significance of proposed corrective actions. The use of this model resulted in rough quantitative estimates of how the recommended corrective actions, which will give a reduction of the reactor scram frequency, contribute to a reduction of the probability of deficient reactor core cooling.

The steps and methods included in the model for analysis and evaluation of opportunities, to improve both the plant reliability and the nuclear safety, are described in detail in Swedish in the main research report "A Systematic feedback of plant disturbance experience in Swedish BWR power plants" [1].

It is known that partially similar projects to this [6], concerning feedback of operating experience or analysis of accident sequence precursors, are being performed in U.S.A. by e.g. the Institute of Nuclear Power Operations [7], Electric Power Research Institute, Nuclear Regulatory Commission [8, 9] and plant vendors and owners and in other parts of the world. For example, the Nuclear Safety Board of the Swedish Utilities has started ERF - a Swedish computerized information and communication system - for feedback of operating experiences [10], where Asea-Atom is also contributing. The present development work at e.g. the Swedish Nuclear Power Inspectorate aims [11] to tie together the systematic reliability analyses (PRA), the event reports and the event analyses in such a way that a systematic feedback is provided to a number of safety activities.

#### SELECTED AREAS FOR FURTHER REDUCTIONS OF THE SCRAM FREQUENCY AND FOR IMPROVING NUCLEAR SAFETY

Several opportunities for reducing the reactor scram and turbine trip frequency in individual units have been identified during this project.

As seen e.g. in Fig. 2 above a large number of failure events, which have contributed to reactor scrams, originate from malfunctions in the turbine plants and from inadvertent reactor protection functions.

The turbine plants in ASEA-ATOM BWRs are designed with 100 percent dumping capacity in order to be able to cope with turbine trips and full load rejections without reactor scram. The analysis results as illustrated by Fig. 5 show that about 50 percent of all generator load rejections from full power have been accommodated without tripping the reactor.

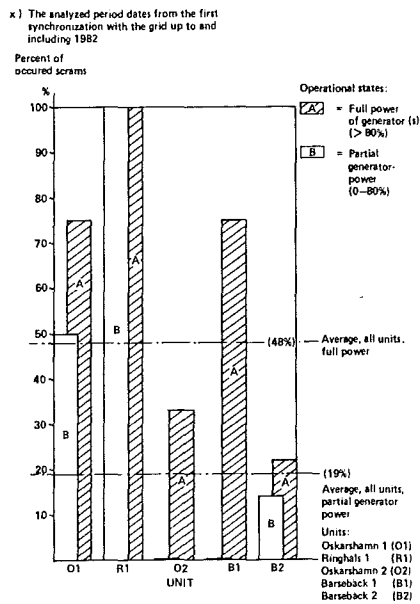


Fig. 5 The proportion of generator load rejections which led to reactor scram

As seen in Fig. 5 the generator load rejections have in the more recently started units studied, Oskarshamn 2 and Barsebäck 2, contributed with a lower, though significant probability to the reactor scrams. Different opportunities for improving this percentage even further, in the case of turbine trips and load rejections in individual units, have been identified during this study. Similar design modifications to these have resulted in an improved performance since being put into effect in the latest BWR nuclear power units now in commercial operation, or in some of the earlier individual units analyzed in this study.

In connection with the evaluation of effected corrective actions, a study has always been made of whether the same initiating failure events have continued to result in scrams. Examples of the proven efficiency, of some of these corrective actions since being put into effect by the vendors and the owners, in reducing scram frequency will be given as follows:

- introduction of a filtration of APRM-scram limit values in the reactor protection system in order to avoid inadvertent scrams. These scrams were caused by very short-lived increase of neutron flux, initiated by pressure transients (turbine control and bypass valve mismatch) in the reactor core.

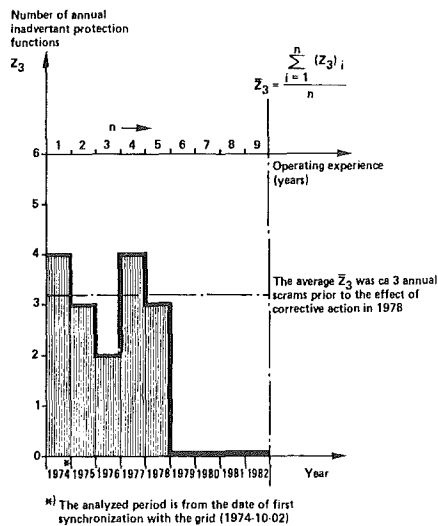


Fig. 6 Oskarshamn, unit 2. Scram analysis. The annual frequency of inadvertent reactor core protection functions

As shown in Fig. 6 corrective actions have given a very promising effect. Operating experience and aforementioned modification in the "oversensitive" reactor core protection system have resulted in a total absence of scrams from this particular problem category compared to an annual average of 3 scrams previously.

- Auto tripping of the partial reactor scram (insertion of only one scram group) in order to achieve rapid reactor power runback necessary in the case of e.g. sudden generator load rejection.

- Improved supervision of the capacity of the operating oil accumulators for the hydraulic operated turbine bypass valves. In this way a prolonged opening time of the turbine bypass valves giving a pressure transient in the reactor core and a reactor scram can be avoided, in the event of turbine trip or generator load rejection.

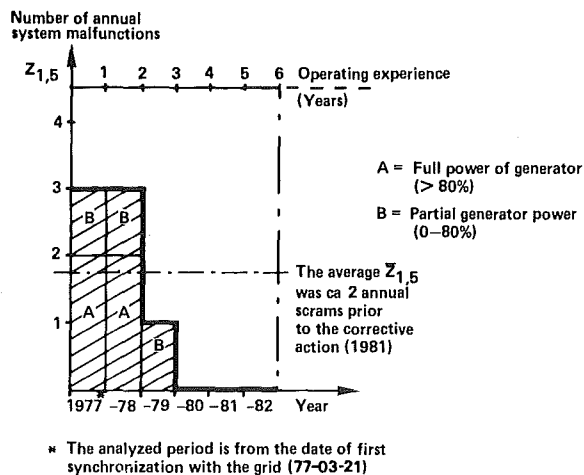


Fig. 7 Barsebäck, unit 2. Scram analysis. The annual frequency of reactor pressure disturbances

As shown in Fig. 7 the corrective action has resulted in an absence of scrams, caused by mismatch of turbine control and bypass valves in the event of turbine trip or generator load rejection.

The expected impact on reducing average scram frequency, of a possible implementation of these aforementioned modifications in the other units studied, was then quantitatively evaluated. These modifications have then been recommended for detailed surveys in the units which by these means, according to the study, exhibit potential opportunities for reducing scram frequency in the event of similar off-site power or turbine plant disturbances. These improvements have afterwards been put into effect, decided or are being surveyed in several applicable units.

The potential quantitative opportunities for reducing scram frequency when implementing corrective actions, in different other problem categories identified in the individual units, were also evaluated and reported in the study.

A pilot analysis was also performed to evaluate which effects some of the proposed corrective actions, for reducing the scram frequency, give on the nuclear safety. In this PRA-application (see Fig. 4 above) e.g. the following proposed actions were found to have a significant improving effect on the nuclear safety in the event of offsite power disturbances.

- automatic tripping of partial reactor scram by the condition of full load rejection of two turbo generators. When implementing this measure the in-house electric load generation, without tripping the reactor scram, can be accommodated to the unit with the second turbo generator, if the first turbo generator trips
- automatic initiation of the rapid switch-over of the backup offsite power to the affected 6 kV-buses in the event of unsuccessful establishment of in-house turbine operation after full load rejection. When implementing this possible measure a loss of feed water flow and loss of condenser vacuum can be avoided if backup offsite power supply is available.

## ESSENTIAL RESULTS

A large number of failure events, which have contributed to reactor scrams, originate from malfunctions in the turbine plants and inadvertent (unnecessary for protection) reactor protection functions. Several opportunities for reducing the reactor scram frequency have been identified during the project and recommendations for improvements in the operating units have been made. These improvements are aimed at eliminating either the primary failures or the secondary contributing causes in the disturbance sequences, otherwise leading to reactor scrams.

The long-term trend of the scram frequency has been decreasing and the average scram frequency in these units of the older BWR generation is about 4 scrams per year and unit in 1980-1982. A clear indication exists, arising from the study, that further reductions in the scram frequency can be achieved by means of design modifications in reactor and turbine systems and improvements of associated procedures.

## ACKNOWLEDGMENT

This research project is performed under the auspices of the Swedish Nuclear Power Inspectorate and in close cooperation with the utilities.

## REFERENCES

1. K J Laakso - Systematisk erfarenhetsåterföring av driftstörningar på blocknivå i svenska kärnkraftverk, Report Asea-Atom KPA 82-114 (in Swedish), Aug. 1983
2. Reactor Safety Study, An Assessment of Accident Risks in U.S. Commercial Nuclear Power Plants, USNRC Report WASH 1400, (Nureg-75/014)
3. J G Kemeny (Chairman) - Report of the Presidents Commission on the Accident at Three Mile Island, U.S. Government Printing Office, October 1979
4. Swedish State Public Investigation, Säker Kärnkraft (Safe Nuclear Power) ?, 1979:68, (in Swedish), Nov. 1979, Stockholm
5. Ringhals 1 Safety Study, Technical Report, the Swedish State Power Board/(AB Asea-Atom), (in Swedish), Aug. 1983, Vällingby, Sweden
6. K J Laakso - A Systematic Evaluation of Transients in Swedish BWR Power Plants, ANS International Meeting on Thermal Nuclear Reactor Safety, Aug. 1982, Chicago
7. E L Zebrovski, S L Rosén - Nuclear Power Plant Safety and Reliability Improvements derived from Operational Experience Analysis, ANS International Meeting on Thermal Nuclear Reactor Safety, Aug. 1982, Chicago, USA
8. C Michelson - Operational Transient Experience-NRC Perspective, Nuclear Power Safety Course, Massachusetts Institute of Technology, USA, July 1981
9. J W Minarick and C A Kukielka - Precursors to Potential Severe Core Damage Accidents: 1969-1979 - A Status Report. June 1982 (NUREG CR/2497).
10. J-P Bento - Experience in Plant Transients. The Swedish RKS Program. ANS Topical Meeting. Anticipated and Abnormal Plant Transients. Sept. 1983, Jackson, USA
11. L Carlsson, L Högberg, L Nordström - Notes on three Key Tools in Safety Analysis and Development: Incident Analysis, Probabilistic Risk Analysis and Human Factors Analysis, International Conference on Nuclear Power Experience, IAEA, Vienna, 82-09-13--17

AN EXAMPLE OF OPERATING EXPERIENCE IN FRANCE  
THE TRICASTIN 1 INCIDENT ON AUGUST 3, 1982

R. Japavaire and B. Fourest

Commissariat à l'Energie Atomique  
Institut de Protection et de Sécurité Nucléaire  
Boîte Postale n° 6  
92260 Fontenay-aux-Roses, FRANCE

ABSTRACT

On August 3, 1982, at the Unit 1 of the Tricastin nuclear power plant, the rupture of the plug of a pressure reducing valve on the compressed air system serving the containment air lock resulted in the loss of air to the inflatable seal of the two air lock doors ; the loss was signalled in the control room by the alarm "air lock 0 m untight".

The containment integrity was lost for 45 minutes ; but the activity released to the outside was very slight. By a rapid intervention of the operator (another plug was put on) the compressed air feeding was restored and consequently the hatch tightness ; the unit remained on power during the intervention.

The basic cause of the incident is a design error : the non-respect of the single failure criterion on one auxiliary system of a function important for safety (containment integrity).

This example of an incident, one of the most significant in French 900 MWe PWR units since their commissioning, will serve as an illustration of the experience feed-back process in France. Difficulties in the implementation of the correctives actions decided after the incident resulted in unjustified delays and in reoccurrences of similar incidents.

INTRODUCTION

From the late seventies both the French utility (E.D.F.) and the French safety authorities have been developing a system to collect, screen and analyze incidents, occurring in pressurized water reactors that came into operation, and to define subsequent corrective actions. For more than two years this system has been fully operational and works satisfactorily.

With the example of one of the most safety significant incidents experienced on a French unit, this paper provides insight on the methodology used for in-depth analysis of incidents in France.

However there are some difficulties in timely implementation of the corrective actions defined after such an analysis. Experience shows that delays in the detailed study of the modifications and in their implementation can result in similar incidents reoccurring.

#### INCIDENTS SCREENING PROCESS [1]

The Safety Analysis Department reviews, on a weekly basis, all the information pertaining to the safe operation of French PWRs. This information may be obtained either by formal report for significant incidents or through the E.D.F. event computer file for less significant events. All this information is classified according to the following four categories :

- 1) Events that do not require specific corrective action are just stored in the computer file (between 500 and 1000 per year : about 1 per unit and per week).
- 2) As a minimum, all incidents notified as significant go through a rapid review in order to detect whether they might be a precursor of a more severe accident and to verify that the corrective actions proposed by the licensee are acceptable and sufficient (about 250 per year).
- 3) Incidents that are potentially expected to be precursors or that are deemed to contain many interesting lessons, are submitted to an in-depth analysis as described below. This analysis leads to detailed recommendations (between 10 and 20 per year).
- 4) Trends or patterns studies cover a series of events with common characteristics, i.e. series of events which affect the same system or component.

#### IN-DEPTH ANALYSIS GENERAL METHODOLOGY

For in-depth incident analysis it is absolutely necessary to obtain additional information through technical discussions on the site with the licensee including, where necessary, with the operators who experienced the incident in order to have a good understanding of the incident sequence and circumstances.

The analysis in itself is done essentially through several interrogations and a search for answers :

- Interrogation about consequences : it is rather easy to determine the actual consequences of an incident in terms of component damage or health effects for the public or plant staff. It is much more difficult to assess its potential consequences. This means how the incident could have resulted in more severe consequences with different initial conditions or with other failures ("what if" process). This very analysis of potential consequences is of major importance to characterize the exact level of significance of the incident and therefore the priority to be attached to the corrective actions.
- Interrogation about causes : this process should go as far as possible to reveal the root causes among the various factors that could have contributed to the incident occurrence. This should be an opportunity to determine whether these causes are generic (i.e. lessons are applicable to a serie of units).



- Interrogation about operator actions and reactions, in order to assess the different factors which have affected their behaviour (training, procedure completeness and clarity, man-machine interface...). This phase also includes a review of technical specifications as they relate to the course of the incident.
- It is also to be underlined that an in depth incident analysis should not be performed apart from the general context of other incidents occurring on operating plants throughout the world and cannot be limited simply to the facts that actually took place in the incident sequence. It is very important to look for analogical incidents and to try to make comparison with similar situations already experienced elsewhere during such or such part of the incident.  
 Putting an incident in the general perspective of worldwide accumulated experience is the best way to identify the general lessons which are undoubtedly the most beneficial for nuclear safety.
- Lastly, an in depth analysis includes an assessment of the corrective actions proposed by the licensee and, if needed, recommendation of additional measures that appear necessary as a result of the preceding steps.

The recommendations resulting from these analyses are discussed with E.D.F. at periodic meetings in order to compare the lessons learned and to follow up on the actions taken by the licensee, up to the implementation on each unit.

#### LOSS OF CONTAINMENT AIR LOCK LEAKTIGHTNESS AT TRICASTIN 1

This incident occurred on August 3rd 1982. It resulted in a temporary loss of the third safety barrier integrity (the  $\beta$  mode of WASH 1400). Because of its safety significance it was analysed according to the process described above. Its main characteristics and the lessons learned are given below.

##### a) Initial condition

The unit was at nominal power. The pressure within the reactor building was 1040 mbars. A controlled purge of the containment by the vent system was planned, but had not yet begun.

##### b) Incident Sequence

At about 1.15 p.m., on August 3, 1982, the appearance in the control room of both alarms : "Air lock 0 m defect" and "Air lock 0 m untight" alerts the control room operator, who reports immediately to the shift supervisor. The latter goes to the air lock. After having checked the local control boards configuration, he hears the sound of an air leak. The plug of the pressure reducing valve EPP 142 VA is ruptured. Consequently, no feeding reaches the air lock door seals. Since the reactor building is in slight overpressure, the pressure drops by 20 mbars ; this depressurisation results in the release of 1000 m<sup>3</sup> into the environment.

Another plug is put on. At 2 p.m., as soon as the plug is in place, the seals are reflat and the containment integrity is restored.

c) Consequences. Significance of the incident

At the time of the incident, the activity of the containment atmosphere was slight ; the actual consequences of the incident as regards the environment were therefore negligible. This was confirmed by the readings of the health physics instrumentations at the site boundary : no variation was noted above the normal background (some  $\mu\text{rad/h}$ ).

This incident resulted nevertheless in a large loss of the integrity function of the third barrier, and had the conditions within the containment been different, the radiological consequences could have been more severe.

To assess more precisely the potential gravity of the incident, several release calculations were made for various initial conditions. The first one corresponds to the maximum technical specifications limits related to the primary coolant activity and leakage. The second one corresponds to LOCA conditions, maximum accident taken into account in the safety reports.

Dose equivalents which would have resulted from the releases made under those conditions would have been :

- in the first case (technical specifications limits) : 0.5 mrem of external exposure and 4 mrem of internal contamination to the thyroid,
- in the second case (loss of containment integrity after a LOCA) : the consequences would have been very severe, and the releases would have exceeded the values considered as acceptable in accident conditions.

d) Causes of the accident

In normal operation, the pressure of the door seals is maintained between 5.6 and 6 bars (relative). By means of an automatic control, air make-up to the seals is provided as soon as the pressure decreases under 5.6 bars. The alarm "air lock defect" is actuated when the periodicity of the air make-up to one of the air lock door seals becomes less than 10 seconds. The alarm "air lock untight" is actuated when the pressure in the seals of the two doors becomes less than 0.5 bar (relative).

From the time the incident was first noticed, the quasi-simultaneous appearance of the two alarms tended to indicate that a very fast deflating of all the seals of the two doors had taken place and therefore the leak tightness of two check valves was questioned. These check valves, EPP 135 VA and EPP 136 VA are located immediately downstream of the pressure reducing valve. However, during tests made to reproduce the incident, it was not possible to reproduce such a rapid depressurization of the whole system. Perhaps when the incident took place, the operator in the control room did not notice the first alarm "air lock 0 m defect" and only became aware of it when he saw the second alarm "air lock untight" appear. Nevertheless this assumption cannot be confirmed, because the information processing system, that records automatically the time of appearance of alarms, was not available at the time of the incident. But it can be noted that the incident occurred just after a staff shift change.

## e) Lessons learned

The incident showed a common mode failure on the air make-up system of the air lock door.

The main following corrective actions were then decided :

- doubling of the pressure reducing valve between the EPP 101 BA tank and the two 135 and 136 VA check valves,
- addition of a device allowing the automatic isolation of the air make-up of the seals of one door, in the event of a pressure drop downstream of the pressure reducing valve serving this door,
- addition of nozzles upstream of the pressure reducing valves and downstream of manual isolation valves of the seals allowing for possible air stand by make-up from a mobile compressor,
- modification of the "air lock defect" alarm setpoints, which will be initiated when the frequency of the air make-up to the seals is less than 2 minutes,
- increase of the "air lock untight" alarm setpoint which will be initiated when the pressure inside the whole of the circuit becomes less than 3.5 bars, a value compatible with the maintaining of the air lock leak tightness under the containment design pressure.

These lessons were discussed and agreed upon between E.D.F. and the safety authorities at a meeting on February 21st 1983. The modifications were supposed to be treated with top priority and be implemented on each unit during the first refueling outage.

In addition E.D.F. decided to replace immediately the plug of the pressure reducing device that failed at Tricastin with a new improved plug on every unit.

## FOLLOW UP ACTIONS

In France, plant management have to submit to the safety authorities two months prior every long outage a program of safety related maintenance activities and modifications to be implemented during the outage [2]. The review of such submittals for several units which were due for refueling outage in the summer of 1983, revealed that the modifications described above for improving the air make-up to the air lock doors seals were not being planned. E.D.F. was required to conduct an investigation which revealed deficiencies in the follow up management after the initial decision about the modifications.

Unit standardization is a characteristic of the French nuclear program. With the full support of the safety authorities, E.D.F. wants all its units of the same design to remain identical throughout their lifetime. That means backfitting has to be decided at the national level and all modifications, unless the minor ones, must receive approval from the headquarter. This implies that every projected modification should be circulated in the various sections of the E.D.F. organization, including those which were involved in the initial design, for detailed studies, review and approval.

This process guarantees better quality of the modifications and better integration in the original design. However this is a lengthy process which requires strong management when a modification has to be implemented on an accelerated schedule.

In the case of the lessons learned from the August 3rd, 1982, incident at Tricastin 1 insufficient management on the follow up decision resulted in about six months delay in the implementation of the modification.

#### REOCCURRENCES

##### - Bugey 2

The design of the air make-up system to the air lock door seals is slightly different on the Bugey units from the other 900 MWe units. However, this design presented the same weakness in sustaining a single failure.

On April 1st 1983 on Bugey 2 a rupture of a filter in the air make-up system resulted in the deflating of all seals on both air lock doors and a loss of containment integrity which fortunately lasted for only about 2 minutes.

##### - Tricastin 1

On April 7th 1984 at the beginning of the annual refueling outage of Tricastin 1 during which the air lock modifications were planned, a similar plug rupture on an other pressure reducing valve of the air make-up system was experienced. However only one air lock door leaked and the containment did not lose its integrity.

##### - Chinon B2

On the eve of a week end May 18th 1984, the unit was running at full power. In violation of quality organization rules, the compressed air system serving the one air lock was valve out for some works without preparing a written temporary operating instruction. Consequently the pressure in the air lock door seals was only maintained by the back up tank 101 BA. Because of the seal natural porosity the pressure began to decrease and the alarm "air lock defect" annunciated it reached 5.6 bars. On May 19th, knowing that some works were being done on the compressed air system the operator did not react to this alarm which sometimes appear frequently. Moreover this alarm regroups several defects none of which require urgent actions. So the pressure in the seals continued to decrease slowly. As the setpoint of the second alarm "air lock untight" had not yet been modified to 3.5 bars, the air lock began to leak in the early morning of May 21st. This loss of containment integrity remained undetected for about 3 hours until a decrease of the pressure inside the containment was noticed.

#### CONCLUSIONS

From the experience reported here several conclusions should be mentioned both from the experience feed-back process and the technical point of view.

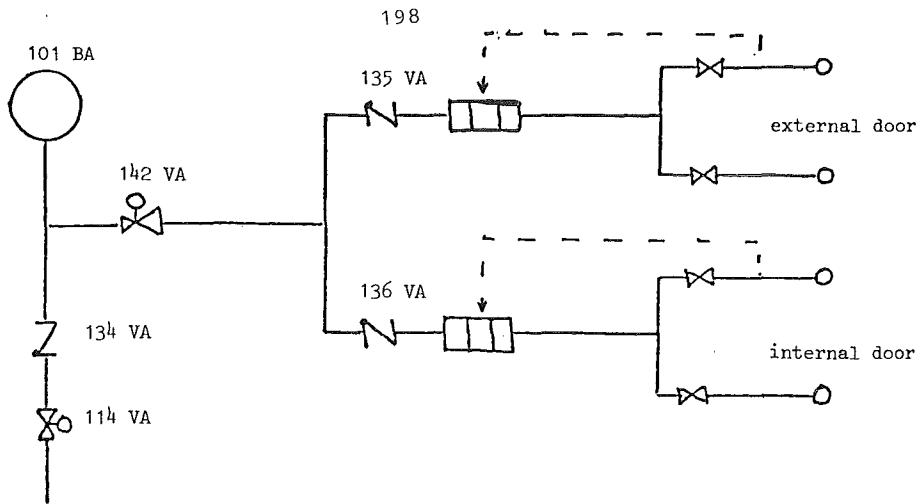
A good system to collect, screen incidents and determine the lessons to be learned is not sufficient for a proper operation of the experience feed back process. Once corrective measures have been defined strong management is essential to ensure timely implementation. In order to avoid conflicting constraints on the various people who have to be involved in the detailed studies of modifications and who sometimes are far away from the actual plant experience, it is necessary to determine priorities in the backfitting process. These priorities should be consistent with the safety significance of the incidents for which corrective measures are defined. Up to now the safety significance of incidents is mainly based on engineering judgement. PRA could be a useful tool in establishing a more quantitative basis for the determination of the time schedule in which to implement corrective actions after significant incidents.

From a technical standpoint these incidents underline once more the importance of support systems, such as the compressed air system, which serve safety related functions.

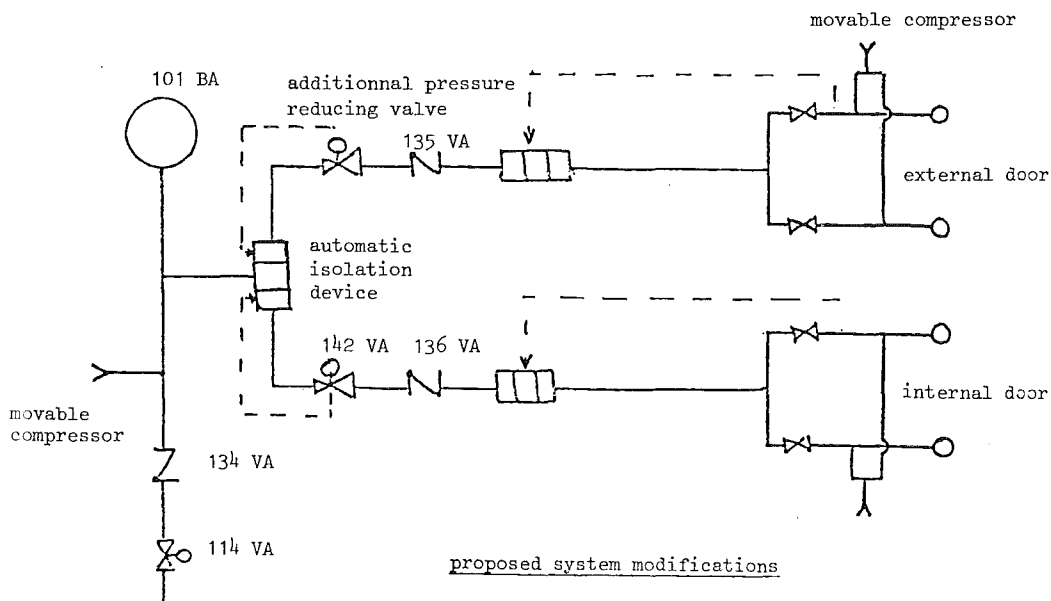
In addition, given these incidents as well as others not mentioned here, the Safety Analysis Department is questioning the reliability of the leak-tightness of the containment air lock doors. The replacement of the inflatable seals on the 900 MWe by a passive system self leak proof under containment pressure, as is already installed on the 1300 MWe units, should be considered.

#### REFERENCES

- [1] Reactor operation feed back in France  
C. Feltin, B. Fourest, J. Libmann  
ANS-ENS Thermal Nuclear Reactor Safety Meeting, Chicago - August 1982
- [2] Le suivi au plan de la sûreté par l'administration française et ses appuis techniques des arrêts prolongés des tranches à eau sous pression des centrales nucléaires.  
D. Favé, JR. Jardel  
IAEA-SM-274/C7 - Karlsruhe - Juin 1984



Containment hatch compressed air system



proposed system modifications

CONTROL ROD GUIDE TUBE SUPPORT PIN CRACKING  
AT FRENCH PLANTS

G. Gros, D. Perrault

CEA/IPSN/DAS  
B.P. n°6, 92260, Fontenay-aux-Roses, FRANCE.

## ABSTRACT

Several ruptures of support pins have occurred in France; some damage was caused to steam generators. The failures were caused by Inconel X 750 stress corrosion; several parameters are assessed. Two safety concerns are analysed: potential control rod guide tube misalignment and consequence of a support pin as a loose part. The conclusion is that a pin failure is of limited safety significance, at least at short term, but the availability can be seriously impaired. That leads to conduct inspections during refueling shutdowns, incorporate a loose parts continuous monitoring system, develop an improved pin design and replace the pins at existing plants.

## INTRODUCTION

The past few years have shown that Westinghouse-designed PWR control rod guide tube pins were subject to a stress corrosion phenomenon which ultimately results in cracking then rupture with potential migration of loose parts into the reactor coolant system.

It was the discovery in autumn 1978, during annual plant inspection, of a pin fragment in a steam generator at the Japanese plant of Mihama 3 which first revealed this anomaly. In 1982, four other discoveries of pin fragments in the reactor coolant system were made: three in France (at Gravelines 1, Fessenheim 1 and Bugey 2) and one in the United States (at North Anna 1).

This paper summarises the action taken in France to remedy this problem: modification of pin design, safety evaluation in case of rupture, protection from loose parts, pin inspection, pin replacement and examination of removed pins.

## PIN DESIGN

1) Pin description and function

Support pins are bolted into the bottom plate of the lower guide tube to align the bottom of the control rod guide tube assembly into the core plate at the top of the fuel assembly. There are two pins per guide tube. They provide lateral support while accommodating thermal expansion of the guide tube relative to the core plate.

The pins are made of Inconel X 750. Each pin incorporates (see figure 1):

- a top section consisting of a shank and a threaded end accomodating the drive nut,
- a collet for precise alignment of the pin in a flange hole,
- a bottom section containing two flexible leaves separated by a groove, which fit into a hole in the upper core plate.

The pin is prevented from rotation relative to the nut by a dowel which radially traverses the nut head. The dowel is welded to a locking device which is prevented from rotation relative to the upper pin section by a slot. Both the dowel and locking device are made of austenitic stainless steel.

To prevent pin fatigue due to alternating stresses exerced by hydraulic loads on the guide tubes, a preload must be provided at joints as follows:

- at the pin/bottom flange joint, preload is provided by tarquing the nut to a value specified on the drawings,
- at the pin/upper core plate joint, flexible leaf size is made to exceed the upper core plate hole diameter, providing a preload during the fit.

## 2) Pin stress corrosion

The anomaly affecting the pin is due to a stress corrosion phenomenon. In most cases this takes the form of intergranular cracks leading to pin cracking and rupture.

The pin stress corrosion phenomenon led to the discovery of two types of rupture (figure 1) :

- at the shank/collet joint,
- in the flexible leaf region.

Note that some cracks have been observed in the thread region (figure 1).

The main parameters influencing stress corrosion are :

- the heat treatment processes undergone by the materials (solution heat treatment and aging)
- stress intensity.

## 3) French pin fabrication and installation characteristics

In France pins have different characteristics for two reasons:

- . the reference specification has been subjected to variations in the following areas :

- solution heat treatment,
- aging heat treatment,
- torquing.

- . Framatome has three different pin manufacturers dealing with three different steelmakers for their INCONEL X750 bar procurement; pin fabrication by these steelmakers varies in certain areas not covered by the specifications (forging sequence, intermediate hardening ...).



During the period preceding the discovery of pin anomalies in Japan, the above factors led to wide pin diversity in France.

Based on the parameters considered as the most important as regards stress corrosion (solution heat treatment and torquing), the pins existing at this time in French power plants were classified into 4 groups.

#### 4) New pins

The occurrence of pin cracking in Japan led Westinghouse to design during 1979 a new pin model capable of being installed in new units. A summary of the design support work for these new pins is given below.

Initial studies were conducted by Westinghouse to reduce the stresses in the pins. But since knowledge was unavailable for the maximum permissible stress value for avoiding the risk of stress corrosion, the new pin was designed to yield the lowest stress compatible with the other design criteria. To meet this requirement, the following modifications were made:

- reduction of torque
- switch from a circular shank/collet joint to a parabolic joint.

It was also realized that heat treatment had a major impact on resistance to stress corrosion; as a result a number of tests on pin strength were performed in France, in the United States and in Japan.

The tests all proved the existence of a solution heat treatment temperature range in which corrosion susceptibility is smaller.

#### 5) Notes on the new design

Note that although the tests showed that the new pins had increased corrosion resistance, no test has proved that they can perform their function throughout unit lifetime. Studies and tests are being conducted as part of a four-way CEA, EDF, FRAMATOME and WESTINGHOUSE agreement. The results obtained up until now are consistent with those obtained in the past.

Note that as regards the flexible leaves, the only modification for upgrading their strength concerns heat treatment. One may well wonder if this will be sufficient.

FRAMATOME is currently also looking into methods for reducing flexible leaf stresses. This study could lead to the beginning of a new family of "second-generation" pins.

Note that the Japanese have carried out a first series of modifications which were slightly different from those proposed by the Americans. They were as follows :

- increased solution heat treatment temperature but to a value less than that chosen by the Americans and which lies outside the temperature range in which corrosion susceptibility appears to be smaller (see above),
- reduction of torque to a value half that used by the Americans,
- reduction of the gap between flexible leaves,
- shot peening.

The Japanese started to instal these new pins in their units as soon as 1979. But during 1983, ultrasonic examinations of the new pins revealed anomalies. This led the Japanese, in conjunction with Westinghouse and Babcock & Wilcox, to design a new type of pin whose heat treatment is practically identical to that adopted by the French and Americans.

#### SAFETY EVALUATION

Since stress corrosion cracking ultimately leads to rupture, it is necessary to assess the risks potentially caused by control rod guide tube pin ruptures. Two questions can be asked as regards safety:

- what are the risks induced by the migration of pin fragments to the reactor coolant system?
- Do guide tubes with one or two broken pins still perform their safety function, which is to guarantee control rod drop?

The answers to these two questions are summed up in the following two paragraphs:

#### 1) Impact of loose parts

##### a) Loose parts considered

The two types of pin ruptures give rise to 2 types of loose parts:

- a flexible leaf weighing 35 grams,
- a pin upper section weighing 190 grams which can disassemble or break up (one case of a pin breaking up into 5 fragments was observed at FESSENHEIM 1 on 16/3/1982).

##### b) Trapping in NSSS systems

Examination of possible trapping in the reactor coolant system and related systems shows that:

- a loose part in the hot leg can either be captured on the RRA (Residual Heat Removal RHR) system suction side in primary loop n°2 or be trapped on the hot side of a steam generators channel head if the loose part cannot enter the SG tubes. A pin upper section may become trapped in a steam generator as at MIHAMA 3, FESSENHEIM 1, NORTH ANNA 1 and BUGEY 2. Extensive damage can be inflicted on the channel head, with greater impact on availability than on safety. A flexible leaf can theoretically enter an SG tube but with a clearance of several tens of millimeters.
- If the loose part is trapped on the RRA suction side, it will circulate through this system upon entry into service. In this case, if the loose part is entrained towards the RRA heat exchangers, it may become trapped there (internal tube diameter 14 mm). But it may also migrate through the heat exchanger by-pass. It will then either be trapped in check valves RIS (Safety Injection System SIS) 01 or 06 VP (as at GRAVELINES 1 of the 13/1/82) or migrate towards the reactor coolant cold legs, from which it will return to the reactor vessel.

c) Trapping in the internals

Examination of the migration of the two postulated loose parts through the reactor coolant system equipment highlights two points liable to have a safety impact:

- jamming of a flexible leaf in a continuous guidance region opening, highly improbable due to the arrangement of the current lines in this region, could cause RCCA (Rod Cluster Control Assembly) blocking during rod drop,
- jamming of a nut (cold) between the lower internals baseplate and the bottom of the reactor vessel (assuming that the nut had calculated without trap by the RRA, and had been reinjected into the cold leg) which could cause local damage to the internals and the claddings at the bottom of the reactor vessel.

in the event of disassembly, breakup or wear of the loose parts, the impact of jamming between the reactor vessel bottom and the lower internals is smaller. However, for fragments of less than 3 mm, migration into the core between the fuel rods or into the guide tubes is possible. The risks of fuel rod damages or RCCA blocking are low, however.

To sum up the risks induced by the presence of a loose part, they are mainly related to small loose parts. Breakup or wear of pin fragments in the reactor coolant system should therefore be avoided. Provision must be made to detect and rapidly remove these fragments from the reactor.

2) Maintenance of the guide tube functiona) During normal operation

Calculations were made and loop tests performed to evaluate the performance of the guide function with time in a certain number of configurations (one pin with a broken leaf and an intact pin-2pins with broken leaves and shanks etc...).

It appears that there is no problem of short-term loss of guide function after breakage of one or more pins.

b) During accident operation

Starting from a situation in which all the guide tubes have broken pins, it was demonstrated that:

- in the event of reactor coolant system breaks under  $0.5 \text{ ft}^2$ , all the rods drop into the core,
- in the event of reactor coolant system breaks over  $0.5 \text{ ft}^2$ , no rod shutdown margin is needed to keep cladding temperature below the safety criterion.

## PROTECTION AGAINST BROKEN PINS

Since loose parts impair the short-term availability and long-term safety of a plant unit, Electricité de France has installed a reactor coolant system acoustic monitoring system at each unit.

This system can be used for continuous surveillance of the signals transmitted by the accelerometers at the bottom of the steam generator channel head (one per steam generator) and one of the 3 sensors at the bottom of the reactor vessel.

Current system performance is such that shank detection is highly probable in a steam generator, but more unlikely in a reactor vessel and leaf detection is problematic in a steam generator, highly improbable in a reactor vessel. However, EDF is currently examining the possibility of upgrading acoustic monitoring, notably by re-analyzing detection setpoint values.

Twice in the past (16/3/82 at Fessenheim 1, 21/7/82 at Bugey 2), the system has led respectively to the detection of a nut and a shank-nut assembly in a steam generator channel head.

#### PIN EXAMINATION

From the outset it has proved necessary to provide a capability for examining the state of in-place pins so as to detect possible cracks before rupture. Actions have been undertaken on two fronts:

- TV camera inspection of the presence of nuts and leaves,
- Ultrasonic examination of pin soundness in both corrosion-affected zones.

##### 1) TV inspection

This system is currently used by EDF to inspect all its guide tube pins. The pins are inspected during refuelling with the upper internals on their storage stand at the bottom of the reactor cavity. It is estimated that it might not be performed this inspection during the first refuelling operation after installation of new pins.

##### a) Verification of the presence of flexible leaves

This inspection is performed by a camera mounted on an automatic trolley moving underneath the reactor internals.

Note that this inspection confirms the absence or presence of flexible leaves but cannot detect cracked leaves, even if cracking is extensive.

Up until now, this inspection has demonstrated the absence of a flexible leaf at GRAVELINES 3 during the second unit refuelling outage in October 1983. The inspection also identified the pin from which a flexible leaf had been discovered in the reactor coolant system of GRAVELINES 1.

##### b) Verification of the presence of pin nuts

Two methods are used:

- One called the "sabre" method, involves the insertion of a horizontal borescope with a vertical viewing mechanism into the gaps separating the guide tube rows; the image was transmitted by a TV camera.
- the other method, developed by FRAMATOME which gave it its name, involves lowering a camera along the guide tube centerline after removing the drive rod. This vertical-axis camera has a horizontal viewed mechanism

which provides scanning of the nut contour through an opening in the guide tube wall behind the continuous guidance system.

At FESSENHEIM 1, this inspection permitted identification of the coordinates of the broken pin whose nut had been discovered in a steam generator. During the same inspection, a pin was revealed to have a slightly slanting nut.

In August 1982, a slanting nut was also discovered at BUGEY 4. In March 1983, a missing shank was found at the bottom of the reactor cavity and a slanting nut was also discovered at BUGEY 3. At the time, the tooling for replacing pins on irradiated guide tubes was not operational. As result it was decided to apply hydraulic loads to all the pin nuts to find out if any pins were at rupture point. The system used, the so-called "hydrolaser", consists of a high-pressure water jet 1 to 2 mm in diameter which is applied to the nut.

This operation revealed a third broken pin. The three affected guide tubes were replaced before startup. The "hydrolaser" examination was also later performed at TRICASTIN 3.

As in the case of the leaf examination, allowance must be made for the limits of the nut examination which does not show if a pin is cracked and is perhaps on the point of rupture. Accordingly, the TV inspection at BUGEY 2 showed nothing but, on re-startup, a pin shank was discovered in a steam generator (21/7/1982).

Due to the limitations of TV inspection, EDF is analyzing another type of examination for detecting cracks, e.g. ultrasonic examination.

## 2) Ultrasonic examination

Ultrasonic examination uses the discontinuity created by a crack in the material to initiate an echo signal which, under certain conditions, should enable identification of the position and size of the defect.

The first laboratory test demonstrated the difficulties of interpreting signals as well as the importance of pin grain size in this type of examination.

To qualify the method, an ultrasonic examination was performed on the pins at TRICASTIN 1. The pins were then removed and analysed. Comparison between the examination results and the ultrasonic indications revealed that the ultrasonic examination only indicated the real condition of the pins in 60 % of cases. Given the fact that the TRICASTIN 1 pins had a fine grain size (ASTM 7 to 8) which lent itself to ultrasonic examination, it is easy to foresee the difficulties which would be encountered with the new larger-grain pins (ASTM 0 to 6).

This led EDF to abandon this method. However, research into another more effective method is now under way.

## PIN REPLACEMENT

EDF systematically replaces old pins by new pins. The first units in which this operation was performed in fact underwent guide tube replacement.

The operation involved replacement of the irradiated guide tubes with old pins by new guide tubes with new pins.

EDF subsequently had problems procuring new guide tubes, as a result of which it decided to carry out "pin replacement", allowing reuse of the guide tubes.

The procedure is as follows :

- removal of irradiated guide tubes with old pins,
- mounting of other irradiated guide tubes with new pins from the pin workshop,
- transport of removed guide tubes to the pin workshop,
- removal of old pins and mounting of new pins on irradiated guide tubes,
- transport of guide tubes with new pins to a site where pins are to be replaced.

On December 31st 1983, 9 units out of 21 had had their guide tube pins replaced. The other units will have their pins replaced according to a schedule spanning 1984 and 1985.

The current status of pins broken during removal is as follows :

Unit	Date	Equivalent hours at full power	Group	Breaks	
				At extraction	after extraction
FESSENHEIM 1	/7/82	26.000	1	32 collets	
FESSENHEIM 2	/1/83	31.500	2	8 collets	2 collets
BUGEY 2	/7/83	19.400	1	20 collets	1 collet 8 leaves
BUGEY 4	/8/82	21.000	2	1 threadtop	
BUGEY 5	/5/83	20.000	2		
TRICASTIN 1	/1/83	15.000	3	4 leaves	2 collets 2 leaves
TRICASTIN 2	/5/83	15.500	4	4 leaves	28 leaves
TRICASTIN 4	/11/83	15.000	4	1 collet	
GRAVELINES B1	/5/83	15.000	4	3 leaves	12 leaves

Note that 2 units out of 9 had no broken pins.

Group 1 seems particularly affected which is not surprising since the pins in this group have undergone solution heat treatment which was unfavourable according to the corrosion test results. Group 2 which has a more favourable solution heat treatment was less affected.

As for group 4, it was considered that lower torque would provide less rupture. This was partly confirmed since only one rupture was observed in the collet region. However, it was observed that the flexible leaf region seemed highly susceptible to breaks : 32 leaves at TRICASTIN 2, 15 at GRAVELINES B1.

Also note that there appears to be no obvious connection between the number of broken pins and the operating time.

#### EXAMINATION OF REMOVED PINS

After being removed from the guide tubes, the old pins undergo a certain number of examinations (visual, liquid penetrant test) to determine their soundness.

At this moment, only the results of the pin examination at FESSENHEIM 1 and 2 are available.

Results are given below :

Batch	Collet defect	Shank defect	Break at 1st thread	No defect
81 pins at FSH 1	75	18	0	4
71 pins at FSH 2	53	13	1	13
42 pins at FSH 1 or 2	23	8	17	4

There are a large number of defects (cracks or ruptures), most of which probably occurred during guide tube removal. Removal force varies between 500 and 1500 daN. Despite this, it can be considered that these defects only occurred because the cracking process was well advanced.

Notethat for the moment there is no obvious connection between pin defects and their locations in the reactor core.

Equally, no correlation could be proved with the pin position (two pins by guide tube).

Also note that a large number of defects observed up until now in the leaves are related to the presence of electric pencil marking (notch effect?).

The results of the examination for the other units will probably have to be awaited before final conclusions can be drawn and comparisons made between pin groups.

#### CONCLUSION

To sum up, it can be said that :

- As regards the causes of the pin stress corrosion cracking phenomenon, we have still no discovered the parameters controlling this phenomenon, even if we now have some idea of the influence of some of them,

- as regards the impact of pin breaks on safety, risks are acceptable, at least on a short-term basis. It is therefore necessary to detect pin breaks for protection against long-term risks.
- as regards the impact of pin breaks on availability, it is necessary to rapidly detect a loose part in order to avoid serious damage, for example to the steam generator channel head.

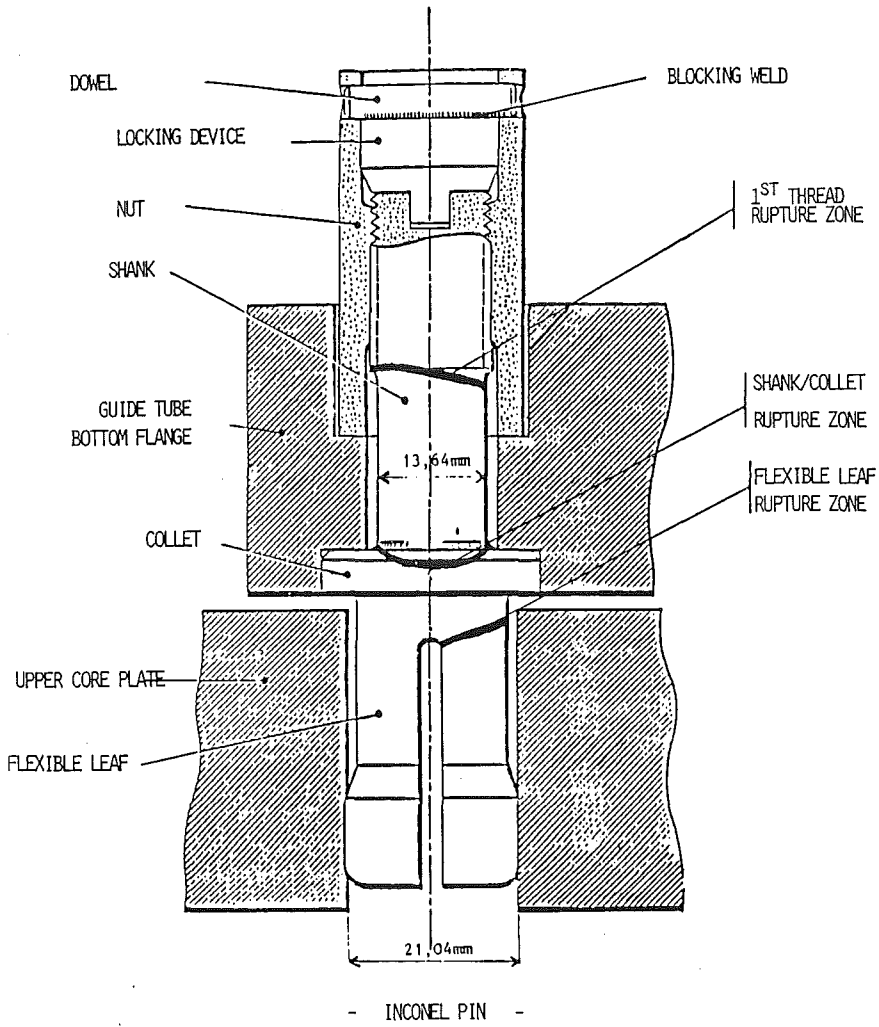
The last two considerations have led to :

- inspect pins during refuelling,
- detect any pin loose parts by means of the acoustic monitoring system,
- replace old pins by new pins with higher resistance to stress corrosion cracking.

Replacement of pins in about twenty power plant units is a large-scale operation. It provides proof that it is possible to successfully carry out difficult plant unit repairs.



FIGURE 1



FAULT TREE ANALYSIS OF WESTINGHOUSE  
SOLID STATE PROTECTION SYSTEM SCRAM RELIABILITY

Paul J. Amico

Applied Risk Technology Corporation  
P. O. Box 175  
Columbia, MD 21045, USA

ABSTRACT

In late 1981 and early 1982, as part of a larger PRA of a Westinghouse nuclear power plant, a fault tree analysis was performed on the solid state protection system (SSPS). Among other findings, this analysis determined that the dominant contributors to unavailability of reactor trip were common mode failure of the reactor trip breakers and failure of the active SSPS train when the other train was undergoing test. This was over one year before common mode breaker failure resulted in scram failure at the Salem plant. A recent expansion of this analysis shows that unavailability can be reduced somewhat (but not significantly) if the testing interval is shortened to once every 72 hours. Any further reduction would begin to increase the unavailability.

INTRODUCTION

In late 1981 and early 1982 a fault tree analysis was performed which quantified the reliability of the solid state protection system (SSPS) of a Westinghouse reactor. This analysis was part of a larger effort to perform a PRA on a Westinghouse nuclear power plant. The analysis included an evaluation of both the reactor scram function and the safety equipment actuation function of the SSPS. With the occurrence of a failure to scram at the Salem plant, which is a Westinghouse plant, the scram failure part of that analysis was reviewed to see what it had shown. The results showed that the dominant contributor to scram failure is common mode failure of the reactor trip breakers, the same failure mode as was seen at Salem. One of the results of the Salem event was suggestions that reactor protection systems such as the SSPS be tested more often than the once per month which is now required. However, the SSPS analysis also had shown that testing of an SSPS train in combination with failure of the trip logic board in the active train was also a large contributor to scram failure. Since testing also contributed to potential scram failure, any change in test interval to improve breaker reliability would bring with it increases in unavailability due to testing. Therefore, in order to properly evaluate the trade-offs involved, the SSPS analysis was recently expanded to determine the optimum testing interval for the SSPS.

SYSTEM DESCRIPTION

The solid state protection system (SSPS) is designed to initiate automatic reactor trips and actuate engineered safety features. It also

provides control signals for some plant systems used in normal operations, signals to control room monitors and annunciators, and inputs to the plant process computer. These functions are provided by an array of sensors tied together by way of a solid state component matrix. For the purposes of this analysis, we are concerned only with the reactor trip function of the SSPS, and all further discussions will address only this function

#### Design and Operation

A simple layout of the solid state protection system is shown in Figure 1. The system consists of two trains of solid state logic and actuating relays that analyze signals developed by four protection channels of bistables and sensors. The solid state logic determines whether the correct combination of sensor inputs are present to initiate a reactor trip. The descriptions below explain the key parts of the system, following the figure from left to right.

#### Process Sensors

The process sensors monitor the plant conditions. In general, a process sensor is a train of components consisting of a sensing device, a transmitter, and a signal modifying device. The signal modifying device takes the raw signal from the transmitter and applies some predetermined function to it. This function varies from sensor to sensor, depending on the desired response characteristics of the signal; it may be as simple as a straight amplification function or it may be more complex, such as a square root function. In some cases the signal is developed from a combination of inputs from more than one sensor, and other devices (e.g., comparators, summing networks, or other calculational circuits) are used to obtain the desired signal. For certain signals that monitor component states like valve positions, the "sensors" are usually local contacts, such as limit switches. The sensors are divided into four channels, each separate from the others, to provide redundancy for each parameter that is monitored. Some parameters have four sensors, while others have only three, thus all four channels are not always used. The signals developed are transmitted by each process device in a given channel to its associated bistable.

#### Bistables

The bistables receive signals from the process sensor channels and change state according to the conditions indicated by the signals as compared to a preset value (or "trip setpoint") which is set within the bistable. Each bistable has two pairs of contacts, one connected to each train of the solid state logic through an input relay. The purpose of the input relays is to provide electrical isolation between the solid state logic trains and the reactor protection sensor channels. Regardless of whether a bistable is normally energized or deenergized, the contact pairs are closed when the bistable is in its normal state. This generates a signal to the logic trains during normal operation. When a parameter passes its setpoint, the bistable changes state and the contact pairs open. This removes the signal to the logic trains and indicates an out of tolerance condition. Each bistable is connected only to the associated process sensor channel. For any given process parameter, usually at least two bistables, in different channels, must change state to actuate a safety system. Conversely, at least two bistables must fail to change state to prevent a system actuation if it is required.

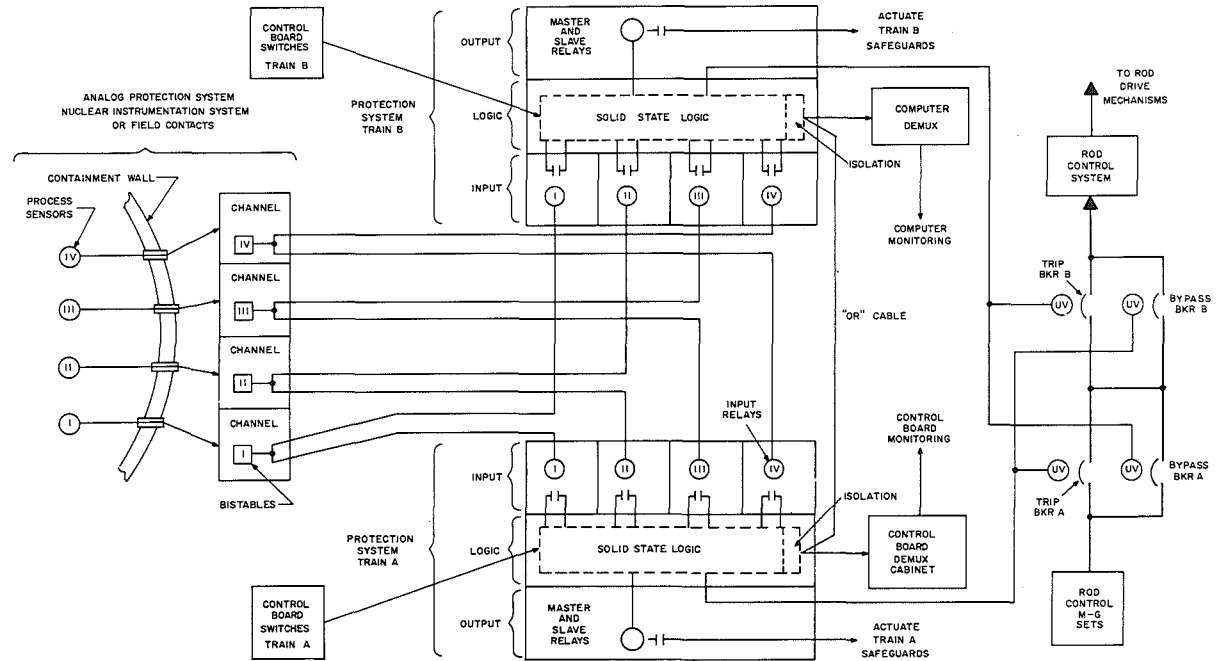


Fig. 1: SSPS Simplified System Diagram

Thus, the failure of any one bistable (or the associated sensor train) will not compromise SSPS functionality, either by causing inadvertent actuation or preventing proper actuation. In addition, each protection channel receives its control power from a different source, and therefore the failure of one power source can cause the failure of the bistables (or sensors) in only one channel. Depending on the type of bistable (or sensor), this failure will be in either the normal or the tripped state. However, since for each process parameter the redundant bistables are in different channels, the same argument applies, and the functionality of the SSPS is not compromised.

#### Solid State Logic Trains

The solid state logic trains interpret the signals from the bistables to determine whether the correct combination of signals exists for the initiation of a plant trip. Each logic train consists of a number of universal logic boards, three safeguards output boards (not used for reactor trip), and an undervoltage output board. These boards perform the various logic functions required to develop the safety system actuation signals using "positive NAND logic." This means that the normal state of the inputs to, and the outputs from, a logic circuit is the presence of a signal (voltage). The presence of a signal is generally referred to as a "high" and the absence of a signal as a "low." When an abnormal condition occurs in one or more process parameters, the bistables associated with these parameters change state, opening the associated contact pairs and thus removing the signal (causing a "low" input) to the associated logic train input. When enough "low" inputs occur in a given circuit to satisfy its particular logic function, a "low" output results. These outputs are fed to other circuits. At any level, the presence of a "low" indicates an abnormal condition, and when a correct combination of "lows" exists, the logic train produces a "low" at one of its ultimate outputs. Each universal logic board contains three circuits (one four-input circuit and two three-input circuits). These circuits can be configured to obtain various combinations of coincidence logic, depending on how the inputs are used. These circuits also allow the use of an "inhibit" input, which can be used to prevent a "low" output during testing or other conditions when a bypass is desired. The undervoltage circuit board is a large OR gate, where the occurrence of a "low" on any of the inputs results in a "low" output. The undervoltage circuit board is used to transmit the reactor trip signal to the reactor protection system breakers.

#### Reactor Protection System (Mechanical)

The mechanical part of the reactor protection system (RPS) consists basically of the control rods and their driver mechanisms, two rod control motor-generator sets, two reactor trip breakers, and two bypass trip breakers. The rods are held out of the core by supplying power from the motor-generator sets to the drive mechanisms, which keeps an electromagnetic clutch energized on each mechanism. Removing power from the drive mechanisms by opening one of the normally closed trip breakers will cause the rods to drop into the core under the influence of gravity, thereby shutting down the nuclear reaction. Each breaker is kept closed by energizing its undervoltage coil using the normally "high" output of the undervoltage output circuit in the associated solid state logic train. When the undervoltage output circuit goes "low," the breaker's undervoltage coil deenergizes and the breaker opens, interrupting power from the motor-generator sets to the control rod drives and causing the rods to drop into the core. The bypass breakers, which are normally open, are

provided to allow testing or maintenance on one of the trains while the plant is in operation. When a bypass breaker is closed, any trip occurring in the associated train will not trip the reactor, since power will still flow through the bypass breaker. A closed breaker is annunciated in the control room to inform the operator that only one RPS train is active. A closed bypass breaker will receive a confirmatory trip signal from the appropriate (active) logic train in the event a trip condition occurs. The bypass breakers are interlocked such that any attempt to close both bypass breakers will result in the immediate trip of all four breakers. In addition to the automatic signals, the operator can manually trip the breakers by means of pushbutton switches in the control room.

#### Testing and Maintenance

Periodic testing is performed on the components of the SSPS in accordance with the plant technical specifications. While a given train is being tested, it is completely out of service. The trip breaker for that train is left open, and the associated bypass breaker is closed. Thus, during testing the reactor can only be tripped by opening one of two closed breakers, both of which get their signal from the single active logic train. Whenever any test switches are in the test position, or a bypass breaker is closed, or an SSPS cabinet door is open, a general warning signal is activated for the affected train, which is annunciated in the control room. If any action is taken on the other train that would result in a general warning, a plant trip will occur. Thus, it is generally impossible for both trains to have a test switch mispositioned in the test mode, since if one train had a switch in the test mode, the plant would trip as soon as any cabinet door on the other train was opened, which would obviously be before any switch positions on that train could be changed. Maintenance is performed only as needed. Thus, there is no contribution to SSPS unavailability from scheduled maintenance. Components found defective during testing or at any other time are repaired as required in accordance with the plant technical specifications. Obviously, the general warning interlocks will also prevent double train outage contributions due to maintenance. Testing and maintenance is discussed in greater detail below.

#### Process Sensors

The process sensors are tested once per refueling cycle. They are tested only while the plant is shut down and are verified serviceable before power ascension. Maintenance is never performed on the process sensors during plant operation. If out-of-service sensors violate the plant technical specifications between refueling outages, the plant is shut down so that they can be repaired.

#### Bistables

The bistables are tested once a month. Each bistable is isolated from its input and output during the test. Since this produces a trip signal from the bistable, the bistable is not considered to be out of service during the test. A dummy signal is applied to the bistable and varied to verify that the point at which the bistable changes state is within the proper limits. A failure to restore the bistable to service after testing will continue to produce a trip signal from the bistable. Maintenance (replacement) of a defective bistable will also result in a trip signal from the bistable output, since it is not present in the circuit. Thus, there is no test or maintenance

contribution to unavailability from bistables.

#### Solid State Logic

Each logic circuit is tested once each month. Each logic train is equipped with a semiautomatic tester that tests a circuit by applying test inputs and pulsing them rapidly between the tripped and nontripped states for all possible combinations of input states. The resultant pulsing of the output of the circuit is monitored, and green lights indicate that the circuit is operating properly. If a circuit is bad, a red light comes on. One train is tested at a time. The operator places the train in test and then tests the circuits one at a time by rotating a set of function selector dials until all circuits have been tested. The pulses are of such short that the trip breakers and safeguards output relays do not have time to change state. The design of the testing system is such that, even though only one circuit is being tested at any instant, the entire train is out of service for the duration of the testing (approximately 2 hours). Maintenance (replacement) of a defective logic board requires taking the entire train out of service in order to prevent inadvertent actuation of safety systems. The out-of-service time for this action is 5 to 6 hours. Logic board replacement is performed only as needed, there are no scheduled replacements.

#### Reactor Protection System Breakers

These breakers are tested monthly during the testing of the solid state logic. The opening and closing of the trip and bypass breakers for the purpose of taking an actuation train out of service provides for the opening and closing of each of the four breakers. The sequence of actions follows the following pattern for each train: close bypass breaker, open trip breaker, test solid state logic, close trip breaker, open bypass breaker. Maintenance is performed on the breakers only when one fails during testing. The plant must be shut down in order to perform maintenance on the breaker, so breaker maintenance does not contribute to overall system unavailability.

#### METHODOLOGY

The system was modeled using standard fault tree techniques, which will not be described in detail in this paper. The top event of the fault tree was "failure to shut down the nuclear reaction." Success was defined as the insertion of control rods such that no five control rods anywhere in the core or no three adjacent control rods remain uninserted. This definition had no effect on most of the analysis, since system failure in most cases resulted in no rod insertion. The only effect was in the evaluation of the probability of common mode control rod failures resulting in a failure to shutdown configuration given that the trip breakers opened. The model included all the components of the SSPS; the sensors, bistables, solid state logic boards, breakers, and control rods. In addition to component faults, test and maintenance and human error fault contributors were included. Common mode failure analysis was applied where appropriate. The data used for the analysis was taken from a data base developed for the overall PRA from a variety of sources. The development of this data base was a separate task, and is not a subject of this paper. Briefly, however, data pertinent to this analysis and contained within the data base was obtained from different sources, including WASH-1400 [1], MIL-HDBK-217C [2], and IEEE STD-500 [3] for

component data, NUREG/CR-1278 [4] for human error rate data, and plant specific experience for test and maintenance data. Additionally, plant experience was included in the component and human factors data where it was considered meaningful. The selection of the data source depended on which source, according to expert judgement, had a better treatment of data for each particular component or other event.

A number of bounding assumptions were made during the analysis and also for the subsequent analysis of the optimum test interval. These assumptions were as follows:

- The failure of all components other than the RPS breakers and the control rods were considered to be independent events, the breakers and rods were evaluated for common mode failure contributions.
- The input relays that serve as an interface between the bistable contacts and the solid state logic were ignored because the failure rate of the relay is much lower than that of the bistable and the relay failure affects only one train, while the bistable failure affects both.
- The nonsafety functions of the SSPS were not considered in the system models because they do not directly affect safety system operation and indirect effects are eliminated by electrical isolation through photo-diode pair coupling of the safety and non-safety parts of the system.
- The failure rate of the solid state equipment, which is always energized, is entirely time dependent; that is, there is no demand contribution to failure.
- The failure rate of the trip breakers is a combination of a time dependent factor and a demand factor, which can be represented by the following equation;

$$\lambda = \lambda_d + \lambda_s T/2$$

For monthly testing, the data base gave a total failure rate,  $\lambda$ , of  $1E-3$ . It also gave a spurious actuation failure rate of  $1E-6/hr$ , which was felt to also be applicable to the standby, or hourly, contribution to the overall failure rate. Applying these numbers to the above equation for the monthly test interval ( $T=720$  hrs), yields a failure rate equation for the breakers for any test interval  $T$  of;

$$\lambda = 6.4E-4 + 1E-6 * T/2$$

Using these assumptions, the unavailability of the SSPS scram function was calculated for the "as built" plant conditions. This determined the expected unavailability of the trip function and the dominant contributors to this unavailability. Since the purpose of this paper is to investigate if altering test intervals will result in a lower unavailability, calculations were also performed for various test intervals, and a curve drawn which shows the optimum test interval.



## RESULTS

The results of the original analysis of the SSPS, which reflect the existing system configuration and test/maintenance conditions, are shown below in the form of dominant cut sets (the most likely combinations of component unavailabilities which would result in system failure).

Cut Set	Demand Unavail.
Common mode failure of trip breakers	1.0E-5
Train A(B) in test AND failure of trip logic board B(A)	8.6E-6
Failure of trip breaker A(B) AND failure of trip logic board B(A)	3.1E-6
Failure of trip logic boards A AND B	2.4E-6
Random failure of trip breakers A AND B	1.0E-6
Train A(B) in test AND common mode failure of trip breaker B(A) with bypass breaker A(B)	5.6E-8
TOTAL RPS UNAVAILABILITY	2.5E-5

As can be seen from these results, common mode breaker failure and test unavailability are relatively close together as dominant contributors. The last cut set is obviously not a dominant contributor, but it has been included because it is partly the key to the test interval optimization, as will be seen next.

As previously stated, the results above were based on the present plant operating conditions, which includes a test interval for most components of once per month (720 hours). In order to evaluate the effect of altering this test interval, the model was reevaluated for test intervals of 2, 8, 24, 72, 168, 336, and 1440 hours. The results of this analysis are shown on Figure 2.

As can be seen in the figure, unavailability is minimized at a test interval of 72 hours (every three days). The cut set values for this test interval are shown below.

Cut Set	Demand Unavail.
Train A(B) in test AND failure of trip logic board B(A)	8.6E-6
Common mode failure of trip breakers	6.8E-6
Random failure of trip breakers A AND B	4.6E-7
Train A(B) in test AND common mode failure of trip breaker B(A) with bypass breaker A(B)	3.8E-7
Failure of trip breaker A(B) AND failure of trip logic board B(A)	2.1E-7

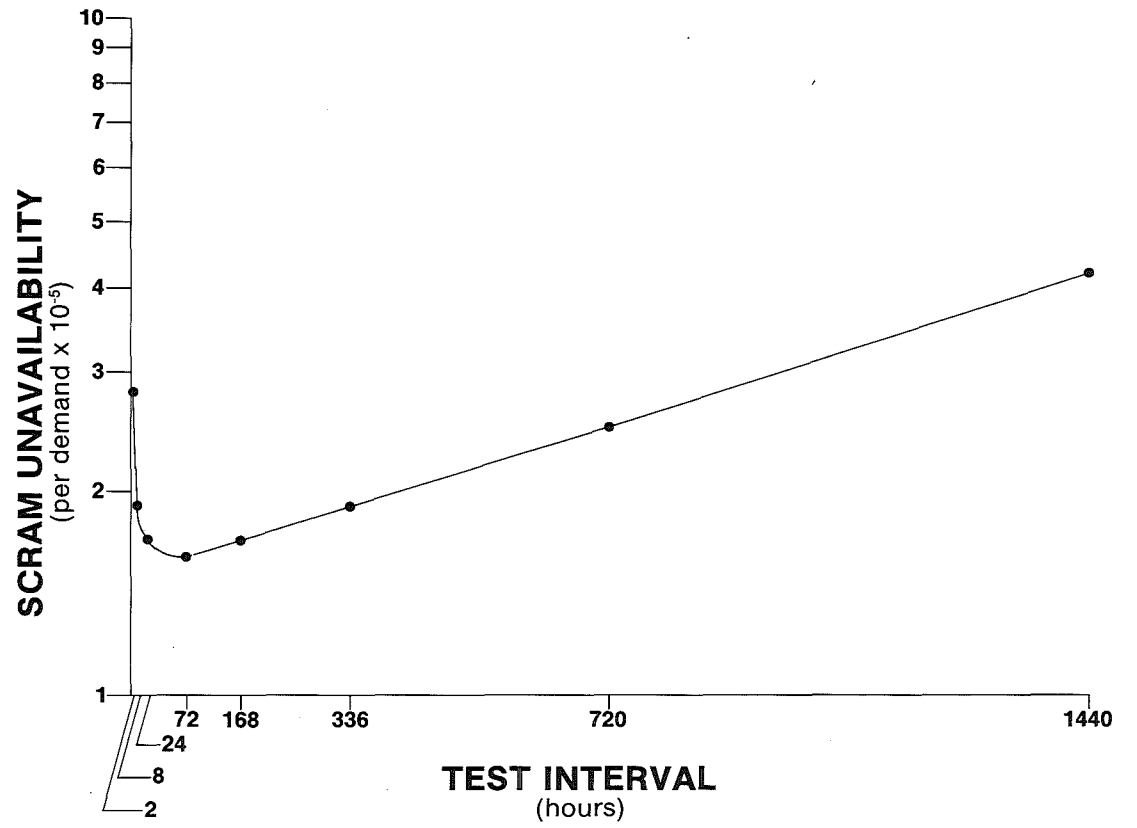


Fig. 2: SSPS Unavailability as a Function of Test Interval

Failure of trip logic boards A AND B	2.4E-8
TOTAL RPS UNAVAILABILITY	<u>1.6E-5</u>

As can be seen from the above table, the unavailability contribution due to test is now dominant. The top cut set has the same value as before, since both the test contribution and the logic board unavailabilities are affected strictly by hourly contributions in equal degree but opposite direction. All of the pure component failure cut sets have declined due to reduction in their unavailabilities from the more frequent testing. The test contribution which is now fourth on the list has increased since the test unavailability is increasing more rapidly than the breaker unavailability is decreasing. Any further reduction in the test intervals causes this cut set to increase more rapidly than all the component failure cut sets can decrease, thus increasing overall unavailability.

Using the results presented above for the 72 and 720 hour test interval cases, the overall reduction in unavailability by changing to 72 hour test intervals from 720 hour intervals can be calculated to be:

$$(2.5 - 1.6) / 2.5 = 36\%$$

#### CONCLUSIONS

The analysis performed gives a calculated reduction of 36% in scram unavailability by changing the test interval for the SSPS to 72 hours. However, it must be remembered that there are uncertainties involved in calculations of this type. In general, most practitioners of PRA techniques do not consider any change less than a factor of three to be significant in a statistical sense. Therefore, while we conclude that shortening the test interval will probably give some reduction in scram system unavailability, it is likely that the reduction will not result in a significant reduction in overall scram failure frequency.

#### REFERENCES

- [1] U.S. Nuclear Regulatory Commission, Reactor Safety Study—An Assessment of Accident Risks in U.S. Commercial Nuclear Power Plants, WASH-1400, October 1975.
- [2] U.S. Department of Defense, Reliability Prediction of Electronic Equipment, MIL-HDBK-217C, April 1979.
- [3] Nuclear Power Engineering Committee of the IEEE Power Engineering Society, IEEE Guide to the Collection and Presentation of Electrical Electronic and Sensing Component Reliability Data for Nuclear Power Generation Stations, IEEE STD-500, June 1977.
- [4] Swain, A.D., H.E. Guttman, Handbook of Human Reliability Analysis with Emphasis on Nuclear Power Plant Applications, U.S. Nuclear Regulatory Commission, NUREG/CR-1278, September 1980.

**STATION BLACKOUT : A TEST ON A PLANT AT POWER  
LESSONS LEARNED FOR SAFETY STUDIES**

T. MESLIN . A. CARNINO . B. PAYEN . A. CAHUZAC

ELECTRICITE DE FRANCE 2 rue Louis Murat 75384 PARIS CEDEX 08 FRANCE

**ABSTRACT**

The paper describes a test of voluntary cut-off of the external electric auxillary sources serving a 900 MWE PWR unit operating at full capacity. With help of the emergency Diesel generators the purpose is then to bring back the unit to a safe cold shut-down state, using natural circulation. Lessons learned during this test are diverse. They deal with the physical transients of the reactor system as well as with ergonomic and human behaviours of the operators under incident conditions. In particular the effectiveness of natural circulation without forming any steam bubble under reactor vessel head was demonstrated.

**INTRODUCTION**

This paper describes a test of voluntary cut-off of external electrical power supplying a 900 MWE PWR unit while operating at full power. With the help of the emergency Diesel generators, the purpose was to bring back the unit to the safe cold shut-down condition using the natural circulation.

Since this test was performed on a nuclear unit in operation, and since one of the purposes was to validate a post-incident operating procedure for the first time on site, the preparation of this transient has been analysed in depth by the operating staff with the collaboration of other E.D.F. specialists. It has to be noted that the Safety Authorities had given their authorisation to implement the test.

**OBJECTIVES****General scope :**

Electricité de France has begun since several years to study and to re-write the operating procedures in case of loss of electrical sources. As far as possible, these procedures are validated on a simulator or a unit in actual operation. This station blackout test takes place within this general pattern of EDF's policy. As the conduct of the test involved numerous aspects, the objectives were also diverse :

**Knowledge of the physical transients :**

- analysis of the reactor system behaviour under natural circulation during the phases of stabilization, boration and safe cold shut-down without formation of a steam bubble under the reactor vessel head ;

- the plant auxiliary systems behaviour during the transient i.e. operation of emergency Diesel generators auxiliary feedwater system (A.F.W.) as well as condensate system.

Validation of the incident operating procedure :

- technical contents
- ergonomic aspects : understanding, task distribution, work load.

Observation of the human behaviour during an unusual and long transient.

Others lessons :

Various lessons will be learned from this test such as technical recommendations for other incidental and accidental procedures and on site validation of the accident program used on the full scale PWR 900 MW training simulator.

## TEST CONDITIONS

- Plant status

- . the test was performed on 1983, August 17 on the Unit n° 3 at DAMPIERRE-EN-BURLY (900 MW 3 loops)
- . a few moments prior to the test, the reactor power was brought down to about 50 per cent of its full capacity.
- . the burn-up was 9577 MWDay/t.
- . the two Diesel generators were started 10 minutes before the test.
- . the plant status was meeting the required technical operating specifications

Operating crews

In the normal framework of the local training program, most of the operating crews had been given a course on the new procedure to be used during this transient. However, on account of the holyday period, a part of the morning crew was not aware of the test. The Safety Engineer was new in his job (1 month) but was aware of the schedule of the test.

Operating means

All the usual operating means were available. A graphic table had been added in order to record the primary pressure and temperature.

Procedure-Scenario of the transient

In case of station blackout, the incident procedure requires, after the stabilization phase, to inquire about the expected time of the return of the external electrical sources. If no source is anticipated within 2 hours, it is required to put the reactor on cold shut-down conditions (scenario of the test).

At first, the loops are borated, then, the pressurizer, after that the primary circuit is cooled down by natural circulation until the Reactor Decay Heat Removal System conditions are reached.

If AC power is available early, it is required to wait in hot shut-down status.

When reaching 177°C, 27 bars, the test is deemed finished. The external electrical supplies are declared available and the plant is re-started with the use of the normal operating procedures.

## TEST ANALYSIS (tables 1-2-3, figures 1-2)

Test chronology (cf. Tables 1-2) :

The station blackout is initiated at 2.24 a.m. The various automatic protective signals are actuated : reactor trip, turbine trip, normal feedwater system isolation, auxiliary feedwater system actuation, emergency Diesel generators actuation...

Table 1 describes precisely the main automatic actions which occurred during the first 5 minutes into the transient.

Stabilization of the primary loops is reached half an hour later. Primary circuit boration is performed from 3 am to 7 am. At 7 am, it is decided to initiate the cooling by natural circulation in order to reach the cold shut-down conditions. The cooling rate is then constant at 10°C/hour. The depressurization is at first "natural" and then monitored by following a track on the left border of the authorized natural circulation operating area (cf. figure 1) in order to prevent bubbling underneath the vessel head. At 7 pm, the conditions are met for switching on the Decay Heat Removal System. The bubble formation under the vessel head highlighted during the 1977 St-Lucie incident has been avoided. No major problem has been met during the course of the test.

Control actions from the operators (figure 1 - 2) :Immediate actions

According to the usual operation practices at E.D.F. the first phase in the case of an incident is to verify and to "confirm" automatic and protective actions.

In the case of this test, the first phase lasted about ten minutes. The main automatic actions occurred correctly, but the operators had to start up manually several auxiliary ventilation systems.

Pressurizer level and pressure

The Charging and Discharging System (CVCS) remains in operation during such a transient. Immediately after the turbine trip signal, the closure of the main steam inlet valves involves a transitory heating of the primary loops with a raise of both pressure and level in the pressurizer. The opening of the turbine by-pass valves and the AFWS start-up lead to a fall in temperature and pressure. The pressure falls down to 148.5 bars and then goes up as a result of the pressurizer heaters. Without the normal pressurizer spray, the pressure can go over 156 bars ; consequently, the operator uses alternately the auxiliary spray or the pressurizer heaters. The pressurizer level follows the pressure. The operator governs it manually and tries to control the auxiliary spray flow. The stabilization of those parameters is reached at 3.30 a.m.

Primary temperature and steam generators levels

The start-up of the whole AFW system leads to a feedwater flow of over 50t/h per steam generator (S.G.) and consequently a rather quick cool-down of the S.G. At first, the temperatures of hot legs and cold legs become equal ; then the  $\Delta t$  increases between the cold point, (S.G. outlet), and the hot point, (vessel outlet). As soon as the  $\Delta t$  is large enough, the natural circulation starts to establish.

The  $\Delta t$  is ranging about 15°C between hot and cold legs during the first hour of the test, and the average temperature of the loops is 272°C.

Boration

The technical specifications require operators to borate the primary circuit while respecting the following rules :

- reach adequate negative reactivity
- maintain a difference smaller than 50 ppm between primary loops and pressurizer.

The primary loops were borated at first during 1 hour 45mn. Then the pressurizer was borated through the auxiliary spray system.

At 6.30 a.m., the negative reactivity condition was widely respected, but the difference of 50 ppm was unachievable. Nevertheless it was decided to continue the test : the boron concentration in the loops was good enough to justify it despite the fact that the pressurizer concentration was too low.

Cool-down and depressurization (table 3)

The cool-down operations begin at 7 a.m. with the cut-off of the pressurizer heaters and the use of the atmospheric relief valves. In this first period, the pressure decreases slowly while the operator conducts the cooling process at a rate of 15°C/h. The goal is to meet and to follow a track on the left border of the authorized thermodynamic domain.

After this first step, the cooling rate will be of about 10°C/h and remains almost constant during the whole test.

In this way, the depressurization is almost natural and does not necessitate particular operations before reaching 130 bars.

After this period, the use of the auxiliary spray system will be more and more frequent and will last longer since its efficiency decreases, while the pressure decreases. It was demanded about 15 times before reaching 27 bars.

The 10°C/h cooling rate is slow enough to enable the operator to control the cooling operations without any perturbation.

On another hand, this rate gives an absolute guarantee against the risk of formation of a steam bubble under the vessel head.

General view

The general results of these different steps are summarized on table 1. The cooling in natural circulation has been on for about 12 hours. The average cooling rate was 9°C/h and the depressurization rate about 9,5 bars/hour.

Special remarks :AFWS behaviour

The AFW system did operate without any major problem except as regards the speed governor of the steam driven pump.

The total water used was  $\approx$  640 tons.

For this reason, the auxiliary water tank must be immediately refilled after the beginning of the transient (from the adjoining unit).

Boration

The boration duration was quite longer than scheduled. It appears practically impossible to make simultaneously homogeneous the boron concentration in the loops and in the pressurizer. Following this test, new directions will be given to borate the primary system in case of natural circulation in order to warrant enough negative reactivity and not to loose too much time.

Primary pump seals

CVCS was in use all through the transient. No major problem was encountered in connection with the pump seals, except some transitory surges of n° 2 seal leakage flow rate.

### Secondary circuit

At 4 a.m., some water hammer occurred in the condensate systems' pipes. This phenomenon was not expected and resulted from some valves staying opened due to the loss of power and thus connecting those pipes with the vacuum of the main condenser.

#### Human behaviour :

During this test, we had the opportunity to observe individual and team behaviour, communication problems, work-load and responsibility sharing. We can stress on the following items.

Written procedures have been used and followed during all the test. We were very impressed by the good quality of team behaviour, first considering the relation between the successive teams during the shift turn-over : every operator explained to his follower what happened and summarized the main events that occurred. Most of the operators stayed in the control room a long time after the planned hours of shift turn-over. Every shift beginning its work checked all the information given by the previous team.

As far as work-load is concerned , it appeared that the planned work-load was not well shared among all the operators.

It was also noted that, when operators have to perform an operation in a way different from the usual one, due to the transient situation, they are reluctant to change their normal operation routines. It then should be recommended that the operating modes required under abnormal conditions be as close as possible to the normal operation modes.

There were some problems regarding communications between the control room and the Nuclear Auxiliary Building and we noted that information feed-back to the control room is not planned in the procedure.

As a final remark, we may say that after 12 hours, the attention of the operators was noticeably less sustained than at the beginning, may be since everybody thought that everything was correctly fixed.

### CONCLUSIONS

The new procedure was validated by the test and will be enhanced only by minor changes in the detail of the operating instructions.

The test did show clearly that it is feasible to bring this PWR system from normal conditions to cold shut-down, when using natural circulation and without formation of a bubble under the vessel head. A cooling rate of about of 10°C/hour gives a comfortable guarantee against this risk. It is also important to follow the left border of the authorized thermodynamic operating domain.

The lessons learned from this test have lead to improve the operation mode used in other procedures linked with the loss of electrical supply.

From an ergonomic point of view, the test observations were important for the new incidental and accidental procedure design under development at EDF.

Eventually, the observation of the operating crew during such a complex transient has significantly increased our knowledge of operator and crew behaviour under disturbed situations and helps to develop pertinent human analysis tools.



**Table I : TEST FIRST 5 MINUTES CHRONOLOGY**

DATE	$\Delta$ TIME	EVENTS
2 h 24' 29"	to = 0 sec	Initiating Event (loss of power)
24' 29"	0,06 sec	Turbine Trip
24' 29"	0,14 sec	Main Breaker opening
24' 30"	1 sec	Turbine by-pass opening
24' 35"	6 sec	Primary pumps Trip
24' 35"	6 sec	Reactor Trip
24' 35"	6 sec	Nuclear power $\leq$ 40 %
24' 36"	7 sec	Nuclear power $\leq$ 30 %
24' 37"	8 sec	AFW Starting
24' 37"	8 sec	Feedwater pumps in service
24' 37"	8 sec	Nuclear power $\leq$ 10 %
24' 38"	9 sec	Electrical supplies switching
24' 41"	12 sec	Steam Generator drains closed
24' 45"	16 sec	Feedwater closed
30' 25"	5mn 56 sec	Primary temperature $\leq$ 284° C

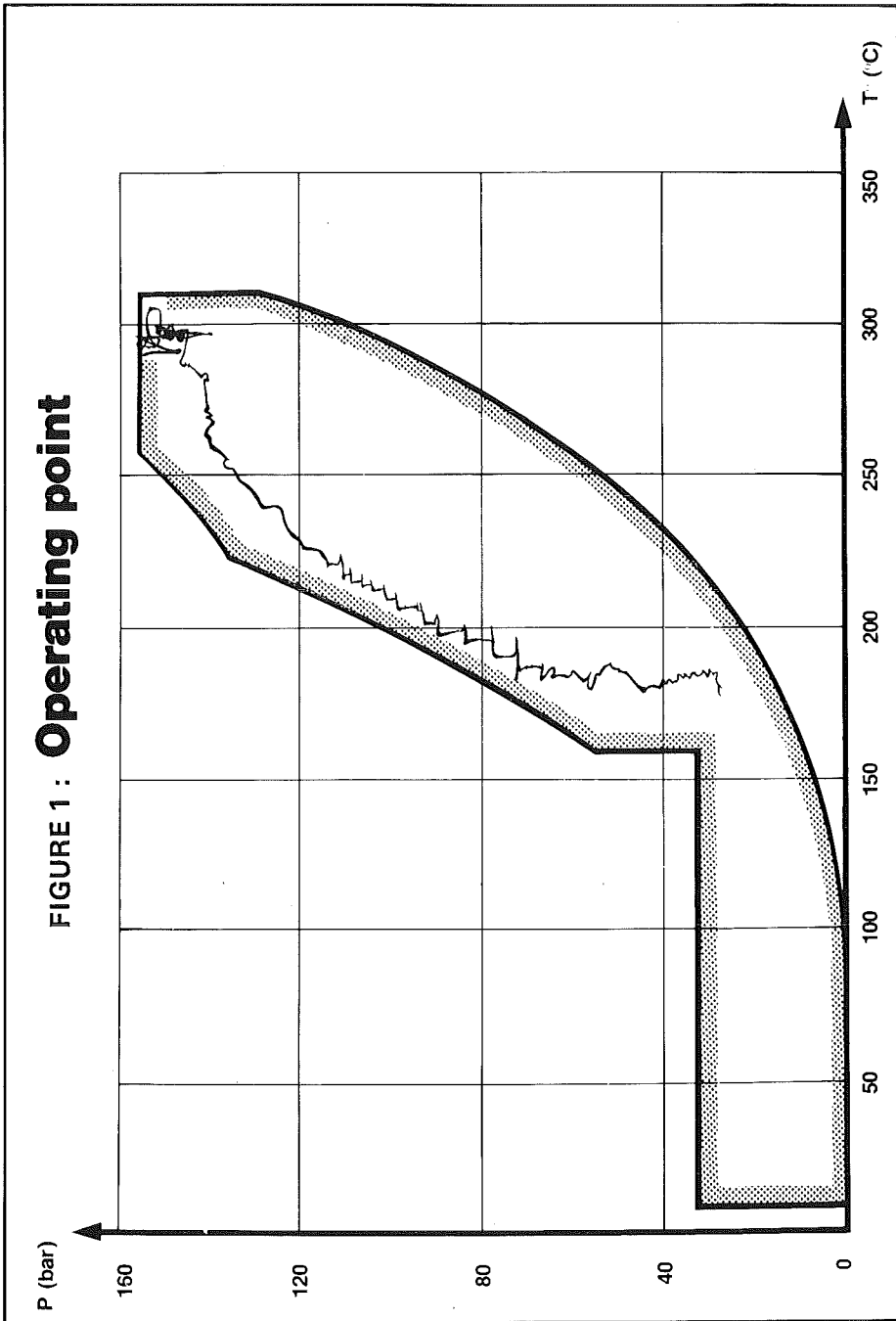
**Table II : TEST CHRONOLOGY**

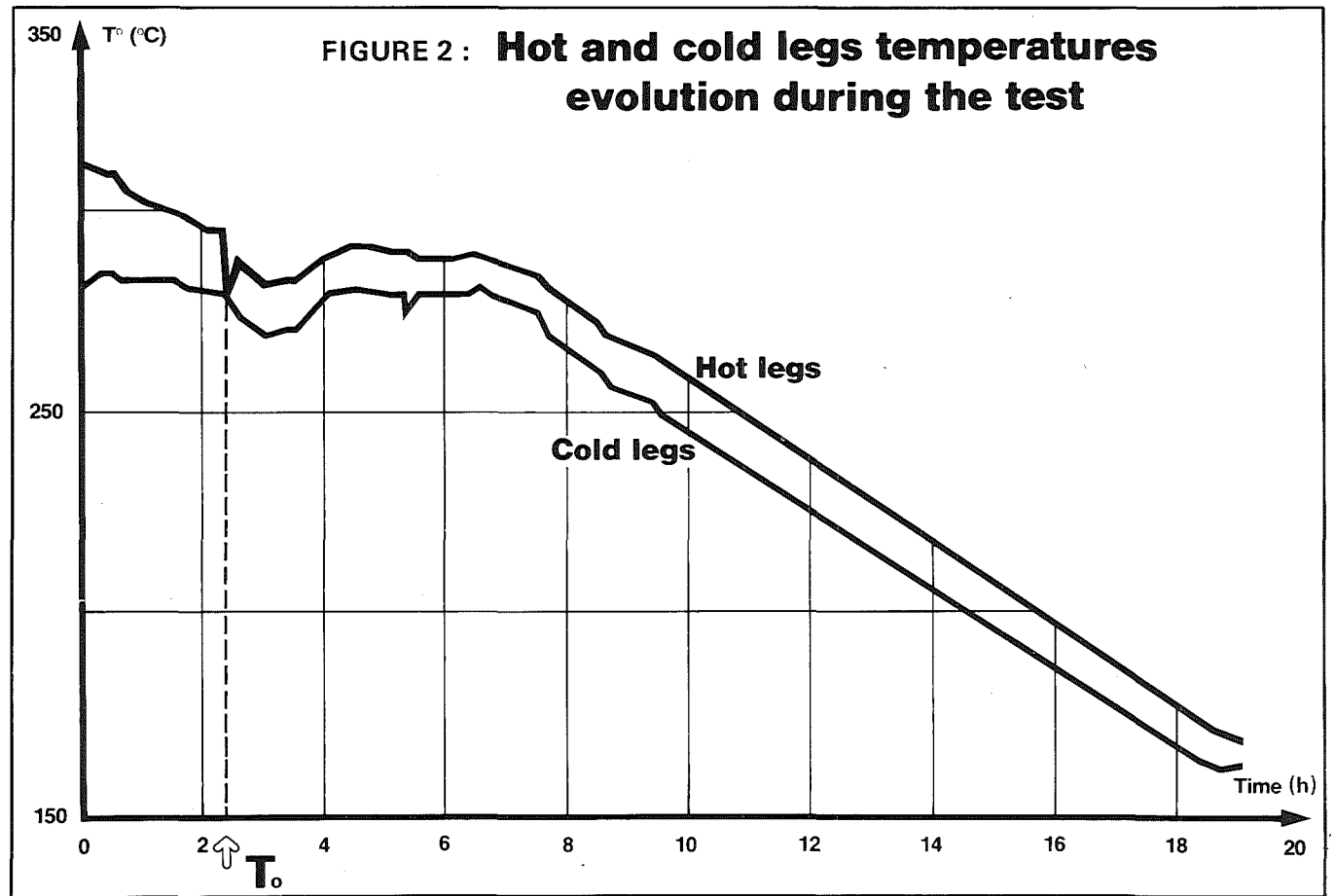
TEST PHASES	MAIN ACTIONS	BEGINNING	END	DURATION	
				PARTIAL	TOTAL
Immediate Actions	Confirmation of automatic protective actions	2 h 24	2 h 30	6 mn	6 mn
Stabilization	Control of L. and P pressurizer Control of S.G. level	2 h 30 2 h 30	3 h 15 3 h	45 mn 30 mn	45 mn
Boration	Loops boration	3 h 15	5 h	1 h 45 mn	3 h 45 mn
	Pressurizer Boration	5 h 10	6 h 30	1 h 20 mn	
	CVCS Relinning	6 h 30	7 h	30 mn	
Cooling/depressurization		7 h	19 h 25	12 h 25 mn	12 h 25 mn
TOTAL					17 h

**Table III : PARAMETRES EVOLUTION**

TEST PHASES		INITIAL T & P	FINAL T & P	DURATION	AVERAGE RATES	
					T	P
1	Stabilization	155 bar	145 bar	5 h	0	
	Boration	303 °C	290 °C			
2	Cooling to the	145 bar	118 bar	7 h	10°C/h	4 bar / h
	Left board	290 °C	225 °C			
3	Cooling following	118 bar	72 bar	4 h	12°C/h	12 bar / h
	the left board	225 °C	177 °C			
4	Depressurization	72 bar	27 bar	1 h 30	0	30 bar / h
	to the RHR conditions	177 °C	177 °C			

**FIGURE 1 : Operating point**





EVALUATION OF PRIMARY COOLANT LEAKS AND  
ASSESSMENT OF DETECTION METHODS

P. Cassette, C. Giroux, H. Roche and J.J. Seveon

Commissariat à l'Energie Atomique  
Institut de Protection et de Sûreté Nucléaire  
Boîte Postale n° 6  
92260 Fontenay-aux-Roses, FRANCE

## ABSTRACT

A review of the French PWR situation concerning primary coolant leaks is presented, including a description of operating technical specifications, of the collecting system of primary coolant leakage into the containment and of the detection methods. It is mainly based on a compilation over three years, 1981 to 1983, of almost all actual leaks, their natures, causes, consequences and methods used for their detection. By analysing these data it is possible to evaluate the efficiency of the primary coolant leak detection system and the problems raised by compliance with the criteria defined in the operating technical specifications.

## INTRODUCTION

The integrity of a PWR primary coolant containment is ensured by strict criteria taken into account at the stages of design, manufacture and production. During normal operation, strict limits are defined in technical specifications.

Nevertheless, the primary containment is not completely leaktight and any leakage of primary water has to be detected. Moreover, the importance for safety of such leaks depends on location, nature, flow rate and duration. Therefore, it is important that, at any time, the operator should be able to detect and locate a leak by means of a reliable and sensitive system intended for that purpose.

This paper aims at reviewing the situation of French PWRs in regard to primary coolant leakage. It is mainly based on a compilation of all actual leaks -their natures, their causes, their consequences, methods used for their detection- between 1981 and 1983. However steam generator tube leakage and reactor coolant pump seal failures are not taken into account. The analysis of these data makes it possible to assess the efficiency of primary coolant leak detection system and to raise problems related to compliance with the criteria defined in operating technical specifications. These two points are presented first.

## OPERATING TECHNICAL SPECIFICATIONS

French regulations related to primary circuit tightness are based on requirements of Regulatory Guide 1-45 : "Reactor Coolant Pressure Boundary Leakage Detection Systems" (1973).

French operating technical specifications distinguish two types of leakage :

- quantified leakage is leakage collected and conducted to a tank and monitored for the flow rate,
- unquantified leakage is all other leakage.

They set up conditions for normal operation and corrective actions as follows :

- with any unquantified leakage greater than  $2.3 \cdot 10^{-1} \text{ m}^3/\text{h}$  hot shutdown should be reached within 4 hours and cold shutdown within 24 hours,
- with any quantified leakage greater than  $2.3 \text{ m}^3/\text{h}$  cold shutdown should be reached within 10 hours.

Moreover leak detection systems have been analysed and approved by safety organisms at the same time as the whole design of the plant. They are described in detail hereafter.

## COLLECTING SYSTEM OF PRIMARY COOLANT LEAKAGE INTO THE CONTAINMENT

Detection methods of primary coolant leakage are strongly dependent on their collecting system design. It is therefore important to describe it, even briefly. For this purpose two kinds of leakage will be distinguished :

- designed collected leakage which is especially conducted to a tank and which may be characterized by the fact it is confined in a closed system from the source to the collecting tank,
- designed uncollected leakage is all other leakage which is, strictly speaking, collected (at least by the containment general sump or another sump or tank) but which is not confined and can spread over the containment atmosphere.

## Collected Leakage

In the reactor building there are three tanks designed to receive collected leakage ; their characteristics are indicated on figures 1 to 3. The three tanks are fitted with monitoring equipment (pressure, temperature, level) ; some of the measurements are recorded in the main control room and alarms and automatic actions are associated with them.

Note that criteria for collecting valve stem leakage are as follows : valves of radioactive circuits (reactor coolant system, chemical and volume control system, residual heat removal system, safety injection system, nuclear island vent and drain system) if their nominal diameter is greater than  $5 \cdot 10^{-2} \text{ m}$  or if they are regulating valves.

### Uncollected Leakage

Uncollected leakage may lead to water or vapor spreading over the containment ; it is collected in the containment sump either straight to it or undirectly for some particular leaks with which specific detection means are associated : they are detailed hereafter.

- Reactor cavity  
The bunker of reactor vessel pit is a water holdup point. Its level is monitored and an alarm warns the operator in the main control room if the water level reaches 5 cm. A draining line, normally isolated, is connected to the containment sump.
- In core instrumentation room  
This room is fitted with a leakage detection system quite similar to that of the reactor cavity. Draining line to the containment sump is normally isolated.
- Settling tank  
It is normally designed for collecting any oil leakage from primary pumps. This tank also collects floor drains from primary coolant pump bunkers. Its level is monitored ; it can be drained into the containment sump and any overflow is conducted to it.

### DETECTION METHODS OF PRIMARY COOLANT LEAKAGE

Among the different means for the operator to know the confinement state of the second barrier especially with respect to the operating technical specifications, we shall distinguish :

- primary leakage quantification methods with which specific detection means are associated,
- primary leakage detection and location methods.

#### Quantification methods

Among the different quantification methods originally envisaged, Electricité de France developed four of them, based on the following measurements :

- chemical and control volume tank level,
- sump level and flow monitoring,
- airborne gaseous radioactivity,
- air cooler condensate flow rate.

The two first methods only are actually operational. Airborne gaseous radioactivity monitoring does not allow quantification of primary leakage but still remains a useful detection means. Monitoring of condensate flow-rate from air cooler allows neither quantification nor detection of any primary leakage. This method therefore has been dropped and plants are no longer equipped with it. A new automatic method was designed and is currently tested at Cruas unit 3.



#### Chemical and volume control tank method (total primary leakage)

This consists of estimating the weight balance of primary coolant during a given period of time by monitoring the chemical and volume control tank level. A part from this, the following parameters are taken into account : pressurizer level variation, primary coolant volume variation, makeup and release volumes during the same duration. When the reactor is in steady-state operation, the operator tries to avoid any makeup or release so as to simplify the method and increase its sensitivity and accuracy (about 150 l/h for a 2 h test and 75 l/h for a 4 h test). In load-follow operation, for application of this method, the release and makeup volumes during the test period are to be evaluated. Installation of volumic counters on the two lines should make this evaluation easier and more accurate.

#### Containment sump method (unquantified leakage)

This method is closely dependent on primary leakage collecting system design in which discrimination between quantified and unquantified leakage is achieved. It is based on level indications and pump operation observation. As this sump collects primary leakage as well as secondary leakage, samples have to be analysed to evaluate the respective part of each type of leakage.

#### Evaluation of quantified leakage flow-rate

It may be done either by measuring leakage flow-rates conducted to the 3 collecting tanks or by calculating the difference between total and unquantified leakage flow-rates.

#### Automatic method of leakage evaluation

A code has been developed which allows, mainly from existing instrumentation (analog instrumentation, on-off signals), calculation of the total amount of primary coolant leakage : total, quantified and unquantified leakage rates.

The total primary leakage is evaluated by calculating at regular intervals the total weight of a reference volume which includes primary coolant system and chemical and control volume system. In order to improve the calculation accuracy, essentially dependent on non linear variations of water density, this reference volume is "meshed" in 19 elementary volumes each weight of which is calculated. The total leakage flow-rate is the difference between two average weights from about 10 calculated values corrected if necessary for makeups and releases.

The quantified leakage rate is also calculated by this code thanks to the collecting tank instrumentation ; the unquantified leakage rate is obtained from the two previous leakage rates provided some validations have been done.

This method, currently tested at Cruas unit 3, would be a great improvement of the primary leakage detection and quantification systems and would decrease the detection delay.

## Detection and location methods

Four types of detection means may be distinguished :

- detection means specifically associated with primary leakage quantification methods (table I),
- detection means associated with particular leaks either unquantified or quantified leaks (table II) ; it clearly appears that for most of them, leakage flow-rates must not reach limiting conditions set up by technical specifications. It would be more consistent to complete them by taking into account these particular leaks,
- detection means such as : airborne gaseous radioactivity in the containment, containment pressure, containment temperature, fire alarms,
- routine inspections.

The second and fourth types allow location of the leakage. For the third type, fire alarms generally give an approximative indication of location. Otherwise the best way to locate leaks remains local inspection.

LEAKAGE NATURE :	DETECTION MEANS
Total leakage :	Chemical and volume control tank :
	- visual detection on the level recording
	- makeup frequency
	- routine measurement
Unquantified leakage :	General containment sump :
	- level alarms
	- lifting pump operation
	- routine measurement
Quantified leakage :	Pressurizer relief tank :
	- level and temperature alarms
	Process drain and reactor coolant drain tanks :
	- level alarms
	- pump operation

Table I - Detection means specifically associated with primary leakage quantification methods

AFFECTED SYSTEM OR COMPONENT		DETECTION AND LOCATION MEANS
Component cooling system	(u)	- Radioactivity alarms - Storage feedwater tank level alarms
Safety injection accumulator tanks	(u)	Level alarms
In core instrumentation room	(u)	Level alarms
Reactor vessel cavity room	(u)	Level alarm
Primary pump bunkers	(u)	Settling tank level monitoring
Primary pump seals n° 2	(q)	High flow-rate alarm
Reactor vessel seal n° 1	(q)	Level alarm
Reactor vessel external seal	(q)	Temperature alarm
Pressurizer relief valves	(q)	Temperature alarms
Various other safety relief valves	(q)	Temperature probes or shift indicators

TABLE II - Particular leaks among unquantified (u) or quantified (q) leakage and specific detection means associated with them

#### OPERATING EXPERIENCE

This study covers 70 incidents which occurred between 1981 and 1983 and collected in Electricité de France incident reporting system. Steam generator tube leakage and reactor coolant pump seal failures are not taken into account.

Initial condition and mode of operation reached after the incident

<u>Initial condition</u>	<u>Mode of operation reached</u>
Power operation 36	Power operation ..... 4 Hot shutdown ..... 18 Cold shutdown ..... 14
Hot shutdown 15	Hot shutdown ..... 6 Cold shutdown ..... 7 Unknown ..... 2

Cold shut down : 12  
Discovered during shutdown : 7

It should be noted that among the 36 incidents which occurred when the reactor was at power, the limit value set up in the technical specifications for the flow rate leakage was reached for only 20 of them ; in those cases implementation of required actions was always correct. In other cases, operators anticipated the required actions.

#### Main causes of primary leakage

The main components involved in primary leakage are as follows :

- a) valves : packing gland leaks, upstream-downstream leaks
- b) reactor coolant pump casing seals
- c) diaphragm flange connections
- d) heat removal exchangers
- e) glass inspection windows on purge lines.

a) Valves : In 1982 and 1983, the behaviour of valves as regards packing gland leakage was considerably improved, through action taken by Electricité de France : manual valve back-seating, implementation of new specifications concerning valve stem leaktightness. Problems still remain on pressurizer continuous spray valves and on motor-operated valve of the charging line inside the containment.

The components affected by upstream-downstream leakage are mainly the pressurizer relief and safety valves. Though these leaks are very low, their potential consequences are important : hydrogen release to pressurizer relief line and tank, suppression of safety valve water plugs thus making safety valves open at a pressure different than their set-point.

- b) Reactor coolant pump casing seals : Although these leaks are very low, these incidents, generally detected during refueling outage by boron deposit on the casing, must be considered as break forerunners. They are essentially due to inadequate stud tightening torque and to insufficient seal quality. Corrective actions have been taken such as improvement in seal quality, increase of tightening torque and reinforcement of periodic controls.
- c) Diaphragm flange connections : These leaks occurred mainly on reactor coolant system temperature by-pass loops during temperature and pressure transients. The replacement of these flange connections by welded joints is still under study at Electricité de France.
- d) Heat removal exchangers : These leaks occurred during reactor heat removal system (RHR) actuation transients on exchanger threaded flange. The improvements of RHR exchangers is still under study (seal modifications, changes in studs tightening torque, modifications of exchanger pipe supports...). Otherwise the RHR actuation procedure has been changed to minimize pressure and temperature transients.
- e) Glass inspection windows on purge lines : The glass inspection window breaks mainly occurred during manual actions on reactor coolant temperature by pass loops. Procedures have been changed to solve this problem.

#### Primary leakage consequences

Reactor coolant leakage may be considered as a forerunner of a break in the second barrier. Besides, these leaks often present some drawbacks which make reactor operating more difficult and reduce plant safety : releases of radioactive and borated water or steam into the containment, reduced capacity of collecting tanks, hydrogen releases, ferritic steel corrosion due to boric acid.

Main problems encountered on French units from 1981 to 1983 due to primary coolant leaks are as follows :

- valve stud corrosion ; EdF is replacing all ferritic steel studs by stainless steel ones on valves in contact with borated water,
- hydrogen fire on a pressurizer relief valve,
- in core instrumentation system spray due to leakage on valve packing glands.

#### Leakage detection and location

As concerns the primary coolant leakage detection the main points drawn from the examination of significant incident reports are as follows :

- a) in normal operation, the main indicator of a primary coolant leakage is the behaviour of the chemical and volume control tank monitoring level,
- b) this indication of primary leakage is often confirmed by simultaneous indicator such as: containment radioactivity, containment pressure, tank and sump levels (reactor coolant drain tank, process drain holdup tank, containment general sump, in core instrumentation room sump, pressurizer relief tank),
- c) some particular leaks are detected by local fire alarm actuations ; for instance leaks into primary coolant pump bunkers and stem leakage of the containment isolating valves on the charging line which are thus easily located,
- d) upstream-downstream leaks of the pressurizer relief and safety valves are detected thanks to alarms generated by the temperature probes on the relief lines.

Primary coolant leakage location, particularly uncontrolled leakage, seems to be rather difficult and is currently visually achieved by local inspections.

#### CONCLUSIONS

The French PWR situation concerning primary coolant leakage was assessed on the basis of the analysis of leaks which occurred over three years, 1981 to 1983 (except steam generator tube leaks and reactor coolant pump seal failures) ; it may be characterized as follows :

- the main components involved in these incidents are valves and, to a lesser extent, primary pump casing seals ; actions have been taken or are planned to reduce their reoccurrence as well as their consequences,
- no problem arised from the primary coolant leakage detection system and thus from the leakage collecting system design. Nevertheless, the leakage detection delay and the method sensitivity can't be accurately appreciated. However, the forthcoming implementation of a new automatic method of primary leakage evaluation should improve its reliability and decrease the detection delay,
- for all reported events, the application of operating technical specifications was correct and in some case, anticipated.

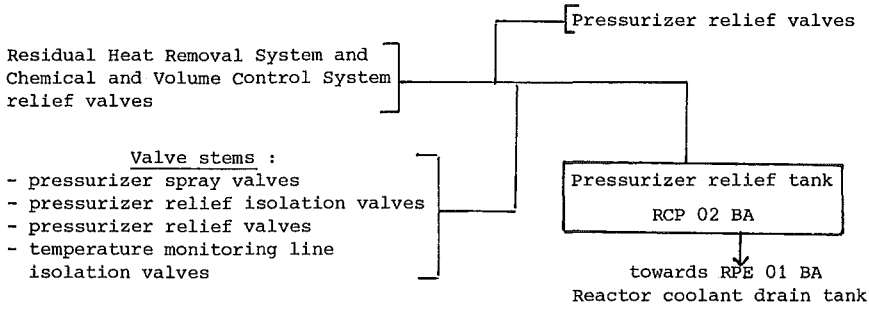


FIGURE 1 - Primary leakage collected by the pressurizer relief tank Schematic presentation

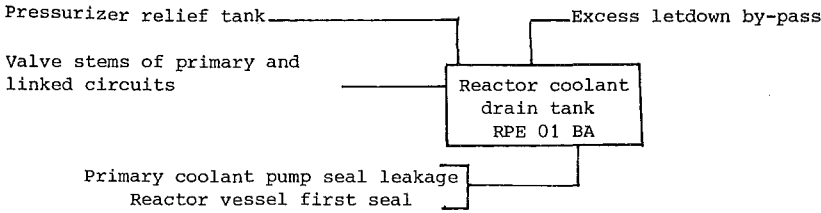


FIGURE 2 - Primary leakage collected by the reactor coolant drain tank Schematic presentation

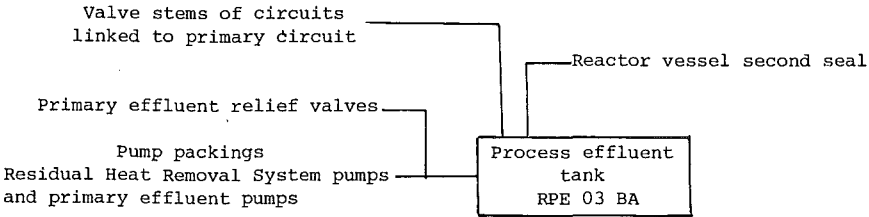


FIGURE 3 - Primary leakage collected by the process effluent tank Schematic presentation

SYSTEMATIC SAFETY EVALUATION OF  
OLD NUCLEAR POWER PLANTS

G. Dredemis et B. Fourest

Commissariat à l'Energie Atomique  
Institut de Protection et de Sûreté Nucléaire  
Boîte Postale n°6  
92260 Fontenay-aux-Roses, FRANCE

## ABSTRACT

The French safety authorities have undertaken a systematic evaluation of the safety of old nuclear power plants. Apart from a complete revision of safety documents (safety analysis report, general operating rules, incident and accident procedures, internal emergency plan, quality organisation manual), this examination consisted of analysing the operating experience of systems frequently challenged and a systematic examination of the safety-related systems. This paper is based on an exercise at the Ardennes Nuclear Power Plant which has been in operation for 15 years. This paper also summarizes the main surveys and modifications relating to this power plant.

## INTRODUCTION

French safety authorities have undertaken a systematic evaluation of the safety of old nuclear plants.

Indeed, it has become apparent that these installations, which were not designed to present safety criteria, should be the subject of a reevaluation primarily designed to establish their global safety level in relation to power plants satisfying current requirements.

The first installation to have been reexamined in this way is the Ardennes Power Plant (CNA) which has been in operation for approximately 15 years. Consequently this paper describes the process adopted by the Institut de Protection et de Sûreté Nucléaire (IPSN) which is the technical arm of the French safety authorities, through a reexamination of the safety of the CNA.

PROCEDURE USED FOR REEVALUATING THE SAFETY OF THE  
ARDENNES NUCLEAR POWER PLANT

The basis for reevaluating this installation was a complete revision of the safety documents undertaken by the licensee at the request of the safety authorities (safety analysis report, general operating rules, internal emergency plan, quality organisation manual). Its preparation included all studies undertaken by the licensee in order to improve the plant's safety and led to modifications both to the design and to the operating rules.

This reexamination therefore involved close cooperation between the licensee and IPSN.

The basic idea behind this safety reevaluation was to endeavour to establish the global safety level of the CNA in relation to 900 MWe pressurized water reactor power plants. For this purpose it was not considered necessary to make a systematic analysis of all systems important from a safety point of view.

Indeed, it seemed more appropriate to adopt different approaches depending on whether the system being analysed was frequently (or even permanently) used or on standby during normal operation of the power plant.

In the case of systems frequently used, experience in operating the power plant provided knowledge of each of them which was considered sufficient in order to assess their suitability for fulfilling the function for which they were designed. The operating evaluation was drawn up on the basis of anomalies and incidents occurring during operation as well as modifications made over the years.

In the case of safety related systems for which there is insufficient operating experience, the procedure adopted was to analyse each systematically, without it being required that they should satisfy all safety criteria applicable to 900 and 1300 MWe pressurized water power plants ; a study was carried out to assess them in relation to what is today considered to be an acceptable safety level and was in two stages :

- a comparison of the system in relation to current design criteria,
- identification of problems in order of importance taking account of the various aspects of the system (incidents, maintenance, periodic testing, procedures...).

Further, two different approaches were adopted with regard to design problems and operating rules.

The design criteria for 900 MWe pressurized water reactor power plants were used as a reference for reexamining safety of the CNA and only those design modifications which were of interest from a safety cost-yield point of view were requested.

On the other hand, with regard to the general operating rules (technical specifications, procedures...) it was considered necessary that CNA should benefit from the considerable improvements made in this field. It was therefore decided to adapt the CNA operating rules on those of 900 MWe pressurized water reactor power plants allowing, of course, for that power plant's specific features.



In some cases the modifications to equipment necessary to bring safety up to a level comparable with that now in force were such (due in particular to the absence of redundancy and/or independence) that it was considered preferable, in agreement with the licensee, to give priority to a study based on complete loss of the function with a view to establishing the procedures to be applied in such a potential occurrence. All the more so, since some specific features of CNA could have a favourable effect on the consequences of total loss of function as compared with the analysis made of 900 MWe pressurized water reactor power plants.

At the same time that this work was proceeding the licensee was also asked to undertake a reevaluation of margins relating to the risk of a vessel embrittlement. This point will not however be considered in this paper.

#### MAIN ACTIONS INITIATED OR UNDERTAKEN DURING THE SAFETY REEVALUATION OF THE ARDENNES NUCLEAR POWER PLANTS

##### - Reexamination of the CNA site

Given the period at which the CNA was designed, site related safety aspects were not considered as comprehensively as now. It was for this reason that it was thought important that a complete reexamination should be made during this reevaluation.

At the end of this work, the only point requiring particular consideration related to checking the power plant's seismic resistance (NRC-RG-1.60 spectrum 0.1 g). In view of the opinion of experts it was decided to limit this study to an examination of the behaviour of the primary system and its supporting structures, to verifying the resistance of the emergency shutdown and removal of residual power systems as well as the spent fuel pool.

##### - Experience of the main nuclear systems

An operating evaluation was made for the following systems :

- chemical and volumetric control system,
- residual heat removal system,
- auxiliaries cooling system,
- raw water system,
- compressed air system,
- ventilation system,
- normal feedwater supply system,
- emergency power supplies.

The reliability of these systems was assessed on the basis of incidents arising on the various items of equipment making them up, on information obtained from preventive maintenance and periodic testing, as well as on modifications made to the systems. This survey was carried out on the operation period of CNA before the safety reevaluation (1968 to 1982).

This operating evaluation showed that the various problems arising during operation had been resolved by corrective measures whose effectiveness has been confirmed by experience.

Only the emergency power supplies were not satisfactory from a safety point of view. Indeed, the CNA having been designed some 20 years ago, the principle of separating redundant trains was not applied : equipment was grouped by function and all power supplies are located in the same building.

Three lines of action were followed in parallel in order to study and improve this situation :

- limitation of potential causes of a loss of power supplies (improved fire protection, physical separation of equipment as far as possible),
- study of the loss of external and internal power supplies,
- installation of new emergency generators as part of the new auxiliary feedwater.

- Systematic analysis of the safeguard systems

. Safety injection and containment spray systems

In this plant, the two "safety injection" and "containment spray" functions are linked and use the same pumps for the recirculating phase. It was for this reason that the systematic study of these two systems was carried out in parallel.

A survey was made on the basis of 900 MWe pressurized water reactor plants of the essential differences in equipment and operating modes during the successive phases of safety injection and containment spray as a function of different break sizes and consequently of the pressure evolution in the primary system.

Following this comparison, the main studies and measures undertaken to improve the safety of the reactor containment, safety injection and spray systems aimed to :

- a minimization of the risks of human failure during switch over from "direct injection" configuration to "recirculating" configuration,
- an accommodation of all possible operating situations and in particular to be able to inject and cool the water in the containment sumps if primary fluid pressure remains high (as in the case of small breaks),
- an improvement of the automatic initiation of the "safety injection" and "containment spray" systems.

Figure 1 shows the main modifications which it has been decided to make to these systems.

In order to reduce the causes of single failure, the licensee intends to double all valves involved in the safety injection sequence and which could by a single failure result in loss of the safety injection and/or containment spray functions.

On the existing circuit, those valves whose position changes during switch over from "direct injection" configuration to "recirculating" configuration are manual, with the exception of the valve located immediately at the sump suction, which is pneumatic. Therefore, such a change in configuration requires local operation by operators in order to align the system. Given the risk of human error involved and the problem of accessibility to the various rooms where the equipment to be operated is located, the licensee intends replacing all the manual valves involved by two motorized valves installed in parallel.

During the recirculating phase, the cooling function for the primary fluid sucked in the sumps is provided by the residual heat removal system exchangers which are not designed for high pressures. In order to ensure the sump water injection and cooling functions should primary fluid pressure remain high, the licensee intends to divide the output of the injection pumps into two : one part will be directly reinjected at high pressure into the primary loops and the other will be depressurized to circulate in the residual heat removal system exchangers so as to cool the water contained in the sumps by means of the spray system.

At the CNA, the safety injection sequence is initiated by a coincidence of the pressurizer low pressure and low level signals. This feature was not modified by the licensee following the TMI in order to avoid spurious safety injection which, in the case of CNA, would involve a delicate operating transient. Indeed, initiation of the safety injection sequence involves complete isolation of the containment and in particular loss of cooling of the primary fluid by the steam generators. Instructions in the control room require the operator to startup safety injection on the "pressurizer low pressure" criterion. After discussion with the plant staff it was decided to eliminate coincidence of the 2 signals and to maintain only the pressurizer low pressure signal, whilst at the same time modifying the containment isolation function by introducing a 2 phases isolation identical to that already existing on 900 MWe pressurized water reactor power plants. This modification will also permit automatic initiation of the spray sequence which is up to now manually controlled from the control room on a containment high pressure criterion.

#### Auxiliary feedwater system

The auxiliary feedwater system was designed to accommodate loss of offsite electric power supplies by ensuring maintenance of the unit at hot shutdown for a period of the order of 15 to 20 h.

The design of the system is such that it does not permit switching from hot shutdown mode to intermediate shutdown mode where pressure and temperature can be controlled by the residual heat removal system.

After systematic analysis of this system it became apparent that it was unable to cover the following situations :

- loss of normal feedwater,
- loss of external and internal power supplies,
- small and medium sized breaks in the primary circuit combined with loss of outside power supplies,
- breaks in secondary system pipes combined with loss of offsite power supplies.

Given this situation, the licensee has decided to install a new auxiliary feedwater system for the steam generator satisfying all present safety criteria (see figure 2).

This modification is the most important resulting from the re-evaluation of this power plant's safety.

- Containment

It was also considered important as part of the CNA safety reevaluation to examine existing arrangements to mitigate, as far as possible, the consequences to the power plant personnel and the environment of accidental and post-accidental conditions.

In the case of CNA, the primary system as well as the auxiliary systems are installed in two separate containment vaults ; given this installation and a few relatively minor adjustments it was considered that the reactor vault containment and that of the nuclear auxiliary vis à vis the environment was satisfactory.

The two main studies undertaken following this examination relate to conditions of access to equipment necessary in a post-accidental situation and also to the qualification of the electrical and mechanical equipment under accidental conditions.

- Revision of safety documents

Simultaneously with these improvements to the power plant, the licensee undertook a revision of the safety documents.

These include the quality organisation manual, the general operating rules, the incident and accident procedures.

Two priorities were established in applying the new quality organisation manual. The first relates to the drafting of the technical specifications for all Q.A. equipment. In carrying out this work the operator came up against many difficulties arising from the age of the equipment, in particular when the supplier of the equipment was no longer the original manufacturer. The second priority relates to the application of the new quality organisation rules for maintenance of the primary system and safety grade systems equipment.

With regard to the revision of the general operating rules, the licensee has been mainly concerned to improve the operating technical specifications. These latter have been improved by adapting technical operating specification of 900 MWe pressurized water reactor power plants to the CNA.

Revision of all the CNA accident and incident procedures is in progress. It is based on studies made for 900 MWe pressurized water reactor power plant procedures and has sought to quantify as much as possible the diagnosis criteria and those applicable to the choice of measures to be taken. The safety authorities have also requested that this revision should include checking consistency between procedures and design ; in particular verifying the accessibility of equipment necessary for the application of accident procedures.

## CONCLUSIONS

Reevaluation of the safety of old nuclear power plants provides an overall view of the plant in relation to safety criteria in force at the time. In the case of the CNA this was not intended to be an exhaustive analysis of the

plant but was directed to highlight those aspects considered to be most important to the safety of that power plant. Given the programme of studies and the modifications undertaken, this examination has resulted in a favourable assessment of the suitability of this power plant for continuing operation under satisfactory safety conditions.

One of the reasons of the success of this programme relates to the good relationship that existed from the very beginning between the licensee and the safety authorities which worked in close cooperation. This seems to be a necessary condition.

The work undertaken as a result of this safety reexamination was spread into three phases :

- phase 1 : overall definition of the modifications,
- phase 2 : detailed design of the modifications,
- phase 3 : implementation of the modification.

At the present time the licensee is completing the second phase of this programme. The target date is to complete all these actions by the end of the 1985 refueling outage.

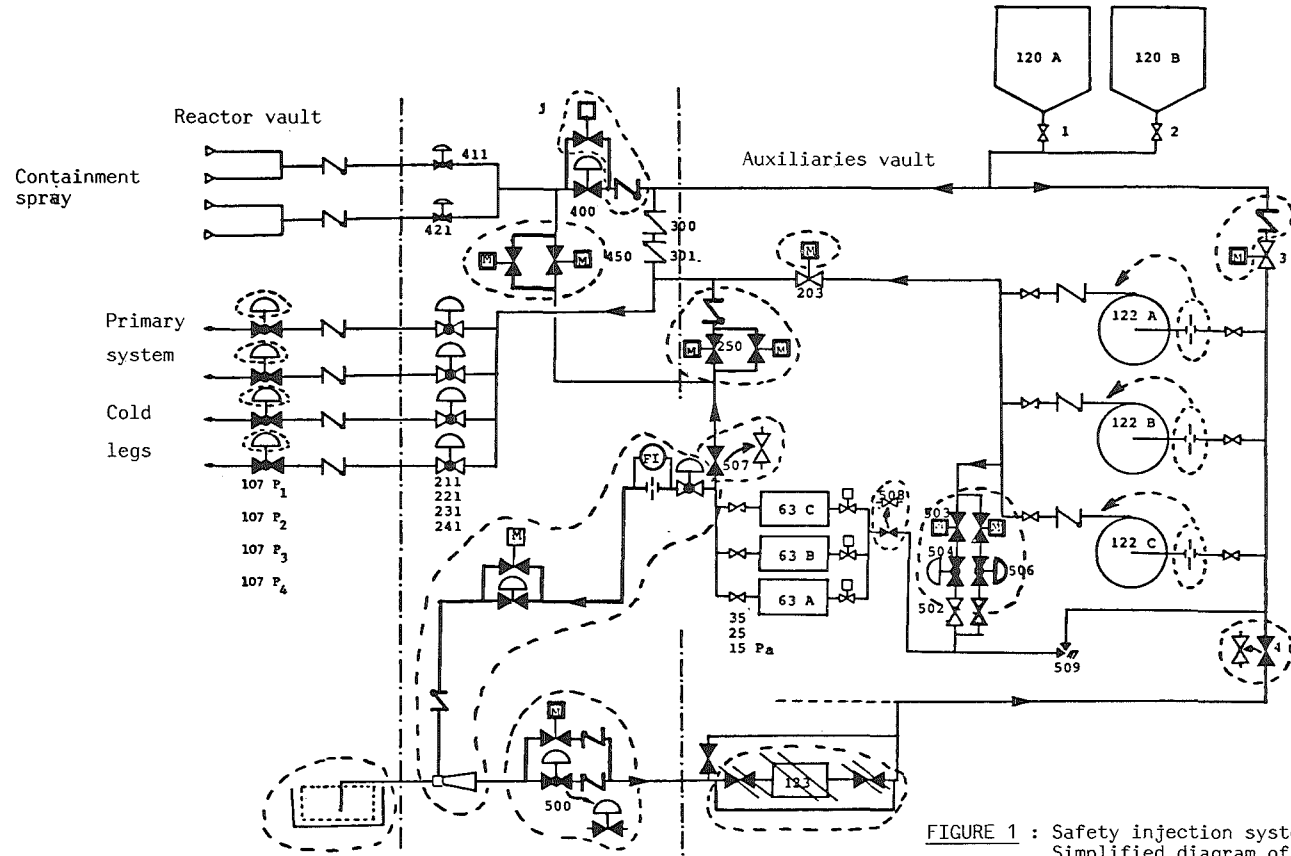


FIGURE 1 : Safety injection system  
Simplified diagram of improvements

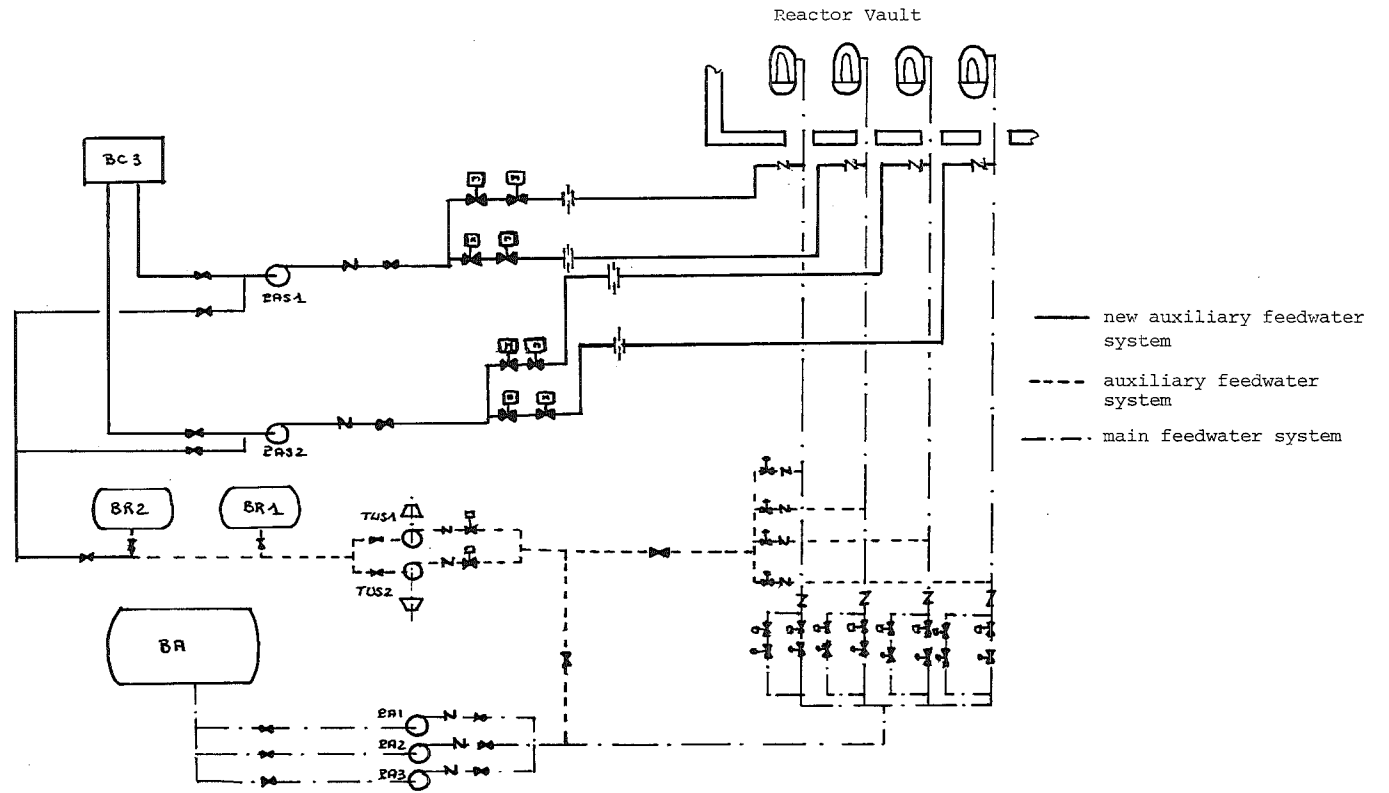


FIGURE 2 : Simplified diagram of feedwater systems

# HYDROGEN WATER CHEMISTRY - A PROVEN METHOD TO INHIBIT INTERGRANULAR STRESS CORROSION CRACKING IN BOILING WATER REACTORS

J. Magdalinski and R. Ivars

ASEA-ATOM  
Box 53, S-721 04 Västerås, SWEDEN

## ABSTRACT

Intergranular Stress Corrosion Cracking (IGSCC) of stainless steel has occurred in several BWR plants in recent years. In Swedish plants the extent of cracking has been limited and the consequences, in terms of operational disturbances, have been quite small. Some cracks have been detected recently in the Ringhals 1 plant, however. As a phenomenon related to ageing, the cracks and their causes must receive the greatest attention.

ASEA-ATOM initiated experimental work in the laboratory and in the Oskarshamn 2 BWR plant in the late seventies. The method chosen for these experiments, the aim of which was crack prevention, was hydrogen addition to the feedwater. Full scale demonstration runs have shown that oxygen suppression by hydrogen addition to the reactor coolant is technically feasible. Materials tests carried out in reactor coolant in the Ringhals 1 plant have demonstrated that intergranular stress corrosion cracking is eliminated when the oxygen concentration is kept low.

The paper will present the main results of the Hydrogen Water Chemistry program. The technique developed has led to the design of a hydrogen injection system which is now commercially available for IGSCC prevention.

## INTRODUCTION

Intergranular stress corrosion cracking (IGSCC) of austenitic stainless steel piping has been a headache for BWR owners for more than a decade. It has caused significant losses in plant availability and costly repairs. The phenomenon has been a problem for metallurgists and corrosion engineers for many years but was first seen in nuclear power plants in 1974-75, when a number of cracks were detected in the stainless pipework of 8 US BWRs.

The extent of cracking in Swedish plants has been limited and the consequences, in the form of disturbances to operation, have been very small. However, as a phenomenon of ageing, the greatest attention must be paid to the cracks and their causes.

IGSCC occurs in the heat-affected zone of welds, an area that is sensitized by the welding process. Three conditions must be satisfied simultaneously for IGSCC to occur: tensile stress, sensitized material and oxidizing environment.

Tensile stress of sufficient magnitude occurs at almost all welds as a result of the presence of normal structural stress, in combination with residual stress from welding.

Sensitization is the result of heat treatment and makes the stainless steel sensitive to corrosion along grain boundaries.



A normal 18 Cr/8 Ni stainless steel with a carbon content of 0.02 - 0.08 % is supersaturated with carbon. If the steel is heated, e.g. in conjunction with welding, the mobility of the atoms increases and, if the heating is of sufficient duration within a critical temperature range (500-900°C), chromium carbides precipitate and grow. The carbide precipitation occurs predominantly on the boundaries of the grains forming the structure of the steel. The precipitation rate is strongly dependent on the carbon concentration, and at concentrations below 0.04-0.05 % carbon the rate is so slow that the risk of sensitization may be neglected. As a result of the carbide precipitation, the grain boundaries become depleted of chromium, resulting in the boundaries losing its stainless properties and becoming "sensitized".

Oxidizing environment, corrosive enough to permit attack on sensitized stainless steel is given primarily by the presence of dissolved oxygen. Boiling water reactors of current design use high-purity water with no chemical additives as primary coolant. A steady state concentration of 100-400 ppb of dissolved oxygen is produced by radiolysis of water in the reactor core. Oxidizing impurities, e.g. from resin intrusions or make-up water, may also be of some importance to the oxidizing potential.

In the case of Swedish boiling water reactors, ASEA-ATOM has set up stringent material and manufacturing specifications to avoid IGSCC. The requirements apply to limitation of the carbon content to a maximum of 0.05 % in steel according to Swedish Standard SS 2333 in contrast to the 0.08 % carbon content of the American steel AISI 304. Certain limitations also apply to heating during welding and to repair welds, to avoid unsuitable heat treatment. These measures have delayed and limited the incidence of IGSCC in Swedish plants, but during 1982-1983, cracks were detected in Ringhals 1, which has been in operation since 1974. Additional preventive measures have been taken in the most recently built plants, including the limitation of the carbon content to a maximum of 0.03 %.

To achieve immunity against IGSCC and to prevent cracking it is sufficient to eliminate one of the three factors mentioned above. In the case of the first - tensile stress - a number of remedies have been developed which to some extent improve the stress situation on the inside of tubes from tensile towards compressive stresses. It is also possible to affect the second factor - sensitization - by choosing a material with a sufficiently low carbon content. Both of these remedies would be demanding and expensive in the case of plants in operation, because they require the treatment of all welds or the replacement of all stainless piping in extensive parts of the primary systems of the plants.

The development of a method to eliminate the third factor, i.e. to prevent corrosion by reducing the oxygen content of the reactor water to very low concentrations has been conducted by ASEA-ATOM. The oxygen content is reduced by the addition of hydrogen to the feedwater system of the plant. This method, which will be known as Hydrogen Water Chemistry (HWC), has also been adopted by General Electric in the U.S.A.

The water chemistry tradition of ASEA-ATOM has its historical roots in the fact that the Swedish nuclear program once started with heavy water reactor concepts, in which the careful treatment of the valuable coolant had high priority. The influence of different additives on the decomposition of the reactor coolant was studied in several research projects during the 1950-60's, for instance in the Halden Boiling Heavy Water Reactor and in the Studsvik R2 Reactor. Based on this broad experience it was natural for ASEA-ATOM to attack the environmental factor and to choose the HWC concept as the potential remedy against IGSCC.

During 1977-78 ASEA-ATOM carried out a pilot study on hydrogen water chemistry for BWRs. An engineering evaluation of the feasibility of hydrogen addition to the reactor feedwater to reduce the reactor water oxygen concentration was performed. The study recommended a short-term demonstration test in the Oskarshamn 2 plant (570 MWe). That test, the first in the world in a full-size commercial BWR, was carried out in November 1979 /1/. Technical feasibility of the hydrogen addition concept was convincingly demonstrated.

Today a number of full-scale test runs have been carried out by ASEA-ATOM in Oskarshamn 2 /2/ as well as in Ringhals 1 (750 MWe) /3/. The testing has produced valuable data on the plant response to hydrogen addition and on the hydrogen addition response to plant behaviour. In Ringhals 1 IGSCC testing was carried out in a test loop using the Constant Elongation Rate Test (CERT) technique. Strongly sensitized test pieces were tested in reactor water with varying oxygen concentrations under full reactor power operation. The conclusion was that IGSCC is completely eliminated when the reactor water oxygen concentration is kept below 5 ppb and no other oxidizing impurity of significant concentration is present. More details regarding materials tests in Ringhals 1 has been reported by Ljungberg and Korhonen /4/.

In order to verify the hydrogen addition technique as a final remedy against IGSCC, necessary follow-up investigations are being carried out. Studies of all relevant physical phenomena and operation-related parameters, including inspection for any side effects, will be continued.

The investigations carried out have been supported by the Swedish power utilities and the Swedish Nuclear Power Inspectorate and have now reached a stage at which operational application of Hydrogen Water Chemistry in Swedish nuclear power plants can be started on a commercial basis.

The main features of the hydrogen water chemistry will be summarized below. Test results will be presented primarily from the hydrogen addition test recently run in the Forsmark 1 plant (900 MWe).

## RESULTS AND DISCUSSION

### Oxygen suppression

It has been known for many years that oxygen production from water radiolysis can be suppressed by addition of hydrogen. A number of tests in the 1960's in experimental reactors confirmed this phenomenon. In the pressure water reactor oxygen suppression was used from the very beginning. However, since the BWR primary loop is not a closed system with regard to noncondensable gases the BWR application of oxygen suppression must be based on continuous hydrogen addition. When the pipe cracking problem made the hydrogen addition concept interesting again, there were doubts that it would be a technically and economically feasible method for BWR plants.

In all reactor tests with hydrogen addition the hydrogen has been supplied from standard compressed gas cylinders. After pressure control, flow monitoring and control the gas has been injected to the condensate downstream of the condensate clean-up system (fig 1). Control and shutdown features are varying in the different plant installations. In the Ringhals 1 plant, which has the most advanced equipment, the system can be operated from the central control room. The hydrogen injection flow is automatically controlled by the preset reactor water oxygen concentration or the preset feedwater hydrogen concentration (fig 2).

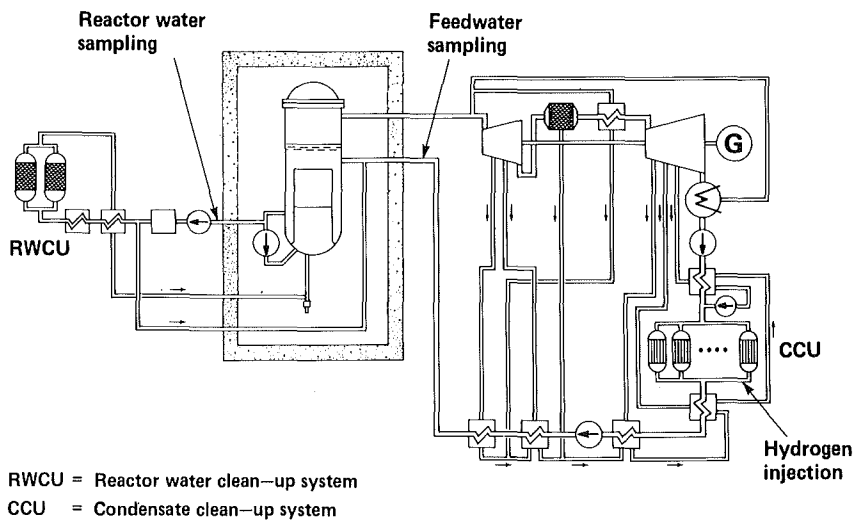


Figure 1. Main flow diagram of Oskarshamn 2

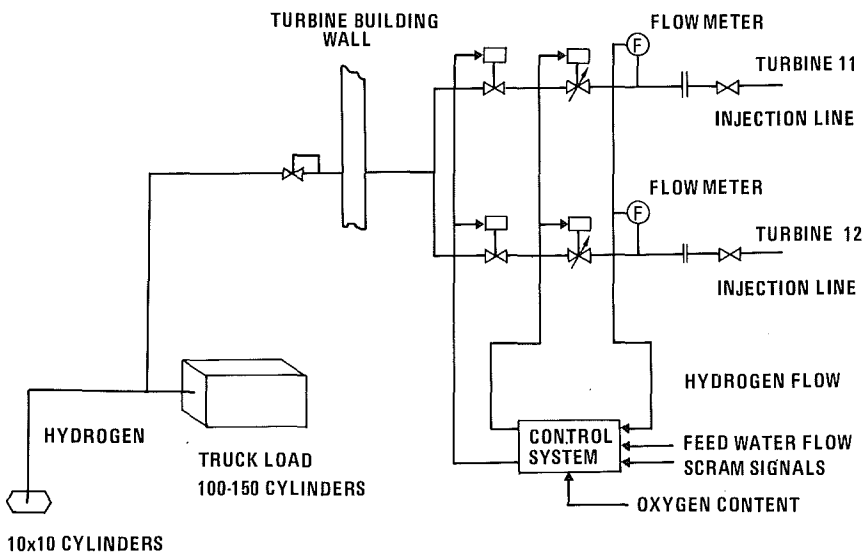


Figure 2. Schematic diagram of hydrogen injection system of Ringhals 1

Data from Forsmark 1 regarding the oxygen concentrations in the core inlet and core exit water as a function of the hydrogen addition rate are shown in fig 3. Apparently the oxygen content in the water below the core is much easier suppressed by hydrogen addition. This phenomenon has been verified in all plants. The reason is that oxygen is consumed to a considerable extent already in the downcomer region by recombination with the added hydrogen. This recombination is catalyzed by the relatively high gamma radiation field in the downcomer close to the core. The fact that the water is subcooled and no gas stripping occurs in the downcomer region also promotes the recombination reaction. This test result is illustrated in fig 4, where oxygen concentrations in the reactor pressure vessel at different hydrogen addition rates are indicated. The two different hydrogen addition rates represents the important concepts of "Partial suppression" with low oxygen concentration in the region below the core, and "Full suppression" with low oxygen concentration in the whole water phase of the reactor pressure vessel.

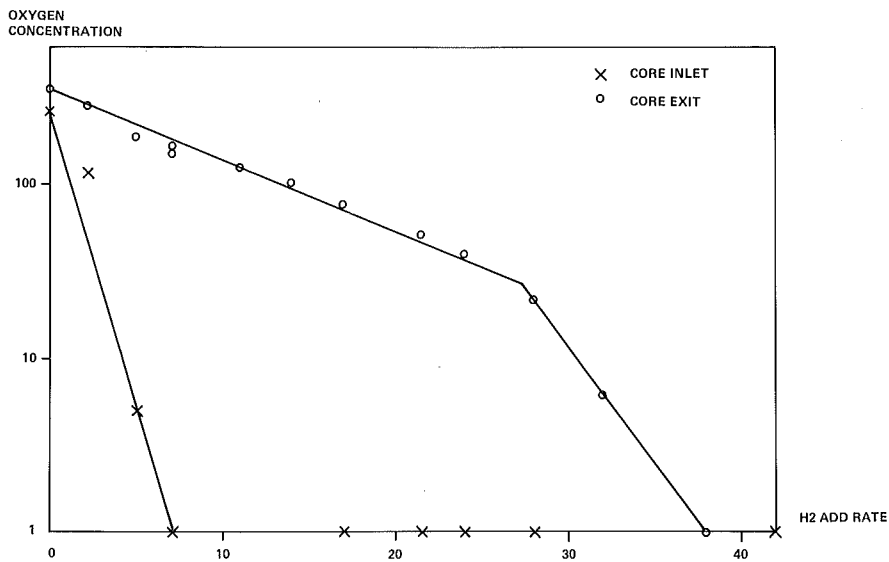


Figure 3. Oxygen concentration in core inlet and core exit water as a function of feedwater hydrogen addition rate (Forsmark 1, April, 1984)

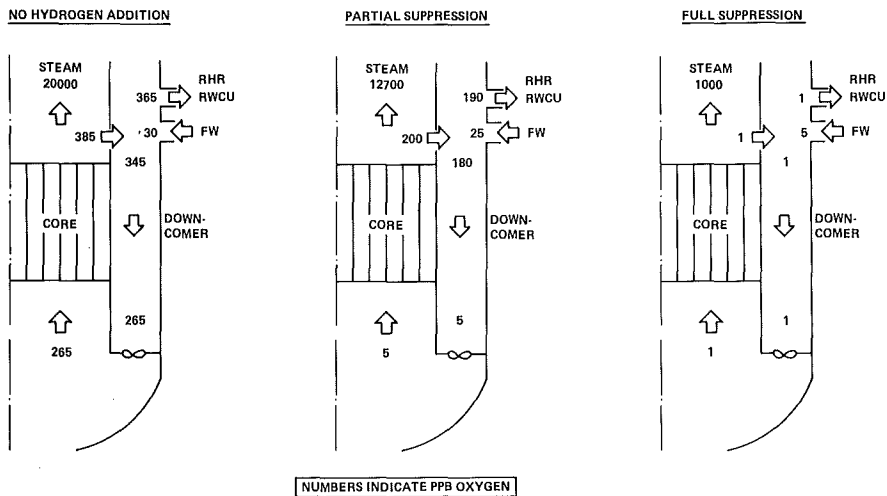


Figure 4. Oxygen concentration in reactor coolant at three feedwater hydrogen addition rate levels (Forsmark 1, April, 1984)

#### Offgas system

With hydrogen addition to the reactor the excess hydrogen suppresses water radiolysis and there is no net consumption of hydrogen in the process. The net production of hydrogen and oxygen decreases. The hydrogen flow to the offgas system is the sum of added and radiolytically produced hydrogen. As shown in fig 5 the hydrogen flow initially decreases and passes through a minimum. At higher addition rates the hydrogen flow increases and approaches the "addition rate line" asymptotically. In a BWR without offgas recombiner the total offgas flow will have approximately the same curve shape as the hydrogen flow.

In a plant with recombiner the radiolytically produced hydrogen and oxygen are recombined. During normal operation the offgases downstream of the recombiner consist mainly of air from in-leakage to the turbine condenser. With hydrogen addition to the feedwater the offgas flow decreases slightly at first, when oxygen from the air in-leakage is being burnt by the added hydrogen. At higher addition rates the offgas flow increases as the hydrogen flow and consists mainly of hydrogen and nitrogen.

In a permanent installation the excess hydrogen in the offgases can be conveniently removed by the addition of oxygen upstream of the recombiner. The offgas flow will be reduced, the time delay increased and a safe operation of the offgas system will be insured (no risk for the occurrence of combustible mixtures of hydrogen and oxygen).

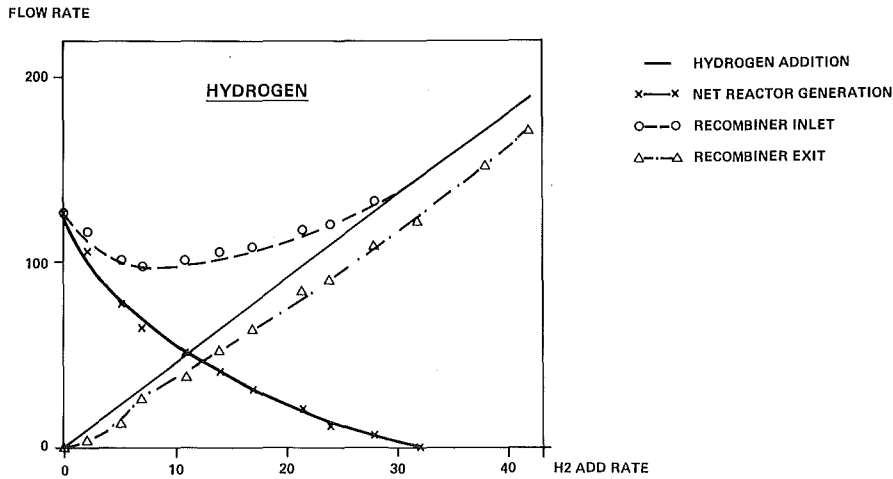


Figure 5. Hydrogen mass balance versus feedwater hydrogen addition rate (Forsmark 1, April, 1984)

#### IGSCC tests

In the Ringhals 1 plant susceptibility to IGSCC was measured with the Constant Elongation Rate Test (CERT) technique. Heavily sensitized test pieces of stainless steel were tested in reactor water at various oxygen concentrations. It was demonstrated that IGSCC is inhibited when the reactor water oxygen concentration is kept below 5 ppb.

The conditions under which a corrosion process can occur are determined by the electrochemical potential (ECP), a fundamental quantity in the thermodynamics of corrosion. ECP of the BWR reactor water is primarily controlled by the oxygen concentration. However, chemical and thermal transients may occur, resulting in oxidizing impurities being transferred to the reactor water. In addition, short-lived products of radiolysis are present in the reactor coolant. Hence, ECP, rather than oxygen, should be used to characterize the environment with respect to the risk of IGSCC, since it represents the integrated effect of all oxidizing species. ECPs of construction materials have been monitored in most of the hydrogen addition tests with metal sensor electrodes against Ag/AgCl reference electrodes at high temperature. However, the measurement technique must be further developed to be suitable for routine application. In-reactor tests to determine the boundary conditions of susceptibility to IGSCC are therefore strongly recommended. Details regarding materials tests and ECP measurements in Ringhals 1 have been reported elsewhere /4/.

## Radiation fields

An important side effect of hydrogen addition is the higher radiation level in the turbine plant. This is caused by an increased stripping by the steam of short-lived N-16 activity. In the reducing reactor water environment during hydrogen addition the fraction of volatile species of nitrogen (e.g. nitrogen gas or ammonia) becomes larger.

Initially the radiation fields at the main steam lines increase very slowly. A sharp increase is followed by a continued slow increase at higher addition rates, fig. 6. Obviously, the main steam line radiation is an additional measure of when the transition regime between oxidizing and reducing conditions is entered.

A typical increase of the main steam lines radiation level is 3-5 times that with no hydrogen addition. As the increase is caused by short-lived N-16 activity, the radiation level is immediately reduced to the original value when hydrogen addition is shut down.

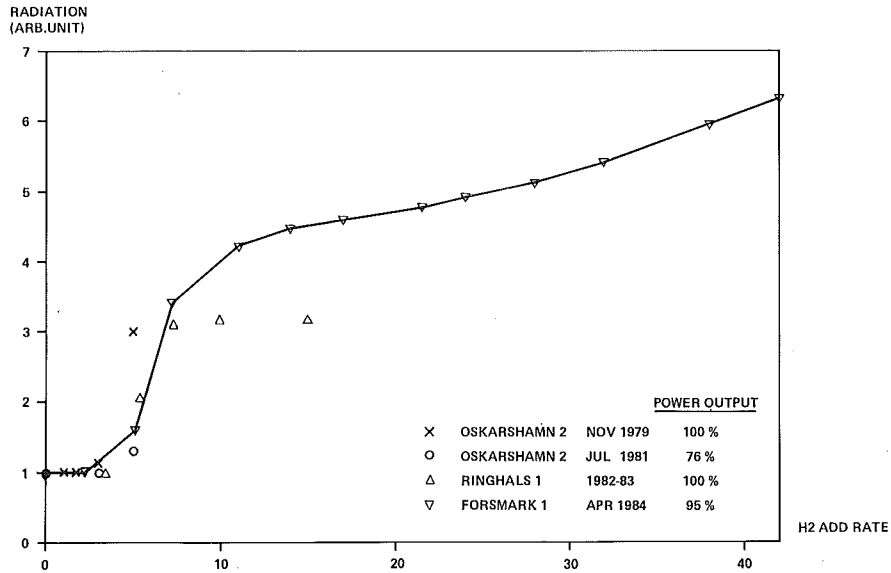


Figure 6. Main steam line radiation field versus feedwater hydrogen addition rate

## Coolant chemistry

Some minor effects on feedwater and reactor water chemistry take place during hydrogen addition.

The condensate and feedwater oxygen concentrations decrease with the decreasing steam oxygen concentration. The order of magnitude of the decrease is determined by the relation between steam oxygen concentration and air in-leakage rate to the turbine condenser. There is no recombination of hydrogen and oxygen in the feedwater train.

The concentrations of chromium and Cr-51 activity in the reactor water decrease significantly (10-fold) with hydrogen addition. This is attributable to the chemical reduction of water soluble chromate into less soluble chromium oxides. The phenomenon is also reflected in a reduced reactor water conductivity.

No other significant side effects of hydrogen addition have been observed, nor are they expected in the long term. However, studies of all relevant physical phenomena and operation related parameters, including inspections for any side effects, will continue.

## CONCLUSIONS

It may be concluded that intergranular stress corrosion cracking (IGSCC) in sensitized austenitic stainless steel in the BWR primary system can be inhibited by hydrogen water chemistry, the detailed specification of which may be specific to a given plant.

A number of full-scale tests under realistic and operational conditions in authentic BWR environment has demonstrated that Hydrogen Water Chemistry, where hydrogen is added to the reactor feedwater, is a viable option for BWRs.

A relatively moderate hydrogen addition to the feedwater achieves a major reduction of the oxygen concentration of the reactor water downstream of the downcomer in the reactor vessel and in connected systems. In the case of the Ringhals 1 plant it has been demonstrated that a reduction of the oxygen concentration to below 5 ppb prevents IGSCC.

Except for an increased radiation level in the main steam lines and in the turbine plant, no important side effects of Hydrogen Water Chemistry have been observed.

The investigations have now reached a stage at which Hydrogen Water Chemistry can be applied on an operational and commercial basis in Boiling Water Reactors.

## ACKNOWLEDGEMENTS

The investigations carried out have been supported by the Swedish State Power Board, the OKG Power Group and the Swedish Nuclear Power Inspectorate. Excellent cooperation and assistance provided by the plant staffs at Oskarshamn 2, Ringhals 1 and Forsmark 1 and by engineers of Studsvik are also gratefully acknowledged.



## REFERENCES

1. Fejes, P., "Deaeration practices in Swedish BWRs", EPRI Seminar on Countermeasures for BWR Pipe Cracking, Palo Alto, California, USA, Jan. 1980.
2. Magdalinski, J. and Ivars, R., "Oxygen suppression in Oskarshamn 2", ANS Winter Meeting, Washington D.C., USA, Nov. 1982.
3. Ivars, R. and Lejon, J., "Hydrogen Water Chemistry Experience in Swedish Boiling Water Reactors", ASME Conference, San Antonio, Texas, USA, June 1984.
4. Ljungberg, L. and Korhonen, S., "Effect of Reduced Oxygen BWR Water Chemistry on Propensity for Intergranular Stress Corrosion Cracking in Sensitized Austenitic Stainless Steel", ASME Conference, San Antonio, Texas, USA, June 1984.

THE FINE MOTION CONTROL ROD DRIVE AND  
REACTOR SCRAM SYSTEM OF KWU; DESIGN,  
LONG TERM OPERATIONAL BEHAVIOUR AND  
EXPERIENCE

R. Schraewer      and      B. Wintermann

Kraftwerk Union              Kraftwerk Union  
Postfach 962                    Postfach 3220  
6050 Offenbach                8520 Erlangen

Abstract

The main feature of the fine motion control rod drive is the ball nut-spindle system inside the guiding tube enabling continuous insertion of the control rod into the reactor core. The mechanical drive of the spindle is an electrically powered motor transmitting the corresponding revolutions over a gear to the spindle.

For reactor scram motion a hydraulic system is used. It comprises a high pressure nitrogen-water reservoir connected by water lines to the control rod housing. In case of demand a fast opening valve allows water to flow into the bottom of the housing to move a piston which in turn moves the control rod upward. Completely satisfactory results have been obtained with this system over 16 years.

1. Concept

One of the goals of reactor technology is to guarantee the safety, reliability and high availability of nuclear power stations. Among all components the control rods possess a key function.

In general they have to perform two important jobs

- . power and burn-up control
- . reactor shut down

The very different demands of the kind of motion /1/ according to task 1, a continuous slow motion with a stay at intermediate positions, and according to task 2 a fast injection, are accomplished for the KWU boiling water reactors with two independent drive systems.

The basic concept is explained in figure 1 as follows:

Each of the control rods is coupled to one trunk piston (figure 1, position 9) by means of a form-closed but flexible clutch. The piston itself is located inside a housing pipe (pos. 19), welded into the bottom of the pressure vessel (pos. 18). The piston is driven by an electric motor at the bottom of the housing and by a hydraulic system, whose pressurized water is injected through a lateral nozzle (pos. 6) into the housing.

## 2. Design

### 2.1 Fine motion control system

The electric motor with its reducing gear and the position finder are protected against the hot reactor water by a flange only penetrated by a sealed drive shaft (pos. 2, 3). This shaft is connected to the ball screw spindle by means of a bayonet clutch; a relative axial displacement over a certain range is possible. With the help of a ball screw nut the rotation of the shaft is transformed into an axial continuous motion with a low speed of about 3 cm/sec. In this manner the trunk piston with the control rod is moved up and down. The piston is surrounded by a concentric guide tube (pos. 13) with holes for pressurized water.

This guarantees together with special rollers (pos. 8) the guidance of the ball screw nut as well as of the piston (together with the screw spindle). At its inside a toothed rack is mounted, enabling the jaws (14) of the piston collar, to fit the gaps between the teeth. During the fine motion the trunk piston rests on the nut due to gravitational force.

Special horns mounted on the nut cause the jaws to leave their snapping position. Therefore a piston motion up and down is guaranteed. The position finder is completed by the following facilities, first a limiting switch and second a disconnecting switch.

#### Limiting Switch

If the piston exceeds its end position during normal operation and lifts the throttle bush, a rod actuates a magnetic switch stopping the drive motor. In addition to that for a reactor scram this switch gives the signal of the arrival of the trunk piston as an input for the reactor control.

#### Disconnecting Switch

The disconnecting spring (pos. 4) between spindle and shaft is compressed due to the weight of the control rod, the spindle and the piston. This way a permanent magnet stays in a zero position. When the weight is taken off for example due to a sticking of the control rod during the downward motion, the spring is discharged and the magnet is lifted. Now a magnet switch gives an electrical signal, which interrupts the motor rotation. The screw nut remains in position and prevents control rod drop out. For a reactor scram this switch gives the signal -removal of the piston from the nut- as an input for reactor control.

In order to reduce the temperature inside the housing pipe during operation time, a small mass flow of rinse water at about 40 °C runs through the scram line. Flowing through a throttle bush arrangement with specially designed gaps (Pos. 11, 20), the water is fed into the pressure vessel. Thereby the warm-up of the housing is diminished, a leakage of hot reactor water into the motor system (pos. 1) is prevented and a lubrication of the rolling and sliding components is reached. Thermometer probes signal a failure of the rinse water system or a leakage of the shaft seal.

## 2.2 Scram System

In case of fast reactor shut down pressurized water is fed through the scram line into the housing and after that it flows through gaps in the guide tube. Due to the arrangement of the throttle bush system, the pressure of the hydraulic system is built up inside the piston. The resultant pressure difference against the reactor water causes a force upon the piston, injecting the control rod into the reactor. As a consequence the piston leaves the screw nut. After the short shut down time the piston (with its collar) is decelerated by disc spring elements behind the throttle bushes.

The short displacement of the bush actuates a magnetic switch and signals the end of the scram stroke. Now the jaws of the piston collar are fitted into the toothed rack and prevent the piston tube sliding down due to gravity as soon as a certain pressure difference across the piston has diminished.

The arrangement of the hydraulic drive system presented in figure 2. Depending on the type of reactor the following solutions were chosen with regard to reliability.

### Common tank system

This KWU system is incorporated in the reactor plants of KWW, KKB, KKP1, KKI1, GKT and KRB-B, C. Some independent operating tanks -for example 6 tanks in KRB2 (figure 2)- pressurized with nitrogen gas provide the control rods by using a twofold installed ring header with the necessary pressurized water. Check valves guarantee an unchanged availability of the whole system, although a hypothetical rupture of the line has been taken into account.

The scram valve is actuated by the reactor control system and opens the path for pressurized water, the shut down procedure can start. The throttle valve limits the speed and therefore the deceleration forces below a maximum at the end of the scram stroke. Furthermore it compensates tolerances of component parts, so that all the control rods show the same velocity at each pressure level.

### Single tank system

This KWU system is incorporated at first in KWL and later in KKK. According to figure 3 each of the control rods is provided with its own water tank. The nitrogen gas, pressurized in a separate tank causes the movement of a piston and starts the injection of the water into the control rod drive.

The functions of the most important components are similar to those of the common tank system.

### 3. Long Term Operational Behaviour and Experience

The drive system here presented was designed in the period from 1959 to 1968 and operated first in the nuclear power station Lingen in 1968. Up to that time an extensive development /3/ was necessary. In addition to modifications of the construction a variety of technological problems was to be solved as for instance corrosion, friction, wear and fretting problems and thermal behaviour under long term operation /4/.

38 control rod drives were selected from the 528 drives of the plants KWW, KKB, KKP1 and KKI over a 12 years period (table 1). The result of their supervision was: Not one of them had any defect, no parts of the components had to be replaced.

Today 16 years later the result of behaviour confirms the KWU concept employing two different systems of the control rod motion. During this time period about 1300 assemblies were manufactured and installed in 9 KWU boiling water reactors with electrical energy of more than 10<sup>7</sup> GWh produced.

Over the whole time only 4 insignificant defects were noticed; not one of them caused a shut down of the reactor. The defects were eliminated during the normal service time.

In addition extensive tests were carried out respecting the scram motion. After starting the scram valve it was observed, that the pressure difference - hydraulic tank to reactor - caused a high pressure in the hydraulic line system at different places. Calculations with fluid dynamic programs and structure dynamic modes were able to simulate the measurements. It was shown that the loads didn't exceed the design limits. The values of shut down time measured were reproducible and confirmed the calculations. The evaluation of probability shows - for example in KKK - with a good approximation a symmetric and reproducible bell shaped curve /figure 5/. 97 % of the measured values had a scattering amplitude of  $\pm 5$  % of the average. This result is an additional confirmation of the design selected and the proven construction of the system.

#### References

- /1/ H. Engel, K. Traube: Besondere Aspekte des KWL-SWR, Atomwirtschaft 13, S. 151-154; A. Reinhard: Die Regelung des Kernkraftwerkes Lingen, Atomwirtschaft 13, S. 161-163, März 68.
- /2/ H. Acher: Entwicklung von Steuerstabantrieben für Siedewasserreaktoren, Kerntechnik 5. Jahrgang, Heft 2, S. 71-75 (Febr. 1963)
- /3/ W. Ullrich: Vortrag auf der Informationstagung über die Weiterentwicklung der LWR in der Gemeinschaft, Brüssel, 23./24.11.66 AEG 3321.552.5E3 1066.
- /4/ H. Acher: Langzeit-Betriebserfahrungen mit neuentwickelten Regelstabantrieben, Atomwirtschaft, Juni 1976

- |                         |                                  |
|-------------------------|----------------------------------|
| 1. Drive Shaft          | 11. Disc Spring Elements         |
| 2. Water Leakage Pipe   | 12. Clutch                       |
| 3. Shaft Seal           | 13. Guide Tube with Toothed Rack |
| 4. Disconnecting Switch | 14. Jaw Arrangement              |
| 5. Ball Screw Spindle   | 15. Limiting Switch              |
| 6. Scram Line           | 16. Gear with Position Finder    |
| 7. Screw Nut            | 17. Electric Motor               |
| 8. Guide Roller         | 18. Reactor Pressure Vessel      |
| 9. Trunk Piston         | 19. Housing Pipe                 |
| 10. Throttle Bush       | 20. Throttle Gap                 |

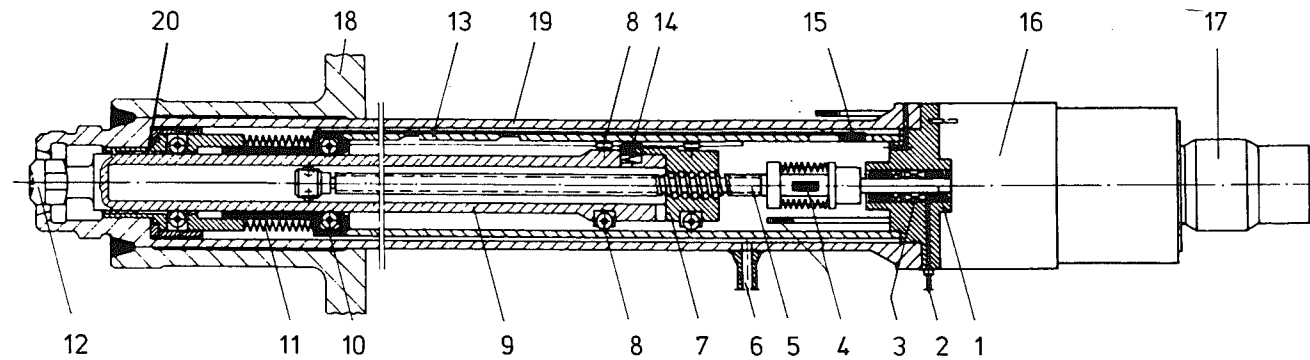


**Figure 1: Principle Assembly of KWU-Fine Motion Control Rod Drive**



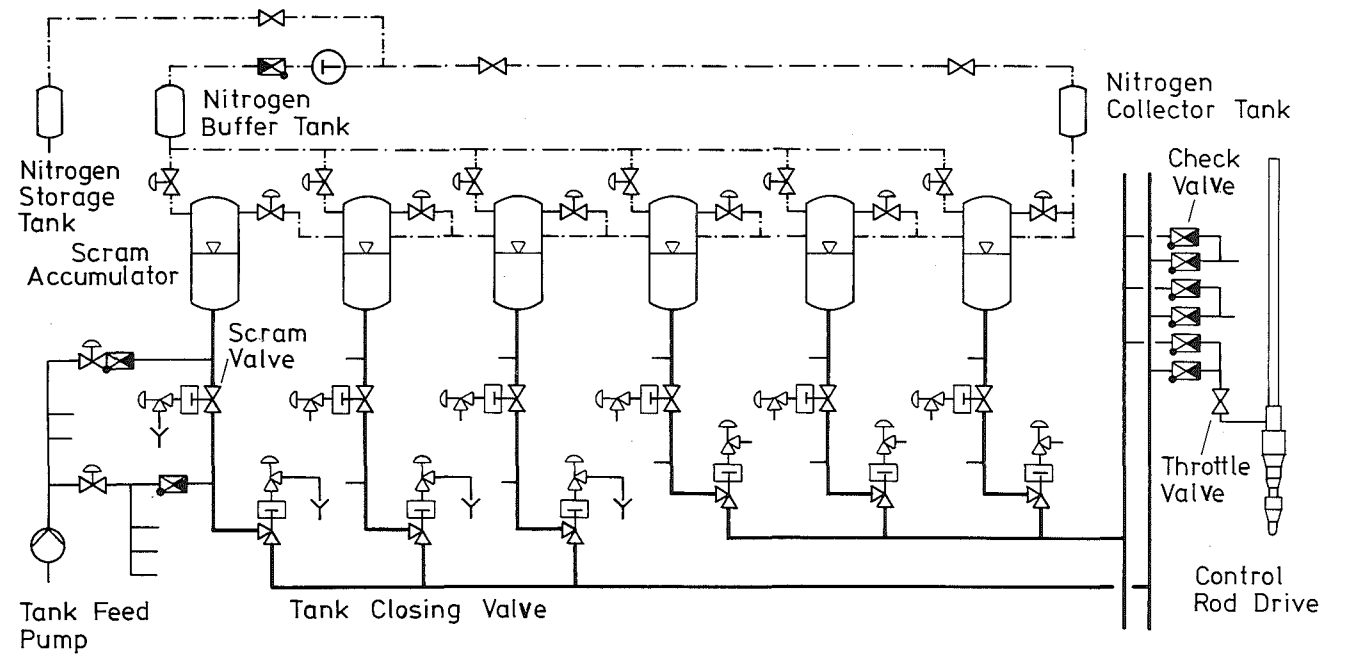


Figure 2: Schematic Diagram of the Common Tank System (KRB)

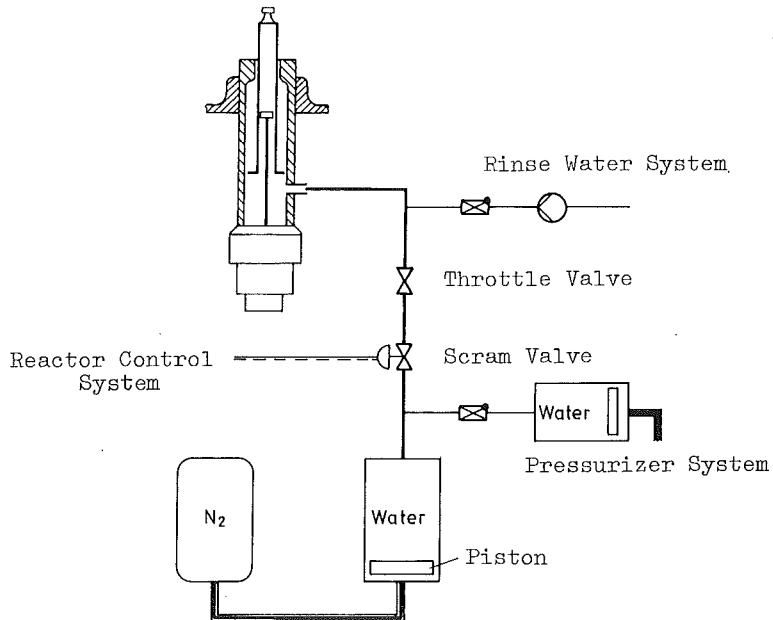


Figure 3: Schematic Diagramm of the Single Tank-System (KKK)

Table 1: Supervised Control Rod Drives of KWU Boiling Water Reactors

Reactor	power	Assembly		Supervision	Tank System
	/MW/	/year/	/number/	/number/	
KWL	250	1967	69	14	Single Tank Syst.
KWW	600	1971	104	16	} 38 6 x 50 % 3 x 100 % 4 x 100 % 3 x 100 %
KKB	900	1974	129	9	
KKP1	900	1975	145	4	
KKI	900	1976	145	9	
GKT	/	1977	113	-	
KKK	1300	1981	205	-	Single Tank Syst.
KRB-B	1300	1982	193	-	6 x 50 %
KRB-C	1300	1983	193	-	6 x 50 %

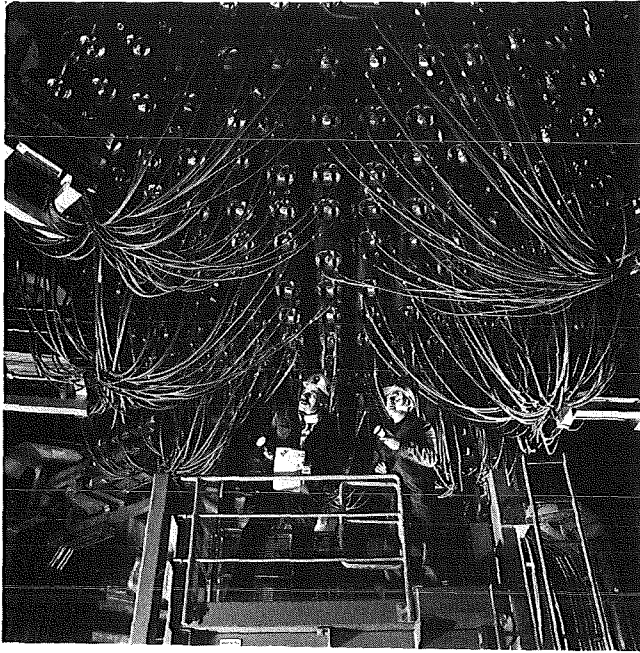


Figure 4: View of the Control Rod Drive System

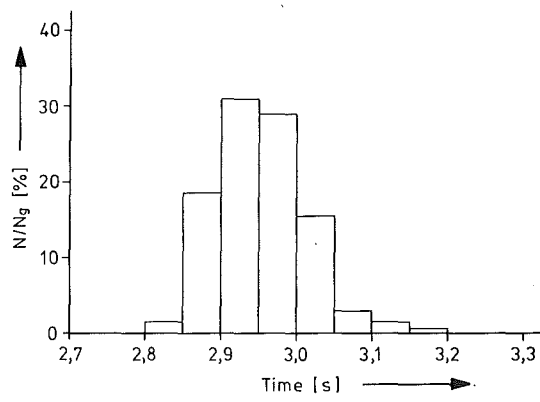


Figure 5: Frequency Distribution of Control Rod Shut Down Time

## POWER UPRATES IN ASEA-ATOM BOILING WATER REACTORS

Ernö Legath

AB ASEA-ATOM  
Box 53, S-72104 VÄSTERÅS, Sweden

## ABSTRACT

Power uprates in the order of 6-10 percent above the contractual power level are possible in Boiling Water Reactors designed and supplied by ASEA-ATOM by using calculated and measured margins.

Before performing the power increase the margins must be proved and necessary equipment modifications identified. Usually only moderate hardware modifications are needed.

The Oskarshamn 2 unit is since November 1982 licensed for operating at 106 percent continuously. The Olkiluoto 1 and 2 units had 1983 a preliminary licence for operation at 103 percent and have from June 1984 a final licence for 108 percent. Five other ASEA-ATOM plants are at present being prepared for power increase to levels between 106 and 110 percent. The Barsebäck 1 and 2 units are expected to be licensed for 106 percent during the fall of 1984.

## INTRODUCTION

A method to increase production and still maintain the safety margins anticipated in the initial operating licence should be of great interest to any utility operating a nuclear power plant. Uprating was believed to be possible by increasing the utilization of the fuel in older plants to data used in plants being built today. Improved calculation methods and numerous verifying measured data have built up considerable extra safety margins in the older plants. This paper is a case description of how ASEA-ATOM BWRs have been or are expected to be uprated. It could be assumed that other light water reactors could be uprated in a similar manner.

Together with the utilities operating the Boiling Water Reactors supplied by ASEA-ATOM and the licensing authorities stepwise programmes for uprating the power of each unit were worked out. The programmes included generally three steps:

- A preliminary study to establish the achievable power level
- Detailed plant studies and calculations to update the safety analysis report.
- Plant modifications and verification tests at increased power levels.

Examples of the work undertaken in each step is given below

## PRELIMINARY STUDIES

These studies concentrated on settling existing margins in the reactor core and in the turbine. ASEA-ATOM had already estimated that power uprates in the order of 6-10 percent would be possible in the BWR's supplied by the company. The uprates could be achieved using existing calculated and measured margins only. In some cases minor plant modifications were anticipated. Core and fuel development had opened the possibility to increase the power density. The preliminary studies aimed at proving that the existing fuel power density of 22.5 W/gU could be increased to 24.2 W/gU and checking how various parts of the plant was affected.

The value of 24.2 W/gU corresponds to the fuel power density of the Forsmark 3 and Oskarshamn 3 units, the two ASEA-ATOM 1060 MWe BWR's to start operation in 1985. Fully used the higher power density would result in 6-10 percent more power output. Also if the detailed studies showed that the increase could be performed partly only, due to real or formal reasons, there would still be great incentives to do so. The foreseen theoretical and practical work was so limited that it would still be economically motivated for the utilities.

The preliminary investigations also proved good prospects for power uprates of the turbine plants with only minor modifications. All but one ASEA-ATOM BWR have turbine plants supplied by ASEA STAL (former Stal-Laval). The investigations undertaken by ASEA STAL indicated that the steam turbines had built-in margins to allow power uprates in the order of 6-8 percent. This could be done with none or minor hardware modifications and still maintaining sufficient control margins, approximately 3 percent. ASEA STAL, however, recommended that this had to be verified by actual overpower tests with each turbine. The investigation also proved sufficient margins in the generator and in the turbine plant auxiliary systems.

The remaining ASEA-ATOM BWR, Ringhals 1, has a turbine plant supplied by GEC, England. The outcome of the GEC studies showed similar results for everything but the turbine itself. To increase power above 104 percent the turbine had to be modified. To reach the planned 110 percent level the inlet nozzle box had to be rebuilt and the high pressure turbine guide vanes had to be replaced.

Plant	Planned uprate	Status of power uprating
Oskarshamn 2	106%, 34 MW	Licensed for 106% since end 1982
Barsebäck 1 and 2	106%, 34 MW	Licensing
Forsmark 1 and 2	108%, 70 MW	Licensing and testing
Ringhals 1	110%, 75 MW	Licensing
Olkiluoto I and II	108%, 50 MW	Licensed for 108% since mid 1984

Table 1 Uprating of ASEA-ATOM BWRs

## ANALYSES

The primary step in the uprating procedure consists of defining available margins and identifying the equipment with the smallest margin, which may require modifications.

The analyses are based upon the condition that margins, either calculated or measured in the plants, will be utilized wholly or partially.

The verification and licensing of the plant for the higher power demand the following work.

- System and function analysis
- Supplementing LOCA analyses
- New dynamic calculations
- Updating of documentation, like FSAR and operating instructions.

The system analyses comprise primarily a qualitative review, resulting in a problem identifying list. For systems which are considerably influenced of the uprating a special note is made on components and functions, which limit the capacity of the system, and on the amount of verifying calculations, which are required to establish system capacity.

In the analysis work the same safety criteria are usually applied which were valid for the plant earlier. Also the earlier calculation models are generally used unless new models are better justified, e.g. by better verification.

After the qualitative review detailed system analyses are carried out for those systems that are affected by the power uprate. The analyses include the necessary supplementary calculations.

In this stage such dynamic and core cooling calculations are made, which are demanded to verify the feasibility of the uprate.

Examples of licensing calculations

Core cooling calculations (GOBLIN)

- largest steam pipe rupture
- largest feedwater pipe rupture
- bottom pipe rupture with 45 kg/s flow
- bottom rupture with 200 kg/s flow

Dynamic calculations for FSAR (BISON)

The documentation, submitted to the authorities for application of approval for tests with higher power, comprises a report of the analyses and a program for modification of the plant.

## IMPLEMENTATION

The need for modifications and supplementation of the plant is elucidated in the analysis work. The experience from the ASEA-ATOM plants shows that only moderate hardware changes are necessary. As typical examples supplementing relief valves and reinforce of cooling systems can be mentioned.

A summary of the specific programmes for the various ASEA-ATOM plants at the power uprate is given below.

Plant	Power uprate %	Specific supplements
Oskarshamn 2	106	Increased opening pressure for safety relief valves from 85 to 87 bar
Barsebäck 1 and 2	106	- " -
Forsmark 1 and 2	108	One additional safety relief valve and modified steam separators
Ringhals 1	110	Modified scram system and modified turbine
TVO I and II	108	One additional safety relief valve, modified steam separators and increased cooling capacity for turbine auxiliary cooling

Table 2 Summary of power uprate supplementation

Parallel with the analysis work tests and measurements have been made in the plants on capacities of relief systems, condensation pool cooling systems and low pressure injection systems for verifying the calculated margins.

After approval for test operation with the higher power the commissioning, testing and evaluation is made in the normal order. The extent of the test programme is assessed in cooperation with the authority.

The final documentation for licensing the plant with the uprated power comprises

- results from the test operation
- updated documents:
  - FSAR
  - operating instructions
  - modification documents

According to the experience from projects carried out until now it is advantageous to divide the power increase in two parts and perform tests in two successive stages.

## RESULTS

Oskarshamn 2 is the first plant licensed for higher power. Since November 1982 the plant is operated with 106% continuously. No hardware changes were necessary.

Application for power uprate in Barsebäck 1 and 2, which are of the same reactor generation as Oskarshamn 2 is being treated by the authority. The plants are expected to be licensed for 106% power during 1984.

The remaining ASEA-ATOM plants Ringhals 1, Forsmark 1 and 2 are presently being prepared for an increase to 108-110%. The analysis work for verification and licensing is in the main being made by ASEA-ATOM at the request of the utilities.

TVO has obtained the permission for operation at 108% power in both plants from the operating season 1984/85, based on stepwise analyses, calculations and tests. During the operating season 1983/84 the plants operated with a power of 103%.

## COST AND TIME SCHEDULE

As an example of costs and time schedules the figures for the two TVO plants are shown below.

Analyses, engineering	2 MSEK
Supplementary equipment: safety valves, heat exchangers	8 MSEK
Total	10 MSEK

## Time schedule

Preliminary study	2nd quarter 1982
Analysis work	
Order of components	1983
Report to the authorities	
Test step 1 (103%-106%)	
Modifications and tests	Refuelling period 1984
108% power	From operating season 1984/85



Dose Reduction by Application of Advanced Methods  
for Testing and Repairing of Steam Generator Tubes

K. Fischer	Kraftwerk Union AG Reaktortechnik Karlstein
H. Kastl	Kraftwerk Union AG Reaktortechnik Erlangen
M. Kurzawe	Kraftwerk Union AG Reaktortechnik Karlstein

TABLE OF CONTENTS

1. INTRODUCTION
2. PREVENTIVE MEASURES
  - 2.1 EDDY CURRENT EXAMINATION
  - 2.2 SPECIAL INSPECTION TECHNIQUES
  - 2.3 VISUAL EXAMINATION AND PROFILOMETRY
3. REPAIR TECHNIQUES
  - 3.1 TUBE PLUGGING
  - 3.2 TUBE PULLING
  - 3.3 SLEEVING
  - 3.4 TUBE REPLACEMENT
4. EQUIPMENT MAINTENANCE AND PERSONNEL TRAINING

## 1 Introduction

The integrity of the tubing of a steam generator has a significant effect on the availability of a nuclear steam supply system.

For this reason, the development of suitable inspection and repair techniques has increasingly grown in importance.

Regular inspection of a representative number of tubes makes it possible for preventive measures to be taken in good time.

The objectives behind KWU's greatly intensified development activities have been to continue to improve the quality of information obtained through inspection and the provision of effective repair techniques.

A considerable amount of effort has also been put into reducing the radiation exposure of inspection and repair personnel.

Through optimization of techniques and equipment, and extensive mechanization and automation, it has been possible to reduce occupational dose rates significantly.

## 2 Preventive Measures

### 2.1 Eddy Current Examination

Mechanized eddy current examination is the standard inspection technique employed in the inservice inspection of steam generator tubing.

Through the application of improved techniques and equipment it has been possible to enhance the quality of information obtained, to cut down inspection preparation time and hence also to reduce the applied dose considerably.

The standard technique uses multifrequency equipment.

To suppress interference due to tube supports, expansion zones and mechanical influences frequency mix techniques are employed.

The data obtained (tube position, defect location and eddy current signals) are transferred to the mobile computerized data acquisition and processing system.

It provides on-line data for further evaluation.

This system identifies suspect-defect tubes automatically.

A special type of manipulator called the "finger walker" is used for positioning. Its advantages include easy and quick setup involving only low radiation exposure, programmable positioning and a broad

range of applications from inspection (standard eddy current examinations as well as special inspection techniques) to repair (plugging of tubes displaying unacceptable defects) and other uses (visual examination using borescopes, profilometry, etc.).

The actual equipment setup also contributes towards reducing radiation exposure.

The control panel, eddy current unit and the data acquisition and processing system are installed in a mobile container set down outside the reactor building and connected to the steam generator via a 200 m-long control and telecommunications cable. Inside the containment a service crew is responsible for all installation and calibration work and for changing the probes etc.

This arrangement allows inspection to be performed with a minimum of personnel inside the containment (see Figure 1).

## 2.2 Special Inspection Technique

A special new inspection technique is being applied to supplement eddy current examination, which uses a rotational ultrasonic probe (USAS) and a rotational eddy current probe (WSAS).

This technique enables precise measurement of wastage as well as exact identification measurement of local defects. Combination of the two into a single combination probe (USAS/WSAS) reduces the number of steps involved in inspection and hence the associated radiation exposure (Figure 2). Furthermore application of this technique has greatly cut down the number of tubes which would have to be plugged on the basis of eddy current examination results alone. Plugging and the inspection techniques described above practically rule out the possibility of leaks arising in the steam generator tubing.

## 2.3 Visual Examination and Profiling

Visual examination methods are inspect tubes from the inside and the outside, to inspect the secondary side of the tube sheet through a vacant tube hole or from a tube lane, and to check the integrity of the tube bundle.

Rigid and flexible borescopes are available for this. When they are equipped with a small camera, the object image can be recorded on magnetic tape. Furthermore, miniature TV cameras with outside diameters of about 18 mm are available for use and new techniques based on miniature, flexible, CCD cameras are being developed.

Remote-controlled inspection equipment and associated manipulating devices have been developed for inspecting large numbers of steam generator tubes from the inside.

The manipulators used by KWU for eddy current examination are designed such that by fitting them with special attachments they can also be used for inspecting the inner surfaces of tubes. Equipment has also been developed for profiling the inner surface of tubing using different variations of profilometers bases either on direct contact or no contact with the tube surface. Useful information in the condition of the tubes as regards expansion zone dimension, tube internal dimensions and any tube deformation can be obtained in this way.

### 3 Repair Techniques

Should one of the inspection techniques described above identify a defect, routine measures such as plugging or other corrective actions are available for implementation.

Tube repairs have not to date been necessary at any nuclear power plants inside West Germany but repair procedures have been developed for implementation at any time in facilities located abroad.

#### 3.1 Tube Plugging

Damaged steam generator tubes used to be sealed off by means of explosive-weld plugs placed into the tubes by hand. Through the development of remote controlled tools and devices, it has been possible to reduce personnel exposure from about 1000 mrem to about 500 mrem per plug. Moreover, they obviate the need for personnel to climb into the primary side in order to place the plugs.

Thanks to even newer plugs which have been in use since 1982, it has become possible to cut radiation exposure down even further to an average, depending on the number of plugs involved, of between 60 and 120 mrem per plug (see Figure 3).

The newer, mechanical plug in use since 1982 can be removed from the tube at a later point in time. Insertion of this type of plug into a steam generator tube does not usually require any preparatory operations such as precalibration, perhaps machining of the tube-to-tube sheet welding, final calibration and cleaning.

A remote-control plugging tool specially developed for this purpose is positioned under the tube to be plugged by the finger-walker manipulator employed for eddy current examination. The tool provided for removing the mechanical plug at a later date is also remote-controlled.

#### 3.2 Tube Pulling

For the purpose of carrying out material examinations and validating inspection results, individual samples of tubing are occasionally removed from the lower region of a steam generator tube bundle.

Steam generator tube sampling has been performed since 1972 with samples being taken from over 30 tubes in 7 nuclear power plants. A cutting tool with retractable blade is employed for cutting off the required length of tube. In order to keep pullout forces to a minimum, the tube is shrunk in its expansion zone using a special deep whole welding tool and is then pulled out with the aid of a self-tapping pull-rod which is automatically retracted by a hydraulic cylinder.

The vacant position in the tube sheet can be sealed off by welding plugs.

In order to avoid the release of radioactivity into the secondary system from the remaining piece of tube, it is possible to decontaminate the tube in question by means of one of the decontamination processes used repeatedly in the past with great success by KWU.

### 3.2 Sleevling

Although KWU has never had to perform sleevling on any of its steamgenerators, it has nevertheless optimized the welding process preferred by it for his application and now offers it as a service for any nuclear power plants.

Through the selection of simple geometries and optimum for sleeve welding, it is possible to establish sleeve weld quality by easy, low-dose methods. Complicated inspection techniques are thus rendered unnecessary.

The use of fully-automatic welding machines, remote controlled tools and manipulators in the future will reduce the number of operations performed in the radiation area.

### 3.3 Tube Replacement

A technique has been developed for replacing sections of steam generator tubes damaged in the vicinity of the tube sheet or tubes which have already been plugged.

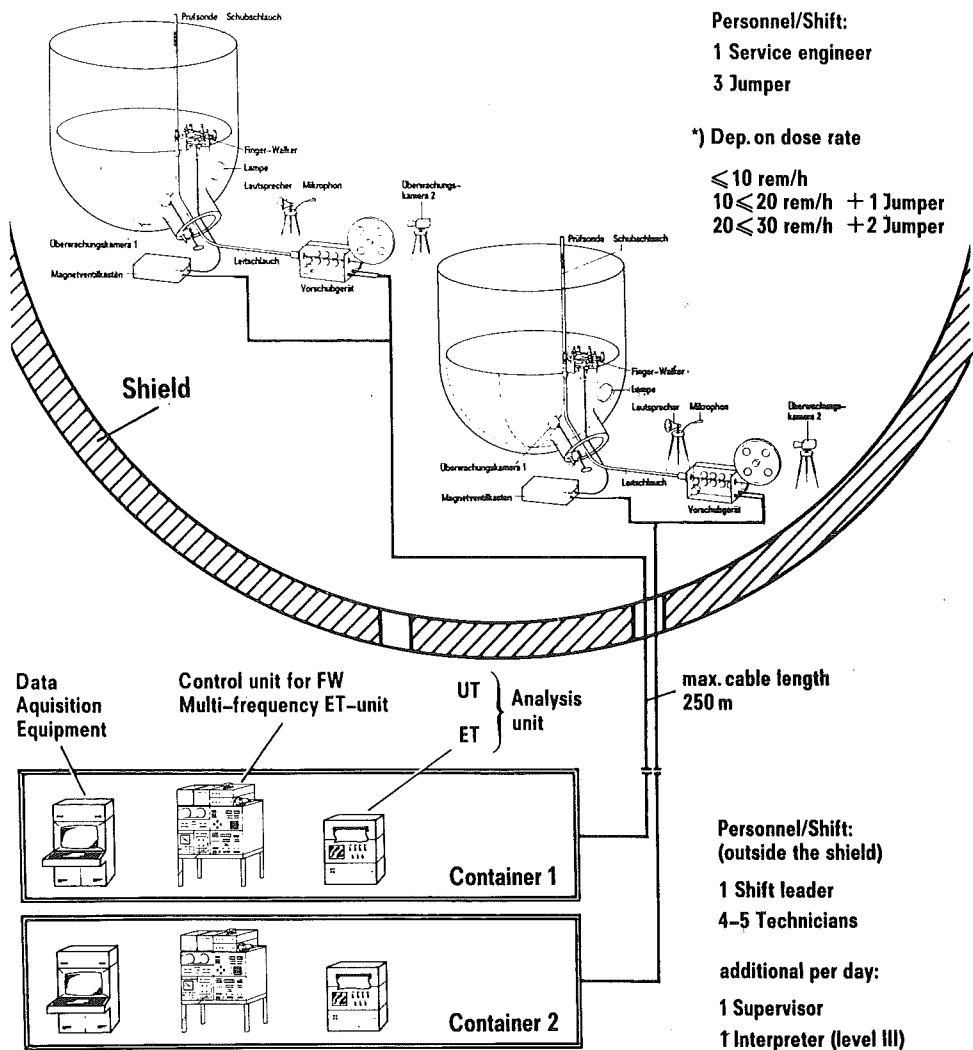
This replacement technique is an alternative to sleevling. Through careful selection of the new materials, damage can be prevented. Also, in this way the full tube cross section is maintained and available for inspection.

Highly advanced welding techniques enable highquality welds to be produced and facilitate weld quality control.

## 4 Equipment Maintenance and Personnel Training.

Thorough preparation and maintenance of equipment as well as intensive training of personnel under simulated conditions contribute to a significant degree towards reducing occupational radiation exposure.

As a basis for this, KKW recently set up a Service Center complete with a controlled access area and a hot shop for storage and maintenance of contaminated equipment. The tools and equipment intended for inspection, maintenance and repair activities inside nuclear power plants can be tested and prepared at the Center under simulated plant conditions. Equipment setup times and downtimes can be reduced through personnel training, practising of operations to determine lowest-dose procedures and equipment life test. Proper equipment maintenance and comprehensive personnel training enhance the performance of inspection activities in the plant and radiation exposure is considerably lowered.

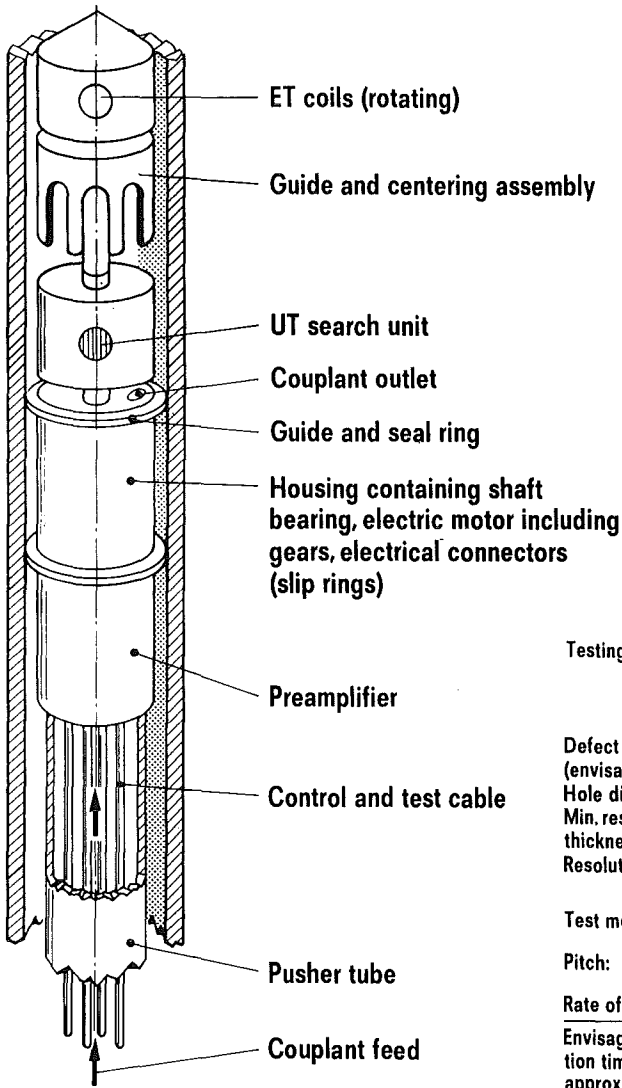


**SG-Tube Examination**

**ET-Equipment Units and Personnel Demand for two simultaneous SG-Inspections**

Fig. 1

E 82 1612 e



Testing range: 500 mm above the tube-sheet to the center of upper roller expanded area

Defect resolution: (envisaged)	UT	ET
Hole dia:	2 mm	0,5
Min. residual wall thickness:	20 %	20 %
Resolution (depth):	±2,5%	< 5%

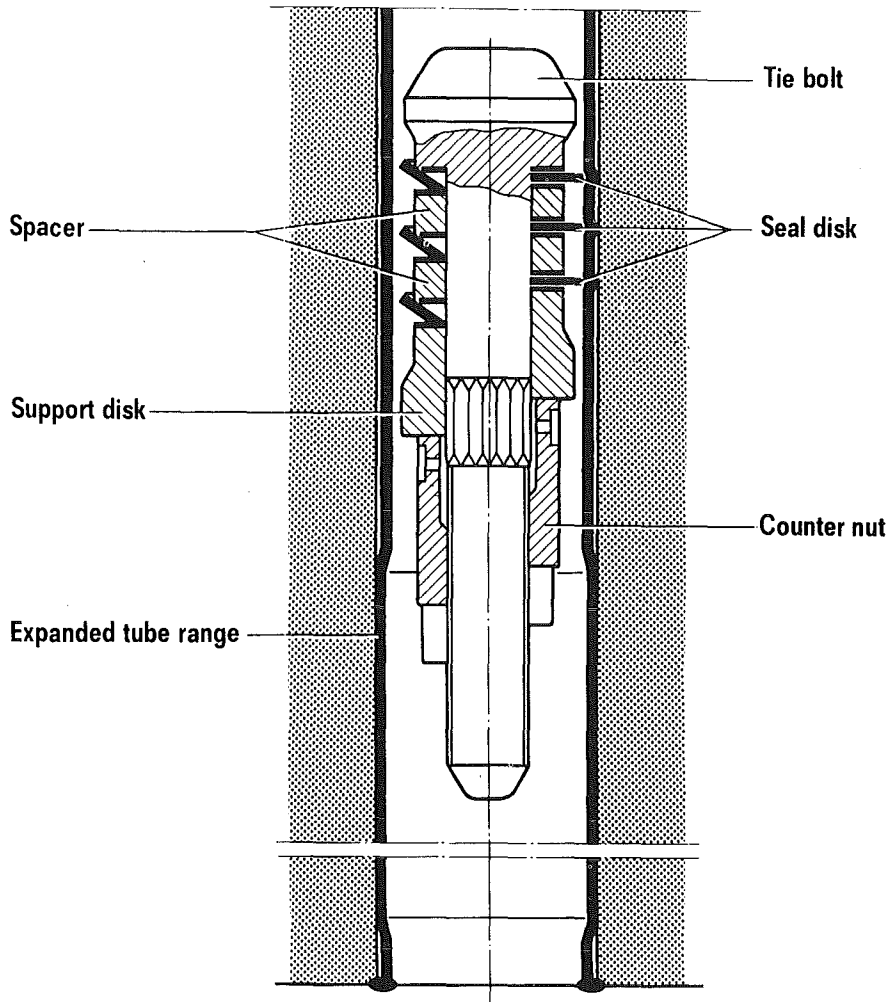
Test motion: helical  
 Pitch: ≤ 2 mm  
 Rate of travel: 10 mm/s  
 Envisaged examination time: approx. 15 min

**Steam Generator Tube Examination  
 Analysis by means of Combined UT/ET Rotating Probe**

Fig. 2

E83 305 e

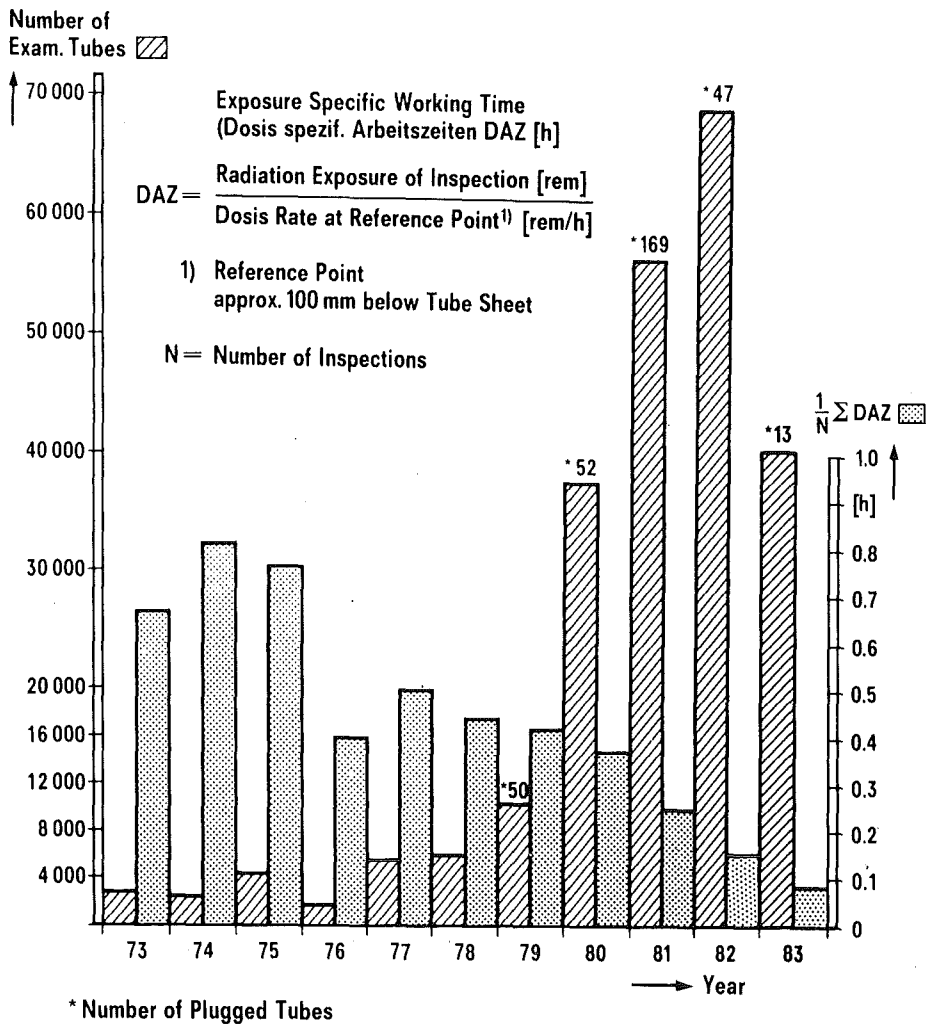




**Mechanical Plug for Steam Generator Tubes**

Fig. 3

E83 329e



**Steam Generator ET-Examination**  
**Number of Examined Tubes and Exposure Specific Working Time**

Fig. 4

E 83145 CeI

INVESTIGATION OF A LIQUID ZONE CONTROL ASSEMBLY FAILURE  
AT A NUCLEAR GENERATING STATION

R.G. Sauvé and W.W. Teper

Nuclear Systems Department  
Ontario Hydro  
Toronto, Ontario, Canada

ABSTRACT

The failure of the Liquid Zone Control (LZC) assembly at a nuclear generating station was investigated. The work was performed in order to determine the cause of structural failure in the LZC assembly guide tube at the location of the bearing pads. The failure resulted in leakage of light water into the moderator. Removal of the defective unit revealed that severe fretting wear had occurred on the guide tube at the location of the bearing pad to calandria bushing contact area. The observed wear pattern was orientated approximately 90° to the direction of the bypass inlet flow. Structural features of the system and results of the investigation including the mathematical simulation models used are described in this paper. Vibro-impact forces were determined in the damaged area using a relatively new and efficient procedure<sup>2</sup>. They were found to be of sufficient magnitude to cause the damage.

INTRODUCTION

This paper describes the analytical investigation of the Liquid Zone Control (LZC) assembly of a nuclear generating station (Figure 1). The system provides a flux distribution control in the reactor core by varying the quantities of neutron absorbing light water. This work<sup>1\*</sup> was performed in

\* Superscripts Refer to References.

order to gain insight into the cause of a structural failure which occurred in the LZC assembly guide tube at the location of the bearing pads which are situated at the calandria nozzle (Figure 1). The failure resulted in the leakage of light water into the moderator. The LZC unit in question is almost directly in line with the exit flow from one of the moderator cooling system inlet nozzles. The orientation of the nozzles is indicated in Figure 2. This analysis was initiated prior to any experimental work, however results of both led to the same conclusions.

Subsequent removal of the defective unit revealed that severe fretting wear had occurred on the guide tube in the bearing pad to bushing contact area<sup>10</sup>. The bearing pads on one side had worn to the point where they no longer provided protection to the LZC guide tube and progressive thinning of the tube wall resulted in a localized crack which lead to leakage. The observed wear pattern was oriented approximately 90° to the direction of the bypass inlet flow. Figure 1 shows the location of the failure. As indicated in the figure, the wear was predominantly on one side of the tube, although some wear was evident on the opposite side.

#### STRUCTURAL FEATURES AND MATHEMATICAL MODEL

The LZC assembly consists of a tube 4.6 inches outside diameter and 4.5 inches inside diameter, approximately 564 inches long. The tube is simply supported at the bottom and at midheight and fixed at the upper end. There are three small diameter vertical tubes tied to the outside tube at several locations.

The mathematical model used to describe the LZC assembly structure is shown in Figure 3. The guide tube and internal tubes were modelled using pipe elements based on the displacement method. Continuity between internals and guide tube was enforced at the bulkheads. The structure material was Zircalloy.

At node 1 restraints were included to simulate the rigid deck plate. Due to the time-dependent nature of the problem and the inherent non-linearities arising from the clearance present at the guide tube/calandria nozzle location, the Ontario Hydro structural dynamic computer code H2DMAP<sup>2</sup> was utilized. This code, is applicable to a wide range of structural dynamic problems including modal analysis, flow induced vibration and transient linear or non-linear dynamic analysis.

The structure's inertial properties were introduced as distributed element masses in accordance to the elements defined. The weight of water inside the tubes was included in the model between nodes 30 and 59, along with the hydrodynamic mass effect of the D<sub>2</sub>O surrounding the guide tube.

The flow distribution was obtained using the MODCIR computer code predictions<sup>3</sup> of the moderator circulation with one moderator pump running. Using these results, the flow velocity distribution was determined and applied to the analytical model as shown in Figure 3. The forcing function was developed from the velocities using the following periodic function<sup>6</sup>:

$$P(t) = \Gamma(x)F \sin(\omega t)$$

$$F = 0.5 \rho V_F^2 d C_L$$

where

$\rho$	=	mass density of surrounding fluid (D <sub>2</sub> O)
$V_F$	=	maximum flow velocity
$d$	=	outside diameter of guide tube
$C_L$	=	lift coefficient
$\omega$	=	driving frequency (rad/s)
$\Gamma(x)$	=	force distribution vector

The value of  $\omega$  was determined by considering the frequency content that the LZC assembly exhibited in a modal analysis and comparing these to the frequency of vortex formation as defined using Strouhal numbers ( $fd/v$ ) in the range of .20 to .40<sup>4,5</sup>. The forcing function was evaluated using a lift coefficient<sup>6</sup>  $C_L = 0.10$ .

These forces were applied to both a linear and non-linear model. The linear model was as shown in Figure 3 except that at node 30 a restraint in the x-direction was included to represent the effect of the calandria nozzle. In the non-linear simulation, the impact behaviour of the guide tube in the calandria nozzle at node 30 was accounted for by incorporating one of the non-linear elements available in H2DMAP with a contact stiffness of 10<sup>5</sup> lb/in. Application of the non-linear dynamic solution technique<sup>2</sup> permitted the interaction forces at this location to be quantified.

## ANALYTICAL RESULTS

### Modal Analysis

A modal analysis of the linear model described in the previous section and illustrated in Figure 3, was performed in order to obtain the dynamic characteristics of the assembly. The results were obtained for two cases:

- (a) restraint at node 30;
- (b) unrestrained at node 30.

These configurations represent the limiting cases of restraint of the assembly because, in reality a significant clearance exists at this location. As a result, the model can be expected to exhibit natural modes of vibration in the frequency range of these two boundary conditions.

In both cases the fundamental mode of the assembly was of a global nature, that is, the fundamental mode shape (eigenvector) indicated overall guide tube motion and no localized excitation. Selected mode shapes for both cases are given in Figure 7. The peak amplitude of relative motion as depicted by the fundamental mode shape occurred at node 30 (X-DIR) in the unrestrained case and at node 48 (X-DIR) in the restrained case. Table 1 lists the first six natural frequencies predicted and a comparison with available experimental data. In reference 9, the dominant frequencies of motion under operating conditions were 4.2 Hz, 6.7 Hz to 7.1 Hz and 10 Hz. These frequencies range between the case of the LZCU restrained and unrestrained at the nozzle location making measurement difficult. Comparison of these results with the predictions (Table 1) indicates good agreement.

#### Flow Induced Vibration Analysis (Linear)

In the linear flow induced vibration analysis the steady state response was obtained using the normal mode method. The first eight modes of vibration were included in the analysis. Using the velocity distribution, the Strouhal numbers were calculated for the two cases under consideration. They were found to be in the range of .078 to .24, corresponding to the maximum flow velocity  $V_f = 7.4$  in/sec (1.9 m/sec).

In Reference 4 it has been shown that response of a cylinder in cross flow is significant for values of  $S$  in the range from 0.14 to 0.66. The region where the frequency of excitation can "lock-in" or synchronize with tube oscillations varies between  $S = 0.14$  to  $S = 0.33$ . In addition, coupling of tube motion in the drag and lift directions may occur when  $0.20 < S < 0.33$ . This results in an orbital (whirling) response path.

#### Guide Tube/Nozzle Impact Simulation

The presence of a clearance at node 30 poses a non-linearity which will render the actual response intermediate between those of the two cases. In order to establish the intensity of fretting wear incident on the guide tube/nozzle interface, the magnitude of the impact forces was required. This necessitated the use of a non-linear simulation model as described earlier. At node 30 a clearance was introduced as shown in Figure 3. The equivalent element force deflection characteristics used to represent this discontinuity in the simulation is shown in Figure 6. To provide a reasonable estimate of the actual in-situ case, the clearance was assumed to be offset. Referring to Figure 3, the total diametral clearance was .070 in. The parameters GAP1 and GAP2 shown in Figure 6 were set to 0.40 in and .030 in respectively. The simulation was run for approximately 11.5 s where the steady state solution was obtained.

The results are displayed as plots in Figures 4, 5 and 6. The maximum response occurring in the span of guide tube in the calandria was found to be approximately 0.045 in. Figure 6 shows the displacement of node 30 at the guide tube/nozzle interface and illustrates the effect of a non-uniform clearance. As seen, the impact occurs predominantly on one side of the nozzle. The corresponding impact forces shown on Figure 5, peak between 15

and 20 lbs. As indicated in the trace of these forces, they are somewhat periodic. Subsequent operation under conditions of severe fretting/wear leads to an increase in clearances and impact forces.

The materials used for the nozzle and guide tube and wear pads were Zircalloy. The available literature on the fretting/wear of Zircalloy tubes does not permit a good quantitative assessment of the current problem. However, the results of short term tests of 16 hours indicate<sup>7</sup>, for example, that under combined rubbing motion and periodic impact forces of approximately 2 lbs, a weight loss of 2.83 mg occurs.

Using this information, three of the small wear pads would wear completely in about two years assuming 7,000 h operation per year. The calculated impact forces are much higher than this but the excitation frequency is lower than that used in Reference 7. However, with high periodic impact forces more severe wear can be expected due to the breakdown of the protective surface oxide film under high impact<sup>7</sup>. The results indicate that severe fretting wear was the cause of failure and that an improved design in the region of the calandria nozzle and guide tube interface would be obtained by an increased wear surface and a better material combination.

#### CLOSURE

The analysis illustrates an application of a new method for computations of vibro-impact forces<sup>2</sup>. Good agreement was obtained between analytical predictions and experiments. Fretting wear of complex structures with clearances, subjected to impact forces, can be analysed at low cost.

#### REFERENCES

1. Sauve, R.G., Teper, W.W., Analytical Investigation of Liquid Zone Control Assembly Failure. Ontario Hydro D&D Report 82327, May 1982.
2. Sauve, R., Teper, W., "Non-Linear Dynamic-Impact Simulation of Process Equipment Tubes with Tube/Support Plate Interaction", Proceedings Vol II, 2nd Intl Topical Meeting on Nuclear Reactor Thermal Hydraulics, Santa Barbara, 1983.
3. Austman, G., "Measurement of In-Core Moderator Temperatures in Unit 3, D&D Report No. 81544, December 1981.
4. Chen and Jendrzejczyk, "Dynamic Response of a Circular Cylinder Subjected to Liquid Cross Flow", ASME Paper 78-PVP-15, March 1978.

5. King and Prosser, "Criteria for Flow Induced Oscillations of a Cantilevered Cylinder in Water", Flow-Induced Structural Vibration Symposium Karlsruhe, Germany, 1972.
6. Pettigrew et al, "Flow Induced Vibration Analysis of Heat Exchanger and Steam Generator Designs", AECL Report No. 5826, August 1977.
7. Ko, P., "Wear of Zirconium Alloys Due to Fretting and Periodic Impacting", AECL Report No. 6518, 1979.
8. Saari, K., Vibration Testng of a Liquid Zone Control Unit, AECL Report IR484, December 1982.
9. Anderson, H., Vibration Monitoring to Study Liquid Zone Control Unit Failure, Ontario Hydro Report 83-124-K, March 1983.
10. Holt, R., Post Irradiation Examination of Defective Zone Control Unit, ZCU-1, AECL Report 2412, August 1982.

NATURAL FREQUENCY (Hz)

MODE	RESTRAINED AT NOZZLE				FREE AT NOZZLE			
	PREDICTED		(EXPERIMENTAL) <sup>8,9</sup>		PREDICTED		(EXPERIMENTAL) <sup>8,9</sup>	
	Normal Condi- tions	In Air	Normal Condi- tions	In Air	Normal Condi- tions	In Air	Normal Condi- tions	In Air
1	1.7	4.1	*	4.5	.56	1.2	*	1.25
2	3.49	6.85		5.9	1.97	4.26		4.3
3	6.16	7.75		8.6	4.11	7.64		
4	7.75	15.5			7.24	9.14		10.1
5	11.0	21.			7.8	16.2		
6	13.6				11.2			

\* See Modal Analysis Section.

TABLE 1

LZCU FREQUENCY RANGE COMPARISON



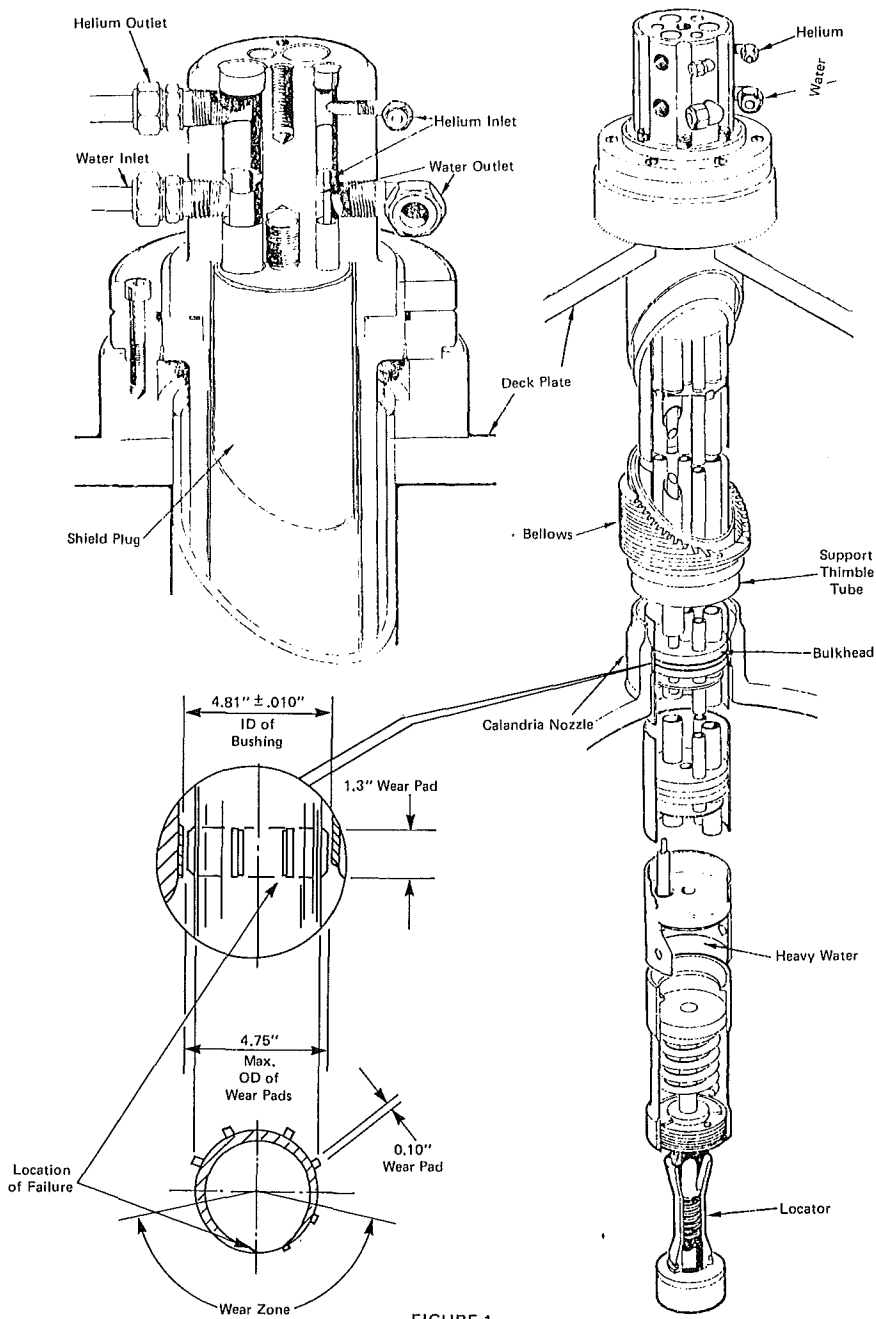


FIGURE 1  
Liquid Zone Control Rod

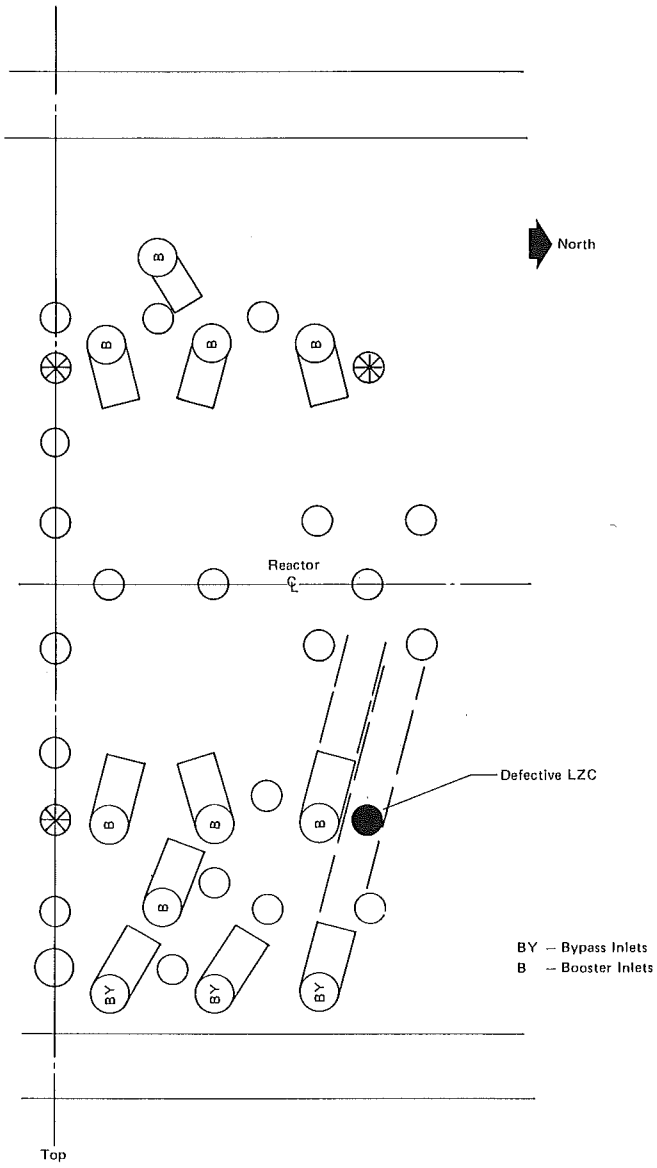


FIGURE 2  
Orientation of Moderator Inlet Nozzles

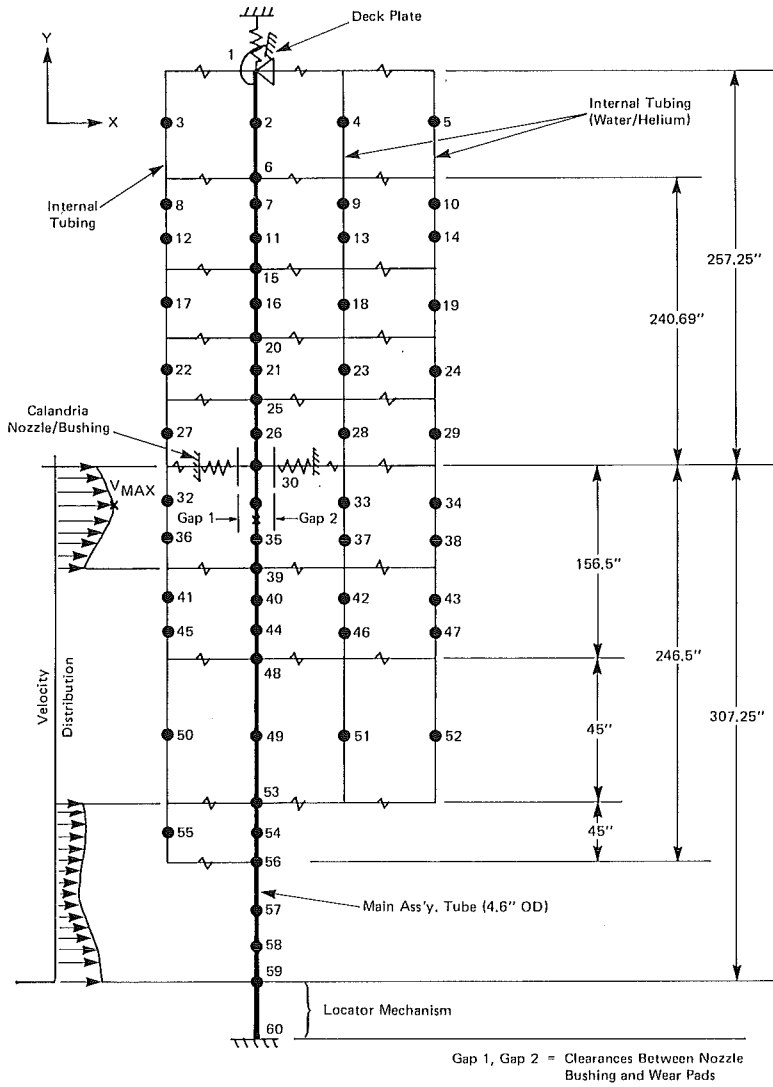


FIGURE 3  
Liquid Zone Control Mathematical Model

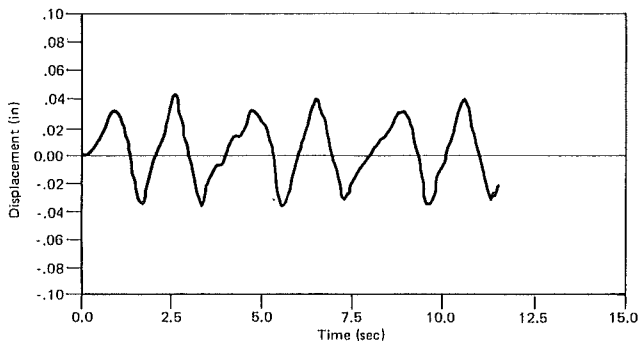


FIGURE 4  
Displacement Response Node 40

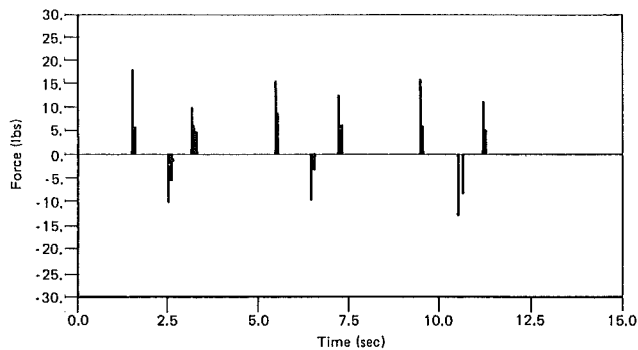
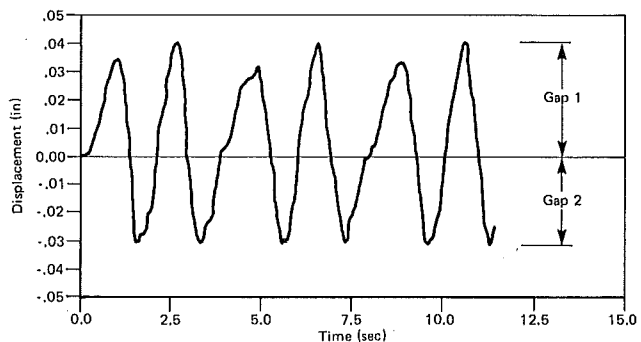


FIGURE 5  
Nozzle/Tube Impact Force Time History at Node 30



Force/Deflection Relationship of  
Non-Linear Element Representing  
Nozzle/Tube Clearance

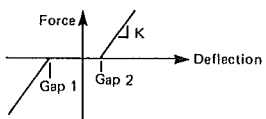


FIGURE 6  
Displacement Response Node 30

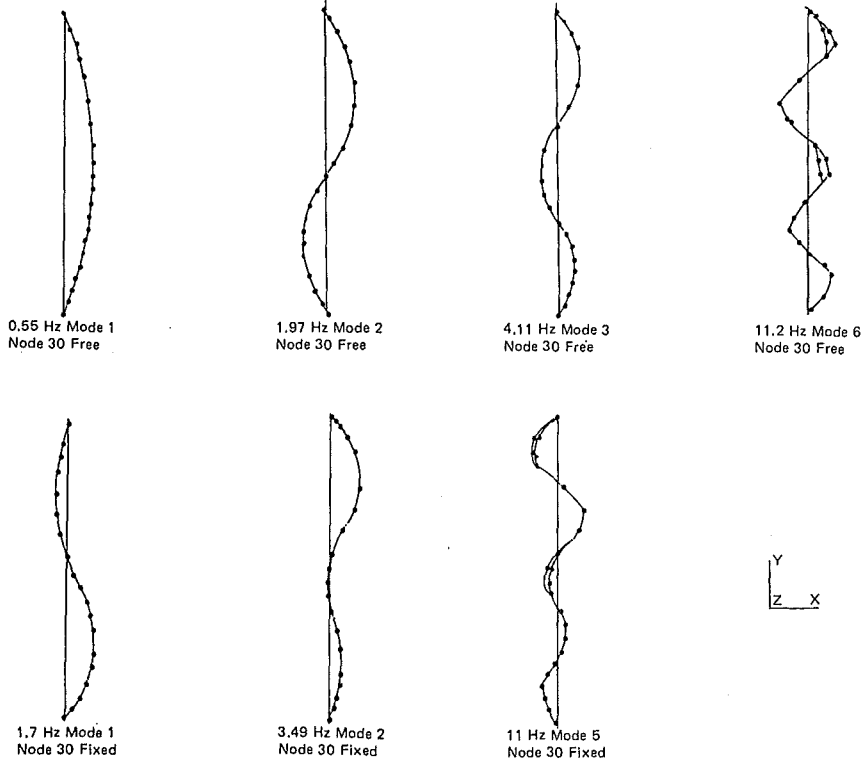


FIGURE 7  
Mode Shapes



## Chapter 3

## System and Component Behavior

	pages
3.1 F.J. Erbacher: Interaction Between Fuel Clad Ballooning and Thermal-Hydraulics in a LOCA	299 - 310
3.2 M.A. Bolander, C.D. Fletcher, C.B. Davis, C.M. Kullberg, B.D. Stitt, M.E. Waterman, J.D. Burttt: RELAP5 Thermal-Hydraulic Analyses of Overcooling Sequences in a Pressurized Water Reactor	311 - 319
3.3 J.E. Koenig, R.C. Smith: TRAP-PF1 Analyses of Potential Pressurized-Thermal-Shock Transients at a Combustion-Engineering PWR	320 - 329
3.4 W. Häfner, L. Wolf: Review and Assessment of American Experiments and Theoretical Models for Thermal Mixing PTS-Phenomena as Basis for Designing HDR-Experiments TEMB	330 - 347
3.5 J.Q. Howieson, L.J. Watt, S.D. Grant, P.G. Hawley, S. Girgis: CANDU LOCA Analysis with Loss of Offsite Power to Meet LWR Acceptance Criteria as Applied in Japan	348 - 356
3.6 U.S. Rohatgi, C. Yuelys-Miksis, P. Saha: An Assessment of Appendix K Conservatism for Large Break LOCA in a Westinghouse PWR	357 - 365
3.7 P. Gulshani, M.Z. Caplan, N.J. Spinks: THERMOSS: A Thermohydraulic Model of Flow Stagnation in a Horizontal Fuel Channel	366 - 375
3.8 N.J. Spinks, A.C.D. Wright, M.Z. Caplan, S. Prawirosoehardjo, P. Gulshani: Thermosyphoning in the CANDU Reactor	376 - 384

	pages
3.9 K.H. Ardron, V.S. Krishnan, J.P. Mallory, D.A. Scarth: Studies of Hot-Wall Delay Effects Pertinent to CANDU LOCA Analysis	385 - 396
3.10 J.T. Rogers: A Study of the Failure of the Moderator Cooling System in a Severe Accident Sequence in a CANDU Reactor	397 - 408
3.11 S.E. Meier: Fluid-Structure Interaction in Pressure Water Reactors	409 - 415
3.12 J.A. Kobussen, R. Mylonas, W.X. Zheng: RETRAN Predictions for Pressure Transients Following a Feedwater Line Break and Consequent Check Valve Closing	416 - 425
3.13 J.A. Desoisa, C.P. Greef: Reactor Fault Simulation at the Closure of the Windscale Advanced Gas-Cooled Reactor: Analysis of Transient Tests	426 - 435
3.14 G. Herbold, E.J. Kersting: Analysis of a Total Loss of AC-Power in a German PWR	436 - 447
3.15 C.A. Dobbe, R. Chambers, P.D. Bayless: Thermal-Hydraulic and Core Damage Analysis of the Station Blackout Transient in Pressurized Water Reactors	448 - 456
3.16 R. Bisanz, B. Burger, U. Lang, M. Schindler, F. Schmidt, H. Unger: Analysis of Severe LOCA Problems Using RELAP5 and TRAC	457 - 466
3.17 R.R. Schultz, Y. Kukita, Y. Koizumi, K. Tasaka: A LSTF Simulation of the TMI-2 Scenario in a Westinghouse Type Four Loop PWR	467 - 476
3.18 E.F. Hicken: Results from the OECD-LOFT Consortium Tests	477



	pages
3.19 P.J. Fehrenbach, I.J. Hastings, J.A. Walsworth, R.C. Spencer, J.J. Lipsett, C.E.L. Hunt, R.D. Delaney: Zircaloy-Sheathed UO <sub>2</sub> Fuel Performance During In-Reactor LOCA Transients	478 - 487
3.20 V.I. Nath, E. Kohn: High Temperature Oxidation of CANDU Fuel During LOCA	488 - 497
3.21 R.M. Mandl, B. Brand, H. Schmidt: The Importance of End-of-Blowdown Phase on Refill/ Reflood for the Case of Combined ECC Injection. Results from PKL Tests	498 - 507
3.22 M. Spiga: Heat Transfer in PWR U-Tube Steam Generators	508 - 515
3.23 F.J. Erbacher, P. Ihle, K. Rust, K. Wiehr: Temperature and Quenching Behavior of Undeformed, Ballooned and Burst Fuel Rods in a LOCA	516 - 524
3.24 D.G. Reddy, C.F. Fighetti: A Study of Rod Bowing Effect on Critical Heat Flux in PWR Rod Bundles	525 - 534
3.25 H. Kianjah, V.K. Dhir, A. Singh: Enhancement of Heat Transfer in Disperse Flow and Downstream of Blockages in Rod Bundles	535 - 545
3.26 D. Saphier, J. Rodnizky, G. Meister: Transient Analysis of an HTGR Plant With the DSNP Simulation System	546 - 555



## INTERACTION BETWEEN FUEL CLAD BALLOONING AND THERMAL-HYDRAULICS IN A LOCA

F.J. Erbacher

Kernforschungszentrum Karlsruhe  
Institut für Reaktorbauelemente  
Projekt Nukleare Sicherheit  
Postfach 3640, 7500 Karlsruhe 1  
Federal Republic of Germany

## ABSTRACT

The state-of-the-art experimental work in several countries on LOCA simulation burst and reflood tests in PWR rod bundles is reviewed concerning the influence of thermal-hydraulics on fuel clad ballooning and coolability of blocked fuel rod bundles.

Representative two-phase flow heat transfer during reflooding limits the mean total circumferential burst strains to approx. 50 %. Reversed coolant flow direction from the refilling to the reflooding phase which is typical of a combined emergency core cooling injection results in a maximum flow blockage of approx. 50 %. With unidirectional flow the maximum flow blockage amounts up to approx. 70 %.

Reflood tests in partially blocked bundles have shown that coolability of PWR fuel rod bundles blocked up to 90 % can be maintained without any unacceptable temperature increase due to the flow blockage.

## INTRODUCTION

In the refilling and reflooding phases of a loss-of-coolant accident (LOCA) occurring in a pressurized water reactor (PWR) Zircaloy fuel rod claddings may reach temperatures which cause them to balloon and to burst due to internal overpressure. Such local ballooning restricts the cooling channels in the fuel element and may lead to local impairment of emergency core cooling.

In the LOCA analysis required for licensing of a PWR, the number of ruptured fuel rods, the cladding deformations and their influence on coolability must be predicted. Flow blockage and quenching are finally the main concerns in the safety assessment, because they determine the maximum cladding temperature which must be limited.

In many countries burst and reflood tests in rod bundles have been performed to furnish experimental data.

## LOCA THERMAL-HYDRAULICS IN A PWR CORE

The thermal-hydraulics in the reactor core depends on the design of the emergency core cooling system. For instance, the injection pressure of the accumulators and the injection mode i.e. cold leg injection only and combined injection, respectively, determine the level of heat transfer and also the flow direction in the core both of which have a dominating effect on clad ballooning. Therefore, a wide range of thermal-hydraulic boundary conditions has been investigated in the LOCA simulation tests.

Figure 1 shows as an example the fuel rod cladding load in a LOCA predicted by conservative evaluation models for a PWR with combined injection.

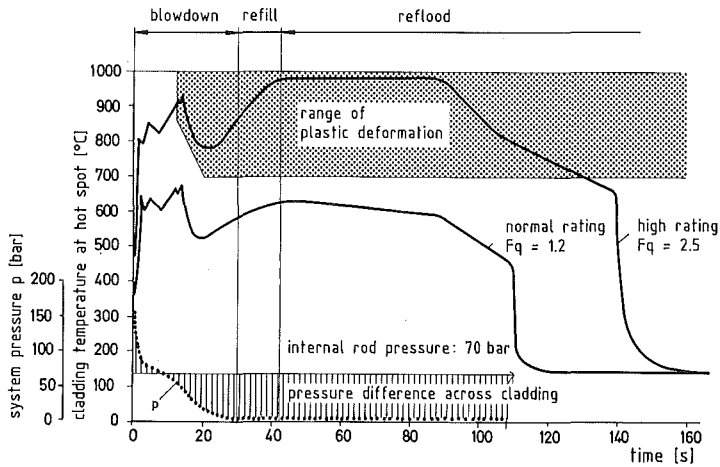


Fig. 1 Fuel rod cladding loading in a 2F-cold leg break LOCA

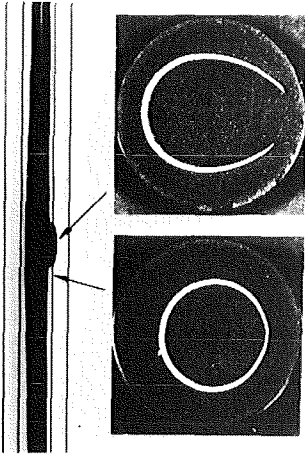
## REVIEW OF LOCA SIMULATION TESTS

To review all tests in detail would be a task beyond the scope of this paper. Therefore only several out-of-pile and in-pile bundle tests have been selected.

Table I summarizes some multi-rod burst tests /1-7/. Only tests using indirectly heated fuel rod simulators and in-pile tests, respectively, are included. From the individual test series only those are listed which have the potential for maximum ballooning i.e. burst in the high  $\alpha$ -phase of Zircaloy around 800 °C. Table II summarizes all relevant out-of-pile reflood tests in partially blocked bundles /8-11/. In these tests the flow blockage due to ballooned claddings has been simulated by sleeves mounted on electrical heater rods.

This paper reviews mainly the effects of thermal-hydraulics on clad ballooning and the effects of flow blockages on coolability. Since the KFK-programs REBEKA /12/ and FEBA /11/ covered a relatively wide range of thermal-hydraulic conditions the essential conclusions will be discussed on the basis of these experimental programs.

EFFECT OF HEAT TRANSFER ON CLAD BALLOONING



In the REBEKA tests Zircaloy has been found to show a specific deformation behavior in the  $\alpha$ -phase region, due to its texture and anisotropy /13/. Since always azimuthal cladding temperature differences exist tube bending occurs where the hot side of the cladding tube during deformation continues to be in more or less close contact with the inner heat source and the opposite cold side is deformed in such a way that it continuously moves apart from the inner heat source (Fig. 2). Via this mechanism heat transfer, which is intensified during reflooding, leads to an increase in azimuthal temperature differences on the cladding tube. Fig. 3 makes evident that increasing azimuthal cladding temperature differences are decreasing the circumferential burst strains /13/.

Fig. 2  
Bowling of Zircaloy tubes during deformation under azimuthal temperature differences and cooling

prox. 30 K were established in the REBEKA bundle tests at the time of burst which limits the mean burst strain to values around 50 %.

Figure 4 illustrates the influence of heat transfer on cladding tube deformation. During the reflooding phase of a LOCA heat transfer coefficients greater than  $50 \text{ W/m}^2 \text{ K}$  are developed during cladding tube deformation. Under these conditions azimuthal temperature differences of approx. 30 K were established in the REBEKA bundle tests at the time of burst

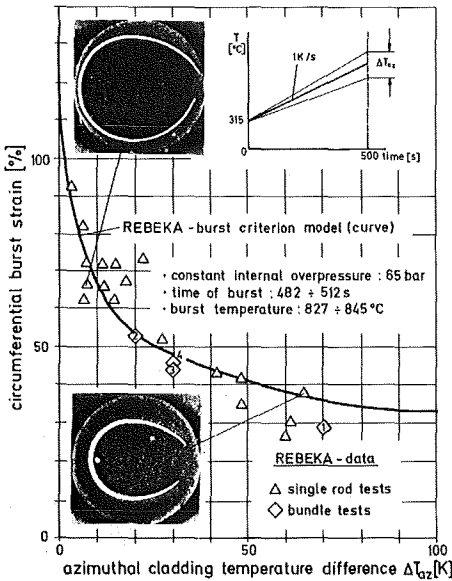


Fig. 3  
Burst strain vs. azimuthal temperature difference

Other bundle tests (see Tab. I) performed in very low heat transfer by steam cooling ( $\leq 5 \text{ W/m}^2 \text{ K}$ ) exhibited higher burst strains. This is consistent with the experience gained within the REBEKA program (see REBEKA-M). However, such high burst strains are not typical of PWR conditions during reflooding.

EFFECT OF COOLANT FLOW DIRECTION ON FLOW BLOCKAGE

The flow blockage caused by the ballooned cladding tubes is also determined by the axial displacement of the bursts between two spacers. Since plastic deformation of Zircaloy cladding tubes reacts very sensitively to the cladding tube temperature, the axial displacement of the bursts is decisively determined by the axial profile of the cladding tube temperature prevailing between two spacers.

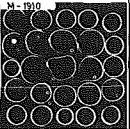
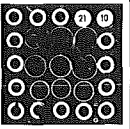
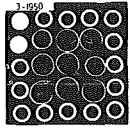
	REBEKA-M	REBEKA-2	REBEKA-3
cross-section at max. flow blockage			
fluid flow	stagnant steam	steam flow	two-phase flow
heat transfer coefficient [W/m <sup>2</sup> ·K]	<10	~ 30	~30 ÷ 100
mean burst strain of inner 3x3 rods [%]	63	54	44

Fig. 4 Influence of heat transfer on clad ballooning

The profile of cladding tube temperature is among others the result of the thermodynamic non-equilibrium in two-phase flow and its being influenced by the spacer grids. Moreover, it is determined by the direction of flow i.e., by the fact whether during cladding tube deformation the flow is uni-directional or whether it changes its direction between the refilling and reflooding phases.

Figure 5 makes evident the influence of a reversed flow direction from the refilling to the reflooding phases on the deformation pattern in REBEKA 5. Due to irregularities in the rod bundle resulting from locally different rod powers and cooling conditions the individual rods show different plots of cladding tube temperature versus time. This implies different times of burst for the individual rods and, because the cladding tube temperature maxima occurring between the spacer grids are shifted as a function of the time, likewise an axial displacement of the bursts. Since the cladding tubes underwent bursting at a relatively flat axial temperature profile, hot spots and cladding tube tolerances contribute in addition to an axial displacement of the bursts on account of the extreme sensitivity to temperature of Zircaloy deformation. The bursts are distributed over an axial length of 242 mm which results in a relatively low flow blockage of 52 %.

Figure 6 shows the deformation pattern obtained in the REBEKA 6 bundle test in which the direction of coolant flow was maintained for the refilling and reflooding phases. Unlike in REBEKA 5, the temperature maximum was shifted towards the upper spacer grid from the beginning of the experiment. After the temperature profile has developed in the refilling phase the temperature maximum remains largely stationary in its axial position. Therefore, irregularities cannot make a contribution to the axial displacement of the bursts. On account of the relatively steep axial temperature profile hot spots and cladding tube tolerances neither make a decisive contribution. Consequently, the bursts are arranged so as to be relatively close to each other and thus give rise to a comparatively large flow blockage. It is apparent from the figure that the bursts are displaced solely over an axial length of 140 mm. The resulting flow blockage is 60 %, i.e., it is greater than in case of reversed flow direction. It remains to be studied whether and to which extent this value is influenced by particularities in this experiment - e.g., by a cold instrumentation tube, a multitude of ther-

mocouples etc. - and flow blockage might have been underestimated for uni-directional flow in this test.

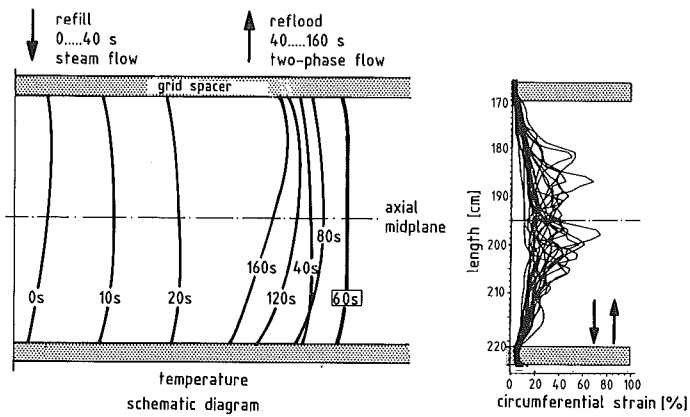


Fig. 5 Influence of reversed flow on axial distribution of clad ballooning (REBEKA 5)

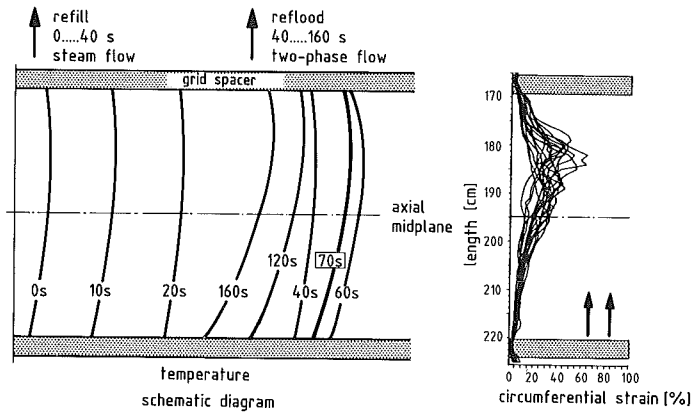


Fig. 6 Influence of unidirectional flow on axial distribution of clad ballooning (REBEKA 6)

Figure 7 illustrates by two photographs the influence of flow direction on cladding tube deformation.

PWR's equipped with a combined emergency core cooling injection into the cold and hot leg exhibit preferentially countercurrent flow of steam and water mainly downwards in the refilling and upwards in the reflooding phase. This situation gives rise to a relatively low flow blockage of approx. 50 %. PWR's

with cold leg injection only have preferentially unidirectional upward flow of steam and water in the refilling and reflooding phases. This may result in a relatively high flow blockage of approx. 70 %.

The full-length bundle tests REBEKA-7 (7x7, all pressurized, unidirectional flow) and NRU-MT 6A (5x5 without corner rods, all pressurized, unidirectional flow) will finally show what maximum flow blockage has to be assumed with unidirectional flow in a LOCA.

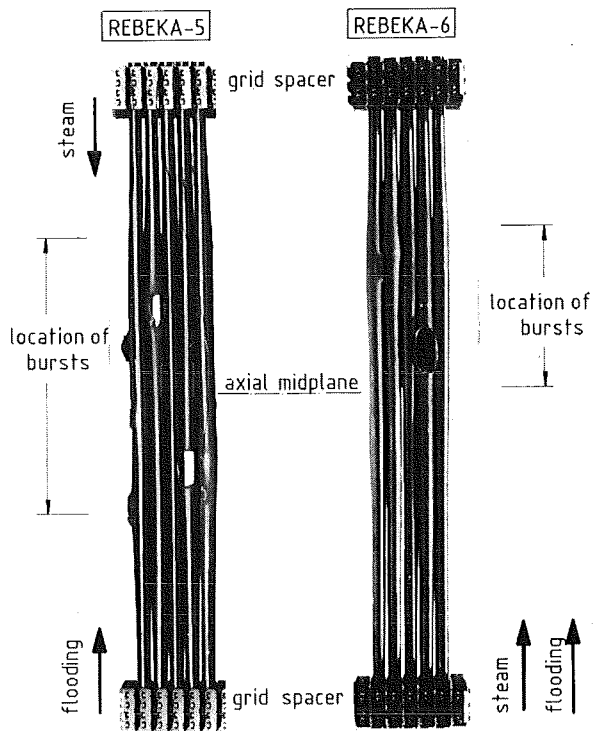


Fig. 7 Influence of flow direction on axial distribution of clad ballooning

#### EFFECT OF FLOW BLOCKAGES ON COOLABILITY

Flow blockages produced by ballooned claddings change the cooling mechanism downstream of the blockage. The increased flow resistance in the blocked region results in a reduction of the coolant mass flow. On the other hand, droplet breakup and turbulence enhancement occur at the blockage, which improve heat transfer. Which of these effects is more dominant depends on a number of boundary conditions.

Within the FEBA program /11/ flooding tests with forced feed have been performed under transient LOCA conditions on a 5x5 bundle with coplanar conical



sleeves simulating the flow blockage. Fig. 8 shows cladding temperature transients in the blocked and the unblocked regions for a flooding rate of 3.8 cm/s and a blockage ratio of 62 % in the blocked region. It is evident from the diagram that under the given conditions the effect of water droplet breakup, which improves the heat transfer, overcompensates the degrading effect of mass flow reduction with the consequence that the cladding temperature downstream of the blocked region is somewhat lower compared to that in the unblocked region.

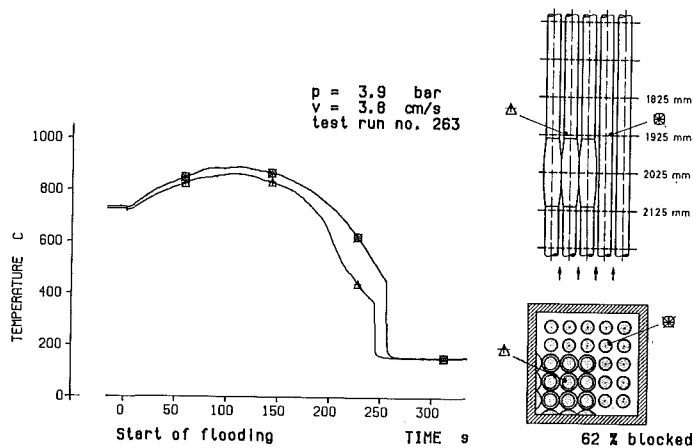


Fig. 8 Cladding temperatures in partly blocked 25-rod bundle (FEBA)

Figure 9 shows corresponding plots for a blockage ratio of 90 % in the blocked region. It makes evident that under these severe conditions the coolant mass flow reduction overshadows the two-phase cooling enhancement effect. However, the temperature rise downstream of the blockage and the delay in quench time are moderate. From this it can be concluded that in fuel elements blocked up to 90 % the coolability in a LOCA can be maintained.

These findings are consistent with the results from other tests listed in Tab. II which were performed with larger bundles, larger bypass regions and partially with gravity feed. The higher temperature rise found in the THETIS blockage experiment is mainly the consequence of a more severe blockage shape and a low rod power both of which tend to deliver very conservative results.

All reflow tests on blocked bundles used solid electrical heater rods with no gap between the cladding and the inner heating element. It has been shown in the REBEKA- and SEFLEX-program that such gapless heater rods exhibit higher peak cladding temperatures and longer quench times compared to nuclear fuel rods and REBEKA fuel rod simulators, respectively. In addition it has been found that burst cladding tubes quench even earlier compared to intact cladding tubes and generate secondary quench fronts /14/.

This recent experience suggests that the test results summarized in Tab. II are still conservative and that there is a higher safety margin in the coolability of a PWR in a LOCA.

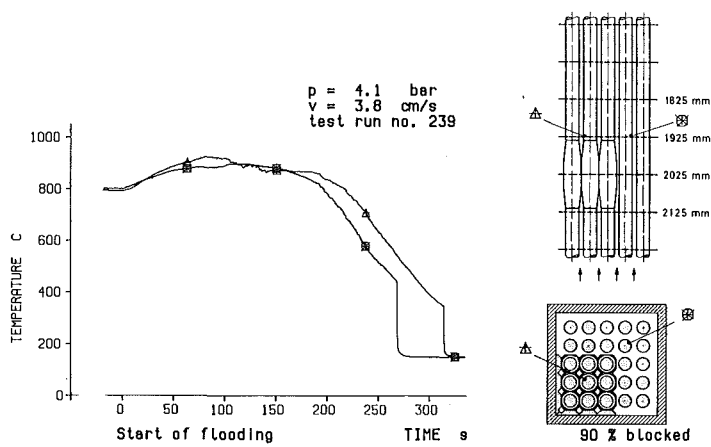


Fig. 9 Cladding temperatures in partly blocked 25-rod bundle (FEBA)

#### SUMMARY AND CONCLUSIONS

- Substantial knowledge and a sufficiently reliable data base on the interaction between fuel clad ballooning and thermal-hydraulics exist in order to prove the safety of a PWR in a LOCA.
- All test data are consistent.
- Differences in the test results are mainly due to different thermal-hydraulic test conditions.
- Heat transfer during reflooding limits the mean total circumferential burst strain of the Zircaloy cladding tubes to approx. 50 %.
- The direction of coolant flow in the fuel element during the refilling and reflooding phases decisively influences the axial displacement of the bursts and the size of flow blockage caused in this way.
- Reversed coolant flow direction from the refilling to the reflooding phases leads to a maximum flow blockage of approx. 50 %.
- Uni-directional coolant flow during the refilling and reflooding phases results in the highest possible flow blockage of approx. 70 %.
- Coolability in a blocked fuel element can be maintained up to a blockage ratio of approx. 90 %.

## REFERENCES

- /1/ S. Kawasaki  
"Multirods Burst Tests under Loss-of-Coolant Conditions."  
OECD-NEA-CSNI/IAEWA-Specialists' Meeting on Water Reactor Fuel Safety and Fission Product Release in Off-Normal and Accident Conditions May 16-20, 1983, Risø National Laboratory, Denmark.
- /2/ R.H. Chapman et al.  
"Effect of Bundle Size on Cladding Deformation in LOCA Simulation Tests."  
Sixth International Conference on Zirconium in the Nuclear Industry, June 28 - July 1, 1982, Vancouver, British Columbia, Canada.
- /3/ G. Cheliotis, E. Ortlieb  
"Parameteruntersuchungen über die Beeinflussung der Hüllrohre durch Nachbarstäbe beim Kühlmittelverluststörfall."  
Abschlußbericht Förderungsvorhaben BMFT RS 185 A, KWU Bericht R 914/022/80, September 1980.
- /4/ B. Adroguer, C. Hueber, M. Trotabas  
"Behavior of PWR Fuel in LOCA Conditions, PHEBUS Test 215 P."  
OECD-NEA-CSNI/IAEA Specialists' Meeting on Water Reactor Fuel Safety and Fission Product Release in Off-Normal and Accident Conditions, May 16-20, 1983, Risø National Laboratory, Denmark.
- /5/ C.L. Mohr et al.  
"LOCA Simulation in the National Research Universal Reactor Program, Third Materials Experiment (MT-3)."  
NUREG/CR-2528, PNL-4166, April 1983.
- /6/ K. Wiehr et al.  
"Bündelexperiment REBEKA-6"  
KFK 3450, Juni 1984, S. 4200-42 bis -96.
- /7/ K. Wiehr et al.  
"Bündelexperiment REBEKA-5"  
KFK 3350, Juli 1983, S. 4200-94 bis - 162.
- /8/ Loftus, M.J. and Hochreiter, L.E.  
"Reflood Heat Transfer in the FLECHT-SEASET 163-Rod Bundle with Flow Blockage and Bypass."  
ASME Paper 83-WA/HT-16 (1983).
- /9/ Joint NRC, JAERI, BMFT 2D/3D Program:  
"SCTF Core I Test Results" (JAERI)  
9th Water Reactor Safety Research Information Meeting, Gaithersburg, MD, Oct. 26-30, 1981.
- /10/ Pearson, K.G., Cooper, C.A.  
"Reflood Heat Transfer in Severly Blocked Fuel Assemblies"  
International Workshop on Fundamental Aspects of Post Dryout Heat Transfer Salt Lake City, April 2-4, 1984, Utah, USA.
- /11/ Ihle, P., Rust, K.  
"FEBA-Flooding Experiments with Blocked Arrays, Evaluation Report"  
KFK-3657, March 1984.

- /12/ F.J. Erbacher, H.J. Neitzel, K. Wiehr  
"Brennelementverhalten beim Kühlmittelverluststörfall eines Druckwasser-  
reaktors - Ergebnisse des REBEKA-Programms"  
KfK-Nachrichten, Jahrgang 16, Heft 2/84, S. 79-86.
- /13/ F.J. Erbacher, H.J. Neitzel, K. Wiehr  
"Effect of Thermohydraulics on Clad Ballooning, Flow Blockage and  
Coolability in a LOCA"  
OECD-NEA-CSNI/IAEA Specialists' Meeting on Water Reactor Fuel Safety and  
Fission Product Release in Off-Normal and Accident Conditions, May 16-20,  
1983, Risø National Laboratory, Denmark
- /14/ F.J. Erbacher, P. Ihle, K. Rust, K. Wiehr  
"Temperature and Quenching Behavior of Undeformed, Ballooned and Burst  
Fuel Rods in a LOCA"  
Fifth International Meeting on Thermal Nuclear Reactor Safety, Karlsruhe,  
FRG, September 9-13, 1984.

Tests		test geometry		thermal-hydraulic test conditions during cladding deformation				test results (averaged)				reference	
		number of rods	heated length	heating rate	coolant flow	flow direction	heat transfer coefficient	burst temperature	burst strain	burst zone within grids	max. flow blockage		
													mm
transient heatup tests (refill)	out - of - pile	JAERI - B 13	7x7 (all pressurized)	850	<1	65 g/s m <sup>2</sup> steam	uni-directional	~2	782	~60	10	90	[1]
		MRBT - B 5	8x8 (all pressurized)	915	10	288 g/s m <sup>2</sup> steam	uni-directional	~5	768	60	40	90 (inner 4x4)	[2]
		KWU - 4	3x4 (2 pressurized)	650	9	forced air	uni-directional	60	838	52			[3]
		PHEBUS - 215P	5x5 (all pressurized)	800	8	steam	uni-directional	50...90	840	50 (inner 3x3)	4	65	[4]
refill and reflood tests	in - pile	NRU - MT 3	6x6 w/o corner rods (12 pressurized)	3660	8...1	steam 5.6...1.0 cm/s reflood	uni-directional	60...70	800	55	10	70	[5]
	out - of - pile	REBEKA - 6	7x7 (46 pressurized)	3900	7...-4	~2m/s steam ~3cm/s reflood	uni-directional	30...100	765	42 (inner 5x5)	14	60	[6]
		REBEKA - 5	7x7 (all pressurized)	3900	7...0	~2m/s steam ~3cm/s reflood	reversed from refill to reflood	30...100	800	49 (inner 5x5)	24	52	[7]

Table I LOCA simulation multi-rod burst tests

Tests	test and blockage geometry						thermal-hydraulic test conditions			results			reference
	number of rods	rod diameter	heated length	blockage ratio (coplanar)	number of fully blocked subchannels	blockage length incl. conical ends	forced feed cold flooding velocity	system pressure	rod power %ANS - standard	max. difference of peak clad temp.			
										downstream of blockage		blockage	
										blockage/bypass	blocked/unblocked	sleeve/bypass	
	mm	m	%		mm	cm/s	bar	%	K	K	K		
FLECHT / SEASET	21	9.5	3.05	up to 90	up to 24	60	1...25	1.4...2.8	50...120	none or negative	none or negative	negative	[8]
	163	9.5			up to 48	60			120	none or negative	none or negative	negative	
SCTF	2000	9.5	3.66	62	~ 400	60	3...10	~ 2.4	120	negative	no tests	negative	[9]
THETIS	49	12.2	3.58	90 80	9 9	450	1.3...5.8	1.3...4.1	30...50		no tests	positive, late about 100 K	[10]
FEBA	25	10.75	3.9	90	9	180	3.8...5.8	2...6	120	max. 50 K mostly none or negative	none	negative	[11]
				62	9	180	2...10			none	negative	negative	

Table II LOCA simulation reflood tests in blocked bundles

RELAP5 THERMAL-HYDRAULIC ANALYSES OF OVERCOOLING  
SEQUENCES IN A PRESSURIZED WATER REACTOR

M. A. Bolander, C. D. Fletcher, C. B. Davis,  
C. M. Kullberg, B. D. Stitt, M. E. Waterman and J. D. Burt

Idaho National Engineering Laboratory  
EG&G Idaho, Inc.  
P. O. Box 1625  
Idaho Falls, Idaho 83415 U.S.A.

## ABSTRACT

In support of the Pressurized Thermal Shock Integration Study, sponsored by the United States Nuclear Regulatory Commission, the Idaho National Engineering Laboratory has performed analyses of overcooling transients using the RELAP5/MOD1.6 and MOD2.0 computer codes. These analyses were performed for the H. B. Robinson Unit 2 pressurized water reactor, which is a Westinghouse 3-loop design plant. Results of the RELAP5 analyses are presented. The capabilities of the RELAP5 computer code as a tool for analyzing integral plant transients requiring a detailed plant model, including complex trip logic and major control systems, are examined.

## INTRODUCTION

The rapid cooldown of a pressurized water reactor (PWR) vessel during a transient or accident accompanied by high coolant pressure is referred to as pressurized thermal shock (PTS). The United States Nuclear Regulatory Commission (USNRC) designated PTS as an unresolved safety issue in late 1981, and developed a task action plan (TAP A-49) to resolve the issue.

The safety issue exists because rapid cooling at the reactor vessel wall inner surface produces thermal stresses within the wall. As long as the reactor vessel wall is ductile, overcooling transients will not cause vessel failures. NRC staff analyses (SECY-85-465) showed, however, certain older plants with copper and other impurities in vessel weldments may become sensitive to PTS as the nil-ductility transition temperature of the weld material gradually increases. The purpose of the thermal-hydraulic analyses presented in this paper is to better understand the behavior of the H. B. Robinson Unit 2 power plant during various kinds of postulated severe overcooling transients with multiple failures of equipment and/or without operator corrective action. The understanding gained in these analyses will be used to determine coolant temperature and pressure responses in the vessel downcomer for other postulated transients using a simplified mass-and-energy balance approach. For each of the thermal-hydraulic transients, Oak Ridge National Laboratory (ORNL) will perform analyses to determine reactor vessel temperature distribution and stresses during the transient and the conditional probability of vessel failure if one of these transients should occur.

The analyses presented in this paper were performed for the H. B. Robinson Unit 2 PWR operated at Hartsville, South Carolina, U.S.A. by Carolina Power and Light Company. The reactor is a Westinghouse three-loop design power plant. This is one of several PWRs the USNRC has identified for which PTS is of concern. The USNRC has contracted with ORNL to integrate the investigation of the PTS unresolved safety issue, and with the Idaho National Engineering Laboratory (INEL) to support ORNL by performing thermal-hydraulic analyses using RELAP5, a state-of-the-art computer code, and a plant-specific model for the H. B. Robinson plant.

The transient simulations were performed from either full power or hot standby operating conditions using "best estimate" modeling assumptions for plant conditions and responses to events specified in the scenario descriptions. The reader is cautioned, however, that for bounding purposes, the scenario descriptions were based on extremely conservative assumptions concerning equipment malfunctions, operator actions and omissions, or combinations of these. While the computer simulations represent "best estimate" plant responses to the scenarios as defined, [Reference 1] they do not represent the "most probable" plant responses to the scenario initiating events.

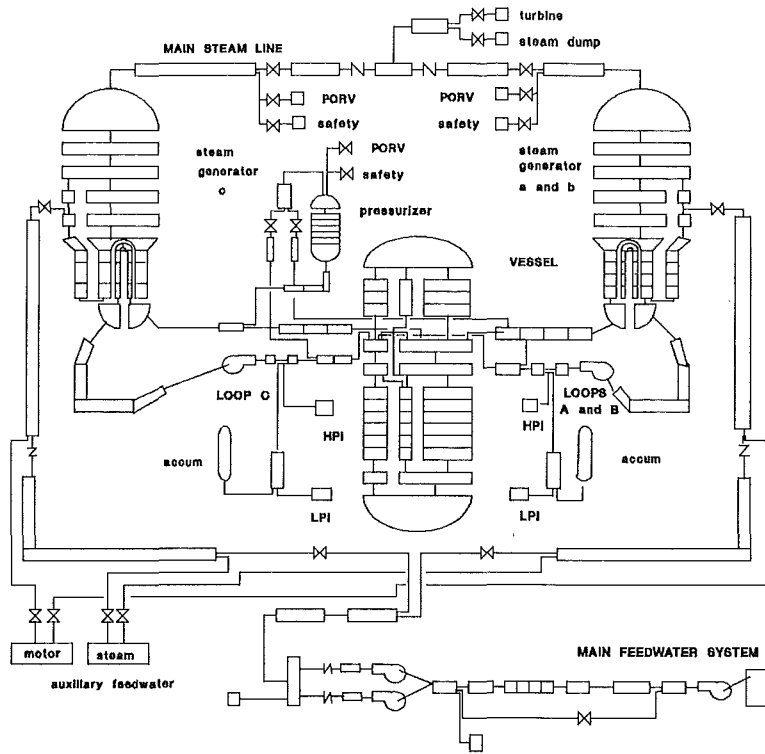
This paper describes the RELAP5 model developed for the H. B. Robinson power plant which was used to perform the transients for the analyses. The paper also describes the 37 transient scenario calculations that were performed with this model. Results of the study are presented by examining base case transients and variations of break size, break location, power level, and/or operator action. Also presented are capabilities of the RELAP5 computer code in performing analyses of this type.

#### Model Description

The transient calculations presented in this paper were performed with a RELAP5 model of the H. B. Robinson, Unit 2 (HBR-2), PWR power plant described herein. The model is a detailed thermal-hydraulic and control system representation of the plant. The thermal-hydraulic model represented all the major flow paths of the plant and is shown in Figure 1. The HBR-2 plant has three primary coolant loops and each loop is represented in the model. The vessel model included all the major flow and leakage paths of the plant. Also modeled on the primary side was the pressurizer and its associated power operated relief valves (PORVs) and safety valves, and the emergency core cooling (ECCs) system. The secondary side model of the plant included: all of the major flow paths in each of the steam generator secondaries; the main steam line out to the turbine including steam dump valves (SDVs), PORVs, and safety valves; and the main feedwater system, including feedwater heaters and auxiliary feedwater systems. To simulate plant control, the major plant control systems were modeled using the control system package contained in the RELAP5 computer code. The systems modeled include the steam dump control system, steam generator level control system, pressurizer pressure control system and pressurizer level control system. Also included in the modeled control system are controllers to simulate feedwater control behavior during steady state and transient modes. The HBR-2 RELAP5 model contained 224 volumes, 242 junctions, 218 heat structures and 300 control system components. For a more detailed description of the model refer to [Reference 1].

As a checkout of the model a simulation of an actual HBR-2 plant trip was performed. Generally, the agreement between measured and calculated data was very good as characterized by the measured and calculated pressurizer pressure responses shown in Figure 2. The comparison provided a limited, but useful, qualification of the plant model.





#### RELAP5 H.B. ROBINSON PLANT MODEL DESCRIPTION

Figure 1. RELAP5 plant nodalization for the H. B. Robinson Unit power plant.

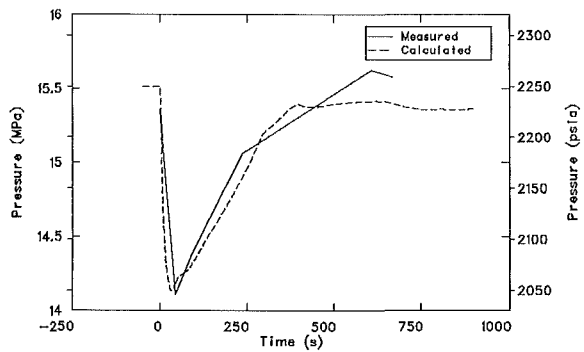


Figure 2. Measured and calculated pressurizer pressure responses of a plant trip transient simulated with the H. B. Robinson model.

## Transient Descriptions

There were 37 transient calculations performed with the detailed model. The scenarios calculated were defined by ORNL and are categorized into five types of transient events: (1) steam line break transients, which include large and medium size breaks, stuck-open PORVs, stuck-open SDVs, and combination stuck-open PORVs and SDVs; (2) loss-of-coolant accidents, which include isolatable or nonisolatable medium and small breaks on either the hot or cold leg, stuck-open pressurizer PORV, and breaks with steam generator overfills; (3) steam generator tube rupture transients, which include a single tube rupture with or without operator action; (4) steam generator overfill and loss of secondary heat sink transients; and (5) combination steam line break and loss-of-coolant accidents which include combinations of stuck-open steam line PORVs or SDVs with stuck-open pressurizer PORV or medium size breaks. In each of the above transient events, the transients were performed at either full power or hot-standby. [References 1 and 2]

## Results

The reactor vessel downcomer pressure and temperature histories for a representative steam line break, loss-of-coolant accident, and combination steam line break and loss-of-coolant accident are presented. Break size, break location, power level, and/or operator action parametric variations are also presented for the first two transient events. The transient calculations were run with the detailed model out to where a stable trend in the response was observed, then, based on past experience, a simplified model of the plant or a simplified mass-and-energy balance approach was used to extrapolate the response to two hours, the period of PTS concern.

The reactor vessel downcomer pressure and temperature responses for a  $0.09 \text{ m}^2$  ( $1 \text{ ft}^2$ ) main steam line break transient from hot standby conditions are shown as Curve 1 in Figures 3 and 4. The break occurred in the Steam Generator A main steam line just upstream from the main steam isolation valves. Primary system pressure rapidly decreased as break induced heat transfer to the A steam generator peaked. As the A steam generator emptied, heat transfer to this generator degraded and primary pressure stabilized. The vessel downcomer temperature response also rapidly decreased during this time period due to the enhanced cooling from the affected steam generator. At approximately 200 s the volumetric addition from HPI exceeded the volumetric contraction from the cool-down and the pressurizer began to refill, repressurizing the primary system. At 600 s auxiliary feedwater was terminated, slowing the decrease in the temperature response shown in Figure 4. When the level in the pressurizer recovered at 650 s, charging flow was automatically throttled and thus slowed the primary repressurization rate. At 1100 s the affected steam generator became dry and heat transfer from the primary was lost, resulting in a turn-around of the downcomer temperature. At 1200 s the primary system pressure exceeded the HPI shut off head, terminating HPI. The system pressure continued to rise to the pressurizer PORV set point due primarily to volumetric expansion as the primary fluid continued to heat up.

Variations to the above transient include operator action, break size, and power level. Curve 2 of Figure 4 shows the reactor vessel downcomer temperature response of a double-ended steam line break where the operator does not terminate the auxiliary feedwater. While the continuation of auxiliary feedwater does not affect the pressure response significantly, the temperature continues to decrease. Had the operator not terminated the auxiliary feedwater in Curve 1 the response would be similar to Curve 2. The dominating factor in the primary pressure and temperature response of steam line breaks is secondary

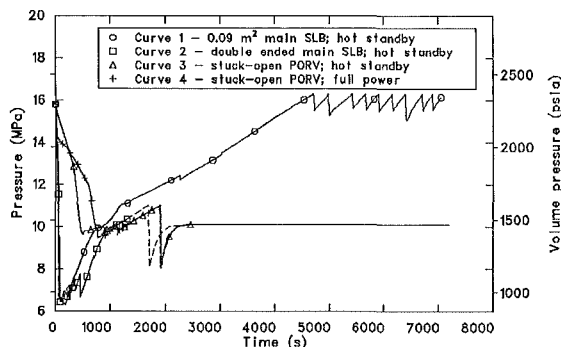


Figure 3. Reactor vessel downcomer pressure for steam line break (SLB) transients.

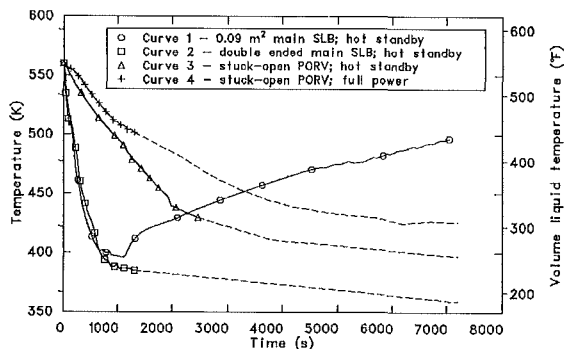


Figure 4. Reactor vessel downcomer temperature for steam line (SLB) break transients.

depressurization. Curve 3 of Figures 3 and 4, a small steam line break representing a stuck-open steam line PORV, shows the pressure and temperature response with respect to break size. Compared with Curve 2, the pressure and temperature response of Curve 3 is slower because of the much smaller break size. Curves 3 and 4 of Figures 3 and 4 show the effects of power level for a stuck-open steam line PORV transient. Because there is more energy to remove at full power (Curve 4) the pressure and temperature responded more slowly than at hot standby (Curve 3).

The reactor vessel downcomer pressure and temperature response for a 6.35 cm, (2 1/2 in.) hot leg break transient at full power are shown in Figures 5 and 6. The initial rapid decrease in primary pressure was a result of a high break volumetric flow due to subcooled liquid at the break and the rapid decrease in core power due to scram. At approximately 150 s the depressurization slowed due to vapor generation throughout the primary system and a decrease in the break mass flow rate which was due to two phase conditions at the break. At approximately 1000 s auxiliary feedwater was terminated and vapor generation due to core decay heat resulted in a primary repressurization. The

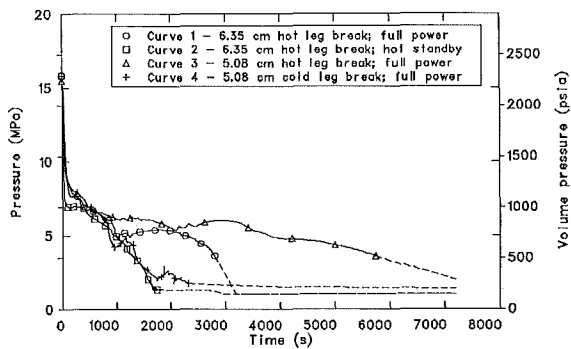


Figure 5. Reactor vessel downcomer pressure for loss-of-coolant accidents.

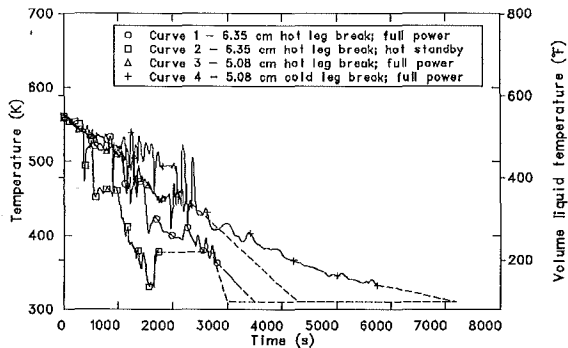


Figure 6. Reactor vessel downcomer temperature for loss-of-coolant accidents.

repressurization continued until the core subcooled reducing the vapor generation rate. After this time, the primary pressure decreased until the energy removal at the break balanced with the energy addition, and break flow equaled total ECC flow.

The temperature response of this transient, shown in Figure 6, decreased due to the cooldown of the system from the depressurization. Cold ECC fluid mixed well with cold leg fluid during this time. As the loops and vessel drained, loop natural circulation was lost and mixing of the ECC fluid with the primary fluid decreased resulting in a faster cooldown of the downcomer temperature. The downcomer temperature was dominated by the ECC fluid temperature due to loop stagnation throughout the remainder of the transient.

The effects of power level, break size, and break location on a loss-of-coolant-accident (LOCA) are shown by Curves 2 through 4 in Figures 5 and 6. Curve 2 is the same type of transient as just discussed except it began at hot standby. The events of the two transients were similar except they occurred earlier in the hot standby case. The higher power kept the system hotter resulting in a slower depressurization and promoted better loop natural circulation due to a larger density difference across the core and better mixing of the primary fluid with the cold ECC fluid.

Curve 3 represents a 5.08 cm (2 in.) diameter hot leg break at full power. The trends in this transient are similar to those of the 6.35 cm (2.5 in.) hot leg break except the events are delayed in time. The delay of events is due mainly to the slower energy removal at the break.

Curve 4 represents a 5.08 cm (2 in.) diameter cold leg break at full power. Compared with Curve 3 the depressurization is faster, due to a higher break volumetric flow rate resulting from colder fluid exiting the break. The temperature response, however, remains about the same. Even though the pressure in the cold leg break is lower, which would induce more ECC fluid into the system, 1/3 of the ECC is going directly out of the break with the net ECC flow being nearly the same in both cases. Thus, approximately the same downcomer cooldown exists in both transients.

The reactor vessel downcomer pressure and temperature responses for a combination LOCA and steam line break are shown in Figures 7 and 8 respectively. As shown, the trend of the pressure response resembles that of the LOCA

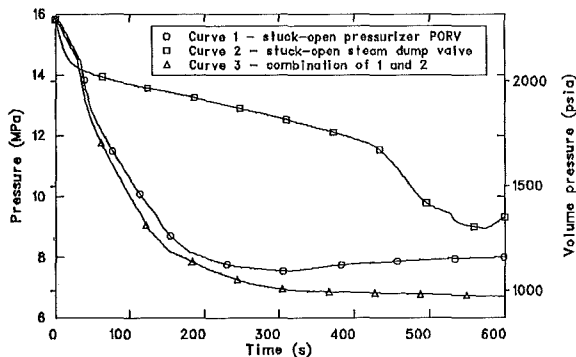


Figure 7. Reactor vessel downcomer pressure for a stuck-open pressurizer PORV transient, a stuck-open dump valve transient, and a combination of the two transients.

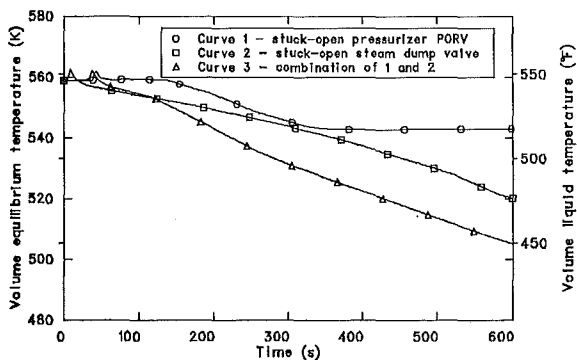


Figure 8. Reactor vessel downcomer temperature for a stuck-open pressurizer PORV transient, a stuck-open valve transient, and a combination of the two transients.

transients because of the break on the primary side. The temperature response in this type of transient, however, resembles that of a steam line break transient because of the dominant enhanced primary-to-secondary heat transfer.

#### Code Capabilities

Capabilities in modeling a complex plant of the nature of the H. B. Robinson plant with the RELAP5 computer code [Reference 3] include control system modeling, trip logic, and user conveniences in the input to constructing models. The control system package included in RELAP5 provides the capability to evaluate simultaneous algebraic and ordinary differential equations. Because the control system used by the H. B. Robinson plant is complex in controlling plant behavior, especially during transient situations, and the inability to monitor this behavior manually, it was necessary to use the RELAP5 control system package to model a majority of the actual control system. The model checkout simulation of a plant transient mentioned earlier has demonstrated the RELAP5 control system modeling adequately represented the actual control system.

Extensive trip logic has been implemented in RELAP5. A combination of variable and logical trips was generated for the H. B. Robinson model to describe the logic involved in determining automatic or manual actions the plant experiences during a transient, such as reactor scram, or emergency feedwater initiation.

Another feature of the RELAP5 code is the user friendliness of the input in constructing large detailed models and the ability to economically perform calculations with these models. Because the input to construct models with RELAP5 is user friendly, the analyst can efficiently and economically build large detailed models. The CPU time to real time ratio (performed on a CDC 176 computer) for the transients performed with the detailed model range from 2.55 to 7.95. Those transients that exhibited high condensation rates or low primary or secondary pressures executed more slowly.

The treatment of condensation effects under specific conditions, such as an surge to a pressurizer is another feature of the RELAP5/MOD1.6 and MOD2.0 computer codes. Condensation occurs at the interface between steam and liquid. When the subcooled primary coolant first enters the superheated steam environment of an empty pressurizer, high condensation rates can be expected. However, once a level has been established within the pressurizer, a layer of saturated liquid is believed to form at the liquid steam interface decreasing the condensation rate significantly. A model which allows vertical stratification of the fluid in RELAP5/MOD1.6 and MOD2.0, and the six field equations in MOD2.0 (which allows subcooled liquid and superheated vapor to exist in the same volume) has greatly improved the calculated pressurizer surge response.

#### CONCLUSIONS

To perform the H. B. Robinson PWR power plant PTS study done at the INEL, a detailed RELAP5 model of the plant was developed. A comparison of code-calculated and measured data from a plant trip transient indicated generally good agreement and thus provided a limited, but useful, qualification of the model. A steam line break transient and a LOCA were examined with perturbations of break size, break location, power level and/or operator action. It was shown that both steam line break transients and LOCAs resulted in cold downcomer temperatures. However, the steam line break transients resulted in a system repressurization, whereas the pressure in the LOCA calculations continued

to decrease. It was also shown that a combination steam line break and LOCA transient exhibited a primary pressure behavior similar to that of a LOCA transient and a downcomer temperature response similar to that of a steam line break transient. The RELAP5 computer code adequately calculated the transient behavior, due in part to its ability to handle complex control and trip logic, which physically controls plant behavior. It was demonstrated that large integral models can economically be run with RELAP5. Inclusion of a vertical stratification model in RELAP5/MOD1.6 and MOD2.0 and six field equations in MOD2.0 has greatly improved calculated pressurizer insurge response.

## REFERENCES

1. C. D. Fletcher et al., RELAP5 Thermal-Hydraulic Analyses of Pressurized Thermal Shock Sequences for the H. B. Robinson Unit 2 Pressurized Water Reactor, EG&G Idaho, NUREG to be published November 1984.
2. C. D. Fletcher et al., Thermal-Hydraulic Analyses of Overcooling Sequences for the H. B. Robinson Unit 2 Pressurized Thermal Shock Study, EG&G Idaho, NUREG to be published October 1984.
3. V. H. Ransom et al., RELAP5/MOD1 Code Manual, Volumes 1 and 2, EG&G Idaho Report NUREG/CR-1826, EGG-2070, November/ 1980.

## NOTICE

This report was prepared as an account of work sponsored by an agency of the United States Government. Neither the United States Government nor any agency thereof, or any of their employees, makes any warranty, expressed or implied, or assumes any legal liability of responsibility for any third party's use, or the results of such use, or any information, apparatus, product or process disclosed in this report, or represents that its use by such third party would not infringe privately owned rights. The views expressed in this paper are not necessarily those of the U.S. Nuclear Regulatory Commission.

This work was supported by the U.S. Nuclear Regulatory Commission, Office of Nuclear Regulatory Research under DOE Contract No. DE-AC07-76ID01570.

TRAC-PF1 ANALYSES OF POTENTIAL PRESSURIZED-THERMAL-SHOCK  
TRANSIENTS AT A COMBUSTION-ENGINEERING PWR\*

Jan E. Koenig and Russell C. Smith

Energy Division  
Los Alamos National Laboratory  
Los Alamos, New Mexico USA 87544

## ABSTRACT

Los Alamos National Laboratory participated in a program to assess the risk of a pressurized thermal shock (PTS) to the reactor vessel during a postulated overcooling transient in a pressurized water reactor (PWR). Using the Transient Reactor Analysis Code (TRAC), Los Alamos studied the thermal-hydraulic behavior of the three following accident categories: steamline breaks, runaway-feedwater transients, and small-break loss-of-coolant accidents. These accidents were simulated for a Combustion-Engineering (C-E) PWR, Calvert Cliffs, and included multiple operator and equipment failures. The results will be used by Oak Ridge National Laboratory (ORNL) to determine the vessel wall temperature and stresses corresponding to the bulk downcomer liquid temperature and pressure predicted by TRAC.

The study identified the importance of the initial plant conditions and loop flows to the PTS issue. If the plant was initially at hot-zero power (rather than full power), the same accident initiator could produce significantly lower downcomer temperatures because of the reduced decay heat and stored energy. Flow stagnation in all reactor coolant loops, which occurred in one transient, could lead to a vessel wall temperature that approached the relatively cold high-pressure-injection fluid temperature. However, routine operator actions would reduce the consequences of any of these simulated accidents if the pressure-temperature relationships prescribed in the operator guidelines are followed. ORNL will extend the results of the Los Alamos study by determining the probability of vessel failure and accident occurrence for an overall assessment of PTS risk.

---

\*Work supported by the US Nuclear Regulatory Commission.



## INTRODUCTION

Los Alamos National Laboratory participated in a program to assess the risk of a pressurized thermal shock (PTS) to a reactor vessel. Our role was to provide best-estimate thermal-hydraulic analyses of 13 postulated overcooling transients using TRAC-PF1.<sup>1</sup> These transients were all hypothetical and included multiple equipment and operator failures. Calvert Cliffs, a Combustion Engineering (C-E) plant, was the pressurized water reactor (PWR) modeled for this study. Calvert Cliffs/Unit 1, located on the Chesapeake Bay in Maryland, began operation in January 1975. Figure 1 shows the configuration of the primary side of the power plant. Unit 1 has a 2 x 4 loop arrangement: two hot legs and two steam generators (SGs) with four cold legs and four reactor coolant pumps (RCPs). The plant operates at 2700 MW<sub>th</sub>.

The reactor vessels of certain older plants containing copper impurities in the vessel welds risk cracking if subjected to a thermal shock concurrent with high system pressure (referred to as PTS). After years of irradiation, the vessel welds in these plants have become more brittle; and therefore, the temperature at which a crack may initiate or propagate increases. Overcooling transients can be postulated that may lead to a PTS. For this reason, in late 1981, the US Nuclear Regulatory Commission (NRC) identified PTS as an unresolved safety issue and developed a task action plan (TAP A-49) to resolve the issue.

An effort to assess the risk of PTS in representative plants of the three US PWR vendors was established. A Westinghouse plant (H. B. Robinson) and a Babcock & Wilcox plant (Oconee) were also studied as part of the program. For the C-E plant (Calvert Cliffs), several organizations participated: the plant owner, which is the Baltimore Gas and Electric Co. (BG&E); C-E; the NRC; Oak

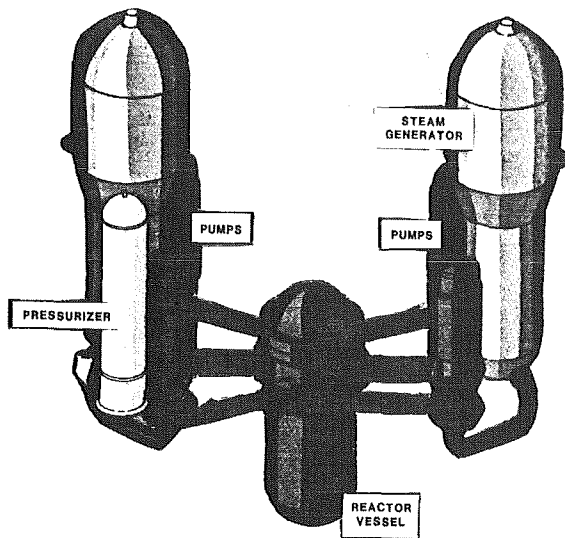


Fig. 1  
Primary side of Calvert Cliffs.

Ridge National Laboratory (ORNL); Brookhaven National Laboratory (BNL); and Los Alamos National Laboratory.

The NRC managed the multi-organizational project. BG&E and C-E supplied extensive information about the plant and its operation. Los Alamos used this information to prepare a comprehensive TRAC-PF1 model of Calvert Cliffs. ORNL identified 13 postulated overcooling transients that could lead to PTS, and Los Alamos simulated most of these transients for 7200 s (2 h) after their initiation. These transients were reviewed by BG&E, C-E, ORNL, and BNL. Our results were provided to ORNL, who plan to extend these results to other postulated PTS transients using a simplified mass-and-energy balance approach. For each of these postulated transients, ORNL plans to determine the stresses in the vessel wall and calculate the probability of vessel failure. ORNL then plans to publish a report<sup>2</sup> that incorporates the entire study and identifies the important event sequences, operator and control actions, and uncertainties.

The purpose of these calculations is to aid the NRC in confirming the screening criterion (the criterion to determine if a power plant is subject to a risk of PTS) in the proposed PTS rule (10 CFR 50.61). The current screening criterion of a power plant is a reference temperature for nil-ductility transition ( $RT_{NDT}$ ) of 405 K (270°F) at 40 effective full-power years. The NRC will also use these analyses to develop requirements for the licensees' plant-specific PTS safety-analysis reports and the acceptance criterion for proposed PTS preventive actions.

#### TRAC-PF1 CALCULATIONS

TRAC-PF1 is a best-estimate finite-difference computer code capable of modeling thermal-hydraulic transients in both one and three dimensions. The code solves the field equations for mass, momentum and energy conservation of both vapor and liquid. The Calvert Cliffs model fully exercised the capabilities of TRAC-PF1.

We performed thermal-hydraulic analyses of three accident categories: runaway-feedwater transients, steamline breaks, and small-break loss-of-coolant accidents (SBLOCAs). These transients were initiated from either hot-zero power (HZP) or full power (FP). The RCPs were tripped 30 s after the safety-injection-actuation signal in all but one transient. Parameters that were significant in assessing the risk of PTS were the downcomer liquid temperature, the system pressure, and the occurrence of flow stagnation in the reactor coolant loops. This paper describes the factors that strongly affected these three parameters in the TRAC PF1 calculations. Table I lists a description of each of the 13 transients, the calculated minimum downcomer liquid temperature, and whether repressurization and/or loop flow stagnation were calculated by TRAC-PF1. This work is documented in detail in Ref. 3.

#### FACTORS AFFECTING DOWNCOMER LIQUID TEMPERATURE

The initial conditions of the plant were important. When a transient was initiated from FP, the decay heat was high enough that a significant decrease in the downcomer bulk fluid temperature did not occur. Uncertainty in the amount of decay heat following FP shutdown exists because the decay heat is dependent on the operating history of the plant and thus, the system energy following FP shutdown can vary significantly. For the TRAC-PF1 calculations, it was assumed

TABLE I  
TRANSIENT RESULTS<sup>a</sup>

Description <sup>b</sup>	Minimum T		Repressurization	Flow Stagnation
	K	°F		
Runaway-feedwater Cases:				
1. Runaway MFW to two SGs from FP	480	404	yes	no
2. Runaway MFW to one SG from FP	490	422	yes	one loop
3. Runaway AFW to two SGs from FP	490	422	yes	no
Steamline Breaks:				
4. 0.1-m <sup>2</sup> MSLB				
a. From HZP	395	251	yes	one loop
b. From FP	468	383	yes	one loop
c. With two operating RCPs from HZP	446	343	yes	no
5. Double-ended MSLB				
a. With failure to isolate AFW to broken SG from HZP	377	219	yes	one loop
b. With two stuck-open MSIVs from HZP	376	217	yes	no
6. Small steamline break (stuck-open TBV)				
a. From FP	530	494	yes	no
b. With one stuck-open MSIV from FP	500	440	yes	no <sup>b</sup>
SBLOCAs:				
7. 0.002-m <sup>2</sup> hot-leg break from FP	440	332	(low flow)	one loop
8. One stuck-open pressurizer valve				
a. With one stuck-open atmospheric dump valve from FP	407	273	no	one loop
b. From FP	350 <sup>b</sup>	171 <sup>b</sup>	no	both loops

<sup>a</sup>No operator intervention assumed except to trip the RCPs.

<sup>b</sup>Estimated.

that the reactor had been in operation for an infinite length of time. An assessment of the effect of the uncertainty of the decay heat following FP shutdown is detailed in the full report (Ref. 3).

Plant features that significantly affected the rate and amount of primary cooldown were:

- (1) SG isolation capability - Valves on the main feedwater (MFW) lines and the steamlines terminate flows (except auxiliary feedwater) into both SGs if the secondary pressure is less than 4.6 MPa (668 psig) in either SG. This limits the cooling potential of a steamline break or stuck-open secondary valve. If the break was downstream of the main steam isolation valves (MSIVs), an overcooling transient was terminated upon receipt of the low-pressure signal (called the SG isolation signal or SGIS). If the break was upstream of the MSIVs, the primary overcooling was still limited to the energy-removal capability of one SG because the other SG was isolated after SGIS.
- (2) SG liquid inventory - The SGs at Calvert Cliffs have relatively large liquid inventories at steady state: ~102000 kg (225000 lb) at HZP and ~63000 kg (138600 lb) at FP. So, even with the capability to isolate one of the SGs, a steamline break would have severe overcooling potential.
- (3) Flow restrictors on the steamlines - Because of a flow restrictor located in each main steamline, the largest effective break size downstream of this restrictor (10 m (32.8 ft) from the SG exit) is 0.2 m<sup>2</sup> (2.0 ft<sup>2</sup>). Hence, the thermal-hydraulics of a 0.2-m<sup>2</sup> main steamline break (MSLB) and a double-ended MSLB (0.52 m<sup>2</sup> (5.6 ft<sup>2</sup>)) would be virtually the same because the effective break size would be the same.
- (4) Auxiliary feedwater (AFW) control logic - AFW is valved out to the SG at a lower pressure if a pressure differential greater than 0.8 MPa (115 psia) exists between the SGs. This limits the overcooling potential of a steamline break to the energy-removal capability of one SG because AFW will not be supplied to the "broken" SG.
- (5) Condenser/hotwell liquid inventory - This determined the overall cooling capability of the runaway-MFW transients.

#### FACTORS AFFECTING SYSTEM PRESSURE

The system pressure and rate of repressurization (if any) are important in assessing the risk of PTS. Because of an assumed operator failure to turn off the charging pumps, all secondary-side-initiated transients repressurized to the pressurizer power-operated relief valve (PORV) setpoint. Figure 2 shows a typical pressure history for a secondary-side transient (0.1-m<sup>2</sup> (1.0-ft<sup>2</sup>) MSLB from HZP). For a potential PTS problem to arise during an SBLOCA, the break size must be small enough for the system pressure to remain high but large enough for high-pressure-injection (HPI) flow to be necessary.

Plant features that strongly influenced the system pressure were:

- (1) Safety-injection and makeup/letdown (charging) flow - HPI flow is delivered by centrifugal pumps with a low shutoff head of 8.8 MPa (1285 psia) and charging flow is delivered by positive-displacement pumps. This means that while the primary can repressurize to the PORV setpoint, the repressurization rate would decrease drastically above 8.8 MPa. Also, the supply of cold water to the downcomer would be limited to charging flow when the system pressure is above the shutoff head of the HPI pumps. This feature was important for postulated secondary-side transients when the primary side repressurized.

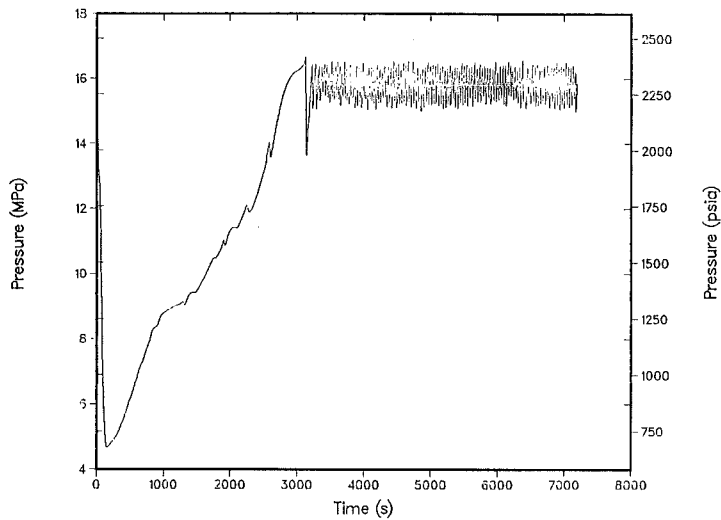


Fig. 2.

Typical primary pressure history for a secondary-side transient.

- (2) Bypass flows into the upper head - Liquid enters the upper head via a controlled flow area through the control-element-assembly (CEA) shrouds and a small bypass leakage flow at the top of the downcomer. This flow was important for all transients when the upper head voided because it strongly affected the condensation rate and thus the depressurization and repressurization rate.

#### FACTORS AFFECTING LOOP FLOW STAGNATION

Flow stagnation is of particular importance to PTS because no mechanism is available to cause significant mixing of the cold-leg fluid with injected HPI fluid and consequently, the HPI fluid may concentrate along the vessel wall. TRAC-PF1 is not designed to predict flows of this nature and hence, calculations were performed at Purdue University<sup>4</sup> and at Los Alamos<sup>5</sup> (using SOLA-PTS code) to resolve the temperature and flow distributions during periods of flow stagnation during the transients.

Figure 3 illustrates the mechanism for producing loop flow stagnation. The SG must be in a reverse-heat-transfer mode for the loop flow to cease. When the driving head (density gradient) produced by heat input from the SG opposed the driving head produced by the heat input from the core, the net force to drive the flow was zero. The higher decay heat from FP transients produced a greater positive driving force for flow than the decay heat at HZP and flow stagnation was more likely in the HZP transients. Thus, the initial conditions also were an important factor in flow stagnation.

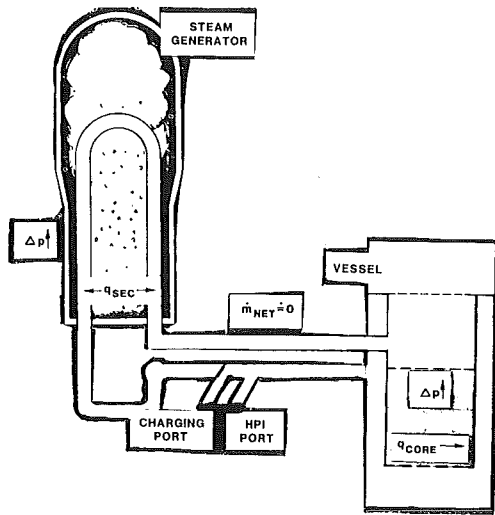


Fig. 3.  
Mechanism for producing loop flow stagnation.

Many transients produced loop flow stagnation in one loop because of asymmetric conditions on the secondary side (resulting from a steamline break or stuck-open valve); however, according to studies at Los Alamos,<sup>5</sup> if one loop is in natural circulation while the other loop is stagnant, the HPI fluid will still mix with the warmer fluid residing in the downcomer. Of the 12 transients initially specified by ORNL, flow stagnation in both loops did not occur. As our understanding of the significant phenomena improved, we were able to identify a transient that produced stagnation in both loops. This calculation is presented in the next section.

Plant features that were significant to flow stagnation were:

- (1) SG isolation capability - During a steamline break or runaway-feedwater transient, one SG may be isolated while the other is not. These asymmetric secondary conditions can lead to cooling of the primary fluid by one SG and heating by the other. The flow may stagnate in the loop where heat is being added by the SG. However, flow stagnation in one loop is currently judged not to be a PTS problem.
- (2) Number of reactor coolant loops - Thorough mixing in the downcomer might not occur if there are more than two loops. If stagnation were to occur in all but one loop of a three- or four-loop plant, it might be of PTS concern.

#### MOST SIGNIFICANT TRANSIENT

The most significant transient (from a thermal-hydraulic standpoint) was initiated by a stuck-open PORV while the plant was operating at HZP. This

transient produced stagnation in both loops leading to a low bulk downcomer temperature with a system pressure of  $\sim 7.2$  MPa (1058 psia).

The calculated downcomer liquid temperature, as shown in Fig. 4, may be divided into two phases. Phase 1 (0-260 s) was before the initiation of HPI flow. The system temperature remained constant at its initial value of 552 K (534 $^{\circ}$ F). Because the primary and secondary sides were already in thermal equilibrium and the decay heat was low, only pressure changes, as shown in Fig. 5, occurred during this portion of the subcooled blowdown. When the pressure dropped below 8.8 MPa (1285 psia), HPI flow started and the primary cooldown began (Phase 2). The entire cooldown was due primarily to the replacement of the initial primary mass by the HPI and charging flow. After the top of the U-tubes in the SGs voided at  $\sim 600$  s, the loop flows ceased and subsequent heat addition from the SGs and pipe walls was small. The system began refilling when the HPI/charging flow exceeded the break flow. When the liquid on one side of the U-tubes spilled into the steam volume on the other side at 1800 s, a rapid condensation process began which caused a pressure drop of  $\sim 0.8$  MPa (117.5 psi). This initiated a small circulation of  $\sim 35$  kg/s (77 lb/s) in the loop without the break because a liquid flow path was re-established.

A minimum pressure of 6.0 MPa (882 psia) was reached before the upper head voided. The system pressure increased as the void in the upper head was compressed by the HPI/charging flow. After the steam in the upper head condensed, the pressure remained relatively constant (1200-2400 s) because of an approximate balance between the break flow and the HPI/charging flow. After 2400 s, significantly cooler liquid had reached the break, increasing the break mass flow and decreasing the system pressure. The pressure leveled off to less than the HPI head as the HPI flow increased and again balanced the break flow.

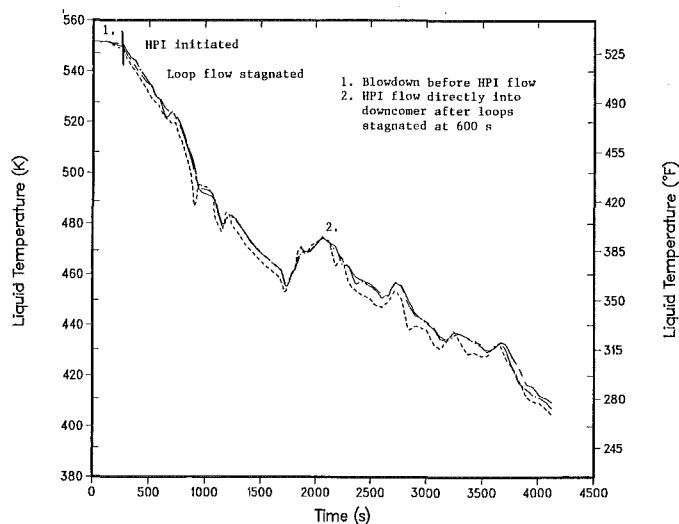


Fig. 4.

Downcomer liquid temperature for stuck-open PORV from HZP.

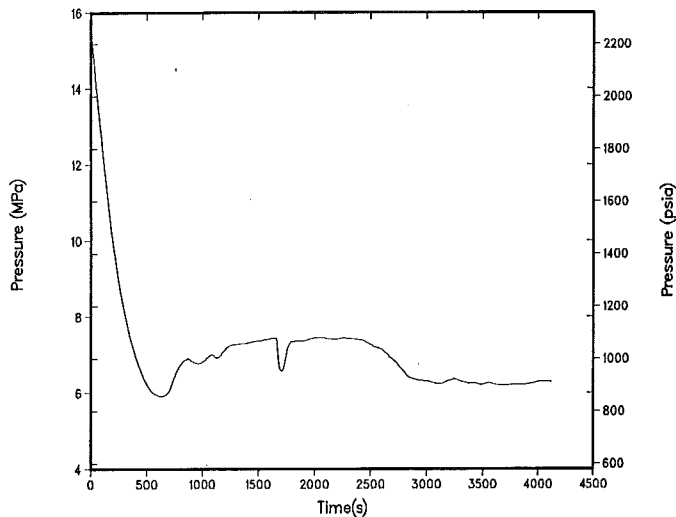


Fig. 5.  
Primary pressure during a stuck-open PORV from HZP.

This transient demonstrated that flow stagnation in both loops was possible during an SBLOCA if the postulated transient is initiated from a low decay-heat level.

#### CONCLUSIONS

In general, those calculations initiated from FP conditions were thermal-hydraulically benign. If initiated from HZP, most of these transients could pose a PTS threat if there was no operator intervention. This is because of the increased likelihood of flow stagnation as well as the reduced heat content of the fluid and the system metal when the plant was at HZP.

Several plant features were identified as significant to the consequences of the postulated potential PTS transients:

1. SG isolation capability.
2. SG liquid inventory.
3. Flow restrictors in the steamlines.
4. AFW control logic.
5. Condenser/hotwell liquid inventory.
6. Safety-injection and makeup/letdown flow.
7. Bypass flows into the upper head.
8. Number of reactor coolant loops.

Steamline breaks possess the largest potential to produce rapid cooldown. If initiated when the SG water mass is large (as at HZP), the subsequent primary-side temperature reduction would be more than if the SG was at FP. SBLOCAs possess a larger potential for overall cooling of the primary system but the rate of cooldown will not be as large as the rate produced by steamline



breaks. Runaway-MFW transients can produce a rapid, but short-lived, cooldown of the primary system.

Simple routine operator actions would have reduced the consequences of any of these simulated accidents. The operator failure assumptions (particularly failure to throttle HPI and charging flow to control the system pressure-temperature relationship prescribed in the operator guidelines) were the single most important contributors to the generation of severe pressure-temperature conditions in all cases.

#### ACKNOWLEDGEMENT

The authors would like to acknowledge the many contributions of Gregory D. Spriggs, of Los Alamos, to this project.

#### REFERENCES

1. Safety Development Group, Energy Division, "TRAC-PF1: An Advanced Best-Estimate Computer Program for Pressurized Water Reactor Analysis," Los Alamos National Laboratory report LA-9944-MS, NUREG/CR-3567 (February 1984).
2. PTS Study Group of Oak Ridge National Laboratory, "Pressurized Thermal Shock Evaluation of the Calvert Cliffs-1 Nuclear Power Plant," Oak Ridge National Laboratory report to be published.
3. Gregory D. Spriggs, Jan E. Koenig, and Russell C. Smith, "TRAC-PF1 Analyses of Potential Pressurized-Thermal-Shock Transients in a Combustion-Engineering PWR," Los Alamos National Laboratory report LA-UR-84-2083 (August 1984).
4. T. G. Theofanus, H. P. Nourbakhsh, P. Gherson, K. Iyer, "Decay of Buoyancy Driven Stratified Layers With Applications to Pressurized Thermal Shock (PTS)," Purdue University report, NUREG/CR-3700 (May 1984).
5. Bart J. Daly, "Three-dimensional Calculations of Transient Fluid-Thermal Mixing in the Downcomer of the Calvert Cliffs-1 Plant Using SOLA-PTS," Los Alamos National Laboratory report LA-10039-MS, NUREG/CR-3704, (April 1984).

REVIEW AND ASSESSMENT OF AMERICAN EXPERIMENTS AND THEORETICAL  
MODELS FOR THERMAL MIXING PTS-PHENOMENA AS BASIS FOR DESIGNING  
HDR-EXPERIMENTS TEMB

W. Häfner and L. Wolf

Battelle-Institut e.V.,  
Am Römerhof 35, 6000 Frankfurt/Main 90, FRG

ABSTRACT

Recent evaluations of high fluence induced embrittlements of some reactor pressure vessel materials have raised the question of vessel integrity during the occurrence of severe pressurized thermal shock (PTS) events. To resolve the PTS issue, both U.S. NRC and EPRI have undertaken a concerted effort to establish a sound data base from scaled model tests and to develop both transient, multidimensional codes as well as simple engineering tools. For Phase II of the HDR Safety Programm, a series of thermal mixing tests, TEMB, in the cold leg and downcomer is planned to establish accurate thermal boundary conditions for a realistic pressurized thermal shock test, at the HDR vessel, NOTZ, at a later point in time. In order to make these efforts most meaningful as well as to use the large-scale, operational HDR-vessel and facility features to the fullest extent, the paper reviews the available American thermal mixing data and highlights those aspects thought to be unique only to the forthcoming HDR experiments and their expected additional contributions to the knowledge base in this area. Additionally, computer codes and models for predicting thermal mixing phenomena will be discussed and their results compared to the available data. Finally, some pre-test predictions by the multidimensional code SOLA-PTS and engineering models, JETMIX and VOLMIX are presented for some of the forthcoming HDR-TEMB experiments.

INTRODUCTION

When high pressure cold emergency core coolant fluid is injected into a PWR cold leg as a consequence of a reactor transient/accident in the primary/secondary system, the inside reactor vessel wall may experience a severe thermal shock which together with an accompanying system repressurization can cause stable crack growth. Given the transient fluid pressure and wall temperature histories, the analysis of crack growth is performed

by fracture mechanics codes. The determination of the transient temperature and pressure histories necessitates the application of such complex system codes as TRAC, RELAP5 throughout the primary, in most instances even secondary systems. However, these systems codes can only accommodate very coarse noding, so that details of thermal mixing in the cold legs and downcomer cannot be assessed by these methods. Rather, much more refined and sophisticated computer codes and/or engineering calculational methods whose input parameters are empirically deduced from a broad data base must supplement the informations gained from system codes.

In order to resolve the important PTS issues, both US NRC and EPRI have undertaken great efforts /1/ for establishing a broad and sound data base from scaled model tests at CREARE /2-6/ and SAI /7/ in order to evaluate the different characteristics of the three American PWR designs in terms of mitigating the injection of high pressure cold emergency coolant.

Parallel to the experimental research, substantial analytical efforts were put in the application and verification of existing multidimensional computer codes, such as COMMIX-1A /8/ and TEMPEST /9/, their necessary extensions and improvements, COMMIX-1B /10-13/ as well as new, special purpose code development such as SOLA-PTS /14,15/. These best-estimate efforts were seconded and supplemented by fast, less expensive engineering models concentrating either on special phenomena, such as HPI-jet mixing under cross-flow Kim /16/, or integrated system behavior based on a control-volume approach supplemented by empirical correlations primarily deduced from the CREARE/SAI-experiments, Sun, Oh /17,18/ or integrated from first principles, Theofanous et al /19,20/, REMIX-code. The development of both methodologies, best-estimate, multidimensional codes and engineering models, gives the potential user the opportunity to choose among various methods according to his needs and resources as well as his desire for insights into physical phenomena. All of the aforementioned tools eliminate the need for overly conservative assumptions for fluid and wall temperature histories as input to deterministic and/or probabilistic fracture mechanic analyses.

Whereas the only purpose of all of the aforementioned experimental facilities was to generate a concise thermal-hydraulic data bank, experimental work on the material and fracture aspects of PTS under more severe pressure and temperature gradients separately goes on at ORNL in the framework of the HSST program.

In contrast to this clearly, separated approach, the integral facility features of the HDR plant allows to examine both thermal-hydraulic and materials research aspects in a truly three-dimensional large vessel under close to real system conditions of 11 MPa and 300 °C. For this purpose a realistic PTS-test, abbreviated NOTZ, is planned for a naturally grown crack at the cylindrical vessel section whose depth of propagation into the vessel base material will be achieved by a cyclic thermal shock test series (THEZ) prior to the HDR-PTS event at the end

of Phase II of the HDR Safety Program sponsored by the BMFT. To achieve this ambiguous objective, a careful planning and approach is in order to attack a variety of obstacles, the first of which is to establish meaningful, (i.e. maximum achievable extremes) reproducible thermal boundary conditions at the cylindrical vessel section under conditions of HPI of 20 °C cold water injection into the cold leg. Thus, a series of thermal mixing tests, abbreviated TEMB, in the cold leg and downcomer is planned /21/ to establish the most extreme downcomer fluid/wall temperature changes which are achievable for various injector geometries and system conditions. In this way, results for the thermal mixing conditions at the injection position and downstream in the cold leg as well as in the downcomer are obtained which supplement and add to the knowledge base established by the American model experiments. With respect to these results, the TEMB experiments stand at the end of an appreciable hard- and software effort in the USA. Therefore, it deemed appropriate to review and assess those efforts in order to plan the HDR-TEMB experiments with due considerations of specific German research needs in this area as well as the feasibility of the NOTZ test in mind. On the other hand, the forthcoming TEMB experiments, besides of enlarging the experimental data base, provide an excellent opportunity to test the validities of the aforementioned analytical tools /8-20/ anew in yet untested more extreme HDR circumstances under truly pre-test conditions.

#### OVERVIEW OF AMERICAN THERMAL MIXING MODEL FACILITIES AND EXPERIMENTAL RESULTS

Table I summarizes the American thermal mixing facilities and their major characteristics. These facilities have been operated under combined EPRI/NRC sponsorship. The first series of mixing tests, MIX1-MIX4 /2-6/ have been performed by CREARE in a 1/5 scale model whose overall geometrical features are shown in Fig. 1 for the example of the MIX3-facility /5/. In addition to these tests series, B&W performed separate tests in a 1/10 scale model /12/. In order to examine any possible effect by the selected model scale, thermal mixing in a full 1:1 model of cold leg/downcomer geometry was tested by SAI /7/. All of these facilities were operated under atmospheric conditions allowing simple facility constructions with transparent materials and thereby visual observations with dye injections as well as inexpensive and proven measurement techniques. This approach insures fast and optimal insights into complex fluid flow phenomena at minimal costs. However, the disadvantages associated with this approach are that only low fluid temperature can be employed for simulating the loop flow, leaving only a slim margin in terms of the applicable temperature of the HPI-flow. Thus, the tested temperature differences between the cold/hot flows are relatively small and so are the density difference ratios, requiring accurate temperature measurements.

To enlarge the examined spectrum of density difference ratios  $\Delta \rho / \rho_{\text{HPI}}$  salt solutions were used as simulating fluids in order to obtain values up to 20 % which are nearly prototypical.

All of the same principles are also applied in the 1/2-scale facility operated at the Purdue University /20/. Whereas most of the aforementioned facilities were used for both natural circulation loop flow conditions as well as limiting condition of stagnant loop flow, Purdue's 1/2-scale model was purposely designed such as to examine only the latter. Special research objectives were to study high Froude number flows, examine any possible effects induced by non-similarities in Re-numbers from strict Froude number scaling as well as to provide consistent sets of space-time distribution of temperatures (simulated by concentrations) and local velocities by hot-film/thermocouple and concentration probes.

Finally, the aforementioned principles were given up for the 1/2-scale facility which is operated by CREARE under a cooperative EPRI/NRC program. It is a non-transparent large scale, heavily instrumented model operating at pressures up to 1.4 MPa allowing the loop flow temperatures to be as high as about 195 °C. Thus far, neither data nor analyses have been published.

It is worth mentioned that according to Table I all American facilities simulated the downcomer as a 90° planar section only with one cold leg penetration. Special attention was given to the simulations of the vendor-specific cold leg designs, such as nozzle curvatures, pipe inclination, loop seal, pump etc.

The major results of the data and their evaluations from the set of the seven American thermal mixing test facilities from which data have been made public can be summarized as follows:

1. Despite of the wide range of possible flow conditions (density difference ratios, volumetric flow ratios, different injector nozzles with respect to diameters, locations and orientations) the degree of mixing between the hot primary coolant flow and cold HPI flow is favourable high.
2. The presentation of the data in terms of the modified Froude-number  $Fr_{\text{CL}} = Q_{\text{HPI}} / A_{\text{CL}} / (g_{\text{DCL}} \Delta \rho / \rho_{\text{HPI}})^{1/2}$  leads to an unique functional relationship over a wide spectrum of the density difference ratio,  $\Delta \rho / \rho_{\text{HPI}}$ , and differently sized and oriented HPI injector nozzles. Fig. 2 /2,3/ demonstrates the primary importance of  $Fr_{\text{CL}}$  for the case of the B&W vent valve facility MIX1. All other experiments indicated the same evidence concerning the controlling character of  $Fr_{\text{CL}}$ .

3. Complete mixing occurs in the downcomer even for very low large flow and steady-state fluid temperatures are close to the ideal mixing temperature there. Fig. 3 /2,5/ indicates the importance of the volumetric flow ratio,  $Q_L/Q_{HPI}$ , for the temperature distributions in the cold leg and thus generally also for downcomer and shows that the steady-state temperatures closely cluster around the curves for the ideal mixing temperatures for water and salt solution conditions even for changes in  $Fr_{CL}$  ranging from 0.025 to 0.075. It is evident from this figure that for a given temperature difference between hot primary and cold HPI flows, the temperatures at the bottom of the cold leg approach the HPI-temperature with decreasing volumetric flow ratio. As can be seen, marked deviations from the hot primary temperature occur only for low values of  $Q_L/Q_{HPI}$  between 0 and 2, with 0 constituting the limiting stagnant loop condition.
4. The characteristic time constant to reach final steady state becomes larger for lower loop flow. The lower the cross-flow effect by the loop flow on the HPI-jet the closer occurs the mixing region at the HPI-nozzle.
5. Counter-current flow reversal of hot primary fluid enters the top of the cold leg region in the direction of the HPI-nozzle for low and stagnant loop flow conditions, enlarging the transverse temperature difference between bottom and upper cold leg regions. Under these conditions, the HPI-jet splits at the bottom and leads to a recirculation pattern upstream.
6. Smaller diameter HPI-nozzles lead to increased mixing because of higher momentum fluxes and jet reflections at the opposite cold leg wall.
7. Under stagnant loop conditions the fluid temperature asymptotically approach the cold leg HPI temperature with time. Gravity effects dominate the flow development and the resultant temperature transients have a very large time constant as shown in Fig. 4 for a sample experiment of the MIX4 test series /6/.
8. The cooldown process can be described in its most simplified form by an exponential time function /6/ whose characteristic time constant is reversely proportional to the volumetric HPI-flow and proportional to a volume factor  $T$ . The size of volumes participating in the mixing processes differently affect the cooldown transient.
9. Reynolds number non-similarities induced by strict Froude number scaling in reduced-scale experiments or mixed scale facilities such as HDR (see below) seem to be unimportant, even for distortions as high as two orders of magnitude in the respective Re-numbers.

The findings were found under the limiting constraints listed for the American experimental facilities in Table I. Yet, they constitute the data base on which together with the analytical tools major decisions for the HDR test matrix were made.

OVERVIEW OF AMERICAN ANALYTICAL METHODS  
FOR PREDICTING PTS THERMAL MIXING PHENOMENA

There are basically two sub-areas which can be identified in classifying methods for computing turbulent buoyant flow and mixing phenomena. These are the methods by which turbulent fluctuations are modeled and the way in which the spatial resolution of the flow in the given geometry is handled. In practice both aspects are coupled. With respect to the problem of turbulence modeling one can differentiate among the following four classes of methods:

1. Correlations giving nondimensional quantities as functions of nondimensional numbers, such as  $Re$ ,  $Fr$ ,  $Gr$ ,  $Nu$ . They are extremely useful but limited especially where geometry affects the fluid and mixing dynamics. New correlations are required each time geometries are changed.
2. Integral methods consider equations (mostly those of class 3) which have been integrated over at least one, mostly over three coordinate directions. This greatly simplifies the mathematical problem through reductions in the independent variables. These methods allow extensive use of experimental data and provide useful physical insights into major phenomena. Their major drawback rests on the need for reformulations and re-qualifications when new type of flow situations are to be computed.
3. Reynolds-Averaged Equations work with averages of the Navier-Stokes equations. The equations describing the mean field contain averages of products of fluctuating velocities, temperatures etc. The averaging procedure leads to fewer equations than unknowns thereby posing the well-known closure problems which necessitates the introduction of a more or less sophisticated turbulence model.
4. Large Eddy Simulation uses equations which are averaged over a small spatial region. This removes the small turbulent eddies from the flow field so that an equation for the large eddies is obtained. The effects of the former on the latter are then modelled.

With the exception of the TURBIT-code /22/ using subgrid scale turbulence modeling with buoyancy effects, none of the available methods fall into class 4 methods. Despite of its proven capabilities and highly scientific standard, TURBIT has not yet been considered for any PTS-thermal mixing application, although it has already demonstrated its value for a different HDR-mixing situation in the downcomer. Its application as the highest-level method available is highly recommended.

Levels 1 and 2 are frequently termed engineering tools, whereas levels 3 and 4 are certainly best-estimate methods. Computations for the latter two levels are limited to institutions with full access to very large, fast computer facilities, preferably vector machines of CYBER-205 and CRAY types.

Worth mentioning is that predictions performed on any level stated above can be used to generate informations useful on the lower level. The problem of treating the flow geometry contains just two categories:

- A. Field Methods use the same set of equations everywhere. No matching is required in the flow interior. However, fine meshes may be needed in some flow regions (boundaries, jet) which make costs for the overall analysis extremely high unless provisions are made to handle non-uniform meshes.
- B. Zonal (Volume) Methods which consider a collection of appropriate "modules" or volumes of the geometry under consideration each of which may be treated by a separate level of turbulence modeling, i.e. integral method or correlation for some zones and full partial differential equations for another. Different solutions in the various zones have to be matched at common boundaries.

Needless to say that in implementing these major categories into useable computer codes a multitude of problems and different solutions arises especially for the combinations of field methods with Reynolds-averaged equations in order to minimize artificial mixing due to numerical diffusion and computational efforts. The published analytical tools and available computer codes can be classified as follows:

- Correlations:
- . Stratification criterium by Theofanous et al /18, 20/
  - . Entrainment under stagnant loop flow by Sun, Oh /18/
  - . Transit time by Fanning, Rothe /6/
  - . Entrainment with loop flow, Kim /16/

Correlation - Integral Method - Zonal Method

- . Buoyant jet injected into pipe flow by Kim /16/; basis for the Battelle-Frankfurt code JETMIX; steady-state; limited to cold leg
- . Mixing model for transient cooldown in cold leg downcomer: with heat transfer to structures by Oh et al /17/; basis for the Battelle-Frankfurt code VOLMIX for stagnant loop condition only.
- . Regional mixing model, RMM and REMIX-code by Theofanous et al /19,20/, transient with heat transfer to structures and one-dimensional heat conduction in vessel wall.



Reynolds-averaged equations and field methods

- . transient, multidimensional code COMMIX-1A /8/ with zero-equation turbulence model and cartesian finite-difference mesh
- . extensions of COMMIX-1A with one-equation turbulence model, fine mesh, slanted surface modeling etc. /11/
- . COMMIX-1B with two-equation turbulence model, with parameters different from the original ones, volume or mass-flow-weighted skew-upwind differencing scheme, implicit difference scheme /10,12,13/ to reduce artificial mixing due to numerical diffusion and allows use for larger mesh sizes to model the plant geometry
- . transient, multidimensional code TEMPEST /9/; treats incompressible flow, numerically very effective; needs matching conditions at interface between cold leg and downcomer; accommodates effectively very fine meshes
- . transient, multidimensional code SOLA-PTS /14,15/ with 2- and 3-equations turbulence models applied selectively, uses the original parameters, differencing scheme of 2nd order accuracy, use of tensor-viscosity method and Filtering Remedy and Methodology, FRAM, to suppress numerical dispersion, solves the conjugated convection/conduction problem without resorting to heat transfer coefficients, multi-loop capability, partly vectorized for CRAY

This variety of analytical tools provides a broad basis to choose from to decide upon the best suited method and approach for the solution of a given problem.

All published numerical calculations are the results of post-test calculations, thus far. Fig. 5 shows a comparison between experimental data, the results of the two best-estimate transient codes COMMIX-1A and SOLA-PTS (TEMPEST results are of the same quality /9/) as well as the result from the steady-state engineering model JETMIX. Both multidimensional codes show excellent agreement with the data for the bottom cold leg temperature near the nozzle exit into the downcomer. But also JETMIX shows a surprisingly close agreement after the initial cooldown transient phase despite of its simplicity. Whereas PTS-thermal mixing behaviors with finite loop flows are feasible to be calculated with multidimensional codes, the lower the loop flow is the higher the computational expenses get because of the increase in time constants of these flows. Thus, best-estimate, multidimensional calculations for stagnant loop condition are only feasible for a limited time span of total problem time and can only be applied for a very limited number of test conditions. Thus, for this most important problem, engineering methods such as EPRI's /17/, Battelle's VOLMIX or Purdue's REMIX /19,20/ are of outmost importance and the only economic tool in the long run.

Fig. 6 demonstrates that integral-zonal methods, such as for instance VOLMIX /17/ are able to perfectly match the long-term transient cooldown data once the empirical correlations and the

fractions of participating volumes have been established by appropriate tuning of the input parameters. Once tuned, it is not known yet how powerful these methods really are to forecast results with the same quality in a different facility and under changed circumstances. It is thought that higher level field methods should have a clear edge versus the lower level-zonal methods in these new situations. To clarify these open points, all of these methods will be challenged by true pre-test predictions for the HDR-TEMB experiments.

#### PLANNING THE HDR THERMAL MIXING TESTS TEMB

Whereas the American test facilities described above have been developed on the basis of strict geometric and Froude number scaling right at the start of the planning stage, the HDR-facility as shown in Fig. 7 as an already existing integral large-scaled plant does not comply with the principle of geometrical similarity as compared to real plants. The downcomer gap width is about half that of the original plant, whereas the cold leg diameter is only about one-fourth. With these distortions in mind, the TEMB-experiments are solely planned for strict Froude number scaling. In fact, as shown by the American data, non-similarities in the Re-numbers should not greatly affect the major objective of the HDR-experiments because, as Fig. 8 demonstrates, they concentrate mainly on low volumetric flow ratios and stagnant conditions anyhow.

As compared to American test sections reviewed above, the HDR offers the following advantages:

- 1) Complete three-dimensional downcomer instead of the planar 90° sections used elsewhere
- 2) High system pressure of 11 MPa and thus high, realistic cold leg temperature of 300°C with HPI-temperatures of 200°C result in the most extreme density difference ratios of 0,29 employed thus far, without resorting to salt solution technique
- 3) Participating heat conducting structures such as RPW-wall with a thickness of 105 mm and a cladding of about 8 mm closely resemble those of real plants
- 4) The installed core barrel though not correctly scaled in its thickness provides a correct thermal boundary opposite to the RPV-inside surface.
- 5) The 3-D HDR downcomer is naturally connected to the lower plenum, which in turn is coupled with the 3-D core region.
- 6) Prior to the initiation of the HPI-injection uniform or axially varying temperature gradients in the core and downcomer regions can be installed simulating as close as possible realistic PWR conditions.
- 7) Provisions are made to test multi-loop conditions with the D2-nozzle operating.
- 8) Constant supply experiments (mass flows and temperatures) as well as transient mass flows and temperatures for cold leg and/or HPI flows can be performed at the HDR
- 9) Besides of the thermal-hydraulic aspects discussed above, the HDR-facility allows to study structural and fracture behaviors at the same time in one and the same experimental facility

with true 3-D thermal-fluiddynamic and structural shell characteristics under nearly realistic system pressure conditions. In this combination, the HDR is unique.

This first test series of about 30 experiments is planned with constant supply fluid boundary conditions. As shown in Fig. 7 three different injector nozzles with the same sizes but different orientations and axial locations will be employed. As Fig. 8 demonstrates emphasis will be placed on low volumetric flow ratios and stagnant loop conditions.  $F_{r_{CL}}$  will range between 0.00625 and 0.22 with emphasis on 0.05 with  $\Delta S/S_{HPI}$  in the range between 0.08 and 0.29 with major emphasis on the latter. This HDR-test matrix covers and extends the American test bed as Fig. 8 amplifies.

Measurement techniques /21/ rest on the reliable and tested sensors which proved excellent in a variety of previous HDR-experiments. Fluid and wall temperatures across and along the flow paths as well as strains will be measured. Velocities in the cold leg and downcomer (?) will be determined by means of temperature fluctuation correlation. Altogether 90 sensors will be installed.

A preliminary set of two experiments ( $Q_L/Q_{HPI} = 2$  and 0) will be performed at the end of November 1984 prior to the RPV-I experiments in order to test facility operation, measurement techniques, data acquisition and reduction procedure as well as to check the validity of the analytical methods in true pre-test predictions early on in order to plan the main test series to be performed in spring 1985 with greater confidence.

Fig. 9 compares SOLA-PTS and VOLMIX pre-test results downstream of the HPI-injection for the stagnant loop experiments early into the transient cooldown. Despite of the 200°C HPI-temperature the opposite cold leg wall experiences a temperature drop of only 100°C down to 200°C from 300°C hot primary fluid within the first second. Afterwards a much slower decay sets on. VOLMIX on the other hand cannot deliver the details of transverse temperature distributions but fits favorably overall given its simplifications and may very well follow the averaged data trend in the long run.

It is felt, that with the aforementioned features and the broad analytical scope, the forthcoming HDR thermal mixing tests will add and supplement the informations obtained from the American model tests, thus far and will foster the international cooperation in reactor safety research.

Facility Characteristics				Test Parameters						
Name	Flow	Facility	Pressure	$Q_{prim}/Q_{HPI}$		Dens.Ratio	Temperature		Froude-Number	
				Range	Center		HPI ( C)	Prim. ( C)	Range	Center
Mix1 1/5	Vent Valve Flow	Bend. Cold Leg	Atmosph.	0.0 - 20.	5.	.02 (.20)	21	65	.010 - .200	.050
Mix2 1/5	High Loop Flow	Horiz.Cold Leg	Atmosph.	2.0 - 50.	10.	.02 (.20)	18	65	.020 - .300	.050
Mix3 1/5	Low Loop Flow	Thermal Shield	Atmosph.	0.0 - 10.	1.-5.	.02 (.16)	21	65	.025 - .075	.050
Mix4 1/5	Stagn.Loop Flow	Lower Plenum	Atmosph.	0.0	0.0	.02, .16	16	65	.015 - .050	.050
SAI 1/1	Loop Flow	Box Sharpe C.L.	Atmosph.	0.6 - 10.7	-	.008 - .02	13.- 26.	40.- 70.	.040 - .070	-
B&W 1/10	Vent Valve Flow	Box Sharpe C.L.	Atmosph.	1.0 - 4.4	-	.03	6	79	.070 - .170	-
Purd.1/2	Vent Val./ Loop	Lower Plenum	Atmosph.	0.0	0.0	.09	15	15	.013, .026	-
CREA.1/2	Vent Val./ Loop	Steel-Facility	15 bar	0.0 - 15.	0.- 5.	.034, .124	27	95 - 195	.025 - .075	.050
HDR	Low Loop Flow	Steel-Facility	110 bar	0.0 - 15.	0.- 2.	.08 - .284	20	300.	.006 - .220	.050
PWR	Vent Val./ Loop	Steel-Facility	110 bar	0.0 - 200.	-	.284	20	300.	.050	-

Table 1: Comparison of Facilities and Operation Conditions

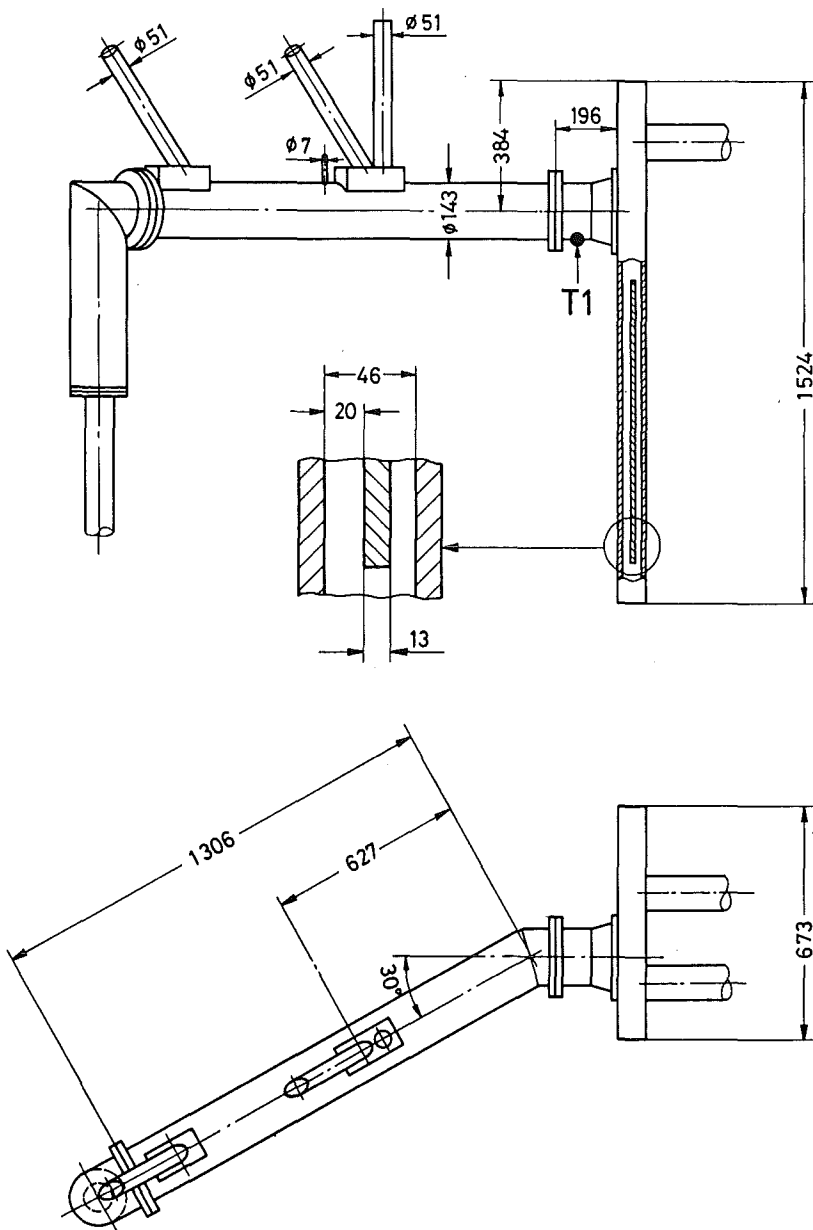


Figure 1: Geometry of 1/5-Scale CREARE Mix 3 Facility

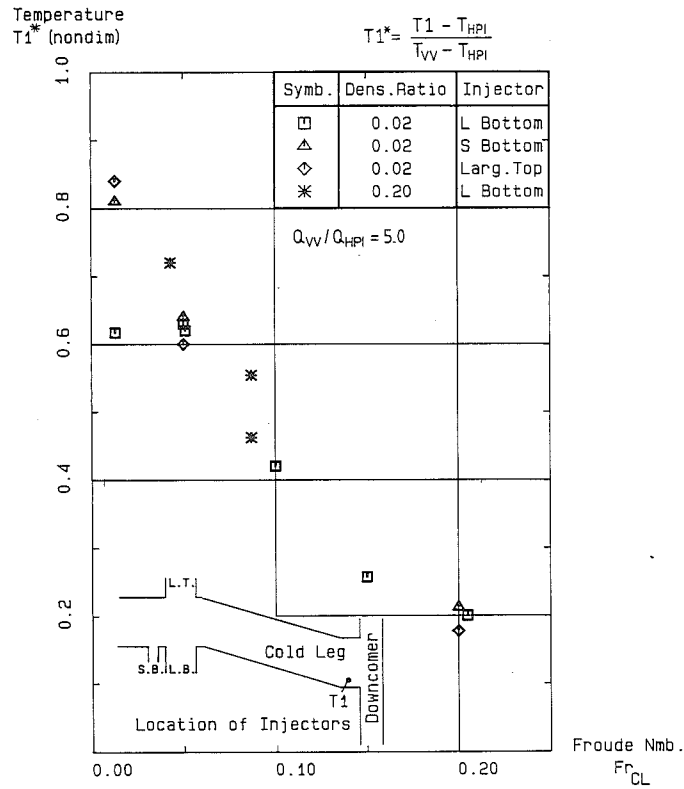


Figure 2: Effect of Froude Number on Steady State Fluid Temperature  
 Experiment: EPRI/CREARE-Mix1

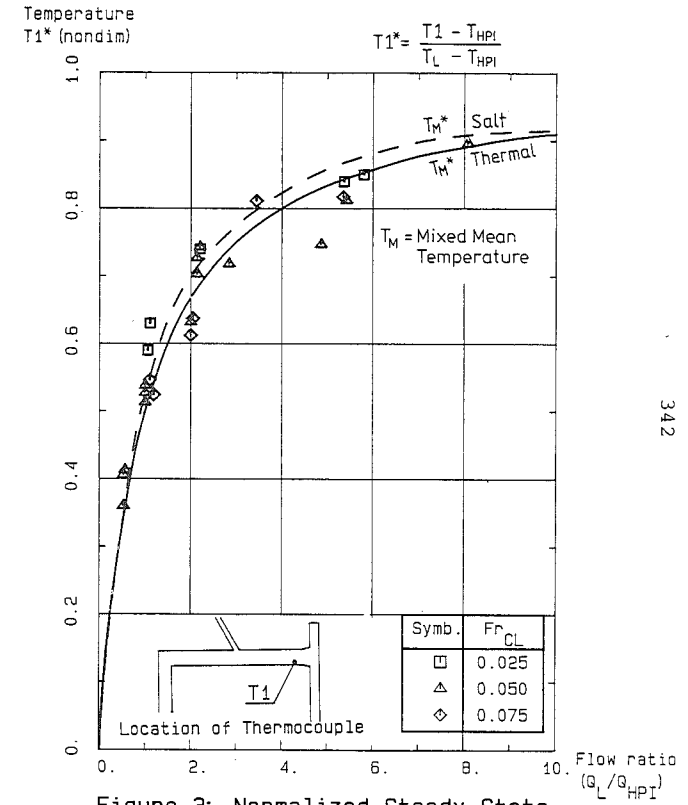


Figure 3: Normalized Steady-State Temperature at Thermocouple T1  
 Experiment: EPRI/CREARE-Mix3

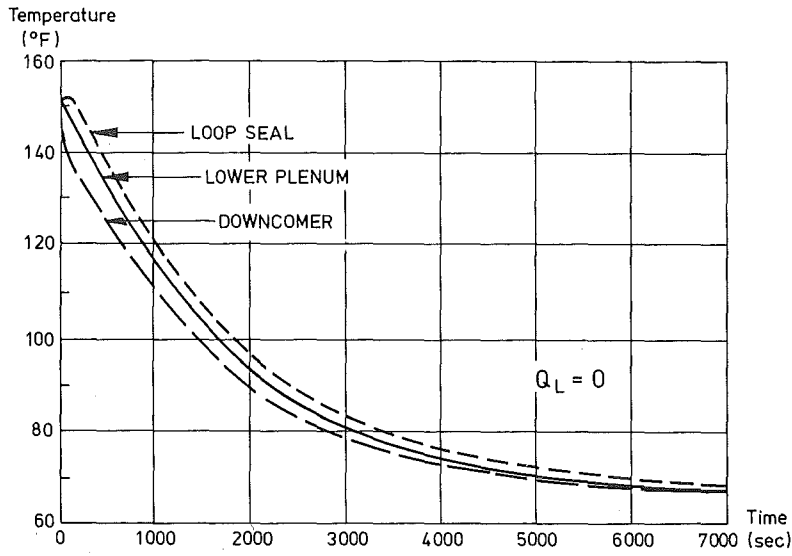


Figure 4: Comparison of Temperature Histories at Different Locations  
Experiment: EPRI / CREARE - Mix 4

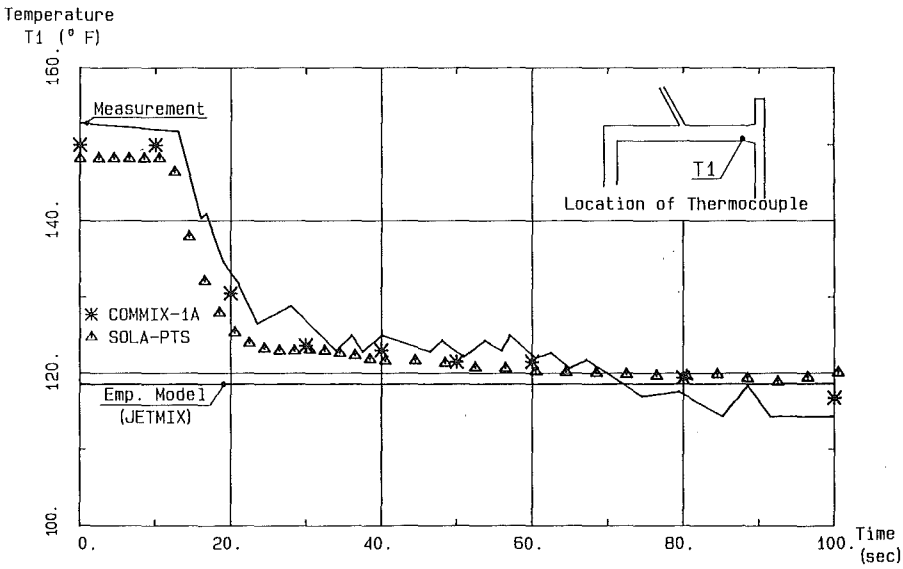


Figure 5: Comparison Between Experimental Data and Calculation  
Experiment: EPRI/CREARE-Mix2 Test #51

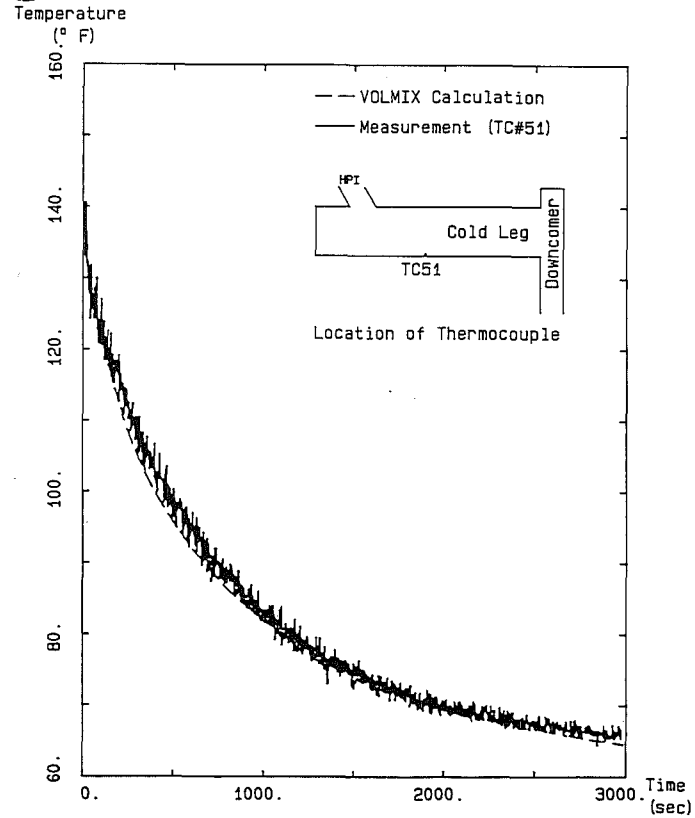


Figure 6: Comparison Between Experimental Data and Predictions of Empirical Model - VOLMIX  
 Experiment: EPRI/CREARE Mix4 Test #73

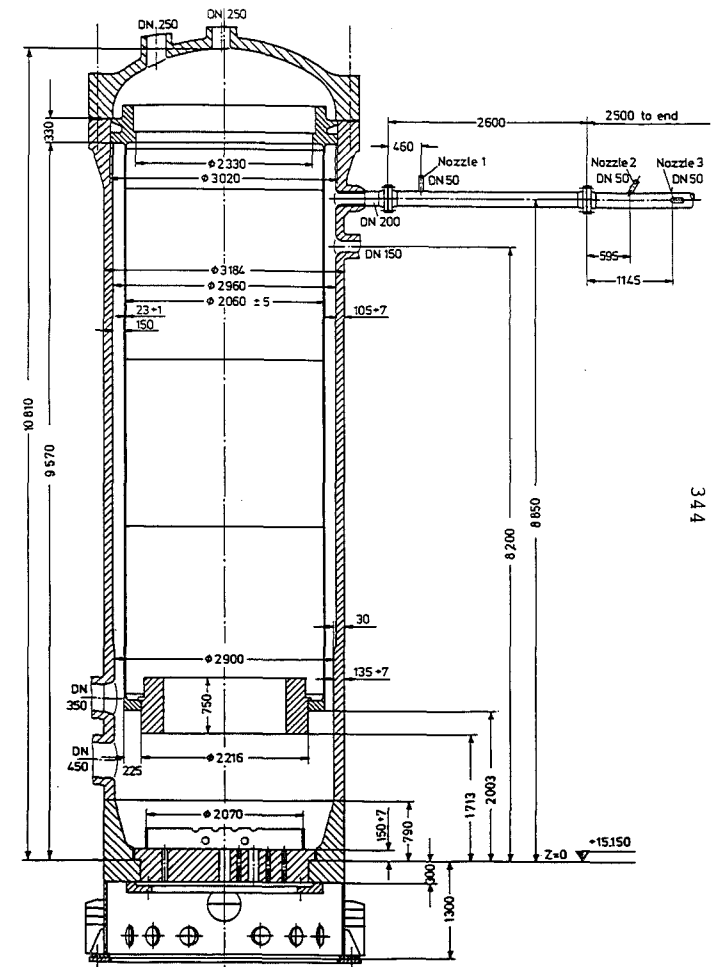


Figure 7: HDR-Test Facility



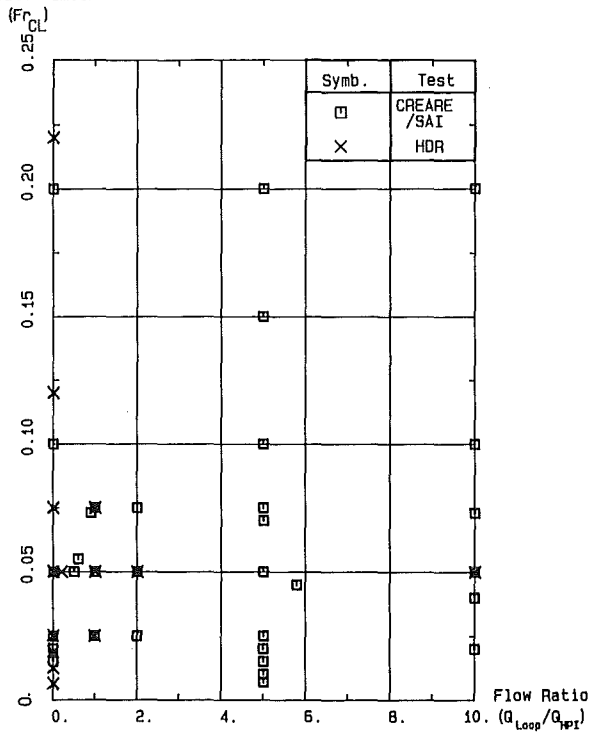


Figure 8: Comparison of EPRI Test Program and HDR Test Matrix

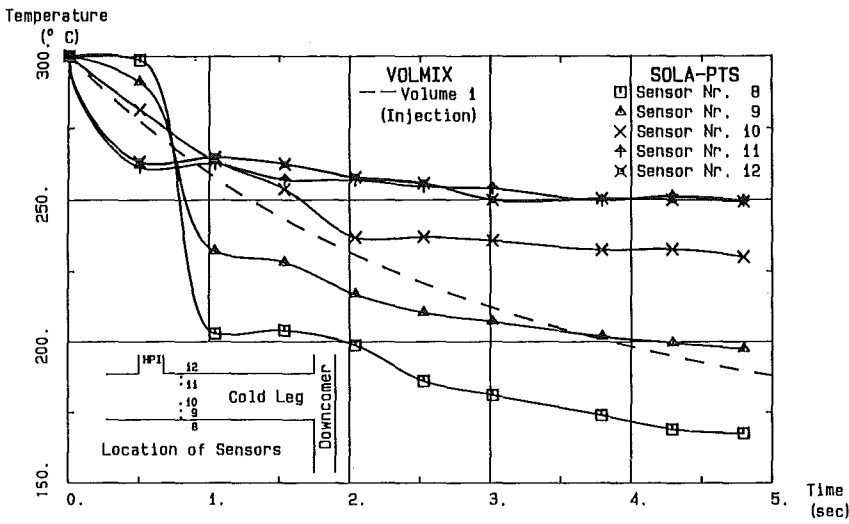


Figure 9: Calculated Transient Temperatures near Injection Nozzle  
 Experiment: HDR-TEMB - with Stagnant Loop Flow

## REFERENCES

- /1/ Chexal, B.; Marston, T.; Sun, B.: EPRI Reserach & Application Efforts on Reactor Vessel Pressurized Thermal Shock, Proc. 11th WRSIM, Gaithersburg, Oct. 26, 1983
- /2/ Rothe, P.H.; Fanning, M.W.: Evaluation of Thermal Mixing Data From a Model Cold Leg and Downcomer, EPRI NP-2773, Dec. 1982
- /3/ Rothe, P.H.; Marcher, W.D.: Fluid and Thermal Mixing in a Model Cold Leg and Downcomer With Vent Valve Flow, EPRI NP-2227, March 1982
- /4/ Rothe, P.H.; Ackerson, M.F.: Fluid and Thermal Mixing in a Model Cold Leg and Downcomer With Loop Flow, EPRI NP-2312, April 1982
- /5/ Fanning, M.W.; Rothe, P.H.: Thermal Mixing in a Model Cold Leg and Downcomer at Low Flow Rates, EPRI NP-2935, April 1983
- /6/ Fanning, H.W.; Rothe, P.H.: Transient Cooldown in a Model Cold Leg and Downcomer EPRI NP-3118, May 1983
- /7/ Hashemi, A; Goodman, J.: Thermal Mixing in a Rectangular Geometry Model of a Cold Leg With High Pressure Injection and a Downcomer, EPRI NP-2924, March 1983
- /8/ Domanus, H.M. et al.: COMMIX-1A: A 3-D, Transient Single-Phase Computer Program for Thermal Hydraulic Analysis of Single and Multicomponent Systems, NUREG/CR-2896, 1983
- /9/ Eyster, L.L.; Trent, D.S.: PTS-TEMPEST Computer Code Simulation of Thermal Mixing in the Cold Leg and Downcomer of a PWR, NUREG/CR-3564, April 1984
- /10/ Chen, F.F. et al.: Turbulence Modeling of Thermal and Fluid Mixing in PWR's During High Pressure Coolant Injection Using COMMIX-1B, Intl. Conf. Numerical Methods in Nuclear Engng., Montreal, Canada, Sept. 6-9, 1983
- /11/ Chen, B.C.-J. et al.: COMMIX-1A Analysis of Fluid and Thermal Mixing in a Model Cold Leg and Downcomer of a PWR, Intl. Conf. Numerical Methods in Nuclear Engng., Montreal, Canada, Sept. 6-9, 1983
- /12/ Hassan, Y.A. et al: Comparison of Measured and Predicted Thermal Mixing Tests Using Improved Finite Difference Technique, Nucl. Engng. Dec. 76 (1983), 153-160
- /13/ Hassan, Y.A. et al.: Implementation of a Mass-Flow-Weighted Skew-Upwind Differencing Scheme in COMMIX.1A, EPRI NP-3518, 1984
- /14/ Daly, B.J.; Torrey, M.D.: 3-D Thermohydraulic Calculations Using SOLA-PTS, Proc. 11th WRSIM, Gaithersburg, Oct. 24-28, 1983, NUREG-CP-0048, 2 (1984) 48
- /15/ Daly, B.J.: Three-Dimensional Calculations of Transient Fluid-Thermal Mixing in the Downcomer of the Calvert Cliffs-1 Plant Using SOLA-PTS, NUREG/CR-3704, April 1984
- /16/ Kim, J.H.: An Analytical Mixing Model for Buoyant Jet Injected into Pipe Flow, ASME-Paper 83-WA/HT-42, 1983
- /17/ Oh, S.; Sursock, J.-P. and Sun, K.-H.: A Mixing Model for Transient Cooldown in a Reactor Cold Leg and Downcomer Under Stagnant Loop Flow, ASME-Paper 83-HT-13, 1983

- /18/ Sun, B. K.-H.; Oh, S.: A Correlation for Entrainment of Water in a Reactor Cold Leg by Coolant Injection into Stagnant Loop Flow, ASME-Paper 83-WA/HT-39, 1983
- /19/ Theofanous, T.G. et al.: Decay of Buoyancy Driven Stratified Layers With Applications to PTS, Proc. 11 WRSIM, NUREG/CP-0048, Vol. 2, pp 91-94
- /20/ Theofanous, T.G., et al.: Decay of Buoyancy Driven Stratified Layers With Applications to PTS, NUREG/CR-3700, May 1984 Pt I: The Regional Mixing Model; Pt II: Purdue's 1/2-Scale Experiment
- /21/ Wolf, L.: Design Report for the HDR-PTS Thermal Mixing Experiments, TEMB, Test Series T 34, in preparation, draft version available upon request
- /22/ Grötzbach, G.: Numerical Evaluation of Radial Mixing Possibilities in the HDR-Downcomer for Achieving Nonuniform. Stable Temperature Distributions - TURBIT-3 Calculations with Buoyancy Affects (in German), IRE /1/ 4125/83/78: PNW/229/78, April 1978

CANDU LOCA ANALYSIS WITH LOSS OF OFFSITE POWER  
TO MEET LWR ACCEPTANCE CRITERIA AS APPLIED IN JAPAN

J.Q. Howieson, L.J. Watt, S.D. Grant,  
P.G. Hawley, S. Girgis

Atomic Energy of Canada Limited  
CANDU Operations  
Sheridan Park Research Community  
Mississauga, Ontario, Canada L5K 1B2

ABSTRACT

The reference CANDU 600, designed under Canadian licensing criteria, has been evaluated for LOCA, under LWR acceptance criteria as applied in Japan. Offsite power is assumed unavailable following a LOCA and reactor trip.

We show that the 1200°C peak cladding temperature criterion can be met with modest changes to the mechanical shutoff rods. The second shutdown system (poison injection), meets the temperature criterion without change. To speed core refill in the absence of forced circulation, the ECC system uses a directed injection to the unbroken end of the core.

Other inherent CANDU safety features such as the availability of the moderator as a heat sink for LOCA without ECC injection, are retained.

INTRODUCTION

A safety assessment is being done to investigate the feasibility of introducing the CANDU reactor to Japan. This paper reports part of that assessment which concerns large loss of coolant accident (LOCA) analysis of a CANDU 600 reactor. This is the single-unit 600 MW(e) model which is operating in Canada and other countries. Reference 1 describes the reference CANDU 600 and the overall safety assessment to meet Japanese licensing regulations. They have evolved primarily from experience with light water reactor (LWR) design and operation. The following assumptions derived from these regulations are made:

- i) the reactor is tripped by mechanical shutoff rods
- ii) offsite power is lost at the time of reactor trip
- iii) the most effective shutoff rod does not drop
- iv) the first reactor trip signal is credited
- v) a second shutdown system, poison injection, is not credited.

A key requirement is that, under these assumptions, the peak cladding temperature (PCT) must not exceed 1200°C.

In Canada, the regulatory agency (the Atomic Energy Control Board) specifies dose limits for accident analysis. Canadian licensing regulations do not have a PCT limit - sheath oxidation is evaluated using a physically-based model. Offsite power is assumed available normally. However, a range of system impairments is also examined from loss of offsite power to a complete loss of emergency core cooling (ECC) supply. The reactor is tripped on the second trip signal of the least effective shutdown system. When that is the mechanical shutoff rods, the two most effective rods are assumed not to drop. This report shows how the key Japanese requirements for LOCA analysis are met, by discussing:

- general system response to a large LOCA in CANDU 600
- predictions of PCT in a large LOCA
- predictions of core refill by the ECC system.

This report considers two representative break locations - the reactor inlet header (RIH) and the reactor outlet header (ROH). Breaks at other locations would behave similarly to one or the other case. The approximate break size in each break location which leads to the highest PCT is identified. Then the thermalhydraulics and fuel analysis is described for the highest PCT case. Longer term analysis is described to show the capability of the ECC system to provide timely refill (within 3 minutes) of the core.

#### GENERAL SYSTEM RESPONSE TO A LARGE LOCA IN CANDU 600

In this section, the general system behaviour is described for large LOCA transients. Events are described in chronological order.

CANDU 600 has two loops with only a small connection between loops. A large break in the primary heat transport (PHT) system causes rapid depressurization of the broken loop. The unbroken loop depressurizes slowly as it loses coolant to the broken loop.

Each PHT loop has two core passes. In the broken loop, the core pass nominally downstream of the break location sees reduced flows, and therefore voids quickly. The increase in coolant void tends to raise the reactor power. The reactor is then tripped, usually within one second of the break. In the accident analysis for the Japan-CANDU, a loss of offsite power is assumed to occur when the reactor trips.

The broken loop pressure continues to drop as coolant discharges out the break. Also, the pressure in the containment building rises due to the coolant discharge. When the combination of low PHT pressure and high containment pressure both reach their respective setpoints, the LOCA signal is generated.

The LOCA signal initiates three main safety actions:

- i) isolates the pressurizer, inventory make-up, and the unbroken loop from the broken loop,
- ii) opens the main steam safety valves (MSSV), and
- iii) opens the high pressure ECC isolating valves.

The LOCA signal isolates the two loops early enough that the unbroken loop inventory remains high (~ 100% of initial, due to pressurizer make-up). Therefore, fuel cooling is maintained in that loop.

The MSSV's are opened to cause a rapid depressurization of the boiler secondary side. For a large LOCA, this helps to limit the extent to which the boilers are a heat source to the PHT fluid. For a small LOCA, this is the major factor in the broken loop depressurization.

The ECC isolating valves are opened to permit core refill. The first ECC stage consists of high pressure accumulator injection. ECC injection is into to the headers (RIH/ROH), and flows through the circuit to the break.

#### BROKEN LOOP THERMALHYDRAULICS FOR PCT

The broken loop thermalhydraulics are simulated with a homogeneous two-phase model which has been modified to include correlations for slip and drift [2]. The CANDU 600 has 95 parallel fuel channels per core pass - these are represented by a single hydraulically averaged channel.

A detailed three-dimensional finite difference reactor physics code is used to generate the reactor power transient [3]. Power transients are generated for the voided-half core (broken loop side), the highest powered channel, and the highest powered bundle (Figure 1). These are used as boundary conditions for the thermalhydraulics calculations. The second shutdown system (which is even more effective than the first) is not credited.

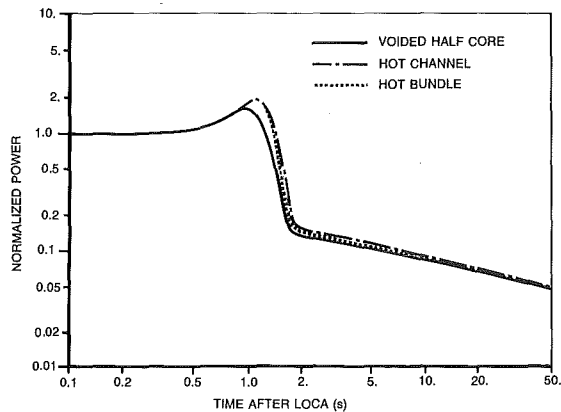


FIGURE 1 POWER TRANSIENTS FOR 90% ROH BREAK

Following the break (taken as a 90% ROH break), the sequence of events is:

- the broken loop pressure decreases rapidly
- coolant void in the core immediately downstream of the break increases causing an increase in reactor power
- the reactor is tripped at 0.5 seconds on high log rate power

- at reactor trip, offsite power is assumed lost which causes loss of power to the PHT pumps and secondary side feed water pumps
- the LOCA signal occurs at 1 second - the ECC valves start to open
- the pressurizer begins to isolate at 3 seconds
- the boiler secondary side cooldown starts at 11 seconds (there is a designed 10 second delay before the valves are opened)
- by 15 seconds ECC water starts flowing into the broken loop

#### CHANNEL THERMALHYDRAULICS FOR PCT

The transient header pressures of the core pass downstream of the break are used as boundary conditions for a single channel simulation. A channel with the highest integrated reactor power during the large LOCA is chosen. The PCT is determined for the hottest fuel element in the hot channel. The channel and element power transients are shown in Figure 1.

Figure 2 shows the hot channel flow for selected ROH break sizes. Breaks of an area equal to about a 90% ROH cause the lowest flows. For RIH breaks, the 15% break size causes the lower flow than either a 10% RIH break or a 20% RIH break. The ROH break which leads to low channel flows is larger in area than the comparable RIH break. This is because of the added resistance to back flow (from the downstream core pass to the break for an ROH break) due to the PHT pump and boiler.

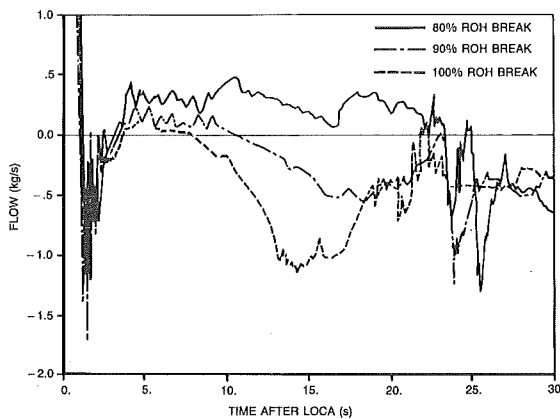


FIGURE 2 HOT CHANNEL FLOW FOR ROH BREAKS

The resulting convective heat transfer coefficient from the hot element clad to the coolant (Figure 3) is small. Even so, about 100 kJ/kg or 2 full power seconds (FPS\*) is removed by the coolant in the first 20 seconds.

\* For peak-rated CANDU fuel, 1 FPS is equivalent to about 50 kJ/kg or about 100°C on PCT.

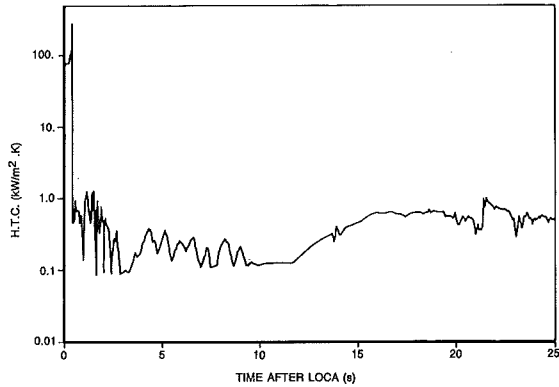


FIGURE 3 HOT ELEMENT CLAD-TO-COOLANT HEAT TRANSFER COEFFICIENT FOR 90% ROH BREAK

#### FUEL RESPONSE FOR PCT

The PCT is determined by the energy in the fuel initially, and energy added and lost in transient. The energy in the hot element (linear rating of 58.5 KW/m) during a large LOCA is at most:

- initial stored energy of 315 kJ/kg (average element temperature 1070°C)
- power transient adds 175 kJ/kg (3.5 FPS)
- convection heat transfer to the coolant subtracts 100 kJ/kg (2 FPS)
- radiation heat transfer to the pressure tube subtracts 50 kJ/kg (1 FPS)
- sheath-coolant (metal-water) reaction adds 15 kJ/kg (0.3 FPS)

Fuel calculations for PCT incorporate the above major components.

Radiation heat transfer is calculated using a two-dimensional (R- $\phi$ ) fuel bundle segment model coupled to a thermal radiation model describing heat exchange among the fuel elements and pressure tube. Pressure tube strain and heat transfer to the moderator in the event of pressure tube/calandria tube contact are also modelled.

The thermal radiation model calculates the interchange of thermal radiation among surfaces using the method of Sparrow and Cess [4]. Thermal radiation from the pressure tube to the calandria tube is calculated throughout the simulation. The Baker and Just correlation [5] is used to calculate the heat generated by the metal-water reaction. The gap heat transfer coefficient between the fuel and the sheath is constant throughout the simulation. The Hobson and Taylor [6] correlation for UO<sub>2</sub> thermal conductivity is used.

Boundary conditions for radiation heat transfer and convective heat transfer (from the channel thermalhydraulics calculation) are next used as input to the final PCT calculation.

The ELOCA-MK2 version of the ELOCA [7] computer code is used to simulate fuel element thermal-mechanical behaviour during high temperature transients.



A single fuel element is considered and axi-symmetric properties are assumed. The fuel modelling includes diametral sheath strain, a dynamic fuel-to-sheath heat transfer coefficient, and the effects of the metal-water reaction on heat generation (Baker-Just). MATPRO9 [8]  $UO_2$  material properties are used. Initial conditions (for the 58.5 kW/m element) are supplied by the steady state fuel performance code ELESIM [9].

The sheath temperature transient for the selected ROH break sizes is shown in Figure 4. The highest PCT of all is 1150°C for the 90% ROH break. The PCT for the 80% ROH break and 100% ROH break is 1090°C and 1110°C respectively.

For RIH breaks, the highest PCT of all is 1140°C for the 15% RIH break.

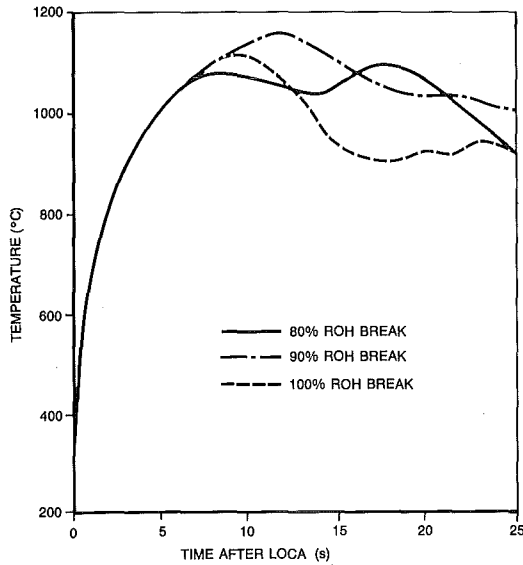


FIGURE 4 HOT ELEMENT SHEATH TEMPERATURE FOR ROH BREAKS

#### DIRECTED ECC INJECTION FOR CORE REFILL

For the reference CANDU 600 design, in the event of a LOCA with offsite power available, ECC injection into all headers is effective refilling the core for all large breaks in less than 3 minutes. To ensure optimum use of emergency core coolant, for LOCA with an assumed loss of offsite power, the CANDU design for Japan has a directed injection system for large breaks. The emergency coolant is injected only into the headers at the "unbroken" end of the core.

The directed ECC injection system has a signal parameter separate from the LOCA signal. The signal is used to detect the break location before the LOCA signal is received.

Figure 5 shows the break detection logic. The break detection logic continuously looks for a difference in the header-to-header pressure drops of the core passes. Normally this difference is essentially zero. Immediately after a LOCA, the upstream core pass header-to-header pressure drop increases and the downstream core pass pressure drop decreases. The difference becomes positive or negative depending on break location.

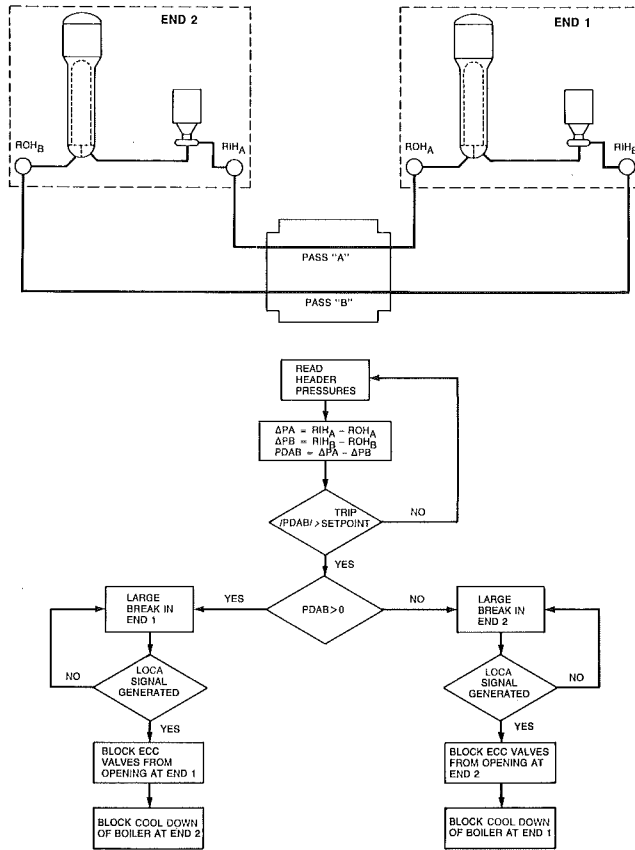


FIGURE 5 BREAK DETECTION LOGIC

The break detection trip setpoint is chosen so that breaks down to the equivalent area of a couple of feeder pipes would initiate directed ECC injection. For smaller breaks, a default to all-header injection and all-boiler cooldown (which is adequate for small break sizes) is used.

Once tripped, and the break location identified, the logic waits for the LOCA signal. When that happens, the directed ECC injection works by:

- i) injection of water into the "unbroken" end of the core
- ii) blocking the secondary side cooldown of the boiler between the points of injection.

A large ROH break with loss of offsite power is used to illustrate core refill with directed ECC injection. The core pass downstream of the break initially has little or no header-to-header pressure drop after blowdown. The directed ECC injection raises the header pressures on the unbroken end of the core relative to the broken end, and forces both core passes to refill towards the break. This is in the positive direction for the upstream core pass, and negative direction for the downstream core pass.

For a RIH break, the scheme reinforces the refill direction since the downstream pass refills in the negative direction even without directed ECC, due to the location of the break.

Figure 6 shows results from an 80% ROH break transient. The downstream core pass refills relatively quickly within 70 seconds of the break. The upstream core pass refills within 130 seconds of the break.

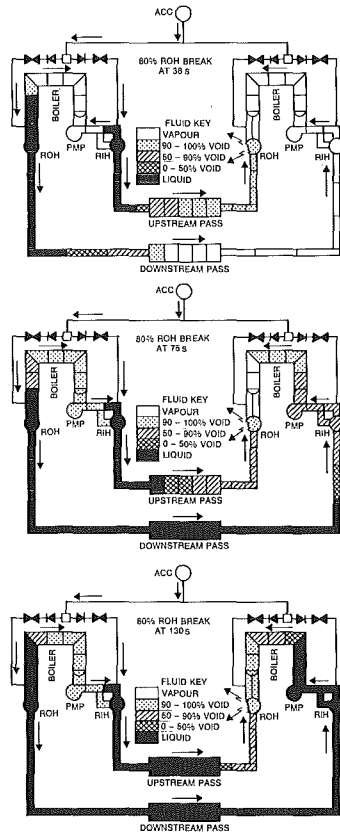


FIGURE 6 80% ROH BREAK REFILL MAPS

The boiler between the points of injection stays hot since the boiler depressurization is blocked. This allows little primary flow through that boiler - most ECC water prefers to go through the downstream core pass. The small amount of fluid that does go over the hot boiler mixes with cool

incoming ECC at the upstream core pass RIH. The warmer incoming water causes the upstream pass to refill slower. However, the fuel is always well cooled by large two-phase flows during the transient, because the pressure drop is so high across the upstream core pass.

The transient header pressures of the downstream pass are used in a channel model to assess two individual channel refill times: a high power channel, and an orificed, high elevation channel. The high power channel has the highest internal stored heat. The orificed, high elevation channel has the highest geometrical resistance to flow.

The refill times for these channels are 88 and 67 seconds, the high powered channel being quicker. Although at steady state the channels are designed to give the same exit quality, in the LOCA transient, the higher resistance due to the orifice is more important for refill than the effect of channel power.

#### CONCLUSION

For large loss-of-coolant accident analysis, the 1200°C peak fuel cladding temperature criterion is met for CANDU 600. In addition, timely core refill is obtained in the absence of forced circulation by a directed ECC injection system.

#### REFERENCES

1. V.G. Snell and M. Bonechi, "CANDU Safety Assessment to Meet LWR Acceptance Criteria as Applied in Japan" paper to be presented to the International Nuclear Power Plant Thermal Hydraulics and Operation Topical Meeting, Taiwan, October 1984.
2. M-R Lin et al, "FIREBIRD-III Program Description", Atomic Energy of Canada Limited Publication AECL-7533, 1979 September.
3. A.R. Dastur, G. Kugler, B. Rouden, and H.Y.M. Li, "Confirmation of CANDU Shutdown System Design and Performance During Commissioning", Atomic Energy of Canada Limited Publication AECL-5914, September 1979.
4. E.M. Sparrow and R.D. Cess, "Radiation Heat Transfer", Brooks Cole Publishing Co., Belmont, California, 1966.
5. L. Baker and J.C. Just, "Studies of Metal-Water Reactions at High Temperatures. Part III: Experimental and Theoretical Studies of the Zirconium-Water Reaction", Argonne National Laboratory, ANL-6548, 1962 May.
6. I.C. Hobson and R. Taylor, "Effect of Porosity and Stoichiometry on the Thermal Conductivity of Uranium Dioxide", UKAEA Report TRG-2323, 1972.
7. H.E. Sills, "ELOCA - Fuel Element Behaviour During High-Temperature Transients", AECL-6357, 1979 March.
8. "MATPRO-Version 09, A Handbook of Materials Properties for Use in the Analysis of Light Water Reactor Fuel Rod Behaviour", TREE-NUREG-1005, 1976.
9. M.J. Nottley, "ELESIM: A Computer Code for Predicting the Performance of Nuclear Fuel Elements", Nuclear Technology, Volume 44, August 1979.

AN ASSESSMENT OF APPENDIX K CONSERVATISM FOR LARGE BREAK LOCA  
IN A WESTINGHOUSE PWR\*

U. S. Rohatgi, C. Yuelys-Miksis and P. Saha

Department of Nuclear Energy  
Brookhaven National Laboratory  
Upton, New York 11973, U.S.A.

ABSTRACT

A 200% cold leg break accident in a Westinghouse four-loop RESAR-3S plant has been analyzed using the best-estimate code TRAC-PD2/MOD1. Two TRAC calculations, one with the best-estimate or realistic initial and boundary conditions, and the other with the licensing conditions, have been performed. These calculations produced the peak cladding temperatures of 800°K and 1072°K, respectively. Comparison of these results with the Westinghouse licensing calculations performed in accordance with the Appendix K rule, shows an overall safety margin of 664°K, of which 272°K is due to the conservative initial and boundary conditions and 392°K is due to the conservative physical models.

INTRODUCTION

This study was undertaken to estimate the conservatism due to the licensing or evaluation models for various thermohydraulic processes and fuel behavior, boundary and initial conditions, and transient scenarios. These were prescribed by the U. S. Nuclear Regulatory Commission in Appendix K of 10CFR50 for the prediction of peak clad temperatures in large and small break LOCA and were based on the understanding of two-phase thermohydraulics and fuel behavior in the early seventies. Significant progress has been made in the knowledge of twophase flow and fuel behavior since then and the current best-estimate models are quite different from those described in Appendix K. The TRAC-PD2/MOD1 code was selected for this study as it was the most assessed best-estimate large break LOCA code available at this time. This code was applied to a Westinghouse RESAR-3S four-loop plant for the analysis of a 200% cold leg break.

The first task in this study was to determine the sensitivity of the peak clad temperature to the nodalization and fuel models. This was accomplished by performing various best-estimate calculations, one of which was finally selected as the benchmark BNL best-estimate calculation. Westinghouse supplied a licensing calculation for RESAR-3S plants taking into account all of the evaluation models, boundary and initial conditions, and scenarios prescribed in Appendix K. The Reactor Coolant Pumps (RCPs) were tripped in the Westinghouse calculations, while they were kept running in the best-estimate calculation. These two calculations provided the lower, i.e., best-estimate, and the upper, i.e., Appendix K, limits for the peak clad temperature and clad temperature histories during the accident.

\*This work was performed under the auspices of the U.S. Nuclear Regulatory Commission.

Besides these two bounding calculations, an intermediate calculation was performed at BNL with the TRAC-PD2/MOD1 code (best-estimate models), but using the evaluation or licensing type initial and boundary conditions and transient scenario used in the Westinghouse licensing calculation. In subsequent sections, two BNL calculations will be described in detail.

#### NODALIZATION

A RESAR-3S plant was modeled with TRAC-PD2/MOD1 with 556 one-dimensional nodes in four loops and a three-dimensional VESSEL with 224 cells as shown in Figure 1. The inner 8 cells from the top of Level 3 to the top of Level 8 represented the core. Each of these cells contained an average rod and an additional hot rod. The average rods had the same axial power peaking but different radial peaking. The models for each loop contained a cold leg, a reactor coolant pump (RCP), a steam generator (SG), a hot leg, and a TEE component connected to safety injection FILLS and accumulator component. The pressurizer was connected to Loop 2. At the time of LBLOCA, the cold leg of Loop 4 was replaced by two pipe sections with BREAK models. TRAC-PD2/MOD1, uses a numerical or self choking model which requires fine nodalizations near the breaks. The containment pressure was supplied as a boundary condition at the BREAK components. This nodalization was arrived at after several calculations and represents the minimum amount of details needed without sacrificing accuracy.

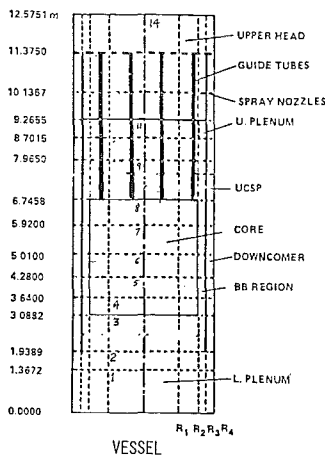


Figure 1 Nodalization in the VESSEL Component

#### BEST-ESTIMATE (BE) CALCULATION

The first calculation performed with TRAC-PD2/MOD1 was with the most probable boundary and operating conditions as shown in Table 1. The safety system performed as designed. The AC power was available throughout the transient.

Figure 2 shows the system pressure as predicted by the code. Initially the system pressure rapidly decreased to saturation pressure due to subcooled blowdown; thereafter, the rate of pressure change slowed down due to choking at

the breaks. At approximately 2.5 seconds, the rate of pressure change decreased again as the vapor generation in the core increased due to flow oscillation at the core inlet as shown in Figure 3. Initially the flow also reversed at the core inlet due to the breaks, but as the break flow decreased below the net cold leg flows, the flow into the core was re-established, enhancing the vapor generation in the core. At approximately 20 seconds the system pressure was close to the containment pressure, indicating the end of the blowdown phase.

Table 1 Comparison of BE and EM Conditions and Scenario

<u>Appendix K/10CFR50</u>	<u>BE/TRAC-PD2</u>	<u>EM/TRAC-PD2</u>
<u>Operating Conditions</u>		
1) Core Power, 1.02 of licensed power.	Licensed power.	1.02 Licensed Power
2) Fuel and clad properties as functions of temperature and other applicable time dependent variables.	Considered	Considered
3) Peaking factor should be realistic.	Most probable values during fuel cycle.	Beginning of fuel cycle.
4) Decay power, 120% of 1971 ANS.	100% Of 1979 ANS.	120% of 1971 ANS.
<u>Boundary Conditions</u>		
1) Containment pressure should be conservative and should account for all pressure reducing devices.	Realistic containment pressure history considered.	Most conservative pressure history considered.
2) Single failure criterion for ECC system requires that at least one equipment with worst effect should be considered.	Not considered.	Disabling one diesel generator results in loss of one HPI pump (Safety injection) and one LPI pump (residual heat removal). This reduces the amount of net injection to all the loops.
<u>Scenario</u>		
1) RCP pump will have locked rotor.	Pump on.	Pump coasting down.
2) Delay in restarting the safety injection pumps after the safety injection signal is activated.	1.5 sec for LPI pumps. 6.5 sec for HPI pumps.	25 sec for all pumps.

Figure 4 shows the clad surface temperatures at four axial locations for the hot rod. There are two temperature peaks in the blowdown phase. The first peak of 800°K at 2.5 seconds represents the peak clad temperature for the transient. This peak occurred when the initial clad heat up due to flow stagnation was quenched when the flow at the core inlet was restored as shown in Figure 3. The second clad heat up was quenched when the flow reversed at the core outlet generating the second peak. All of the axial locations were quenched by 45 seconds. Figure 5 shows the liquid fraction in the core, which increased rapidly during the reflood phase (time > 39 seconds). At the time of quenching the liquid fraction was around 35%.

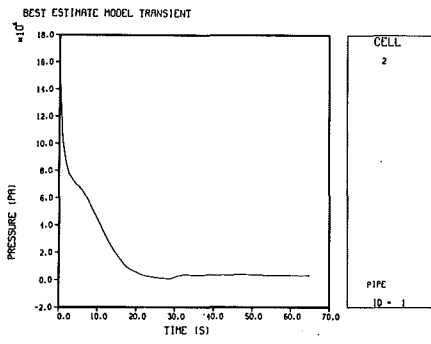


Figure 2 System Pressure in the Best-Estimate Calculation.

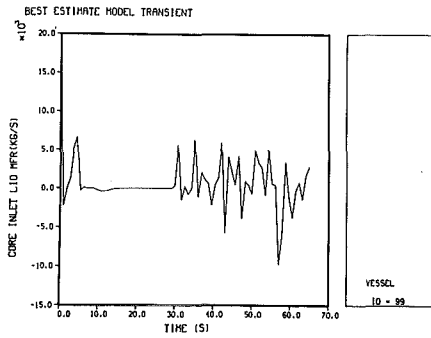


Figure 3 Core Inlet Liquid Mass Flow Rate For Best-Estimate Calculation.

The sequence of these and other events during the transient have been summarized in Table 2. The accumulators started the water injection at 10.5 seconds while the safety injections started at 2.5 to 7.6 seconds due to the built-in delay of 1.5 to 6.5 seconds in their initiation. The lower plenum was full (95%) at 39 seconds indicating the end of refill and the beginning of the reflood phase.



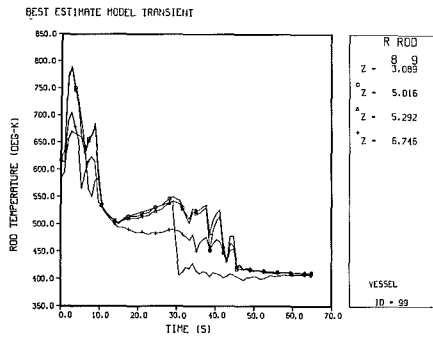


Figure 4 Clad Surface Temperatures for Hot Rods in BE Calculation.

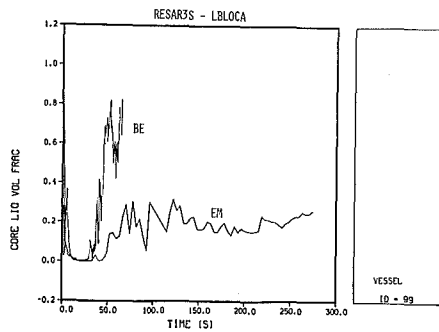


Figure 5 Comparison of Core Liquid Volume Fractions in Two BNL Calculations.

#### EVALUATION MODEL (EM) TYPE CALCULATION

The second BNL calculation with TRAC-PD2/MOD1 was performed using the licensing type boundary and operating conditions as shown in Table 1. The single failure criterion as prescribed in Appendix K was satisfied by eliminating one of the two safety injection trains. Furthermore, the loss of AC power was also assumed which resulted in tripping the RCPs. Initially the core power was 102% of the licensed power, while the decay power was 120% of the ANS 1971 Standard. This calculation consisted of best-estimate models, but evaluation model type (licensing) boundary and operating conditions. Therefore, it is called the Evaluation Model (EM) type calculation.

The nodalization in this calculation was the same as in the previous best-estimate calculation. However, there were some changes in the placement of the rods and their radial peakings. Appendix K requires at least two channel analysis, one of which should be the hot channel and the hot rod should be placed there. This requirement was satisfied by designating one of the inner quadrants as the hot channel as shown in Figure 6. The average rod in this quadrant had the highest radial peaking (1.38). The hot rods in the other inner quadrants have the same power density. This arrangement brought the conditions in this calculation closer to the Westinghouse licensing calculation<sup>2, 3</sup>.

Table 2 Comparison of Sequence of Events for BE and EM Calculations

EVENTS	TIME (s)	
	BE/BNL	EM/BNL
1. Break	0.0	0.0
2. Safety Injection Signal Generated.	1.1	5.1
3. Broken Loop Accumulator Injection	2.2	N/A
4. Intact Loop Accumulator Injection	10.5	11.3
5. Pressurizer Empties (Water Level < 0.005 m)	16	17.5
6. Safety Injection (Charging, Residual Heat Removal, High Head Safety Injection).	2.6 to 7.6	30.1
7. Lower Plenum Refilled (Liquid Fraction 0.95) and Beginning of Reflood.	39	48.5
8. Peak Clad Temperature.	2.5	65
9. Accumulator Empty.	Did Not	86.5
10. Quenching of Hot Spots Begins	44	244

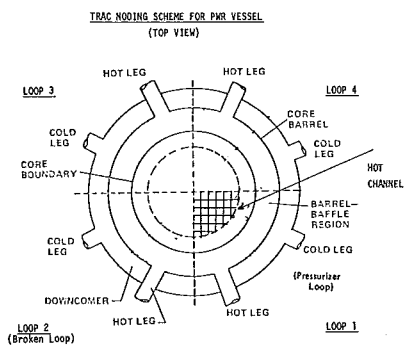


Figure 6 Vessel Cross Section for EM Calculation

Figures 7 and 8 show the rod surface temperatures at four axial locations for the hot rods in the hot channel and an adjacent channel. The peak clad temperatures for both rods occurred in the reflood phase and the highest clad temperature of 1072°K occurred for the hot channel rod at 65 seconds. The peaks in the blowdown phase were relatively smaller and were governed by the core inlet and outlet flows as were explained earlier for the BE calculation.

All the rods were either quenched or close to quenching by 270 seconds. The long duration between the timings of PCT and quenching was due to smaller safety injection and accumulator flows, and because they together were of the same order of magnitude as the break flows. The hot channel did affect the clad temperature history as can be seen from Figures 7 and 8. The difference between the PCT of the hot channel and the other channels in the blowdown phase was of the order of 50°K, and in the reflood phase it varied from 20°K to 100°K.

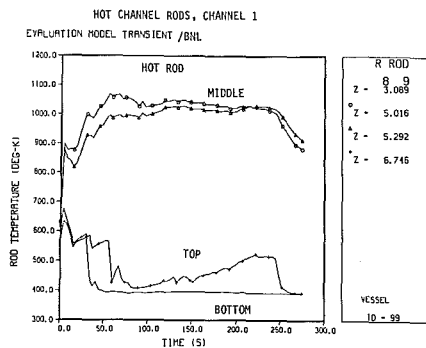


Figure 7 Clad Surface Temperatures For Hot Rod in Hot Channel For EM Calculation.

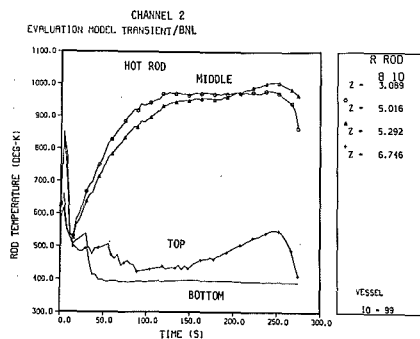


Figure 8 Clad Surface Temperatures for Hot Rod in Other Channel in EM Calculation.

The timings of the sequence of events for this calculation are summarized in Table 2. The safety injections came on quite late due to the assumption of 25 seconds delay in starting the diesel generators. The lower plenum was full by 48.5 seconds and the reflood phase began. The core liquid fraction as shown in Figure 5 was increasing at the termination of calculation indicating that the core was in the process of complete quenching.

## DISCUSSION

The best-estimate (BE) calculation was performed with the best-estimate code (TRAC-PD2/MOD1) and with all safety systems working as designed. The evaluation model (EM) type calculation was performed with licensing type boundary and operating conditions but with the best-estimate code. Besides these two calculations, results of a third calculation performed by Westinghouse<sup>3</sup> with licensing or evaluation model type boundary and operating conditions and physical models were also available. The clad temperatures for these three calculations have been compared in Figure 9.

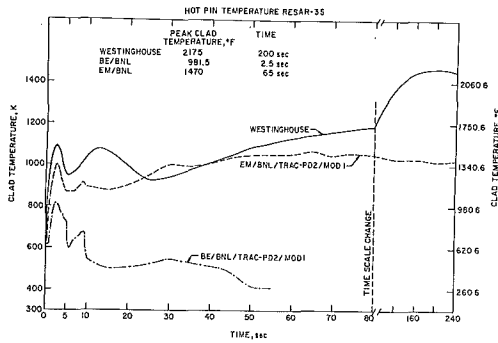


Figure 9 Comparison of Clad Temperature for Hot Rods for Westinghouse and Two BNL Calculations.

A comparison between the Westinghouse and the BNL BE calculations indicates that the licensing or Appendix K requirements contribute to a conservatism of 664°K in the PCT prediction. A comparison of the EM type calculation with these two bounding calculations indicates that the licensing type operating and boundary conditions and scenarios are responsible for 272°K conservatism in PCT while Appendix K required physical models contribute about 392°K to the conservatism of PCT estimation. The peak clad temperature in the best-estimate calculation occurred very early in the transient, and was not affected by the ECC system. On the other hand, the ECC system did affect the other two calculations.

## CONCLUSIONS

This study indicates that there is a large safety margin in the licensing or Appendix K requirements and most contribution is due to the required physical models such as subtraction of safety injection fluid collected during the blowdown phase from coolant inventory and restriction on return of nucleate boiling or transition regime in the core before the reflood phase, etc. Furthermore, a hot channel analysis is conservative, and if licensing type calculations are to be performed with TRAC, then one of the quadrants should represent a hot channel.

## ACKNOWLEDGEMENT

The authors gratefully acknowledge the valuable assistance and advice provided by Dr. Fuat Odar of USNRC, D. R. Hochreiter and Mr. R. Kemper of Westinghouse Electric Co., and Dr. K. Williams of LANL in performing this study. The typing of Ms. A. Fort is genuinely appreciated.

## REFERENCES

1. Liles, D. R. et. al., "TRAC-PD2, An Advanced Best Estimate Computer Program for Pressurized Water Reactor Loss-of-Coolant Accident Analysis," USNRC Report, NUREG/CR-2054, 1981.
2. Kemper, R., Private Communication.
3. Fujita, R. K, et. al., "Comparison Between a Most-Probable and a Licensing Calculation of a 200% LOCA in a Four Loop 17 x 17 Westinghouse PWR," National Heat Transfer Conference, Niagara Falls, NY, August 5-8, 1983.

THERMOSS: A THERMOHYDRAULIC MODEL OF FLOW STAGNATION  
IN A HORIZONTAL FUEL CHANNEL

P. Gulshani, M.Z. Caplan, N.J. Spinks

Atomic Energy of Canada Limited  
Sheridan Park Research Community  
Mississauga, Ontario, Canada L5K 1B2

ABSTRACT

A model, called THERMOSS, is developed to compute the duration of stagnation in a CANDU reactor fuel channel with subcooled, stagnant initial conditions. The model solves, in closed form, the one dimensional, two-fluid conservation equations. In the computation of the duration of stagnation, the channel water level is an important intermediate variable because it determines the amount of steam production. A feature of the model is that water level is determined by a momentum balance between frictional pressure drop in the steam phase and hydrostatic head in the liquid phase. This is in contrast to an earlier model in which the level was determined from mass balance considerations. A satisfactory agreement between the predicted and experimentally observed channel water level and duration of stagnation is obtained.

INTRODUCTION

Following a postulated break in the CANDU reactor, emergency coolant is injected to refill the horizontal fuel channels and remove the decay heat. As part of the accident analysis, the effects of loss of forced circulation during the accident are predicted. A break size exists for which, at the end of pump rundown, the break force balances the natural circulation force and the channel flow is reduced to near zero. This subcooled, stagnant channel condition is referred to as the standing-start initial condition.

The sequence of events that follows this initial condition is depicted in Figure 1. The channel coolant boils and stratifies. Eventually the steam flow from the channel heats up the endfitting to the saturation temperature and reaches the vertical feeder. The resulting buoyancy-induced flow then refills the channel.

To compute the duration of channel stagnation and, hence, assess temperature excursions of the fuel pins and that part of the pressure tube exposed to steam, the channel water level needs to be known because it determines the steam generation rate. The level also directly affects the pressure tube circumferential temperature distribution. The steam generation rate influences the convective cooling of exposed pins.

The THERMOSS (THERmohydraulic Model of Standing Start) model developed in this paper solves, in closed form, the one-dimensional, two-fluid conservation equations and computes the channel water level and duration of stagnation. The model predictions are compared with test results. THERMOSS differs from an earlier (IBIF) model<sup>1</sup>, in that the channel water level is determined from momentum rather than mass balance, and hence is more physically based.

#### EXPERIMENTAL RESULTS

To study the standing-start phenomena, a large number of tests were conducted in the Cold Water Injection Test (CWIT) facility (Figure 2) at Westinghouse Canada Inc. Gamma densitometers on the vertical feeder pipes measured the presence of any void. Thermocouples on the channel fuel rods measured rod surface temperature as well as channel water level.

The tests were conducted as follows: channel power was raised from zero to the desired value after the loop was brought to the desired subcooled stagnant condition in pressure and temperature. It was difficult to achieve perfectly stagnant initial conditions but this was attempted by making the configuration as left-right symmetric as possible (Figure 2).

Temperatures in Figure 3 show sequential uncovering of fuel rods (top first). Turn-around temperatures in Figure 3 coincide with the arrival of steam at the vertical feeder (Figure 4). The duration of channel stagnation is the time interval between the start of top pin uncovering and steam arrival at the vertical feeder.

A typical channel water level transient is shown in Figure 5. Each bar corresponds to the uncertainty in the location of the thermocouple on the pin circumference. The level drops rapidly initially and then gradually to its final position just before steam vents through the vertical feeder. All test results have been studied. Results are presented below for a typical test series covering a wide range of conditions.

Figure 6 shows final fractional water level versus power. The level is bounded between 0.1 and 0.4 and appears to be independent of subcooling. It decreases with power and, for a given power, increases with pressure (compare O with ■ at 100 kW).

Figure 7 shows duration of stagnation versus power. The data show some scatter attributable to the difficulty in achieving perfectly stagnant initial condition. Therefore, upper bound curves through the data points at each subcooling are drawn to show trends. The duration of stagnation decreases with power for a given subcooling and increases with subcooling for a given power. For a given power and subcooling, it decreases with pressure. This is clear from a comparison of the two data points at 100 kW and 90°C subcooling on Figure 7. These are the only data points of equal subcooling and significantly different pressures - 0.2 and 1 MPa. This pressure effect has also been observed in other test series.

#### THE IBIF MODEL

This model<sup>1</sup> envisages the fuel channel as a pot of water: the level

drops as water is boiled off. It calculates the mass of steam needed to heat up the endfitting to the saturation temperature. This mass of steam gives the final channel level. The duration of stagnation is then calculated using a constant level which is an average of the final and full-channel level. The level and duration depend primarily on the degree of subcooling in the endfitting.

#### THERMOSS: A THERMOHYDRAULIC MODEL OF STANDING START

The THERMOSS model calculates the time interval between the onset of boiling in the fuel channel and the arrival of steam at the vertical feeder.

During this time the large axial steam flow requires a significant pressure gradient to overcome friction. This pressure gradient depresses the water level in the channel below that in the endfitting. Eventually a quasi-steady state is reached where the hydrostatic head from the endfitting to the channel balances the steam pressure gradient. To replace water lost through boiling and maintain this steady state, water flows back to the channel.

For simplicity, the THERMOSS model ignores the initial rapid transient period. The level is assumed to be in the quasi-steady state from time zero. In this state, the level is determined from momentum balance between the frictional pressure drop in the steam and hydrostatic head change in the water phase, noting that volumetric flow rates in the water phase are negligible compared to those in the steam phase.

The model solves for the level profile in each channel assembly component (Figure 8) and for the steam flow rate out of the channel. The steam flow rate and an energy balance is then used to compute the time of heat up of each channel assembly component.

#### Water Level Profile

Figure 9 shows a fluid element  $dz$  in a channel assembly component. The balance of frictional pressure drop in the steam and hydrostatic head change in the water phase gives the (momentum) equation:

$$\frac{d}{dz} h = v u^2 \quad \text{with} \quad v \equiv \frac{f \rho_G}{2 D g \rho_L} \quad (1)$$

where  $f$  is the D'arcy friction factor,  $D$  is the hydraulic diameter,  $g$  is gravitational acceleration and the remaining symbols have their usual meaning.

The other equation needed to solve (1) is given by mass balance in the steam phase:

$$\frac{d}{dz} (\alpha u) = \begin{cases} \lambda(1-\alpha) & \text{in fuel channel} \\ 0 & \text{elsewhere} \end{cases} \quad (2)$$

where  $\alpha$  is the void fraction and

$$\lambda \equiv \frac{\dot{q}}{\rho_G \cdot h_{LG} \cdot V} \quad (3)$$

assuming axially uniform power  $\dot{q}$  and ignoring radial power depression. In equation (3)  $V$  is the component volume.



Equations (1) and (2) are solved in each channel assembly component and the level is matched at the junctions as in Figure 8. For a given level profile, the steam flow rate  $Q$  out of the fuel channel is calculated in closed form. To obtain closed form solutions, circular cross-sections are replaced by square ones of equal area. Detailed derivation of the results is reported elsewhere<sup>2</sup>.

The channel water level is found to be a function of geometry, power and pressure but not of subcooling as in IBIF model. The level decreases with power. It increases with pressure as steam specific volume is smaller at higher pressure.

#### Duration of Stagnation

The time  $\tau_k$  ( $k=1,2,3,4$ ) needed to heat up each channel assembly component to the saturation temperature is computed as follows:

The interface tip at any point along a channel assembly component (Figure 10) advances, in time  $dt$ , a distance  $dz$  as the steam flow from the channel heats up piping and water within  $dz$ . Energy balance on the pipe-water element in Figure 10 gives:

$$\rho_G \cdot Q \cdot h_{LG} \cdot dt = \frac{C_k}{\lambda_k} \cdot \Delta T \cdot dz \quad (4)$$

where  $\Delta T$  is the subcooling. This equation is integrated to obtain the time needed to heat the component to the saturation temperature:

$$\tau_k = \frac{C_k \cdot \Delta T}{\lambda_k \cdot \rho_G \cdot h_{LG}} \cdot \int_0^L \frac{dz}{Q} \quad (5)$$

The duration of channel stagnation  $\tau$  is then the sum of all  $\tau_k$ 's:  $\tau = \tau_1 + \tau_2 + \tau_3 + \tau_4$ , where the initial time is taken to be when steam extends just to the end of the heated channel.

#### COMPARISON OF MODEL PREDICTIONS WITH EXPERIMENT

THERMOSS predictions have been compared to all tests using a single friction factor  $f = 0.02$  for the entire channel assembly. Results are presented below for a typical test series covering a wide range of conditions.

Open circles in Figure 11 show a typical level transient predicted by the THERMOSS model. Figure 12 shows the predicted final water level at the channel centre for the test series. The predicted level is bounded between 0.2 and 0.5. It decreases with power and for a given power, the level increases with pressure. THERMOSS overpredicts the level but the observed trends with power, pressure and subcooling in Figure 6 are well predicted. The error in level could easily be improved by a more careful choice of friction factor.

Figure 13 shows that THERMOSS overpredicts the duration of stagnation by about 20% with a further uncertainty of about  $\pm 20\%$ . There is no systematic effect of power, pressure or subcooling on this error. Note, however, that the error would increase to about  $30\% \pm 20\%$  if the calculation of level were improved, for example, with an improved friction factor. The following

factors contribute to this error:

**Test conditions:** The tests rarely have exact standing start conditions. There is usually some asymmetry and this biases steam flow towards one end or the other. Thus, the channel vents earlier than in a completely symmetrical case. Since the model is symmetric, its tendency to overpredict the duration is expected.

**Steam superheat:** There is experimental indication of steam superheat which has been ignored in the model. Superheat would cause an additional flow of energy to the endfitting which would reduce the duration.

**Algebraic simplification:** Simplifications have been made which cause an overprediction of the duration by about 20%.

#### CONCLUDING REMARKS

The endfitting in the CWIT facility has a geometry different from that in the CANDU reactor. THERMOSS predicts that the level and, hence, the duration of stagnation depend on the channel assembly geometry. Thus, THERMOSS is a reliable extrapolatory tool.

The THERMOSS model computes the channel water level following refill of a horizontal fuel channel and subsequent flow stagnation. It predicts and explains the observed trends:

- i) The level behaviour is explained in terms of a simple momentum balance rather than a mass balance. It follows that the level is independent of subcooling as water flows back to the channel to replace that lost through boiling.
- ii) The effect of pressure on the level and on the duration of stagnation is explained in terms of steam specific volume.

The predicted duration of channel stagnation shows satisfactory accuracy being overpredicted by about 20% with no systematic dependence of the error on the independent variables. This error will increase with an improved calculation of level but will decrease if steam superheat is modelled.

#### ACKNOWLEDGEMENT

The experiments reported in this paper were funded in part by Ontario Hydro.

#### REFERENCES

1. Y. Feyginberg, P. Sergejewich and W.I. Midvidy, "A Method For Assessing Reactor Core Cooling Without Forced Circulation", 2nd Int. Topical Meeting on Nuclear Reactor Thermal Hydraulics, Vol. II, p. 808, Santa Barbara, California, January 1983.

2. P. Gulshani, M.Z. Caplan and N.J. Spinks, THERMOSS, A Thermohydraulic Model of Flow Stagnation in a Horizontal Fuel Channel, AECL report 8330, September 1984, Atomic Energy of Canada Limited, CANDU Operations.

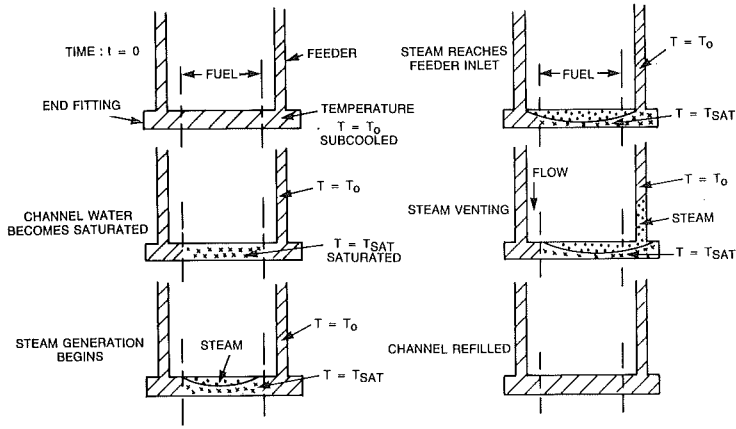


FIGURE 1 CHANNEL-REFILLING SEQUENCE OF EVENTS

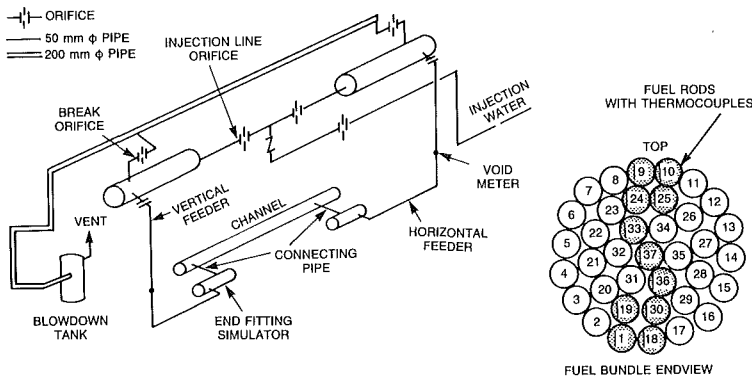


FIGURE 2 SCHEMATIC OF CWIT FACILITY

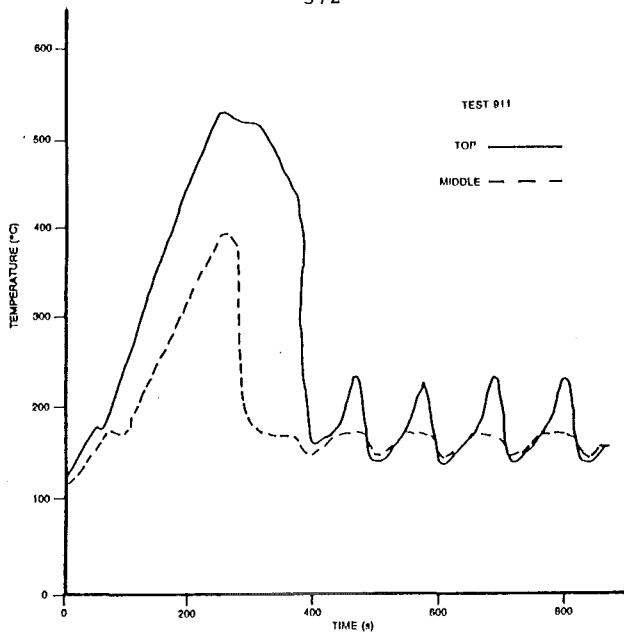


FIGURE 3 TOP AND MIDDLE PIN SURFACE TEMPERATURES

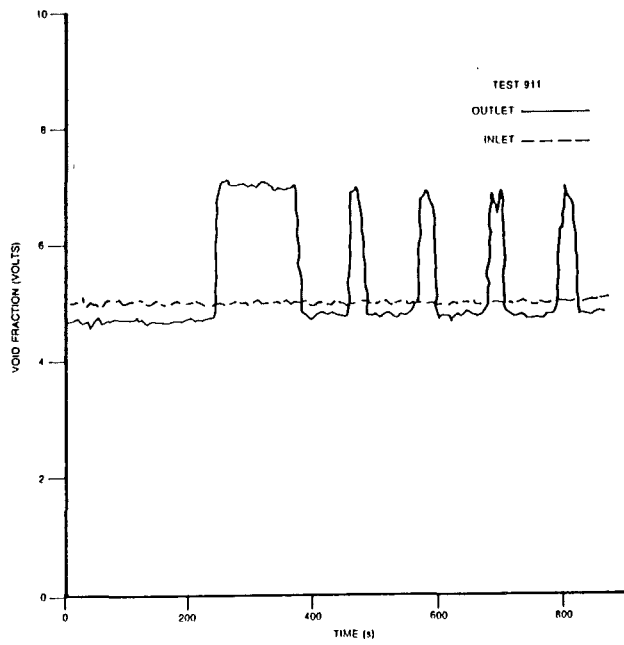


FIGURE 4 INLET AND OUTLET FEEDER VOID FRACTIONS

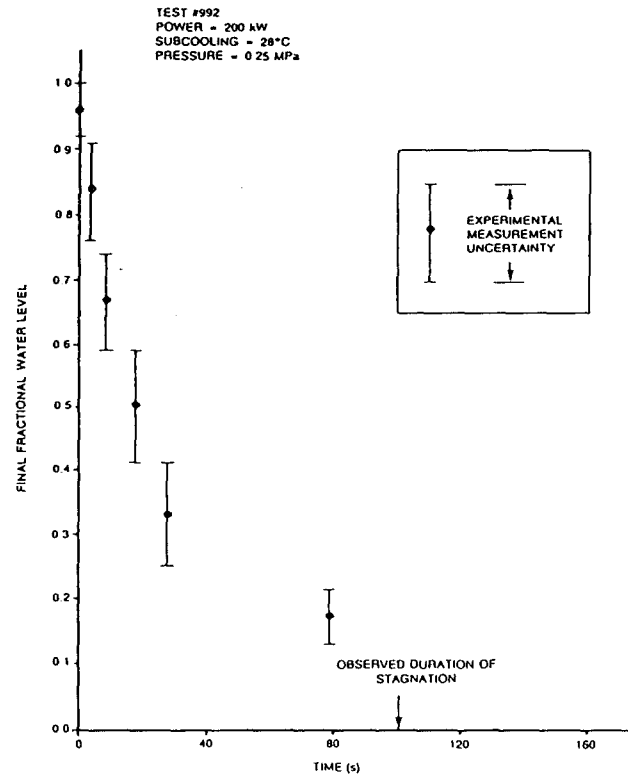


FIGURE 5 OBSERVED TRANSIENT WATER LEVEL

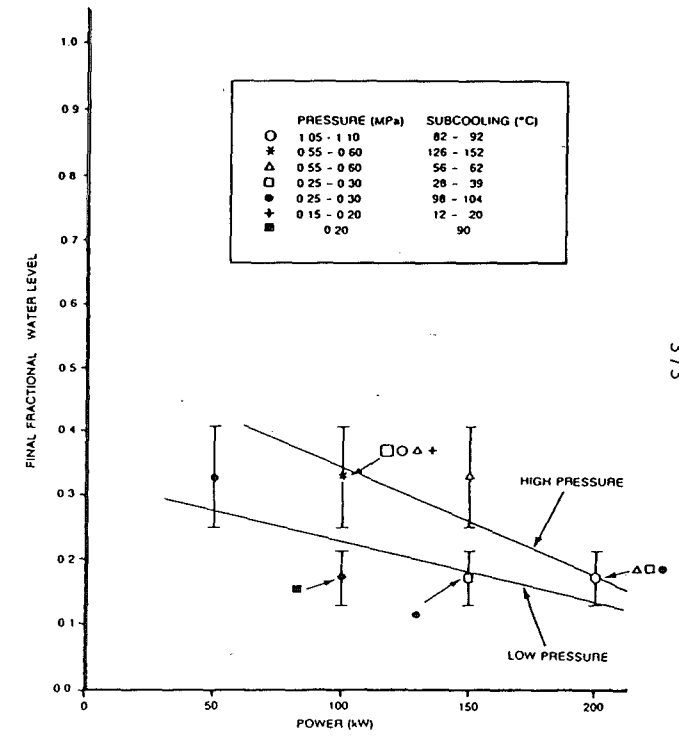


FIGURE 6 OBSERVED FINAL FRACTIONAL WATER LEVEL

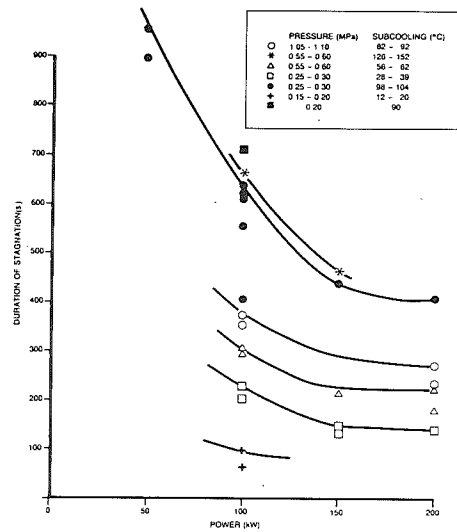


FIGURE 7 OBSERVED DURATION OF STAGNATION

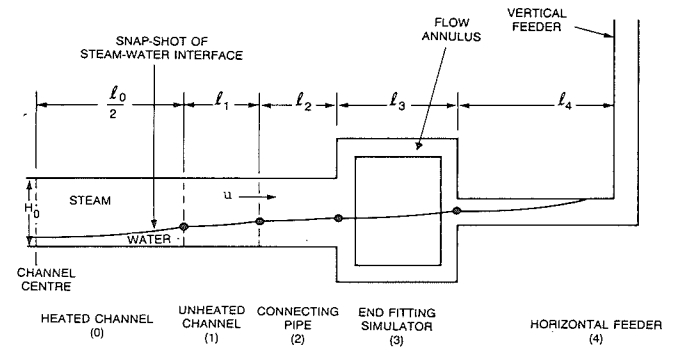


FIGURE 8 (ONE HALF OF) CWIT TEST CHANNEL ASSEMBLY

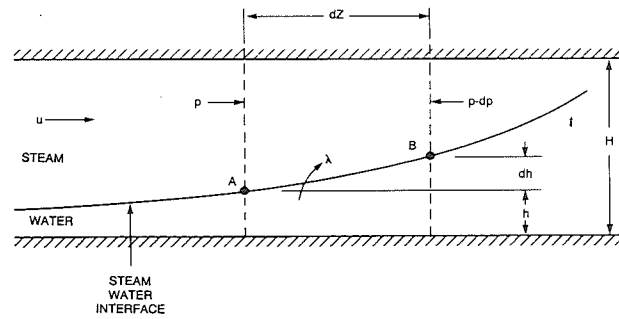


FIGURE 9 CHANNEL ELEMENT

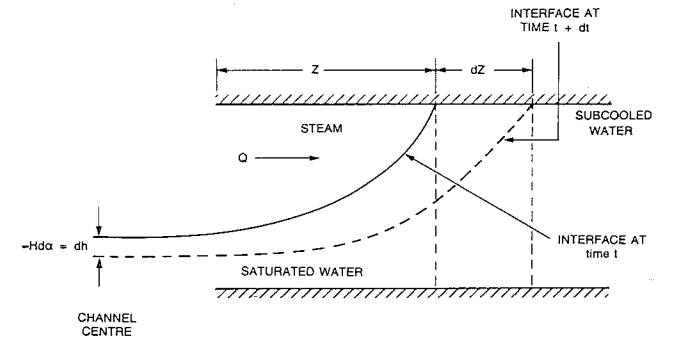


FIGURE 10 MOTION OF INTERFACE

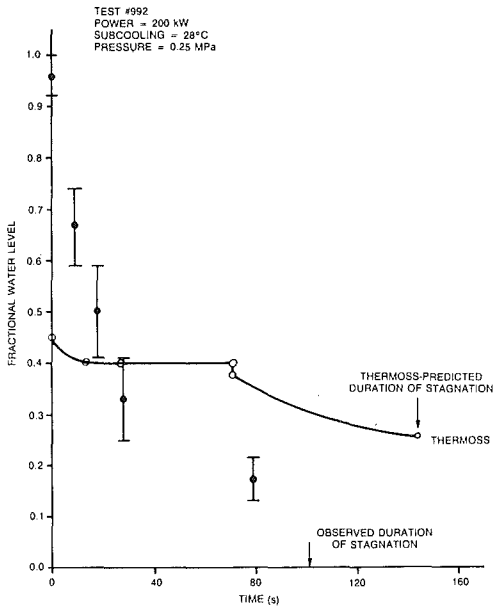


FIGURE 11 TRANSIENT WATER LEVEL

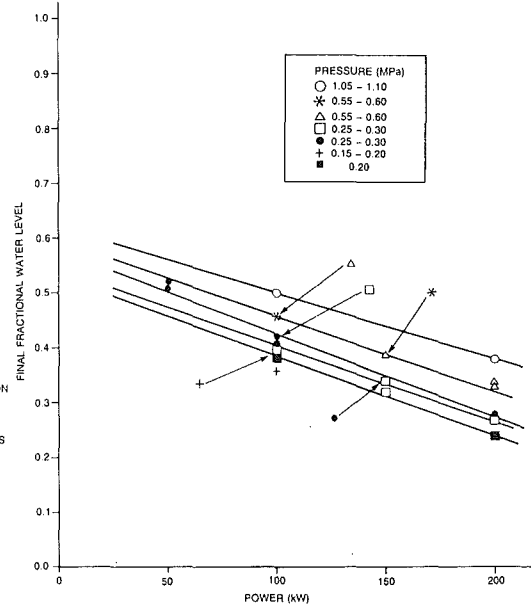


FIGURE 12 THERMOSS FINAL FRACTIONAL WATER LEVEL

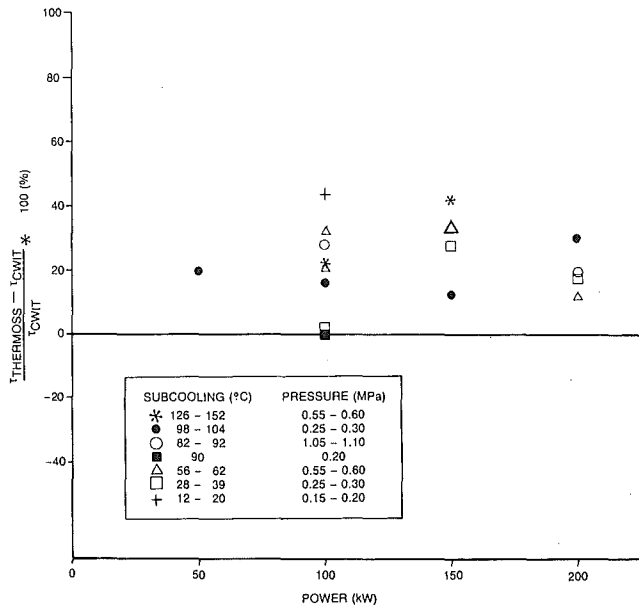


FIGURE 13 PERCENTAGE DIFFERENCE BETWEEN THERMOSS AND MEASURED DURATION OF STAGNATION

## THERMOSYPHONING IN THE CANDU REACTOR

N.J. SPINKS, A.C.D. Wright, M.Z. Caplan, S. Prawirosoehardjo, P. Gulshani

Atomic Energy of Canada Limited  
CANDU Operations  
Sheridan Park Research Community  
Mississauga, Ontario, Canada L5K 1B2

## ABSTRACT

Thermosyphoning is defined as the natural convective flow of primary coolant over the boilers. It is the predicted mode of heat transport from core to boilers in many postulated scenarios for CANDU reactor safety analysis.

The scenarios encompass a wide range of boundary conditions in reactor power, secondary temperature and primary coolant inventory. Loss of pumping of the primary coolant is a common feature.

Thermosyphoning is single or two-phase depending on the boundary conditions. The paper describes the important thermohydraulic characteristics of thermosyphoning in CANDU reactors with emphasis on two-phase thermosyphoning. It utilizes predictions of a transient thermohydraulics computer code and describes experiments done for the purpose of verifying these predictions. Predictions are compared with single-phase thermosyphoning tests done during commissioning of the Gentilly-2 and Point Lepreau CANDU 600 reactors.

## INTRODUCTION

The CANDU reactor has several modes of decay heat removal. The boilers and primary pumps provide the normal mode. The shutdown cooling system has independent heat exchangers and pumps and can remove decay heat at pressures up to nominal primary system pressures. Thermosyphoning is the mode of heat transport to the boilers in the absence of any forced circulation of the primary coolant, with secondary water being provided by the normal feedwater system, the auxiliary feedwater pumps or, on depressurization of the secondary side, by an emergency supply system.

Thermosyphoning is defined as the natural convective flow of primary coolant over the boilers. It is the predicted mode of heat transport from core to boilers in many postulated scenarios for CANDU reactor safety analysis. The scenarios encompass a wide range of boundary conditions in reactor power, secondary side temperature and primary coolant inventory. Loss of pumping of the primary coolant is a common feature. Reactor power is at decay levels.



Figure 1 is a schematic diagram of one loop of a CANDU primary heat transport system. It comprises two passes of the coolant past the fuel. Thus the coolant sees core 1, boiler 1, pump 1, core 2, boiler 2, pump 2, core 1, etc. Each core pass includes about 100 horizontal fuel channels each of which is connected by an inlet and an outlet feeder to larger diameter inlet and outlet headers. Large diameter piping connects the headers to the boilers and pumps. The tops of the boiler U tubes are located typically 11 m above the headers and the headers are located typically 7 m above the channels. The total height is 18 m and density differences in this height provide the buoyancy force for thermosyphoning.

Thermosyphoning is single-phase or two-phase depending on the boundary conditions. Two-phase thermosyphoning is predicted for high reactor decay power, low primary coolant inventory and/or low secondary temperature. For example, two-phase thermosyphoning is predicted for scenarios without coolant make up following a secondary depressurization.

CANDU thermosyphoning characteristics have been studied analytically and experimentally. The basic approach is to use a transient thermohydraulics computer code for reactor predictions supported by comparison of additional code predictions with relevant experiments. This approach is supplemented by algebraic modelling to enhance understanding of specific phenomena.

#### THERMOHYDRAULIC CHARACTERISTICS

A transient thermohydraulics computer code FIREBIRD [1] has been used to study the characteristics of thermosyphoning in the CANDU primary heat transport system as a function of coolant inventory and secondary temperature. The important characteristics are:

##### SYSTEM VOID DISTRIBUTION

As system void is increased, the excess void first appears in the outlet side of the loop. At very high system voids ( $\sim 20\%$ ) steam penetrates to the cold leg of the boiler and eventually to the inlet headers. Phase separation in a header could result and would be expected to cause steam to accumulate in and pressurize the header. Thermosyphoning may not continue. Figure 2 indicates the region where the inlet header is subcooled. It extends up to 25 to 40% system void depending on secondary temperature, and covers the scenarios of interest.

At low secondary temperature (say  $100^\circ\text{C}$ ), primary pressure is low and the liquid saturation enthalpy,  $h_L$ , is a strong function of pressure. Hot water from the core flashes to steam as its pressure reduces en route to the boilers. Thus the void is located towards the upper part of the outlet-feeders and the boiler inlet. There is no steady boiling in the core at relevant system void fractions.

At the nominal secondary temperature of  $260^\circ\text{C}$ , primary pressure is high,  $h_L$  is virtually constant, and boiling occurs in the core even at low system void fraction.

## SYSTEM FLOW

The system flow increases with increasing system void up to a maximum at about 20% void, see Figure 2. Thereafter steam penetrates past the top of the boiler reducing the buoyancy head whereas frictional forces continue to increase, so the flow decreases.

Single phase flows increase slightly with increasing secondary temperature because density is more sensitive to temperature change. At given system void, two-phase flows increase with decreasing secondary temperature, see Figure 2, because with flashing, the void is located more in vertical than in horizontal components. This enhances the buoyancy force.

## CHANNEL FLOW STRATIFICATION

Steady stratified flow is possible, for the scenarios of interest, only at high secondary temperature when steady boiling can occur in the fuel channel.

Full size horizontal channel experiments show that the flow will not be stratified above a value of 0.8 kg/sec. The tests also show that the Nusselt number will be at least 4.36 for the heat transfer from the fuel to steam. These limiting values were used in the following individual-channel studies.

Channel flow depends on channel geometry, header-to-header pressure drop, coolant inlet subcooling and channel power. We will consider these parameters in turn.

Upper channels have the most restrictive geometry for thermosyphoning with the smallest buoyancy head and with more resistive inlet feeders than central channels.

System calculations show that inlet subcooling ranges up to 20°C, depending on system void fraction. Header to header pressure drop is virtually zero, at high pressure, so channel flow is driven by buoyancy forces below the headers. Low channel decay power gives low exit quality, low outlet feeder void fraction, low buoyancy head and flows which could be stratified. Higher channel decay power gives flows too large to stratify.

Stratified flow exposes fuel elements to steam cooling, but this is adequate because channel power is low and boiling takes place only near the channel exit where the heat flux is low.

For a limiting condition of stratified flow in an upper channel an exposed fuel temperature of 580°C is predicted [2], an increase of only 280°C above the saturation temperature. Fuel damage is not expected at this temperature.

## FLOW OSCILLATIONS

Channel and system flow oscillations are possible depending on coolant inventory and secondary temperature. Periods range from 1 to 3 minutes and are governed by fluid transport time. Amplitudes reach limit cycles where the channel flow is subcooled during the high-flow part of a cycle but stratified during the low-flow part of a cycle. The temperature rise of exposed fuel in each cycle is not large (about 200°C). Even with channel flows that, on

average, would stratify, oscillations give periodic rewetting and therefore provide good fuel cooling.

The oscillations themselves have been the subject of separate detailed studies [3,4]. Channel flow oscillations [3] are caused by the delayed response of buoyancy force to flow change. During the low flow interval, steam generated in the horizontal channel is transported to the vertical feeder. On arrival at the feeder the large buoyancy force induces a large flow that in turn floods both channel and feeder. The process repeats.

System oscillations [4] can be described as a periodic redistribution of system void at the two ends of the reactor. An excess of steam between core and boiler at one end displaces liquid and so reduces the flow in the upstream core pass and increases the flow in the downstream core pass. Less upstream flow produces even more steam at this end. More downstream flow produces even less steam at the other end. At the limit cycle, void collapses completely but momentarily at one end and then similarly, a half cycle later, at the other end.

#### VERIFICATION

The above predictions are supported by comparing code predictions to full-size horizontal channel tests, reduced-size system tests and reactor commissioning tests.

Early CANDU 600 reactor predictions with FIREBIRD and a similar code, HYDRA-3, have been compared to more recent single-phase thermosyphoning commissioning tests at the Gentilly-2 and Point Lepreau reactors. Tests were done for a range of powers typical of decay power. Test flows were obtained by a heat balance using the measured core power and measured temperature rise from inlet to outlet header. Predicted flows were within the measurement uncertainty for the Gentilly-2 tests, as can be seen in Figure 3. The Point Lepreau flows are smaller but are consistent with a lower secondary temperature.

System thermosyphoning experiments were done in a reduced-size electrically-heated single-channel-per-pass representation of CANDU, called RD-12. Following pump rundown, flows, pressures and temperatures were measured as the loop was drained at given secondary temperature. Pass-to-pass flow oscillations started at low system void and continued to high void. Thermosyphoning provided good heater cooling up to a very high system void.

Code comparisons have been made with a range of RD-12 tests. All significant trends and phenomena were captured. The occurrence of oscillations at the onset of boiling was predicted as was the growth of the limit cycle with increasing system void. Figure 4 compares predicted to measured flow in each of the two non-boiling regions (between boiler and core in each core pass). This particular test had a pressurizer connected to one outlet header so the flow in one pass was not perfectly out of phase with that in the other pass. The period was somewhat overpredicted.

Single channel and parallel channel tests have been done in another electrically-heated facility employing full-size components below the headers. Tests were done by supplying water to the headers usually at a small header-to-header pressure drop as is characteristic of thermosyphoning. The

tests showed the flow to be generally oscillatory, converging to steady two-phase flow at small inlet subcooling and steady non-boiling flow at high inlet subcooling. The flow stratification threshold was taken directly from steady two-phase flow tests in this facility.

Figure 5 compares predicted to measured upper-pin temperature for a channel test which exhibited flow oscillations. This particular test had a near zero flow or "standing-start" initial condition with a near zero header-to-header pressure drop boundary condition. Temperatures above saturation were caused by exposure of upper pins to steam during periods of flow stratification in the horizontal channel. Rewetting was caused by a large buoyancy-induced flow which developed when steam from the channel penetrated to the vertical feeder.

The timing of rewetting is overpredicted. This is caused by a weakness in modelling the difference in phase velocities in stratified two-phase flow. The predicted steam flow rate from the channel is too small, delaying the time of steam penetration to the feeder. This modelling deficiency makes the FIREBIRD code conservative for application to "standing-start" scenarios. Instead an algebraic model, called, THERMOSS [5] is used for predicting the timing of the first rewetting.

FIREBIRD overpredicts the time below saturation (predicted 770-560 seconds, measured 470-350 seconds, see Figure 5) because the flow in the low-flow part of the cycle is overpredicted. However, some uncertainty in predicting the oscillations can be tolerated because the temperature rise during an oscillation is small.

#### CONCLUSION

The effectiveness of single-phase thermosyphoning in CANDU has been demonstrated in reactor commissioning tests. Code predictions show that two-phase thermosyphoning is particularly effective at low pressure because system void is concentrated in vertical components where the buoyancy force produces flows considerably greater than in single phase. Two-phase thermosyphoning flows are lower at high pressure and the channel flow can be stratified but only near the channel exit where heat fluxes are low. Fuel damage is not expected. Two-phase thermosyphoning may not continue for a system void fraction greater than 25 to 40% when steam is predicted to penetrate to the reactor inlet header, but such high void fractions are not relevant to thermosyphoning scenarios arising from accident analysis.

Code calculations have successfully predicted reactor commissioning tests and semi-scale system tests, the latter including tests which exhibited flow oscillations. Code predictions capture the qualitative features of channel tests but overpredict the period of oscillations. This leads to some uncertainty when applied to reactors but the temperature rise during oscillations is small.

#### REFERENCES

1. Lin, M-R. et al, "FIREBIRD-III Program Description", Report AECL-7533, September 1979.

2. Prawirosochardjo, S., Spinks, N.J., "CANDU 600 MW(e) Reactor-Analysis of Abnormal Transient Events Under Japanese LWR Licensing Assumptions", to be presented at the International Nuclear Power Plant Thermal Hydraulics and Operating Topical Meeting, Taipei, Taiwan, 22-24 October 1984.
3. Feyginberg, Y., Sergejewich, P., Midvidy, W.I., "A Method for Assessing Reactor Core Cooling Without Forced Circulation", in proceedings of the Second International Topical Meeting on Nuclear Reactor Thermal-Hydraulics, Santa Barbara, California, January 11-14, 1983, American Nuclear Society, Volume II, p. 808, 1983.
4. Gulshani, P., "A Figure of Eight Thermosyphoning Stability model and its Verification", in proceedings of the Second International Topical Meeting on Nuclear Reactor Thermal-Hydraulics, Santa Barbara, California, January 11-14, 1983, American Nuclear Society, Volume II, p. 840, 1983.
5. Gulshani, P., Caplan, M.Z., Spinks, N.J. "THERMOSS: A Thermohydraulic Model of Flow Stagnation in a Horizontal Fuel Channel", in proceedings of this meeting.

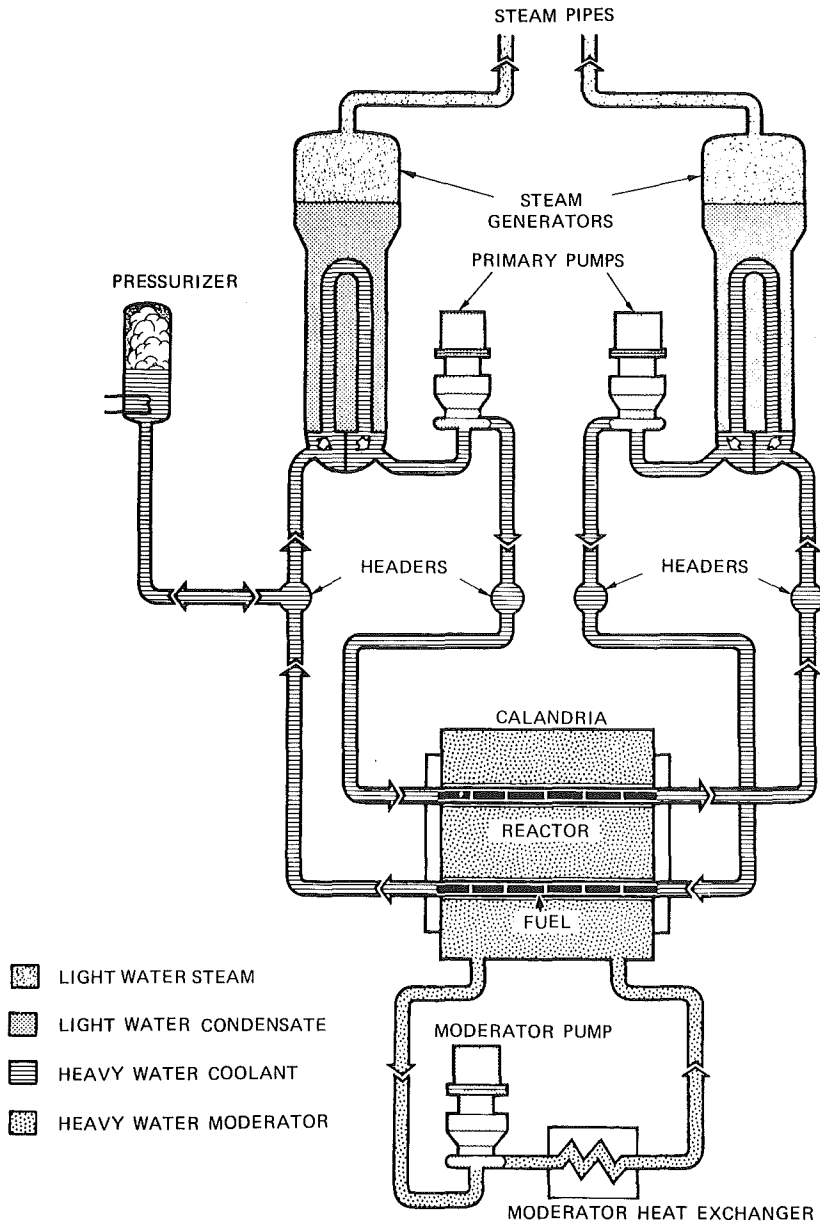


FIGURE 1 CANDU REACTOR – SIMPLIFIED FLOW DIAGRAM

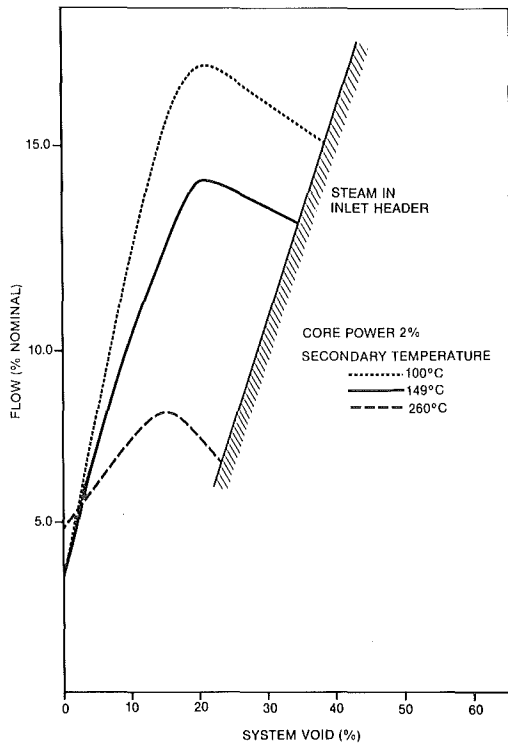


FIGURE 2 CANDU THERMOSYPHONING FLOW PREDICTIONS

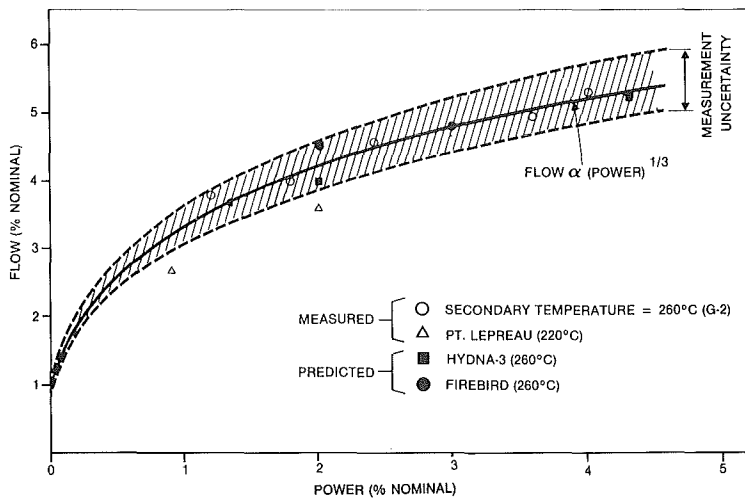


FIGURE 3 CANDU SINGLE-PHASE THERMOSYPHONING FLOW-MEASURED AND PREDICTED

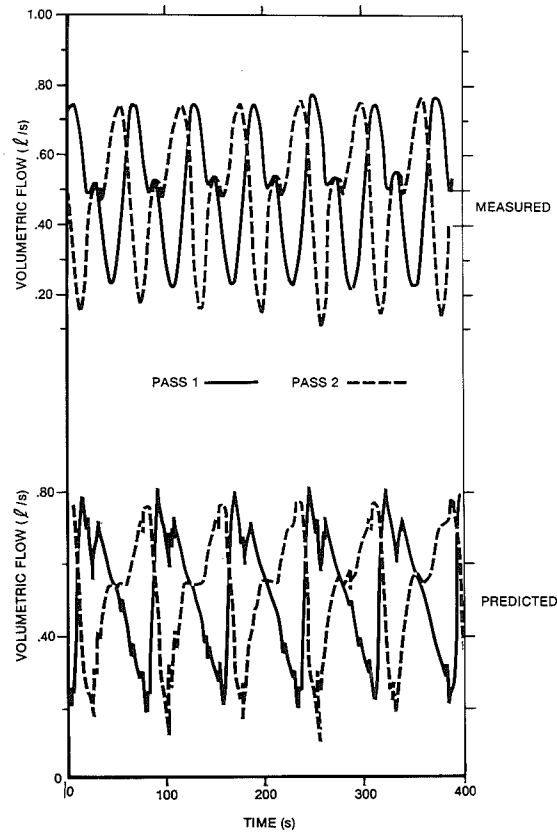


FIGURE 4 RD 12 FLOW OSCILLATIONS DURING TWO PHASE THERMOSYPHONING-MEASURED AND PREDICTED

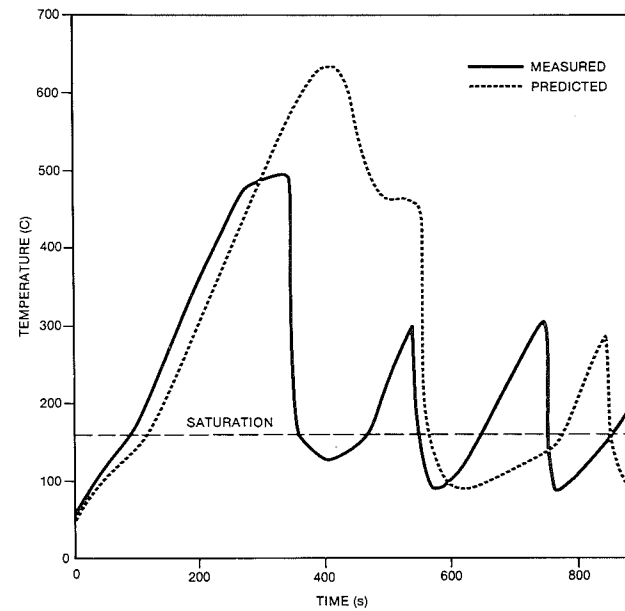


FIGURE 5 HOT PIN TEMPERATURE DURING A STANDING-START TEST



STUDIES OF HOT-WALL DELAY EFFECTS PERTINENT TO  
CANDU LOCA ANALYSIS

K.H. Ardron, V.S. Krishnan, J.P. Mallory and D.A. Scarth

Atomic Energy of Canada Limited  
Whiteshell Nuclear Research Establishment  
Pinawa, Manitoba R0E 1L0, Canada

## ABSTRACT

Experiments designed to simulate certain types of postulated loss-of-coolant accidents in CANDU reactors show that, for some conditions, long time delays occur before the injected water is able to penetrate down the feeders to reach the horizontal fuel channels. The time delays are identified as a "hot-wall" effect, caused by countercurrent flow flooding in the feeders, due to the interaction between the water downflow and the upflow of steam generated by release of heat from the feeder pipe walls.

This paper describes results of full-scale tests to measure the hot-wall delays for the CANDU reactor core geometry. A theoretical model is described that predicts the measured time delays reasonably well.

## INTRODUCTION

The core of a CANDU reactor consists of groups of horizontal fuel channels connected by individual feeder pipes to headers located above the core. In a postulated loss-of-coolant accident (LOCA) emergency cooling water is injected into the headers by pumped or accumulator injection systems.

In certain LOCAs in CANDUs it is predicted that the pressure difference between the inlet and outlet headers may remain close to zero for an extended time period. Experiments in a large-scale test facility have shown that under these conditions a long time delay may occur before the injected water is able to penetrate down the feeders to reach the heated channel. The time delay appears to be caused by the occurrence of countercurrent flow flooding in the feeders, due to the interaction between the liquid downflow and the upflow of steam generated as water contacts the hot walls of the feeder pipes. Such "hot-wall delays" have been extensively studied for the case of vertical tubes and annuli, because of their potential importance in some LOCAs in PWRs [1,2].

The present paper describes the results of full-scale tests carried out to study hot-wall delays for the CANDU reactor core geometry. A theoretical model is described that predicts the measured delays reasonably well.

## EXPERIMENTAL

Test Facility and Test Procedure

Experiments to measure the hot-wall time delays were carried out in the Cold Water Injection Test (CWIT) facility at Westinghouse Inc. Canada Systems Test Laboratory. The CWIT facility (shown schematically in Figure 1) simulates a CANDU header/feeder/channel system at full geometrical scale. The fuel channels are represented by 100 mm diameter 6 m long horizontal pipes containing electrical heater rods simulating CANDU reactor fuel rods. The channels are connected below the headers by feeders that consist of sections of horizontal and vertical steel pipe of either 50 mm or 75 mm internal diameter. For each channel the geometries of the inlet and outlet feeders are the same; details of the feeder geometries are shown in Figure 2. A pumped injection system is provided to inject cold water into the headers, to simulate the action of the reactor Emergency Coolant Injection System.

In the present experiments the penetration of injected water into the feeders was measured using thermocouples strapped to the outside of the pipes at the locations shown in Figure 2. Further information was provided by gamma-ray densitometers positioned just above the base of the feeders.

The test procedure was to pre-heat the loop pipework to an initial temperature in the range 150 - 300 °C by circulation of dry pressurized steam. The steam flow was then shut off and the loop depressurized through discharge lines connected to the headers. When the loop pressure fell below the injection pressure (which was controlled at a pre-determined value), cold water entered the headers through the check valve. In order to ensure that the header-to-header pressure drop was as close as possible to zero during the refilling of the system, the discharge line orifice areas and injection line orifice areas were made equal (so-called symmetric injection arrangement).

Tests were carried out with either both channels in circuit (parallel channel tests) or with the top channel isolated by insertion of blanking flanges in the feeders just below the header (single channel tests). The range of test conditions was as follows:

Feeder pipework initial temperature	150 - 350 °C
Channel power	0 - 50 kW/channel
Injection pressure	0.5 - 1.5 MPa
Discharge line orifice area (% of 50 mm i.d. feeder pipe area)	1 - 100%

Test Results

Forty-seven tests were carried out, consisting of 26 parallel channel tests and 21 single channel tests. Because of space limitations it is not possible to describe the observations from all tests in detail. However the main trends can be summarized as follows:

- (1) In all tests it was observed that water penetrated preferentially into one of the feeders of each heated channel (subsequently referred to as the "refilling feeder"). In the single channel tests, the refilling feeder was always the geometrical outlet feeder; in the parallel channel tests the refilling feeder varied randomly from test to test. In all but three of the parallel channel tests, opposite feeders refilled for the top and bottom channels.
- (2) There was an extended time delay (referred to as feeder refill time delay) before the refilling feeder became completely filled with subcooled water. During this delay period, which exceeded 600 s in some tests, no water was observed to enter the heated channel.
- (3) At the end of the feeder refilling period, rewetting of the heated channel began, starting from the end connected to the feeder that had refilled. The rewetting was apparently driven by the hydrostatic pressure imbalance between the refilled feeder and the opposite feeder, which was still partially voided.
- (4) The feeder refilling time delay depended strongly on initial pipework temperature and on the break orifice size (which determined the pressure in the loop during the injection phase). However, the delay did not appear to be sensitive to channel power, injection pressure, etc.

#### THEORETICAL MODEL

In this section we describe a theoretical model for calculating the length of the feeder refill time delay. The main assumption is that during the time delay period, the inflow of water into both feeders is restricted by countercurrent flow flooding (CCFL), as a result of the reverse flow of steam produced by boiling as the water contacts the hot feeder pipe walls. When the stored heat is completely removed, the reverse steam flow, and hence the flooding restriction, is assumed to cease, so that water can run freely under gravity to reach the heated channel. Thus, in our model the feeder refill delay is identified with the time taken for the incoming water flow, restricted by flooding, to cool the feeder pipework to  $T_{SAT}$ .

Calculation of the flooding limit, and the rate of energy extraction from the pipework, is described below.

#### Flooding Equation

In the CANDU system the feeder pipework consists of a series of horizontal-to-vertical pipe elbows. Experimental and theoretical investigation of countercurrent flow flooding in an elbow geometry were described in references [3] and [4]; in this work it was observed that the flooding point occurs in the horizontal leg of the elbow. The theoretical analysis in reference [4] showed that, for the limit of ideal frictionless flow, the flooding limit for the elbow could be expressed by the equation:

$$\sqrt{j_g^*} = 0.447 - 0.176 \sqrt{j_l^*} - 0.263 j_l^* \quad (1)$$

where the  $j^*$  parameters are calculated based on the diameter of the horizontal leg of the elbow. This convenient equation was adopted for the present analysis.

#### Calculation of Rate of Removal of Stored Heat

The rate of extraction of stored heat from the feeder pipework is determined by performing mass and momentum balance. The situation considered is shown in Figure 3. When water enters the headers it is assumed to penetrate both feeders A and B. However a net steam flow in the channel is established from A to B. A fraction of the steam generated in feeder A is assumed to flow in the reverse sense, while the remaining fraction  $(1 - f)$  flows in the forward sense. As described above, the liquid downflow in the feeders is assumed to be limited by CCFL in a horizontal pipe section below the header. It is also assumed that 100% of the liquid flowing downwards past the flooding point is vaporized on contacting the hot walls of the feeder pipework further downstream.

For feeder A the water downflow and the steam upflow are related by:

$$W_{gA} = f W_{lA} \quad (2)$$

which is the statement of the condition that a fraction  $f$  of the incoming liquid flow is converted into steam that flows in the reverse direction. For feeder B the water inflow and the steam upflow are related by:

$$W_{gB} = W_{lB} + (1 - f) W_{lA} \quad (3)$$

Equation (3) is a statement of the condition that the steam upflow in feeder B is equal to the steam generated by vaporization of 100% of the incoming water, plus the forward flow fraction generated in feeder A.

During the feeder refill phase we have postulated that steam upflow and water downflow in both feeders are related by the flooding Equation (1). Thus, if  $f$  is known,  $W_{lA}$ ,  $W_{gA}$ ,  $W_{lB}$  and  $W_{gB}$  can be determined by simultaneously solving Equations (1) and (2), and Equations (1) and (3), respectively. The procedure is shown diagrammatically in Figure 4, which illustrates the general case where the diameters of feeders A and B are different. It is seen by inspection of this figure that  $W_{lA} > W_{lB}$ , indicating a faster rate of heat extraction from feeder A.

Assuming that the removal of stored heat from the feeders is brought about solely by vaporization of the incoming liquid, the heat removed from the walls of feeder A in time increment  $dt$  is given by:

$$dE_{WA}(t) = W_{lA} h_g \lambda dt \quad (4)$$

A similar equation can be written for feeder B.

The hot-wall time delay  $\tau_{HW}$  is defined as the time taken to cool either feeder wall to  $T_{SAT}$ . Thus  $\tau_{HW}$  is given when the following equation is satisfied for either feeder:

$$\int_{t_0}^{t_0 + \tau_{HW}} dE_W(t) = \sum_I C_{WI} M_{WI} (T_{WIo} - T_{SAT}(t_0 + \tau_{HW})) \quad (5)$$

In Equation (5) the left-hand side is the energy removed from the feeder during the time interval  $t_0 \rightarrow t_0 + \tau_{HW}$ . The right-hand side is the stored heat that must be removed to cool the feeder to the saturation temperature at time  $t_0 + \tau_{HW}$  (the summation is taken over all pipe segments comprising the feeder). In applying the model, the integration in Equation (5) is performed numerically by using the trapezoidal rule.

As in reference [1] the total feeder refill delay time is taken as the sum of hot-wall delay time and the gravity refill time:

$$\tau_f = \tau_{HW} + \tau_{grav} \quad (6)$$

$\tau_{grav}$  is the time taken by water to fall freely through the feeder under gravity, in the limit where the pipe walls are cold.

#### Determination of Flow Split Factor f

The flow split factor  $f$  is determined by performing a momentum balance for the steam flow during feeder refilling. The presence of liquid in the feeders is ignored for this calculation. In practice the form of the equations depends on where in the feeders the steam is generated, which is not known. For our simplified analysis we have assumed that in each feeder the steam is generated at a point close to the junction between the base of the feeder and the channel end-fitting, as shown in Figure 3.

Now the pressure loss in a series of  $N$  pipe sections is given by the equation:

$$\Delta P = \frac{W_g^2}{2\rho_g} \sum_{i=1}^N \frac{\lambda_i}{A_i^2} [(f_{gwi}/D_{ei}) + (K/\lambda)_i] = W_g^2 \gamma \quad (7)$$

Here  $(K/\lambda)_i$  refers to the minor loss coefficients due to fittings, elbows, area changes etc., and  $f_{gwi}$  is the pipe wall friction factor for the  $i$ th pipe segment. In the present analysis the pipe wall friction factor is expressed in terms of the Reynolds number and the wall roughness, using standard correlations. The steam is assumed to be at the saturation temperature in both the feeders, but at the heater rod temperature inside the heated channel.

Referring to Figure 3, if  $P_H$  denotes the pressure in the headers (the header pressures are assumed equal) we have:

$$P_1 - P_H = \gamma_A W_{gA}^2 = \gamma_{CH} W_{gCH}^2 + \gamma_B W_{gB}^2 \quad (8)$$

We also note that by mass conservation, since 100% of the incoming liquid is assumed to be vapourized:

$$\begin{aligned} W_{\lambda A} &= W_{gA} + W_{gCH} \\ W_{\lambda B} &= W_{gB} - W_{gCH} \end{aligned} \quad (9)$$

The flow split factor  $f$  is defined by:

$$f = \frac{W_{gA}}{W_{gA} + W_{gCH}} \quad (10)$$

Hence, using Equations (8) and (9)

$$f = \frac{(\gamma_{CH} + \phi^2 \gamma_B)^{\frac{1}{2}}}{(\gamma_{CH} + \phi^2 \gamma_B)^{\frac{3}{2}} + \gamma_A^{\frac{1}{2}}} \quad (11)$$

where

$$\phi = 1 + \frac{W_{\lambda B}}{W_{gCH}} = 1 + \frac{W_{\lambda B}}{(1-f) W_{\lambda A}} \quad (12)$$

#### Numerical Solution Procedure

A computer program was written to solve the above equations for cases of interest. The steps in the calculation of  $\tau_{HW}$  are as follows:

- (1) Estimate a value for the flow split factor  $f$  at  $t_0$ ;
- (2) using Equations (2) and (3) and the flooding curve, Equation (1), calculate  $W_{\lambda A}$ ,  $W_{gA}$ ,  $W_{\lambda B}$  and  $W_{gB}$  at  $t_0$ ;
- (3) calculate  $\gamma_A$ ,  $\gamma_B$  and  $\gamma_{CH}$  from Equation (7) (note that these quantities are functions of  $W_{gA}$ ,  $W_{gB}$  and  $f$  because of the Reynolds number dependence of the wall friction factors);
- (4) calculate  $f$  from Equation (11);
- (5) repeat steps (1) - (4) until a converged value for  $f$  is obtained;
- (6) advance the time by  $\Delta t$ ;
- (7) calculate  $\gamma_A$ ,  $\gamma_B$  and  $\gamma_{CH}$  from Equation (7) (by using fluid properties at current time-step and velocities at previous time-step);
- (8) calculate updated values for  $f$  from Equation (11);
- (9) calculate updated values for  $W_{gA}$ ,  $W_{\lambda A}$ ,  $W_{\lambda B}$  using Equations (1), (2) and (3);
- (10) update the value of the integral on the left-hand side of Equation (5), using the old-time and new-time values of the integrand;
- (11) repeat steps (6) - (10) until Equation (5) is satisfied for either feeder.

#### COMPARISON WITH DATA

Predictions of the model were compared with data from the CWIT tests described above.

The feeders in the CWIT facility contain multiple horizontal sections, as shown in Figure 2. The internal diameter of the uppermost horizontal section is 50 mm, and that of the lower sections is 75 mm. Inspection of the thermocouple data indicates that, as water penetrates the refilling feeder, the flooding point moves downward through the feeder, proceeding from one horizontal section to the next. However, the flooding point in the "outlet" feeder (in the sense of the refilling) remains located in the uppermost horizontal section (50 mm dia.) for a much longer time period. In

view of this the effective diameter of the refilling feeder for use in the flooding equation (1) was taken as the length-average diameter of all the horizontal pipe sections above the feeder base (= 71.2 mm). The effective diameter of the "outlet" feeder was taken as 50 mm. The summation in Equation (5) was taken over all sections of feeder pipework below the header, including flanges and valves. Finally the gravity refill time [ $\tau_{\text{grav}}$  in Equation (6)] was taken as 10 s in all cases, based on a single-phase flow calculation.

Model predictions obtained on this basis are compared in Figure 5 with all data for pipework initial temperatures above 200°C. Outwardly the agreement does not appear to be particularly good; in some cases the measured time delays are a factor of two larger than the predicted values. The picture alters strikingly, however, when the single channel tests and the three parallel channel tests, in which refilling of both channels occurred in the same direction, are removed from the data-set. Figure 6 shows a comparison with the remaining parallel channel test results (14 tests in all). Agreement is now seen to be excellent.

The explanation for the discrepancies in the single channel test cases is probably that pressurization of the "outlet" header (see Figure 1) occurred during feeder refilling, as a result of the preferential venting of steam to this header. A similar asymmetry would have been expected to develop in the three anomalous parallel channel tests where both channels refilled in the same sense. Such a pressure "imbalance" would tend to increase the factor  $f$  to a value greater than that calculated by our model, which assumes equal header pressures. For all remaining parallel channel cases, opposite feeders refilled in the bottom and top channel, so there is no reason why a pressure imbalance should have developed between the headers. The implication is that the present model predicts the hot-wall delay time reasonably well when the condition of equal header pressures, for which it was derived, is realised.

#### CONCLUSIONS

Experiments designed to simulate certain postulated LOCAs in CANDU reactors have shown that, for some conditions, significant time delays can occur before the injected water is able to penetrate through the feeder pipes to reach the horizontal channels. The time delays have been identified as a "hot-wall" effect, caused by the occurrence of countercurrent flow flooding in the feeders.

A theoretical model developed on this basis agrees with the measured time delays reasonably well.

#### ACKNOWLEDGMENT

The experiments described in this paper were funded jointly by Ontario Hydro and Atomic Energy of Canada Limited. The analysis was developed in support of an Ontario Hydro funded project to investigate the performance of CANDU Emergency Coolant Injection Systems.

## REFERENCES

- [1] Block, J.A. and Wallis, G.B., AIChE Prog. Symp. Series 74 (1978) 73-82.
- [2] McPherson, G.D., Nuclear Safety 18, (1977) 306-316.
- [3] Siddiqui, H., Banerjee, S. and Ardron, K.H., Countercurrent Flow Flooding in Horizontal-to-Vertical Pipe Elbow. Part I: Experiments. Submitted to International J. Multiphase Flow, June 1984.
- [4] Ardron, K.H., Banerjee, S. and Siddiqui, H. Countercurrent Flow Flooding in Horizontal-to-Vertical Pipe Elbow. Part II: Theory. Submitted to International J. Multiphase Flow, June 1984.

## NOTATION

$C_W$	Heat capacity of section of feeder pipework.
$D_e$	Hydraulic diameter.
$E_W$	Stored heat in feeder walls.
$f$	Flow split factor
$f_{GW}$	Pipe wall friction factor for steam flow.
$h_{g,l}$	Latent heat.
$j_k$	Phase k superficial velocity.
$J_k$	$= j_k \{ \rho_k / gD \rho_{lg} \}^{3/2}$ ; non-dimensional superficial velocity.
$K$	Minor loss coefficient.
$l$	Length of pipe segment.
$M_W$	Mass of section of feeder pipework.
$P$	Pressure.
$t$	Time.
$T$	Temperature.
$W$	Mass flow rate.
$\gamma$	Flow resistance parameter.
$\phi$	Parameter defined in Equation (12).
$\rho_k$	Density of phase k.
$\tau_f$	Feeder refill time.
$\tau_{HW}$	Hot-wall delay time.
$\tau_{grav}$	Gravity fill time.

## Subscripts

$g$	Gas phase.
$l$	Liquid phase.
SAT	Saturation property.
A,B	Property of feeder A or B.
CH	Property of channel plus channel end fittings.
$i$	Property of $i$ th pipe segment.
$o$	Property at beginning of feeder refilling.



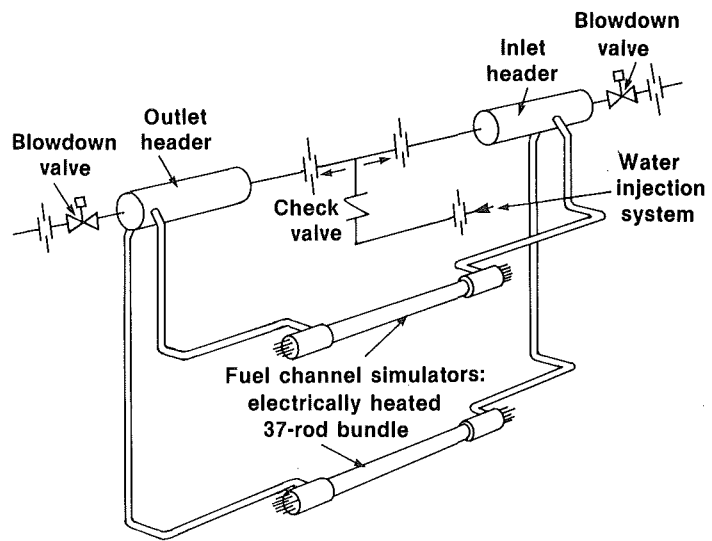


Figure 1: Schematic of Experimental Facility

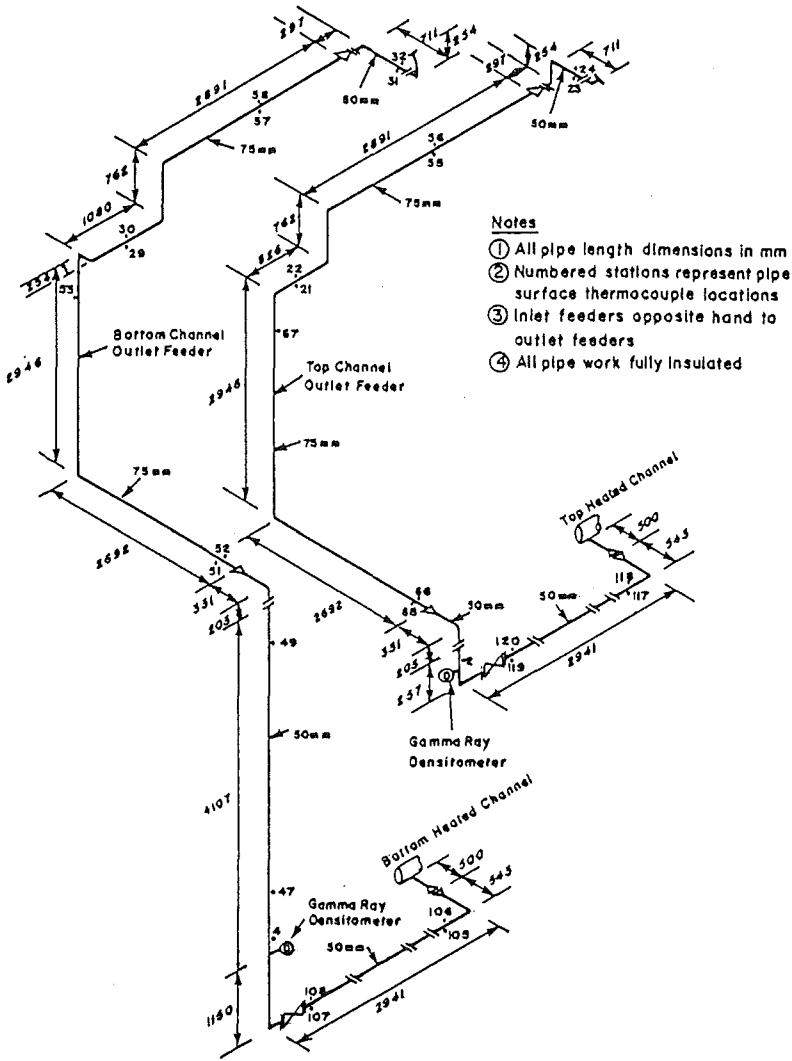


Figure 2: Feeder Pipework Geometry

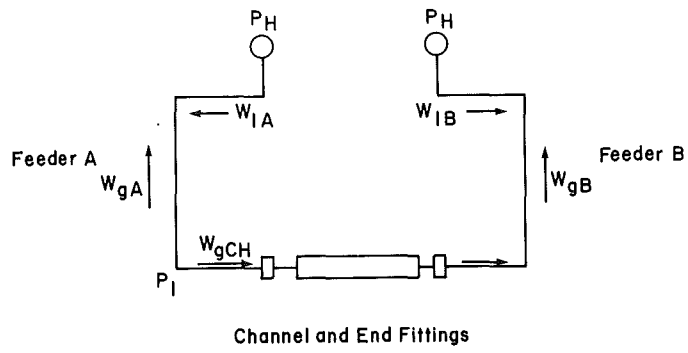


Figure 3: Feeder/Channel System During Feeder Refilling, Showing Direction of Steam and Water Flows

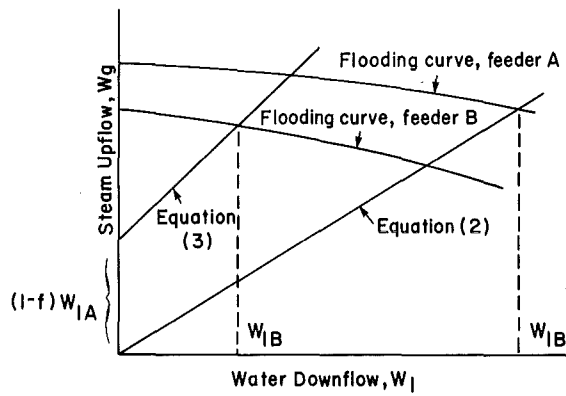


Figure 4: Diagram Showing Liquid Flow Rates into Feeders A and B

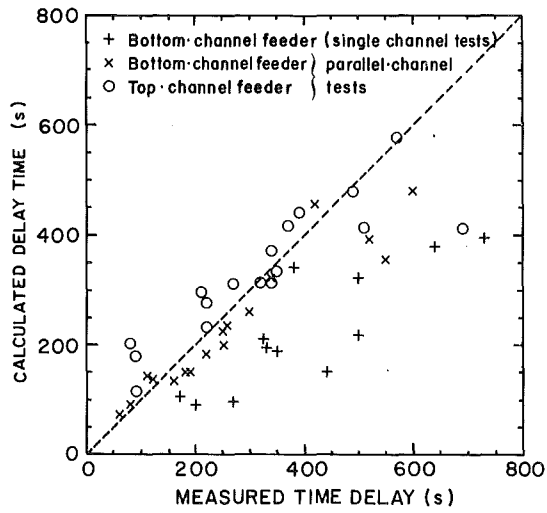


Figure 5: Comparison of Model with All Data

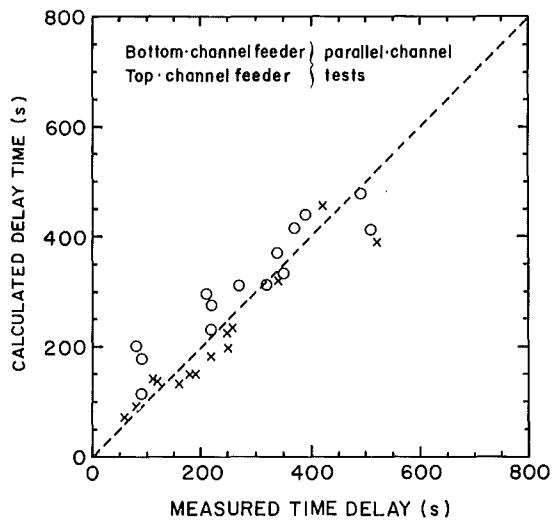


Figure 6: Comparison of Model with Reduced Data

A STUDY OF THE FAILURE OF THE MODERATOR COOLING SYSTEM  
IN A SEVERE ACCIDENT SEQUENCE IN A CANDU REACTOR

J.T. Rogers

Department of Mechanical and Aeronautical Engineering  
and  
Energy Research Group  
Carleton University  
Ottawa, Ontario, K1S 5B6, Canada

ABSTRACT

In a CANDU power reactor, failure of emergency coolant injection (ECI) following a large LOCA will not result in fuel melting because of heat transfer from the fuel channels to the separately-cooled moderator in the calandria. This paper reports the results of a study of a severe accident sequence in which a large LOCA with failure of ECI is followed by failure of the moderator cooling system. Results show that the core debris will be contained in the calandria vessel, which acts as an effective core catcher. Implications of the results for CANDU safety and risks are discussed.

INTRODUCTION

In a CANDU nuclear power reactor, the short (0.5m long) fuel bundles, 12 per channel, are supported in horizontal Zircaloy pressure tubes about 6m long through which the heavy-water coolant flows. The number of pressure tubes depends on the thermal power of the reactor; there are 480 in a Bruce-A reactor unit ( $\sim 2700$  MW(th)). Surrounding each pressure tube is a concentric calandria tube. A trickle flow of gas ( $\text{CO}_2$  or  $\text{N}_2$ ) occurs along the channel in the annulus between the two tubes. Outside the calandria tubes is the cool heavy-water moderator contained in the calandria itself. The purpose of the gas-filled annulus is to keep heat losses from the coolant to the moderator at acceptably low levels during normal operation. The moderator is maintained at a low temperature ( $\sim 80^\circ\text{C}$ ) by a separate cooling circuit. The cool moderator surrounding the calandria tubes provides a potential heat sink following a LOCA should the emergency coolant injection (ECI) fail or be impaired. Studies have shown

that fuel will not melt in such an accident because of heat transfer to the moderator [1,2,3,4].

Figure 1 is an isometric view of a typical CANDU reactor core. It should be noted that the calandria vessel is surrounded by separately-cooled ordinary water in the shield tank which is contained within the calandria vault wall which forms the main concrete shield.

A study has been undertaken for the Atomic Energy Control Board to assess the behaviour of CANDU reactor cores, in particular, a Bruce-A reactor core, under accident conditions more severe than those considered in normal licensing processes. The study was not intended to be a comprehensive risk investigation; only a limited number of severe accidents was examined, mainly thermo-hydraulic physical processes were analyzed and no calculations of event-sequence probabilities were made. The complete results of the study are given in reference [5]. Certain aspects of the study are described in references [6] and [7].

In this paper, the results of the study are given for an accident sequence in which the moderator cooling system (MCS) fails together with failure of ECT following a large LOCA.

#### DESCRIPTION OF ACCIDENT SEQUENCE

In the accident sequence considered here, a late-stagnation LOCA with failure of emergency cooling injection results in the pressure tubes overheating and sagging onto the calandria tubes, providing an effective heat flow path to the moderator [1]. The moderator cooling system fails, the moderator heats up and the calandria pressure increases until the rupture disks on the calandria relief ducts break, at about 140kPa(g). See Figure 1. The calandria pressure drops to that of the reactor vault. Some moderator is lost through the ducts by liquid swell and sub-cooled void generation. The moderator begins to boil. As boiling develops, liquid moderator is rapidly expelled through the relief ducts by void formation and additional moderator is lost by vaporization. As the void fraction near the top of the calandria increases, the top row of calandria tubes becomes uncovered, causing a rapid temperature rise of these tubes, now cooled by convection and radiation to steam generated by the boiling moderator. Pressure tube and fuel temperatures also increase. The exothermic reaction between the Zircaloy calandria tubes and the steam causes further increases of fuel channel temperatures. Eventually, other rows of tubes are also uncovered and similar subsequent behaviour occurs.

Uncovered fuel channels eventually disintegrate by melting or other mechanisms and fall to the bottom of the calandria, probably causing disintegration of any lower uncovered fuel channels as they fall (Cascading failure). The hot debris from these channels is quenched by moderator remaining in the calandria. Mixing of molten debris with moderator may result in vapor explosions. Deuterium gas from the Zircaloy-heavy water reaction escapes to the reactor vault. The steam and deuterium discharges, and possible deuterium combustion, cause pressure increases in containment, which may result in containment failure.

Eventually, all the moderator is expelled from the calandria and the quenched debris is uncovered and heats up again. The debris melts and forms a molten pool, supported by the calandria wall, which is cooled by the shield tank water. The molten pool may boil. The calandria wall may melt or fail and the molten material mix with the shield-tank water which may result in a vapor explosion and which, once again, would quench the debris. The shield tank water may be expelled and/or boil off into containment and the core debris may heat up and melt once more. Molten material may melt through to the fuelling machine duct and through the floor of the duct into the underlying rock. Interaction of the molten pool with concrete would generate non-condensable gases which may cause containment failure, if it has not already occurred. Eventually, molten material would solidify in the concrete or the underlying rock.

## ANALYTICAL APPROACH

It is recognized that the behaviour of core components under the extreme conditions of this accident sequence is, in general, quite speculative since little experimental information on CANDU core component behaviour and physical phenomena under these conditions is available. The approach used has been to attempt to model the essential features of the behaviour of core components and the moderator on a physically-sound basis, as far as possible, and to undertake sensitivity studies of the effects of the important parameters at the different stages of the accident sequence. In some cases, bounding analyses have been used.

## METHODS AND RESULTS

## Heat Source to Moderator

For the large LOCA considered here, the primary system blowdown lasts about 170 seconds [2,5]. After this time, decay heat, stored heat and heat generated by the Zircaloy-steam reaction within the fuel channels are transferred from the fuel channels to the moderator. The total heat source to the moderator was determined by grouping fuel channels according to average powers into four groups and applying the IMPECC program [2,3,4,5,8], which uses the ANS decay heat source, to each group to establish the heat flow rate to the moderator, for the case of pressure tubes sagging onto calandria tubes, at a pressure tube temperature of 1000°C [1]. Allowance was made for heat generated within the channels by the exothermic Zircaloy-steam reaction, using information from the Whiteshell Nuclear Research Establishment of AECL [9]. The result is shown in Figure 2. The peaks in the curve during the period that the heat source is increasing represent the rapid discharges of stored energy from the pressure tubes as those in each group sag onto the calandria tubes [10]. The heat source shown in Figure 2 applies as long as all the calandria tubes are submerged in the moderator.

## Expulsion of Moderator and Behaviour of Uncovered Fuel Channels

An explicit, finite-difference computer program, MODBOIL [5,6,7], has been developed to analyze the thermo-hydraulic behaviour of the moderator in this accident sequence.

In MODBOIL, the moderator is divided into 24 horizontal slices, one for each row of fuel channels, which are the control volumes in the analysis. The time-dependent heat source for each slice is pro-rated from the overall heat source in Figure 3, accounting for the number of fuel channels in each slice and their average power ratings. Transient heat and mass balances are made on each slice for non-boiling, sub-cooled boiling and bulk boiling conditions. Under non-boiling conditions, two options are available, perfect mixing or no mixing of liquid among slices. No significant differences in overall moderator behaviour were found for these two extreme cases.

MODBOIL calculates the moderator swell, the pressure over the moderator, the time to failure of the calandria rupture disks, the initiation and development of sub-cooled and bulk boiling of the moderator, the void fractions in each slice, the pressure distribution throughout the calandria allowing for static head effects, two-phase flow-pressure losses and choked flow in the relief ducts and the rate of moderator expulsion from the calandria. It also determines the times of effective uncovering of fuel channel rows and allows for heat source redistribution from any moderator slice to the bottom slice to model the disintegration of uncovered fuel channels. Criteria for fuel channel disintegration were established using IMPECC-UCZ [5,6,7] which models the thermal behaviour of uncovered fuel channels allowing for radiative and convective heat transfer to steam flowing over the calandria tubes and for heat generated by the reaction

between this steam and the Zircaloy calandria tubes. For representative channel uncover times, steam flow rates and temperatures, IMPECC-UCZ shows that the fuel in uncovered channels will still be well below the  $UO_2$  melting temperature up to the times of channel disintegration [5,6,7], as can be seen in Figure 3. Some melting of calandria tube Zircaloy may occur in this period, as indicated, for example, in Figure 4, but the amounts will be limited since most Zircaloy will have been oxidized before its melting temperature is reached and predicted temperatures do not reach the melting point of  $ZrO_2$ .

The MODBOIL program models the quenching of disintegrated fuel channel debris in the bottom slice of moderator, allowing for stored and decay heat and assuming film boiling (plus radiation) or nucleate boiling as appropriate.

Moderator Behaviour Before Channel Uncovery Results show that rupture disk failure occurs at about 9.2 minutes and that liquid begins to spill from the relief ducts at about 9.4 minutes. Bulk boiling begins in the top slice just before 16 minutes and propagates downwards rapidly until it becomes fully developed across the calandria at about 17.6 minutes. The rapid increase in void fraction in this period results in a large fraction of moderator being rapidly expelled from the calandria, as can be seen in Figure 5. Moderator is expelled in surges during this period, as shown in Figure 6, but the accompanying pressure surges are not severe (peaks < 220kPa abs) because of the low steam qualities at the exit of the relief ducts ( $\leq 4\%$ ) during this period.

Moderator Behaviour After Channel Uncovery After channel uncover begins, reference conditions used to define the behaviour of the core are:

- a) Delay times between channel uncover and disintegration established from IMPECC-UCZ runs, as described in references [5 and 7].
- b) Fraction of channel mass disintegrating = 1.0 (FRCMAS=1.0)
- c) Fraction of Zircaloy molten at disintegration = 1.0 (FRMELT=1.0)
- d) Average temperature of fuel at disintegration =  $1750^\circ\text{C}$ (TF)
- e) Average temperature of Zircaloy (solid or molten) at disintegration =  $1750^\circ\text{C}$ (TZIRC)
- f) Uncovered channels disintegrate when struck by falling debris (Cascading failure)

It is judged that these are the most severe conditions for core and moderator behaviour that might occur in this accident sequence. The rationale for the choice of these reference conditions is discussed in reference [5].

For these conditions, MODBOIL predicts that the top row of channels becomes uncovered at about 21 minutes and that the initial disintegration of fuel channels occurs at about 23 minutes, when the top three rows collapse simultaneously. This and subsequent channel disintegrations cause the later flow rate surges shown in Figure 6; with pressure peaks <470kPa abs. Essentially all the moderator is expelled from the calandria in about 48 minutes, as shown in Figure 5.

As the reference condition temperatures, as established from IMPECC-UCZ [5,7], indicate, the fuel material will not be molten at the times of disintegration and MODBOIL shows that it will be rapidly quenched as it falls into the moderator. Although the reference conditions assume that all channel Zircaloy is molten at disintegration, only a fraction of the calandria tube Zircaloy is likely to be molten at this time since the fuel sheaths and pressure tubes will have already been oxidized and a significant fraction of the calandria tube Zircaloy will also have been oxidized, as discussed earlier. The melting point of  $ZrO_2$  ( $\approx 2700^\circ\text{C}$ ) is well above the anticipated peak temperatures of the non-fuel materials in the channels. See Figure 4. Thus, almost all of the non-fuel debris also will fall into the moderator as solid material. MODBOIL shows that, whether molten or not, all non-fuel debris will also be rapidly quenched in the moderator. Finally for the reference conditions, average debris temperatures will be about  $110^\circ\text{C}$  just before the last of the moderator is expelled from the calandria at about 48 minutes and only a few fuel channels



(at an average temperature of  $\sim 1750^{\circ}\text{C}$ ) will remain intact at that time.

Results of sensitivity studies, as given in references [5 and 7], show that the average moderator expulsion rate and time to complete expulsion are not likely to be much different from those for the reference conditions, even for the case in which no delay is assumed to occur between calandria tube uncovering and channel disintegration ("instantaneous disintegration"). The study has also shown that steam superheated by, and deuterium gas generated from, the uncovered calandria tubes will not have any significant effect on calandria pressure nor on discharge rates from the calandria [5].

The investigation also concluded that no vapor explosion would occur as the core debris falls into the remaining moderator [5].

#### Thermal Behaviour of Bed of Core Debris

Following moderator expulsion, a bed of solid core debris is left at the bottom of the calandria. It is not possible to predict the physical and geometric characteristics of this debris bed with any confidence, so that a simple one-dimensional thermal model which would facilitate sensitivity studies was developed.

In the model, it is assumed that the debris forms a uniform porous bed of  $\text{UO}_2$  and  $\text{ZrO}_2$  material with porosity and average pore size to be specified as inputs to the computer program DEBRIS. Mechanisms of heat transfer considered are conduction through solid material, allowing for random contact thermal resistances, and conduction and radiation through the steam-filled pores. Considering these mechanisms, an equivalent effective thermal conductivity of the bed was determined. The volumetric heat source used is based on the ANS decay heat source, with the dilution effects of structural material and bed porosity accounted for.

The upper surface of the debris bed is assumed to be cooled by natural convection to steam and radiation to the calandria walls above the bed, which are cooled by the shield-tank water. The lower surface of the bed, resting on the calandria wall, is cooled by conduction through the wall and natural convection or sub-cooled boiling to the shield-tank water, with the program selecting the appropriate mechanism, depending on the existing conditions at any time.

Figure 7 shows maximum, upper and lower surface temperatures of the debris bed as functions of time for the selected reference conditions. The maximum temperature in the bed reaches the melting point,  $\sim 2700^{\circ}\text{C}$ , at about 85 minutes after the start of re-heating, or about 135 minutes after the initiation of the accident. The upper and lower surface temperatures of the bed are well below the melting point at this time. The lower surface temperature is well below the melting temperature of the stainless steel calandria wall and the lower surface heat flux into the shield tank water,  $15.5 \text{ W/cm}^2$ , is well below the critical heat flux, estimated at about  $280 \text{ W/cm}^2$  for these conditions [5]. Thus, the calandria wall will remain well-cooled and will retain its integrity up to the least the time at which bed melting begins.

The reference conditions used for porosity ( $\epsilon_v$ ) and average pore size, 0.5 and 0.03m respectively, are arbitrary, although the large pore size selected reflects a judgement as to the nature of the debris, considering that little or no melting will have occurred before bed uncovering. However, sensitivity studies show that predicted results are very insensitive to wide variations, separately and jointly, in these parameters as well as to significant variations in solid material thermal conductivity and the contact conductance parameter [5]. For example, Figure 7 shows that the predicted temperatures for bed porosities of 0.1 and 0.8 are only slightly different from those for the reference condition porosity of 0.5.

### Thermal Behaviour of a Molten Pool of Core Debris

Once melting begins in the debris bed, some time will be required for the transition to a completely molten pool. Because of the complexity of this transition stage [5], no attempt was made to develop an analytical model for the debris during this period. Instead, the time required for this period and the accompanying heat source decay were ignored, giving a conservative analysis. Thus, for the reference conditions, the earliest time for complete molten pool conditions was taken as 135 minutes.

A quasi steady-state, modified one-dimensional energy balance is the basis of the model in the program MOLTENPOOL for the thermal behaviour of the pool, in which allowance is made for the curvature of the calandria wall forming the lower surface of the pool.

Internal radiation heat transfer, which is important in high-temperature molten pools [11], is accounted for using the method of Anderson [12]. Molten pool internal heat transfer for non-boiling and boiling conditions was determined using established correlations and models [5].

A major uncertainty in this analysis is that of liquid and vapor property values for the molten pool materials. Four different sets of consistent property values were used to determine the sensitivity of results to uncertainties in property values.

Results for the reference conditions were inconclusive as to whether the pool would boil or not, with two sets predicting no boiling and two sets predicting boiling. Nevertheless, the maximum predicted downward heat flux, i.e., the heat flux through the calandria wall into the shield tank water, did not exceed  $20 \text{ W/cm}^2$  for any of the four sets of property values.

Heat fluxes of  $20 \text{ W/cm}^2$  are still well below the estimated critical heat flux of  $280 \text{ W/cm}^2$  for the conditions in the shield tank water [5], so that the calandria wall will be well-cooled throughout this stage of the accident sequence, irrespective of the uncertainties in molten pool liquid or vapor property values and whether the pool boils or not.

Sensitivity analysis showed that even much shorter initial times for molten pool formation, ~30 minutes, did not result in heat fluxes to the shield tank water exceeding  $30 \text{ W/cm}^2$ , still well below the critical heat flux [5].

### Interaction of the Molten Pool with the Calandria Wall

Although the calandria wall should remain well-cooled during this stage of the accident sequence, provided that the shield-tank water cooling system is operational, the possibility of partial calandria wall melting and failure exists.

To investigate this question, the asymptotic behaviour of the molten pool on the calandria wall under quasi-steady state conditions was analyzed using a one-dimensional model. From this analysis, the conditions for wall melting were established, as shown in the non-dimensional plot in Figure 8, where  $\phi$  represents a non-dimensional source heat flux from the molten pool and  $Bi_{ac}$ , the coolant Biot number, represents the cooling capability of the shield tank water.

For the highest predicted heat flux from the non-boiling molten pool for the reference conditions, the shield tank water will be undergoing subcooled nucleate boiling on the calandria wall [5]. For these conditions,  $\phi = 0.285$  and  $Bi_{ac} = 5.10$ , so that Figure 8 shows that there will be no melting of the calandria wall, and that, furthermore, these conditions ensure that the wall is very far from the melting point. The analysis also showed that a solidified crust of core material about 2.3cm thick would form on the wall, thus providing a protective shield. Further analysis showed that the heat flux from the pool would have to be about  $100 \text{ W/cm}^2$ , about five times the maximum predicted value for the reference conditions, before any melting of the calandria wall would begin [5].

For the property values which predict that the molten pool will boil, the heat flux into the calandria wall is less than the maximum for non-boiling conditions, so that the calandria wall under the surface of the pool will be also well protected and cooled and far from the initiation of melting in this case [5]. However, the vaporized core debris will condense on the calandria wall above the pool surface, and the resulting high heat fluxes may cause melting of the calandria wall. A simple model of this process was developed and embodied in the computer program CONFILM. The model assumes that a quasi-equilibrium state would be established between evaporation of core material from the surface of the pool and its condensation on the calandria walls above the pool. The condensation heat transfer coefficient was established assuming that conventional correlations apply and that the condensing film was under laminar flow conditions. Results show that the average condensation heat flux for the reference conditions in this case is considerably higher than that from the molten pool itself, about 50 to 55 W/cm<sup>2</sup>, depending on the property values used. However, these values are still well below the critical heat flux for these conditions so that the calandria wall above the pool surface will remain well cooled. Also, the interaction of the condensate film with the calandria wall was assessed using the quasi-steady state model discussed earlier. This assessment showed that this portion of the wall would also be far from any initiation of melting and would be protected by a solidified layer of debris about 1.0cm thick [5].

#### End Point for the Accident Sequence

The analysis of the accident sequence shows that the core material debris, whether solidified or molten, will not jeopardize the integrity of the calandria vessel, irrespective of whether the molten pool boils or not. Calculations with MOLTENPOOL show that, eventually, the molten pool would begin to re-solidify at a time between 10 and 50 hours, depending on the molten material property values. Thus, we can conclude with good confidence that essentially the entire mass of core material will be contained within the calandria, as long as the shield-tank cooling water system functions properly. The calandria, in effect, acts as an effective inherent core catcher in a CANDU reactor.

Therefore, we also conclude that the subsequent stages of the accident sequence, as listed earlier in this paper, would not be experienced should this accident actually occur.

#### Containment Pressurization and Effects

A single-node model was developed to estimate additional containment pressurization resulting from the loss of MCS and was incorporated into a computer program BLDG. Sensitivity studies with BLDG predicted maximum absolute pressures in containment in the range of 140 to 165 kPa, well within the test pressure. The additional maximum concentration of deuterium gas in containment resulting from this accident sequence is about 0.6%, so that there would be no significant increased probability of deuterium combustion. When major releases of bound fission products occur, after debris melting begins, maximum absolute containment pressure is predicted to be in the range of 123 to 147 kPa.

Thus, we can conclude that this accident sequence will not cause containment failure and that radioactivity releases would be relatively low because of low pressure differences across containment boundaries.

#### CONCLUSIONS

Important conclusions reached in the study of this accident sequence are:

- a) The operators would have about 20 minutes to provide an alternate heat sink for the moderator before channel uncover and disintegration begin.

- b) The moderator would be completely expelled from the calandria in about 45 to 50 minutes.
- c) No gross fuel melting would occur even when fuel channels are uncovered, and fuel in the core debris in the bottom of the calandria would not begin to melt until about 135 minutes after the accident begins.
- d) The calandria walls would not melt nor suffer significant damage from molten core debris, even though boiling of the molten pool may occur, provided that the shield-tank water cooling system remains operational.
- e) Core debris would be contained within the calandria and would begin to re-solidify in the period of 10 to 50 hours after the initiation of the accident. The calandria serves as an inherent core catcher in a CANDU reactor.
- f) Pressurization of containment during the accident sequence would not cause containment failure nor result in excessive releases of fission products outside containment.

Of course, there are considerable uncertainties in the properties and behaviour of CANDU core materials under the extreme conditions encountered in this accident sequence, so that the results must be treated with caution until such time as work on these topics [e.g., 13,14] yields further information.

It is judged that core debris would also be contained within the calandria for an early - stagnation LOCA in which the pressure tubes balloon, rather than sag, onto the calandria tubes [1].

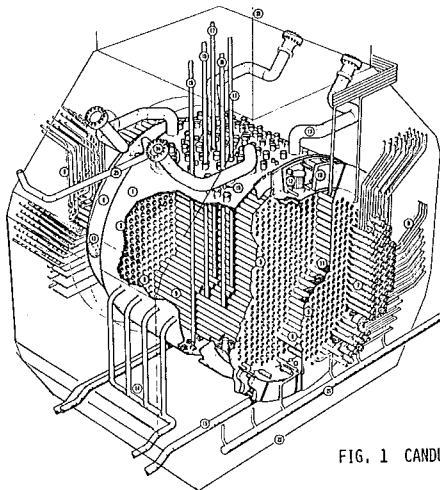
While no assessment of event probabilities was made as part of this study, rough estimates of the probability of this accident sequence indicate a value considerably less than  $10^{-7}$  per reactor year. With such a low probability, the recommendations of reference [15] would not require that this accident sequence be considered in a licensing application.

#### ACKNOWLEDGEMENTS

The work described in this paper was done under contract to the Atomic Energy Control Board. Significant support was also provided by the Natural Sciences and Engineering Research Council of Canada.

The important contributions of T.C. Currie, J.C. Atkinson and R. Dick to this work are gratefully acknowledged.

L. Seabrooke is thanked for typing the paper.



1. CALANDRIA
2. CALANDRIA MAIN SHELL
3. CALANDRIA-SIDE TUBESHEET
4. CALANDRIA SUB-SHELL
5. FUELLING MACHINE-SIDE TUBESHEET
6. LATTICE TUBES
7. END FITTINGS
8. FEEDERS
9. CALANDRIA TUBES
10. SHIELD TANK SOLID SHIELDING
11. STEEL BALL SHIELDING (END SHIELD)
12. MANHOLE
13. CALANDRIA RELIEF DUCTS
14. MODERATOR INLETS
15. MODERATOR OUTLETS
16. SHUT-OFF UNIT
17. ADJUSTER UNIT
18. VERTICAL FLUX DETECTOR
19. CONTROL ABSORBER
20. LIQUID ZONE CONTROL UNIT
21. END SHIELD COOLING PIPING
22. SHIELD TANK
23. SHIELD TANK EXTENSION
24. RUPTURE DISC ASSEMBLY
25. MODERATOR OVERFLOW

FIG. 1 CANDU REACTOR ISOMETRIC DIAGRAM

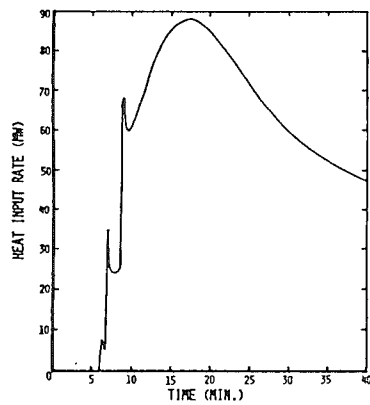


FIG. 2 TOTAL HEAT INPUT RATE TO MODERATOR, BRUCE-A UNIT

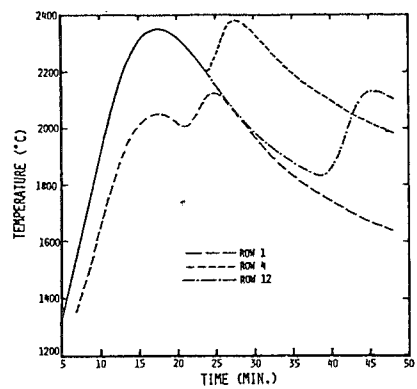


FIG. 3 MAXIMUM FUEL TEMPERATURES IN DIFFERENT ROWS

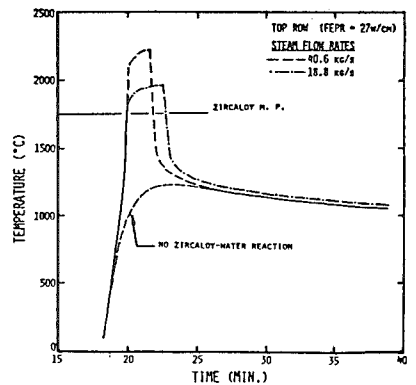


FIG. 4 MAXIMUM CALANDRIA TUBE TEMPERATURES FOR TOP ROW

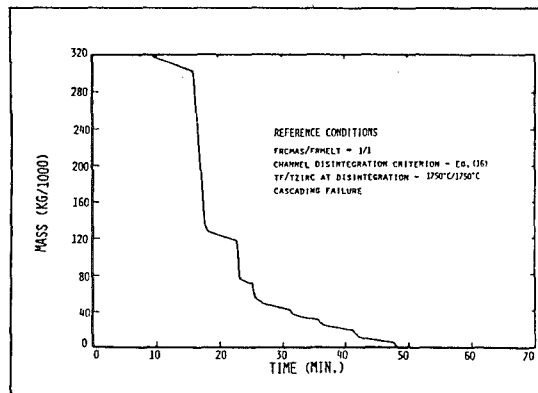


FIG. 5 MASS OF MODERATOR REMAINING IN CALANDRIA VS TIME. REFERENCE CONDITIONS

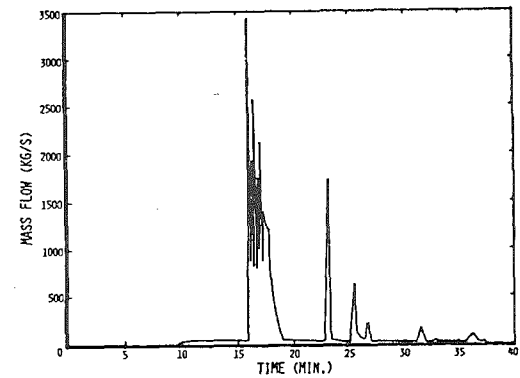


FIG. 6 MODERATOR EXPULSION RATE. REFERENCE CONDITIONS

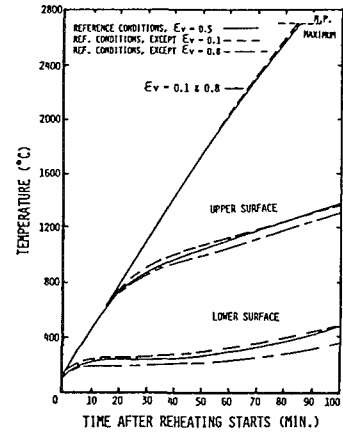


FIG. 7 TEMPERATURES IN POROUS BED OF SOLID CORE DEBRIS

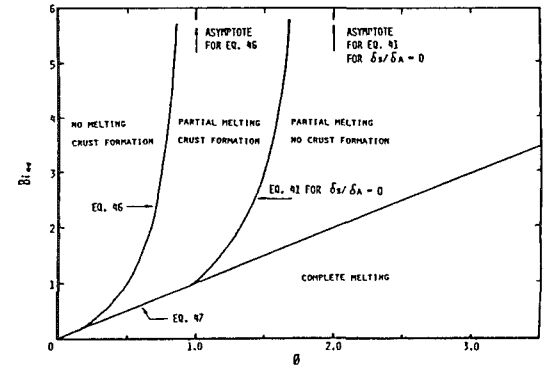


FIG. 8 MAP OF CONDITIONS FOR MELTING OF CALANDRIA WALL

## REFERENCES AND FOOTNOTES

1. Meneley, D.A., and W.T. Hancox, LOCA Consequence Predictions in a CANDU-PHWR, Paper 145, IAEA International Conference on Nuclear Power Experience, Vienna, September, 1982.
2. Rogers, J.T., CANDU Moderator Provides Ultimate Heat Sink in a LOCA, Nuclear Engineering International, 24, 280, p.38, January, 1979.
3. Rogers, J.T. and T.C. Currie, Analysis of Transient Dry-Patch Behaviour on CANDU Reactor Calandria Tubes in a LOCA with Late Stagnation and Impaired ECI, Proceedings, International Meeting on Thermal Nuclear Reactor Safety, Aug.29-Sept.2, 1982, Chicago, U.S.A.
4. Rogers, J.T. and T.C. Currie, Heat Transfer and Thermohydraulic Studies Related to the Moderator Heat Sink in a CANDU Nuclear Power Plant, Invited Paper, Proceedings VIIth All-Union Heat and Mass Transfer Conference, Minsk, U.S.S.R., May, 1984.
5. Rogers, J.T., Thermal and Hydraulic Behaviour of CANDU Cores Under Severe Accident Conditions, Final Report, Report to the Atomic Energy Control Board, Dept. of Mechanical and Aeronautical Engineering, Carleton University, AECB INFO- , June, 1984.
6. Rogers, J.T., T.C. Currie, J.C. Atkinson and R. Dick, Analysis of Effects of Calandria Tube Uncovery Under Severe Accident Conditions in CANDU Reactors, Proceedings, Fourth Annual Conference, Canadian Nuclear Society, June 15, 1983.
7. Rogers, J.T., J.C. Atkinson and R. Dick, Analysis of Moderator Expulsion from a CANDU Reactor Calandria Under Severe Accident Conditions, ASME Paper 84-HT-16, August, 1984.
8. Rogers, J.T. and T.C. Currie, A Model for Thermal Analysis of a CANDU Fuel Channel Following a LOCA with Delayed ECC Flow, Paper presented at CNA International Conference, Ottawa, June 1978. Also, report of: Department of Mechanical and Aeronautical Engineering, Carleton University, Ottawa, May, 1978.
9. Hancox, W.T., Whiteshell Nuclear Research Establishment, AECL, Pinawa, Manitoba, Personal Communication, July, 1980.
10. Only three peaks are shown instead of the expected four since the first peak, being small, was obscured in the computer plot.
11. Stein, R.P., L. Baker, Jr., W.H. Gunther and C. Cook, Heat Transfer from Heat Generating UO<sub>2</sub>: Interpretations of the Available Experimental Data, ASME 79-HT-115, August, 1979.
12. Anderson, E.E., Radiative Heat Transfer in Molten UO<sub>2</sub> Based on the Rosse-land Diffusion Method, Nuclear Technology, 30, 65, July, 1976.
13. Rosinger, H.E. The Severe Fuel Damage Program at WNRE: Status and Future Direction, AECL Report WNRE-556, February, 1984.
14. Hadaller, G.I., G.H. Archinoff and E. Kohn, CANDU Fuel Bundle Behaviour During Degraded Cooling Conditions, Proceedings Fourth Annual Conference, Canadian Nuclear Society, June 15, 1983.
15. Recommended General Safety Requirements for Nuclear Power Plants, Advisory Committee on Nuclear Safety, ACNS-4, June, 1983.



FLUID-STRUCTURE INTERACTION IN PRESSURE WATER REACTORS

S. E. Meier

Gesellschaft für Reaktorsicherheit mbH  
Schwertnergasse 1, D-5000 Köln 1

## ABSTRACT

A leak or a break in the primary system of a pressure water reactor (PWR) generates fluiddynamic loads in the coolant system and specially on the reactor internals. Fluid-structure interaction (FSI)-codes were developed and validated during the last years to determine the realistic height, frequency and location of the maximum load.

The FSI-code DAISY is validated at several Heiß Dampf Reaktor (HDR)-blowdown experiments and extended by special features to describe a PWR primary system. The loads and the stresses are determined in the core barrel of a PWR, initiated by a 0.1 area leak in the cold leg of the coolant system near the entrance nozzle of the pressure vessel.

## INTRODUCTION

During the last years coupled fluid-structure interaction (FSI)-codes have been developed and validated at the Heiß Dampf Reaktor (HDR)-blowdown experiments. Today these codes can determine realistic fluiddynamic loads on the reactor internals. The FSI-program DAISY, developed by the Gesellschaft für Reaktorsicherheit (GRS), participated with success in the validation program by pre- and postshot calculations. In consistent application of the obtained experiences with this program the complete 4 loop primary circuit of a pressure water reactor together with the core internals is simulated for the first time. This demands possibilities to model pumps and heatexchangers, the adequate description of the vessel internals and the thermodynamic states as well. Consequently the requirements to the code are much higher as for the simulation of the HDR-experiments.

Comprehensive extensions of the code concerning the behaviour of pumps under decompression waves and the determination of the stationary twodimensional flowdistribution in the downcomer region enable the coupled calculation of the fluiddynamic loads and the structural response of the vessel internals.

## THE DAISY-CODE

The calculations were performed with the GRS-code DAISY, which consists of a fluid part, the network code DAPSY, a structure part, the FE-program ASKA and a coupling interface. This interface calculates from the displacements of the structure the new volumina which are passed to the fluid part. The calculated pressures are converted into forces which are used in the structure part.

DAPSY is developed by GRS and is recently used in the licensing procedures. In the program the onedimensional equations for mass, momentum and energy are solved in Euler coordinates with the method of characteristics. The two phase flow is described with a homogeneous thermodynamic nonequilibrium model. The slip between the phases is not regarded but an additional fourth equation describes the delayed attainment of the thermodynamic equilibrium for fast dynamic transients. That means the mass equations for liquid and vapour are connected by the mass transfer rate. The flow velocity in discharge orifices or contractions is limited by the local soundspeed of the two phase mixture. 2D and 3D geometries are simulated in connecting the onedimensional flowchannels by the network-technique. By this technique the modelling is very flexible and orifices combined with pressure drops, characteristic in the downcomer of a PWR, are easy to simulate.

With the FE-code ASKA the structure of the RPV internals are modelled with the appropriate elements (shells and beams) and the stiffness, mass and damping matrices of the complete system are determined. To optimize the computation time, the number of degrees of freedom is reduced to the essential one (radial, tangential) by a static condensation. For the solution of the differential equation system for the structure an explicit central difference method without iterations is used. This method requires matrices, which depend on the time step and are determined prior to the dynamic calculation. With an elastic material behaviour these matrices need not be changed during the whole calculation.

The coupling interface obtains the displacements of the core barrel from the structure part, calculates the new volumina for the downcomer and transfers this to the fluid part where the new pressures are calculated. These pressures multiplied by the accompanying areas are the new loadvector for the structure part.

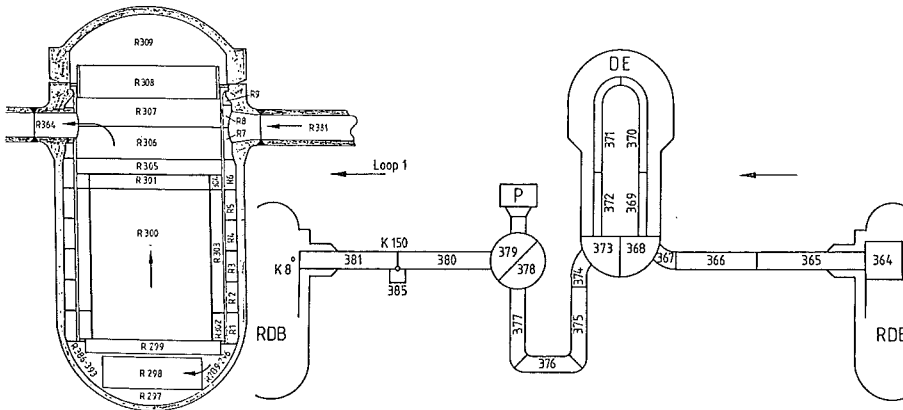


FIG. 1: FLUID MODEL OF RPV FOR DAISY FIG. 2: FLUID MODEL OF LOOP 1 FOR DAISY

MODELLING AND RESULTS

For the calculation of the loading and structural response of PWR internals in case of a blowdown the whole four loop primary circuit and the RPV (Fig. 1, 2) is modelled with 1652 fluid discretisation points. Figure 3 shows the 2D-network of the downcomer region. The blowdown assumption is a 0.1A-leak with 15 ms opening time according to the German Reaktor-Sicherheitskommission (RSK) guidelines. The RPV internals (core barrel, core shroud, core supports) are represented by 656 ASKA elements (Fig. 4). Because of the non-symmetric position of the blowdown loop and the mutual in-

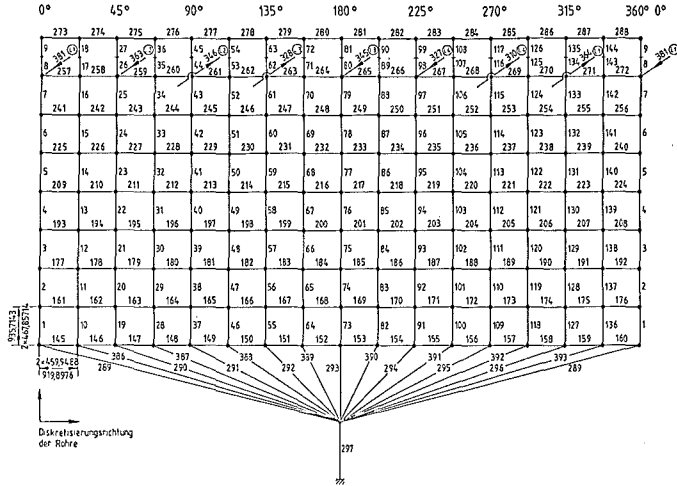


FIG. 3: FLUID MODEL OF THE DOWNCOMER FOR DAISY

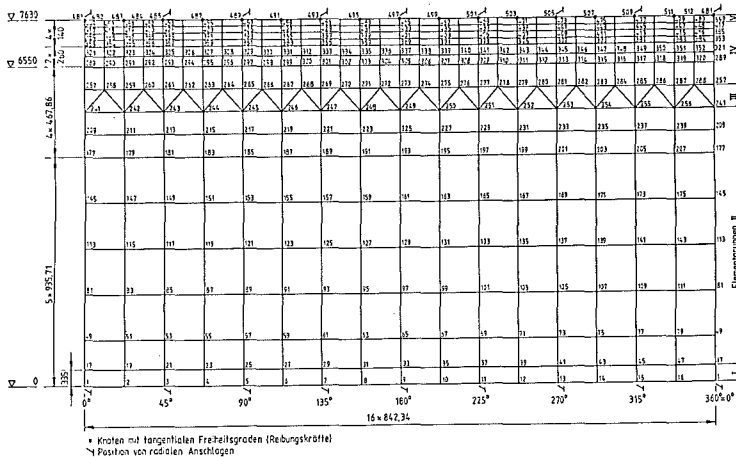


FIG. 4: STRUCTURE MODEL OF THE CORE BARREL FOR DAISY

fluence of the other three loops the whole RPV (360°) and primary system had to be modelled. A realistic computation of the blowdown implies an accurate description of the thermodynamic initial conditions. Therefore the correct reproducing of the flow conditions and pressure losses were considered to be important. The flexibility of the network technique allows the consideration of the changing cross-section in the downcomer near the nozzle-region (see Fig. 1). Furthermore the pump model was adapted to the requirements of decompression waves and a calculation for stationary flow conditions was carried out to determine the 2D-flow distribution in the downcomer region.

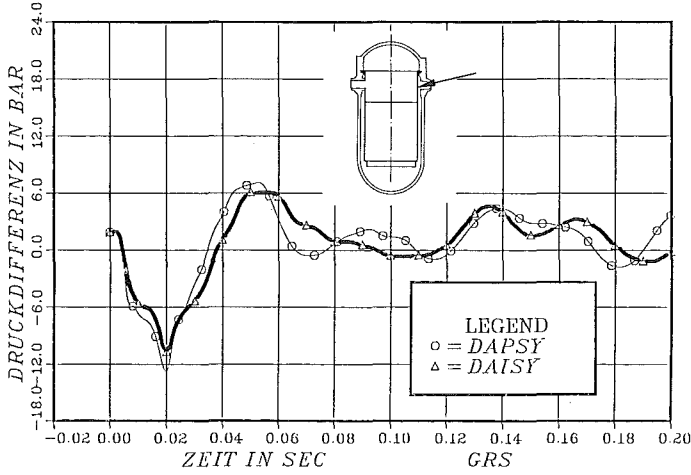


FIG. 5: PWR, 0.1A-LEAK, PRESSURE DIFFERENCE ACROSS CORE BARREL COUPLED (DAISY) AND UNCOUPLED (DAPSY) CALCULATION

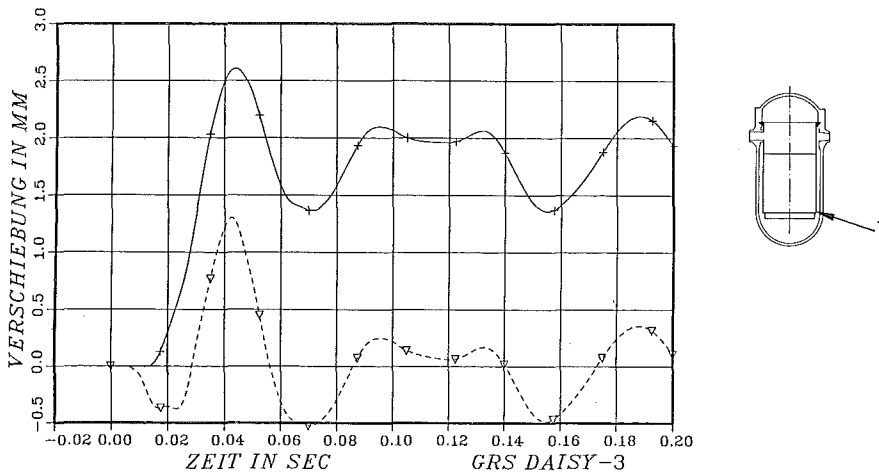


FIG. 6: PWR, 0.1A-LEAK, ABSOLUTE AND RELATIVE RADIAL DISPLACEMENT OF LOWER CORE BARREL, RELATIVE = DISPL. OF LOWER END - DISPL. OF UPPER FLANGE

Figure 5, 6 and 7 show pressure difference and radial displacements of the core barrel. The thermodynamic state of this calculation corresponds to normal operating conditions, i.e. 100 % load. The comparison between a coupled and uncoupled (DAPSY) calculation (Fig. 5), i.e. without FSI, shows a slight influence on the pressure difference across the corebarrel opposite to the blowdown loop. Because of the large stiffness of the core barrel the maximum pressure difference of 13.0 bar decrease only to 10.5 bar in the coupled DAISY-calculation. This loading results in a maximum radial displacement of 2.0 mm at this point (Fig. 7) while the lower core support hits the core stops at 2.5 mm (Fig. 6). The core barrel flange slides 1.9 mm (gap: 7.5 mm) and stops after ca. 60 ms because the circumferential pressure field is in equilibrium (Fig. 7).

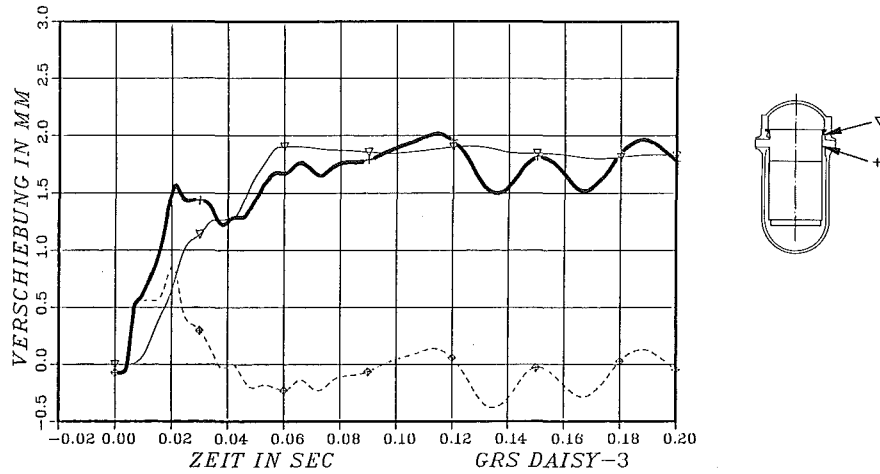


FIG. 7: PWR, 0.1A-LEAK, ABSOLUTE AND RELATIVE RADIAL DISPLACEMENT OF UPPER CORE BARREL FLANGE AND POINT WITH HIGHEST LOADS

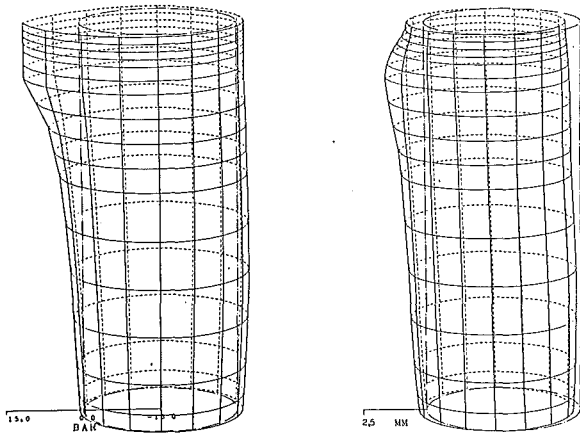


FIG. 8: PWR, 0.1A-LEAK, SPATIAL DISTRIBUTION FOR PRESSURE AND RADIAL DISPLACEMENT AT T = 20 ms

The calculated pressure- and displacement-fields of the core barrel at 20 ms and 60 ms are shown in figures 8 and 9. At these times the highest local load (20 ms, see fig. 5) and largest displacements (60 ms, see fig. 7) are reached.

The structural response on the fluiddynamic load follows nearly without delay in the flange region with local bulge (right site fig. 8) and then with sliding. The lower part with the core mass moves later. The initially nonuniform pressure field (fig. 8) reaches at 60 ms a uniform circumferential distribution (fig. 9) while the displacements due to sliding are strongly asymmetric.

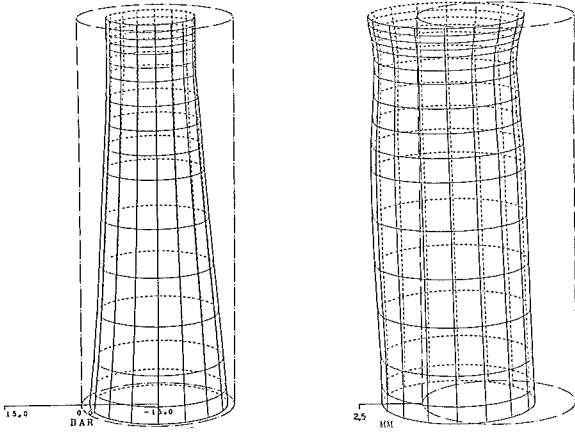


FIG. 9: PWR, 0.1A-LEAK, SPATIAL DISTRIBUTION FOR PRESSURE AND RADIAL DISPLACEMENT AT T = 60 ms

The highest stresses in the core barrel appear opposite to the break nozzle and in the flange region (fig. 10) but they are still in the elastic domain. On the other side (180° from the break nozzle) the highest axial membran stresses (fig. 11) are calculated at about 40 ms. They result from the global movement of the core

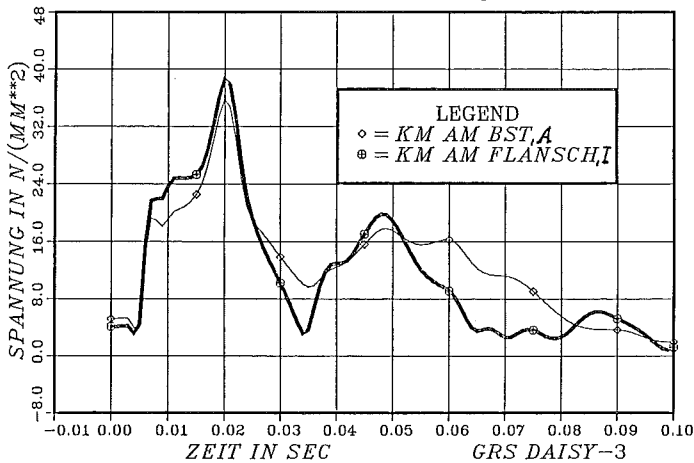


FIG. 10: PWR, 0.1A-LEAK, EQUIVALENT STRESSES IN THE CORE BARREL

barrel (fig. 6). In this analysis the flange was considered as fixed in the axial but sliding in the horizontal direction. In reality the flange is able to twist if it is axial loaded caused by an asymmetric flange support. Detailed FE analysis were performed by several institutions. They found a stress amplification factor for the outer surface of the core barrel wall in dependence of the art of flange support (clamped, fixed, loose) which varies between 3 and 10. With the highest factor a slight local plastification at the outer surface cannot be excluded which does not affect the structural integrity of the flange.

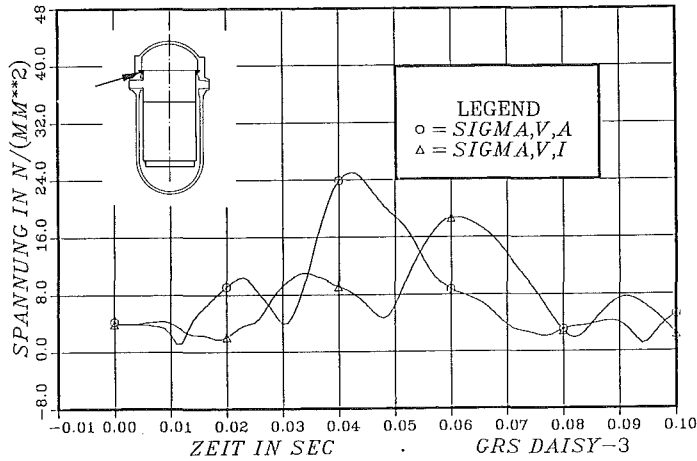


FIG. 11: PWR, 0.1A-LEAK, EQUIVALENT STRESSES IN THE CORE BARREL

#### CONCLUSION

The coupled FSI-code DAISY is able to simulate all important effects in the primary system of a PWR during a blowdown accident. This analysis includes the simulation of critical two phase flow in orifices, thermodynamic non-equilibrium states near the discharge orifice as well as the description of pressure wave propagation with structure interaction within the RPV. The application of the code to a real PWR leads in case of a 0.1 area leak to loads which do not challenge the core barrel integrity.

#### ACKNOWLEDGEMENT

This work was performed with support of the German Federal Minister of the Interior.

RETRAN PREDICTIONS FOR PRESSURE TRANSIENTS FOLLOWING  
A FEEDWATER LINE BREAK AND CONSEQUENT CHECK VALVE CLOSING

J.A. Kobussen, R. Mylonas and W.X. Zheng (\*)

Swiss Federal Institute for Reactor Research (EIR)  
CH-5303 Wuerenlingen, Switzerland

ABSTRACT

Two subroutines describing the conventional swing type and damped plug type check valve have been developed and implemented into the thermo-hydraulic transient code RETRAN. Both models have been used to simulate a postulated feedwater line rupture of the KKB PWR plant (Kernkraftwerk Beznau) and to analyse pressure responses following the closing of the check valve. The conventional undamped swing type check valve yields pressure transients that may jeopardize the integrity of the isolated part of the feedwater system. With a properly designed damped plug type check valve, the pressure peaks can be suppressed almost totally.

1.0 INTRODUCTION

The main feedwater line supplying a steam generator (SG) usually contains a check valve (CV). A function of this CV is to prevent the SG from blowing down during the event of a feedwater pipe rupture upstream of the valve.

In case of a feedwater pipe rupture, the CV should close as soon as possible, in order to allow a minimal loss of water from the SG only. On the other hand, a fast closing valve can produce severe pressure transients (water-hammer) in the feedwater line between the SG and the CV. These pressure transients can potentially lead to violation of the isolated part of the feedwater system. To overcome this problem, it has been suggested that the use of a damped CV can diminish the severity of the pressure transients /1-3/.

Since no models in RETRAN /4/ are available that accurately can predict the closing time of a CV under reverse flow conditions, two models have been developed and implemented in RETRAN. The first model describes a conventional swing type CV that may close and open. The dynamics of this valve is described by an inhomogeneous second-order linear differential equation. The second valve model describes a damped plug type CV. The damping term in the equations of motion for the valve piston is proportional to the velocity squared. The proportionality factor may be a function of piston position. It allows an increased damping when the valve is almost closed. Both CV models have been tested with a RETRAN model describing a postulated feedline rupture at one of both Westinghouse designed KKB plants (Kernkraftwerk Beznau) in Döttingen, Switzerland, that is run by the utility NOK (Nord-Ostschweizerische Kraftwerke). The results for the swing type CV have been compared with earlier NOK results obtained with the ITCH-MULTIFLEX code /5/.

2.0 THE RETRAN SIMULATION MODEL

RETRAN-02 is a thermal hydraulic code that can be used in the best estimate analysis of light water reactor systems. It is based on a homogeneous one-dimensional hydrodynamic model and describes a piping network by dividing the

\* present address: Institute of Nuclear Energy Technology, Tsinghua University, P.O. Box 1021, Beijing, China



system into a series of control volumes. The control volumes are connected by flow paths called junctions. Components can be placed at either control volumes or junctions.

Both Beznau PWR plants are almost identical in construction and equipped with two SG which both are supplied with feedwater (FW) through the main feedwater line (MFL). The MFL has two loops that meet each other in a mixing section. In each loop a CV is built in to prevent the SG from blowing down after a MFL break. For the present analyses a MFL break is postulated in one of the loops near the mixing section. To analyse the pressure and mass flow transients in this loop with the RETRAN code, the following assumptions were made.

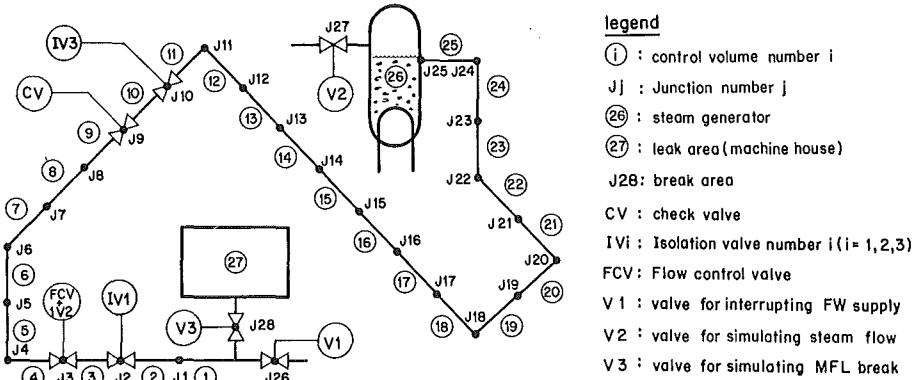


Figure 2-1: RETRAN nodalization scheme for analysing CV closure transients

- The SG is represented as one control volume with Wilson's bubble rise model built in and a constant internal heat production ( representing the primary system) of 814.2 MW and a constant vapour outflow of 359.33 kg/s. The pressure in the SG is assumed to be 6.89 MPa.
- No heat transfer occurs from the environment during the transient.
- The initial flow rate is 359.33 kg/s with a specific enthalpy of 514.2 kJ/kg.
- At the beginning of the transient, a double ended pipe break is assumed. This break is represented as two valves V<sub>3</sub> and V<sub>1</sub> which are opened/closed with a ramp function with a raising time of 1 ms. The break cross sectional area is assumed to be equal to 0.114 m<sup>2</sup>.
- In the loop, three isolation valves (IVi) and one feedwater control valve (FCV) are built in. During the transient the IV are assumed to remain fully open. The FCV remains in a half-open position.
- The total length of the piping between SG and broken end is 60.9 m. The CV is located at a distance of 21.2 m from the broken end.

Based on above assumptions a proper RETRAN input model has been developed. The model can be used for calculations for both the conventional swing type CV and the damped plug type CV when appropriate CV parameters are supplied to the relevant CV routine. A nodalization scheme of the RETRAN input model is given in Figure 2-1.

### 3.0 MODEL FOR THE CONVENTIONAL SWING TYPE AND THE DAMPED PLUG TYPE CV

A conventional swing type CV consists of a disc (or door) in a flow channel and can (under influence of gravity and fluid forces) rotate around a rotation axis to vary the effective flow area in the flow channel. For a flow into the positive direction the valve disc is raised to enlarge the valve opening area. Under influence of gravity and of reversed flow forces, the motion of the valve disc is reversed.

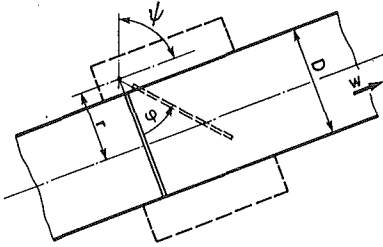


Fig. 3-1: Conventional swing type CV

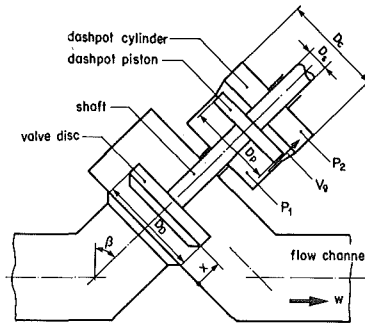


Fig. 3-2: Damped plug type CV

With the assumption of decoupling of the dynamical equations for the fluid and for the valve disc, the influence of the position of the disc on the fluid motion is fully described by the effective opening area and the pressure drop across the valve. In principle they can be measured under stationary conditions and may depend on the flow direction. In Figure 3-1 a scheme of the physical model for the conventional swing type CV is given. The angular form of Newton's equation of motion is:

$$J \cdot \ddot{\phi} + K \cdot \dot{\phi} = M \quad (1)$$

$$\text{where } M = -A \cdot r \cdot \Delta P_v - m \cdot g \cdot r \cdot \cos(\phi - \psi) \quad (2)$$

and

- A : valve disc area
- r : distance of geometrical center of the disc to its rotation axis
- ψ : angle of the feedwater line to the vertical
- φ : angle of the disc relative to the closed position
- K : linear damping factor
- g : gravitational acceleration
- J : inertial momentum of disc, relative to its rotation axis
- m : mass of the disc

The second term in Eq. 1 represents a linear damping term that might be present. The first term in Eq. 2 is due to the pressure differential  $\Delta P_v$  across the valve. The second term represents the torque due to the weight.

In Figure 3-2 a model for a (non-linearly) damped plug type valve with dashpot is given. The allowance (or gap area) between the dashpot cylinder and the dashpot piston depends on the disc position  $x$ . For an almost closed valve ( $x$  small) the gap area is small yielding a strong damping. In case the valve is almost completely open ( $x$  large), the gap area is large, yielding an almost undamped valve behaviour. The total force on the moved mass (valve disc, valve shaft and dashpot piston) then has four terms due to the weight, to the

atmospheric pressure, to the pressure difference across the valve disc and due to the pressure difference across the dashpot piston. Assuming the fluid in the dashpot is incompressible, the flow is stationary and the shaft diameter is negligibly small, the following equation of motion can be established:

$$m \cdot \ddot{x} = f; \quad f = -G - \frac{\alpha}{2} \cdot \dot{x} \cdot |\dot{x}| \quad (3)$$

$$\text{where } G = \Delta P_v \cdot A_D + m \cdot g \cdot \cos(\beta); \quad \alpha = \xi_g \rho_D A_D^3 / (A_C - A_D)^2 \quad (4)$$

and

- x : position of valve disc, relative to the closed position
- $A_D$  : valve disc area
- m : total moved mass (shaft, piston and disc)
- g : gravitational acceleration
- $\beta$  : angle of shaft to the vertical
- $\xi_g$  : pressure loss coefficient for flow through the allowance between dashpot cylinder and piston
- $\rho_D$  : density of fluid in dashpot
- $A_D$  : dashpot piston cross sectional area
- $A_C$  : internal dashpot cylinder cross sectional area

Based on the Eqs. 1 and 3 two subroutines have been developed and implemented into the RETRAN code. Assuming M is a constant during a RETRAN time step, Eq. 1 is solved analytically. Eq. 3 is solved numerically during each RETRAN time step (see /6/). The coupling between the CV subroutines and the RETRAN code is as follows. RETRAN provides the subroutine the proper variables to calculate the torque M or force f. The subroutine, on the other hand, provides the value of the angle  $\phi$  or lift x to the RETRAN code. This enables RETRAN to calculate the junction area (area-angle or area-lift table) that enters directly into the momentum equation for the fluid.

#### 4.0 RESULTS FOR THE CONVENTIONAL SWING TYPE CHECK VALVE

For the conventional swing type CV actually built in in the KKB plant, the following quantities were determined:

- maximum opening angle 0.87 rad (=50°)
- moment of inertia I = 6.9641 kg m<sup>2</sup>
- area moment A · r = 0.0402 m<sup>3</sup>
- angle of flow channel to the vertical  $\psi = \pi/2$  rad (= 90°)

Using these data, the swing type CV model and the RETRAN simulation model of Figure 2-1, a transient analysis has been performed. The results are summarized as follows:

After rupture of the feedwater line (upstream of the CV) a decompression wave propagates from the rupture to the SG. The SG acts as a constant pressure boundary condition (fixed end), such that the pressure wave reflects at the SG with an inversion of its phase. The result is a compression wave that travels back to the break. At the break this wave reflects again to strike the check valve which closes soon after that (110 ms after break).

Simultaneously and parallel to the pressure wave a mass flow wave propagates from the break into the direction of the SG. This mass flow wave reflects at the steam generator without phase inversion and travels further with doubled amplitude into the direction of the break. When the wave hits the CV, the reversed mass flow closes it.

After closing of the valve, the mass flow through the valve is stopped abruptly. As a consequence, the kinetic energy of the flow is transformed into

pressure energy. The result is a damped standing pressure wave between the closed CV and the SG. The magnitude of the first pressure peak is 16.71 MPa. The numerical results show a good agreement with results obtained with the ITCH-MULTIFLEX code.

In the Figures 4-1 through 4-3 the disc position, its closing velocity and the torque on the disc are given as a function of time. The disc position and the torque on the disc are compared with results from the ITCH-MULTIFLEX code /5/. For more details see /6/

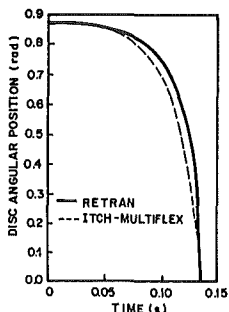


Fig. 4-1: Angular position of CV disc as function of time

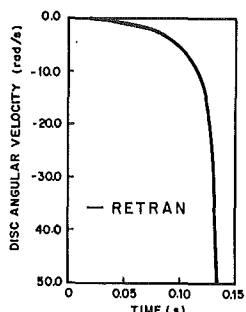


Figure 4-2: Angular velocity of CV disc as a function of time

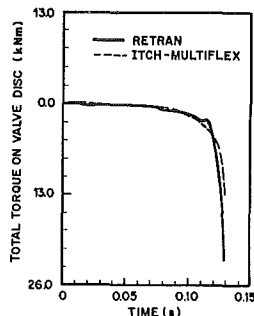


Figure 4.3: Torque on CV disc as a function of time

## 5.0 PARAMETRIC STUDIES FOR THE SWING TYPE CHECK VALVE

Some system parameters used in the transient analyses do contain several uncertainties. Therefore parametric studies have been carried out to specify the influence of these uncertainties on the transient. The results of these studies are summarized in Table 5-1 and discussed below.

### 5.1 Inertia and Form Loss Coefficient of the Check Valve

It can easily be demonstrated that the valve dynamic behaviour during a transient is mainly affected by the form loss coefficient and the inertia of the valve. Unfortunately, an exact value of the valve inertia could not be obtained from the valve drawings. Furthermore, the reverse form loss coefficient of the valve remains unknown. Consequently, it is necessary to investigate the influences of these uncertainties on the transient.

Case 1,2,3 and 4 of Table 5-1 show the effects of the valve inertia on the valve closing time and on the pressure peaks. The influences of the reverse form loss coefficient of a valve on the transient are given by case 2,5 and 6. One observes that a larger form loss coefficient and a smaller inertia of a check valve will cause the valve to close earlier and this, in turn, will more or less reduce the pressure peak because the reverse flow through the valve has not fully developed at the moment when the valve closes completely. On the other hand, it is also seen that the form loss coefficient and the inertia of a CV have greater influence on the valve closing time than on the magnitude of the pressure peaks. In other words, the pressure peaks following a CV slam are less sensitive to the form loss coefficient and inertia of the valve.

### 5.2 The Pipe Break Time

For safety analyses one usually assumes an instantaneous double ended guillotine break. For the present analyses, the instantaneous break has been mo-

delled by assuming a junction area that, up to the full open area, increases linearly in time. The time passed between the begin of the break and the moment where the full open area has been achieved - the break time - was set equal to 1 ms. A more realistic value, however, might be 20 ms. In order to see how sensitive this break time is for the magnitude of the pressure peaks to be expected after the CV slam, three different break times have been considered: 1 ms (case 2), 20 ms (case 7) and 200 ms (case 8). From the results it is seen that the pipe break time in the given range will affect the valve closing time, but it has not much influence on the magnitude of the pressure peaks.

Case	$I^*$	$\xi_v^*$	$t_{br}$	$\xi_f(3)$	$\xi_r(3)$	$A_{eff}$	$t_{cl}$	$P_{max}$
1	0.5						110	16.71
2	1.0	0.4	1	12.38	30.95	0.0418	134	17.37
3	2.0						178	17.17
4	4.0						228	17.18
5							150	17.99
6		1.0					115	16.73
7	1.0	0.4	20				136	17.75
8			200				144	17.31
9					12.38			130
10			1	2.27	3.41	0.1143	126	25.52

Legend:  $I^*$  : normalized disc inertia (-)  
 $\xi_v^*$  : ratio of reverse and forward form loss coeff. of CV (-)  
 $t_{br}$  : pipe break time (ms)  
 $\xi_f(3)$  : forward form loss coefficient junction 3 (FCV + IV) (-)  
 $\xi_r(3)$  : reverse form loss coefficient junction 3 (FCV + IV) (-)  
 $A_{eff}$  : effective flow area FCV (m<sup>2</sup>)  
 $t_{cl}$  : closing time of CV (ms)  
 $P_{max}$  : highest pressure peak after CV closure (MPa)

Table 5-1: Results of parametric studies for the swing type CV

### 5.3 Flow Restriction on the Feedwater Line

In the KKB plant, a flow control valve (FCV) is fitted into the main feedwater line. A quite large pressure drop across the FCV has been found in the NOK supplied documents. This suggests that the FCV might play a role of a flow restriction during a blowdown transient. However, uncertainty in the pressure loss across the FCV is encountered once again. In particular, the reverse form loss coefficient is unknown.

Three cases considered for the FCV flow resistance are shown as cases 2, 9 and 10 in Table 5-1. Case 9 represents the situation where the reverse form loss coefficient of the FCV is set equal to the forward form loss coefficient. Case 10 represents the situation without FCV fitted into the feed line. For

both cases the reverse flow will develop more rapidly and reach a higher value just before the CV closes. As a result, the CV will close earlier and produce higher pressure peaks.

#### 6.0 RESULTS FOR THE DAMPED PLUG TYPE CHECK VALVE

For the damped plug type CV the following quantities were adopted:

disc area	A	= 0.1018 m <sup>2</sup>
moved mass	m	= 70 kg
max disc lift	x <sub>max</sub>	= 0.13 m

The damping parameter  $\alpha$  as a function of disc position  $x$  (damping characteristics) is given in Figure 6-1. The values of  $\alpha_1$ ,  $\alpha_2$ ,  $x_1$  and  $x_2$  have been subject of a parametric study.

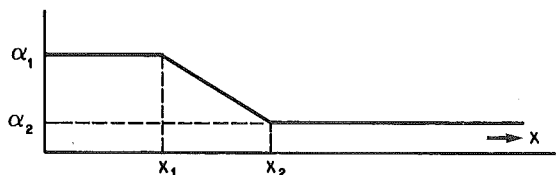


Figure 6-1: Damping characteristics of the damped plug type CV

A survey of the calculations and the most important results (closing time and pressure peak) are given in Table 6-1 and discussed below. A graphical representation of some of the results is given in Figures 6-2 and 6-3. The calculation designed as case 1 is considered as the reference case. With the assumed valve data a valve closing time of 350 ms and a pressure peak of 9.7 MPa was found.

#### 6.1 Influence of the Damping Parameter (cases 2,3,4 and 5)

To see the influence of the region of weak damping, one calculation has been performed for which the damping parameter was taken constant over the entire range of the disc travel (case 2) and equal to the value for case 1 in the region of weak damping. The result is an almost undamped fast closing valve. A closing time of 100 ms and a pressure peak of 15.8 MPa was found. This pressure peak is not as high as found for the swing type check valve (section 5, case 1) due to the faster closing of the valve.

For the calculations indicated as cases 3 and 4, the damping parameter (region of strong damping) has been decreased. The result is a shorter valve closing time, and consequently higher pressure peaks. An increased damping for the region of weak damping (case 5), on the other hand, enlarges the valve closing time slightly and consequently slightly higher pressure peaks are predicted.

#### 6.2 Influence of the Damping Characteristic (cases 6,7,8,9 and 10)

The damping characteristic of the damped valve is not only determined by the values  $\alpha_1$  and  $\alpha_2$ , but also by the transition points  $x_1$  and  $x_2$ . With smaller values of  $x_1$  and  $x_2$  the dashpot piston enters into the region of strong damping later. Because the early phase of the valve closing process does not influence considerably the mass flow through the valve, an early entering into the region of strong damping causes a later closing of the valve without diminishing the pressure peaks. On the other hand, if the valve enters into the region of strong damping too late, the valve will slow down more abruptly. This

Parameter-Table with :  $0 \leq x \leq x_1 \rightarrow \alpha = \alpha_1$  ;  $x_2 \leq x \leq x_{\max} \rightarrow \alpha = \alpha_2$   
 $x_{\max} = 130 \text{ mm}$  ; initial pressure = 7.1 MPa

case Nr.	$x_1$ mm	$x_2$ mm	$\alpha_1$ $10^6 \text{ kg/m}$	$\alpha_2$ $10^3 \text{ kg/m}$	closing time ms	pressure peak MPa	
1	40	55	38.7	0.42	350	9.7	reference case
2	--	0	--	0.42	100	15.8	almost no damping
3	40	55	19.3	0.42	266	11.2	decreased SD
4	40	55	3.87	0.42	160	14.7	decreased SD
5	40	55	38.7	4.2	358	10.3	increased weak damping
6	25	40	38.7	0.42	262	13.9	smaller region of SD
7	25	40	193.0	0.42	490	12.5	as case 6, increased SD
8	50	65	38.7	0.42	424	8.49	larger region of SD
9	50	65	19.3	0.42	324	9.6	as 8, decreased SD
10	60	75	38.7	0.42	536	8.48	very large region of SD
11	As Case 1, but no FCV				341	12.7	
12	As Case 8, but no FCV				400	10.7	

Table 6-1: Parametric study for damped plug type CV (SD = strong damping)

in turn might cause higher pressure peaks. The calculations, indicated as cases 6, 8 and 10 indeed show this behaviour. For case 8, where  $x_1 = 50 \text{ mm}$ , obviously an optimal situation has been reached. A closing time of 424 ms and a pressure peak of 8.49 MPa was obtained. A value of  $x_1 = 60 \text{ mm}$  (case 10) influences the pressure peak only slightly (8.49 MPa instead of 8.48 MPa) whereas the closing time is enlarged considerably (536 ms instead of 424 ms). Smaller values of  $x_1$  (case 1 and 6 with  $x_1 = 40 \text{ mm}$ , and  $x_1 = 25 \text{ mm}$ , respectively) yield higher pressure peaks. The cases 7 and 9 have been calculated to see, in comparison with case 6 and 8, the influence of the damping parameter  $\alpha_1$ . As expected a higher/lower value of  $\alpha_1$  yields a larger/shorter closing time and lower/higher pressure peaks.

### 6.3 Flow Restriction on the Feed Water Line (cases 11 and 12)

The aim of the calculation case 11 and 12 was to determine the influence of the FCV when simulating a damped valve in the feedwater line. The calculation of the reference case 1 and of the optimal case 8 were repeated with the assumption of no FCV being in the feedline. For case 1 the closing time reduces slightly from 350 to 341 ms. The pressure peak increases from 9.7 to 12.7 MPa. Similar results were obtained for case 8. The closing time of the CV reduces from 424 to 400 ms and the pressure peak increases from 8.49 MPa to 10.7 MPa.

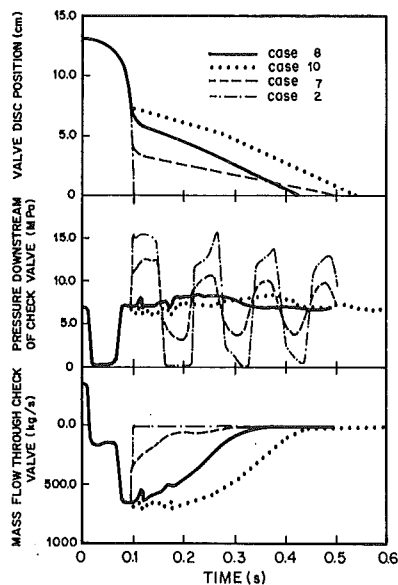


Figure 6-2: Dynamic response to CV closure for the cases 2, 7, 8 and 10

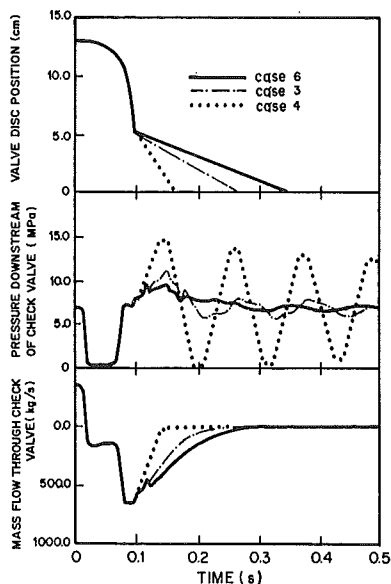


Figure 6-3: Dynamic response to CV closure for the cases 3, 4, and 6

## 7.0 SUMMARY AND CONCLUSIONS

Two subroutines describing the conventional swing type and damped plug type CV have been developed and implemented into the thermo-hydraulic transient code RETRAN. Both models have been used to simulate a postulated feedwater line rupture of the KKB PWR plant and to analyse pressure responses following the closing of the CV. The results obtained with the undamped swing type CV have been compared with results obtained with the ITCH-MULTIFLEX code. The main conclusions are listed below.

- The RETRAN calculations performed with the conventional swing type CV, as actually built in in the KKB plant, show a good agreement with results obtained with the ITCH-MULTIFLEX code.
- For the postulated feedwater line rupture both codes predict a valve closing time of 134 ms and pressure peaks after closing of 17 MPa. These pressure peaks may jeopardize the integrity of the isolated part of the feedwater system.
- The assumption of an instantaneous rupture is neither conservative nor non-conservative. Even with an unrealistic large break time of 200 ms the magnitude of the highest pressure peak remains almost unchanged.
- For accurately predicting the pressure responses, the reversed mass flow after the break should be calculated correctly. For that reason it is inevitable to have reliable values of the pressure loss coefficients of all fitting in the feedwater line for reversed flows.



The damped plug type CV considered in the present analyses has two different damping regions. If the valve is almost completely opened (large lift of the valve piston) there is only a small damping. If the valve is nearly closed (small lift of the valve piston) the damping is very strong. In both regions a constant damping parameter is assumed. In the transitional region the damping parameter is interpolated linearly. The main conclusions that could be drawn from the analyses with the damped plug type CV can be summarized as follows:

- During the first phase of closing, whereas the valve damping is small, the closing process does not influence the mass flow, nor the pressure peaks after closing.
- There exists an optimal value of the lift of the valve piston at which the valve enters into the region of strong damping. With this optimal value, the pressure peaks after closing can be suppressed almost completely.
- Larger values of the damping parameter for the region of strong damping yield longer closing times and lower pressure peaks after closing.
- When the valve enters into the region of strong damping earlier than in the optimal situation, longer closing times and unchanged pressure peaks are predicted.
- When the valve enters into the region of strong damping later than in the optimal situation, shorter closing times and higher pressure peaks are expected. These higher pressure peaks cannot or only scarcely be suppressed by higher values of the damping parameter.

#### 8.0 REFERENCES

- /1/ E.B. Pool, H.B. Brinkman: Nuclear containment of postulated feedwater linebreak. Flow line, 1978, No.3, Rockwell International, Flow control Division, Pittsburg PA 15208, USA
- /2/ T. Grillenberger, W. Ch. Mueller, W. Winkler: Vergleich zwischen Vorausrechnungen und HDR experimenten, Uebersicht zu den deutschen Standardproblemen Nr. 4 und Nr. 4a: 5. Statusbericht des Projektes HDR-Sicherheitsprogramm des Kernforschungszentrums Karlsruhe, PHDR Arbeitsbericht 5/8/81, (Dezember 1981)
- /3/ K. Grotloh: Verhalten von Dampfsolventil und Speisewasserrueckschlagventil in Kernkraftwerken beim Bruch der Reaktor-Kuehlmitteleitung. Technische Rundschau Sulzer 2/1980, P 48-52
- /4/ J.H. McFadden et. al.: RETRAN-02 - A Programm for Transient Thermal-Hydraulic Analysis of Complex Fluid Flow Systems. Electric Power Research Institute, EPRI-NP-1850-CCM, Palo Alto, CA (May 1981)
- /5/ NOK Feedwater System Requalification Programm, Hydraulic Transient Analysis of Check Valve Slam Event, NOK 354-D2 (Oct. 1982)
- /6/ J.A. Kobussen, R. Mylonas, W.X. Zheng: Check Valve Closure Transients and the RETRAN Code, Proceedings of the 3rd International RETRAN Meeting, Las Vegas, NV, 9-11 April 1984, to be published.

REACTOR FAULT SIMULATION AT THE CLOSURE OF THE  
WINDSCALE ADVANCED GAS-COOLED REACTOR: ANALYSIS OF TRANSIENT TESTS

J.A.Desoisa and C.P.Greef

Central Electricity Generating Board  
Berkeley Nuclear Laboratories, Berkeley,  
Gloucestershire, GL13 9PB, ENGLAND

ABSTRACT

The closure of the Windscale prototype advanced gas-cooled reactor (AGR) offered a unique opportunity to test fault study calculational methods under extreme conditions, relatively unfettered by economic constraints. Three major types of experiment were carried out: fast reactivity transients from very low to near full power, large amplitude reactivity ramps at power and gas circulator trip experiments. Preliminary modelling of the more extreme tests using the CAGR fault study code has previously demonstrated agreement to within 5-10% in both power and temperature transients. More refined analyses have now been completed. These take account of detailed fuel stringer geometry and certain transient effects, have enabled uncertainties to be quantified and have led to further increased confidence in the computer model.

INTRODUCTION

Computer codes to simulate reactor behaviour in a postulated fault play an important part in the safety cases for Commercial Advanced Gas-Cooled Reactors (CAGR's) in the U.K. Testing the adequacy of these fault study codes is a continuing process, helping to increase confidence in the safety case and potentially enabling increases in power output to be achieved. A great deal of relevant testing can be carried out with analytical and computer studies and by comparison with laboratory experiments. However, the direct simulation of fault sequences on a commercial reactor is clearly excluded on safety grounds and the scope for any type of measurement on commercial plant is severely restricted by economic constraints.

The closure of the prototype AGR at Windscale (WAGR) therefore offered a unique opportunity to test fault study methods under conditions well beyond those experimentally and economically achievable on commercial reactors and an experimental programme which included a comprehensive series of reactor transient tests was jointly funded and performed by the Central Electricity Generating Board, the South of Scotland Electricity Board and the United Kingdom Atomic Energy Authority.

A detailed description of the execution of these tests and preliminary analysis has been reported [1]. This work demonstrated in general terms the

adequacy of the fault study code KINAGRAX [2] used in the analysis of the experimental data. Subsequently a more detailed and comprehensive analysis has been undertaken in an attempt to quantify the uncertainties in the code. This has involved the modelling of several features of the experiments not considered in the preliminary analysis and sensitivity studies for the more important input parameters of the computer code. It is this work that is reported in this paper.

#### EXPERIMENTAL MEASUREMENTS

The planning and execution of the experiments have been described in some detail elsewhere [1]: only the main points are given here.

The WAGR has a thermal output of 100 MW compared with about 1500 MW for CAGR. The reactor cores are very similar, with the same configuration of re-entrant flow passages and almost identical fuel pins supported in similar grids and braces. Fuel ratings and temperature distributions throughout the reactor core are comparable. The major distinction concerns the fuel stringer: the WAGR stringer has four elements each of nine fuel pins in a single ring whereas the CAGR stringer has eight elements with 36 pins in three rings.

The experiments were designed to simulate the major characteristics of CAGR pressurised faults. Three types of transient were investigated to test the performance of the computer code over the range of relevant conditions.

Fast symmetric reactor power transients were initiated from low power (down to 200 watts) up to near full power by withdrawing the bank of 18 in-line control rods uniformly across the reactor core. Measurements were carried out at two flow rates, from different power levels and, in successive tests, with increasing reactivity additions to produce a minimum neutron flux doubling time of 2.3 seconds in the most extreme case. The objective of these measurements was to simulate the rapid flux rise time associated with uncontrolled start-up reactivity faults.

At-power reactivity transients were also carried out, starting from a number of initial power and flow levels. In the most extreme of these tests, starting from an initial state of 72 MW and 57% flow, peak recorded fuel can temperatures of 1000°C were achieved at a power of 130 MW (i.e. 130% full power). This was well in excess of the corresponding full power operating temperatures (800 - 850°C) although for economic reasons it was not possible to extend the tests to the temperatures postulated for the severest CAGR faults (around 1100°C).

The third main category of experiment was the gas circulator trip tests. In these, all four main gas circulators were tripped simultaneously with the result that the gas flow fell over a timescale of a few tens of seconds to 15% full flow at which level pony motors automatically operated to maintain that flow. Temperatures initially rose and were ultimately stabilised by the combined effects of the negative fuel temperature reactivity feedback and the pony motors. In addition to these three major types of test, comprising some 35 transients in all, subsidiary measurements were made to provide values of control rod slope and fuel temperature coefficient of reactivity required for the analysis. The rod slope was determined from conventional low-power doubling and halving measurements, the results being used directly in the analysis. The fuel temperature coefficient was determined by the dynamic technique applied successfully to CAGR's [3], the measurements in this case

being used simply to verify the values derived theoretically from reactor physics lattice codes.

Extensive reactor instrumentation was available in WAGR for recording reactor behaviour, including coolant gas and fuel can thermocouples, gas flow recorders, and in-core and ex-core neutron flux chambers. Arrangements were made for the computerised logging of all the relevant data at appropriate sampling rates.

#### METHOD OF ANALYSIS

The computer code upon which CAGR fault studies are largely based is KINAGRAX [2] and accordingly it is with this code that the experiments have been analysed. The KINAGRAX calculation is for a single fuel channel representation of average reactor transient behaviour, including fuel and moderator temperature reactivity feedback. A one-dimensional single energy group neutron diffusion equation is used to determine the axial rating distribution. This is coupled to a thermal hydraulic calculation which models the various heat transfer processes between fuel pins, coolant flows and moderator components and provides radial temperature distributions at each axial plane in the calculation (see Fig. 1). In addition, provision exists for the modelling of two specific reactor channels in which the thermal hydraulic calculations are driven by the flux in the average channel enhanced by user specified multipliers to give the required initial channel powers and in which the coolant flow rates may be different from the average channel.

The thermal hydraulic data used in the analysis have been obtained from previous WAGR investigations and prepared according to CAGR recommended methods. This was to ensure that the use of the computer code in the experimental analysis was fully consistent with its use in CAGR fault studies (except that some items of data are deliberately pessimised in fault studies, whereas best estimate data were used throughout in the WAGR analysis).

The nuclear data were in general obtained from lattice calculations averaged to a mean core irradiation of 10.5 GWD/Te on the assumptions of fuel cycle equilibrium and a flat radial flux. Where necessary the data were also axially averaged using the flux shape appropriate to the mean position over fuel life of the bank of eighteen in-line control rods.

The fuel temperature coefficient measurements spanned a range of mean fuel temperatures from 400 - 800°C and gave agreement to within about 5% (1 $\sigma$ ) with lattice calculations, allowing the use of calculated coefficients for the higher fuel temperatures reached in some experiments. Likewise, the modelling of the measured control rod slope in KINAGRAX led to a total uncertainty in rod worth of 5% (1 $\sigma$ ) for the range of transients of interest. The axial flux shapes input to KINAGRAX were obtained from an extensive correlation of measured flux shapes (from wire plots) as a function of rod insertion: the error in this data was 3% (1 $\sigma$ ) relative to mean.

Certain features of the experiments were not modelled in the preliminary analyses reported previously [1] but have been included here because they have a measurable effect on the predictions.

Firstly, it was necessary to modify KINAGRAX to model the central graphite tie tube (Fig. 1) whose thermal inertia is very large compared with the corresponding CAGR tie bar which is not modelled. The effect of the tie tube, which is to retard the response of temperatures to power and flow changes, is most

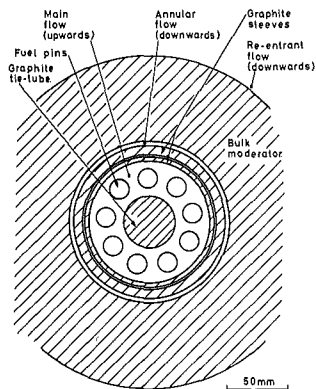


FIG. 1. Plan of WAGR Fuel Cluster as Modelled by KINAGRAX.

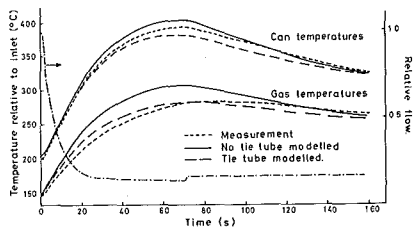


FIG. 2. Circulator Trip Test - Temperature Transients.

clearly seen in the circulator trip tests (Fig. 2): the initial rate of rise of temperature is reduced as heat is absorbed in the tie tube and similarly the reduction in temperature following flow stabilisation is slowed down, with the tie tube now acting as a heat source.

Can temperatures were measured by thermocouples mounted in thick-walled cans having the same outer diameter as standard cans and so containing a smaller volume of fuel of higher enrichment in order to maintain linear fuel rating. The KINAGRAX model was extended to predict dynamic effects associated with the thicker cans (1.9 mm compared with the standard 0.4 mm) as well as the temperature drop through the can, taking account of the small rating mismatch that developed with irradiation. In practice, none of these effects alone was greater than about  $10^{\circ}\text{C}$  in can temperature and, because of self-cancelling, the net effect was itself less than this.

The coolant flow through the reactor core was significantly influenced by gas temperature changes during the transients: in the most extreme case, a transient from low to high power involving a large increase in gas temperature, the flow reduced by 13% by the peak of the transient. This effect was not modelled in preliminary analyses, but has been incorporated now, calculating the flow variation from the experimental record of core pressure drop and coolant temperature, and inputting this variation as a boundary condition to KINAGRAX. In consequence, the calculated temperatures have increased but not as much as in inverse proportion to the flow decrease because of the negative fuel temperature reactivity feedback.

#### RESULTS OF SIMULATIONS

About one half of the 35 major transients has been simulated with KINAGRAX. In each case calculated powers have been compared with measured fluxes from logarithmic and linear chambers, and calculated can and coolant temperatures with measurements from four different instrumented fuel stringers, encompassing a range of power level, flow rate and axial location of can thermocouples. Sensitivity studies have also been carried out on a few selected transients, varying the principal input parameters of the computer code to assess the effect of uncertainties in the parameters. The sensitivity studies are presented in the

next section and here the main results are discussed, using in general the most extreme transient of each type as an illustration.

### Start-up Transients

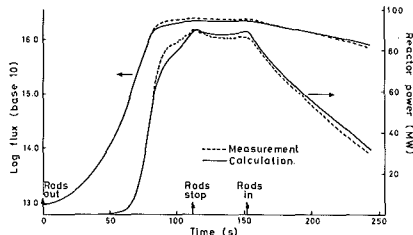


FIG.3 Start-Up Transient - Log and Linear Powers.

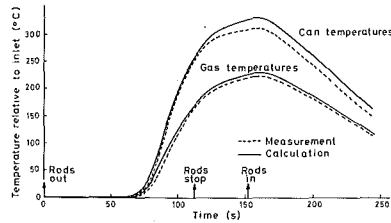


FIG.4 Start-Up Transient - Temperature Transients.

Figures 3 and 4 show results obtained for a transient at full flow, starting at 38 kW reactor power and rising to a peak of 91.7 MW, with a reactivity addition of 523 mN ( $\beta_{0.75}$ ). The initial reactor power for the calculation was determined from the log chambers, so the log fluxes in Figure 3 are effectively normalised at the start. The linear power chambers were reliable only as an indicator of relative power, hence in this case measurement has been normalised to calculation at the peak to emphasise the shape of the transient in the region where feedback becomes operative and the control rods stop, pause and then reinsert. The temperatures in Figure 4 are from one of the four channels analysed: the flow rate for this channel was determined by the position of the coolant gag at the channel outlet, and the channel power was obtained from high power steady state reactor surveys of channel gas outlet temperatures, assuming that the power distribution did not change significantly with reactor power.

The excellent agreement in power in the early part of the transient demonstrates the accuracy of the KINAGRAX model for this type of fast, no-feedback transient and also shows that the rod slope used in the calculation has a small error: a 3% change in the rod slope produced a significant discrepancy towards the peak. The total reactivity feedback is also well predicted, since the discrepancy in peak power evident from the log flux comparison is equivalent to only a 1% error in the chamber calibration (compared with  $\sim 3\%$   $1\sigma$  assessed uncertainty) or to a 5% reduction in the fuel temperature reactivity coefficient ( $\sim 5\%$   $1\sigma$ ). That the peak power is predicted closely is also supported by the temperature comparisons (Fig. 4): for the eight comparisons available, the average discrepancy (calculation - measurement) / (measurement) at the peak of the start-up transients is  $4.5\% \pm 4.0\%$  for the gas temperature and  $4.4\% \pm 4.7\%$  for the can.

There is an interesting discrepancy occurring towards the peak of the transient, most apparent in Fig.3. It appears that, although the calculation is predicting the total reactivity feedback correctly, the rate at which it operates is different from measurement. Sensitivity studies on the calculation failed to reveal any phenomenon that could be responsible and so the discrepancy, although small in magnitude, remains unresolved.

A similar series of start-up transients was also carried out at 44% coolant flow. The principal difference from those just discussed was that, because of

the lower flow rate, the fuel temperature rise for a given power rise was greater. In consequence, the power tended to overshoot before the fuel temperature feedback became effective: in the most extreme case the overshoot in power was 35%. This was well modelled by the computer code, with no evidence of the feedback discrepancy found in the full flow transients.

A third series of start-up transients commenced at subcritical power levels (and full flow). In the most extreme of these the initial subcriticality was  $-560 \text{ mN}$  ( $-\$0.80$ ) and the reactor power 144 W. Fig.5 shows the measured and calculated temperatures superimposed on the flux doubling time throughout the transient. In this case, the main difference from the full flow critical start-up transients was the lower power at the start (or as the rods passed through the critical balance point to be precise). This meant that faster doubling times were achievable (2.3s as opposed to 4.0s for the transient of Fig.3). Again the KINAGRAX code modelled the reactor behaviour well, demonstrating its ability to handle the transition from subcritical to supercritical multiplication.

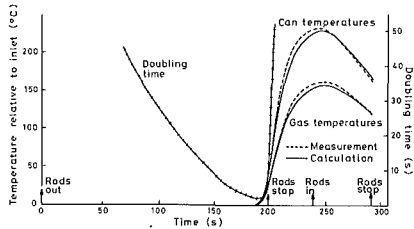


FIG.5. Sub-Critical Start-Up Transient: Doubling Time and Temperatures.

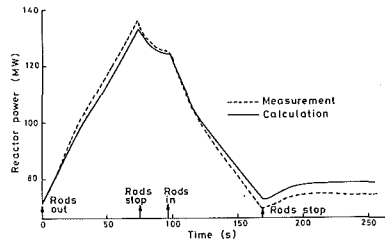


FIG.6. Reactivity Ramp at Power - Reactor Power Transient.

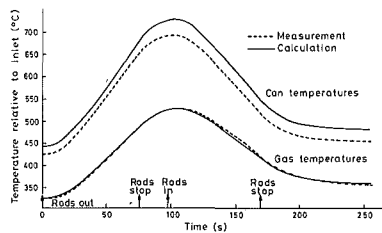


FIG.7. Reactivity Ramp at Power - Temperature Transients.

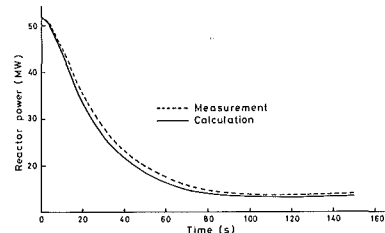


FIG.8. Circulator Trip Test - Power Transient.

#### At-Power Reactivity Transients

Figs.6 and 7 show the results of the most onerous at-power reactivity test: the reactivity addition was  $320 \text{ mN}$  ( $\$0.46$ ) and the peak can temperature achieved in the channel shown was  $994^\circ\text{C}$  (the channel inlet temperature was  $300^\circ\text{C}$ ). The initial reactor power for the calculation was obtained from a flow and temperature survey and the output from the flux chambers was normalised to this. The initial power in the individual channels modelled (Fig.7) was normalised to the channel gas outlet temperature. The results obtained (see Table) show that peak power is systematically underpredicted for the eight

transients of this type that have been analysed, but by an amount small compared with data uncertainties.

A tendency towards overprediction of the power at the end of the transient is apparent both in the at-power and start-up reactivity tests. The effect is not of direct significance to faults of the types being simulated in the tests since it is peak powers that are of interest. Nevertheless it is symptomatic of a deficiency in either modelling and data which might, in principle, be important in some circumstances. Likely contributors to this effect are therefore discussed in the next section.

The gas temperature transient (Fig.7) is essentially a reflection of the power transient and consequently the errors involved are likewise small. The can temperature, on the other hand, is influenced not only by the overall power but also by local rating and heat transfer uncertainties. Any errors due to these additional factors will result in discrepancies between measurement and calculation that persist throughout the transient, as is shown in the Figure and fairly generally in the cases examined (see also the Table, which shows the errors to be small, typically a few percent). Can temperature behaviour in a postulated fault is often crucial (an important safety limit being that the fuel cans should not melt) and so the capabilities of KINAGRAX in predicting this parameter are particularly reassuring.

KINAGRAX only calculates a mean can temperature, without cross-channel or cross pin tilts. The measured temperatures used in the comparisons are the average from two thermocouples mounted on opposite sides of the fuel cluster and on the outward facing surface of the fuel pin. Thus although cross-channel effects are eliminated, cross-pin effects are not. However, a more detailed steady state calculation modelling cross-pin tilts indicated these effects to be small, of order 2-3°C at most, so no correction has been made to the KINAGRAX values.

#### Circulator Trip Tests

Figs.2 and 8 show comparisons for a circulator trip test at high flow, the measured circulator rundown characteristic being superimposed in Fig.2 to show the operation of the pony motors. The impact of the tie bar modelling is most pronounced for this type of test, and with its inclusion the quantitative agreement between measured and predicted temperatures is broadly comparable with that for the reactivity transients. Qualitatively, however, there does appear to be a small but genuine dynamic discrepancy, unlike the reactivity transients. No satisfactory explanation of this effect has been forthcoming; the obvious possibility of an error in the measured flow transient is excluded by the virtually identical flow estimates obtained from circulator speeds and core pressure drop.

### SENSITIVITY STUDIES AND UNCERTAINTIES

The results of analyses carried out using best estimate data are shown in qualitative terms in the Figures, which demonstrate the close agreement between experimental data and the KINAGRAX predictions. The Table summarises quantitatively the results obtained for the at-power reactivity transients, and also the results from a selection of the sensitivity studies carried out to ascertain the extent to which data uncertainties contribute to the observed discrepancies between experiment and theory.



TABLE

## SENSITIVITY STUDY OF AT-POWER REACTIVITY TRANSIENTS

Time in Transient:-	Percentage Differences						
	Power		Gas Temperature		Can Temperature		
	Peak	End	Peak	End	Start	Peak	End
	Base Calculation - 4 Fuel Channels Examined						
Fuel Channel No.1	-1.6±1.1	4.0±2.5	-0.3±1.2	1.4±1.7	3.1±0.8	3.3±1.5	6.4±2.5
Fuel Channel No.2			0.9±1.4	1.8±1.8	2.6±0.6	2.7±1.5	6.4±2.8
Fuel Channel No.3			3.5±2.3	3.6±2.9	4.8±1.5	6.2±2.0	8.7±4.0
Fuel Channel No.4			3.6±2.4	4.7±3.6	-0.5±1.5	1.1±2.6	4.4±4.0
	Sensitivities to Parameter Changes						
Rod Slope x 1.05	+3.1	-0.2	+1.6	+0.6	0	+1.7	+0.9
Fuel Feedback x 0.9	+6.2	+1.6	+3.9	+2.0	0	+4.3	+2.8
Heat Transfer x 1.05	+0.5	-0.2	+0.5	-0.1	-1.7	-1.2	-1.8
Moderator Feedback x 0.5	-1.6	-4.3	-1.5	-3.9	0	-1.3	-3.4
No Xenon	-0.9	-3.0	-1.1	-1.7	0	-0.5	-2.1
Coolant Flow x 1.05 -in average channel	-0.8	-0.9	-1.5	-0.3	0	-0.9	+0.4
-in driven channel	0	0	-0.1	-0.3	+0.6	+0.2	+0.4
Fuel-can Conduct- ance x 0.5	-0.9	-1.0	-1.5	-0.8	0	-1.5	-0.4
Flux Shape Change	0	0	-0.7	+0.6	-0.3	-2.5	+0.4

Note: The normalisation of the comparisons for these tests makes the differences on power and gas temperature zero at the start of the transient.

The first part of the Table gives the results from the best estimate calculations. The numbers given are (Theory-Experiment)/(Experiment)% relative to total power or inlet gas temperature as appropriate. Four fuel channels have been analysed and the results shown separately. The first two channels are both well removed from the edge of the reactor core, neither is adjacent to a control rod channel and both have thermocouples in fuel element 3 (i.e. at about  $\frac{1}{2}$  height): the similarity in results is remarkably close. Channel number 3 is right on the core-reflector boundary and has element 2 thermocouples, and channel 4 is close to the core edge, immediately adjacent to a control rod channel and has element 1 thermocouples. The results for these two channels show somewhat larger systematic discrepancies and scatter.

The second part of the Table summarises the sensitivity studies, showing the change in the percentage differences due to the stated parameter variation. To a first approximation, adequate for the purposes of the present discussion, the changes are linear in the parameter variation and the same for all fuel channels and all the at-power reactivity transients.

The first parameter variation considered in the Table is a 5% increase in rod slope. The change has a direct effect on the peak power and consequently on peak temperatures and it is clear that the small discrepancy in the peak power prediction is well within the uncertainties in rod slope. By the end of the transient the rods have returned to their initial position, so clearly the sensitivity at this stage is very low.

The uncertainty in the fuel temperature coefficient of reactivity is about  $0.1 \text{ mN}^{\circ}\text{C}^{-1}$  in a value of  $-1.0$  to  $-1.5 \text{ mN}^{\circ}\text{C}^{-1}$  depending on mean fuel temperature. The sensitivity at the peak of the transient is, as expected, very similar to the rod slope sensitivity for the same percentage change in parameter. There is, however, a greater sensitivity at the end of the transient.

The standard deviation of the heat transfer coefficient in this fuel clus-

ter geometry is about 6%. The principal effect of variations in this parameter is on can temperature. The uncertainty in heat transfer could be responsible for a significant part, if not all, of the small systematic can temperature discrepancy.

The moderator temperature feedback coefficient used in the basic calculations was  $4.8 \text{ mW}^{\circ}\text{C}^{-1}$ . Because of the large thermal inertia associated with the moderator, the effect of any change in coefficient becomes more apparent towards the end of each transient. In fact, the power overprediction observed towards the end of all the transients investigated would be largely eliminated by halving the feedback coefficient. However, although there is a significant uncertainty associated with the coefficient, it is unlikely to be this large, and so the observed discrepancies may be due in part to deficiencies within the KINAGRAX bulk moderator temperature model.

Long term behaviour is also influenced by Xenon drift. The calculations assumed equilibrium Xenon concentration for each transient, although this was never, in fact, the case. To assess the effect of this assumption a single calculation was carried out with no Xenon modelling at all. It was deduced from this that the neglect of Xenon drift leads to only small errors.

The sensitivity of the results to uncertainties in the coolant flow rate in either the average reactor or driven channel, the fuel-to-can conductance and axial flux shape was also examined. No significant points emerge.

Sensitivity studies have also been carried out for the start-up and circulator trip tests. Limitations of space preclude their detailed discussion here but it is sufficient to note that broadly similar results emerge and to quote the overall errors on the base calculations carried out on all transients analysed (including at-power tests):

Error in peak power prediction =  $-0.4 \pm 2.7\%$   
 Error in peak gas temperature =  $1.7 \pm 4.0\%$   
 Error in initial can temperature =  $2.2 \pm 2.7\%$   
 Error in peak can temperature =  $1.4 \pm 5.0\%$

In summarising the results of the sensitivity studies, it appears that three minor unresolved systematic discrepancies have been identified. These are an anomaly in the operation of fuel temperature feedback in some start-up transients, an apparent error in long-term bulk moderator modelling and a discrepancy in transient shape in the flow transients. With these exceptions all of the errors observed in the comparisons could be explained by identified uncertainties in input data. However, the data uncertainties are small and the errors in the base calculations themselves are small, as shown above. Consequently, it may be concluded that the residual uncertainties in KINAGRAX are at a low level.

#### DISCUSSION

The modelling and data used in KINAGRAX are extensively supported by experimental and theoretical work. However, the severity of the experiments carried out on WAGR has greatly extended the range of experimental evidence available for validating fault study codes for AGR's. The high quality of the results of the comparison with KINAGRAX, therefore, further increases confidence in the adequacy of the code. In particular the scope for unforeseen effects arising in large amplitude or fast transients, that would not be apparent from previous experimental data, must be greatly reduced by the WAGR tests.

## CONCLUSIONS

The reactor transient tests carried out on the Windscale AGR have greatly extended the range of experimental evidence in support of the safety case for the CAGR's. Tests of direct relevance to postulated CAGR faults have been simulated, including fast start-up reactivity transients, at-power reactivity ramps and circulator trip tests.

A large number of these tests have been simulated with KINAGRAX, a computer code on which fault studies are based. Agreement with measurement is very good, and sensitivity studies show that such discrepancies as exist may be due largely to input data errors. It is concluded that KINAGRAX is able to predict steady state conditions and transient amplitudes in both power and temperature to within a few percent. This level of agreement greatly increases our confidence in the CAGR fault study code and significantly reduces the likelihood of unforeseen effects not apparent in steady state or small amplitude tests.

## ACKNOWLEDGEMENTS

The authors are grateful to the large team of people from the CEGB, UKAEA and SSEB who enabled the experiments to be carried out. This paper is published by permission of the CEGB.

## REFERENCES

1. The Windscale AGR Concluding Experiments: Reactor Transient Tests by J.A. Desoisa, C.P.Greef, J.H.Leng and G.P.Snape, BNES Conference on Gas-Cooled Reactors Today, Bristol, 1982.
2. A One Dimensional Advanced Gas-Cooled Reactor Kinetic Program by J.Ellis, CEGB Report RD/C/N109, 1967.
3. Measurements and Calculations of the Fuel Temperature Coefficient of Reactivity for the Hinkley Point 'B' AGR by A.R.R.Telford, Nuclear Technology, 1982, 56, January, 33-39.

ANALYSIS OF A TOTAL LOSS OF AC-POWER IN A GERMAN PWR

G. Herbold, E.J. Kersting

Gesellschaft für Reaktorsicherheit (GRS) mbH  
Köln, Schwertnergasse 1, FRGABSTRACT

Risk studies and the TMI-2 accident demonstrated the significance of events involving multiple equipment failures.

Severe accident analysis are currently performed for a 1300 MW<sub>e1</sub>-PWR using the advanced code DRUFAN-02. Special attention has been focused on the detailed representation of the primary and secondary side. The purpose of those studies is to simulate postulated accident initiators including equipment malfunctions and determine primary system response, timing and significance of events and the adequacy of plant operator responses. A base calculation was performed, simulating a total loss of AC-Power. Furthermore an operator controlled primary depressurization at various times has been studied. With this procedure it could be possible to mitigate the accident due to accumulator water injection.

INTRODUCTION

The TMI-2 accident has focused attention on the potential for multiple equipment failures and their consequences during accidents beyond the design basis. It has been recognized how important recovery procedures and operator responses are to control these types of accidents and to mitigate their severity. The "Station Black-out" case as initiating event was selected because of its great implication to the overall risk of nuclear power plants. This case covers also the total loss of feedwater in an emergency power case. The main assumptions for our calculation will be described in the following chapter.

CALCULATIONAL RESULTS

The investigations have been performed using the advanced best estimate Code DRUFAN-02 /1/.

The code DRUFAN has been developed initially for the simulation of the blowdown and the initial refill phase of LWR-reactors. The code can be used for the analysis of large, medium sized and small breaks /1, 2/ and transients as well.

The numerical method applied in DRUFAN is the "lumped parameter approach". The physical system is described by "lumped parameter" control volumes which are connected by flow paths. The ordinary differential system of the thermo- and fluiddynamic model is based on the conservation laws for vapor mass, liquid mass, overall energy and overall momentum. The liquid and vapor phases are treated as a homogeneous mixture, or in case of mixture level-tracking as a nonhomogeneous mixture.

The nodalization chosen for the following calculations is shown in Figure 1. The reactor system has been simulated in a very detailed manner especially the secondary side. In all vertical junctions the drift flux option was used in order to determine a realistic void distribution in the system. Typical best estimate assumptions have been used for all calculations (e.g.: 100 % initial operating power, simplified DIN 25463 decay heat, etc.)

In the figures 2 to 5 the important results of the Station Black-out (total loss of AC-Power) without intervention are presented.

After the closure of the main steam valves the pressure on the secondary side increases from 64 to 86 bar and initiated the automatic blowdown operation of the relief valves (Fig. 2). After a short time of depressurization the pressure on the secondary side is kept at a level of 75 bar. During this period natural circulation on the primary side is established and the fluid on the secondary side of the steam generators is boiled away through the relief valves. Due to the decrease of the liquid level on the secondary side the energy generated by the core cannot completely be transferred to the secondary side from about 50 min on. This effect leads to a gradually heatup of the primary system causing the system pressure to increase and the pressurizer liquid level to rise (Fig. 2 and 3). After 1 h the pressure setpoint of the pressurizer relief valve is reached and the valve opens. During the first period of about 1000 s only vapor is leaving the pressurizer causing a rapid increase of the liquid level in the pressurizer. At about 4700 s the pressurizer is entirely filled with fluid and the valve flow rate increases due to the loss of two-phase-mixture (Fig. 3). The second increase of the valve massflow-rate occurs at 5500 s, when flashing begins in the upper plenum of the vessel. This causes a rapid insurge of fluid into the pressurizer. In order to save CPU-time the pressurizer relief valve in DRUFAN was modelled as a continuous opening valve in connection to a time dependent volume. For that reason the valve setpoint used in the calculation was the average value between the opening and closing pressure setpoint.

During the heatup phase of the primary side a constant natural circulation flow of about 800 kg/s through the core is established. Just before the complete primary system becomes saturated an increase in natural circulation occurs due to voiding in the core which causes an increasing density difference. A short time after boiling of the entire primary system the natural circulation stops.

At the same time the primary side of the steam generators starts to empty. The liquid level in the steam generator of the pressurizer loop drops faster than in the steam generator of the other loops. This is caused by the suction effects of the surge-line massflow (Fig. 4). During this period the DRUFAN code determines counter current flow conditions in the loops.

At about 7000 s the liquid level drops below the top of the active core and uncovering of the core begins (Fig. 5). The excursion of cladding temperature occurs at about 7300 s with an average rate of increase of about 0,6 K/s at the hot spot. At about 8100 s the core is completely dry and only the lower plenum and the loop seals are still filled with liquid.

Due to the lack of adequate models describing the effect of local disturbances of the core geometry in the DRUFAN-Code the calculation was terminated at about 9000 s. Without additional preventive measures the core would further heat up followed by core-meltdown.

Calculations with interventions:

Two additional DRUFAN-Calculations of a station black-out-transient were performed to study possible operator actions which could mitigate or prevent core damage. Among the various existing possibilities to influence the course of this kind of an accident is the primary depressurization with the objective to make use of the passive water reservoir stored in the accumulators. Contrary to the current possibilities in the plants we assumed that the opening of the safety- and the relief - valves of the pressurizer could be activated by operator intervention. In the following we investigated the effectiveness of this measure to prevent or mitigate core uncovering leading to core melt-down. The beginning of operator intervention was selected at times after the secondary side has emptied.

In the 2nd calculation, the operator activity is initiated shortly after the steam generators have emptied (ca. 3500 s) and after the pressure in the primary system has increased abruptly due to unavailable heat sink (Fig. 6).

At this time the pressurizer is only half filled with water. This is the reason for fact that only the steam discharges after opening of all pressurizer valves. Combined with this process, the high volume flow leads to a rapid depressurization of the primary system and to almost simultaneous "flashing" of the liquid in pressurizer and upper plenum of the Reactor Pressure Vessel (RPV).

These effects cause an expansion of the fluid volume in the RPV. This acts to slow down the rate of depressurization leading the fluid to surge into the pressurizer. In turn this produces a rapid increase of the already high swell level in the pressurizer (Fig. 8).

Some seconds after the initiation of the operator action the liquid level in the pressurizer attains the height of the valve lines and the fluid mixture flows out through the valves (Fig. 7).

The resulting strong reduction of the volume flow combined with the flashing in the RPV causes an abrupt stop in pressure decrease (Fig. 6). Simultaneously with the transition from steam to mixture

essentially more mass will be carried out of the primary system (Fig. 7). As soon the void in the pressurizer increases the mass flow through the valves reduces and thus gradually the depressurization in the primary system increases. Approx. 4400s after the occurrence of the accident, the swell level in the pressurizer begins to decrease and consequently steam flows out of the valves (Fig. 8). At 5300 s the primary pressure reaches a value lower than 26 bar and the injection from the accumulators starts (Fig. 6). At this time the liquid level has almost fallen to the bottom of the core (Fig. 10). The water injection causes the liquid level to increase and prevent further heat up of the fuel rods. DRUFAN calculates for the high powered fuel rods a max. temperature of 900 K (Fig. 11).

In the 3rd calculation, the operator action is initiated at a later time (ca. 5300 s) and therefore deviates from the other calculation. Up to this time the pressurizer is totally filled with two-phase mixture and its relief valve has responded to the function of limiting the pressure in the Primary. Corresponding to the high swell level in the pressurizer the massflow through the valves is two phase.

Additional opening of the remaining pressurizer valves by the operator (safety valves and the opening of pressurizer relief valve) causes a large increase of loss of coolant (Fig. 7). Compared to the previous calculation the results show an accelerated decrease of the liquid level in the pressurizer and in the upper region of the RPV (Fig. 10).

"Flashing" in the RPV (upper plenum) starts already at a pressure level of about 135 bar due to prolonged heat up of the liquid by decay heat. Contrary to the first calculation the rate of the depressurization in the primary system is more pronounced (Fig. 6). This is firstly due to essentially higher energy discharge through the valves caused by the higher pressure and enthalpy levels in the RPV.

Because of the specific characteristic of steam properties during "flashing" at 135 bar about 30 to 40 % less steam volume is produced than at a pressure of 85 bar.

Due to the higher loss of coolant and the resulting lower residual inventory in the Primary compared to the previous case the rate of depressurization is higher and the injection of the accumulator starts 400 s earlier (Fig. 6).

In spite of the shorter period of depressurization, the maximum fuel rod temperature was slightly higher than in the previous case. This is the result of higher loss of the coolant (Fig. 11).

These last two calculations have shown that by this measure the primary side can be depressurized effectively without core destruction down to the pressure level of the accumulator injection. Therefore the blowdown of the primary side could be initiated by the operator in the time range between 1 to 1,5 hours after loss of AC-Power.

It is even possible to select the blowdown at a later time without causing extensive damage to the core. This conclusion can be drawn by extrapolation of the calculated fuel rod temperatures.

A depressurization of the primary side before one hour is not rational for this case because during this period the steam generator secondary side is still available as a heat sink and can transmit almost the total decay heat. Only after the secondary side of the steam generator has almost emptied and accordingly the energy inventory in the primary system has increased, then the assumptions for the action of the operator become more favourable. This condition is reached after 50 to 55 min.

It is difficult to comprehend the complex flow situation in the hot leg and at the entrance of the surgeline. This may lead to uncertainties in the determination of the quality in the pressurizer and subsequently in the calculation of the two-phase discharge flow.

An underestimation of the discharge flow has been ruled out by a conservative input permitting a high entrainment of the surgeline entrance. Therefore the upper time limit for blowdown estimated by this calculation is pessimistic and can be accepted for a first-hand orientation.

If in the other case an overestimation of the discharge flow would occur, then it would have been caused by the higher quality in the pressurizer. The result would have been a faster depressurization in the primary system and an earlier injection of the accumulators. Simultaneously a higher liquid level in the core would exist during water injection. Under these assumptions the resulting core heat up would have been lower than in our calculation and would leave more time for intervention.

Final refilling of the primary system with the water from accumulators is only a preliminary estimation as the quench and condensation models in DRUFAN are not yet sufficient. Therefore in the figures they are given with dotted lines. This estimation is based on the assumption that during reflooding the pressure in the primary system drops to approximately 6 bar as a result of condensation and only steam is discharged out of the pressurizer valves. After the refilling of the system it will take 1,5 to 2 h time before uncovering of the core begins again.

Compared to the course of an accident without any operator intervention one will gain approximately 2 h. This time can be well used for carrying out tasks like reactivation of emergency power supply or other unconventional measures to secure long time cooling.

#### SUMMARY

Using the advanced Computer Code DRUFAN-02 a "Total Loss of AC-power transient" in a typical German commercial PWR (1300 MW<sub>e1</sub>) has been analysed in a detailed manner.



The results indicate that in case of no intervention the core would heat up after 2 h ending in core melt-down. An opening of all the 3 pressurizer valves within a definite time range is sufficient to depressurize the system down to the pressure setpoint (26 bar) for the ECC-injection in order to make use of the stored reservoir in the accumulators. By this action the core can be kept undamaged, the system could be reflooded and additional 2 h could be gained for recovery of AC-power supply. Furthermore other unconventional measures could be undertaken to prevent core melt.

#### REFERENCES

- /1/ M.J. Burwell, D. Znix, G. Lerchl, F. Steinhoff  
DRUFAN-01/MOD2, Volume I,  
Program Description - System Code  
GRS-A-646, November 1981
- /2/ F. Steinhoff  
DRUFAN-02 Interim Program Description Part 1  
GRS-A-685, März 1982

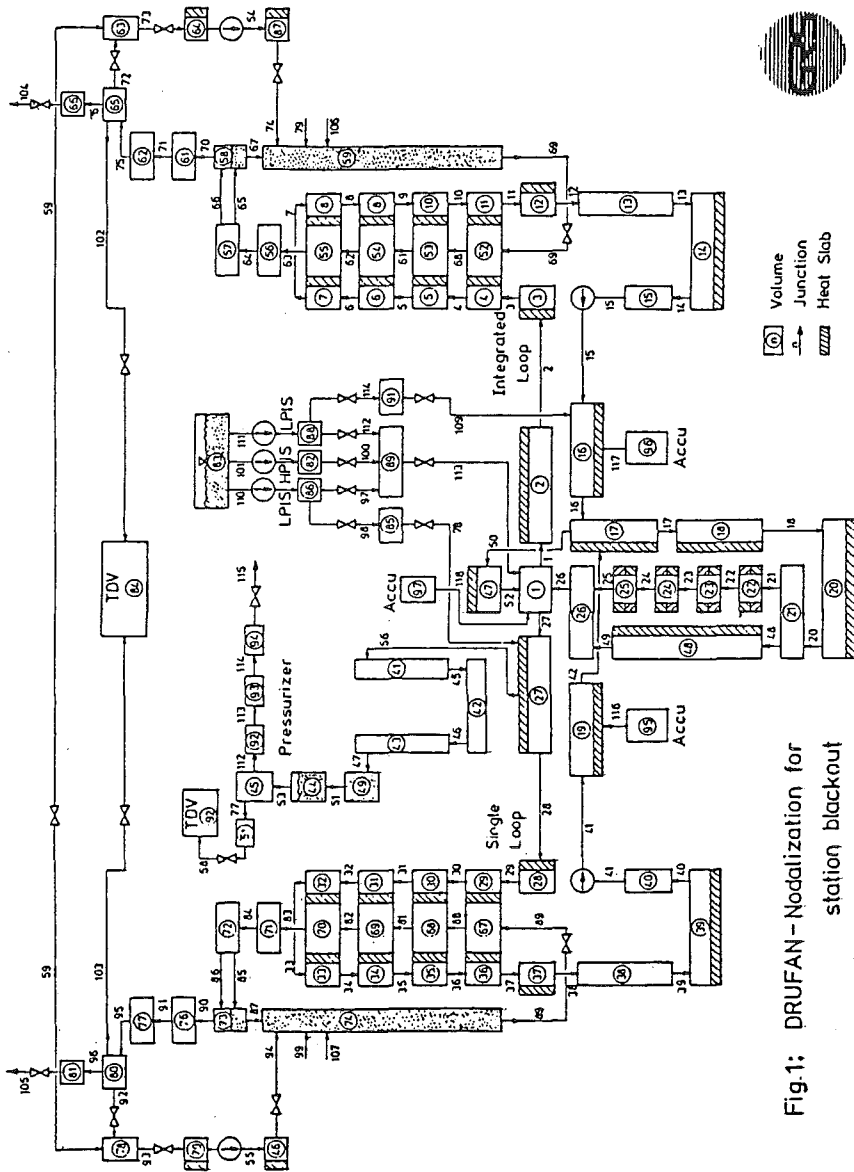


Fig.1: DRUFAN - Nodalization for station blackout



STATION BLACK-OUT WITHOUT OPERATOR INTERVENTION

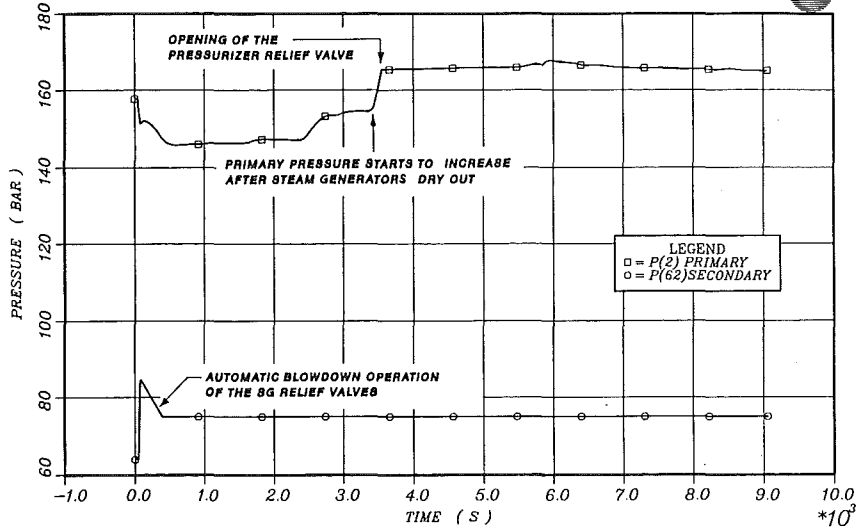


FIG. 2: PRIMARY AND SECONDARY SYSTEM PRESSURE

STATION BLACK-OUT WITHOUT OPERATOR INTERVENTION

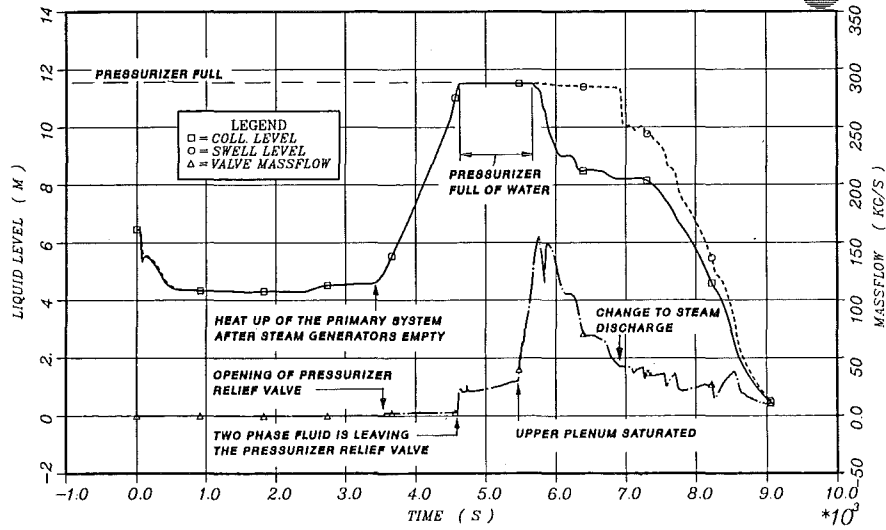


FIG. 3: PRESSURIZER LIQUID LEVEL / RELIEF VALVE MASSFLOW

STATION BLACK-OUT WITHOUT OPERATOR INTERVENTION

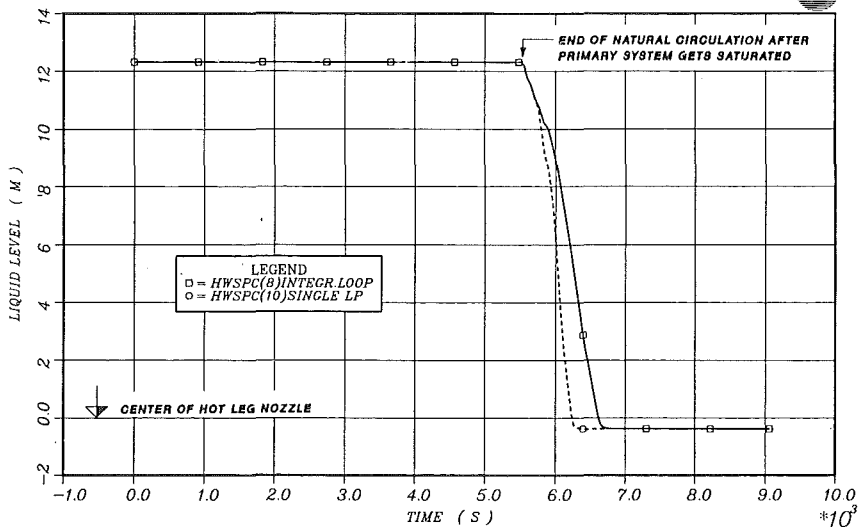


FIG. 4: STEAM GENERATOR U-TUBE LEVEL ( UPFLOW SIDE )

STATION BLACK-OUT WITHOUT OPERATOR INTERVENTION

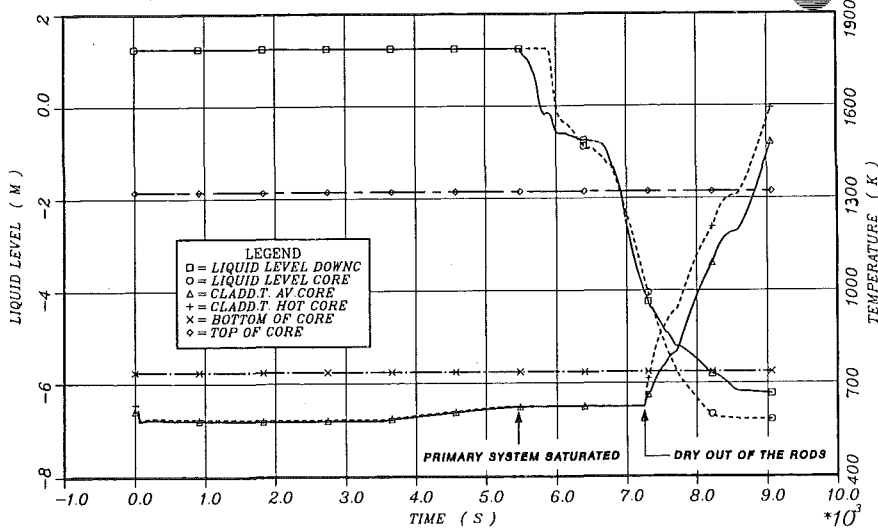


FIG. 5: LIQUID LEVEL IN VESSEL / CLADDING TEMPERATURE

STATION BLACK-OUT TRANSIENT ANALYSIS

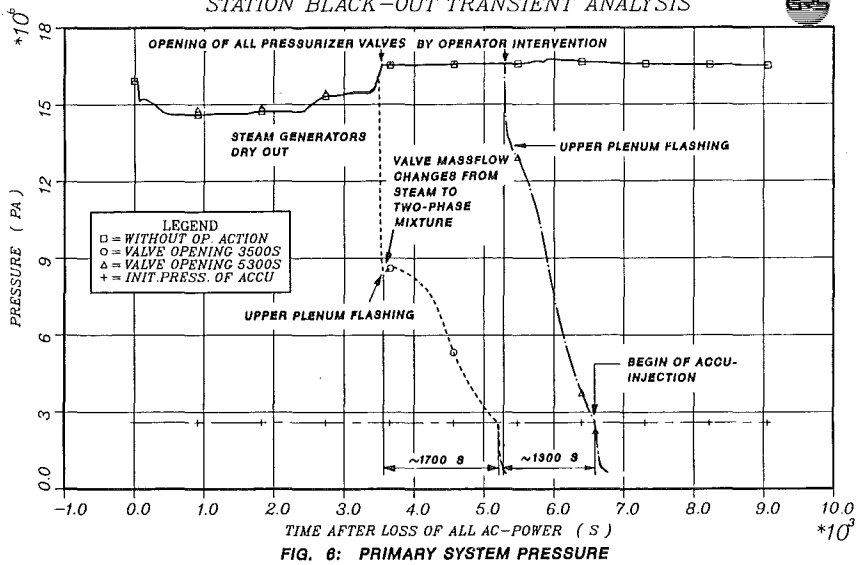


FIG. 6: PRIMARY SYSTEM PRESSURE

STATION BLACK-OUT TRANSIENT ANALYSIS

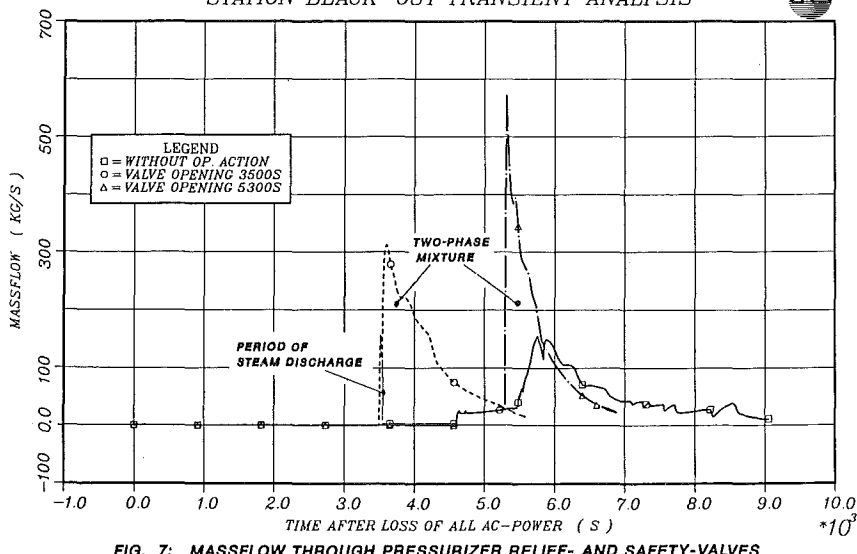


FIG. 7: MASSFLOW THROUGH PRESSURIZER RELIEF- AND SAFETY-VALVES

STATION BLACK-OUT TRANSIENT ANALYSIS

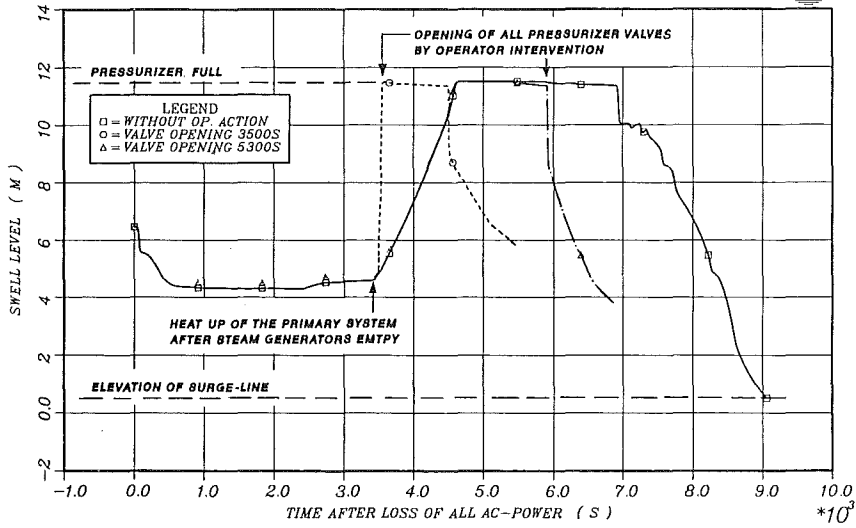


FIG. 8: PRESSURIZER SWELL LEVEL

STATION BLACK-OUT TRANSIENT ANALYSIS

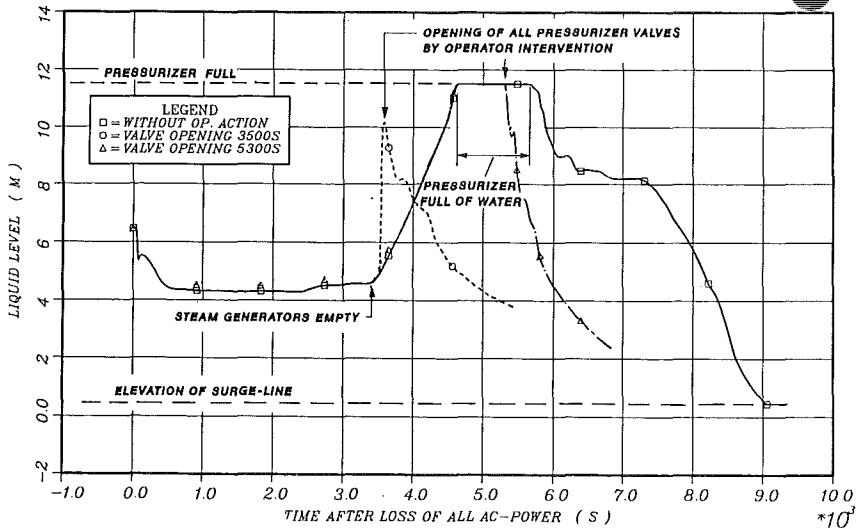


FIG. 9: PRESSURIZER COLLAPSED LEVEL

STATION BLACK-OUT TRANSIENT ANALYSIS

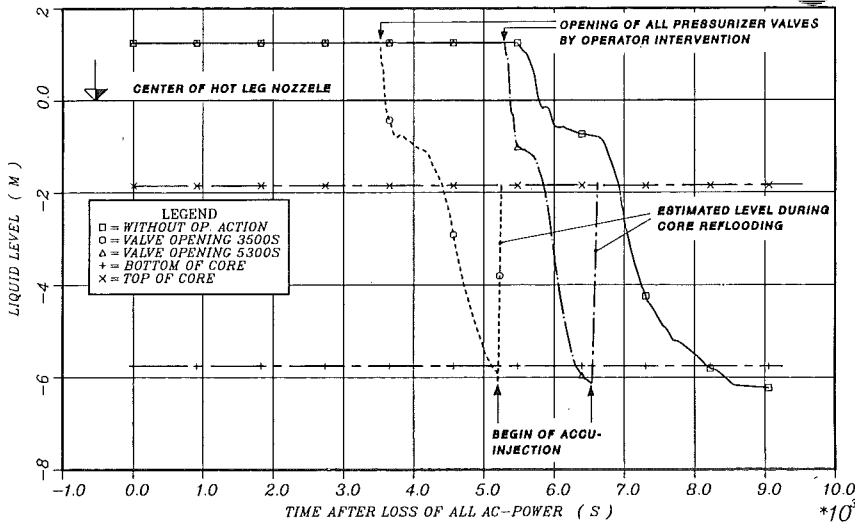


FIG. 10: COLLAPSED LEVEL IN REACTOR VESSEL

STATION BLACK-OUT TRANSIENT ANALYSIS

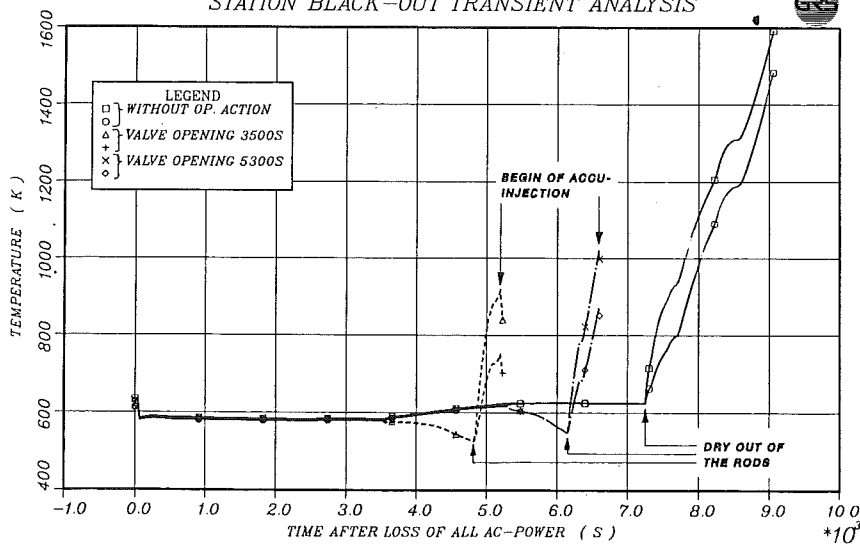


FIG. 11: CLADDING TEMPERATURE IN HOT AND AVERAGE CORE

THERMAL-HYDRAULIC AND CORE DAMAGE ANALYSIS OF THE  
STATION BLACKOUT TRANSIENT IN PRESSURIZED WATER REACTORS

C. A. Dobbe, R. Chambers, and P. D. Bayless

EG&G Idaho, Inc., P. O. Box 1625  
Idaho Falls, Idaho 83415, U.S.A.

## ABSTRACT

Analyses of a Pressurized Water Reactor (PWR) station blackout transient performed by EG&G Idaho in support of the U.S. Nuclear Regulatory Commission's Severe Accident Sequence Analysis (SASA) Program are presented. The RELAP5 and SCDAP computer codes were used to calculate the effects of concurrent loss of off-site power, on-site power, and emergency feedwater on the Babcock and Wilcox (B&W) designed Bellefonte PWR and the Westinghouse designed Seabrook PWR. Results provide insight into the timing of significant events, severity of core damage, and effect of differences between the two PWR designs on transient results.

## INTRODUCTION

The Severe Accident Sequence Analysis (SASA) Program was formulated by the United States Nuclear Regulatory Commission (USNRC) to evaluate postulated reactor accidents over a broad spectrum of accident sequences. These postulated sequences may extend beyond the current design basis in terms of core damage, system failures and release of fission products to the environment. The objectives of the Idaho National Engineering Laboratory (INEL) SASA programs are: to evaluate nuclear steam supply system (NSSS) response for accident sequences that could lead to partial or total core melt; to determine the timing of significant events; to determine the magnitude and timing of fission product release from the fuel rods and the hydrogen generation rate; and to evaluate the effect of operator actions on accident mitigation. The INEL pressurized water reactor (PWR) SASA effort is currently directed toward the evaluation of station blackout transients from accident initiation through severe core damage.

The station blackout sequence has been identified by the Accident Sequence Evaluation Program [1] as one of the highest frequency accidents leading to core melt. The station blackout sequence, designated the TMLB' sequence, is initiated by a loss of off-site power followed by a failure to establish on-site power with the diesel generators. The scenario further assumes failure to provide coolant to the steam generator via the emergency feedwater system and no operator intervention. The TMLB' sequence results in eventual core degradation and a challenge to the reactor containment boundaries.

The TMLB' sequence was calculated with the RELAP5 [2] and SCDAP [3] computer codes. The RELAP5 computer code was used to evaluate the thermal-hydraulic response of the NSSS; the SCDAP computer code was used to evaluate the core thermal-mechanical response following core uncovering. The TMLB' sequence was evaluated for both a Westinghouse and a Babcock and Wilcox design



PWR to determine the significance of design features on the timing and severity of key events for the TMLB'. This paper briefly describes the computer codes, PWR plant and input models used, the analytical procedure, the TMLB' transient sequence, and the calculated results. Detailed discussions of these items are documented in References 4 and 5 for the Westinghouse and the Babcock and Wilcox PWR analyses, respectively.

#### COMPUTER CODE DESCRIPTION

RELAP5/MOD2 is an advanced one-dimensional, two-fluid, nonequilibrium computer code utilizing a full six equation hydrodynamic model providing continuity, momentum and energy equations for each of two phases within a control volume. The energy equations contain source terms which couple the hydrodynamic model to the heat structure conduction model by a convective heat transfer formulation. The code contains special process models for critical flow, abrupt area changes, branching, cross-flow junctions, pumps, valves, core neutronics, and control systems.

SCDAP/MOD1 provides the capability to perform phenomenological analysis of the thermal, mechanical, and chemical behavior of a light water reactor core during severe accidents where core support structure integrity is maintained. SCDAP simulates core and vessel plena disruption by modeling heatup, geometry changes, material relocation, and formation, heatup and melting of debris. A coolant boiloff model was used to calculate vessel thermal-hydraulic conditions utilizing RELAP5 analytical results for initial and boundary conditions in the upper plenum, core inlet and core.

#### NSSS PLANT AND INPUT MODEL DESCRIPTIONS

The TMLB' sequence was analyzed for both a Babcock and Wilcox and a Westinghouse PWR design. The Babcock and Wilcox design selected was Bellefonte, a 3600 MW(t) PWR design with 205 fuel assemblies and raised coolant loops. Bellefonte has two primary coolant loops connected to the reactor vessel, each consisting of a hot leg, a once-through steam generator, two pump suction legs, two reactor coolant pumps, and two cold legs. A pressurizer is connected to one of the hot legs via a surge line. The RELAP5 input model simulated the hot legs and four cold legs explicitly and represents the primary and secondary systems with 183 volumes, 190 junctions, and 185 heat structures. The SCDAP input model used 16 volumes to represent the portion of the core inlet, core, and upper plenum associated with a single fuel assembly. Three components were used to model the fuel assembly representing the fuel rods, the control rods and control rod guide tubes, and the instrument tube.

The Westinghouse design selected was Seabrook, a 3411 MW(t) four loop PWR design with 193 fuel assemblies. Seabrook has four primary coolant loops connected in parallel to the reactor vessel. Each loop contains a hot leg, U-tube steam generator, pump suction leg, reactor coolant pump and cold leg. A pressurizer is connected to one of the hot legs via a surge line connection. The RELAP5 input model of Seabrook simulated two coolant loops. The first loop, representing the primary coolant loop containing the pressurizer, modeled the volumes and flow areas of a single coolant loop. The second loop modeled was a composite of the remaining three loops with the volumes and flow areas increased by a factor of three for correct loop mass and fluid velocities. The Seabrook RELAP5 model utilized 143 volumes, 147 junctions, and 175 heat structures to represent the primary and secondary systems. The SCDAP input model used 12 volumes to represent the portion of the core inlet, core, and upper plenum

associated with a single fuel assembly. Components used to model the fuel assembly represented the fuel rods, and the control rod guide tubes and instrument tube.

The system conditions at the initiation of the TMLB' sequence are compared in Table I for the two RELAP5 models.

TABLE I. COMPARISON OF COMPUTED STEADY STATE PARAMETERS FOR THE BELLEFONTE AND SEABROOK NSSS

Parameter	Bellefonte	Seabrook
Core thermal power $M\bar{w}^a$	3600.	3411.
Pressurizer pressure (MPa)	15.2	15.5
Hot leg temperature (K)	603.9	598.5
Cold leg temperature (K)	574.2	565.2
Total loop flow (kg/s)	19833.	17741.
Steam generator pressure (MPa)	7.31	6.53
Steam generator liquid mass (kg) <sup>b</sup>	29584.	182340.
Steam generator feedwater flow (kg/s) <sup>c</sup>	1034.	474.2
Steam generator feedwater temperature (K)	520.	500.

a. Core axial power shape and initial fuel stored energy are based on end of cycle (460 effective full power days for Bellefonte, 275 effective full power days for Seabrook).

b. Total for all steam generators.

c. Per steam generator.

The system conditions shown represent best estimate plant operating conditions for the two facilities. Core parameters for both models were based on end of first cycle to maximize the fission product inventory and therefore the decay heat. Of particular interest for the TMLB' sequence is the comparison between the once-through and U-tube steam generator secondary liquid masses. The total inventory for the Bellefonte once-through steam generator secondaries is only 16% of that contained in all of the Seabrook U-tube steam generator secondaries. Since emergency feedwater is unavailable for the TMLB' sequence, the initial inventory represents the total secondary heat sink for the transient.

#### ANALYTICAL PROCEDURE

The evaluation of the TMLB' sequence involved two separate calculational steps. Appropriate boundary conditions were applied to the RELAP5 steady state NSSS model to simulate the TMLB' sequence. The RELAP5 analysis was terminated when peak fuel rod cladding temperatures were about 1500 K. The SCDAP calculation was then initiated at a point in the transient where cladding surface temperatures were about 1000 K, the temperature at which zirconium cladding oxidation was computed to begin. Coolant temperatures, pressures, and void fractions from the RELAP5 analysis were used to initialize the SCDAP calculation. The core inlet flow was adjusted to produce a core dryout in SCDAP that agreed as closely as possible with that calculated by RELAP5. The SCDAP calculations were terminated when significant melting and relocating of cladding and fuel had occurred.

## RESULTS

The system thermal-hydraulic response to a TMLB' sequence is characterized initially by a complete boiloff of the steam generator secondary side liquid mass. The primary system then heats up and, as the coolant in the loops expands, pressurizes to the setpoint of the primary coolant system relief valves. The primary system saturates and loop voiding terminates natural circulation of coolant. The remaining fluid in the loops drains into the pump suction and reactor vessel, with the reactor vessel fluid being boiled off by fission product decay heat. Fuel cladding dryout and heatup produce cladding oxidation, deformation and failure, resulting in hydrogen generation and fission product release to the primary coolant system. Continued core heatup results in core and structural material liquefaction and relocation within the vessel. Failure of the primary coolant system boundary is then highly probable.

The sequences of significant events for the TMLB' transient are summarized in Table II.

TABLE II. TMLB' SEQUENCE OF EVENTS FOR BELLEFONTE AND SEABROOK

Event	Time (s)	
	Bellefonte	Seabrook
Scram initiation, reactor coolant pump trip, feedwater trip	0.0	0.0
Loss of effective heat sink	45.	4900.
Primary system saturates (hot legs)	950.	6510.
Loss of natural circulation	1100.	6800.
Fuel cladding heatup begins	1800.	8290.
Fuel cladding oxidation initiation	2550.	9060.
Fuel cladding failure	2840.	9820.
Steam starvation observed in upper core	3100.	9840.
Cladding oxide shell ruptures - clad-fuel melt relocates	3550.	11400.

The loss of effective heat sink event refers to the time when core decay heat transfer to the primary system exceeded the heat removal capacity of the steam generators. The large difference in the timing of this event for the two NSSS designs was due to the difference in steam generator secondary side heat capacity, and was directly related to the initial secondary side liquid inventory. The timing differences became even larger as the transient progressed due to the reduced decay heat levels in the Seabrook calculation, decay heat being a decreasing function of time after scram.

The primary system pressure response, calculated by RELAP5, is shown in Figure 1 for the two TMLB' calculations. Following the loss of an effective heat sink, both calculations show a primary system repressurization to the respective power operated relief valve (PORV) setpoints. For the Seabrook case, the capacity of the two PORVs was sufficient to relieve primary system overpressure for the remainder of the transient. The Bellefonte PORV was not of sufficient capacity to relieve primary system overpressure and the primary repressurized to the safety relief valves opening pressure of 17.2 MPa by 1000 s. The primary

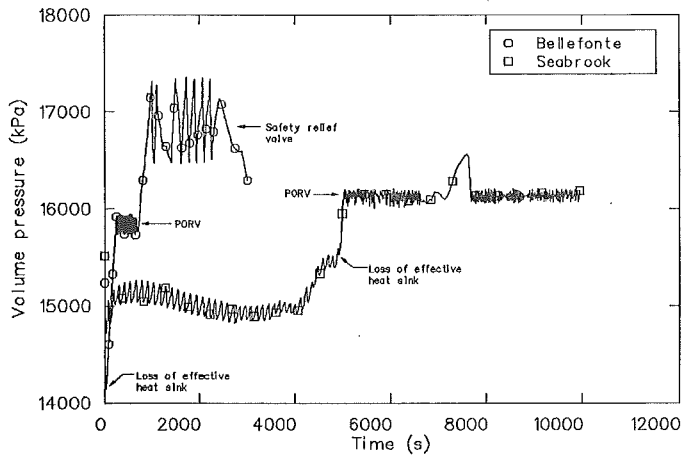


Figure 1. RELAP5 calculated primary system pressure histories for the Bellefonte and Seabrook TMLB'.

system pressure then cycled between the safety relief valve opening and closing pressure (16.4 MPa) for the remainder of the transient.

The RELAP5 calculated fuel cladding surface temperature response for the Bellefonte and Seabrook TMLB' analyses are shown in Figure 2 for three representative core locations. The temperature response shows that the core dryout in both cases was from the top down. The heatup rate in the Bellefonte analysis was more rapid than that calculated for Seabrook because of the higher decay power in the transient.

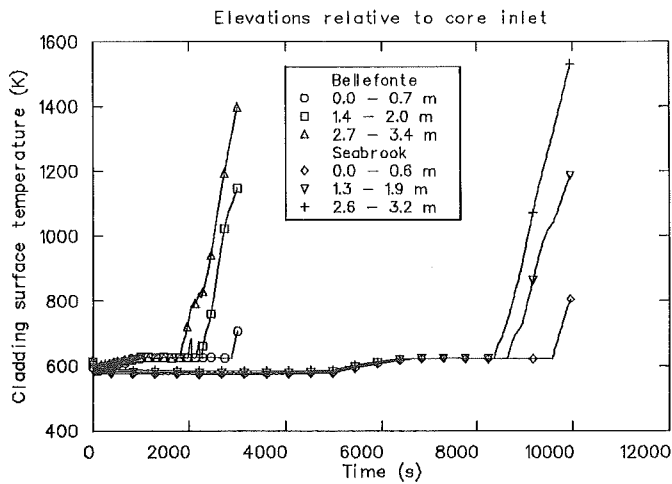


Figure 2. RELAP5 calculated fuel cladding surface temperature histories for the Bellefonte and Seabrook TMLB'.

The fuel rod cladding surface temperature histories, calculated by the SCDAP code, are shown in Figures 3 and 4 for the Bellefonte and Seabrook nuclear power plants, respectively. The temperatures at three of the ten axial elevations are given in each figure. The results of the calculations will be discussed in four areas: cladding ballooning, subsequent cladding failure with the associated fission gas release, cladding oxidation and the resultant hydrogen generation, and rupture of the cladding oxide shell and relocation of core materials.

Cladding ballooning was calculated at 2750 s at a temperature of 1230 K in the Bellefonte plant; the cladding ballooned over only 10% of the rod length. Because the fuel-cladding gap size increased, the cladding surface temperature rise slowed, as seen in Figure 3. The effect of the ballooning in the Seabrook calculation can be seen in Figure 4 in the curves corresponding to nodes 4 and 9 at 9270 s. Ballooning was calculated over 80% of the rod length at temperatures of 1290 - 1670 K. This sausage-type ballooning is calculated at higher temperatures, after lower temperature increase rates, than the localized ballooning that was calculated for the Bellefonte plant. The lower temperature increase rate resulted from the lower decay power in the Seabrook calculation than in the Bellefonte calculation. Ballooning caused partial flow blockage corresponding to a 90% flow area reduction in both calculations.

The cladding failed shortly after ballooning at the 2.8 m elevation in both calculations, at a lower temperature for the Bellefonte plant (1370 K) than for the Seabrook plant (1710 K). When the cladding failed, fission products were released to the coolant. Fission product release is highly temperature dependent. As temperatures increased, fission products were continuously released from the fuel to the fuel-cladding gap and from the gap to the coolant. Very little difference between the calculated fission product release rates for the two plants at any given temperature was seen. The accuracy of SCDAP calculations at temperatures in excess of 2400 K has not been established because of an insufficient data base. When that temperature was calculated (at 3900 s in Bellefonte and 12000 s in Seabrook), a total of about 0.3 kg of soluble fission products (CsI and CsOH) had been released from the rods in the core in both cases. At the completion of the Bellefonte calculation, maximum fuel and cladding temperatures were about 2900 K, and 0.6 kg of soluble fission products had been released from the cladding in the core. At the same temperature, a similar amount had been released in the Seabrook calculation. However, when the Seabrook calculation was terminated, fuel and cladding temperatures had exceeded 3000 K and fuel melting had occurred. At liquefaction, all fission products are calculated to be released instantaneously from the fuel. Consequently, the total soluble fission product release from the cladding for the Seabrook plant was much higher - 9.8 kg.

Zircaloy oxidation was calculated by SCDAP when temperatures reached 1000 K (at 2550 s and 9060 s for the Bellefonte and Seabrook plants, respectively). The heat resulting from cladding oxidation was about 20% of the heat from rod decay power at 2750 s in the Bellefonte calculation and 25% at 9500 s in the Seabrook calculation. However, because the water level had decreased considerably, very little steam was being generated by 3100 s in the Bellefonte calculation, and by 9840 s in the Seabrook calculation. All of this steam was being used in the oxidation reaction at lower elevations. Consequently, no steam was flowing past the cladding in the upper half of the rod. Oxidation ceased in these nodes as a result of steam starvation and no heat was generated by the oxidation reaction. The temperature rise slowed and the fuel rods did not form a thick oxide shell. When dryout at the bottom of the fuel was calculated, oxidation ceased completely. Because of the steam starved environment, only about 40 kg of hydrogen were generated in the Bellefonte core and 30 kg in Seabrook. About 4% of the cladding was oxidized in both cases.

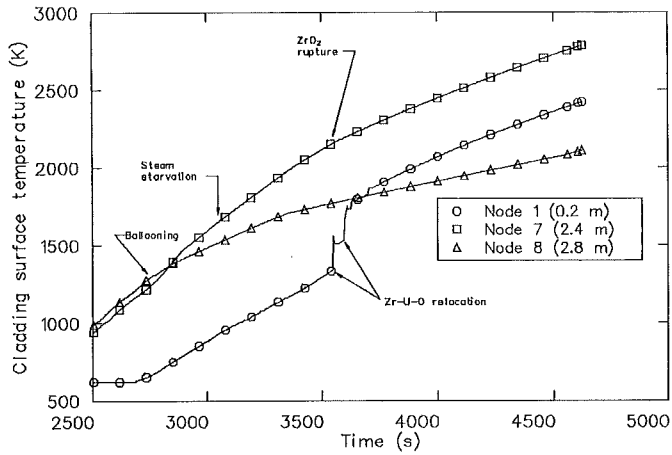


Figure 3. SCDAP calculated fuel cladding surface temperature histories for the Bellefonte TMLB'.

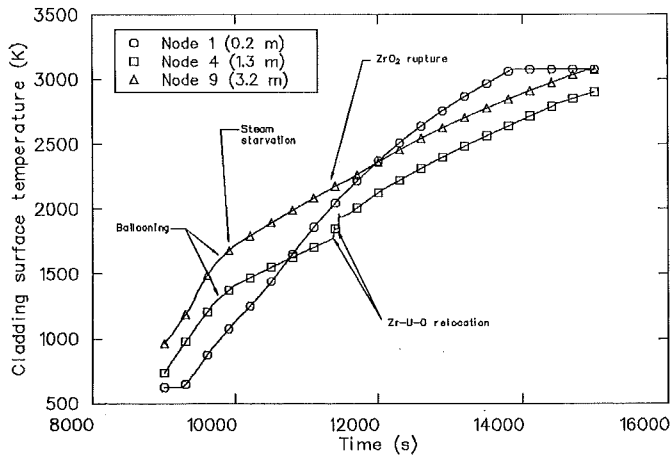


Figure 4. SCDAP calculated fuel cladding surface temperature histories for the Seabrook TMLB'.

When temperatures increased to 2125 K (3500 s at node 7 in the Bellefonte calculation, 11200 s at node 9 in the Seabrook calculation), the zircaloy inside the oxide shell began to liquefy and dissolve the outer portion of the fuel pellets. Shortly thereafter (3550 s and 11400 s) the relatively thin  $ZrO_2$  shell ruptured because of increased stress and decreased strength at a temperature of about 2200 K. A hot mixture of liquefied fuel and cladding relocated downward. As a result, a step change in the cladding surface temperature can be seen in Figure 3 at 3550 s at the 0.2 m elevation, and in Figure 4 at 11400 s at the 1.3 m elevation, where the liquefied mixtures solidified again. At 3900 s and 12000 s, the latest times at which accuracy in SCDAP has been documented, 60% and 25% of the Zr and 0.6% and 1.0% of the  $UO_2$  in the core had

relocated below the bottom of the core in the Bellefonte and Seabrook calculations, respectively. At the end of both calculations, 84% of the zircaloy had dripped below the bottom of the fuel rod. Of the original  $UO_2$  in the Bellefonte calculation, 0.8% had dripped below the bottom of the core while, because of the higher temperatures, 4.6% of  $UO_2$  in the Seabrook core had relocated below the fuel rods.

#### CONCLUSIONS AND RECOMMENDATIONS

The results presented here represent calculations of a TMLB' sequence through the core damage phase of the transient. The analysis assumed no interaction between the core damage activity and loop thermal-hydraulics. Cladding oxidation and the resultant hydrogen production and heatup rate were severely limited by a lack of available steam. If early oxidation-induced hydrogen production were accounted for in the loop thermal-hydraulic analysis, the steam supply to the core could be altered. Additionally, the heatup rate affected the extent of the rod ballooning which in turn, changed core geometry and coolability. In fact, the slower heatup rate computed for Seabrook resulted in a larger percentage of the rod length ballooning which could result in co-planar flow blockage.

The linking of the thermal-hydraulic analysis to the fuel damage analysis is particularly important for future analysis of fission product transport through the primary coolant system (PCS), and for estimation of the most probable failure point in the PCS boundary. Heating of ex-vessel structures (hot legs, steam generator tubes, pressurizer surge lines, for instance) by superheated steam-hydrogen mixtures may result in failure in the coolant loops prior to lower plenum melt-through of molten core material. These two scenarios could provide radically different containment loadings and fission product transport activity. Analyses are currently underway to evaluate phenomena which affect source term tracking in the system. Plant models incorporating parallel flow paths through the core and upper plenum are being used to evaluate the effect of recirculatory flows on the heatup of the core and vessel structure. Evaluation of loop piping penetrations and fittings is also planned to identify potential weaknesses in the PCS boundary.

#### REFERENCES

1. A. M. Kolaczowski et al., Interim Report on Accident Sequence Likelihood Reassessment (Accident Sequence Evaluation Program), February 1983.
2. V. H. Ransom et al, RELAP5/MOD2 Code Manual, Vol. 1, EGG-SAAM-6377, April 1984.
3. G. A. Berna, C. M. Allison, and L. J. Siefken, SCDAP/MOD1/VO: A Computer Code for the Analysis of LWR Vessel Behavior During Severe Accident Transient, IS-SAAM-84-002, Rev. 1, July 1984.
4. P. D. Bayless, R. Chambers, Analysis of a Station Blackout Transient at the Seabrook Nuclear Power Plant, to be published.
5. C. A. Dobbe, R. Chambers, Analysis of a Station Blackout Transient for the Bellefonte Pressurized Water Reactor, to be published.

## NOTICE

This report was prepared as an account of work sponsored by an agency of the United States Government. Neither the United States Government nor any agency thereof, or any of their employees, makes any warranty, expressed or implied, or assumes any legal liability or responsibility for any third party's use, or the results of such use, or any information, apparatus, product or process disclosed in this report, or represents that its use by such third party would not infringe privately owned rights. The views expressed in this paper are not necessarily those of the U.S. Nuclear Regulatory Commission.

Work supported by the U.S. Nuclear Regulatory Commission, Office of Nuclear Regulatory Research under DOE Contract No. DE-AC07-761D01570.



## ANALYSIS OF SEVERE LOCA PROBLEMS USING RELAP5 AND TRAC

R. Bisanz, B. Burger, U. Lang, M. Schindler, F. Schmidt, H. Unger

Institut für Kernenergetik und Energiesysteme (IKE)  
University of Stuttgart, Pfaffenwaldring 31, 7000 Stuttgart 80, FRG

## ABSTRACT

The codes RELAP5 and TRAC-PF1 have been applied to accident scenarios with incipient-to-complete loss of primary system water inventory. Under such conditions the fuel rods in the steam covered regions within the core will heat up and degrade. The results of the analyses performed have been compared against water boil-off experiments. The paper describes the limitations of the codes in view of the high temperatures and the experiences in the code applications.

With respect to the temperature development and water boil-off, the influence of the nodalization has been assessed. RELAP5 has been applied to risk relevant scenarios. Especially in the high temperature range, the code has been coupled with the core heatup and slumping code MELSIM3 of the core melt system KESS-2, which is recently under development. Results of the codes application show the necessity of the coupled analysis as well as the required code improvements.

## INTRODUCTION

Several computer codes have been developed which allow the analysis of the thermalhydraulics behavior of fluid and structures during reactor accidents. The objective of the advanced best estimate codes RELAP5/Mod1 /1/ and TRAC-PF1 /2/ is to provide a capability for the analysis of loss-of-coolant accidents (LOCA) and non-LOCA transients.

At elevated temperatures, severe accident codes like MELSIM3 /3/ treat the core heatup and slumping under water boil-off conditions. In order to prove the applicability of the codes with respect to accident scenarios with incipient-to-complete loss of primary system inventory and temperatures far beyond the regulatory guidelines up to core melt situations, model as well as program capabilities have been analyzed.

In order to allow a detailed analysis of severe accident conditions the thermal hydraulic codes may be coupled with fuel/core behavior or structural mechanics codes within the Plant Simulation and Analysis System (SASYS) of the IKE /4/ (s. Fig. 1). Interfaces exist also between the RELAP5 or TRAC codes and the RSYS graphic system /5/. The codes run on a CRAY-1M machine.

#### SEVERE ACCIDENT SCENARIOS

During the course of severe accidents in light water reactors, the heat transfer conditions between the fuel rods or steam generator tubes and the fluid are mainly affected by the uncovering of the fuel rods, tubes or the dry out of the flow channels. For the case of the uncovering transients a relevant parameter is the level of the two-phase mixture. The height of the so called mixture level is generally marked as a sharp increase of the void fraction and the surface temperature.

After uncovering, the fuel rods will heat-up because of the relatively low heat transfer rates between rod and steam. At temperatures above approx. 1500 K the metal-water reaction predominates the fuel rod behavior. It also reduces the steam to hydrogen, which possibly may limit the chemical reaction /3/.

The processes described below are typical for the situations analyzed in the frame of risk studies (/6/, /7/). Especially in small break accidents and transients the system response on core behavior is substantial. The codes are applied in order to contribute to the following questions:

- Find out the minimum availability of safety components to avoid uncoolable conditions.  
Calculations with the severe accident code MELSIM3 have found the degree of core uncovering which lead to coolable core conditions /8/, /9/. The core temperatures of the TMI-2 reactor were much higher than the regulatory limits.
- Provide a better understanding of the plant behavior leading to severe core damage conditions.
- Reduce the conservatism in the risk assessment.

#### THERMALHYDRAULIC MODELING USING RELAP5 AND TRAC

With respect to modeling capabilities of the entire system behavior, both codes predict the fluid flow with similar accuracy. RELAP5 and TRAC are based on a nonhomogeneous, nonequilibrium hydrodynamic model. The models include component process models for pipes, branches or tees, pumps, control system and heat structures, for example. Whereas RELAP5 has a one-dimensional vessel model, TRAC-PF1 allows a three dimensional discretization.

The main weaknesses with respect to the severe core damage application are the lack in

- fuel rod deformation modeling
- metal-water reaction modeling in RELAP5
- consideration of slumping phenomena
- modeling of fission product release
- structural mechanics response.

#### CORE MELT CODE MELSIM3

With respect to the elevated temperature range, the core melt code system MELSIM3 has been developed in order to allow the analysis of core melt phenomena in light water reactors.

MELSIM3 treats the core behavior in a two dimensional (r,z) geometry including representative fuel rods, fluid channels and surrounding structures.

However, the thermalhydraulic conditions, e.g. inlet mass flow and temperature, as well as pressure, have to be provided by the thermalhydraulic codes.

MELSIM3 is also part of SASYST and represents the best-estimate part of the German core melt system KESS-2, which has been reported elsewhere /10/.

#### APPLICATIONS OF RELAP5 AND TRAC-PF1

The codes have been applied to a core uncovering experiment which was performed in 1975 in the Westinghouse Laboratory in Forest Hills /11/.

Twenty-two constant pressure boiloff, or core uncovering tests were performed in the G-2-loop test facility using a bundle of 336 full length heater rods with different power classes. The test number 718 has been modeled with RELAP5 and TRAC-PF1. The test section consisting of the bundle, downcomer, upper and lower plenum, was filled with water through a feedwater line up to a predefined level (s. Fig. 2). Then, the valve was closed and the heater rod power was switched on. Fig. 3 represents the calculated mixture level versus time compared with the experimental data. During the first 100 s the mixture level as predicted by RELAP5 decreases faster than observed in the experiment. This may be due to more complicated initial conditions. However, after 200 s the results match each other. The cladding temperature history at the 3.75 m level agrees quite well (Fig. 4).

In order to assess the sensitivity of the chosen axial nodalization, the number of axial marks in the RELAP5 calculation has been reduced from 20 to 6. The initial void fraction and the power shape were adjusted according to the finer mesh case. Fig. 5 demonstrates, that the finer nodalization leads to higher temperatures. This is due to a different boiloff rate and varying heat transfer modes as predicted by RELAP5.

At 500 s the difference is approx. 100 K. This effect demonstrates, that the analysis of core uncover transient, such as small break LOCA's, requires a finer mesh instead of a coarse one, which usually is applied for large break LOCA's. This holds especially for the RELAP5 code, because it does not predict the fuel rod behavior with a finer mesh than used for the fluid behavior.

#### APPLICATION OF RELAP5 WITHIN THE FRAME OF THE GERMAN RISK STUDY, PHASE B

The RELAP5 code has been applied in order to simulate the thermal hydraulics response of severe accident conditions. In this paper calculational results for the primary system of a typical pressurized water reactor shall be presented which have been performed with RELAP5.

Fig. 6 represents the pressure histories in the upper plenum and the steam generator secondary side. In order to achieve steady-state conditions within the entire system, the code had to run until 100 s. At that time a 80 cm<sup>2</sup> break has been opened in the primary system. Simultaneously, station black-out and a failure of the safety pumps on the secondary side is assumed. Additionally only one high pressure injection system is active. Accordingly to the opening of the break the primary pressure decreases rapidly.

After reaching 132 bar the reactor scrams and the turbines are turned off. Consequently, the secondary pressure increases until 88 bar, when the safety valves open and close again. This pressure level is held until 1000 s and decreases further on. After approx. 1000 s the secondary pressure is higher than the primary one.

Fig. 7 shows the cladding temperature histories in the upper half of the core. Approx. 700 s after initiation of the accident the fuel rods were partly reflooded because of the water flow from the steam generator to the core. Afterwards the water inventory in the core boils down, the fuel rods are cooled only by steam flow and therefore their temperature increases continuously.

Another calculation was performed considering a 20 cm<sup>2</sup> cold leg break. Again it is assumed, that the reactor scrams due to the pressure drop. Simultaneously, station black out is anticipated, which causes a primary coolant and main secondary feedwater pump trip. Neither the primary sided high pressure injection systems nor the secondary sided auxiliary feedwater systems are taken into account in this calculation.

The primary pressure history is shown in Fig. 8. A rapid pressure drop occurs immediately after break opening. Further on, a slow approach to the level of 80 bar is reached, which is governed by the operation of the safety relief valves on the secondary side.

Appr. 4000 s after break opening, the steam-generators are dried out. As a result, the primary pressure rises slightly. The pressure drops again, after the stagnant water in the pressurizer is evaporated totally.

Total dryout of the core is reached appr. 4000 s after break opening. The core begins to heat up (Fig. 9). The temperature rise, calculated with RELAP5 is appr. 0,6 K/s. In the coupled calculation, which combines the

thermo hydraulics from RELAP5 with the more sophisticated core behaviour modeling of MELSIM3, core heat up is more rapid, mainly due to consideration of metal-water reaction.

#### CONCLUSIONS

The analyses performed demonstrate the necessity of a detailed coupling of thermal hydraulics codes with severe accident codes. The SASYST concept is shown to be an appropriate tool for the analysis of severe accident phenomena.

However, in order to allow an adequate coupling, the codes applied need yet to be improved further.

#### REFERENCES

- /1/ V.H. Ransom, et al.: "RELAP5/Mod1 Code Manual", Vol. I and II, NUREG CR-1826, March 1981
- /2/ Safety Code Development Group, Energy Division: "TRAC-PF1: An Advanced Best Estimate Computer Program for Pressurized Water Reactor Analysis", Los Alamos National Laboratory
- /3/ R. Bisanz: "Modellierung und Analyse des Verhaltens von Leichtwasserreaktoren bei Störfällen mit schweren Kernschäden", Dissertation, University of Stuttgart, submitted May 1983
- /4/ R. Rühle, R. Bisanz, W. Scheuermann, F. Schmidt, H. Unger: "SASYST - A New Approach in Total Plant Simulation During Severe Core Damage Accidents", Int. Meeting on Thermal Reactor Safety, Chicago, 1982
- /5/ R. Lang, B. Schlecht: "Farbgrafik in RSYST", IKE 4 R-9, Mai 1983
- /6/ WASH-1400, NUREG-751014, 1975
- /7/ Deutsche Risikostudie Kernkraftwerke, Verlag TÜV Rheinland, 1979
- /8/ F. Schmidt, G. Bleher, R. Bisanz: "Bedingungen für die Kühlbarkeit eines teilweise unbedeckten Reaktorkerns", Jahrestagung Kerntechnik der KTG, Berlin 1983
- /9/ R. Bisanz, F. Schmidt: "Analysis of the TMI Incidence Using EXMEL and MELSIM3", Int. Meeting on Thermal Reactor Safety, Chicago, 1982

- /10/ F. Schmidt, R. Bisanz: "KES2 - Recent Development and Perspectives",  
Int. Meeting on Light Water Reactor Severe Accident Evaluation, Vol. II,  
Cambridge, Mass., USA, Aug./Sept. 1983
- /11/ T.S. Andreycheck: "Heat Transfer Above the Two-Phase-Mixture Level Under  
Core Uncovery Conditions in a 336-Rod Bundle", Vol. I and II, EPRI NP-  
1692, Jan. 1981

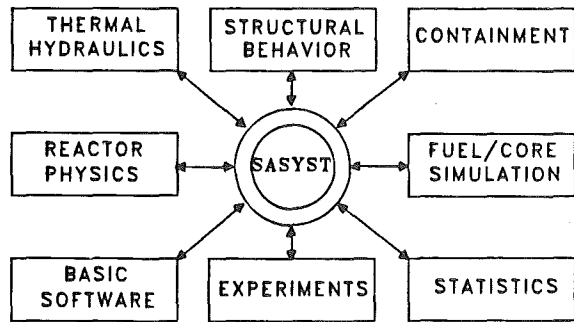


FIG. 1 : S A S Y S T  
PLANT SIMULATION AND ANALYSIS SYSTEM OF IKE

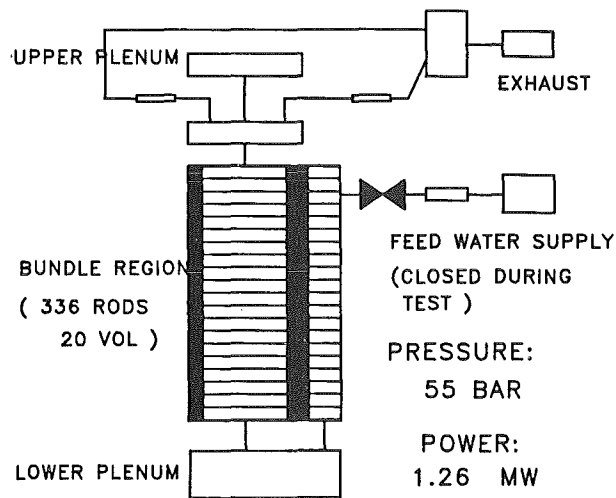


FIG. 2 RELAP5/MOD1 NODALIZATION  
OF THE BOILOFF EXPERIMENT

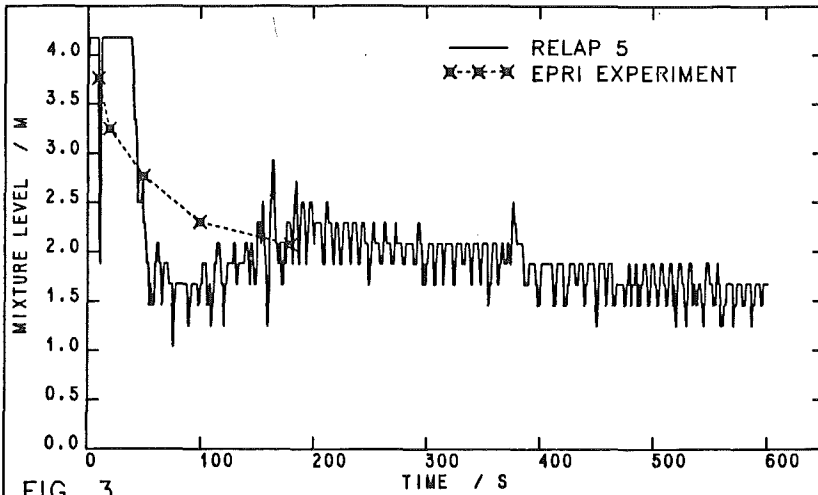


FIG. 3  
RELAP 5 PREDICTED MIXTURE LEVEL HISTORY  
AGAINST THE EPRI BUNDLE WATER BOILOFF EXPERIMENT

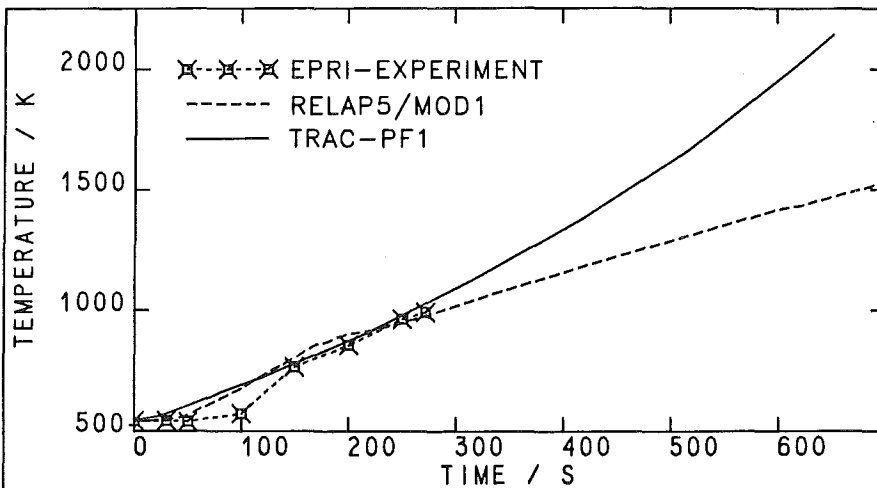
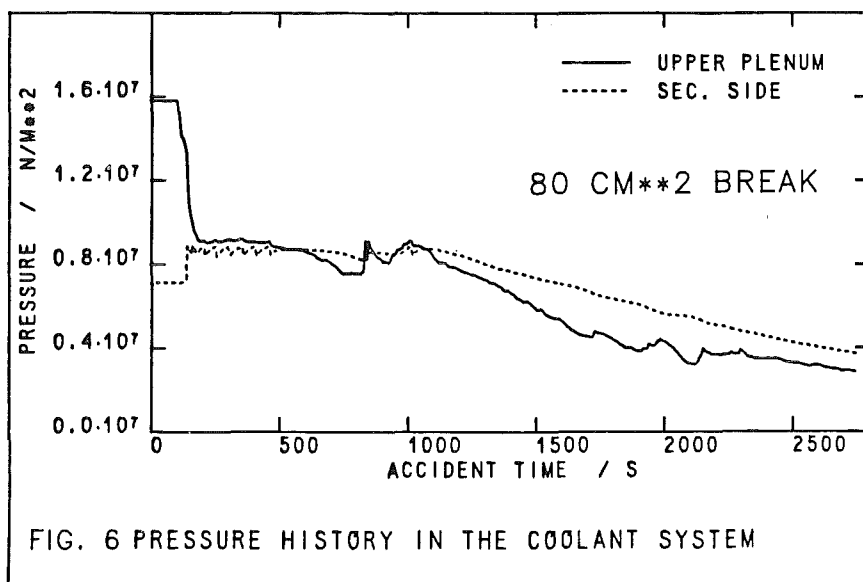
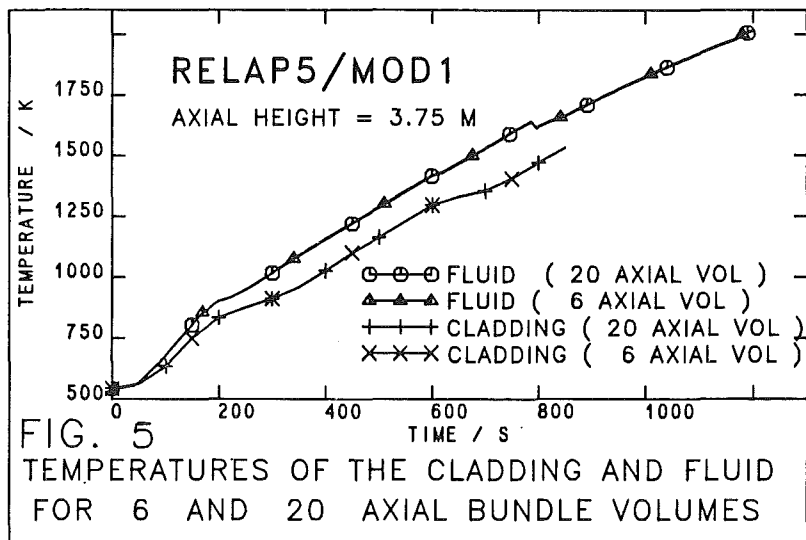
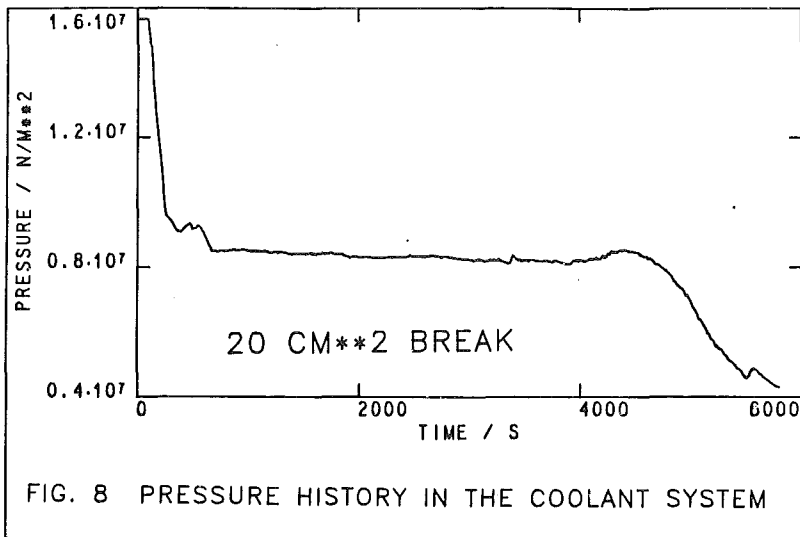
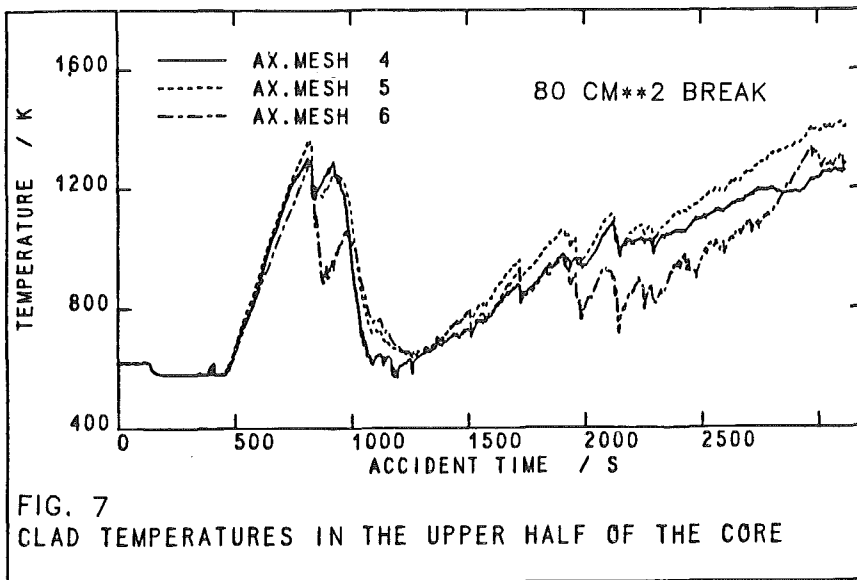
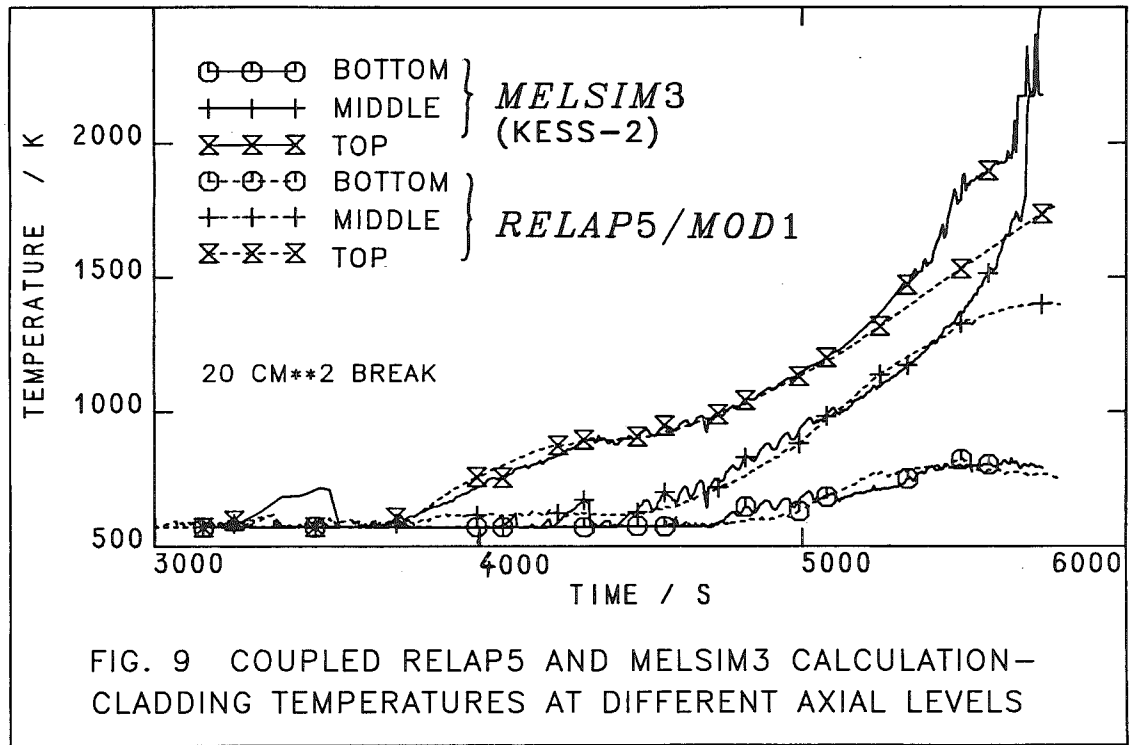


FIG.4: RELAP5 AND TRAC-PF1 PREDICTED CLADDING  
TEMPERATURES COMPARED AGAINST BOILDOWN EXPERIMENT









A LSTF SIMULATION OF THE TMI-2 SCENARIO IN A WESTINGHOUSE  
TYPE FOUR LOOP PWR

Richard R. Schultz\*, Yutaka Kukita, Yasuo Koizumi  
and Kanji Tasaka

Japan Atomic Energy Research Institute  
Tokai-Mura, Ibaraki-Ken, Japan

\* USNRC Resident Engineer at JAERI  
(on leave from EG&G, Idaho,  
Idaho National Engineering Laboratory)

ABSTRACT

The Three Mile Island-2 (TMI-2) scenario in a Westinghouse (W) type four loop pressurized water reactor (PWR) was studied in preparation for upcoming tests in the ROSA-IV Program's Large Scale Test Facility (LSTF). The LSTF is a 1/48 scale simulator of a W type four loop PWR with full scale component elevation differences.

TMI-2 scenario simulation analyses were conducted to establish a pretest prediction data base for RELAP5 code evaluation purposes and to furnish a means of evaluating the LSTF's capability to simulate the reference PWR. The basis for such RELAP5 calculations and the similarities between the LSTF and reference PWR thermal-hydraulic behavior during a TMI-2 scenario are presented.

INTRODUCTION AND APPROACH

The Rig of Safety Assessment (ROSA)-IV Program was initiated by the Japan Atomic Energy Research Institute (JAERI) in 1980. The ROSA-IV Program was formed in response to the need for data characterizing small break loss-of-coolant accidents (SBLOCAs), abnormal and operational transients in Westinghouse (W) type pressurized water reactors (PWRs).

The ROSA-IV Program is international in scope. The United States Nuclear Regulatory Commission (USNRC) joined informally in 1981 and as a participant by cooperative agreement in 1984.

The Large Scale Test Facility (LSTF) is the heart of the ROSA IV Program. The LSTF has two loops and has the same component elevation differences as a W type four loop PWR (the reference PWR) to simulate

natural circulation [1]. The LSTF hot and cold leg pipe sizes, i.e., 207mm inner diameter, were constructed to have the same length to root diameter ( $L/\sqrt{D}$ ) ratio as the reference PWR to simulate flow regime transitions isochronously [2]. Further, the LSTF is operational at representative primary pressure levels, i.e., 16 MPa, and plant power levels sufficient to simulate the core decay heat several seconds after scram. The LSTF volumes were scaled at 1/48 of the reference PWR.

The objective of the present study was to construct a portion of the LSTF test matrix relating to the TMI-2 scenario. In summary, the incident at TMI-2 was characterized by: (1) Continuous primary system mass loss through a stuck open power operated relief valve (PORV) and letdown valves. (2) Reduction of the emergency core cooling system (ECCS) injection mass flow by the operator following misinterpretation of high pressurizer water level. (3) Continuous operation of the reactor coolant pumps (RCPs). (4) The loss of main and auxiliary feedwater systems. (Although the auxiliary feedwater system was restored after 8 minutes, the flow was throttled by the operator.)

However, several significant differences between the Babcock & Wilcox (B&W) TMI-2 plant and the reference PWR assure that a W type plant will have dissimilar behavior to the TMI-2 plant. Perhaps the most significant difference between W type reactors and the B&W TMI-2 class reactors is in the steam generator (SG) design [3]. The once-through B&W SG design contains much less secondary fluid than the W U-tube design.

Another significant difference centers on the reactor coolant pump (RCP) trip logic. All the Japanese built W type plants trip their RCPs on low primary system pressure, whereas B&W plants did not in 1979.

Because of major differences between the reference PWR and the TMI-2 plant, the approach taken in the following analyses was to study reference PWR transients of a similar nature to the TMI-2 accident in the sense that analogous primary thermal-hydraulic conditions were obtained. Thus, transient variations which are peculiar to the TMI-2 plant characteristics will not be examined herein.

#### THE CODE, MODELS AND CALCULATIONAL MATRIX

The pre-core uncover portion of the TMI-2 scenario (peculiar to a W four loop plant) was simulated using the RELAP5/MOD 1 Cy 18 [4] computer code. Calculations were conducted assuming the initiating event to be a main feedwater system trip concurrent with a failed open PORV or a break in the PORV manifold. The auxiliary feedwater system was assumed inoperative. Thereafter, plant boundary conditions were determined by combining reference PWR automatic trip conditions with the known events at the TMI-2 plant to obtain thermal-hydraulic phenomena similar to those present in the TMI-2 accident.

## RELAP5 Code/Model Development

The LSTF calculations were conducted using the RELAP5 model shown in Figure 1. The reference PWR model nodalization is not shown; the LSTF and reference PWR model nodalizations are similar [3].

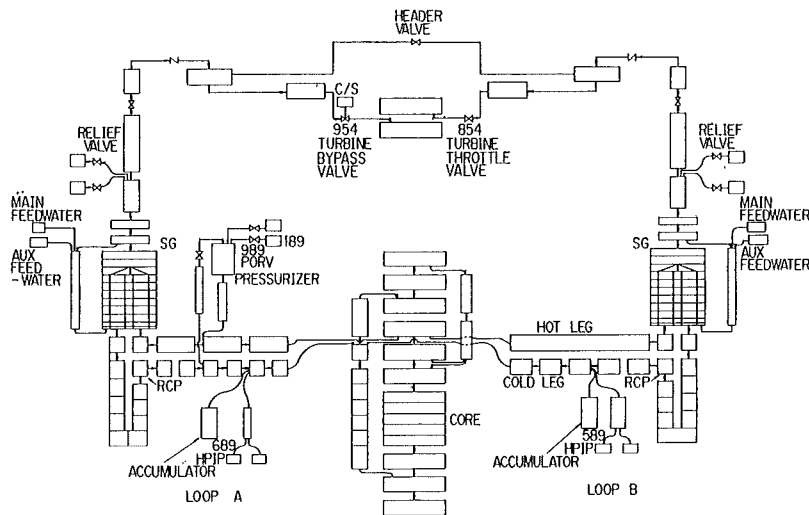


Fig. 1 LSTF nodalization

The reference PWR models and the LSTF model were assumed to be at 100% rated power, i.e. 3423 MWt: reference PWR and 10 MWt: LSTF, as the transient began (Note that 100% rated power for the LSTF is 14% of 1/48 scaled reference PWR rated power).

#### Calculational Matrix

The calculational matrix (see Table I) was constructed to examine the effect of an open PORV (or break flow area variations in the pressurizer manifold) i.e., junction 989, combined with variations in the available emergency core cooling system (ECCS) flow i.e., junctions 589 and 689. All these calculations assumed the PORV to fail open (or a break to occur) at the beginning of the transient. In addition, the main and auxiliary feedwater systems were assumed to fail.

The effect of the high pressure injection pump's (HPIPs) ECCS flow was examined by assuming one of four HPI pumps (shutoff head = 10.7 MPa) was available in one calculation and no HPI pumps in the remaining calculations.

The zero HPI pump flow calculations were conducted to simulate the thermal-hydraulic conditions in the TMI-2 accident which resulted from an operator who responded to a full pressurizer, i.e. an apparently "solid-system" by reducing the ECCS flow.

The baseline transient (No 1) has no HPI pumps and one stuck-open PORV. Transients No 2 and 3 assume break areas in the PORV manifold line midway between one stuck-open PORV and a fully severed PORV manifold line. Transient No 4 assumes a fully severed PORV manifold line, i.e. roughly a flow area equivalent to 13 stuck-open PORVs.

Transient 5 was the only case examined assuming HPI pumps were available. This transient was examined assuming a flow area equivalent to two stuck-open PORVs and with one available HPI pump.

#### BASELINE TRANSIENT: REFERENCE PWR THERMAL-HYDRAULIC BEHAVIOR

Loss of the main feedwater system concurrent with a stuck-open PORV caused an immediate decrease in the secondary (Fig. 2) and primary (Fig. 3) inventories. The secondary inventory decreased to the 25% (narrow range) water level scram setpoint in 4.6s. Thus, at 4.6s the turbine throttle valve began to close and the turbine bypass valves were tripped to open as the primary system hot/cold leg average temperature exceeded 567.7K.

TABLE I: TMI-2 SCENARIO SEQUENCE MATRIX

<u>TRANSIENT</u>	<u>EQUIVALENT No of FAILED PORVs</u>	<u>AVAILABLE ECCS EQUIPMENT</u>
1(1)	1	Accumulators (Ac), low pressure injection pumps (LPIP)
2	2	Ac, LPIP
3	6	Ac, LPIP
4(2)	13	Ac, LPIP
5	2	1 high pressure injection pump (HPIP), Ac, LPIP

(1) Baseline calculation.

(2) The flow area of a fully severed PORV manifold is roughly equivalent to 13 stuck-open PORVs.

Concurrently the primary system pressure decreased (Fig. 4) as primary system mass was exhausted through the PORV. Following scram, the depressurization rate increased as the core power decreased. In addition, the turbine bypass valve opened, increasing the primary to secondary heat transfer. Thus, the primary system fluid shrank as the primary system

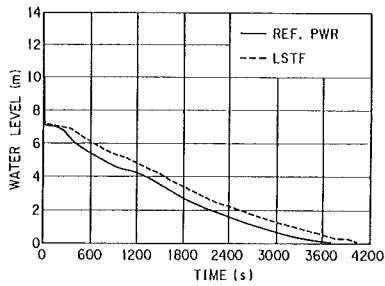


Fig. 2 SG collapsed water level

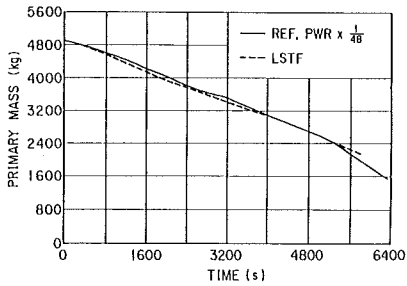


Fig. 3 Primary mass inventory

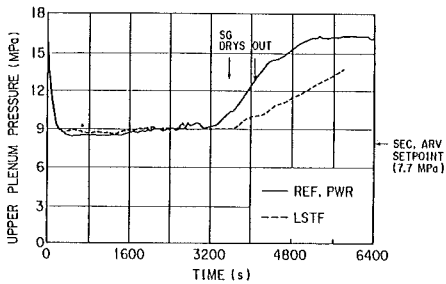


Fig. 4 Primary system pressure

average temperature decreased. Consequently, the pressurizer water level decreased (Fig. 5).

Following closure of the turbine bypass valve, the primary system average temperature slowly began to increase. At the same time, the primary system depressurization continued. The reactor coolant pumps (RCPs) were tripped off at 53.4s as the primary pressure became less than 12.27 MPa, i.e. the safety injection (SI) setpoint pressure. The SI signal also deactivated the turbine bypass valves.

The secondary inventory continued to decrease (Fig. 2) even after the turbine bypass valves were shut, due to the action of the atmospheric relief valves (ARVs) which opened at 75s on high secondary pressure (greater than 7.72 MPa). The secondary pressure remained between 7.72 and 7.9 MPa from 75s until the end of the calculation.

As the primary depressurization continued, voids began forming at the core upper elevations at 190s as the saturation pressure was reached. Thus, liquid mass began to move from the hot leg into the pressurizer causing the pressurizer level to increase (Fig. 5). The primary pressure reached a quasi-equilibrium value at 400s (Fig. 4) as an energy transfer balance was achieved between the core decay power, the primary to secondary heat transfer and the PORV exhaust flow.

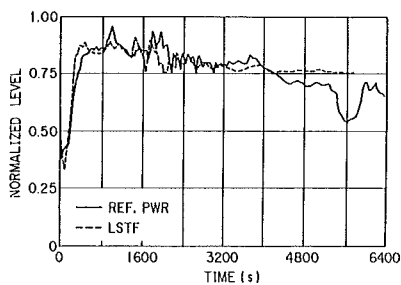


Fig. 5 Pressurizer collapsed water level

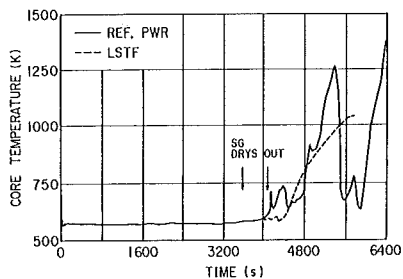


Fig. 6 Core temperatures: upper elevations.

of the calculation. The core was fully dried out at 6320s and a sustained heatup (Fig. 6) was calculated throughout the core.

The pressurizer collapsed water level behavior is of great interest, since the TMI-2 plant operator's misinterpretation of the pressurizer water level [5] resulted in premature ECCS flow reduction during the TMI-2 accident. The reference PWR pressurizer water level reached 86% full by 610s (Fig. 5) and peaked at 93% full at 980s.

The primary system pressure remained relatively constant (Fig. 4) from 400s until 3240s. However, as SG dryout became imminent (Fig. 2) the primary to secondary heat transfer decreased and the primary pressure began to increase. Following SG dryout at 3580s, the primary repressurization rate increased. Along with the increasing primary pressure, the core fuel rod temperatures also increased (Fig. 6). At 4120s intermittent fuel rod heatup was calculated to begin. The primary pressure reached the setpoint (16.2 MPa) of the two operational PORVs at 5300s. The primary pressure remained at or near that value for the remainder

#### BASELINE TRANSIENT: LSTF THERMAL-HYDRAULIC BEHAVIOR

The LSTF initial conditions were set to have the same primary system energy distribution as the reference PWR. However, since the LSTF rated power was limited to 10 MW, i.e., 14% of the scaled reference PWR power, the LSTF primary loop flow rates were also limited to 14% of the reference PWR. In addition, since the LSTF's SGs are geometrically scaled, the LSTF steady-state secondary pressure was maintained at 7.1 MPa (instead of the reference PWR value: 5.7 MPa) to limit the primary to secondary heat transfer to 10 MW.

These differences caused the LSTF to have a different thermal-hydraulic



behavior from the reference PWR early in the calculated transient. For instance, the SG water level, used to trip the PWR core power, behaved differently. Consequently, the LSTF's core power was programmed to trip off at the same time as the reference PWR.

As the transient began, the secondary (Fig. 2) and primary (Fig. 3) inventories began to decrease. The core power began to decay at 7.4s, when the reference PWR core power had decayed to 10 MW (scaled value). The LSTF turbine throttle valve began to shut at 7.4s and the turbine bypass valve opened. However, because the LSTF primary loop flows were a factor of seven less than the reference PWR and the LSTF secondary pressure was at 7.1 MPa, the LSTF primary to secondary heat transfer at scram was lower than the reference PWR. As a result, the LSTF turbine bypass valve remained open longer and depressurized the LSTF secondary below that of the reference PWR. When the primary pressure reached the SI signal setpoint (at 54.5s), the turbine bypass valve was shut. The RCPs were programmed to begin to coastdown at 62.5s in conjunction with the reference PWR.

The primary inventory decreased at much the same rate as the reference PWR. However, the secondary inventory decreased more rapidly than the

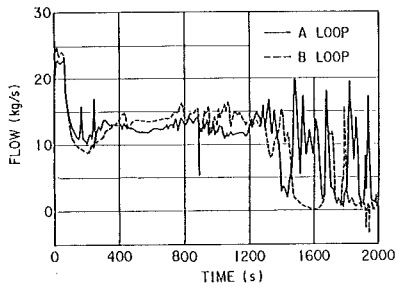


Fig. 7 LSTF A and B loop flows

reference PWR initially. No secondary inventory was lost from the LSTF after 54.5s until 300s when the secondary pressure reached the ARV setpoint. Thereafter, the LSTF secondary inventory also decreased at the same rate as the reference PWR.

The LSTF primary system pressure (Fig. 4) and pressurizer water level (Fig. 5) behaved very similar to that of the reference PWR. However, the A and B loop (Fig. 1) flows prior to stagnation (at 1800s) showed a manometric loop to loop oscillation (Fig. 7) believed to be induced by the rapidly changing PORV mass flux (due to rapid changes in upstream quality).

As the transient progressed, the LSTF SGs began to dry out and the primary pressure began to climb at 3640s. The LSTF SGs dried out at 4060s. However, the LSTF primary pressure did not climb at the same rate as the reference PWR since the LSTF PORV flow had a higher quality than the reference PWR. Core dryout occurred at 4500s and the heater rods began a sustained heatup.

Discounting the LSTF/reference PWR hydraulic behavior mismatch early in the transient, i.e. prior to 300s (resulting from the power/loop flow mismatch), the LSTF/reference PWR correspondence was excellent. Both the LSTF and the reference PWR calculations predicted the onset of extended core heatup in the same time period.

## SYSTEM BEHAVIOR WITH LARGER PRESSURIZER BREAK SIZES

The excellent correspondence between the reference PWR and the LSTF, observed in the baseline calculation, was also observed for transient Nos 2 through 5 (see Table I). All the calculations are shown in Figures 8, 9 and 10 and are summarized in Table II.

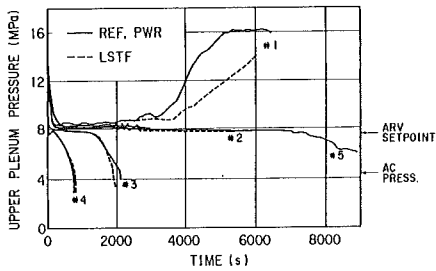


Fig. 8 Primary system pressure

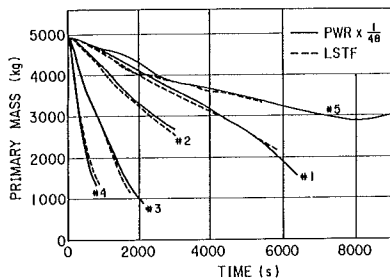


Fig. 9 Primary mass inventory

Transient No 4 behaved very similar to No 3, but the accumulator injection pressure was reached before core dryout occurred. Again low pressure recovery was achieved.

The results of transient No 5, with one available HPI pump, indicated

Transient No 2, assuming a pressurizer leak size equivalent to two stuck-open PORVs, depressurized more rapidly to a primary quasi-equilibrium pressure (7.8 MPa) than the baseline (Fig. 8). A larger primary system mass loss rate (Fig. 9) resulted in the time of core dryout occurring before SG dryout. Consequently, core heatup (Fig. 10) began at 2600s (1500s earlier than the baseline). The reference PWR and LSTF showed good agreement and both predicted extended core heatup.

Transient No 3 showed the primary to depressurize much more rapidly than the baseline. The primary pressure remained at a quasi-equilibrium value for only 1000s before the primary mass loss was sufficient to allow higher quality PORV effluent and rapid depressurization. Dryout at 1700s (Fig. 10) caused the core to rapidly heatup. However, by 2100s the system had depressurized to the accumulator injection pressure (4.5 MPa). Thus, low pressure recovery was achieved.

Transient No 4 behaved very similar to No 3, but the accumulator injection pressure was reached before core dryout occurred. Again low pressure recovery was achieved.

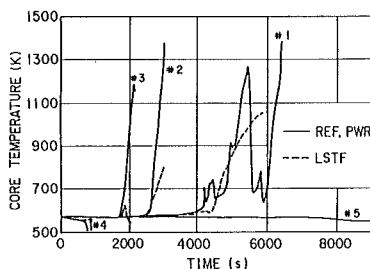


Fig. 10 Core temperatures:  
upper elevations.

system conditional recovery. The primary pressure, with initial behavior the same as that of transient No 2, remained at a quasi-equilibrium value until 7450s. Although the primary mass was still decreasing at 8000s, the core collapsed liquid level was increasing (and the primary pressure decreasing) as the HPI flow moved from the cold leg into the core region. By 8300s the primary mass began to slowly increase as the core steaming rate continued to decrease. Thus, full system recovery was likely (conditional recovery). Again good correspondence between the reference PWR and the LSTF were observed.

TABLE II: Calculation Summary

<u>TRANSIENT</u>	<u>CHARACTERISTICS</u>
1	Core dryout occurred; SG dryout time ( $t_{SG}$ ) < core dryout ( $t_{CD}$ ); primary repressurization prior to core heatup; extended core heatup (ECH).
2	Core dryout occurred; $t_{CD}$ < $t_{SG}$ ; ECH.
3	Core dryout occurred; $t_{CD}$ < $t_{SG}$ ; accumulator injection; recovery.
4	Accumulator injection; recovery.
5	Conditional recovery.

#### CONCLUSIONS AND OBSERVATIONS

Conclusions and observations resulting from the above calculations are:

1. The basic characteristics of a TMI-2 type scenario in a  $\bar{W}$  type four loop plant may best be simulated with a loss of feedwater in conjunction with an open PORV using transient No 1 (see Table I) or a variation of transient No 1 with partial high pressure ECCS. Although transient No 1 repressurized (uncharacteristic of the TMI-2 accident), the "high" pressurizer water level following core dryout (even with no high pressure ECCS present) was characteristic of the accident. Test boundary conditions would include failure or partial failure of the high pressure ECCS. The test would proceed until core temperatures

- reached a specified value.
2. The transient No 5 calculation has demonstrated that the reference PWR ECCS have sufficient capacity to allow conditional recovery of the system with a pressurizer leak equivalent to two stuck-open PORVs, even when only one HPI pump is operative.
  3. Transient Nos 3 and 4 have demonstrated that core heatup during PORV manifold break sizes equivalent to six or more PORVs will be mitigated by the low pressure ECCS.
  4. The loop to loop oscillations observed in the LSTF RELAP5 analyses (see Fig. 7) are thought to be characteristic of the symmetrical two loop construction. Thus, early test data must be carefully monitored to determine whether such behavior is present in the LSTF.
  5. The TMI-2 sequence calculations discussed herein have shown the LSTF to have the same qualitative thermal-hydraulic response as a W type four loop plant for such transients.

## REFERENCES

1. K. Tasaka, et al., Conceptual Design of Large Scale Test Facility (LSTF) of ROSA IV Program for PWR Small Break LOCA Integral Experiments, JAERI-M 9849, December, 1981.
2. N. Zuber, Problems in Modeling of Small Break LOCA, NUREG-0724, October, 1980.
3. R. R. Schultz, Y. Kukita and K. Tasaka, Simulation of a TMI-2 Type Scenario at the ROSA-IV Program's Large Scale Test Facility: A First Look, (to be published).
4. V. H. Ransom, et al., RELAP5/MOD1 Code Manual, Volumes 1 and 2, NUREG/CR-1826, EGG-2070, March 1982.
5. Mitchell Rogovin and George T. Frampton, Three Mile Island - A Report to the Commissioners and the Public, NUREG/CR-1250, January, 1980.

RESULTS FROM THE OECD-LOFT CONSORTIUM TESTS

E.F. Hicken

Gesellschaft für Reaktorsicherheit (GRS) m.b.H.  
Forschungsgelände, 8046 Garching, FRG

This paper is excluded from publication due to the strict rules for publication issued by the Management Board of the International LOFT Consortium.

ZIRCALOY-SHEATHED UO<sub>2</sub> FUEL PERFORMANCE DURING IN-REACTOR LOCA TRANSIENTS

P.J. Fehrenbach, I.J. Hastings, J.A. Walsworth, R.C. Spencer,  
J.J. Lipsett, C.E.L. Hunt and R.D. Delaney

Atomic Energy of Canada Limited - Research Company  
Chalk River Nuclear Laboratories  
Chalk River, Ontario, KOJ 1J0

## ABSTRACT

Four in-reactor transient tests with maximum fuel sheath temperatures up to about 1000°C have been performed at Chalk River Nuclear Laboratories (CRNL) to measure fission product releases and verify sheath deformation calculations in the transient fuel performance code ELOCA. The two Zircaloy-sheathed elements survived the test transients intact and post-irradiation sheath strain measurements compare favourably with code predictions using measured fuel sheath temperature and coolant pressure transients. Sweep gas measurements of activity release to the fuel-sheath gap during high temperature transients with stainless steel-sheath fuel rods indicated increased release rates during high temperature operation. However, the largest releases were associated with rapid heatup and rewet quench.

## INTRODUCTION

Transient fuel performance codes such as ELOCA [1,2], which are capable of predicting the amount of sheath deformation, the occurrence and timing of fuel sheath rupture, and the inventory of short-lived fission products in the fuel/sheath gap at rupture, can be used to assess the development and consequences of fuel damage resulting from hypothetical accidents. Individual ELOCA sub-models, such as that for deformation of Zircaloy during high temperature transients in steam, are based on extensive out-reactor test data [3]. Although data describing the release of short lived fission products during steady state operation has been obtained at CRNL [4] and elsewhere [5,6], in-reactor data on transient release required for model verification are less common. This paper describes four in-reactor tests performed at CRNL to provide data at sheath temperatures up to 1000°C for:

- (1) verification of ELOCA sheath deformation predictions, and
- (2) development of a transient fission product release model to be incorporated in ELOCA.

## FUEL DESIGN AND TEST PARAMETERS

Because the primary test objectives were development and verification of our models, fuel design parameters were chosen for experimental convenience and were not typical of CANDU fuel. All tests were performed using single 20 mm diameter fuel elements instrumented to measure fuel and sheath temperatures, and when appropriate, internal element pressures. Fuel element details and major test parameters are presented in Tables 1 and 2.

In the two tests designed to produce sheath deformation (FIO-130, 131) the elements were sheathed in Zircaloy-4 and contained internal element gas pressures relevant to CANDU fuel. The larger diameter fuel and sheathing, internal clearances for fuel thermocouples, and volume associated with capillary tubing and pressure transducers resulted in an internal volume about three times larger than for CANDU fuel. Sheath strain would not therefore be expected to reduce internal pressures as effectively as in CANDU fuel with smaller internal volume [7].

The two fission product release test elements (FIO-133, 138) were sheathed in 304L stainless steel and connected to an in-reactor sweep gas system. During normal and transient operation, short-lived fission products were swept from the element by a carrier gas and measured on-line by gamma ray spectrometry [4,8].

The high temperature fuel sheath transients were produced in three of the tests by depressurizing the test section while the reactor was at power, to simulate a LOCA condition. As in previous LOCA tests [8,9] the amount of fission heat produced between blowdown initiation and reactor shutdown was used to control the magnitude of temperature rise in the fuel and sheath. The blowdown transients were terminated automatically by cold water injection (rewet) at a pre-set test section pressure. The time between blowdown initiation and rewet was therefore controlled by the rate of depressurization and the selected rewet initiation pressure.

Transients in the remaining test (FIO-133) were obtained by increasing the quality in two-phase coolant flow to induce sheath dryout during full power operation of the fuel element. Rewet was achieved by reversing the procedure and reintroducing hot water into the steam flow. The rates of dryout and rewet were increased from the first to the third dryout transient.

## TEST RESULTS

### Thermo-mechanical Response

Fuel and sheath temperatures, together with reactor power and coolant and internal element pressures are shown in Figure 1 for the two Zircaloy-sheathed tests. Although the two elements contained different pre-transient internal gas pressures, a positive driving force for sheath strain existed during the high temperature portion of the transient for both tests. Both elements survived the transient without experiencing sheath rupture.

Resulting sheath strains were measured by post-irradiation profilometry and typical axial profiles of diametral strain for both tests are shown in Figure 2. As expected, the average strain experienced in the FIO-130 fuel element with the lower internal pressure was much less. The distinct ridges on the sheath at pellet interface locations indicated that strong pellet-sheath mechanical interaction (PCMI) had occurred. The arrest in the peripheral fuel temperature rise and the coincident sharp rise in sheath temperatures as shown in Figures 1 and 2 suggests that much of this PCMI occurred during the early part of the high temperature transients.

The comparison in Table 3 of the post-transient measured sheath strains at each sheath thermocouple position with those calculated by ELOCA shows good agreement. The maximum measured strain was 3.3% to 4.1% at the bottom thermocouple location (875°C) of the FIO-131 element compared with the predicted value of 4%.

The single element test geometry resulted in circumferential temperature variations less than 35°C and circumferential variations in measured strain were less than 1.5%, even at the location of the thermocouples. However, the axial variation in average diametral strain was more significant, consistent with the large axial variation in measured sheath temperature (240°C).

Figure 3 shows the ELOCA predictions of internal gas pressure and sheath strain at the bottom thermocouple location during the FIO-131 transient, and the comparison with measured values. Again the agreement is good. The small overprediction of gas pressure early in the transient is due primarily to the existence of axial variations of temperature and sheath strain which were not taken into account by ELOCA. Both the calculations and measurements show that the internal element pressure decreases rapidly once the sheath begins to strain. For a pre-transient internal pressure of 8 MPa, the driving force for sheath strain is lost after about 4.5% sheath strain and the rate of strain drops to zero before rewet occurs. This sensitivity of internal pressure to sheath strain is a consequence of the relatively small internal volume in these test elements.

CANDU power reactor fuel elements contain an even smaller internal volume. Using the ELOCA code to apply the measured sheath temperature and coolant pressure transients for the FIO-131 test to a regular CANDU fuel element with the same starting internal gas pressure therefore resulted in a smaller calculated sheath strain of about 2%, as shown in Table 3. Further ELOCA calculations showed that even for the higher temperature transient of the FIO-130 test, CANDU fuel elements would remain intact for pre-transient internal pressures up to about 9 MPa.

### Fission Product Release

#### Dryout Conditions

Figure 4a shows release of Kr-88 during the second dryout transient of the FIO-133 test. During normal operation we measured fuel peripheral and sheath temperatures of 800°C and 300°C, respectively; during the transient the maximum corresponding temperatures were 1365°C and 695°C respectively. Integrated release of Kr-88, an example of the short-lived fission products, during the transient, was 0.5%. Figure 4b shows release for Xe-133 during the more severe third transient, with maximum temperatures similar to those for Figure 4a, but achieved in a shorter time. Integrated release in this case was 1.4%. The data in Figures 4a and b show similar features:

- i) an initial burst of release accompanying run-up to maximum temperatures,
- ii) a steady release period at the maximum transient temperature where release was characterized by a  $\lambda^{-1}$  relationship, and
- iii) a major burst of release during rewet.

For the third transient (Figure 4b) rewet was accompanied by a reactor trip. In both cases, about 80% of the release accompanied rewet or rewet/reactor trip, and is consistent with enhanced transport and release of fission products accompanying fuel cracking due to thermal shock. We previously reported [10] that no iodine exited from the fuel element during the transient. None was detected at the spectrometer, and the piping downstream of the test section showed a maximum of only 0.026 Bq (500  $\mu$ Ci). Also, despite the severe thermal shock of the final rewet and trip, the fuel maintained good integrity; there was no sign of powdering.



## Blowdown Conditions

Figure 5 gives initial release results for FIO-138 Blowdown #3, in which the maximum sheath temperature of 850°C was reached 21 s after the blowdown was initiated. Gross gamma activity in the exit sweep gas stream, corrected for transport time to the element, is plotted against time; corresponding reactor power, coolant pressure, and fuel peripheral and sheath temperatures are also shown. The gamma activity is directly proportional to the short-lived fission product release. Activity begins to increase about 15 s into the transient, corresponding with the increase in sheath temperature, and continues to a value about 30% above the pre-transient level. The increased release continues for about 1 min, then falls off as temperatures decrease with the introduction of rewet. An interesting contrast in behaviour with the dryout testing is that there is no significant release during rewet in the blowdown transient. Also, release remained constant during the high temperature periods. The heatup rate is more severe in the blowdown case, and we postulate that fuel cracking permits release during this period. The cracks which form remain open and subsequent release is due to enhanced diffusion of the short-lived species to the fresh surfaces. Radial temperature gradients in the fuel are decreasing during this period but there is insufficient time for crack healing. There is little additional cracking, and thus release, during rewet. In contrast, during the dryout experiment, the fuel temperature distribution is similar to that under normal operating conditions, and crack-healing occurs during the high temperature excursion. Also plotted in Figure 5 is the increase in sweep gas activity accompanying the reactor trip in which there was no temperature increase. This will permit us to determine the release due to the temperature transient alone. Data analysis is being performed to produce integrated release for individual short-lived isotopes.

## CONCLUSIONS

The Zircaloy-sheathed LOCA tests have shown that the transient fuel performance code ELOCA is able to predict sheath strain adequately in superheated steam cooling conditions up to about 1000°C for single element geometry in fresh or irradiated fuel elements.

A small amount of sheath strain reduces the internal element pressure rapidly because of the relatively small internal volume in CANDU fuel elements.

Application of the measured temperature transients (970°C sheath temperature for 40 seconds) to a single CANDU geometry fuel element using the fuel code indicates that the element would survive intact with starting internal pressures up to about 9 MPa.

Under dryout conditions, release of short-lived fission gases is dependent on transient temperature, but most release occurs during rewet, probably caused by fuel cracking.

Under blowdown conditions, most release occurs during the high temperature portion of the transient, prior to rewet.

No iodines were detected at the spectrometer under dryout or blowdown conditions.

## ACKNOWLEDGEMENTS

Part of the work described here was funded by CANDEV, a co-operative development program between Atomic Energy of Canada Limited and Ontario Hydro. The authors also gratefully acknowledge significant contributions to the fabrication and instrumentation of these tests by D. Rose, L.R. Bourque, A.R. Yamazaki, R.L. Stoute and M.G. Jonckheere, to the operation and monitoring of the tests by L.L. Larson, P.G. Anderson, K.G. Heal, M. O'Kane, and D.C. Howell and J. Thomas, and to the data analysis by W.R. Chase and E.P. Penswick.

## REFERENCES\*

- [1] H.E. Sills, "ELOCA - Fuel Element Behaviour During High-Temperature Transients", AECL-6357, 1979 March.
- [2] J.A. Walsworth and H.E. Sills, "High Temperature Transient Fuel Performance Modelling - ELOCA.Mk4", AECL-7693, in preparation.
- [3] S. Sagat, H.E. Sills, J.A. Walsworth, D.E. Foote and D.F. Shields, "Deformation and Failure of Zircaloy Fuel Sheaths Under LOCA Conditions", Presented at the 6th International Conference on Zirconium in the Nuclear Industry, Vancouver, British Columbia, Canada, 1982 June 28-July 01, also as AECL-7754.
- [4] I.J. Hastings, C.E.L. Hunt, J.J. Lipsett and R.D. MacDonald, "Behaviour of Short-Lived Fission Products Within Operating UO<sub>2</sub> Fuel Elements", Res. Mechanica 6 (1983) 167.
- [5] M. Bruet, J. Dodelier, P. Melin and M.L. Pointud, "CONTACT 1 and 2 Experiments: Behaviour of PWR Fuel Rod up to 15000 MW.d.tU<sup>-1</sup>", IAEA Specialists' Meeting on Water Reactor Fuel Element Computer Modelling, Blackpool, U.K., 1980 March 17-21, IAEA Report IWGFPT/7, 1980.
- [6] A.D. Appelhans and J.A. Turnbull, "Measured Release of Radioactive Xenon, Krypton and Iodine From UO<sub>2</sub> During Nuclear Operation and a Comparison with Release Models", Eighth Water Reactor Safety Research Information Meeting, Gaithersburg, Maryland, 1980 October 27-31.
- [7] A.W.L. Segel, "CANDU Design Features that Influence Fuel Modelling for Transients", Nuclear Engineering and Design, 56 (1980) 189.
- [8] P.J. Fehrenbach, "Facilities and Techniques for Instrumented Fuel Irradiations in the NRX Reactor at Chalk River", Irradiation Technology, P. van der Hardt, H. Röttger ed., D. Reidel Publ. Co. Dordrecht Holland, 1983, also as AECL-7994, 1983.
- [9] V.J. Langman, R.D. MacDonald and P.J. Fehrenbach, "Recent CANDU Transient Fuel Behaviour Data from Research Reactor Irradiations", AECL-7415, 1982 May.
- [10] I.J. Hastings, C.E.L. Hunt, J.J. Lipsett and R.G. Gray, "Transient Fission Product Release During Dryout in Operating UO<sub>2</sub> Fuel", International Meeting on Thermal Nuclear Reactor Safety, Chicago, Ill., 1982 August, also as AECL-7832, 1982.

\* AECL-xxxx is a published report of Atomic Energy of Canada Limited.

TABLE 1

FUEL ELEMENT DETAILS			
TEST OBJECTIVE	SHEATH STRAIN	FISSION PRODUCT RELEASE	-
TEST DESIGNATION	FIO-130, 131	FIO-133, 138	CANDU FUEL
<b>UO<sub>2</sub> FUEL</b>			
Diameter (mm)	18	18	12
Length (mm)	462	379	480
Enrichment (wt% U-235)	1.38	1.38	0.7
<b>FUEL SHEATH</b>			
Material	Zircaloy	304L S. Steel	Zircaloy
Diameter (mm)	20	20	13
Thickness (mm)	0.8	0.8	0.4

TABLE 2

MAJOR TEST PARAMETERS				
TEST OBJECTIVE	SHEATH STRAIN		FISSION PRODUCT RELEASE	
Test Designation	FIO-130	FIO-131	FIO-133	FIO-138
<b>Pre-Transient Conditions</b>				
Coolant Type	PW	PW	2 Phase	PW
Temperature (°C)	260-288	260-285	260-350	260-290
Pressure (MPa)	9.7	9.8	8.5	9.8
Flow (kg/s)	0.8	0.9	0.24-0.15	0.8
<b>Fuel</b>				
Power (kW/m)	65	65	60	60
Burnup (MW·h/kg U)	35	3	55	50 (1)
Central temperature (°C)	1975 (2)	1900	1700 (2)	1900 (2)
Peripheral temp. (°C)	860	785	800	725
Sheath temperature (°C)	300-320	289-325	300	280-320
Internal pressure (MPa)	1.5	8.1	-	-
<b>Transient Conditions</b>				
Max. central temp. (°C)	2275 (2)	2200	2300 (2)	2300 (1)
" Peripheral temp. (°C)	1450	1398	1365	1300
" Sheath temp. (°C)	971	875	695	1000
No. of Transients	1	1	3	6
Time at Maximum Temp. (s)	45	25	2400	55
Differential Pressure Across Fuel Sheath (MPa)	0-1.5	2 to 3	-	-

(1) Nominal values.  
(2) Calculated values.

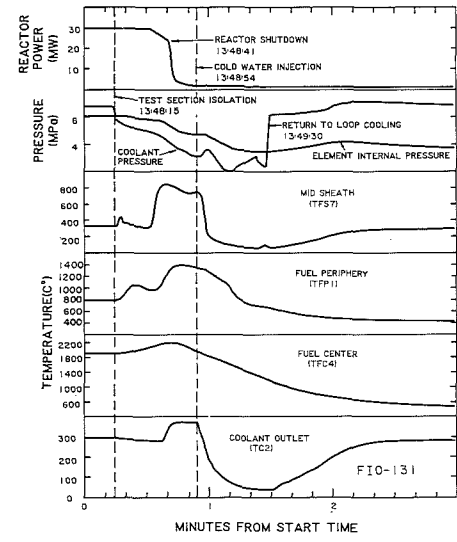
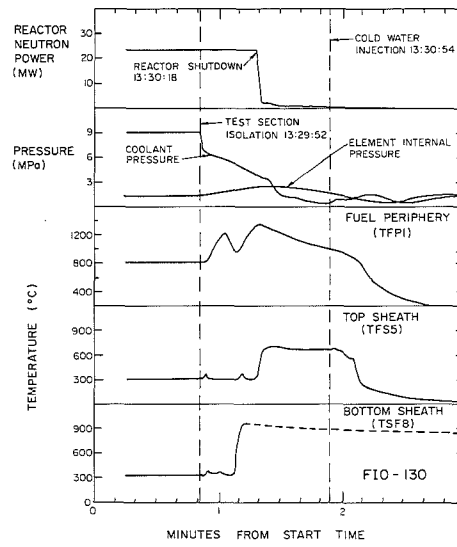


Figure 1 Selected test parameters versus time during the blowdown transients from in-reactor tests FIO-130 and FIO-131

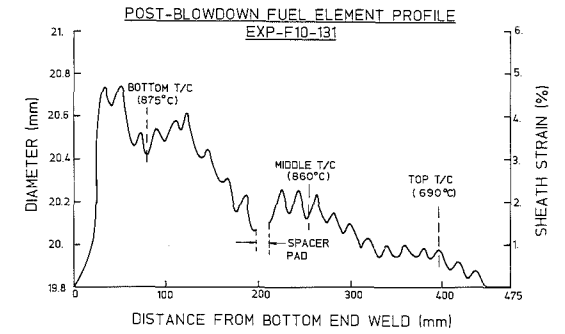
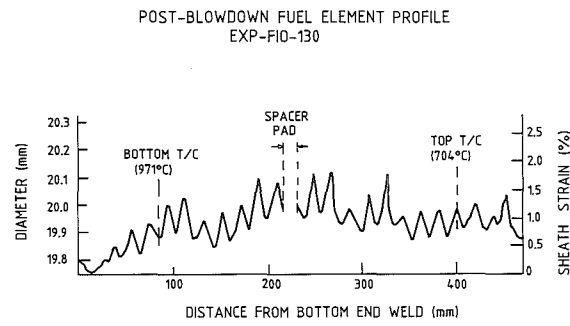


Figure 2 Post-transient diametral element profiles for tests FIO-130 and FIO-131.

TABLE 3

TEST	LOCATION	TEMP (°C)	STRAIN (%)		
			MAXIMUM	MINIMUM	PREDICTED
FIO-130	Top	704	0.75	0.3	0
	Bottom	971	0.80	0.30	2.0
FIO-131	Top	690	1	0.7	0.2
	Mid	860	2.5	1.8	3.2
	Bottom	875	4.1	3.3	4.0
CANDU FUEL		875	-	-	2.0

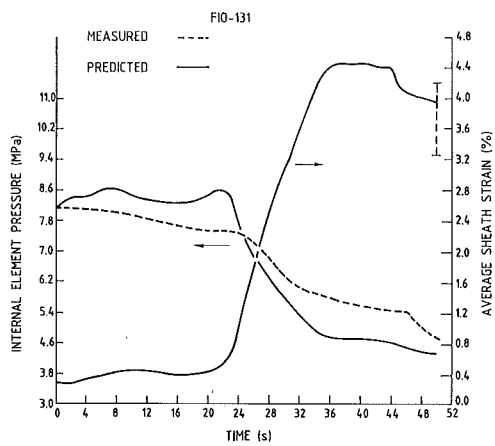
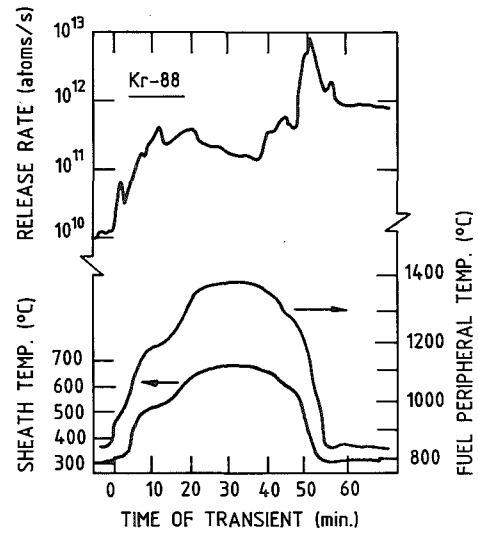
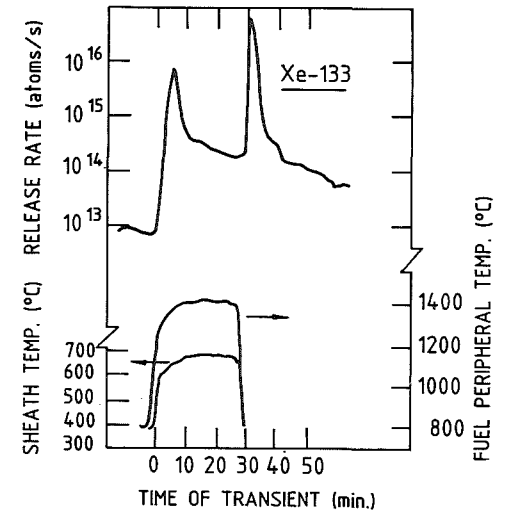


Figure 3 Comparison of measured internal pressure during transient and post-test sheath strain at the bottom thermocouple location (875°C) for FIO-131 with values predicted by ELOCA.



4a



4b

Figure 4 Release rate of selected isotopes during the a) second and b) third dryout transients of the FIO-133 test.

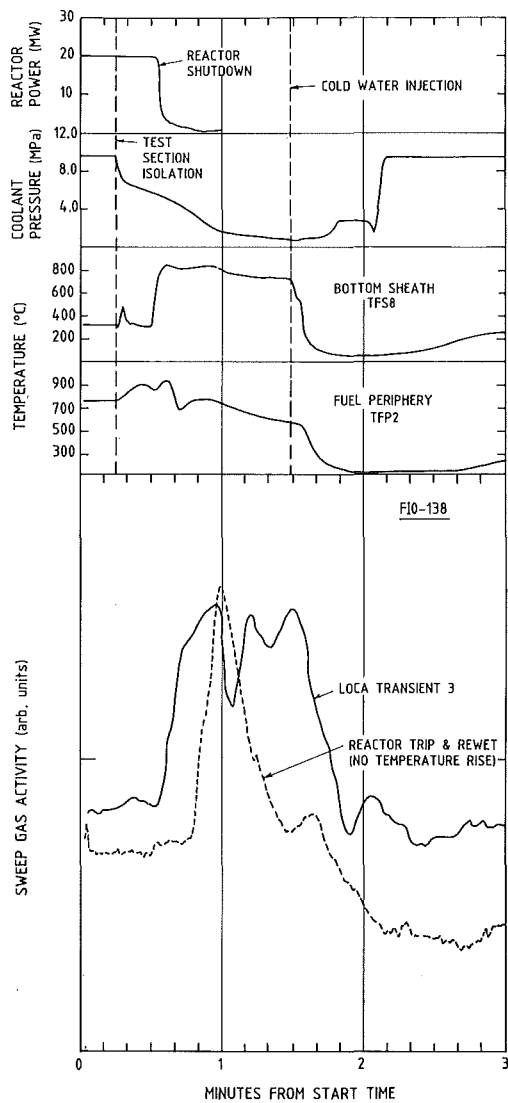


Figure 5 Reactor power, coolant pressure, and fuel and sheath temperatures, together with gross gamma activity of the sweep gas for the third blowdown transient in the FIO-138 test. The sweep gas activity measured during a blowdown cycle performed without a fuel or sheath temperature increase is shown for comparison; the timing of the release curve is displaced arbitrarily for clarity. Also, note the time scale is different than in Figure 4.

## HIGH TEMPERATURE OXIDATION OF CANDU FUEL DURING LOCA

V.I. Nath and E. Kohn

Atomic Energy of Canada Limited  
Sheridan Park, Mississauga, Canada

## ABSTRACT

Oxidation effects on CANDU fuel after a loss of coolant accident (LOCA) are significant only if the fuel cladding temperature exceeds about 1000°C. To reach such temperatures effectively requires the flow to stagnate in the reactor core. This requires a specific break size. The duration of low flow depends on the thermohydraulic characteristics of the circuit. The stagnation influences fuel clad temperatures, but to first order, the temperature is determined by the operating temperature, hence power, of the fuel. For the CANDU reactor second order effects on the cladding temperature arise from the power transient, metal water reaction, blowdown heat removal and radiation. The high temperature duration is short, i.e. less than a minute.

We show that radiative heat transfer from the fuel to the pressure tube is an important inherent mechanism for limiting metal water reaction rates. Further, we establish that the duration and temperature of the transient is well within established embrittlement criteria.

1.0

## INTRODUCTION

With water cooled reactors, a loss of coolant accident causes a cladding temperature rise. If unchecked, this will lead to oxidation of the cladding and eventual embrittlement. Various criteria have been advanced to determine if embrittlement has occurred which would result in fuel failure and/or loss of fuel geometry especially when the cladding rewets at the end of the transient.

The basic purpose of the present work is two-fold:

- (a) to evaluate the importance of radiative heat transfer from the fuel to the pressure tube as a self-limiting mechanism for metal water reaction (MWR) rates in a CANDU reactor, and
- (b) to derive therefrom the time to cladding embrittlement for various linear bundle powers in order to show that realistic fuel transients would not cause embrittlement.

To accomplish this, a sensitivity study is performed at various bundle powers.



## 2.0 MODELS, ASSUMPTIONS AND BOUNDARY CONDITIONS

The study is performed under artificial undercooling assumptions for a 37 element bundle (Figure 1) used in CANDU 600 reactors. The cladding temperatures, the heat generated by the MWR and the heat transferred to the pressure tube (PT) are calculated by a transient 2-dimensional, thermal model of the bundle with the following assumptions:

- (1) The GE correlation [1] is used to evaluate the heat generated due to MWR. The GE correlation applies up to 1577°C or the range of application in this study. The reacted metal,  $w$ , measured in weight/unit area is assumed to be of the form:

$$w^2 = kt$$

where  $t$  is the time of reaction and  $k$ , referred to as rate constant, depends upon the universal gas constant (cal/mole K), absolute temperature (K) and activation energy (cal/mole). The method of Sparrow and Cess [2] is used to calculate the thermal radiation. This thermal model of a CANDU fuel bundle was developed by Ontario Hydro and is known as HOTSPOT.

- (2) The power transient, the heat transfer coefficient (HTC) between the cladding and the coolant, the coolant pressure, and the coolant temperature are boundary conditions for these calculations. The last three variables are obtained from thermohydraulic predictions. The power transient used in the present study, shown in Figure 2, is based on a fast-voiding LOCA and the slower shutdown system (solid rods). (The CANDU 600 reactor has two independent shutdown systems.)
- (3) The contribution of  $UO_2$ /zircaloy interaction to the total heat produced is insignificant and, therefore, not considered. The effect of such an interaction on the phenomenon of embrittlement is discussed in the next section.
- (4) Typical CANDU fuel cladding LOCA temperature transients have a duration of less than a minute (Figure 3).

The cladding heatup duration was artificially prolonged to show the tolerance of the CANDU design to conditions much more severe than those expected in a large LOCA, and therefore to give some idea of the available margins to embrittlement. The boundary conditions are fixed as follows.

For the first ten seconds, the boundary conditions were taken from the thermohydraulic predictions which are in themselves pessimistic due to assumptions such as not crediting the faster shutdown system (liquid poison injection into the moderator). Convection cooling was then artificially minimized as follows: The heat transfer coefficient was instantaneously decreased to  $0.1 \text{ kW/m}^2 \text{ K}$  (appropriate for dry steam at low flow) and kept constant for the rest of the calculation. The coolant temperature was conservatively kept constant at 900°C. These conditions were chosen from thermohydraulic predictions as the minimum value of heat transfer coefficient and a high coolant temperature chosen during the stagnation period in the channel. The transients are run to 100 seconds; going further is meaningless since best estimate predictions show clad temperature turnaround by about 50 seconds.

It is assumed that the pressure tube (PT) does not strain to contact the calandria tube (CT) which is surrounded by subcooled moderator. This is not real for the prolonged transients but keeps the pressure tube temperature higher and the resulting heat loss from the fuel lower. Even without contact, heat from the fuel will still be radiated to the CT via the PT and thus go to the moderator - an inherent heat sink.

The resulting boundary conditions thus form an envelope to the expected behaviour during a LOCA.

We studied four bundles with powers ranging from 1560 to 2140 kW/m. In the reactor at any given time, most of the fuel bundles have power less than 1450 kW/m, with peak powers not expected to exceed 1870 kW/m.

### 3.0 EMBRITTLEMENT CRITERION

Embrittlement of Zircaloy-4 fuel cladding has been a concern since Hobson and Rittenhouse [3] observed that a specimen exposed at 1315°C in steam for two minutes (and then cooled) fractured when tested in slow compression, while one held at 1200°C did not. Hesson et al [4] heated UO<sub>2</sub> fuel clad in Zircaloy-2 at high temperatures in steam for short times and then quenched it with water. Only those claddings failed which had oxidized more than 0.17 times the total cladding thickness before quenching. This led to the establishment of the 1200°C/0.17 oxidation embrittlement criterion.

It is well recognized (Hobson [5], Pawel [6], Sawatzky [7], Tong [8]), that ductility of the cladding after oxidation is determined by the oxygen concentration in the  $\beta$ -phase. Embrittlement is, therefore, a function of temperature and time. In this assessment, we use the embrittlement criterion developed by Sawatzky [7], from which can be derived a time at temperature relationship shown in Figure 4.

The fuel sheath has the potential to interact with the fuel pellets and thus be oxidized. The rate at which this occurs has been studied by Hofmann [9] and Rosinger [10]. Rosinger's study included the effect of CANLUB graphite deposited on the inner surface of the CANDU fuel sheath. At 1373 K and 1473 K at times up to 7200s no interaction occurred. Therefore, the UO<sub>2</sub>-zircaloy interaction is unimportant for the short transients we are considering here.

### 4.0 RESULTS AND DISCUSSION

Zero to one hundred second temperature histories of the fuel cladding for the 1790 and 2140 kW/m power bundle are shown in part (a) of Figures 5 and 6. Part (b) of these figures show the heat generated by the MWR as compared to the heat removed by radiation to the PT. There is significant heat storage in both the fuel and the pressure tube which reduces the rate of cladding temperature increase.

The heat removed from the fuel bundle by radiation is always greater than the heat generated by metal water reaction. The cooler pressure tube is a significant "brake" on the fuel cladding heatup rate, even without crediting significant heat transfer to the moderator via the PT/CT. Even at a high cladding temperature of approximately 1450°C (Figure 6), the MWR amounts to only about one-fourth the decay power (Table 1). Table 1 gives the power generation and heat losses from the fuel, and the time to embrittlement at the peak cladding temperature (PCT) for the four bundle powers studied.

The neutron flux gradient across the CANDU bundle acts as a significant equalizer to element temperatures. The outermost elements, which have the highest ratings, are most affected by radiation to the pressure tube while the centre element, which has the lowest rating, is almost unaffected. Thus the temperatures of all elements after about 100 seconds are within 125°C of each other (Table II).

For the maximum power CANDU bundle (1870 kW/m), time to embrittlement at the peak cladding temperature under the arbitrary undercooling assumptions presented, is of the order of 100 seconds; the actual period of overheating is ~ 50 seconds (Figure 3), and at lower temperatures. For powers well above the maximum, the time decreases, but not drastically. For lower powers, the time to embrittlement grows to 200 seconds for 1790 kW/m and 950 seconds for 1560 kW/m bundle. The peak cladding temperatures for the four bundles are 1443°C, 1353°C, 1293°C, 1204°C.

Thus CANDU fuel is tolerant to severe LOCA transients which are terminated in the short times expected when the emergency coolant injection system operates. However, even if the transients were so severe as to cause embrittlement of the fuel, for example if the ECC system were impaired, it would still be maintained inside the fuel channel [11], so that core geometry would be preserved.

## 5.0

### CONCLUSIONS

The radiative heat transferred to the pressure tube is significantly more than the heat generated by the metal water reaction. This slows significantly the temperature escalation due to exothermic reaction.

Even with convection cooling artificially minimized, so that temperatures ~ 1300°C result, the times at such temperature for CANDU fuel bundles are factors of 2 or greater below physically-based embrittlement criteria.

## 6.0

### REFERENCES

1. P.W. Ianni, Metal Water Reaction - Effects on Core Cooling and Containment, APED-5454 (March 1968)
2. E.M Sparrow and R.D. Cess, Radiation Heat Transfer, Brooks Cole Publishing Co., Belmont, California (1966)
3. D.O. Hobson and P.L. Rittenhouse, Embrittlement of Zircaloy-Clad Fuel Rods by Steam during LOCA Transients, ORNL 4758 (1972)
4. J.C. Hesson et al, Laboratory Simulations of Cladding - Steam Reactions Following Loss-of-Coolant Accidents in Water-Cooled Power Reactors ANL-7609 (1970)
5. D.O. Hobson, Ductile-Brittle Behaviour of Zircaloy Fuel Cladding, Proc. Topical Meeting on Water Reactor Safety, March 26-28, 1973, Salt Lake City, Utah, Conf. 73034
6. R.E. Pawel, Oxygen Diffusion in Beta Zircaloy During Steam Oxidation, J. Nucl. Mat. 50 (1974) 247
7. A. Sawatzky, A Proposed Criterion for the Oxygen Embrittlement of Zircaloy-4 Fuel Cladding, Zirconium in the Nucl. Industry (Fourth

Conference), ASTM STP 681, American Society for Testing and Materials, 1979, pp. 479-496

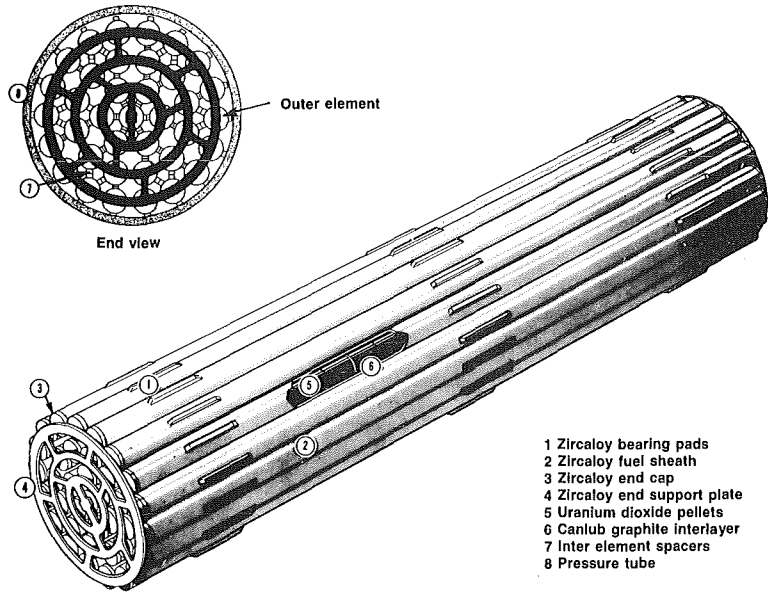
8. L.S. Tong, Issues Concerned with Future Light-Water Reactor Designs, Nuclear Safety Vol. 23, No. 2, March 1982, pp. 127
9. P. Hofmann, Out of Pile UO<sub>2</sub>/Zircaloy-4 Experiments Under Severe Fuel Damage Conditions, Proceedings of the OECD-NEA-CSNI/IAEA Specialist's Meeting on Water Reactor Fuel Safety and Fission Product Release in Off-Normal and Accident Conditions - RISØ National Laboratory Denmark May 16-20, 1983
10. H.E. Rosinger, A Study of Pellet/Clad (Uranium dioxide/Zircaloy-4) Interaction at 1372 K and 1473 K, Atomic Energy of Canada Ltd. Report AECL 7785, February 1983
11. P.D. Thompson and E. Kohn, Fuel and Fuel Channel Behaviour in Loss of Coolant Accident without the availability of the Emergency Coolant Injection System, Proceedings of the Meeting on Water Reactor Fuel Safety and Fission Product Release in Off-Normal and Accident Conditions - RISØ National Laboratory Denmark May 16-20, 1983

TABLE I  
EFFECTS OF DIFFERENT BUNDLE POWERS  
at 100 SECONDS

Bundle Linear Power (kW/m)	Outer Element Linear Power (kW/m)	Decay Power (kW/m)	MWR (kW/m)	Radiation to PT (kW/m)	Power to Coolant (kW/m)	'Time to Embrittlement at PCT(s)
1560.	48.	64.	11.	19.5	39.5	950
1790.	55.	73.	15.	22.	51.	200
1935.	59.	79.	18.	23.5	59.	90
2140.	65.	87.5	22.5	27.	71.	20

TABLE II  
TEMPERATURE DISTRIBUTION IN BUNDLES AT  
DIFFERENT TIMES

ELEMENT	1790 kw/m Bundle Temp. (°C) at			2140 kw/m Bundle Temp. (°C) at		
	5 s	20 s	100 s	5 s	20 s	100 s
OUTER	1012	1118	1198	1152	1256	1322
INTERMEDIATE	911	1106	1287	1038	1278	1429
INNER	841	1005	1280	926	1146	1435
CENTRE	809	956	1255	890	1081	1413



Pressure tube, calandria tube, bundle configuration

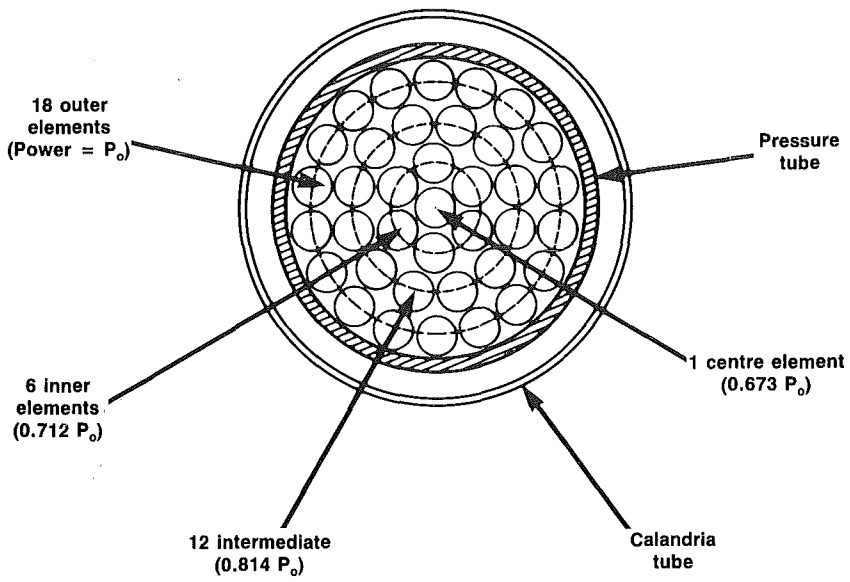


FIGURE 1 600 MW(e) 37-ELEMENT FUEL BUNDLE

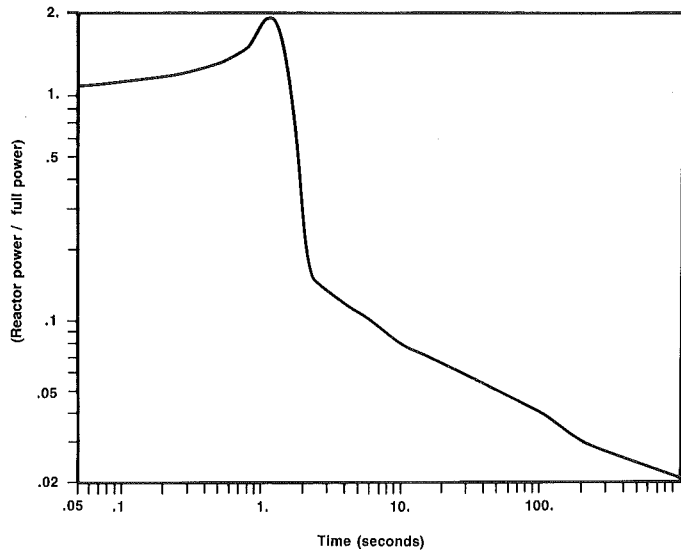


FIGURE 2 POWER TRANSIENT FOLLOWING LOCA

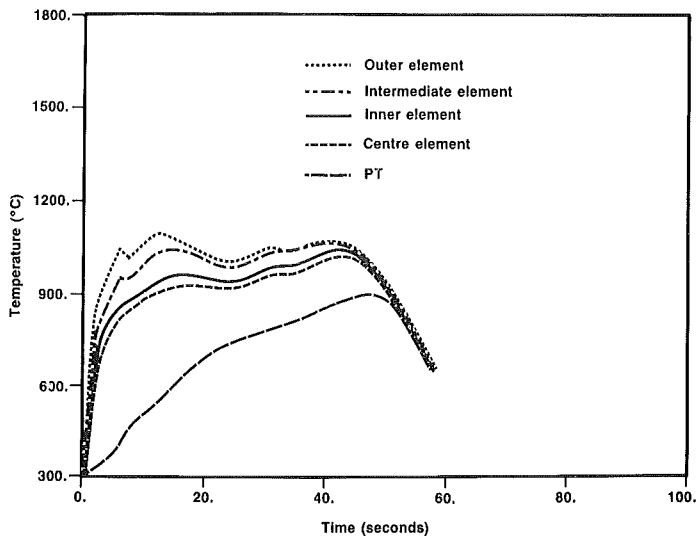


FIGURE 3 TYPICAL "CANDU" FUEL CLADDING TEMPERATURES FOLLOWING CRITICAL LOCA (OFFSITE POWER UNAVAILABLE)

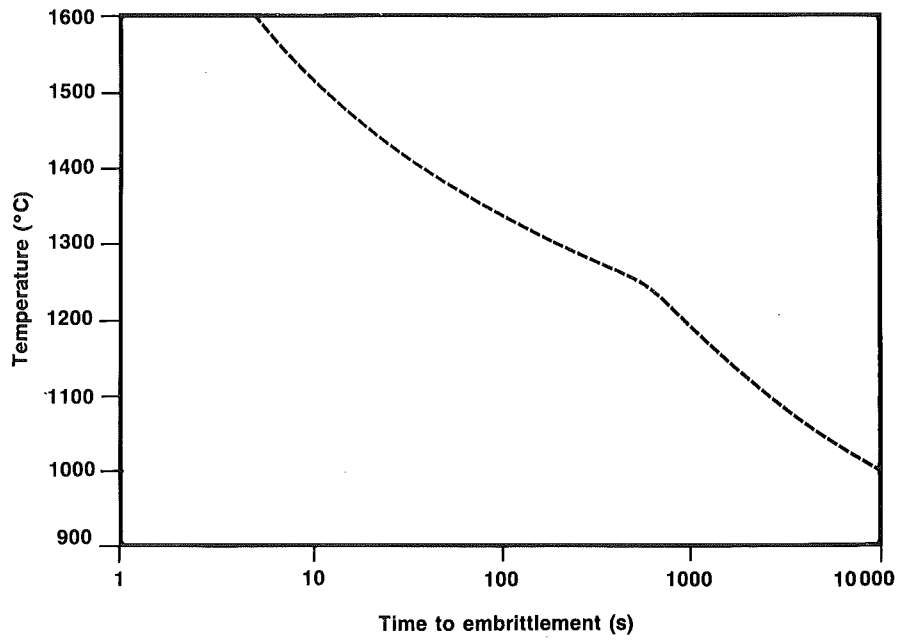


FIGURE 4 SAWATZKY'S CURVE



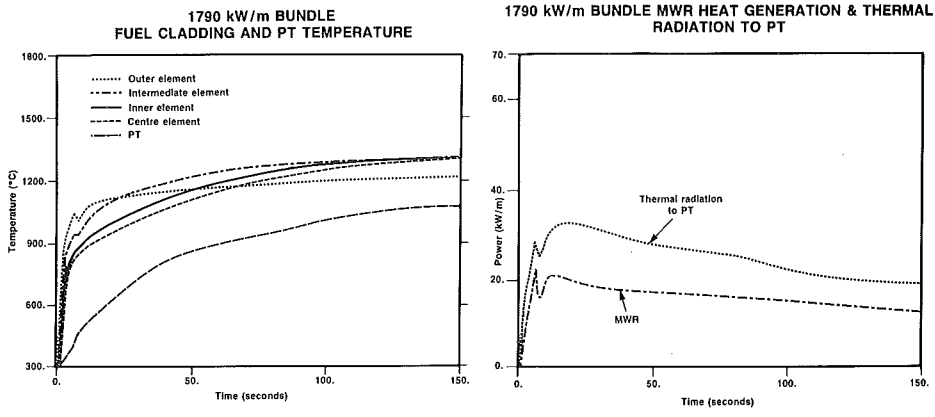


FIGURE 5 1790 kW/m BUNDLE

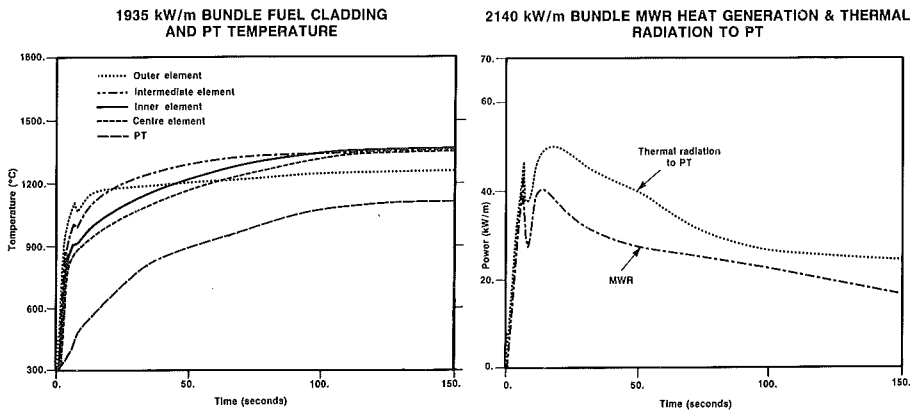


FIGURE 6 2140 kW/m BUNDLE

THE IMPORTANCE OF END-OF-BLOWDOWN PHASE ON  
REFILL/REFLOOD FOR THE CASE OF  
COMBINED ECC INJECTION. RESULTS FROM PKL TESTS

R.M. Mandl, B. Brand, H. Schmidt

Kraftwerk Union AG, Erlangen

ABSTRACT

To simulate the latter stage of a large break loss of Coolant Accident (LOCA) more realistically the end phase of blowdown (EOB) has to precede the refill/reflood. The appropriate tests were carried out in the PKL (Primärkreisläufe) facility. The results, confirming TRAC (Transient Reactor Analysis Code) calculations show that the EOB phase has a considerable influence on the course of a large break LOCA in case of combined ECC-injection. Residual water as well as the water injected into the hot legs effect good core cooling, lead to early rewetting and energy transport out of the core and thus speed up core reflooding.

1. INTRODUCTION

Design basis criteria as well as licensing procedures call for proof of core coolability during postulated loss of coolant accidents (LOCA). To this purpose complex computer codes capable of predicting the thermohydraulic core behaviour have been developed. These codes have to be verified by their correctly predicting the course of a LOCA simulated in test facilities. These facilities, called System Test Facilities must in turn, be capable of simulating, normally on a reduced scale, the behaviour of a PWR under LOCA conditions.

From technical point of view (e.g. fuel rod simulation) it is extremely difficult to build a test facility capable of simulating the full pressure and power of a PWR and at the same time having sufficiently large dimensions to correctly model phenomena which occur in the refill and reflood phase of a LOCA. The time (at the end of blowdown) of pressure equalization with containment - about 4 bar - appeared to be a natural dividing line between the predominantly homogeneous flow during blowdown and the refill/reflood characterized by a pronounced separation of the liquid and vapour phases of the coolant. The acceptance of this dividing line enabled the simulation of blowdown and refill/reflood in two kinds of test facilities. Full pressure, full-power scaled test facilities with 25 - 70 fuel rod simulators modelled successfully the blowdown conditions whereas test facilities with low pressure capabilities, decay power smaller than ten percent and scaled with 300 - 2000 fuel rods, simulated under conservative assumptions the low pressure refill/reflood phase. Conservative

assumptions were applied where uncertainties were encountered - one of them being that at the beginning of refill (4 bar) the primary side was devoid of water and filled with stagnant steam.

This and conservatively predicted clad temperatures constituted the initial conditions for all previous refill/reflood tests. No credit was taken for the presence of either blowdown residual water or for ECC water already injected in the latter phase of blowdown by accumulators (p < 26 bar). To bridge the gap in modelling blowdown and refill/reflood phase the Primärkreisläufe (PKL) test facility, Fig. 1, designed for 40 bar, was adapted to simulate refill/reflood preceded by End-of-Blowdown (EOB) thereby creating more realistic boundary conditions.

This presentation describes the logical basis for and way of performing these tests. The first results confirming the influence of EOB are presented.

## 2. PKL II TEST OBJECTIVES

In order to simulate the latter stage of large break LOCA more realistically it is necessary to relax some of the conservative assumptions applied up till now. More representative boundary conditions are achieved by preceding refill/reflood with End-of-Blowdown (EOB) and simultaneously applying the so called 'Best Estimate' (BE) conditions. Some of the important differences between licensing and Best-Estimate assumptions are the following:

- power level and power density distribution
- decay power
- stored energy in core
- availability of emergency core cooling systems.

In case of a combined injection ECC-system however, the most significant contribution is made by considering the cooling effect of accumulator water in the EOB phase. This water, injected in the latter phase of blowdown and largely ignored in the conservative analysis, assists in early cooling of fuel rods especially in core of large sized cold leg breaks. Calculations made using the American TRAC PF 1 Code, developed for Best-Estimate analysis, showed for the case of a KWU-line PWR (combined injection) that taking into account the cooling effect of the accumulator water not only reduces the maximum fuel rod temperatures by several hundred degrees K but also prevents the usually expected second temperature peak during the refill and reflood phase Fig. 2.

It is the objective of the current PKL test series to perform refill/reflood experiments under Best-Estimate conditions as described above and initiated before End-of-Blowdown. For this purpose the PKL facility was modified and a new test procedure introduced.

## 3. TEST FACILITY

The PKL (Primärkreisläufe) test facility in which the EOB tests are carried out represents a typical KWU 1300 MW(e) four loop PWR on a scale of 1 : 145. It was designed to simulate the behaviour of the entire primary system during the refill and

reflood phase of a LOCA. In view of the importance of the driving gravity forces during reflood all elevations correspond to actual reactor dimensions (1:1)

The test facility is designed for a maximum pressure of 40 bar. In Fig. 1 the PKL test facility is shown as modified for EOB tests. The test bundle simulating the core consists of 314 electrically heated rods. These are subdivided into 3 independently heated zones. 25 heater rods are instrumented with over 150 thermocouples.

The three loops (one of them of double capacity simulating two loops) contain steam generators with original-size tubes. Their secondary sides are also volume-scaled and are filled during the test with water at 55 bar and its corresponding saturation temperature in order to simulate the energy transfer to the primary side and the resulting pressure drop.

In addition to the scaled components PKL is equipped with a separator (mass flow rate downstream of break) and three conditioning-water tanks which inject water into the system during the conditioning phase (26 bar  $< p < 40$  bar).

The facility is instrumented with over 600 measuring points. Apart from the conventional measurement of temperature, pressure and single-phase mass flow two-phase flow instrumentation also exists. The test data are recorded at sampling frequencies of 25 Hz (pressure, diff. pressure, mass flow) and 5 Hz (temperature).

#### 4. TEST PROCEDURE

The so called 'Conditioning Phase' (Fig. 3) is started at 40 bar with stagnant-steam filled system by opening the break and injecting hot water into the pipes to the left and right of the break as well as into the upper plenum for cold leg break and into downcomer for hot leg break.

The objective is to achieve, on reaching 26 bar

- pressure gradient
- core mass flow rate
- fluid density distribution
- clad temperature
- containment backpressure

identical to what these would be if the facility had experienced a complete blowdown starting at 160 bar. The prevailing conditions at 26 bar are precalculated by system codes TRAC and DRUFAN.

For a specified break size and location three calculations are made:

1. A prototype PWR transient starting from normal operating conditions, i.e. 160 bar, full power.
2. A PKL transient starting from normal operating conditions assuming PKL were designed for 160 bar and full power.
3. A PKL transient starting at 40 bar with a steam-filled system and simultaneous injection of hot water to the left and right of the break as well as into the upper plenum or downcomer.

The first two calculations are made in order to demonstrate the suitability of the PKL test facility for the proposed tests. The amount of 'injected' water which causes calculations 2 and 3 to be identical is the amount to be used for the conditioning of the specified test.

## 5. RESULTS

According to the original schedule it was intended to complete the current End-of-Blowdown test series (PKL IIB) by July 1984. Due to unexpected multiple failure of heater rods repairs had to be carried out and the test series was delayed. For this reason the results shown are limited to the first test in the test matrix i.e. double ended guillotine break in the cold leg between the pump and reactor pressure vessel inlet. The initial and boundary conditions, Fig. 4, were those of a Best Estimate case as described in chapter 3. The results and conclusions are consistent with several shakedown test runs under similar conditions.

It can be said that the conditioning procedure consisting of injecting water to the left and right of the break to control the pressure gradient and simultaneously injecting water into the upper plenum to effect the correct mass flow direction and distribution is practicable and was successfully carried out.

The rate of change of pressure during EOB is identical to that predicted by TRAC calculations, the absolute values differ only slightly, Fig. 5. The maximum velocity indicated in the downcomer is of the order of 70 m/s which compares favourably with the predicted value of 80 m/s. There is no velocity measurement available in the core but correct velocity in the downcomer allows the assumption of correct velocity in the core. The mass distribution at these high velocities will be more or less homogeneous.

As expected from precalculations a large number (about 30 %) of the heater rod thermocouples quench in the EOB-phase (0 - 30s) confirming the fact that presence of water in the core (1.0) particularly at elevated pressure produces considerable cooling effect in the unwetted region leading to faster quenching. The temperature rise is limited to ca. 50 K, Fig. 6.

Comparing the flow pattern in the system with the predictions it can be seen that during EOB hot leg oscillations take place only in the broken loop. The hot leg of the single intact loop experiences high negative flow due to surge line depressurization, during this phase the flow in the double loop is almost negligible. During reflood all three hot legs show periodic oscillations. The highest amplitude is recorded in the broken loop where subcooled water penetrates into the steam generator tubes (Fig. 7) and partly evaporates thereby reinforcing the oscillations. The single and double loops show similar oscillations in horizontal sections of their respective hot legs, however hardly any water enters the steam generators.

Oscillation in the hot legs are transmitted through the upper plenum and influence, among others, a periodic breakthrough of subcooled water into the core. In certain regions the subcooled water penetrates the whole length of the core (Fig. 8).

During EOB the downcomer and core are exposed to negative flow at high velocities. In the reflood phase downcomer oscillations (typically - 1.0 m/s + 0.6 m/s) can be correlated with oscillations in core and hot legs.

The overall system behaviour during cold-leg-break reflood is typical of combined injection experiments i.e.

- net negative flow through core and downcomer
- penetration of subcooled water through the upper tie plate
- no significant steam flow through steam generators.

#### 6. FUTURE WORK

The results discussed here are based on a 200 % cold leg guillotine break and combined ECC injection. The PKL II test matrix contains five additional cold leg break tests as well as two with break in the hot leg. Parameters are amount and location of injected water i.e. cold leg only, hot leg only or combined injection.

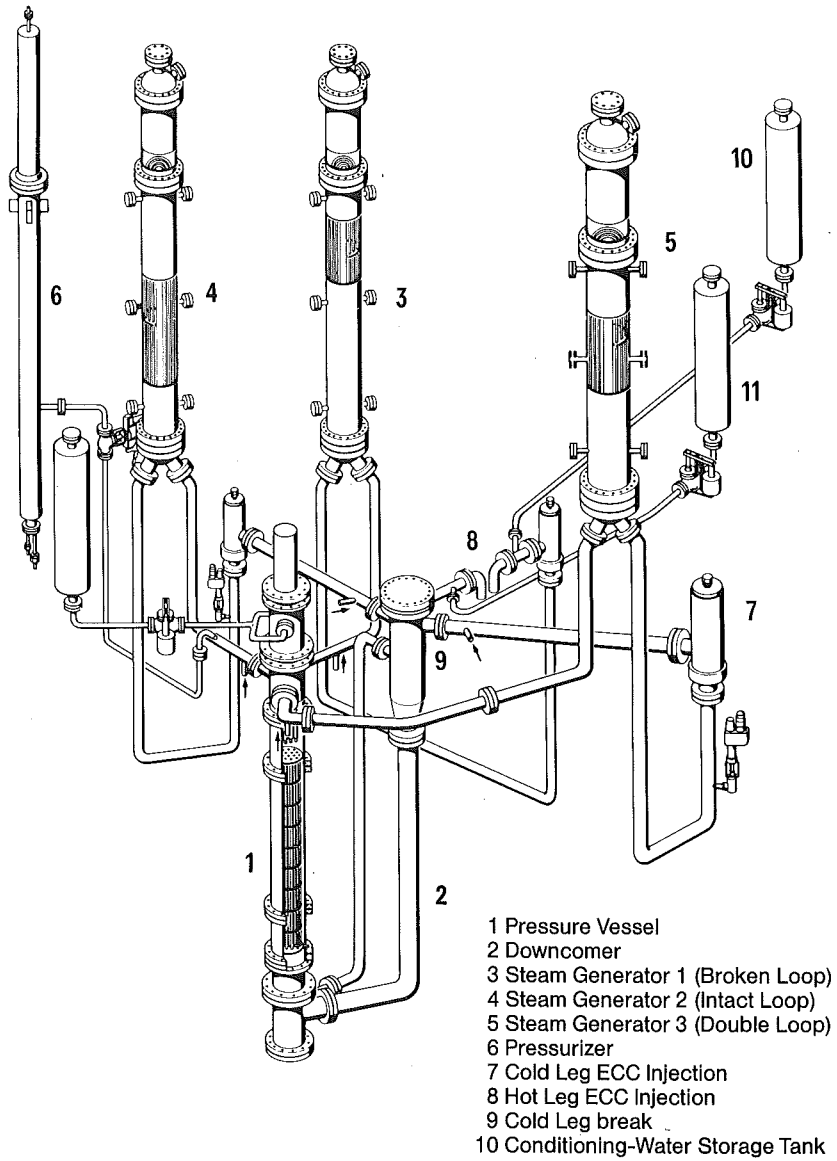
#### 7. CONCLUSIONS

Realistic initial and boundary conditions in refill/reflood tests are achieved by preceding these tests with End-of-Blowdown. This procedure together with Best-Estimate conditions for decay power, ECC rates and core temperatures form the basis for PKL IIB test matrix.

The first test (200 % double-ended cold leg break, combined injection) proved that the envisaged conditioning procedure can be realized in practice. By injection of a specified amount of hot water the depressurization gradient ( $p \leq 26$  bar) was effectively controlled. The ECC water injected into the hot legs penetrated the core before refill/reflood causing efficient fuel rod pre-cooling during the EOB phase. This in turn led to limited temperature rise (ca. 50 K) and rapid core quenching.

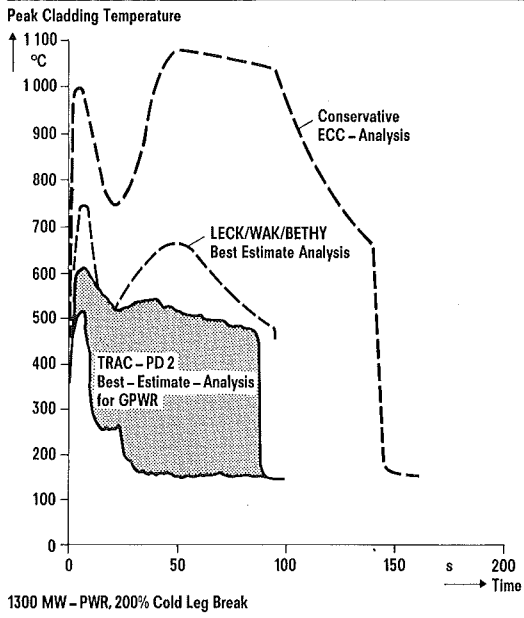
#### References:

Brand B., Sarkar J.: "Wiederauffüll- und Flutversuche mit Berücksichtigung der Primärkreisläufe (PKL)"; Band 1 Ergebnisse der Versuchsserien PKL IB + IE, Abschlußbericht Förderungsvorhaben BMFT 1500 287

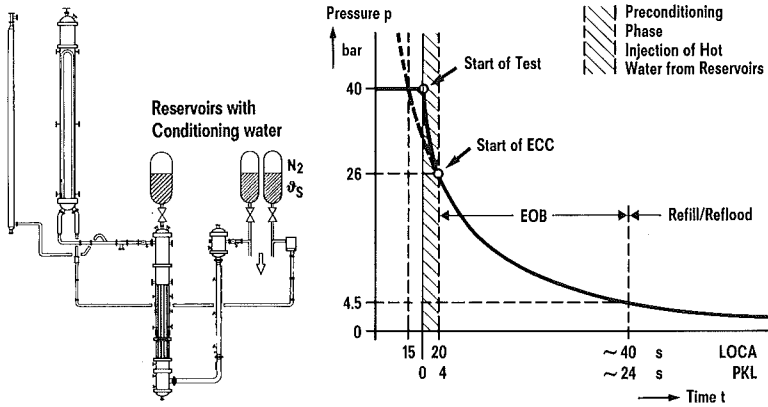


PKL II B - TEST FACILITY

Fig. 1



PEAK CLADDING TEMPERATURES WITH CONSERVATIVE AND BEST-ESTIMATE ANALYSIS Fig. 2



PKL II B - TEST PROCEDURE FOR END-OF-BLOWDOWN TESTS Fig. 3

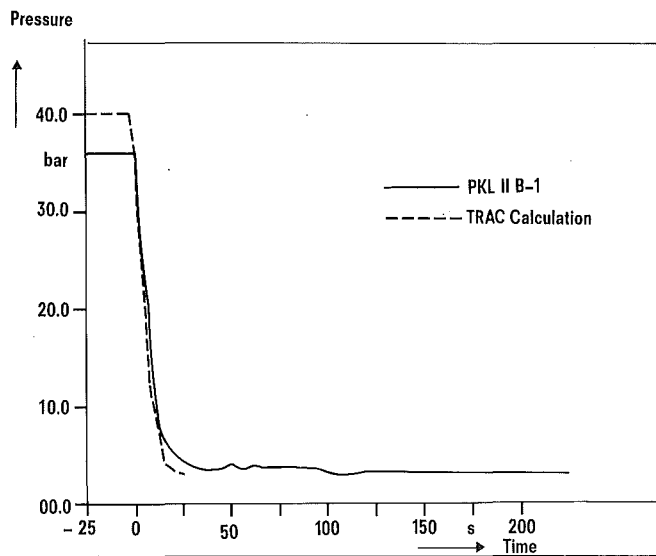




No.	Break		Coolant Injection (8/8 Acc. + Pumps)		Comments	Required Calculations
	Location	Size	Cold Leg	Hot Leg		
Shake-down Test	Cold Leg	200%	3/8	4/8		R = Reactor calculations K = Conditioning calculations
1	Cold Leg	200%	3/8	4/8	Best Estimate, EOB-Base Test	R, K
2	Cold Leg	200%	2/8 Acc. 3/8 P	3/8	Licensing Conditions	R, K
3	Hot Leg	200%	--	2/8 Acc. 3/8 P		R, K
4	Hot Leg	200%	3/8 P	3/8 Acc. 3/8 P		Reference Values
5	Cold Leg	200%	W	--	ECC-Rates according to W K-factors	
6	Cold Leg	100%	3/8	4/8	Best Estimate with	R, K
7	Cold Leg	200%	3/8	4/8	Best Estimate Alternative Conditioning	K

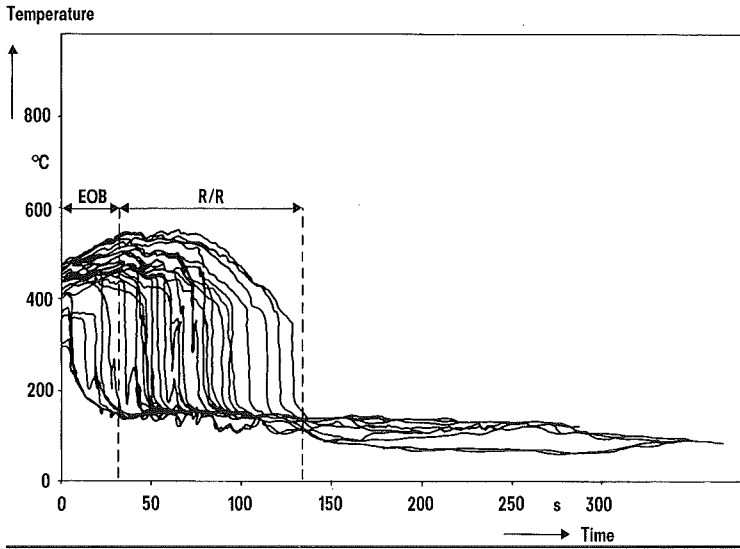
PKL II B - TEST MATRIX

Fig. 4



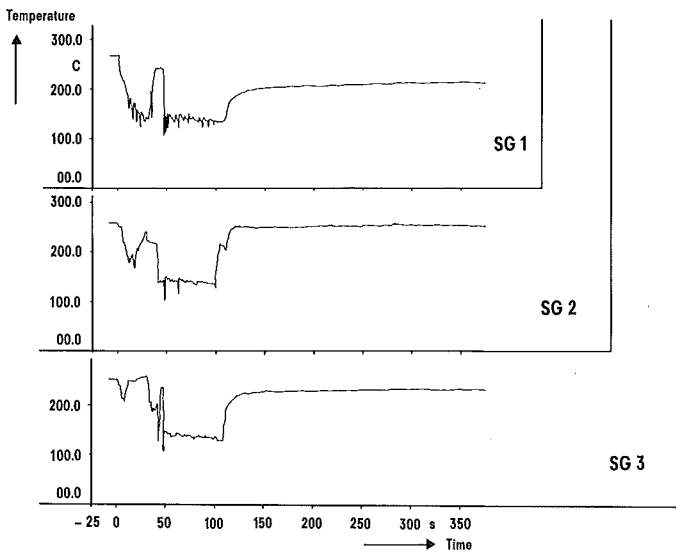
PKL II B-1 - SYSTEM PRESURRE

Fig. 5



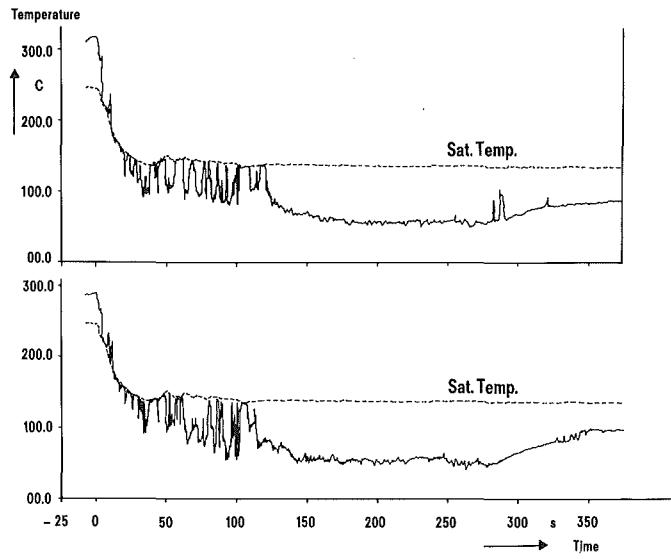
PKL II B-1 - HEATER ROD CLAD TEMPERATURE

Fig. 6



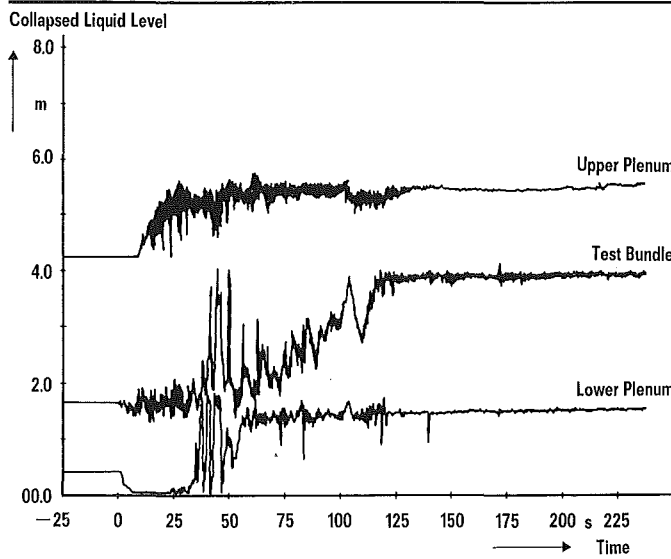
PKL II B-1 - PRIMARY SIDE SG INLET TEMPERATURE

Fig. 7



PKL II B-1 - TEMPERATURE 40 mm BELOW UPPER TIE PLATE

Fig. 8



PKL II B-1 - COLLAPSED LIQUID IN RPV

Fig. 9

## HEAT TRANSFER IN PWR U-TUBE STEAM GENERATORS

Marco Spiga

Istituto di Fisica Tecnica, Facoltà di Ingegneria  
Università di Bologna

## ABSTRACT

A non linear multinode computer code used for steady state modelling of vertical natural circulation U-tube steam generators, for pressurized water reactor plants, is described. The methods employed for the physical and mathematical representation of steam generator performance, numerical solution techniques and empirical correlations for two phase flow and heat transfer are related. Aim of the paper is the determination of pressure, temperature and steam quality for the fluids in both primary and secondary sides. Particular attention is devoted to the analysis of the heat transfer coefficients in the boiling region. The method proposed is very simple and has the merit of predicting reliable results with very small computational time.

## INTRODUCTION

A deep knowledge of the steam generator thermal-hydraulic behaviour is essential in the analysis of PWR plants, since this component provides a dynamic link between the core and the turbo-generator system. In licensing new power plants several steady state and perturbation situations are to be considered to assure the safe and reliable running of the plants; it is necessary therefore to predict accurately the steady state and transient heat transfer in the steam generator.

Within the reactor safety research, the interest in steam generator behaviour has considerably increased [1], leading to numerical [2-3] and experimental [4-5] works. However there are relatively few computer codes developed specifically for steam generator analysis; presently this analysis is performed using a wide variety of general purpose codes, describing the entire nuclear steam supply system and including the steam generator as only one component of the whole system. Such codes (RELAP, TRANFLO, SATAN,

TRAP...) can be flexible enough to be applicable to the same generator analysis in a stand-alone fashion, but they require an extremely large computational time and their adaptation is far from trivial.

The paper presents a simple one-dimensional non-linear model to predict the steady state behaviour of U-tube steam generators; the numerical solution requires a very small computer time, hence this model can give the designer an immediate and inexpensive tool for the system benchmark. The one-dimensional approach, justified by the high degree of turbulence, is very useful as a first approximation; at the last stage eventually the designer can resort to the more detailed but onerous three-dimensional codes.

#### MODEL DESCRIPTION

U-Tube steam generators, used in Westinghouse and Combustion Engineering PWR plants, are vertical tube-and-shell heat exchangers. In the primary side the reactor coolant enters the inlet plenum, flowing inside the U-tubes upward first and then downward, and exits from the outlet plenum. On the secondary side, a wrapper divides the shell region into tube bundle and downcomer. Feedwater is introduced into the downcomer through an annular ring to mix the recirculating water returning from the steam-water separation devices. The water flows downward in the downcomer, at its bottom this flow enters the tube bundle region upward.

The mathematical model here proposed does not consider the separation devices, so the system boundaries are formed by the water inlet and steam outlet (at the top of the U-tubes) on the secondary side (Fig. 1).

In the secondary fluid exchanges of mass, momentum and energy occur between the parallel and counter flow sections due to the considerable radial gradients in thermodynamic properties; mixing effects are properly considered in the mathematical model.

In the one dimensional approach, for every section all parallel tubes are represented by a single tube. For the primary single-phase flow only the energy equation is considered, since in steady state the influence of pressure and compressibility are quite negligible. In the secondary side a distinction is made between single and two phase flow regions; in the latter the momentum and energy transfer processes require a distributed parameter description; in this model complete separation of the phases is assumed (slip flow). The wall tube is modelled as a single resistance (including fouling) with zero axial heat conduction; the thermophysical properties of water and wall are considered depending on temperature.

The conservation equations (mass, momentum, energy) for the secondary two phase flow are:

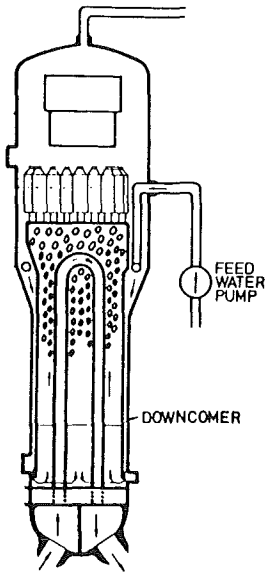


Fig. 1 - U-tube steam generator.

The term  $dP/dz$  appearing in the equation (2), as usual, represents the head loss; the friction factor is given by empirical correlation. The local steam void fraction is

$$\alpha = (x \rho_1 / \rho_v) / \{(1-x)S + x \rho_1 / \rho_v\}$$

being the quality

$$x = (h - h_1) / (h_v - h_1)$$

and the slip ratio  $S$  given by the Bankoff-Jones correlation

$$S = (1 - \alpha) / (k_{bj} - \alpha)$$

with:

$$k_{bj} = k_b + (1 - k_b) \alpha^a$$

$$k_b = 0.71 + 0.29 p / p_c$$

$$a = 3.53 + 2.66 \cdot 10^{-8} p + 1.18 \cdot 10^{-14} p^2 \quad (p \text{ in Pa})$$

Of course the equations (1-3) describe the behaviour of the secondary single phase in the subcooled region, setting  $\alpha = 0$ .

$$\frac{d}{dz} \{ \rho_1 (1 - \alpha) v_1 + \rho_v \alpha v_v \} = 0 \quad (1)$$

$$\frac{d}{dz} (\rho V_2^2 + p) + \rho g + \frac{dP}{dz} = 0 \quad (2)$$

$$\frac{d}{dz} (\rho V_1 h) = q_s \frac{W}{A_s} \quad (3)$$

where  $\rho$  is the mean density of the thermal equilibrium mixture:

$$\rho = \rho_1 (1 - \alpha) + \rho_v \alpha$$

and  $V_1, V_2$  are mean velocities defined as:

$$V_1 = \{ \rho_1 (1 - \alpha) v_1 h_1 + \rho_v \alpha v_v h_v \} / \rho h$$

$$V_2^2 = \{ \rho_1 (1 - \alpha) v_1^2 + \rho_v \alpha v_v^2 \} / \rho$$

The energy balance for the primary fluid leads to an equation analogous to the equation (3), in which the temperature appears directly.

At last the energy exchange between the primary and secondary flow is simply given by the steady state algebraic conditions (in cylindrical geometry) depending on the heat transfer coefficients (water (or steam)-wall) and the tube thermal conductivity.

In the preheat region the heat transfer coefficient for the secondary fluid is corrected [6] to take account of the triangular or square tube bundle arrangement; effects of U-tube bending on heat transfer are neglected.

#### EMPIRICAL CORRELATIONS

Some empirical correlations are incorporated in the model for heat transfer and pressure drop. In the subcooled region the water Nusselt number is given by the Bugger correlation

$$Nu = 0.02 Re^{0.83} Pr^{0.4} \quad (Re > 10^4)$$

while in the nucleate boiling region the fluid temperature is given by the Jens Lottes correlation:

$$T_w - T = 33.3 (q/3.15 \cdot 10^6)^{0.25} / \exp(p/6.2 \cdot 10^6)$$

being  $q$  in  $W/m^2$ ,  $p$  in Pa,  $T$  in  $^{\circ}C$  ( $3.4 \cdot 10^6 < p < 13.8 \cdot 10^6$  Pa).

The model includes also correlations for DNB and post dry out analysis (which could be used in a future transient version of the model for accident analysis).

For the friction factor in the single phase fluid the Colebrook correlation is applied

$$\frac{1}{\sqrt{f}} = -4 \text{ Log} \left( \frac{1.255}{Re \sqrt{f}} + \frac{1}{3.71} \frac{\epsilon}{D} \right)$$

To obtain the frictional pressure loss for two phase flow the single phase factor is corrected by a two-phase multiplier (function of steam quality, pressure and mass flow rate) [7].

#### NUMERICAL SOLUTION AND RESULTS

The equations (1-3) constitute a set of ordinary non linear differential equations; together with the energy balance for the primary fluid and the wall exchange condition, they allow to determine the velocity, pressure and enthalpy for the secondary fluid and

the temperature for the primary one. The temperature of the secondary fluid is found by a function  $T_s(h_s, p_s)$  given in [7].

The tube bundle length is spatially discretized and the differential equations are solved by means of a finite difference method; the code provides optionally for the Runge Kutta or the Merson integration rule. The cold and the hot leg of the bundle are analysed independently; they are coupled only by a mixing condition for the secondary flow (in every discretized section) and by a congruence relation at the top of the bundle).

For the hot leg, the input data are the inlet enthalpy of the primary side and a trial inlet enthalpy of the secondary fluid (together with both mass flow rates and pressures).

For the cold leg, the input data are the enthalpy of the secondary fluid at the top of the U-tubes (obtained as output in the hot leg) and a trial outlet enthalpy of the primary fluid.

Applying the congruence principle for the primary fluid at the top of the U-tubes, the exact enthalpy of the inlet primary water is found. Analogously, with few iterations, the temperature of the inlet secondary water is found, taking account that saturated water (from the separator devices) is recirculated and mixed with the feedwater entering the bottom of the tube bundle. The model validation has been performed comparing the numerical results with the experimental data available in [8-9], related to the steady state inlet and outlet conditions for the fluids in the U-tube steam generator of the Robinson nuclear plant. The agreement is very good, in particular the steam quality at the top of the U-tubes and the outlet temperature of the primary water are quite coinciding.

In figure 2 the pressure and steam quality for the secondary flow are shown versus the axial coordinate, in the tube bundle; the term  $dp_p/dz$  decreases in the boiling region because of the buoyancy effects.

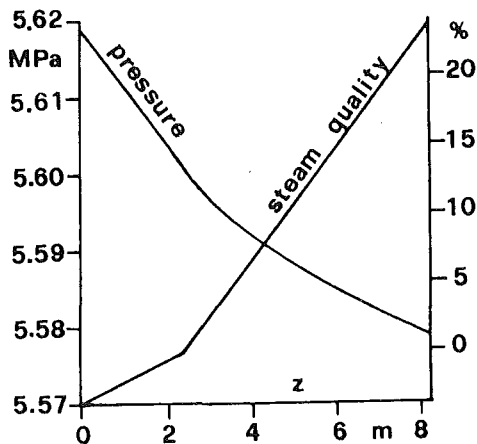


Figure 2  
Pressure and steam  
quality for the se-  
condary flow.



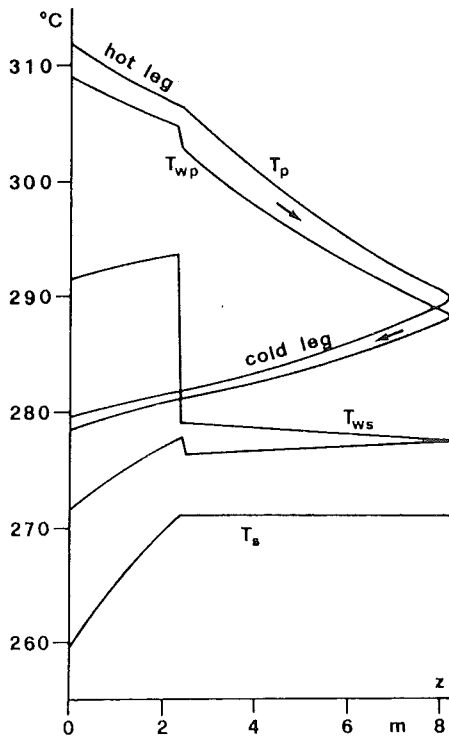


Figure 3 - Temperature distribution for fluids and walls in the steam generator.

In figure 3 the temperature profiles are shown for the primary water, the inner tube wall (primary side), the outer tube wall (secondary side), the secondary fluid. The discontinuities of the tube wall temperature are amenable to the sudden heat transfer coefficient variations (from the single phase region to the boiling one); these discontinuities can be eliminated modifying the heat transfer coefficient with an interpolation in the transition (single phase-two phase) region.

These results are obtained using the input data shown in table 1 and assuming that the tube is made of AISI 304 stainless steel.

The computational time required (resorting to the Runge Kutta numerical solution) is about 12 seconds on a CDC Cyber 76 computer.

TABLE 1

$W_p$	= 5.255 cm	$W_s$	= 6.0 cm
$A_p$	= 2.18 cm <sup>2</sup>	$A_s$	= 7.58 cm <sup>2</sup>
$m_p$	= 0.9058 kg/s	$m_s$	= 0.3826 kg/s
inlet $p_s$	= 5.619 MPa	inlet $p_p$	= 15.51 MPa
inlet $T_s$	= 259.45°C	inlet $T_p$	= 311.89°C
mixing factor	= 1	outlet $T_p$	= 279.85°C
$L$	= 8.2 m	spatial step	= 10 cm

## NOMENCLATURE

A	cross sectional area
D	tube diameter
f	friction factor
g	acceleration of gravity
h	specific enthalpy
L	tube length
m	mass flow rate
Nu	Nusselt number
p	pressure
$p_c$	critical pressure (22.12 MPa)
Pr	Prandtl number
q	heat flux
R	two phase multiplier
Re	Reynolds number
S	slip ratio
T	temperature
v	velocity
W	watted perimeter
x	steam quality
z	axial co-ordinate (z = 0 at the bottom of the tube bundle)
$\alpha$	volumetric void fraction
$\epsilon$	absolute surface roughness
$\rho$	density

## Subscripts

l	saturated liquid
p	primary
s	secondary
v	saturated steam
w	wall

## ACKNOWLEDGEMENTS

This work was financially supported by the CNR.

## REFERENCES

1. J.C. Lee, Z.Z. Akcasu et al.: Review of transient modelling of steam generator units in nuclear power plants; NP-1576, Research Project 684-1, University of Michigan, Interim Report, October 1980.
2. A. Hoeld: A theoretical model for the calculation of large transients in nuclear natural circulation U-tube steam generators; Nuclear Engineering and Design, Vol. 47, pp. 1-23, 1978.
3. N.W.S. Bruens: U-tube steam generator dynamics modelling and verification; 2nd Int. Conf. Boiler Dynamics and Control in Nuclear Power Stations, BNES, Bournemouth, October 1979.
4. S.P. Kalra: On the natural circulating PWR U-tube steam generators, experiments and analysis; Int. Seminar Advancement in Heat Exchangers, ICHMT, Dubrovnik, September 1981.
5. G. Cattadori, G. Masini, L. Mazzocchi: Experimental tests on U-tube steam generator thermal hydraulics; European Two Phase Flow Group Meeting, Zürich, June 1983.
6. J. Weisman: Heat transfer to water flowing parallel to tube bundles; Nuclear Science Engineering, Vol. 6, pp. 78-79, 1959.
7. M. Ferrero: Funzioni per il calcolo di precisione dell'entalpia dell'acqua e del vapore, NIRA report, SEC I/102-20.
8. T.W. Kerlin, E.M. Katz, J. Freels, J. Thakkar: Dynamic modelling of nuclear steam generators, 2nd Int. Conf. Boiler Dynamics and Control in Nuclear Power Stations, BNES, Bournemouth, October 1979.
9. T.W. Kerlin, E.M. Katz, J.G. Thakkar, J.E. Stronge: Theoretical and experimental dynamic analysis of the H.B. Robinson nuclear plant, Nuclear Technology, Vol. 30, pp. 299-316, September 1976.

TEMPERATURE AND QUENCHING BEHAVIOR OF UNDEFORMED, BALLOONED  
AND BURST FUEL RODS IN A LOCA

F.J. Erbacher, P. Ihle, K. Rust, K. Wiehr

Kernforschungszentrum Karlsruhe  
Institut für Reaktorbauelemente  
Projekt Nukleare Sicherheit  
Postfach 3640, D-7500 Karlsruhe 1  
Federal Republic of Germany

## ABSTRACT

In the HALDEN program it has been shown that the thermal behavior of REBEKA fuel rod simulators is representative of nuclear fuel rods.

In the SEFLEX program of KFK it has been found that the quench velocity in a LOCA transient is higher and the maximum cladding temperature in the unwetted portion of the rod bundle is lower for fuel rod simulators with a gap between the heat source and the cladding compared to gapless heater rods.

In the REBEKA program of KFK it has been shown that burst Zircaloy cladding tubes quench earlier than non-deformed claddings. It was found that premature local quench fronts are generated at the bursts long before the regular quench front had reached these axial elevations, they propagate in the axial and lateral directions and cause a fast quenching of the hot fuel rod bundle regions around burst claddings.

These new findings indicate a higher safety margin of coolability in a LOCA of a PWR. They have not yet been modeled in existing computer codes.

## PROBLEMS

In the refilling and reflooding phases of a loss-of-coolant accident (LOCA) in a pressurized water reactor (PWR) Zircaloy fuel rod claddings, depending on the size and location of the rupture in the primary system may reach temperatures which cause them to balloon under the impact of internal overpressure.

In thermal-hydraulic experiments i.e. FEBA, PKL, FLECHT, THETIS, CCTF and SCTF the temperature and quenching behavior has been investigated using electrical solid heater rods without gap inside the cladding. Ballooned fuel rod claddings have been simulated by sleeves fixed on the outer surface of such heater rods.

The development of computer codes was based mainly on experimental data obtained from tests performed with such gapless heater rods. However, the application for the prediction of the quenching of the fuel rod claddings in in-pile experiments showed large discrepancies, i.e. the fuel rods quenched much earlier than the codes had predicted.

## OBJECTIVES

A comparison of the behavior of a nuclear fuel rod with that of fuel rod simulators of different design during the reflood phase of a LOCA will be discussed. Emphasis is placed on the overall and local quench phenomena and the peak cladding temperatures. The main features and the corresponding programs are shown in Fig. 1.

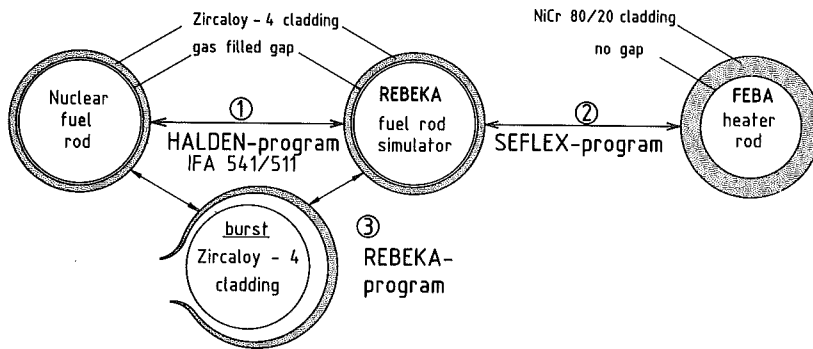


Fig. 1 Experimental approach to investigate the temperature - and quenching behavior of nuclear fuel rods and different fuel rod simulators (schematic)

## EXPERIMENTS

## HALDEN-program

In the HALDEN-program IFA 541 and 511 rod bundle experiments with 5 and 7 rods, respectively, with controlled forced feed reflooding have been performed in the Halden reactor [1]. In these experiments nuclear fuel rods and REBEKA-fuel rod simulators, respectively, have been used. The heated length of both the types of rods was about 1.5 m. The test series were carried out under comparable operational procedures and boundary conditions in order to compare the thermal behavior of such simulators with nuclear rods.

## SEFLEX-program

(Fuel Rod Simulator Effects in Flooding Experiments)

The aim of the SEFLEX-program [2] is to quantify the influence of the design of different fuel rod simulators on quench front progression and heat transfer in rod bundles during the reflood phase of a LOCA.

For thermal-hydraulic reflood experiments usually electrically heated rods are used which are characterized by a close thermal contact between the stainless steel cladding tube and the electrical insulation containing the embedded heating coil. However, nuclear fuel rods are characterized by heat generating fuel pellets stacked in a Zircaloy tube with a specified radial gap between the cladding tube and the pellets. For transient cooling conditions the thermal behavior is different for the different design of the rods described.

Experimental data from FEBA reflood tests using heater rods without gap serve as a data base [3]. For comparison forced feed bottom reflood tests have

been performed using a 5x5 REBEKA rod bundle in the FEBA test facility to minimize the influence of the boundary conditions of different test rigs. The REBEKA fuel rod simulators consist of a Zircaloy cladding of 0.72 mm wall thickness containing  $\text{Al}_2\text{O}_3$ -pellets. The gap between the pellets and the cladding is filled with either helium (fresh fuel) or argon (high burnup). An electrically heated rod of 6 mm diameter is placed in the center of the pellets. The cross sections of a FEBA rod and a REBEKA rod are shown in Fig. 2. The remaining characteristics are the same for both types of rods used for the comparison of the reflood behavior: Heated length: 3.9 m, cosine shaped axial power profile approximated by 7 power steps, peak to average rod power: 1.19, rod diameter: 10.75 mm, rod pitch: 14.3 mm, 7 original PWR grid spacers without mixing vanes.

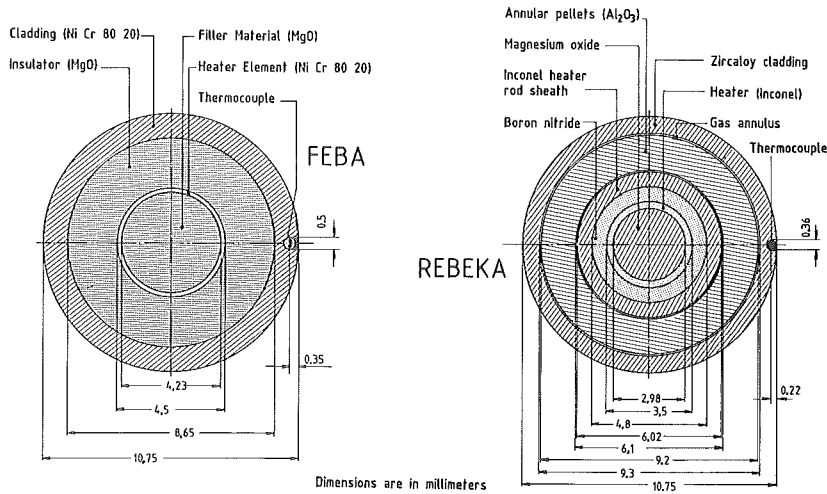


Fig. 2 Fuel rod simulator cross sections

Both test series using bundles of 5x5 FEBA rods or 5x5 REBEKA rods have been carried out under the same operational procedures, e.g. initial bundle power of 200 kW followed by a 120 % ANS standard decay heat transient for system pressures of 2 bar and 4 bar, and flooding velocities of 3.8 cm/s and 5.8 cm/s.

REBEKA-program  
(Reactor typical Bundle Experiments Karlsruhe)

In the REBEKA-program the plastic deformation behavior of pressurized Zircaloy-4-clad fuel rod simulators in 7x7 rod bundles has been investigated under thermohydraulic conditions of the refilling and reflooding phases of a LOCA [4]. The flooding conditions were simulated by forced feed bottom flooding. The REBEKA fuel rod simulator of the 2<sup>nd</sup> generation used in the test REBEKA 6 has the same design as described in the SEFLEX-program except a continuous cosine shaped power profile. In these experiments among others the initiation and the progression of additional quench fronts on ballooned and burst claddings have been investigated.

## RESULTS

HALDEN-program

Figure 3 shows a comparison of nuclear fuel rods and electrically heated REBEKA fuel rod simulators. The good simulation quality of the REBEKA-simulators in respect to the temperature and quenching behavior can be seen. Therefore, it can be concluded that results obtained with REBEKA fuel rod simulators are representative of nuclear fuel rods.

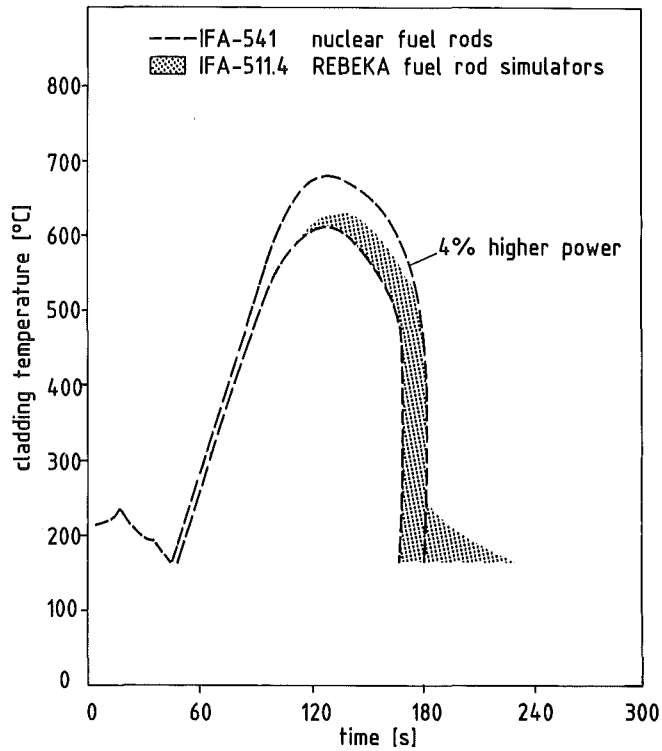


Fig. 3 Comparison of nuclear fuel rods vs. REBEKA fuel rod simulators

SEFLEX-program

The reflooding behavior of both the bundles consisting of either 5x5 FEBA rods or 5x5 REBEKA rods is significantly different. The main effects are evident using results of tests performed with a system pressure of 2 bar, a flooding velocity of 3.8 cm/s in the cold bundle, and a feed water temperature of 40 °C. The quench front progression in the REBEKA rod bundles is faster than that in the FEBA rod bundle (see Fig. 4). For the upper bundle portion it even increases again for the bundle of REBEKA rods with argon filling.

The corresponding cladding and housing temperatures measured at the bundle elevation indicated in the sketch are shown in Fig. 5. The peak cladding temperatures are lower for the REBEKA rod bundles as a result of increased precursory cooling compared with the conditions in the FEBA rod bundle. The maximum cladd-

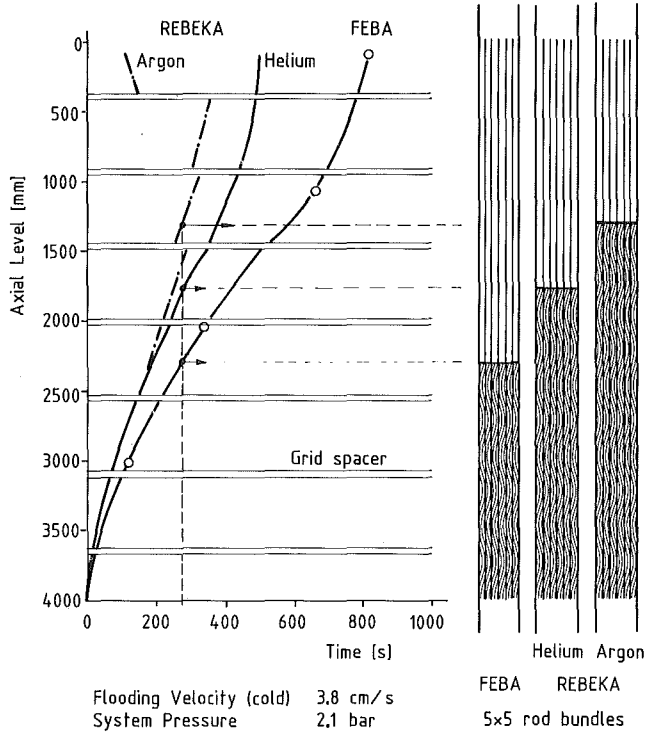


Fig. 4 Quench front progression in FEBA and REBEKA rod bundles

ing temperatures again are lower for the case of argon in the REBEKA rods. The temperature transients of the bundle housing which is identical for all of the tests proves that the precursory cooling is influenced by the different radial design of the rods applied.

The reasons for the lower cladding temperatures and the faster quench front progression at the REBEKA rod bundles are the lower heat capacity of the Zircaloy claddings and the more pronounced decoupling of the cladding from the heat source. The same effect can be observed for ballooned claddings as well as for blockage sleeves simulating ballooned claddings. The consequences of the different reflooding behavior of the individual rod bundles on the fluid conditions within the bundle subchannels are indicated by the different water carry over rates.

Figure 6 shows the water carry over collected downstream of the bundle exit versus reflood time. A higher amount of water entrained by the steam is being evaporated within the REBEKA rod bundle subchannels removing more heat per unit of time. Less water is carried over.



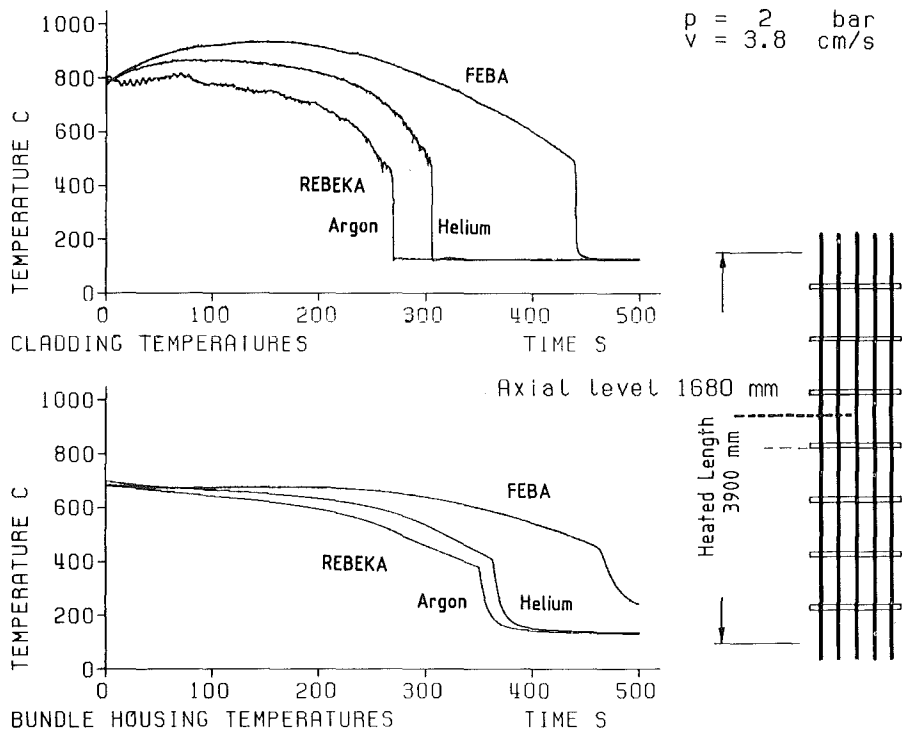


Fig. 5 Cladding and housing temperatures in 5x5 FEBA and REBEKA rod bundles

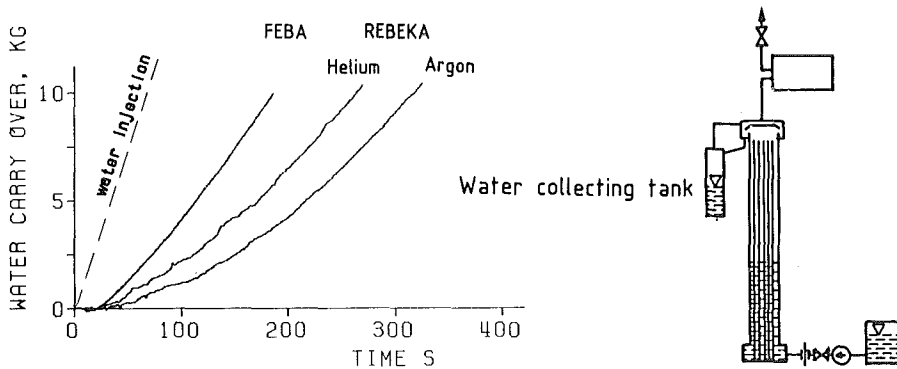


Fig. 6 Water carry over in 5x5 FEBA and REBEKA rod bundles  
 ( $p = 2 \text{ bar}$ ,  $v = 3.8 \text{ cm/s}$ )

REBEKA-program

The highest degree of the decoupling of a cladding will be reached when the cladding had burst. Then the gas has escaped and replaced or mixed by steam with its much poorer heat conductivity and burst lips are penetrating into the coolant channels. The two-phase flow coolant is able to cooling down the cladding in the region of the burst very fast and the water droplets will quench it. Two new quench fronts begin to propagate from the burst. One of them moves relatively fast upwards in flow direction, the other downwards opposite to the direction of flow. This is illustrated schematically in Fig. 7, the experimental results are plotted in Fig. 8. The axial quench front propagation initiated by a burst cladding is evident. In comparison to the cladding temperature of the burst rod at 1850 mm, the temperature history of an undeformed cladding at the same axial position is plotted. It shows that the regular quench front has a time delay of 135 seconds.

Figure 9 demonstrates the lateral quench front propagation initiated by a burst cladding. The axial position of 1850 mm of the non-deformed rod 14 quenched earlier than the axial midplane of 1950 mm (TC positions are measured in mm from top). The reason for that off-normal behavior is the touch of a burst cladding of the neighbouring rod 36 with its early quenching. In that way a lateral propagation will occur. - Fig. 10 illustrates the quench sequence.

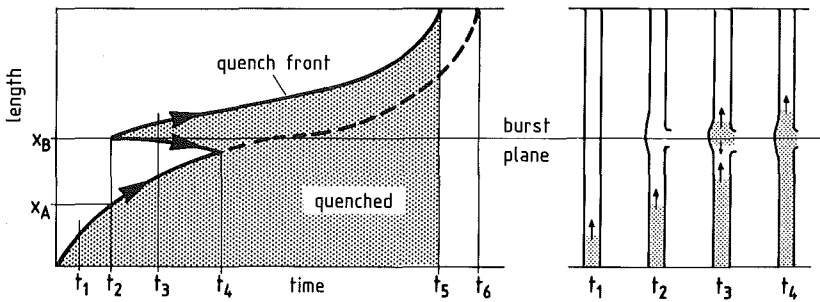


Fig. 7 Premature quenching of burst Zircaloy claddings (schematic)

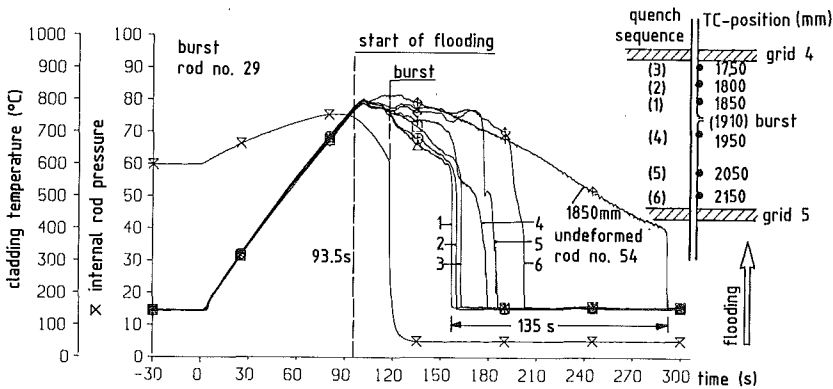


Fig. 8 Cladding temperatures and internal rod pressure of a burst rod (REBEKA 6)

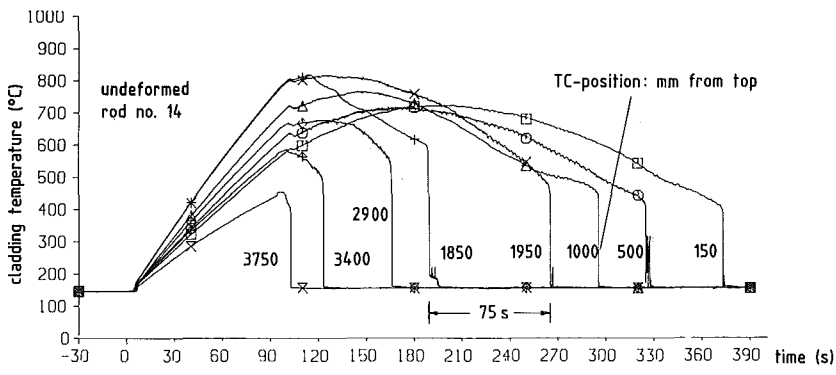


Fig. 9 Cladding temperatures of an undeformed rod (REBEKA 6)

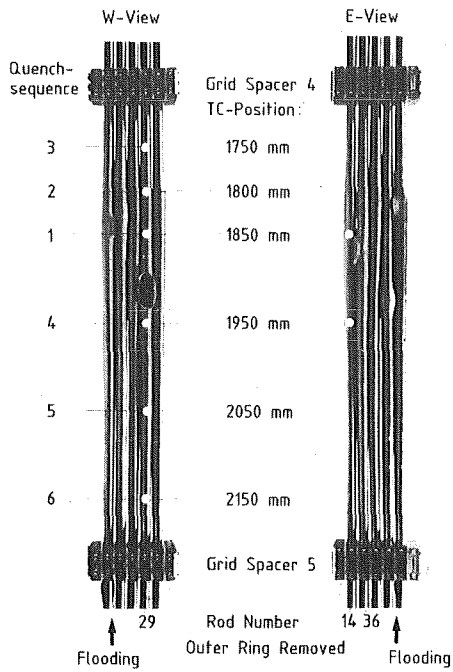


Fig. 10 View of a burst rod bundle with indication of the quench sequence (REBEKA 6)

## SUMMARY AND CONCLUSION

- The short quench times of nuclear fuel rods observed in in-pile tests can be explained,
  - they can not be simulated with solid heater rods,
  - however, REBEKA fuel rod simulators represent a good simulation.
- REBEKA fuel rod simulators exhibit lower peak cladding temperatures and earlier quenching compared to solid heater rods.
  - This is the result of the lower heat capacity of the cladding and of the heat resistance in the gap between pellet and cladding.
- Burst cladding tubes quench earlier compared to intact cladding tubes and generate secondary quench fronts.
- The secondary quench fronts propagate relatively fast in the axial direction and have also effects in the lateral direction.
- This leads to a fast cooling of the hot zones in a fuel element.
- All these favorable effects have not yet been modeled in existing computer codes.
- They suggest a higher safety margin in assessing the coolability of a pressurized water reactor in a loss-of-coolant accident.

## REFERENCES

- [1] Vitanza, C., Johnsen, T.  
"Results of Blowdown/Reflood Tests with REBEKA Electric Simulators (IFA-511.4, Cycle 2)"  
OECD Halden Reactor Project, HWR-85, May 1983.
- [2] Ihle, P., Rust, K. and Schneider, H.  
"Fuel Rod Simulator Effects in Flooding Experiments (SEFLEX-Program)",  
in Projekt Nukleare Sicherheit, Annual Report 1983, Report No. KFK 3450,  
pp. 4200-93 to 4200-111, June 1984.
- [3] Ihle, P. and Rust, K.  
"FEBA-Flooding Experiments with Blocked Arrays, Evaluation Report",  
Report No. KFK 3657, Kernforschungszentrum Karlsruhe, March 1984.
- [4] Erbacher, F.J., Neitzel, H.J., Wiehr, K.  
"Brennstabverhalten beim Kühlmittelverluststörfall eines Druckwasserreaktors  
- Ergebnisse des REBEKA-Programms",  
KFK-Nachrichten, Jahrgang 16, Heft 2/84, S. 79-86.

A STUDY OF ROD BOWING EFFECT ON CRITICAL HEAT FLUX  
IN PWR ROD BUNDLES

D.G. Reddy and C.F. Fighetti

Heat Transfer Research Facility  
Columbia University  
New York, NY 10027, U.S.A.

ABSTRACT

A broad overview of the experimental and analytical results of several experimental programs to determine the effect of rod bowing on critical heat flux (CHF) conducted at Columbia University are presented. First, an accurate generalized subchannel CHF correlation, which covers both PWR and BWR operating conditions as well as postulated loss-of-coolant accident (LOCA) conditions, developed at Columbia University based on the local conditions obtained with the COBRA IIIC subchannel code from heretofore unpublished rod bundles CHF data is presented. Second, the results of a comprehensive study of rod bowing effect on CHF in PWR type rod bundles using CHF data points from seven bowed rod tests with various degrees of reduced clearance between heated rods are discussed.

INTRODUCTION

Boiling crisis in nuclear reactor fuel elements is characterized by sudden drop in the heat transfer rate due to change of heat transfer mechanism and a temperature excursion of the fuel rod surface. The heat flux just before the occurrence of boiling crisis is called Critical Heat Flux (CHF). Since the operating criteria for nuclear reactors specify that they must operate under conditions below critical heat flux, the prediction of CHF is a subject of vital importance in nuclear reactor design. Because of the complexity of the CHF phenomenon in fuel rod array geometry and lack of analytical methods for the prediction of CHF in rod bundles, the understanding of the CHF in rod bundles depend upon interpreting correctly the vast amount of data obtained in electrically simulated reactor fuel elements. The research work presented in this paper is a step in this direction. Two topics of interest related to CHF are presented in this paper are: the prediction of CHF in rod bundles; and the effect of rod bow on CHF PWR rod bundles

At present a generalized critical heat flux (CHF) correlation based on local conditions obtained with a non-proprietary subchannel code is not available in the open literature. Experience has shown that existing CHF correlations such as W-3, B&W-2, CE-1, and WSC-2 developed with proprietary subchannel codes are not very accurate when used with subchannel codes available in the open literature, such as COBRA. Therefore, a need exists for the development of a CHF correlation using experimental data obtained in fuel assemblies representative of nuclear reactor rod bundles and local conditions obtained with a subchannel code available in the open literature. Such an objective can be accomplished because of the availability of the following two items:

- A large data base of about 11 000 CHF data points obtained in fuel assembly models is available at the Heat Transfer Research Facility of Columbia University.
- A widely used and well documented subchannel code COBRA is available in the open literature.

The second objective of the present study is to evaluate the effect of one of the fuel abnormalities, that of a bowed rod on Critical Heat Flux (CHF) in PWR type rod bundles. Results of several experimental programs to determine the effect of rod bowing on CHF conducted at the Heat Transfer Research Facility of Columbia University are presented in this paper. These tests were performed in 4X4 and 5X5 rod bundles simulating a section of a full sized PWR fuel assembly by electrically heating the test sections. The CHF data from seven bowed rod tests with various degrees of reduced clearance between heated rods were used in this study.

### TEST FACILITIES

There are two major thermal-hydraulic facilities for CHF testing at the Heat Transfer Research Facility. They are known as the Medium Pressure and the High Pressure Heat Transfer Loops. The operating limits of these loops are given in Table I and schematic drawings of these flow loops are shown Figures 1 and 2 respectively.

Flow was maintained by a centrifugal pump in the Medium Pressure Loop and by a set of four canned rotor pumps in the High Pressure Loop. A throttle valve upstream of the test section automatically controlled the flow, and also maintained its stability during the tests. A turbine flow meter, a calibrated platinum resistance thermometer (RTD) and thermocouples located at the inlet of the test section measured flow and temperature, and a large-scale Bourdon pressure gauge with transducers monitored the outlet pressure. All of these measurements were recorded continuously during the tests.

Heating to test sections was provided by six motor-generator sets operated in parallel for a maximum DC output of 50,000 Amps at 230 Volts (i.e., 12 Megawatts). Heat rejection in both loops was accomplished by shell-and-tube heat exchangers with constant temperature water as the coolant. A detailed description of the power system is provided in Reference 1.

### TEST PROCEDURE

Each of the test sections had a different configuration, but all tests were performed in the same fashion. The test section outlet pressure, inlet temperature and mass flow rate was established and maintained constant. The total power to the test section was then increased in small increments and the loop brought to the corresponding equilibrium conditions each time. This process was continued until a temperature excursion was observed to start in one or more of the rods in the bundle. The temperature increase varied depending on system conditions, from a minimum of 5 Deg. C to 50 Deg. C or more. When the indication was judged to be sufficient to have established the presence of CHF, the power to the test section was reduced and the test conditions prior to the temperature excursion were recorded both manually and by a computer controlled data acquisition system.

TABLE I Heat Transfer Loop Operational Limits.  
 (a) Medium Pressure Loop (b) High Pressure Loop

	(a)	(b)
Maximum Pressure, $\times 10^6$ N/m <sup>2</sup>	16.5	17.2
Maximum test section flow, m <sup>3</sup> /hr	125	115
Total head developed by pump, m of water	180	160
Test section housing length, cm	510	500
Test section housing I.D., cm	16.6	17.8
Heat exchanger capacity, kw	6000	4000
Maximum secondary water Flow, m <sup>3</sup> /hr	150	150
Maximum well water temperature, DEG. C.	15	15

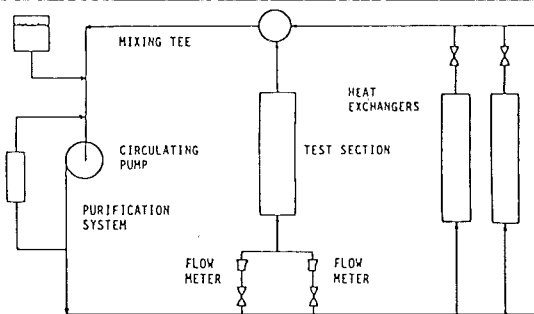


FIGURE 1. Medium Pressure Heat Transfer Loop.

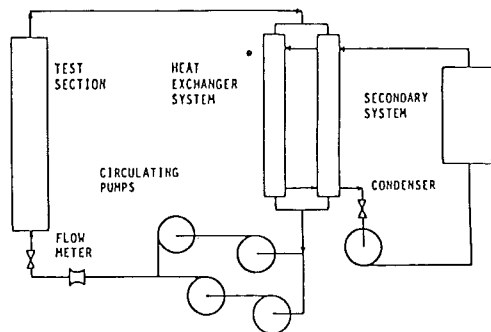


FIGURE 2. High Pressure Heat Transfer Loop.

## THE COLUMBIA CHF CORRELATION

An accurate generalized subchannel CHF correlation, which covers both the PWR and BWR operating conditions as well as postulated loss-of-coolant conditions, was developed at Columbia University based on the local conditions obtained with the COBRA IIIC subchannel code from heretofore unpublished rod bundle CHF data. The basic form of the Columbia CHF correlation [2,3] is

$$q_c'' = (A - X_{in}) / (C C_G^* + L'') \quad (1)$$

where,

$$A = P_1 Pr^{P_2} (Gk'')^{(P_5 + P_7 Pr)} \quad (2)$$

$$C = k' P_3 Pr^{P_4} (Gk'')^{(P_6 + P_8 Pr)} \quad (3)$$

$$C_G^* = 1.3 - 0.3 C_G \quad (4)$$

and

$$L'' = (X_1 - X_{in}) / q_1'' \quad (5)$$

$q_c''$  and  $q_1''$  are the critical and local heat fluxes ( $W/m^2$ ),  $X_{in}$  is the inlet quality,  $X_1$  is the local quality,  $Pr$  is the reduced pressure (pressure/critical pressure),  $G$  is the local mass flux ( $Kg/m^2 \cdot s$ ),  $C_G$  is the grid loss coefficient,  $k'$  &  $k''$  and  $P_1$  through  $P_8$  are constants.

The coefficients  $P_1$  through  $P_8$  were optimized using non-linear regression analysis. The optimized values of the coefficients  $P_1$  through  $P_8$  are 0.5328, 0.1212, 1.6151, 1.4066, -0.3040, 0.4843, -0.3285, and -2.0749 respectively. The values of constants  $k'$  and  $k''$  are  $3.1706 \times 10^{-7}$  and  $7.3659 \times 10^{-4}$  respectively.

The Columbia CHF correlation utilized 3607 CHF data points from 65 fuel assembly test sections. The data cover a wide range of rod bundle geometries (Rod diameter: 9.7 to 17.3 mm, and Heated length: 76 to 427 cm) and operating parameters (Pressure: 1.4 to 16.9 M.  $N/m^2$ , Mass flux: 270 to 5600  $Kg/m^2 \cdot s$ , and Quality: -0.25 to 0.75).

The accuracy of the correlation was ascertained by evaluating the average ratio of predicted to experimental CHF, standard deviation (STD), and root mean square error (RMS). Also distribution of residuals within error bands of 5%, 10%, 15%, and 20% was determined. The correlation predicts the source data of 3607 data points from 65 test sections with an average ratio of 0.995. The standard deviation is 7.20% and the RMS error is 7.20%. The distribution of residuals is as follows: 51% of CHF data are correlated within 5% error band, 82% of the points within 10%, 97% of the points within 15% and 99.9% of the points within 20%.



Residual analysis was performed by plotting the ratio of predicted CHF to experimental CHF versus parameters appearing in the correlation, such as, mass flux, pressure, average exit quality, inlet quality, and average heat flux. Examination of these residual plots (not presented here) shows that the ratios of predicted to experimental CHF are more or less evenly distributed within the error band of 20%, thus confirming the adequacy of the general form of the correlation and its dependence on various parameters.

#### EFFECT OF GRID SPACERS ON CHF

In nuclear reactor fuel bundles, the basic purpose of grid spacers is to maintain relative position of rods (rod-to-rod clearances) fixed through-out the core length. The grid spacer in a rod bundle increases flow resistance (pressure drop) and turbulence, which in turn promote mixing, thus reducing any flow and enthalpy imbalance between subchannels. Simple grids, in general, do not, significantly increase flow resistance or promote mixing. However, in certain instances, grid spacers with mixing vanes are used whose purpose is not only to keep relative rod positions fixed but also promote mixing by selectively diverting flow from hot subchannels to cold subchannels and vice versa. This type of spacers increase flow mixing and thus reduce enthalpy rise in hot channels. They also peel off the bubble layer of the rods to some degree. The combined effect of the above two actions is increase in CHF limits. From the above discussion, it is clear that a grid spacer correction factor is required to account for the flow mixing effect of the spacers on CHF.

One of the major tasks of developing a unified CHF correlation with data from different fuel bundles is to characterize the grids of various types of reactors. Any transverse momentum exchange due to the presence of grids should result in an increase in the bundle overall pressure drop. Based on this assumption, one could use the pressure drop due to grids in the evaluation of the effectiveness of the grids in mixing and thus enhancing the CHF limits. In general, the grid loss coefficient, which is a measure of the pressure drop due a grid, is higher for mixing vane grids than for simple grids. Therefore the effect of grid spacers on CHF was accounted for in the CHF correlation in terms grid loss coefficient ( $C_G$ ).

The grid loss coefficient is defined as,

$$C_G = (2 DP_G g_c) / (n G^2 v) \quad (6)$$

where,  $DP_G$  is the pressure drop due to grid spacers,  $G$  is the mass flux,  $n$  is the number of grids,  $v$  is the specific volume, and  $g_c$  is the Newton constant.

The spacer coefficients used in this work were calculated using isothermal pressure drop data. The pressure drop due to grid spacers is,

$$DP_G = DP_T - f G^2 L v / (2 D_e g_c) \quad (7)$$

where,  $DP_T$  is the total frictional pressure drop,  $f$  is the McAdams single phase friction factor,  $L$  is the length of the bundle, and  $D_e$  is the equivalent diameter of the bundle.

## EFFECT OF ROD BOWING ON CHF

The effect of rod bowing on CHF is of interest for the design of PWR fuel assemblies. In order to achieve a higher level of reliability of reactor components several CHF tests with bowed rods were carried by various reactor vendors. The results of three series of experimental programs to determine the effect of rod bowing on CHF conducted at the Heat Transfer Research Facility of Columbia University are discussed in this paper.

Markowski et al. [4] evaluated the results of the first series of tests using the TORC subchannel code and the CE-1 CHF correlation. The second series of tests were studied by Hill et al. [5] using THINC computer code and modified W-3 CHF correlation. Some of the data from the third series of tests were analyzed by Nagini et al. [6] with the aid of COBRA IIIC subchannel code and modified W-3 correlation. In the present study, a comprehensive study of all these data was carried out with one set of subchannel code and CHF correlation to evaluate the rod bowing effect on CHF.

## TEST SECTION DESCRIPTION

The first series of bowed rod tests were conducted with electrically heated rod bundles representative of a portion of a Combustion Engineering (CE) 14X14 fuel assembly. Three bundles were tested (Test sections 58, 67, and 69). These test sections consisted of 21 heated rods of diameter 11.18 mm and one unheated rod of diameter 28.32 mm in a 5X5 square rod array with a rod pitch of 14.73 mm. The heated length of the bundles was 3.81 m. The rods were supported by 9 reinforced CE standard grid spacers with a grid spacing of 336 mm. The rod bundles had uniform radial and non-uniform axial heat flux distribution. The radial geometry is presented in Fig. 3 and the axial heat flux distribution is given in Fig. 4. Details of the radial and axial geometry parameters are given in Reference 4.

Test section 58 had all the rods straight. The bowed rod test sections 67 and 69 were identical to test section 58 except for the rod bow. In test section 67, the heated rod in position 17 was bowed towards rod 21 to contact rods 16 and 18 at 3.36 m elevation. The point of maximum bow was located 203 mm upstream of the last grid. In test section 69, the heated rod in position 18 was bowed away from rod 6, reducing the gap between rod 21 and the guide tube from 3.55 mm to 1.65 mm. The point of maximum bow was the same as in test section 65.

The second series of bowed rod tests consists of three bundles (test sections 131, 148 and 151), representative of Westinghouse 15X15 fuel assemblies, all of which had top skewed axial heat flux profile and were 4.27 m long. These rod bundles consisted of 16 heated rods of diameter 10.72 mm arranged in a 4X4 square array with a pitch of 14.1 mm. These rods were supported by mixing vane grid spacers placed 660 mm apart, with simple support grids in the middle of the mixing vane grids. These test sections had non-uniform radial heat flux distribution with inner four rods at about 18% higher power level than twelve outer heater rods. Figures 5 and 6 show radial geometry of the test sections and the axial heat flux distribution respectively. Additional details of these test sections are given in Reference 5.

Test sections 131 and 148 had all the rods straight. Test section 151 was identical in all respects to these tests except for a bowed rod. The rod in position 16 was bowed towards rod 14 to contact rods 15 and 13 at the 345 mm elevation.

The third series of bowed rod tests (test sections 166, 167, 168, 169, and 170) were also representative of the Westinghouse 15X15 fuel assemblies (10.7 mm rod diameter, 14.1 mm rod pitch, and 4.27 m heated length). The heater rod in position 14 was replaced with an unheated rod of diameter 13.8 mm. The radial geometry of these test sections is shown in Fig. 7 and the axial heat flux distribution is given in Fig. 6.

Test section 166 was a straight rod bundle. In test section 167, the rod in position 16 is bowed towards rod 14 to contact rods 15 and 13 at 345 mm elevation, as in test section 151. In test section 168, heated rod located in position 15 was bowed towards rod 13 to contact rod 16 and the thimble tube located in position 14. The point of maximum bow is the same as in test section 167. In test section 169, rod in position 15 was bowed towards rod 13, reducing the gap between rods 15 and 16, and 15 and the thimble tube in position 14 to 15% of the normal gap. The point of the maximum bow is the same as in test section 168. Test section 170 is identical to test section 169, except that the gap at the point of maximum bow was reduced to only 50% of the normal gap.

#### ANALYSIS OF BOWED ROD DATA

The bowed rod effect was quantified by evaluating matching experiments with all rods straight and with one rod bowed. Analysis of these data was carried out pairing bowed and unbowed runs taken at the same flow conditions. Since in practice it is difficult to match test section inlet conditions exactly, the measured heat fluxes were normalized by their corresponding heat flux at critical power as predicted by a correlation. The COBRA IIIC computer code was used to determine the local fluid conditions. The measured-to-predicted critical power ratio was then calculated by using the Columbia CHF correlation. The differences between the bowed and the unbowed measured-to-predicted ratios were further normalized by the measured-to-predicted ratios for the unbowed runs to obtain the rod bow effect parameters.

The dependence of bow parameter on pressure, mass flux and local quality was evaluated by dividing the data into several groups and compiling bow parameter statistics. Table II gives compilation of number of points in each group and the average bow parameter of that group at different pressures. Similarly, statistics for mass flux and local quality are given in Tables III and IV respectively.

A careful study of the statistics lead to the following important conclusions:

1. The rod bow parameter is strangely dependent on pressure and local quality but shows little or no dependence on mass flux. The adverse effect of rod bow on CHF increases monotonically with increasing pressure. The effect is significantly high at 16.5 M. N/m<sup>2</sup>. The rod bow parameter increases with decreasing local quality.
2. These results also demonstrate that if small gap exists between rods the adverse effect of rod bow on CHF decreases considerably. The bow effect calculated by interpolating the data between no bow and rod bowed to

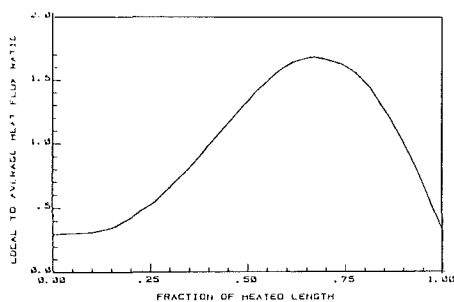
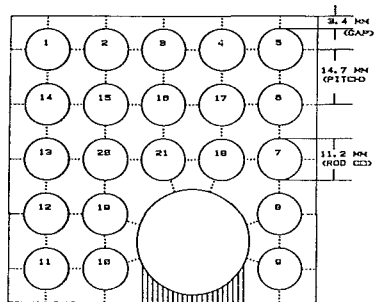


Fig. 3 Radial geometry of test series I Fig. 4 Axial geometry of test series I

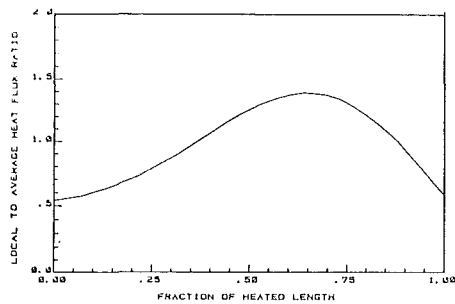
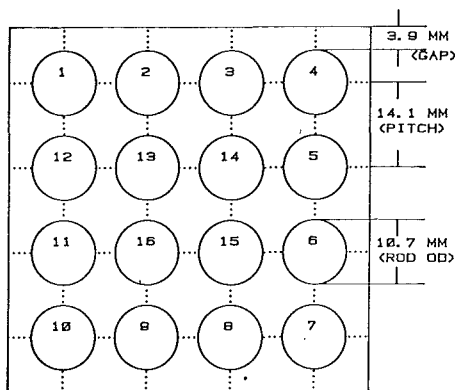


Fig. 5 Radial geometry of test series II Fig. 6 Axial geometry of test series II

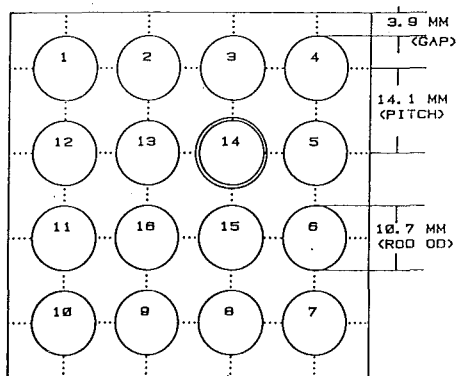


Fig. 7 Radial geometry of test series III

Table II Number of data points (NPTS) and Average Bow Parameter (A.BP) broken down by pressure (Million N/m<sup>2</sup>)

Pressure			Test Sections					
	65	67	151	167	168	169	170	
10.3	NPTS		14	8	8	8	7	
	A.BP		1.7	0.0	-1.7	-1.3	3.5	
12.1	NPTS	11	7					
	A.BP	2.3	-2.2					
12.4	NPTS		3	5	5	5	4	
	A.BP		-0.7	3.0	0.2	1.0	5.4	
13.8	NPTS	12	9					
	A.BP	5.2	-2.3					
14.5	NPTS		13	11	12	11	11	
	A.BP		2.9	11.4	6.3	1.8	2.7	
15.2	NPTS	16	14					
	A.BP	4.9	-2.8					
16.5	NPTS	9	11	10	12	13	11	
	A.BP	10.4	-1.8	5.7	19.2	15.6	-1.5	0.7

Table III Number of data points (NPTS) and Average Bow Parameter (A.BP) broken down by mass flux (Kg/m<sup>2</sup>.s)

Mass Flux			Test Sections					
	65	67	151	167	168	169	170	
1350	NPTS	13	10					
	A.BP	10.8	-1.6					
2025	NPTS	2	1	8	4	7	7	
	A.BP	0.9	0.8	1.1	6.6	9.8	2.9	4.0
2700	NPTS	19	18	15	12	11	7	
	A.BP	3.3	-3.2	2.9	10.8	7.1	2.5	6.8
3375	NPTS	2	1	8	7	8	8	
	A.BP	-0.3	-1.6	3.7	13.2	6.8	-1.1	1.9
4050	NPTS	12	11	6	6	5	5	
	A.BP	4.6	-1.8	3.0	11.6	6.3	-3.6	-1.5
4725	NPTS			3	7	7	8	
	A.BP			5.7	7.7	4.7	-1.6	-0.9

Table IV Number of data points (NPTS) and Average Bow Parameter (A.BP) broken down by local quality range

Quality			Test Sections					
	65	67	151	167	168	169	170	
-0.1 -	NPTS	8	7		5	5	5	
	A.BP	10.5	-3.3		15.1	11.9	-6.2	-6.4
0.0 -	NPTS	12	21	13	23	24	21	
	A.BP	5.4	-3.1	5.4	12.6	8.5	1.1	4.3
0.1 -	NPTS	16	12	22	8	9	9	
	A.BP	3.1	-1.1	1.5	0.9	0.2	0.7	1.4
0.2	NPTS							
	A.BP	3.8	4.8	2.7				

contact overestimates the degradation of CHF due to partial bow closure.

#### SUMMARY AND CONCLUSIONS

- An accurate generalized subchannel CHF correlation based on local conditions obtained with the COBRA IIIC code, developed utilizing over 3600 CHF data points from 65 test sections simulating PWR and BWR fuel assemblies is presented.
- The effect of grid spacers on CHF was investigated and this effect was accounted for in the CHF correlation in terms of grid loss coefficient.
- The rod bowing effect on CHF was studied. The results of this study lead to the following conclusions:
  1. There was no adverse effect on CHF of a heater rod bowed to contact at low pressures and at high pressures the degradation of CHF due to rod bow was insignificant.
  2. The rod bow effect increases with decreasing quality.
  3. When a small gap exists between the rods the adverse effect of rod bow on CHF decreases significantly.

#### REFERENCES

1. Hovemeyer, W. E., Sreepada, S. R., and Casterline, J. E., "Upgraded DC Power System and Thermal-Hydraulic Facilities at Columbia University", EPRI Report NP-773, 1978.
2. Reddy, D. G., "A Generalized Subchannel CHF Correlation for Water Cooled Nuclear Reactors", D.Eng.Sc. Dissertation, Columbia University, 1981.
3. Reddy, D. G., and Fighetti, C. F., "A Generalized Subchannel CHF Correlation for PWR and BWR Fuel Assemblies", EPRI Report NP-2609, January 1983.
4. Markowski, E. S., et al., "Effect of Rod Bowing on CHF in PWR Fuel Assemblies", ASME Heat Transfer Conference, 1977 77-HT-91.
5. Hill, K. W., et al., "Effect of a Rod Bowed to Contact on Critical Heat Flux in Pressurized Water Reactor Rod Bundles", ASME Winter Annual Meeting, 1975 75-WA/HT-77.
6. Nagino, Y., et al., "Rod Bowed Contact Departure From Nucleate Boiling Tests in Cold Wall Thimble Cell Geometry", Journal of Nuclear Science and Technology, 15(8) pp 568-573 August 1978.

ENHANCEMENT OF HEAT TRANSFER IN DISPERSE  
FLOW AND DOWNSTREAM OF BLOCKAGES IN ROD BUNDLES [1]

H. Kianjah, V. K. Dhir and A. Singh [2]

School of Engineering and Applied Science  
University of California, Los Angeles  
Los Angeles, CA 90024

## ABSTRACT

Results of experiments conducted to study the effect of a discontinuous phase and blockages in rod bundles on heat transfer are presented. The test section consists of a 4-rod bundle with the rod diameter and pitch of typical PWR fuel elements housed in a plexiglass tube. The rod bundle is 184 cm tall and is heated electrically. The blockages are of sleeve type and they block 60% of the inner flow channel area while leaving a virtually infinite flow bypass region. In the experiments the discontinuous phase is simulated with 30 and 100  $\mu\text{M}$  spherical glass particles entrained in air. The mass flow rate ratio of particles to air was varied from 0 to about 4 or the volume fraction,  $\beta$ , of particles to air was varied from 0 to about  $2 \times 10^{-3}$ .

The results indicate significant enhancement in heat transfer in the presence of particles. The enhancement is also appreciable downstream of blockages. However the relative enhancement under two phase flow conditions is smaller than that for the single phase.

## INTRODUCTION

During reflood phase of a loss of coolant accident in light water reactors, entrained flow conditions exist over a large extent of the rod bundles downstream of the quench front. The maximum temperature attained by the rods prior to complete cooling significantly depends on heat transfer rate under entrained flow condition. In certain instances, prior to flooding the overheated cladding may swell as a result of large pressure in the fuel pins. The swollen cladding may block the flow channels between the fuel pins. The resultant flow distribution will affect the local heat transfer coefficient. Knowledge of heat transfer mechanisms in the vicinity of blockages in rod bundles is essential to describe the thermal-hydraulic response of the core during the reflood phase of the accident. The purpose of this work is to determine experimentally under simulated conditions the enhancement in heat transfer resulting from agitation or turbulence created by the presence of droplets in steam flow in both undeformed and deformed rod bundles.

Several studies documenting the two phase gas-liquid heat transfer coefficients have been reported in the literature. These studies which have been reviewed by Drucker *et al* [3] among others unequivocally show that the presence of small amounts of gas in a flowing liquid can significantly enhance the heat transfer from the wall. It is found that the magnitude of the ratio of two phase to single phase heat transfer coefficient for bubbly and slug flow increases with the cross-sectionally averaged void fraction. The enhancement in

heat transfer coefficient however decreases with an increase in the liquid Reynolds number. Drucker et al correlated most of the two phase flow heat transfer data available in the literature as well as their own rod bundle data as

$$\psi \equiv \frac{Nu_{tp}}{Nu_{sp}} = 1 + C_1 \left( \frac{\alpha Gr}{Re^2} \right)^{1/2} \quad (1)$$

where  $\alpha$  is the void fraction and Gr is the Grashof number defined as

$$Gr = \frac{(\rho_d - \rho_c) g D_h^3}{\rho_c \nu_c^2} \quad (2)$$

In equation (2),  $\rho_d$  and  $\rho_c$  are the densities of the discontinuous phase and the continuous phase respectively,  $\nu_c$  is the kinematic viscosity of the continuous phase,  $g$  is the gravitational acceleration and  $D_h$  is the hydraulic diameter. The Nusselt numbers and Reynolds numbers in equation (1) are defined in the usual fashion with a characteristic length given by the hydraulic diameter. The constant  $C_1$  was found to be 2.5 for flow in tubes and 3.25 for flow over a four rod bundle. Drucker et al proposed that similar enhancement mechanism and a correlation similar to equation (1) should be valid when solid particles are entrained in a gas. Theofanous and Sullivan [4] have also made similar observations.

Many studies of heat transfer in flowing solid-gas mixtures have also been reported in the literature. The earliest quantitative study out of these is that of Farbar and Morley [5]. In their experiments Farbar and Morley entrained alumina-silica catalyst particles in air and passed the mixture through a 17.5 mm I.D. tube with its wall maintained at a nearly constant temperature. They observed that the heat transfer coefficient increased with the ratio of mass flow rate of solids and air and with the flow velocity. However for turbulent flow of air, the enhancement in heat transfer was found to decrease with flow Reynolds number. For mixtures of particles lying in the size range 20-210  $\mu$ m, they correlated their data as

$$Nu_{tp} = 0.14 Re^{0.6} \left( \frac{W_s}{W_a} \right)^{0.45} \quad (3)$$

In equation (3),  $W_s$  and  $W_a$  are the mass flow rates of solids (discontinuous phase) and air (continuous phase) respectively.

Subsequently Farbar and Depew [6] conducted experiments on nearly uniform particle sizes of 30, 70, 140 and 200  $\mu$ m. In these experiments they observed that the smallest particles resulted in highest enhancement in heat transfer whereas the largest size particles had no appreciable effect. The thermal entry length was found to increase with particles and Depew and Farbar [7] report, it could be three times higher than that for flow with no particles. A very comprehensive review of heat transfer in solid gas flows has been presented by Depew and Kramer [8].

Studies related to effects of blockages in tubes and rod bundles on heat transfer have shown that considerable enhancement in heat transfer coefficient



occurs just downstream of blockages. Experiments of Koram and Sparrow [9] for an unsymmetric blockage in a tube indicated that the increase in heat transfer downstream of the blockage could be attributed to the flow's reattachment to the tube wall. Murakami, Kikuchi and Michiyoshi [10] observed the same effect in a rectangular channel. They concluded that the downstream enhancement is a function of the ratio of blocked to unblocked area in the channel. Experimental Results of Drucker *et al* [3] for single phase flow agreed qualitatively with the aforementioned results. However, two phase bubbly and slug flow results showed much smaller relative enhancement.

The purpose of this study is to quantify for both blocked and unblocked rod bundles the enhancement in heat transfer as would occur in disperse flow regime due to the turbulence generated by the droplets. During reflood phase of a LOCA the droplets continue to evaporate as a result of heat transfer from the wall and from the steam. The continuous evaporation coupled with different modes in which heat can be transferred to the droplets, makes it difficult to discern in a real system the role the droplets play in improving the heat transfer from the wall. Thus in this study experiments are conducted by entraining glass particles in air. The density ratio of glass to air is about the same as of water to steam at expected system pressure during a LOCA.

#### EXPERIMENTAL APPARATUS AND PROCEDURE

Apparatus: The main components of the test apparatus are: the test section, a mixing chamber, variable area nozzle for metering flow of particles and a filtering system. Figure 1 shows a schematic diagram of the apparatus. The glass particles are stored in the feeder tank which is placed on a weighing machine. The variable area nozzle connects the feeder tank to a horizontal plexiglass tube which acts as a mixing chamber. One end of the mixing chamber is connected to utility air supply via a rotameter. The other end is connected to a flow establishing section preceding the test section. The flow establishing section is 77 cm long and is a 5.08 cm I.D. plexiglass tube. To re-establish the flow soon after it leaves the mixing chamber, a secondary air supply line is connected to the flow reestablishing section at the bottom. After passing through the test section, the mixture of particles and air is fed into a dust collector.

The test section consists of 4 rods arranged in a square grid and housed in a 5.08 cm I.D. plexiglass tube. The rods are 1.1 cm O.D. stainless steel tubes with a wall thickness of 0.84 mm and a length of 184.2 cm. The rods are held together with spot welding at discrete locations with wire wraps made out of 0.6 mm diameter stainless steel wire. For blocked rod bundle experiments, sleeve type blockages are placed in the mid plane of each rod. The diameter of the blockages is chosen such that with the same rod spacing as the unblocked case the blockages would barely touch each other. The orientation of the rods is secured by soldering the blockages together. For both set of bundles two of the four rods are instrumented with 30 gage chromel-alumel thermocouples. The thermocouples are spotwelded on the inner wall of the stainless steel tubes. Figure 2 shows the location of these thermocouples and a cross-sectional view of the test section. The rods are positioned such that the thermocouples on one of the instrumented rods face the inner channel while those on the other rod face the outer channel. The rod thermocouples and the thermocouple placed at the inlet of the test section to measure the incoming fluid temperature are connected to a data logger.

Procedure: Prior to initiation of experiments with a new rod bundle, the

thermocouples mounted on the rods are calibrated with respect to the thermocouple placed at inlet of the test section. Thereafter the flow rate of air is adjusted to a desired value and the electrical heating of the rods is initiated by maintaining a constant AC voltage across the rod bundle. The voltage is adjusted with the help of a variac and current and voltage are noted with a multimeter. During initial heating period and after steady state conditions are achieved, the data are scanned every fifteen seconds from all the thermocouples. To allow for any variation in the inlet temperature of air, an average of three sets of steady state data is used for calculations.

The solid particles are then entrained by opening the valve connecting the mixing chamber with the feeder tank. The choice of a particular nozzle is made a priori depending on the desired flow rate of the particles. The reduction in the weight of the feeder tank is recorded every ten minutes. In a manner similar to the single phase experiments, the thermocouple output is continuously recorded on the data logger. Because of the fluctuations in wall temperature due to the turbulence created by the particles, the instability of the flow and the electrostatic charge developing between glass particle, an average of 6 to 12 data sets is taken.

Data Reduction: The thermocouple output recorded in millivolts was converted into temperature by using appropriate conversion factor. The evaluation of heat transfer coefficient requires outer wall temperature rather than the inner wall temperature as noted from the thermocouple output. Therefore assuming axial symmetry, no axial conduction and insulated inner wall, the steady state one dimensional conduction equation with heat generation was solved. For the highest heating rates employed in the present experiments, the maximum temperature difference between inner and outer wall was found to be 0.01K. This difference is extremely small in comparison to the temperature difference between the wall and the fluid. Thus the thermocouples can be considered to give the outer surface temperature.

Knowing the current, the voltage, the inlet temperature of the mixture, the total length of the rods and the mass flow rate of solids and air, the bulk mixture temperature at any axial location was calculated as

$$T_b(z) = T_i + \frac{EI}{(W_a c_{pa} + W_s c_{ps})} \frac{z}{L} \quad (4)$$

In writing equation (4), it is assumed that the fluid and the particles are at the same temperature. In equation (4)  $T_i$  and  $T_b$  are the inlet and bulk temperatures respectively;  $E$  is the voltage difference,  $I$  is the current,  $z$  is the axial distance measured from inlet,  $L$  is the total height of the rods,  $c_{pa}$  and  $c_{ps}$  are the specific heats of air and solid respectively. Knowing at a given location the wall temperature,  $T_w$ , and the bulk temperature from equation (4), the local heat transfer coefficient,  $h$ , is calculated as

$$h = \frac{EI}{4[T_w(z) - T_b(z)] A_s} \quad (5)$$

In equation (5),  $A_s$  is the outer surface area of one rod.

While developing the correlation for enhancement in heat transfer, the volumetric fraction of particles rather than ratio of mass flow rate of solids

to air is used. With the assumption that the particles attain their terminal velocity very quickly and that Stoke's drag law is valid, a relation between mass flow rate ratio and volumetric fraction of solids was found.

#### RESULTS AND DISCUSSION

The single and two phase entrained flow experiments for heat transfer from a four rod bundle were conducted with Reynolds number varying from 14,500 to 21,000. In the experiments particles of 30  $\mu\text{m}$  and 100  $\mu\text{m}$  nominal size were used with mass flow rate ratio of particles to air varying from 0 to about 4. These mass flow rate ratios resulted in the variation of solid volume fraction,  $\beta$  from 0 to  $2 \times 10^{-3}$ . All of the results presented here pertain to the inner channel of the rod bundle.

Disperse Flow Heat Transfer in the Unblocked Rod Bundle: The Nusselt numbers obtained with various ratios of mass flow rates of 30  $\mu\text{m}$  particles and air and for flow Reynolds number of 20,500 are plotted in Figure 3 as a function of number of hydraulic diameters from inlet. The plotted data are for the inner channel. The arrows on the abscissa indicate the location of wire wraps. With increase in mass flow rate of solids the heat transfer coefficient is seen to increase all along the rod bundle. At higher mass loadings of particles a sudden increase in heat transfer coefficient is observed downstream of the wire wraps. This is probably due to separation and re-attachment of the flow. In the presence of the particles the distance from inlet at which the flow fully develops thermally is observed to increase somewhat. Figure 4 shows the dependence of Nusselt number on axial distance from inlet for 100  $\mu\text{m}$  particles. Again with increase in the ratio of mass flow rate of particles to air, the Nusselt number is found to increase. In comparison to the data plotted in Figure 3 for 30  $\mu\text{m}$  particles, the enhancement for the same  $Re$  and  $W_s/W_a$ , is found to be smaller with 100  $\mu\text{m}$  particles. Also with bigger particles no significant increase in heat transfer just downstream of the wire-wraps is observed.

The relative enhancement,  $\psi-1$ , in heat transfer obtained from the data such as that plotted in Figures 3 and 4 was found to be nearly independent of the axial distance from inlet. This observation is in contradiction to the conclusion drawn by Depew and Farber from their data [7] in which they found enhancement to die down with distance from inlet. The flow became fully developed at about 50 hydraulic diameters from inlet. The present data also show that the relative enhancement decreases with increase in Reynolds number but increases with increase in the loading ratio,  $W_s/W_a$ . For the same Reynolds number and the loading ratio, the relative enhancement is larger with 30 $\mu\text{m}$  particles as compared to that with 100  $\mu\text{m}$  particles.

Correlation of the Heat Transfer Data: The functional form of the correlation equation (1) developed by Drucker, Dhir and Duffey [3] based on bubbly and slug flow data should be valid for solid particles entrained in air when the void fraction,  $\alpha$ , is replaced by,  $\beta$ , the volume fraction of the solids. The volume fraction,  $\beta$ , can be easily related to the mass flow rate of the particles if the particle velocity relative to the fluid is known. In the present work the value of  $\beta$  is evaluated by assuming that the particles attain their terminal velocity very quickly. For the range of  $Re$  studied in this work, it is found that for 100  $\mu\text{m}$  particles

$$\beta \approx 0.558 \times 10^{-3} \left( \frac{W_s}{W_a} - 1.3 \right) + 7.19 \times 10^{-4} \quad (6)$$

and for 30  $\mu\text{m}$  particles

$$\beta \approx 0.538 \times 10^{-3} \left( \frac{W_s}{W_a} - 2.8 \right) + 1.51 \times 10^{-3} \quad (7)$$

In Figure 5 the relative enhancement obtained with 30  $\mu\text{m}$  and 100  $\mu\text{m}$  particles is plotted as a function of  $\beta\text{Gr}/\text{Re}^2$ . The 30  $\mu\text{m}$  data covering more than an order of magnitude variation in  $\beta\text{Gr}/\text{Re}^2$  are correlated within  $\pm 40\%$  as

$$\psi = 1 + 71.5 (\beta\text{Gr}/\text{Re}^2)^{0.85} \quad (8)$$

The large variability of the data with respect to the best fit through the data results from the significant uncertainty associated with the data for which the enhancement is only 10-15%. The 30  $\mu\text{m}$  data show a much stronger dependence on  $\beta\text{Gr}/\text{Re}^2$  in comparison to the bubbly flow data of Drucker *et al* [3].<sup>2</sup> The enhancement with 100  $\mu\text{m}$  particles for a rather narrow range of  $\beta\text{Gr}/\text{Re}^2$  is correlated as

$$\psi = 1 + 2.6 (\beta\text{Gr}/\text{Re}^2)^{0.5} \quad (9)$$

The correlation (9) shows a similar dependence of relative enhancement on  $\beta\text{Gr}/\text{Re}^2$  as was obtained in reference [3] with bubbly flow. However the relative enhancement obtained with bigger particles is about 25% lower than that found in the bubbly flow.

Disperse Flow Heat Transfer in the Blocked Rod Bundle: The enhancement in heat transfer in the vicinity of blockages located at the mid plane of the rod bundle are plotted in Figure 6 for a flow Reynolds number of 16700. The plotted data are for pure air flow and for the cases when the ratio of mass flow rate of 30 $\mu\text{m}$  particles to air is 1.7 and 4.4 respectively. The dotted and chain lines represent the enhancement in the absence of the blockages. In cases for which the data for the unblocked bundle at the same loading was not available, equation (8) was used. Referring to the case of  $W_s/W_a = 0$ , a significant enhancement in heat transfer rate is observed downstream of the blockage. As has been discussed by Koram and Sparrow [9] and Drucker *et al* [3], this enhancement is attributed to the separation and reattachment of flow in the downstream wake of the blockages. Immediately downstream of the blockages is the separation region featuring high turbulence which enhances the heat transfer rate. The heat transfer coefficient reaches a maximum value when the flow reattaches to the surface of the rod. Following the peak an exponential decay of heat transfer coefficient characterizes the flow redevelopment region. The undisturbed value of the heat transfer coefficient is seen to occur within about 10 hydraulic diameters. The maximum enhancement in heat transfer rate downstream of the blockages is about 35%. This value is significantly lower than an increase of about 135% predicted from the correlation of Drucker *et al* developed with water data. In the reattachment region, the boundary layer just begins to form and conditions closer an inviscid flow exist. For this case the heat transfer rate is probably limited by Peclet number rather than Prandtl and Reynolds numbers. This observation needs to be substantiated with data obtained with fluids other than water and air.

With particles an abrupt increase in heat transfer just upstream of the blockages is observed. This increase in heat transfer is caused by the cross flow conditions that develop as the flow trying to avoid the high resistance

region in the inner channel diverts to the outer channel. Downstream of the blockage, the enhancement attains a maximum value and then exponentially decreases to the undisturbed value for the unblocked bundle. For a loading of 1.7, the maximum enhancement is about 20% where as it decreases to about 15% when  $W_s/W_a$  is increased to 4.4. Both these values are lower than the maximum enhancement observed with air alone. This indicates that increase in turbulence in the separated and reattachment regions downstream of the blockage is smaller when the main flow turbulence is already augmented because of presence of particles. This inference is reinforced by the observed reduction in enhancement as the loading ratio,  $W_s/W_a$ , or turbulence of the main flow is increased.

Figure 7 shows the relative enhancement in heat transfer in the vicinity of blockages for a flow Reynolds number of 14500. The observed enhancement for both the single and two phase flow conditions is similar to that observed in Figure 6. The maximum enhancement downstream of the blockages is smaller under two phase flow conditions than that for the single phase flow and is consistent with the earlier observation of Drucker *et al.*

The presence of droplets in the steam region far downstream of the quench front during reflooding will thus definitely enhance heat transfer. The smaller particles in the size range of about 30  $\mu\text{m}$  will mainly contribute to this enhancement. Though the mass fraction of the smaller particles under entrained flow conditions during reflooding may be small, the number density of these particles can be easily larger. As observed in FLECHT SEASET [11] experiments, an enhancement of 70-80% above the single phase flow conditions is easily possible. In order to precisely quantify the enhancement, data with different distributions of particles are needed. It should also be pointed out that the effect of evaporation of droplets on the local temperature profile need to be included when using the correlation developed with the particles.

If blockages are present, heat transfer downstream of blockages will be augmented beyond that caused by the droplet created turbulence. Some droplets may shatter as they hit the blockages. The present data do not include the effect of droplet shattering and subsequent change in the droplet size distribution on heat transfer downstream of the blockages.

#### CONCLUSIONS

1. The presence of a discontinuous phase in a continuous phase leads to enhancement in heat transfer. The enhancement is found to increase with the loading ratio or the volume fraction of the discontinuous phase and decrease with increase in the base flow Reynolds number. For the same flow and loading conditions, the enhancement is higher with 30  $\mu\text{m}$  particles than with 100  $\mu\text{m}$  particles.
2. The enhancement data has been correlated with the dimensionless group  $\beta Gr/Re^2$ . For a base flow Reynolds number of 16700, and  $\beta$  of about  $2 \times 10^3$  an enhancement of 120-150% has been observed in the four rod bundle.
3. In addition to the enhancement created by the discontinuous phase, the rate of heat transfer is further augmented downstream of the blockages as a result of separation and reattachment of flow.

## NOTES

1. Work supported by EPRI, Palo Alto, Ca.
2. Safety and Analysis Department, EPRI.

## REFERENCES

3. Drucker, M.I., V.K. Dhir, and R.B. Duffey, "Two Phase Heat Transfer for Flow in Tubes and Over Rod Bundles with Blockages", presented at Winter ASME meeting Nov. 1982, and to be published in Journal of Heat Transfer.
4. Theofanous, T.G., and J. Sullivan, "Turbulence in Two-Phase Dispersed Flows", Journal of Fluid Mechanics, Vol. 116, 1982, pp. 343-362.
5. Farbar, L., and M.J. Morley, "Heat Transfer to Flowing Gas-Solids Mixtures in a Circular Tube", Industrial and Engineering Chemistry, Vol. 49, No. 7, 1957, pp. 1143-1150.
6. Farbar, L., and C.A. Depew, "Heat Transfer Effects to Gas-Solids Mixtures Using Solid Spherical Particles of Uniform Size", Industrial and Engineering Chemistry, Vol. 2, No. 2, 1963, pp. 130-135.
7. Depew, C.A., and L. Farbar, "Heat Transfer to Pneumatically Conveyed Glass Particles of Fixed Size", Journal of Heat Transfer, Vol. 85, 1963, pp. 164-172.
8. Depew, C.A. and T.J. Kramer, "Heat Transfer to Flow Gas Solid Mixtures", Advances in Heat Transfer, Vol. 9, 1979.
9. Koram, K.K., and E.M. Sparrow, "Turbulent Heat Transfer Downstream of an Unsymmetric Blockage in a Tube", Journal of Heat Transfer, Vol. 100, 1978, pp. 588-594.
10. Murakami, S.; Y. Kikuchi and I. Michiyoshi, "Heat Transfer in Downstream of Blockage with Discrete Permeability in Rectangular Channel", Journal of Nuclear Science and Technology, Vol. 16, 1979, pp. 929-931.
11. Personal Communication with L.E. Hochreiter Westinghouse Electric Corporation, Pittsburgh, March, 1982.

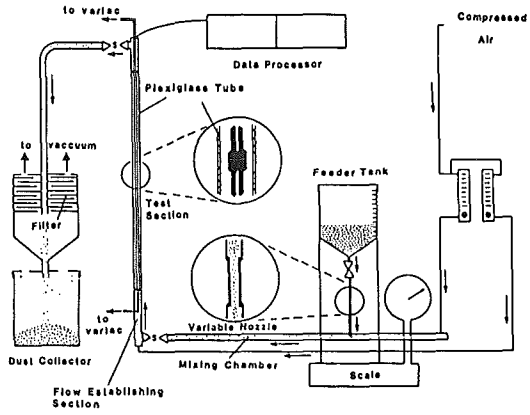


Figure 1 Schematic Diagram of the Experimental Setup

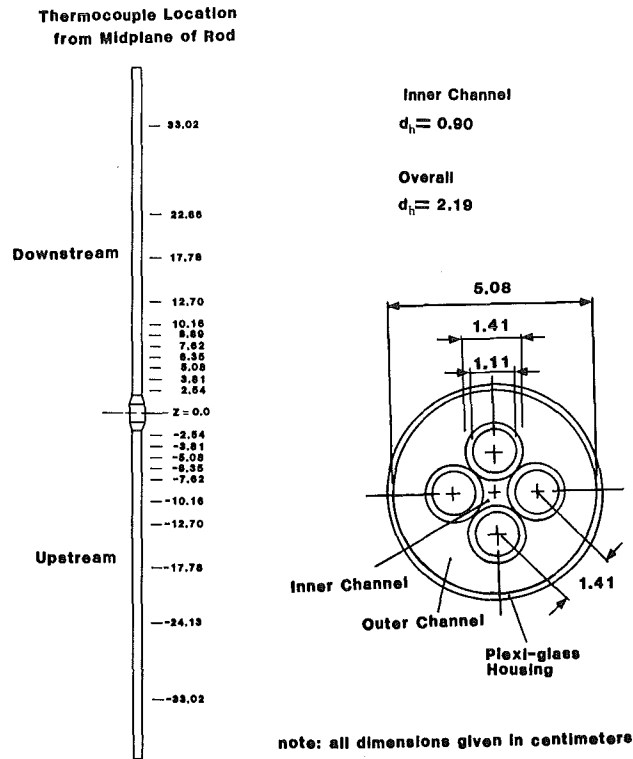


Figure 2 Details of the Test Section Cross-Section and Thermocouple locations

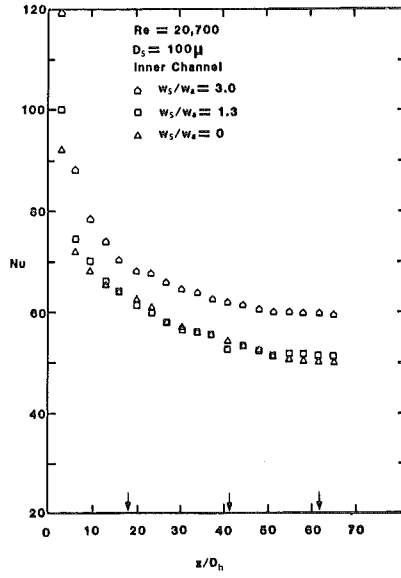
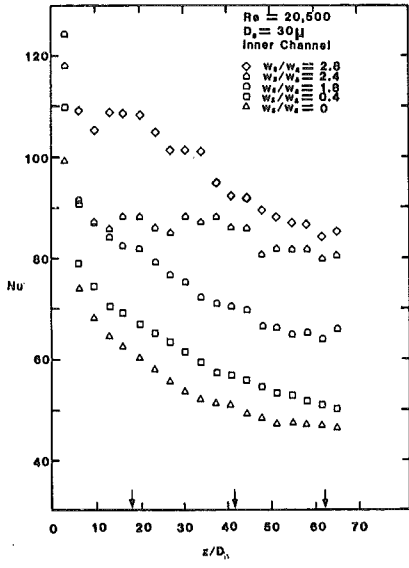


Figure 3 Nusselt Number in unblocked channel for 30 μm particles

Figure 4 Nusselt Number in unblocked channel for 100 μm particles

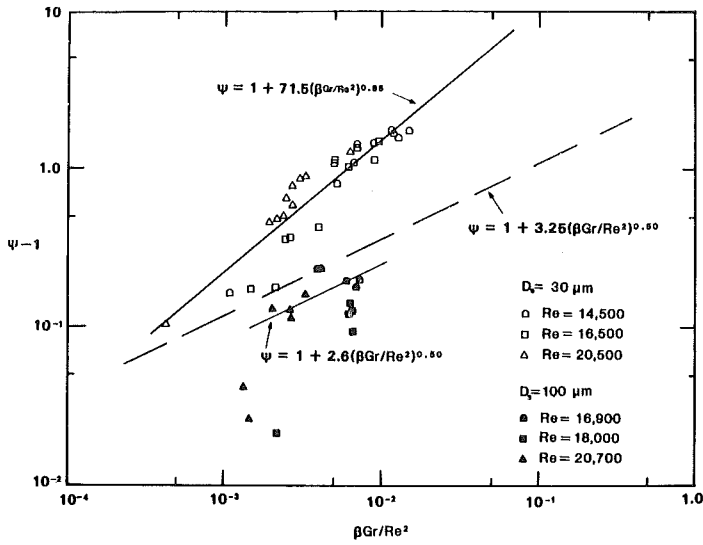


Figure 5 Correlation of  $\psi-1$  with  $\beta Gr/Re^2$  for 30 μm and 100 μm particles



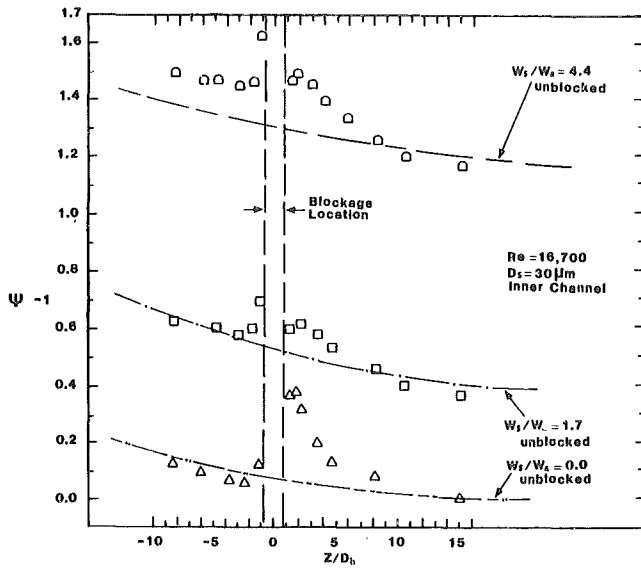


Figure 6 Variation of Heat Transfer Enhancement in the Vicinity of Blockages for  $Re=16,700$

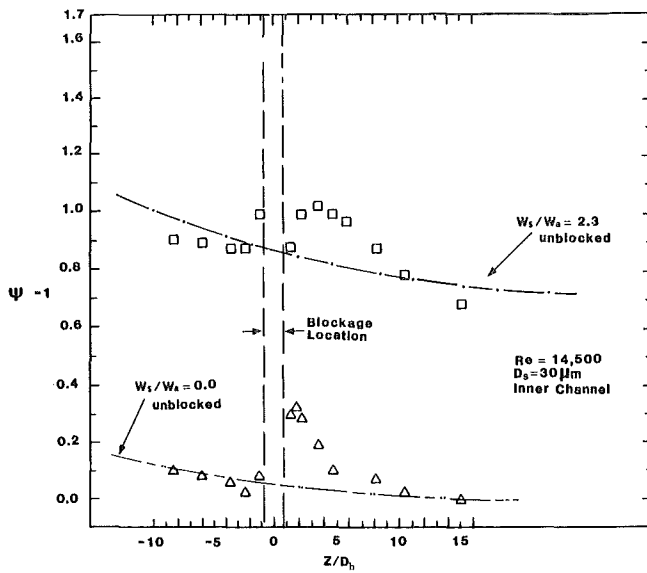


Figure 7 Variation of Heat Transfer Enhancement in the Vicinity of Blockages for  $Re=14,500$

TRANSIENT ANALYSIS OF AN HTGR PLANT  
WITH THE DSNP SIMULATION SYSTEM

D. Saphier, J. Rodnizky

SOREQ Nuclear Research Centre, Yavne, Israel

and

G. Meister

KFA Jülich, Germany F.R.

ABSTRACT

This article presents an analysis of the transient behaviour at a high temperature gas cooled reactor plant. The analysis has been performed by means of simulation programs which are generated by the DSNP program system ("Dynamic Simulator for Nuclear Power Plants"). The simulation includes the reactor core, the heat removal system comprising several heat removal loops with different design and the turbine/generator set. Several perturbations of the heat removal balance caused by different types of initiating events are investigated.

1. INTRODUCTION

DSNP is a special purpose program system for the simulation of the dynamic behaviour of the heat generation and heat removal system of nuclear power plants.

The dominant feature of DSNP is its ability to transform the flow chart or a block diagram of a heat removal system directly to a simulation program by means of a relatively small amount of DSNP instructions. The programming effort required for the development of a simulation program for a new or a modified design of a power plant is thus drastically reduced. The inherent flexibility of the DSNP system permits the simulation of a large variety of different designs within short times so that plant optimization can be achieved with improved efficiency.

The DSNP includes several libraries containing program modules which model particular components or subsystems of the heat generation and heat removal system. The libraries contain in addition a large variety of auxiliary routines such as materials properties functions and engineering correlations for two-phase flow and heat transfer. Materials properties functions, for instance, are available for water and steam, for helium, graphite and most of the metals used in reactor design.

DSNP statements are available to include an arbitrary number of component modules into a simulation program and to link them together in such a way that their mutual dependence is taken into account. Other statements serve to define the components design by assigning geometrical data, materials and boundary conditions.

The simulation program generated in this way consists of a system of coupled and (normally) nonlinear differential equations supplemented by a set of additional algebraic relations. Different numerical algorithms are available in the DSNP library which can be assigned to the program by choice.

The DSNP control language is a higher level programming language which requires a special "precompiler". This precompiler translates the DSNP statements into FORTRAN and searches the libraries for the requested component modules, auxiliary routines and design data. Finally it generates the simulation program together with the requested output routines for the display of results.

## 2. PLANT DESCRIPTION

The system underlying the present analysis resembles a projected power plant of the high temperature gas cooled type containing a pebble bed graphite core and a heat removal system designed to supply partly process heat for chemical processes such as coal gasification and partly heat for electricity generation. This plant which has a much more complicated heat removal system than that of a plant designed for electricity generation only, has been selected to demonstrate the capabilities of DSNP.

The core of the reactor is a packed bed of spherical fuel elements consisting of graphite with fuel embedded in form of small coated particles. Heat is removed from the core by forced flow of helium through the bed in downward direction.

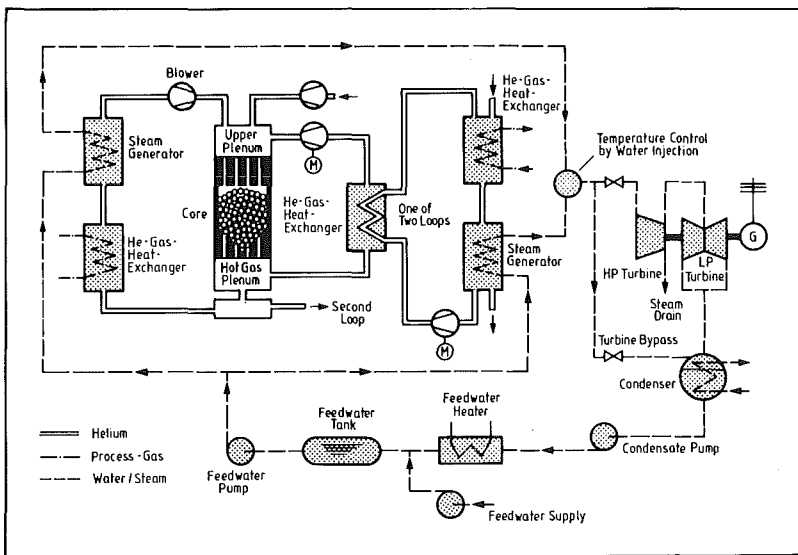


Fig. 2.1: Schematic flow chart of the analyzed HTGR plant

The heat removal system includes several loops of different design in order to meet the different tasks simultaneously. A simplified flow diagram of the system is shown in Fig. 2.1. The loop shown on the left of the reactor core includes a steam reformer and a steam generator in series. The loop on the right is separated from the primary circuit by an intermediate gas-gas-heat exchanger. Two loops of this type exist with the same performance. The total number of heat removal loops, therefore, is three.

The plant is designed for a nominal power of 500 MWth with core dimensions chosen such that the average core power density is 4.0 MW/m<sup>3</sup>. The average helium pressure in the primary circuit is 4.0 MPa.

The core inlet temperature is chosen to be 300°C and the gas mass flow through the core such that the outlet temperature attains 950°C. Half of the generated power is carried away via the loop of type 1 while the other half is removed via the two loops of type 2 by equal parts.

### 3. SIMULATION OF THE HTGR PLANT

DSNP was originally developed for the simulation of water and sodium cooled reactors /1/, /2/. Since 1980 new component modules have been developed and included into the DSNP library which extend the applicability to the simulation of gas cooled reactors /3/, /4/.

Essential differences with regard to modelling assumptions arise from the compressibility of the coolant and from the modelling of the pebble bed core. Considerable simplifications, in turn, arise from the fact that normally phase changes of the primary coolant have not to be considered.

The secondary water-steam cycle in HTGR plants may operate under different conditions compared with that in a liquid cooled reactor but from the modelling standpoint it does not exhibit essential new aspects. Most of the modules describing components in the secondary circuit of LWR and PWR, therefore, can be used for HTGR plants too.

### 4. MODELLING OF THE HTGR PEBBLE BED CORE

The HTGR-core is modelled in the present study by means of the following set of DSNP library modules:

- The core thermohydraulics module CORPB2,
- the core power distribution module TPOWR1,
- the neutron kinetics module NEUTR1,
- the reactivity feedback module FDBEK1,
- the decay heat module GAMAR1.

CORPB2 models the thermohydraulics of the pebble bed in a spatial one dimensional approach.

TPOWR1 provides the axial distribution of the power generation density in the core. (For the plant under consideration the distribution has a distinct maximum in the upper half of the core.)

NEUTR1 calculates the instantaneous reactor power as a function of reactivity from the point reactor kinetics equations with one prompt neutron group and six delayed groups.

FDBEK1 calculates the feedback effects resulting from temperature coefficients of reactivity. Fuel and moderator temperature coefficients related to average temperatures inside the active part of the core can be taken into account. This module is normally directly linked to the kinetics module NEUTR1.

GAMAR1 evaluates the decay heat generation after shutdown. The empirical ANS-standard function is used with this module.

Fig. 4.1 shows this complex of core modules with their mutual interactions. Included in addition are the modules SAFTY1 and CONTR1 which act directly on the core complex. SAFTY1 simulates the plant protection system. This module may receive several prescribed variables of the heat removal system and will initiate a scram at prescribed trip settings. Scram initiation acts on the module CONTR1 which generates the reactivity transient associated with the movement of control and shut down rods.

The core thermohydraulics module CORPB2 models the interaction of a gas flow with a packed bed of heated spheres. The equations for continuity, energy and momentum of the gas flow together with the equation for the heat diffusion inside the fuel sphere form a coupled set of differential equations.

The module is based on an approach which is commonly used in simulation codes for a gas flow in a packed beds. This approach is based on the customary gas dynamic equations with the real gas density  $\rho$  replaced by the effective density  $\rho_{eff} = \alpha \rho$  where  $\alpha$  is the void fraction of the bed. The continuity and the energy equation, therefore, can be written in the form

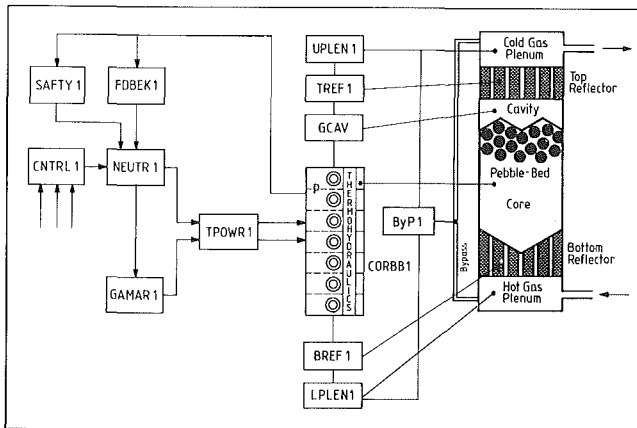


Fig. 4.1: DSNP modules used to simulate the HTGR core

$$\alpha \frac{\partial \rho}{\partial t} = -\text{div}(\alpha \rho \vec{v}) \quad (1)$$

$$\alpha \frac{\partial (\rho c_v T)}{\partial t} = -\text{div}(\alpha \rho \vec{v} c_p T) + \text{div}(k_e \text{grad } T) + Q \quad (2)$$

where  $T$  is the gas temperature,  $c_v$  and  $c_p$  the specific heat capacities for constant volume and constant pressure respectively,  $k_e$  an effective gas conductivity and  $Q$  the heat generation density.

The effective gas conductivity is evaluated from a correlation which, in addition to the molecular conductivity of the gas, takes the radiative energy exchange between neighbouring spheres into account.

The thermal coupling between the gas flow and the fuels spheres is achieved by a heat transfer coefficient which is calculated from existing correlations. The differential equation governing the heat diffusion inside the fuel spheres is solved by a commonly used implicit finite difference algorithm. The core is subdivided into a prescribed number of axial sections as shown in Fig. 4.1 in order to account for the axial variation of the heat generation density inside the core. For each section the heat diffusion is evaluated for a representative sphere with a sphere power corresponding to the local nuclear power generation density.

## 5. ANALYSIS OF SYSTEMS PERTURBATIONS

Three types of initiating events which cause a perturbation of the plant energy balance have been analysed by means of DSNP simulation programs with different degrees of complexity. These events are

1. a stepwise increase of the reactivity from zero to a constant value of  $\beta$  0.1. The imposed reactivity pulse is terminated after 4.5 s,
2. a depressurisation of the primary circuit by an anticipated leak to the atmosphere with a free flow area of 0.012 m<sup>2</sup>,
3. a 25 % decrease in turbine power demand.

All programs included the complex of core modules described in section 4. Heat exchangers, steam generators, blowers, valves and other components are represented by modules available from the DSNP library. The primary circuit is represented by a series of gas cavities and pipe segments which form the gas flow paths between the cavities.

Two programs have been used for this purpose. The first program (PRPL6) includes the core and all heat exchanging equipment of the three loops. The secondary steam-water circuits are not included and replaced by constant inlet conditions at the secondary side of the heat exchangers and steam generators. The second program (PRPL8) comprised the total heat removal system as shown in Fig. 2.1. The corresponding DSNP flow chart representing the interconnection of DSNP-modules is shown in Fig. 5.1. Steam generators and heat exchangers, for instance, are represented by more than one module. Gas cavities representing the entrance and exit plenum of these components are additionally included into the simulation network.

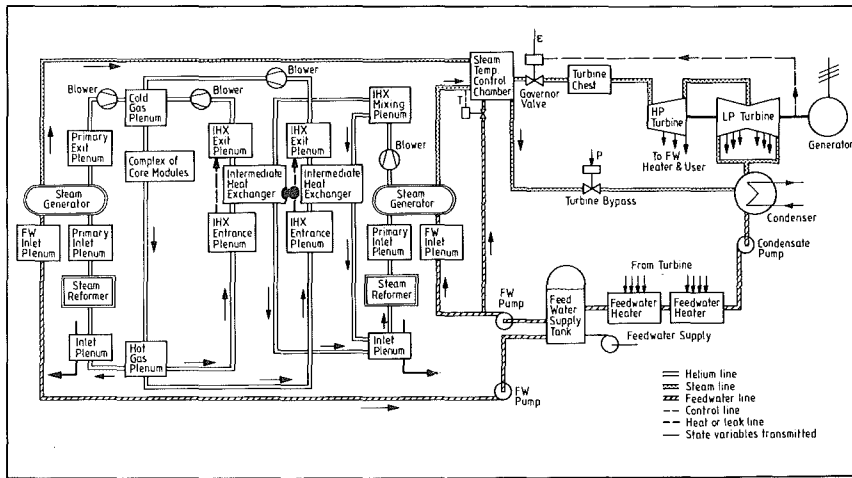


Fig. 5.1: DSNP-flowchart showing DSNP-modules required for a full scale simulation of the plant shown in Fig. 2.1

### 5.1 REACTIVITY TRANSIENTS

The response of the reactor power is determined by the imposed reactivity pulse modified by the temperature feedback. During the time interval shown in Fig. 5.2, however, this feedback effect is rather small because the core temperature follows the power transient with considerable delay. This slow response is typical for HTGR reactors and results from the large heat storage capacity of the core. The temperature feedback becomes visible after termination of the pulse. Since the imposed reactivity is reduced

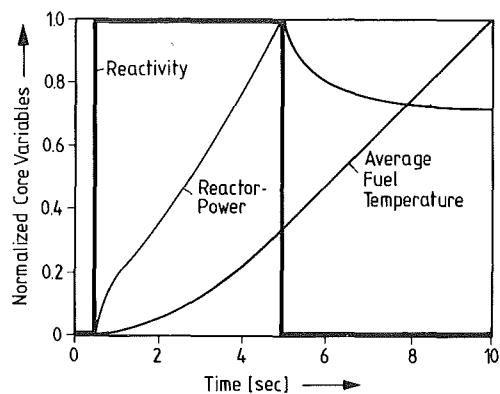


Fig. 5.2: Change of reactor power and average fuel temperature resulting from a reactivity perturbation

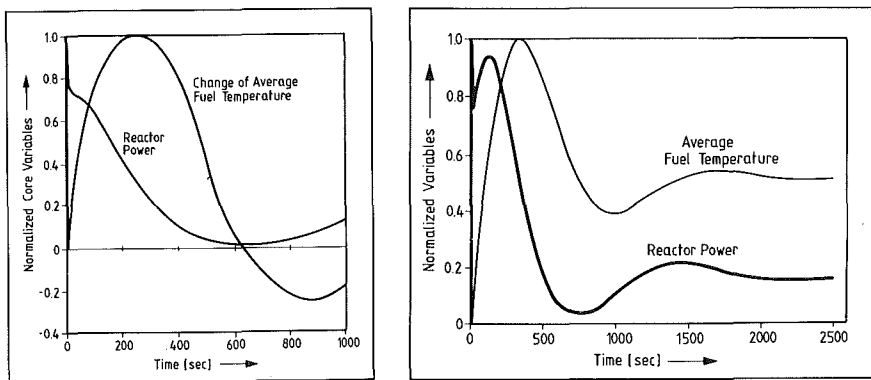


Fig. 5.3: Change of reactor power and average fuel temperature resulting from a reactivity perturbation. Long term range. Left: simplified simulation, right: full scale simulation.

to zero the temperature induced self-shutdown mechanism becomes immediately effective at this time point. Fig. 5.3 displaying on the left side the transient over a larger time interval shows that the reactor power is forced down while the fuel temperature passes after the initial increase through a maximum about 260 s after initiation of the perturbation.

The corresponding transient obtained with the full scale program PRLP8 is shown in Fig. 5.3 on the right side. The imposed reactivity pulse is the same as before, but after termination of the pulse a small amount of positive reactivity is left and kept constant throughout the transient. The short term behaviour during the reactivity pulse does not exhibit any essential difference compared with the previous case. The long term behaviour, however, shows deviating features. The reactor power drops initially at the instant of termination of the reactivity pulse in the same manner as before but rises again to a maximum which is attained after 120 s. This is a consequence of the delayed response of the core average temperature. At the instant of termination of the reactivity pulse the temperature feedback is not yet sufficient to compensate completely the small amount of imposed reactivity being left. About 120 s of temperature rise are needed to attain this compensation. In the course of the long term behaviour, which is governed by the self-shutdown mechanism, power and temperature show some minor damped oscillations which are caused by the lag of the temperature response. The core temperature as well as the other temperatures in the primary circuit stabilize at much higher level than in the previous case. This results from the thermodynamic response of the intermediate and the steam-water loops. While in the previous case all temperatures on the secondary side of the heat exchanging devices are kept constant they rise in the present transient thus counteracting the acceptance of heat from the primary circuits.



## 5.2 DEPRESSURIZATION

The leak was presumed to be located in the cold gas plenum above the top reflector of the core. It was further assumed that the gas blowers continue operation and that no reactor scram is initiated. The analysis has been performed with the full scale program PRPL8 but no external perturbation to the secondary circuits has been imposed. With the anticipated leak size an initial relief mass flow of about 32 kg/s results. The pressure equilization is practically obtained after about 720 s. Fig. 5.4 shows different gas flows within the first 20 s after initiation of the depressurization.

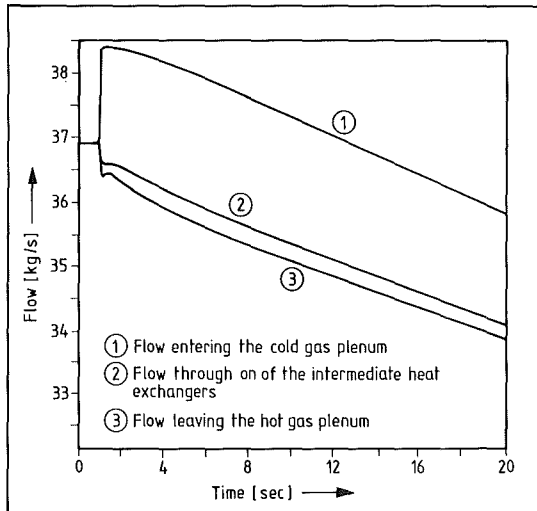


Fig. 5.4: Gas flow rates at different locations in the primary circuit during depressurization

The flows from the heat removal loops to the cold gas plenum experience a sudden increase while the flow from the hot gas plenum to the heat exchangers show a corresponding decrease. This indicates that the gas mass in the hot gas plenum is discharged essentially via the heat removal loops which have a much lower flow resistance than the pebble bed core.

The flow rate for the hot gas plenum shown in Fig. 5.4 is essentially that of the core flow. The decrease of this flow results in an increase of core temperatures which, in turn, cause a "self shut-down" of the reactor by the negative reactivity feedback. The long term behaviour of the reactor power and the average fuel temperature is shown in Fig. 5.5. The fuel temperature increases within the first 1000 s and decreases afterwards monotonically.

The transients of the gas temperature in the cold gas plenum and in the core inlet cavity as well as the temperature of the top-reflector (situated between the two gas cavities) are shown in Fig. 5.6. These temperatures decrease initially due to gas expansion and rise again after passing through a minimum at about 300 s. In the long term range they follow a moderate increase.

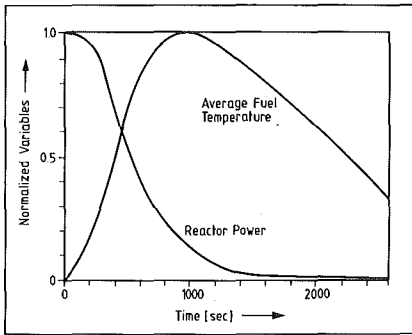


Fig. 5.5: Change of reactor power and of the average fuel temperature during a depressurization of the primary circuit

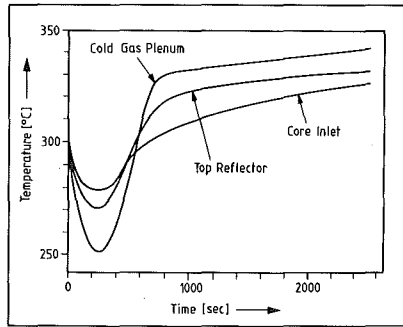


Fig. 5.6: Temperature transients at different locations during depressurisation

### 5.3 CHANGE OF TURBINE LOAD

The turbine response has been analyzed with a simulation program which includes all heat exchanging equipment of the heat removal system and the components of the secondary circuits as shown in Fig. 2.1. The steam temperature control chamber is represented by a two-phase control volume which allows water injection.

The turbine admission valve was assumed to be operational. All other valves, including the turbine bypass valve, are kept in their initial state. The turbine admission valve is assumed to be actuated by a PI controller which is designed to maintain constant turbine speed under various load conditions. The reduction of power demand with simultaneous failure of the bypass valve has the effect that the secondary system will, at least temporarily, not be able to accept the full power generated by the reactor. The resulting increase of temperature in the primary circuit in connection

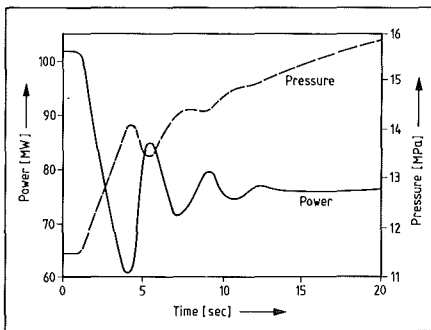


Fig. 5.7: Transients of turbine power and pressure at the steam generator exit

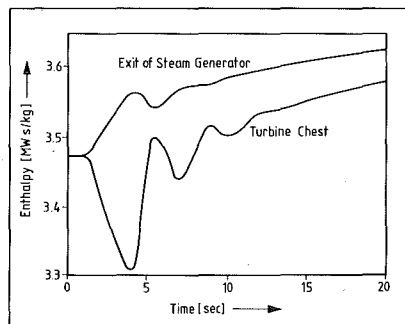


Fig. 5.8: Transients of the steam enthalpy of the exit at the steam generator and at the turbine chest

with the negative temperature feedback of reactivity determines the plant behaviour in the long term range. A safe and stable power plant should readjust itself to a new steady state power level without excessive temperature and pressure changes in the system.

Fig. 5.7 shows the response of the turbine power to a stepwise reduction of power demand by 25 % together with the corresponding pressure rise in the exit plena of the steam generators. The turbine power undergoes a damped oscillation and stabilizes at the new level of 75 % of the initial power within about 20 s. This transient is strongly determined by the setting of the PI controller acting on the turbine admission valve. The long term transients of the plant involve considerable changes in pressure and temperatures but do not affect the turbine significantly because it is isolated by the fast acting admission valve. The initial pressure transient as shown in Fig. 5.7 exhibits a significant increase. Under normal operating conditions a relief valve would limit this pressure increase. Fig. 5.8 shows the enthalpy transient at the steam generator exit and at the turbine chest. The enthalpy in the turbine chest drops initially due to the decrease of pressure and flow but then follows the same transient as the enthalpy leaving the steam generator.

#### ACKNOWLEDGEMENT

This research is partly supported by the National Council for Research and Development, Jerusalem and by the Kernforschungsanlage Jülich.

#### REFERENCES

- /1/ D. Saphier, The simulation Language of DSNP, Argonne National Laboratory, ANL-CT-77-20 (1978)
- /2/ D. Saphier, The Precompiler for the DSNP, Argonne National Laboratory, ANL-CT-77-22 (1978)
- /3/ D. Saphier, Transient Analysis of the Pebble-Bed HTGR with the DSNP Simulation Language, RASG-107-84 (1984)
- /4/ D. Saphier, DSNP Models Used in the Pebble-Bed HTGR Dynamic Simulation, RASG-108-84 (1984)



Chapter 4

## Safety Systems and Function Optimization

	pages
4.1 R. Martin, H. Guesnon: Safeguard Pumps Qualification for French Nuclear Plants The EPEC Test Loop	559 - 573
4.2 P. Wietstock: Hydrodynamical Tests with an Original PWR Heat Removal Pump	574 - 580
4.3 G. Depond, H. Sureau: Steam Generator Tube Rupture Risk Impact on Design and Operation of French PWR Plants	581 - 587
4.4 L. Cave, W.E. Kastenberg, K.Y. Lin: A Value/Impact Assessment for Alternative Decay Heat Removal Systems	588 - 596
4.5 H.A. Maurer: Cost Benefit Analysis of Reactor Safety Systems	597 - 606
4.6 A. Renard, R. Holzer, J. Basselier, K. Hnilica, Cl. Vandenberg: Safety Assessment from Studies of LWR's Burning Plutonium Fuel	607 - 616
4.7 J.L. Platten: Periodic (Inservice) Inspection of Nuclear Station Piping Welds, for the Minimum Overall Radiation Risk	617 - 625
4.8 P. Grimm, J.M. Paratte, K. Foskolos, C. Maeder: Parametric Studies on the Reactivity of Spent Fuel Storage Pools	626 - 633

	pages
4.9 W. Geiger: The CEC Shared Cost Action Research Programme on the Safety of Thermal Water Reactors: Results in the Sub-Area "Protection of Nuclear Power Plants Against External Gas Cloud Explosions"	634 - 642
4.10 G.P. Celata, M. Cumo, G.E. Farello, P.C. Incalcaterra: Physical Insight in the Evaluation of Jet Forces in Loss of Coolant Accidents	643 - 654
4.11 A. Singh, D. Abdollahian: Critical Flow Thru Safety Valves	655 - 665
4.12 A. Aust, H.-R. Niemann, H.D. Fürst, G.F. Schultheiss: Chugging-Related Load Reduction for Pressure Suppression Systems	666 - 674
4.13 S.A. Andersson, S. Helmersson, L.-E. Johansson: Improved Fuel Cycle Flexibility and Economy: Verification Tests with BWR Coolant Flow Range Extension	675 - 682
4.14 M. Bielmeier, M. Schindler, H. Unger, H. Gasteiger, H. Stepan, H. Körber: Investigation of the ECC-Efficiency in the Case of Small Leaks in a 1300 MW <sub>e1</sub> Boiling Water Reactor	683 - 692
4.15 H. Fabian, K. Frischengruber: Safety Concept and Evaluation of the 745 MW KWU- Pressurized Heavy Water Reactor (PHWR)	693 - 711
4.16 P. Antony-Spies, D. Göbel, M. Becker: Survey of KWU's Safety Related Containment Work for American Boiling Water Reactors	712 - 719

SAFEGUARD PUMPS QUALIFICATION FOR FRENCH  
NUCLEAR PLANTS

---

THE EPEC TEST LOOP

---

R. MARTIN - H. GUESNON  
EDF and FRAMATOME - FRANCE

---

SUMMARY

---

Because of their size, it has not been practical to qualify full safeguard pump assemblies, by testing alone. Recourse to other methods, such as qualification by analysis (mathematical proof, operating experience) and individual qualification of pump components, has been necessary.

Nevertheless, tests run on a specially-design full-train pump test loop have given a good indication of the ability of pumps to perform as required, particularly during thermal transients and with high-solids-content fluid. The loop, known as EPEC, was financed jointly by Framatome and the French state-owned utility EDF.

This paper reviews the specifications to which nuclear power plant safeguard pumps must be qualified, and surveys the qualification methods and program used in France to verify operability of the pump assembly and major pump components. The EPEC test loop is described along with loop capabilities and achievements up to now. It is demonstrated that qualification by testing could be given greater prominence, provided that significant investments in new test facilities are made.

---

INTRODUCTION

---

Safeguard pumps perform the essential function of ensuring safe reactor shutdown after an incident or an accident. It is essential that pump design guarantee utmost reliability.

As active components, these pumps must be qualified as a unit, i.e. all auxiliaries necessary to pump operation (motor, lube system, seal system, coupling, etc.) must be considered together with the pump.

It is common industry practice to use computer codes and design standards to guarantee the mechanical strength of the pump equipment, while overall system operability under various operating conditions is generally verified by qualification testing.

For particularly complex equipment, such as electronics assemblies and valves, comprehensive qualification tests can be run systematically on the entire unit. For these assemblies, qualification by analysis, when used, is sometimes of secondary importance.

Until now, however, safeguard pump size and the inadequacy of existing test facilities has made it impractical - from both a time and cost standpoint - to qualify safeguard pumps by full - train testing.

Nevertheless and as far as possible, qualification testing of pump assemblies does give a good indication of pump operability, particularly during thermal transients and in heavily-laden fluid service as will be shown below.

The present paper describes the qualification procedure adopted for French nuclear power plant safeguard pumps. The paper presents the EPEC test facility built specially for this purpose, and shows, through results from tests performed on a number of pumps (including the Medium Head Safety Injection (MHSI) Pump designed for service in 1300 MW nuclear power stations), the interesting possibilities offered by full-train qualification testing.

## 2. Safeguard pump specifications for PWR plants

Safeguard pumps are intended to function under upset, faulted and emergency conditions. Each of these conditions corresponds to a specific operating environment which is substantially different from that encountered during normal service ; these pumps must be capable of reliably performing their intended function under these extreme operating conditions, and off normal operating requirements must thus be integrated into pump design bases.

Typical safeguard pump specifications are shown in the table below. These specifications are for a 1300 MW 4 Loop Medium Head Safety Injection (MHSI) pumps.

	Flow Rate Value (CM/hr)	Capacity as % of BEP
BEP (1)	300	100
minimum	56	19
design flow	245	82
runout	490	163

The MHSI is a multistage horizontal-shaft pump running at 4300 rpm and with Power Input 1400 KW. Weight is approximately 16,000 kg and dimensions (l+w+h) are 7,3 x 2,5 x 1,9 m.

(1) BEP : Best Efficiency Point



The pump takes suction from :

- . the refueling water storage tank (during periodic tests and initial safety injection phase). Pumpage is cold borated water having the following characteristics :
  - boric acid concentration : 2000-2250 ppm
  - ph : 4,7
  - solid suspended particles : 0,5 ppm
- . reactor containment sumps (recirculation safety injection phase).

Pumpage is hot and heavily laden with particles.

It is required that the MHSI pump ensure its design flow rate within 5 seconds from receipt of the startup signal. This means that the pump must start up without waiting for its auxiliary oil pump to cut in and without allowing sufficient time for it to come up to temperature.

In addition, the pump must be capable of remaining operable during a seismic event and under the effects of irradiation from pumped fluid.

### 3. Qualification principle applied to safeguard pumps

Qualification of equipment is the demonstration that the equipment can perform as required under the most severe operating conditions that are likely to be encountered.

#### 3.1 - Qualification methods

Two main methods may be employed for qualification purpose :

- qualification by analysis
- qualification by testing

Qualification by analysis consists in furnishing mathematical or logical proof, or demonstrating from past experience with similar equipment, that the equipment will work as required. This method is only valid if the mathematical model or other input data are representative of actual equipment operating conditions. If operating parameters are known and measurable, the method is termed quantitative. Otherwise, it is considered qualitative.

Qualification by testing requires that one or more samples (generally one is sufficient) of the equipment be subjected to a series of tests representative of service conditions under which the equipment is expected to operate.

Combined qualification combines these two methods. It is employed especially when qualification by testing alone is impractical.

When qualification by testing is employed, it must be borne in mind that equipment may be subjected to more than one influence factor at the same time.

It is difficult if not impossible to precisely reproduce all accident conditions simultaneously without employing large, costly test setups. For this reason, a test sequence comprising a number of different tests is employed. Each test is intended to verify operability under a given set of environmental conditions.

Although certain equipment, e.g. valves and electric actuators, can be qualification-tested as a whole, this is not always practical with large components. The MHSI pump assembly, for example, is 7,3 m long and 1,9 m high and weighs 16.000 kg. Placing a unit this size on a shake table or inside an irradiation chamber would require extremely large test rigs and considerable capital outlay.

For this reason seismic, irradiation aging, and other tests are often run on individual pump components. This is also done when testing highly sensitive components or equipment subjected to particularly severe service, e.g. bearings and mechanical seals. Such subsystem-testing may employ a full or partial test sequence.

For one particular Equipment, and in order to prove his qualification, any or all of the above methods may be used in qualifying safeguard pumps. Both full-train and individual component testing may be employed. The exact method utilized in each case depends on the characteristic to be qualified, the size of existing test facilities, and representativity and exhaustivity criteria.

Prior to qualification by testing, test conditions, control parameters, and components to be tested are determined. At the completion of testing, test results may serve to validate the test or calculation methods used.

### 3.2. - Typical qualification program

The table below shows the qualification program for a typical safeguard pump tested at the EPEC facility, the MHSI pump .

TABLE 1 : Typical qualification program  
(MSHI pump)

characteristic	qualification method	Equipement qualified
resistance to pressure	combined (math proof + hydrostatic test)	pressure-retaining parts . main pump . booster pump . sealwater heater
hydraulic performance (w. cold water) (H, NPSHR Output for specified flow-rates)	testing (supplier rig+ EPEC loop)	motor-pump assembly on provisional test-loop
hydraulic performance (hot water)	testing (EPEC loop)	motor pump assembly on provisional test-loop
seismic resistance	analysis (math proof)	- rotor assembly - pump supportage - lube and cooling system
resistance to temperature of mechanical seals (1)	testing (bench + EPEC loop)	- mechanical seal assy. - cooling and filtration system
resistance to temperature transients	testing (EPEC loop)	motor-pump assembly on provisional test-loop
Rapid startup with and w/o startup of aux. lub. pump	testing (EPEC loop)	motor pump assembly on provisional test-loop
startup time	testing (EPEC loop)	motor pump assembly on provisional test-loop

(1) Loop test was performed on mechanical seal provided by usual supplier.  
Bench test was run to qualify seal from alternate supplier.

TABLE 1 : (continued)

Characteristic	qualification method	Equipment qualified
dynamic behavior (e.g. critical speed)	analysis (math and logical proof)	- rotor assy. - bearings - coupling
shaft mechanical strength (e.g. fatigue resist.)	analysis (math + proof)	shafting
operation in heavily particle-laden water	testing (EPEC loop)	full train
radiation resistance	analysis (logical proof + testing)	gaskets, oil, grease
dynamic behavior (e.g. natural freq. search)	combined (logical proof + field test)	full train

An important secondary objective of the test program has been to prove the validity of computer codes and analytical methods used in qualification. Tests conducted on the low Head Safety Injection (LHST) Pump at the Tournesol Test facility located in the CEA DDMT Research Center at Saclay, have demonstrated the validity of calculation models employed. The tests were run on a 2-axis shake table and conducted under the auspices of the Research and Development agreement among CEA, EDF, FRAMATOME and WESTINGHOUSE.

Note : the MHSI pump discussed in this paper served as the 1300 MW plant series model. Tests run on the pump at the EPEC facility were thus type (first off) tests, and therefore more comprehensive than standard duplicate tests run on other pumps which are already in service or plants.

#### 4. EPEC TEST LOOP

Qualification methods and programs are, of course, considered valid only if tests and calculations are shown to be representative of site equipment operating conditions.

Generally speaking, existing acceptance test loops at supplier facilities are not adequate to reproduce accident conditions. And then acceptance tests cannot be considered as representative. The EPEC test loop was devised specifically to afford a representative test setup for safeguard pumps under site environmental conditions and particularly hot conditions. This facility which has rapidly become an essential link in the qualification process, is briefly described below.

##### 4.1. - Simulation capabilities

The following safeguard pump functions are capable of being simulated on the EPEC loop :

###### Normal operation

- reactor coolant charging and makeup
- unit cooldown at low pressure startup and shutdown.
- filling of accumulators and other vessels

###### Upset, faulted and accident conditions

- high pressure and low pressure safety injection of boric acid to prevent uncovering and to ensure proper residual core cooling
- containment spray to counteract release of steam during a loss of coolant accident (LOCA) or steam line break (SLB)

- auxiliary feedwater flow to the steam generators.

#### 4.2. - Loop design

The EPEC test loop is the result of a joint effort by Framatome and EDF. It was engineered and built by "les Etablissements des Constructions et Armes Navales (ECAN)" in Indret, France.

The EPEC facility contains a number of capabilities which are not provided on standard pump supplier test loops, e.g. :

- hydraulic and mechanical characteristics measurement under hot and cold conditions (see footnote, p. 10).
- thermal shock simulation under hot and cold conditions
- startup and shut down transient simulation with fast-response recording system
- simulation of process flow heavily laden with suspended solid particles.

The test loop comprises :

- the main loop with pump to be tested. Pressure is controlled by a pressurizer and temperature is kept in the range of 20-140°C by means of a cooler. Orifices with a range of 4 to 1500 CM/hr are provided to measure system flows.
- 12 CM transfer tank and 3 way valve for simulation of rapid thermal transients
- suspended particles injection system for simulation of recirculation phase of safety injection or containment spray
- vacuum pump for simulation of pump cavitation tests and determination of NPSH
- central data acquisition system for recording and display of operating parameters and fully automatic operation of the test loop.

The recording system is designed for extra-fast acquisition of startup, shutdown and thermal shock transient data.

## EPEC TEST LOOP CHARACTERISTICS

flowrate	4 - 1500 m <sup>3</sup> /h
temperature	ambient -140°C continuous (180°C MAX.)
Pressure	BP 12 bar HP 200 bar
Reactor coolant pipe dia.	273 - 355 mm
transfer tank volume	12 m <sup>3</sup>
pressurizer volume	2 m <sup>3</sup>
cooler output	6 MW
Pump power input	1,4 MW (provisionnal)
Pump type which can be tested	- multistage - horizontal - vertical - wet-pit

All instrumentation and associated equipment installed on the EPEC test loop (flowmeter, primary elements, pressure gauges, etc...) were designed, built and erected to French standards, in particular NF X 10-602.

#### 4.3. - Test program

A typical EPEC qualification test program includes :

- verification of pump hot and cold hydraulic and mechanical characteristics (1)
- NPSH test, hot and cold conditions
- low-flow test (temp. vibration, steady-state performance)
- performance during startup and shutdown transients, with and without startup of auxiliary lube pump ; fast-response recording hydraulic and mechanical characteristics.
- pump performance during rapid temperature transients (steep front thermal shock gradients from 20 to 140°C or cold shock from 140 to 70°C over several min)
- endurance tests, steady state conditions (200 - 400 h)
- verification of pump performance in heavily-laden fluid service, with or without shutdown/restart
- vibration measurement(integrated into other tests).

(1) cold : room temperature  
hot : 140°C, occasionally up to 180°C



## 5. EXPERIENCE TO DATE USING EPEC TEST LOOP

The EPEC test loop was commissioned in 1981. To date, 3 pumps have been tested on the EPEC loop, two low capacity high head units and one high capacity low head assembly.

- charging pump for 900 MW 3-loop plants (this pump being also used as High Head Safety Injection (HHSI) pump)
- MHSI pump for 1300 MW 4-loop plants
- containment spray pump for 1300 MW 4-loop plants

In all, the current qualification program is scheduled to cover 6 safeguard pumps intended for service in French 3 and 4-loop power plants.

### 5.1. - Improvements in test equipment

A number of improvements have been made in the EPEC test loop to enhance performance. In particular, steps have been taken to ameliorate measurement accuracy and to improve control of particle injection for closer simulation of mixing conditions at pump suction and closer representativity.

An extra-fast recording system has been installed to monitor major pump parameters (speed, motor current draw, etc.). This makes it possible to check with greater accuracy that there are no friction losses during transients.

### 5.2. - Main test results

The EPEC loop has enabled a number of critical pump criteria to be verified. In particular, it has demonstrated that safeguard pumps can function as required in conditions of severe service such as steep temperature gradients and heavily particle-laden water. Also, additional pump data concerning the way pumps operate has been obtained.

Main test results can be summarized as follows :

- pump hydraulic and mechanical characteristics such as NPSH and efficiency were not influenced by temperature.
- pumps showed good behaviour while running hot. Steady-state performance and vibration were satisfactory
- thermal isolation of bearings and mechanical seals and cooling system efficiency were found to be adequate
- understanding of pump behaviour during startup and shutdown transients was improved. No instability was detected at startup, and startup time was within specified values in all cases.

Emergency startup without help of the auxiliary pump did not in any way impair pump performance. Lube circuit pressurization time for different operating conditions (startup, switchover to standby pump, restart following diesel generator startup) was found to be adequate :

- pumps proved to be insensitive to thermal transients (positive or negative gradients). No vibration or instability was observed
- good extreme flow (minimum flow and runout) capabilities were evidenced (1). Vibration and internal temperature rise levels were acceptable
- pumps did not exhibit evidence of malfunction in the presence of solid particles suspended in pumped fluid, either during steady-state or transient (startup/shutdown) operation. Particle dilution, segregation and disintegration phenomena were observed. There was no sign of binding at the impeller wearing ring clearances . Areas particularly sensitive to wear were identified and some progress was made in evaluating ring wearing rate. Influence of solid suspended particles on pump hydraulic characteristics was studied.
- no solid-particle-induced hydrostatic line bearing malfunction was observed

#### Other tests

The EPEC test loop is a versatile facility, and can be utilized for tests which are not normally included in qualification test programs. High temperature tests are one example.

The facility can be useful not only to verify equipment operability, but to test unit design as well. Faulty thermohydraulic isolation at the mechanical seal is one major design error discovered using the EPEC loop.

- (1) minimum flow was 0,04 x BEP  
runout flow was 1,5 x BEP

## 6. CONCLUSION

We are convinced that comprehensive full-train qualification tests are essential to determine pump operability under extreme conditions of high-temperature and heavily-particle-laden water service. Although full-train test facilities are expensive, their cost can be justified if the number of pumps in the series to be qualified is sufficiently high.

The results of qualification tests run on test loops such as EPEC can serve as major factors (albeit not the sole ones) in qualification programs.

By combining full-train testing with qualification by analysis and bench testing of selected individual components, real assurance that nuclear safeguard pumps will function as required in the event of an incident or accident can be provided.

## APPENDIX 1

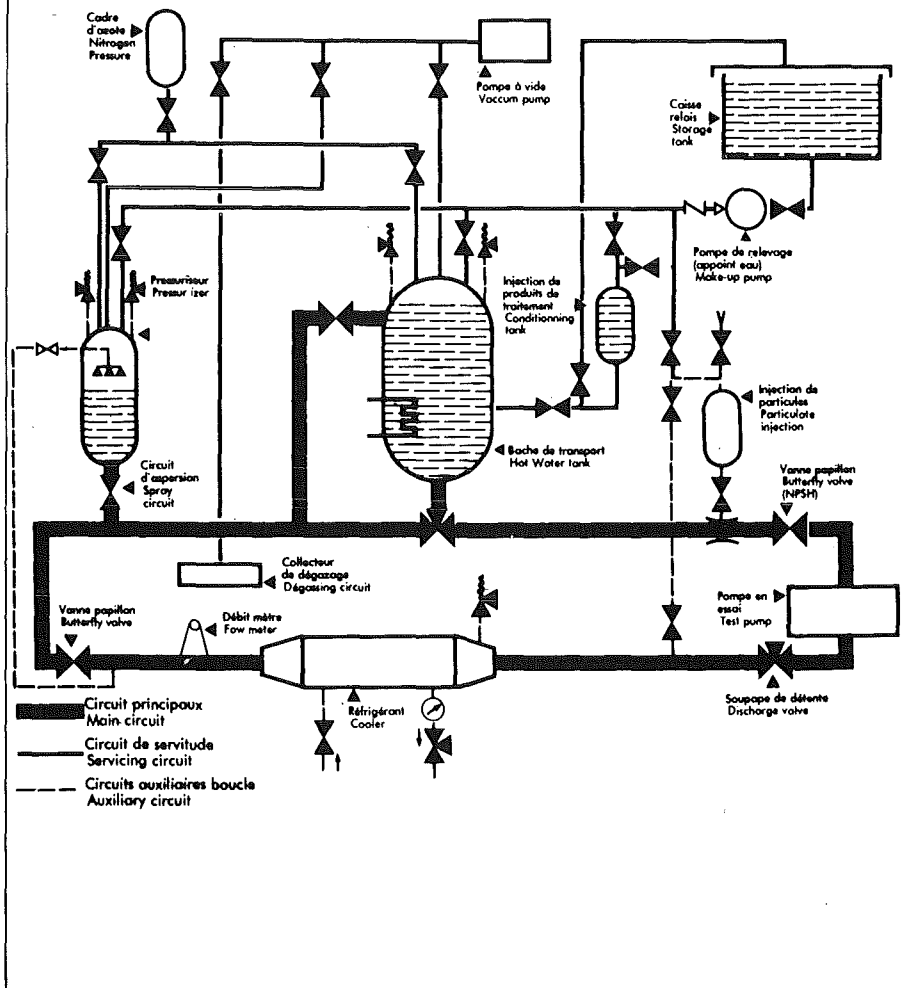
## CHARACTERISTICS OF SUSPENDED PARTICLES

- max. size of particles passing through filters	2,5 x 2,5 mm
- concentration	500 ppm
- particle makeup	
. screened crushed concrete	300 ppm
. thermal insulation (wet shredded rock wool)	
. paint flakes	50 ppm
. sand	40 ppm
. crushed glass	10 ppm
- injection method	gradual until 500 ppm concentration is obtained (pump in operation)

# Boucle D'essai de Pompes

## Pump Test Loop

"EPEC"



## HYDRODYNAMICAL TESTS WITH AN ORIGINAL PWR HEAT REMOVAL PUMP

P. Wietstock

GKSS-Forschungszentrum Geesthacht GmbH  
Institut für Anlagentechnik  
2054 Geesthacht, Federal Republic of Germany

## ABSTRACT

GKSS-Forschungszentrum performs hydrodynamical tests with an original PWR heat removal pump to analyse the influences of fluid parameters on the capacity and cavitation behavior of the pump in order to get further improvements of the quantification of the reached safety-level.

It can be concluded, that in case of the tested heat removal pump the additional loads during transition from cavitation free operation into fully cavitation for the investigated operation point with 980 m<sup>3</sup>/h will be smaller than the alteration of loads during passing through the total characteristic.

The results from cavitation tests for other operation points indicate, that this very important consequence especially for accident operation will be valid for the total specified pump flow area.

## INTRODUCTION

The normal decay heat and emergency heat removal system represents an essential part of the safety system of a PWR-plant. The heat removal pumps, being part of this system, must fulfil different tasks with manifold operation conditions. Some of these operation conditions are characterized by a very small distance of the NPSH-value of the system from the required NPSH-value of the pump. For this reason disturbances in the pump suction area may initiate cavitation within the pump with consequences on the capacity of the pump and possible additional loads on the pump unit.

GKSS-Forschungszentrum carries out hydrodynamical tests with a heat removal pump simulating operation conditions similar to those in a PWR. The pump unit is an original pump as operated in german PWR-plants at present. Tests are made to analyse the influences of fluid parameters on the capacity and cavitation behavior of the pump in order to get further improvements of the quantification of the reached safety-level.

## TEST-PROGRAM

The investigations are subdivided in three main phases, from which two phases refer to stationary tests and the third phase enlarges instationary investigations of the pump /1/. Main points of the experimental program are

especially

- Investigation of the total head of the pump as function of the NPSH when full cavitation has developed (total pressure head against zero). Parameters are load, fluid-temperature and gas content.
- Determination of the mentioned NPSH-characteristics as function of impurities within the fluid.
- Determination of instationary capacity and cavitation behavior and investigation of failure-reducing operation modes.

The tests should enable an evaluation of the hydraulic and vibration behavior of the system. At first the field of test parameters is similar with normal operation conditions of the reactor plant and independent from anticipated accident procedures. For evaluation of test results however some anticipated reference accident procedures will be considered in the test-program.

The test program with the original heat removal pump on the NKP-test rig of the GKSS-Forschungszentrum in parallel will be supported by basis investigations with a low pressure test rig of glas material, especially analysing problems of cavitation and transport of impurities within the fluid.

#### PWR HEAT REMOVAL PUMP

The technical development in German PWR-plants had lead to three different PWR heat removal pump-types with the same principle of construction of the emergency heat removal system.

The first stage of development represents a horizontal single-stage volute pump. The speed of this standard chemical pump is about 1490 rpm. For the several PWR-plants the hydraulic data could be different.

The second stage of development are single-stage pumps with circular-space casings and vaned diffusers. The motor is a four-pole-motor with a speed of about 1490 rpm.

In the case of the third stage of development it is a single-stage pump with circular-space casing and vaned diffuser. The motor is a six-pole motor with a speed of about 980 rpm. The reduction of speed to 980 rpm was necessary by reason of a recommendation of the German Reaktor-Sicherheitskommission /3/.

For the GKSS tests an original pump according to the first stage of development was selected. This pump-type is in operation at present in most of the German PWR power plants.

#### EXPERIMENTAL FACILITIES

For the investigation of the above mentioned problems a pump test rig is operated (Fig. 9) at pressures up to 21 bar and temperatures up to 180°C

with fully desalinated water with or without defined impurity. The pipe diameter of the loop is 400 mm at the suction side and 300 mm at the discharge side of the pump. The test pump is an original unit with special additional measuring equipment /2/.

Separate studies regarding the phenomenology of the cavitation and transport of impurities within pipes including the pump are performed in a model glass loop with a pipe diameter of 100 mm (Fig. 10). This loop is operated at atmospheric pressure up to 90°C. Furthermore, this loop is used to test measuring equipment.

#### EXPERIMENTAL RESULTS

In the following some examples of test results will be presented, which give an information about load variations on the pump initiated by flow alterations or cavitation alternatively.

Fig. 1-4 give for stationary and cavitation-free operation over the total pump flow rate characteristics for head, radial deflection, radial amplitude of vibration and axial deflection as function of pump flow for basis and comparison. The fluid in the test rig is clean. It is water from the communal supply with an air content lower than 3 ml/l.

These characteristics are compared with results from a cavitation test with a flow rate of 980 m<sup>3</sup>/h, speed of 1500 rpm and 30 °C water temperature from the same quality and gas content (Fig. 5-8).

- Fig. 1 shows a normal Q-H-characteristic.

Fig. 5 shows the total head as function of the NPSH-value for the above mentioned cavitation test. The cavitation test was characterized by decreasing NPSH-values - starting with high value - by reduction of the pressure in the suction vessel step by step. There is no throttle valve installed in the suction pipe.

- Fig. 2 shows the radial deflection of the impeller against the pump casing in the front split ring area as function of the pump flow measured at two positions displaced by 90°. The test value of 0 mm corresponds with an original split width of 1.68 mm resp. 1.43 mm. Negative values in the figures represent an increase of the original split width. The alteration of the pump flow from 1400 m<sup>3</sup>/h down to 100 m<sup>3</sup>/h results in an enlargement of the split to 0.4 mm in one measuring position.

Fig. 6 shows relevant values for the cavitation test given in Fig. 5. During transition to fully cavitation the alteration of the split ring width amounts to 0.15 mm in maximum.

- Fig. 3 shows the radial amplitude of vibration as function of the flow for mentioned measuring position. During alteration of the pump flow the maximum change of this parameter amounts to 150 µm.



Fig. 7 shows again the conditions for the cavitations tests, the alteration of the amplitude of vibration during transition into cavitation amounts about 50  $\mu\text{m}$ .

- Finally fig. 4 represents the axial deflection of the impeller back-side against the pump casing in a special measuring position as function of the pump flow. With start conditions of 2.15 mm the maximum alteration amounts to about 0.8 mm for a pump flow variation from 1400 to 0  $\text{m}^3/\text{h}$ .

The conditions for the cavitation tests shows fig. 8; the maximum alteration of the deflection results in less than 0.15 mm for transition in fully cavitation.

Finally it can be concluded, that in case of the tested heat removal pump the additional loads during transition from cavitation free operation in fully cavitation for the investigated operation point with 980  $\text{m}^3/\text{h}$  will be smaller than the alteration of loads during passing through the total Q-H-characteristic.

The results from cavitation tests for other operation points confirm, that this very important consequence especially for accident operation will be valid for the total specified pump flow area.

It might be still mentioned, that these results are test results with the GKSS test facility. The flow on the suction side of the pump passes before entering the pump a straightener and after that a contracting channel. Therefore the flow is a full developed turbulent flow with very small variation in axial direction (bulb-shaped flow).

It is expected, that a disturbed flow after a bend or a valve will have an influence on the above mentioned results. Tests in next time will quantify this influence.

Test results relative to determination of the mentioned NPSH characteristics show, that the required NPSH-value (3% head decrease) will be influenced by temperature and gas content. For nominal capacity a reduction of the required NPSH-value of about 0.5 meter or 11% by increasing the temperature from 90°C to 125°C was measured. In this case the gas content was less than 2 ml/l. The determination of the influence of gas content lead to more scattering tests results. But the tendency shows, that an increasing gas content leads to an increasing required NPSH-value.

A more detailed description of these NPSH-characteristic-tests will be presented at the Pumpentagung Karlsruhe '84 /4/.

Results of tests relative to instationary pump flow and cavitation behavior were presented at the Jahrestagung Kerntechnik '84 /5/.

#### REFERENCES

- /1/ P. Wietstock:  
Untersuchungen an DWR-Nachkühlpumpen-Problemstellungen und Untersuchungsprogramm.  
(persönliche Mitteilung)

- /2/ H. Domann:  
Beschreibung des Nachkühlpumpen-Versuchsstandes der GKSS  
GKSS 83/E/28
- /3/ Empfehlungen der Reaktor-Sicherheitskommission auf ihrer 119. Sitzung am 15. Dez. 1976, Pkt. 11  
GRS-Kurz-Information Nr. 28, Reihe C 1977
- /4/ P. Wietstock, H. Domann:  
Einfluß von Fluidparametern auf das Kavitationsverhalten einer Chemienormpumpe.  
Pumpentagung Karlsruhe '84 2.-4. Oktober 1984
- /5/ H. Domann, H. Schwan, D. Seeliger:  
Experimentelle Untersuchung zum Verhalten einer originalen Nachkühlpumpe bei schneller Druckabsenkung.  
Tagungsbericht; Jahrestagung Kerntechnik '84, Frankfurt

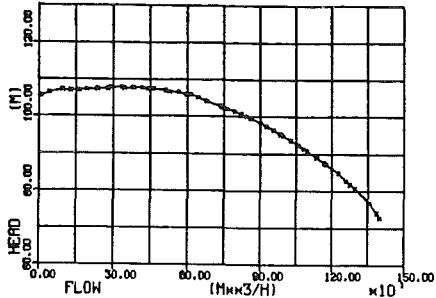


FIG. 1: HEAD - F (FLOW)

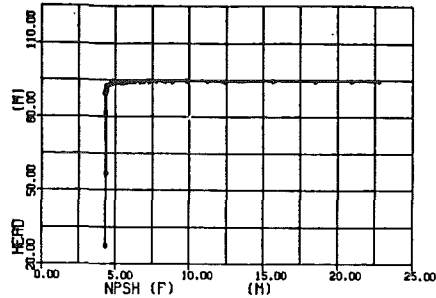


FIG. 5: HEAD - F (NPSH)

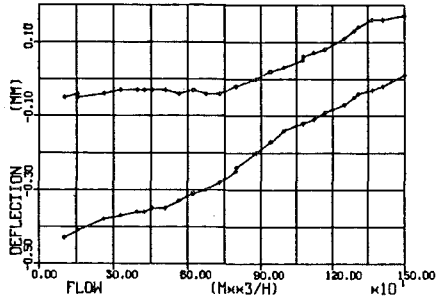


FIG. 2: RAD. DEFLECTION - F (FLOW)

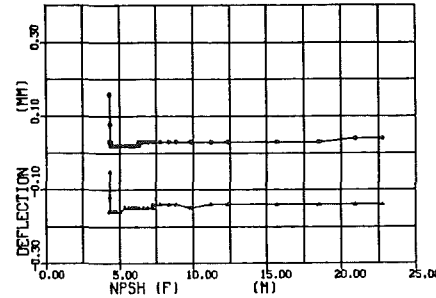


FIG. 6: RAD. DEFLECTION - F (NPSH)

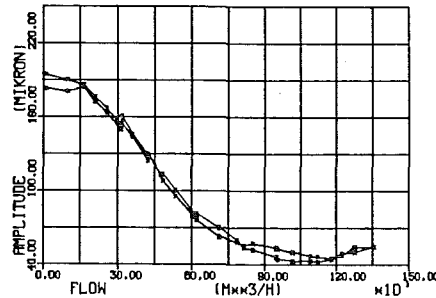


FIG. 3: RAD. AMPLITUDE - F (FLOW)



FIG. 7: RAD. AMPLITUDE - F (NPSH)

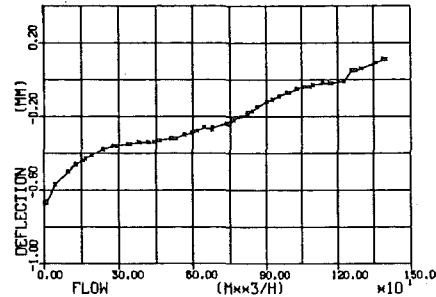


FIG. 4: AXIAL DEFLECTION - F (FLOW)

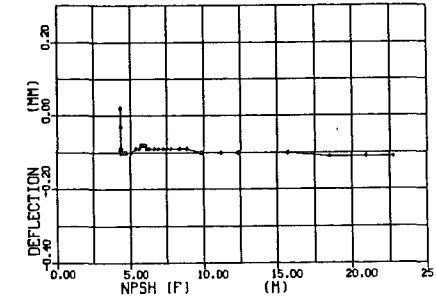


FIG. 8: AXIAL DEFLECTION - F (NPSH)

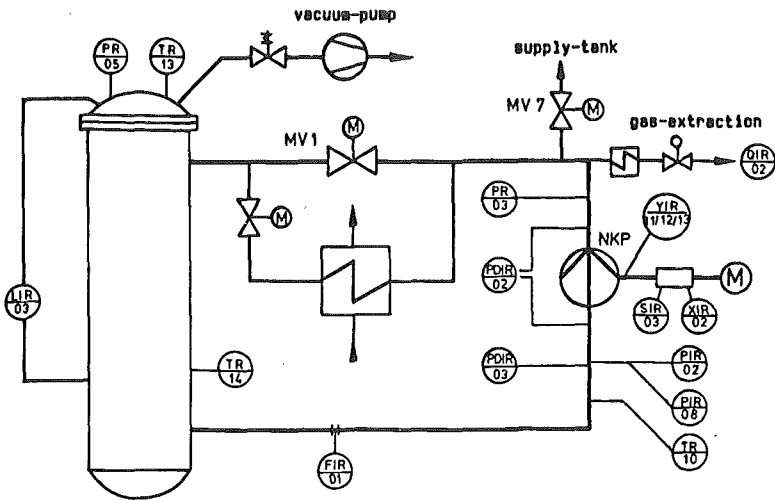


Fig.9: NKP-Test rig with main measuring equipment

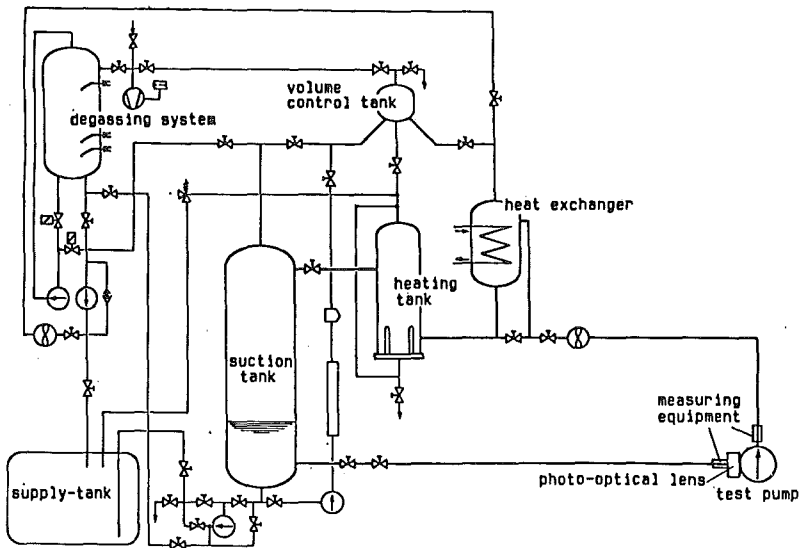


Fig.10: Low pressure glass loop

STEAM GENERATOR TUBE RUPTURE RISK IMPACT ON DESIGN AND  
OPERATION OF FRENCH PWR PLANTS

G. DEPOND, H. SUREAU

ELECTRICITE DE FRANCE  
Service Etudes et Projets  
Thermiques et Nucléaires  
12-14, avenue Dutriévoz  
69628 VILLEURBANNE Cédex

ABSTRACT

The experience of steam generator tube leaks incidents in PWR plants has resulted in an increase of EDF analysis leading to improvements in design and post-accidental operation for new projects and operating plants.

The accident consequences are minimized for each of the NSSS three barriers :

- first barrier : safeguard systems design and operating procedures relying upon core safety allow to maintain a low level of primary radio-activity,
- second barrier : steam generator design and periodic inspection allow to reduce tube ruptures risks,
- third barrier : atmospheric releases are reduced as a result of optimal recovery procedures, detection improvements and atmospheric steam valves design improvements.

INTRODUCTION : STEAM GENERATOR TUBE RUPTURES CONSEQUENCES

The experience of steam generator tube leaks incidents in PWR plants has resulted in an increase of EDF analysis and developments to improve steam generator tube rupture accident treatment. The paper presents this analysis which leads to an evolution in design and post-accidental operations for new projects and operating plants.

The EDF approach can be summarized as follow :

- . a steam generator tube rupture consists of a second and third barrier simultaneous failures resulting in radiological releases of RCS fluid,
- . automatism and safety devices designed to cope with the LOCA are able to maintain clad and core integrity even in the case of multiple tube ruptures,
- . to recover third barrier integrity and to stop the leak, manual intervention is necessary,

. if initial primary activity is low (according to severe operating specifications) and if primary activity remains low during accidental transient (according to emergency procedure relying upon core safety priority) radiological consequences are low and leakage termination delay time has a low contribution to the amount of releases provided steam and not liquid is released to the environment.

Nevertheless too long recovery transient could result in filling up the faulted steam generator and in releasing secondary liquid leading to atmospheric PORV (power-operated relief valve) failure risks. This risk emphasizes the benefit of recovery time minimization and atmospheric PORV design improvements.

#### IMPACT ON DESIGN AND OPERATION

These improvements will mainly apply to nuclear plant project under development (N4 project) but some of them will too be used on operating and starting plants in a near future.

Design and operating procedures are optimised for design basis accident : one tube rupture for operating plants, two tubes rupture for N4 project ; but "beyond the design basis situations" are also investigated in order to mitigate their consequences in any case.

The purpose of the presentation is to show how these improvements succeed in minimizing accident consequences for each of the three barriers :

##### 1) first barrier :

The objective is to minimize primary fluid activity. This can be obtained using the following measures corresponding to :

- safety systems design : high head safety injection pumps maximum outlet pressure is maintained higher than steam valve automatic operating set point ; this choice allows a safe automatic behaviour of NSSS during any kind of LOCA.

- operating guide-lines conception : safety injection operating guideline does not rely upon event diagnosis (steam generator tube rupture diagnosis) but is based on physical states diagnosis (RCS inventory) ; this provides sufficient core cooling in any case.

- complementary instrumentation : water level in reactor vessel for example allows to define more accurate criteria for safety injection termination resulting in leakage termination without reducing safety level.

##### 2) second barrier :

Measures are taken to reduce steam generator tube ruptures risk occurrence :

- steam generator design : selection of tube material, reduction of possible stagnation zones

- secondary water chemistry

- periodic inspection.

3) third barrier :

- Detection :

Existing instrumentation consists of a continuous activity measurement in condenser and of steam generator blowdown-system (one measurement per steam generator) which can detect small leaks (a few liters/hour). Otherwise faisability studies have been performed to set up redundant safety device based on N 16 detection through steam lines ; this additional device could detect lower leaks.

- Post-accidental operating guide-lines :

In the beginning of the accidental transient, core integrity is ensured by automatic safety systems actuation. There is no risk of core uncover, even in case of multiple tubes ruptures, as far as no failure of the faulted steam generator secondary side is taken into account.

Then operator actions must be optimised to mitigate the situation as well as possible. For that purpose, numerous steam generator tube ruptures transients calculations have been performed with EDF's code AXEL (1). This code has a specific modelisation to describe steam generator realistic behaviour ; activity transfers and releases are also calculated by this code, using :

- a global evaluation on RCS

- an evaluation of each volume element of the steam generator secondary side.

Two kinds of hypothesis are used :

Table 1 : Hypothesis used for activity releases calculations

Hypothesis	"Realistic"	Conservative
RCS activity ( $I_{131}$ )	0.06 Ci/t	11 Ci/t
Source increase after scram	$S/S_0 = 500$ (peak of iodine at scram)	$S/S_0 = 1$ (peak of iodine before accident)
Fraction of water exhausted into the atmosphere with steam	1 %	10 %

The optimisation allows to define one or two emergency procedures to cover all possible steam generator tube ruptures situations with following aims :

- a) core safety (safety injection actuation and termination on RCS inventory criteria)
- b) activity releases reduction (faulted steam generator isolation)
- c) leakage termination as quick as possible (by reduction of primary temperature and pressure).

One example of a calculated transient is given figures 1 to 6 : two ruptured tubes without coolant pumps after scram according to the use of single failure criterion (2) :

- scram and safety injection actuation occur automatically nearly 400 s after transient beginning ; important part of the releases (as far as the faulted steam generator is not filled up) occurs at that moment, because turbine steam by-pass is supposed to be unavailable.

- operator intervention takes place 900 s after safety injection actuation : faulted steam generator isolation, opening of its blowdown-system and beginning of RCS cooling, using the other steam generators (56° C/h)

- 2100 s after transient beginning, safety injection termination occurs on RCS inventory criteria (subcooling margin greater than 40° C and pressurizer level greater than 50 %) which leads to leakage termination 2750 s after transient beginning.

In order to be relevant, this steam generator tube ruptures emergency procedure requires a sufficient redundancy level and safety qualification for the steam generator atmospheric PORV, so the non faulted steam generator atmospheric PORV must be available to cool down RCS quickly enough in all situations and the faulted steam generator atmospheric PORV must be available to open and close for steam or/and liquid operating conditions to prevent any failure (PORV stuck open for example).

Table 2 gives mass and activity releases in following cases :

- design basis situations :
  - . class 3 : 1 ruptured tube with blowdown system failure
  - . class 4 : 2 ruptured tubes without coolant pumps
- "beyond design basis situations" :
  - . 10 ruptured tubes
  - . 2 ruptured tubes with a stuck open and not isolated PORV on the faulted steam generator.

Furthermore the following "beyond the design basis situations" steam-line break outside containment without isolation, with multiple steam generator tube ruptures (one to ten ruptured tubes) are studied to define an operating procedure which avoids core uncover and mitigates radioactive releases.



2 SG RUPTURED TUBES WITHOUT COOLANT PUMPS

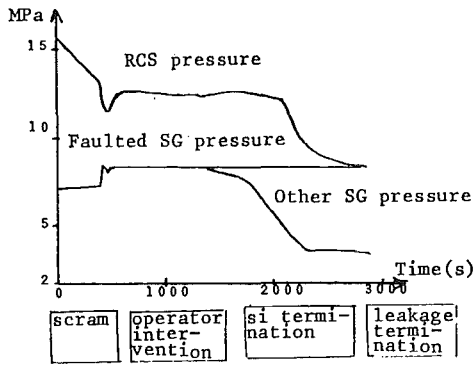


Fig. 1 : RCS and SG pressures

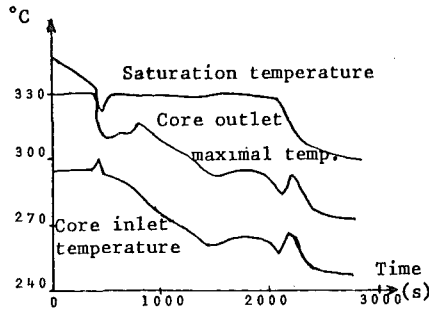


Fig. 2 : RCS temperatures

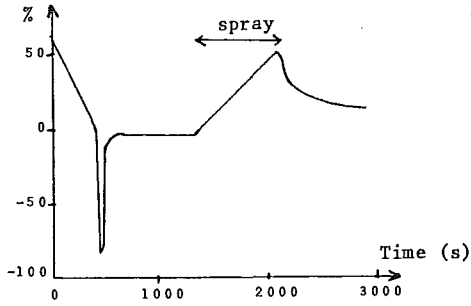


Fig. 3 : Pressurizer level

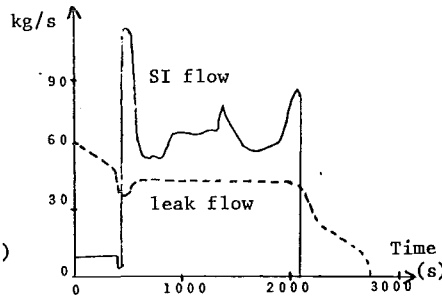


Fig. 4 : HHSI and leak flows

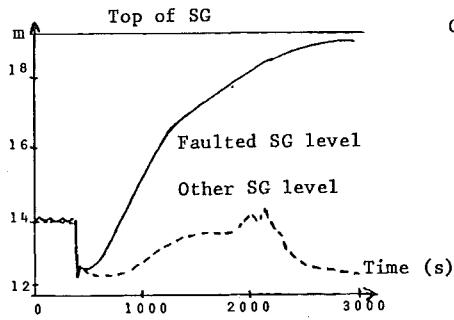


Fig. 5 : SG levels

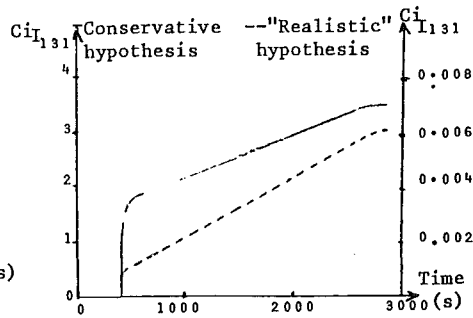


Fig. 6 : Activity releases to the atmosphere

TABLE 2 : S G T R RESULTS

	DESIGN BASIS SITUATIONS		"BEYOND THE DESIGN" BASIS SITUATIONS	
	3rd CLASS	4th CLASS		
	1 tube without blow- down system	2 tubes without coolant pumps	10 tubes	2 tubes with a stuck open PORV
TIME SCRAM(S)	1018	396	55	396
SI TERMINATION(S)	3440	2097	1475	2341
LEAKAGE TERM. (S)	3810	2750	1700	3 h 15 mn
Margin/FSG filled up (m3)	32	5	FSG filled up at 760 s	FSG filled up at 2 h
Mass transfers prim → sec (t)	79	104	188	282
sec → atm (t)	9 steam	9 steam	9 steam 66 liquid	149 steam 33 liquid
Activity transfers with "realistic" hypothesis				
prim → sec ( $C_{i131}$ )	59	71	110	296
sec → atm ( $C_{i131}$ )	0.006	0.006	13.5	47
Dose (rem at thyroid 500 m)	$0.12 \cdot 10^{-3}$	$0.12 \cdot 10^{-3}$	0.27	0.94
Activity transfers with conservative hypothesis				
prim → sec ( $C_{i131}$ )	370	1143		
sec → atm ( $C_{i131}$ )	3.5	3.5		
Dose (rem at thyroid 500 m)	0.07	0.07		

## CONCLUSION

Taking into account all precedent measures and optimal recovery procedures, the consequences of any type of steam generator tube rupture accident fulfill safety requirements concerning activity releases.

- For the design basis situations : a maximum of two ruptured tubes with single failure assumption on all required systems ; the secondary side of the faulted steam generator does not get full during accidental transient, there is only steam discharge to the environment. The dose to the thyroid is evaluated lower than 70 millirem to the maximally exposed individual (at 500 meters from the site) with Final Safety Analysis Report assumptions and lower than 0,1 millirem with more realistic assumptions.

- For "beyond the design basis situations" : more than two ruptured tubes simultaneously or not with a steam break ; it is not possible to avoid filling up the secondary side of the faulted steam generator and liquid discharge to the environment. In these cases the doses are ten to thousand times greater than those calculated for design basis.

## REFERENCES

- [1] Code AXEL - Formulation physique EDF - SEPTEN 1984
- [2] Projet N4 : Rupture de deux et dix tubes de générateur de vapeur EDF - SEPTEN 1984
- [3] Projet N4 : Rupture d'un tube de générateur de vapeur EDF - SEPTEN 1983.

A VALUE/IMPACT ASSESSMENT FOR ALTERNATIVE DECAY HEAT REMOVAL  
SYSTEMS

L. Cave, W.E. Kastenberg and K.Y. Lin  
Mechanical, Aerospace and Nuclear Engineering Department  
University of California, Los Angeles  
Los Angeles, California 90024, USA

ABSTRACT

A Value/Impact assessment for several alternative decay heat removal systems has been carried out using several measures. The assessment is based on an extension of the methodology presented in the Value/Impact Handbook and includes the effects of uncertainty. The assessment was carried out as a function of site population density, existing plant features, and new plant features. Value/Impact measures based on population dose are shown to be sensitive to site, while measures which monetize and aggregate risk are less so. The latter are dominated by on-site costs such as replacement power costs.

INTRODUCTION

A survey of core-melt accidents found in the Reactor Safety Study for Pressurized Water Reactors (PWRs), shows that about 75% of the sequences considered are attributable to loss of the decay heat removal (DHR) function and about 25% to others. More recent probabilistic risk assessments (PRAs) support the general conclusion that loss of DHR is a dominant contributor to core melt frequency for both PWRs and Boiling Water Reactors (BWRs). This result has led to increased interest in the study of alternative decay heat removal systems for various combinations of plant configuration and concepts.

A study of alternative decay heat removal concepts for Light Water Reactors (LWRs) has been conducted by Berry and Sanders [1]. Their results, based on an evaluation of nine alternative DHR concepts, shows that for PWRs an add-on auxiliary feedwater (AFW) train, or an add-on high pressure injection (HPI) feed-and-bleed train are, in general, the most favorable alternatives based on their reduction of core-melt frequency. However, more recent studies have shown that in some cases, correction of a minor design error (e.g. inadequate fire protection of a vital cable route) may achieve a substantial decrease in the probability of core melt.

The main purpose of this paper is to develop a methodology to determine whether or not such improvements in DHR systems as described above, or anticipated in the future, are "cost-effective" with respect to various criteria. Such criteria might include a limit on population dose/dollar spent or a net benefit which is positive. The methodology presented here is based in part on the recently published Value/Impact (V/I) Handbook [2]. It extends the methodology for the treatment of uncertainty, both in the V/I assessment and in the use of the assessment by the decision maker.

Improvements such as alternative DHR systems, which are intended to reduce core melt frequency (and hence risk) fall under the general category of "prevention", rather than "mitigation", wherein improvements are aimed at ameliorating the consequences of core-melt once it has occurred. It should be noted then, that the V/I methodology presented here, as well as the conclusions drawn from the examples treated, have as their focus accident prevention.

#### METHODOLOGY

Value/Impact (V/I) assessment is a general approach used by decision makers as an aid in determining whether or not an action should be undertaken. The Handbook mentioned above lists a number of "decision attributes", i.e. the "values" (or benefits) and the "impacts" (or costs) which can be considered in a V/I assessment. These include public health effects, occupational exposures (routine and accidental), off-site and on-site property damage, regulatory efficiency, improvements in knowledge, industry development and implementation costs, and NRC development and implementation costs. The methods for quantifying these attributes, so that values can be compared with impacts within the DHR context have been proposed by Cave and Kastenbergl [3].

There are two principal methods for displaying the results of a V/I assessment [2]:

1. Ratio Method. In this method the result is presented as the ratio: value/impact. In this context, "value" may be expressed simply in terms of the expected reduction of radiation dose to the public within some specified radius of the plant and impact is the expected cost of the proposed action. This ratio could have mixed units (e.g. person-rem averted/\$M) or if the value were expressed in monetary terms, the resulting ratio would be dimensionless.

2. Net Benefit Method. In this method all attributes are quantified in monetary terms to the extent possible, and if the difference (value minus impact) is positive, there is a net benefit from the proposed action.

In this paper, a third method is introduced:

3. Complex Ratio Method. To the extent possible, all attributes are quantified in monetary terms and the result is presented as the ratio: value/impact. In this context "value" is expressed as the sum of health effects averted and off-site costs averted; on-site costs averted may also be included in the value term. In the regulatory context, there is disagreement over whether or not on-site costs should be included. Pending resolution, these can be treated separately.

The relative advantages and disadvantages of these methods are summarized in the Handbook, but the main ones can be summarized as follows:

1. In its simplest form, the ratio method has the major advantage that it can be compared with some "decision value", (e.g. \$1,000/ person-rem averted, or 1,000 person-rem averted per \$ M) to provide a perspective on the action. It has the disadvantage that only one form of the "value attribute" can be accommodated in the numerator. Thus, a benefit such as the monetary value of an averted accident has to be treated as a negative cost, or the population dose has to be considered a surrogate for all benefits.

2. The net-benefit method has the advantage that any attribute which can be expressed in monetary terms can be introduced. Because the net-benefit may be the difference between two large and nearly equal numbers, each subject to large uncertainty, presentation of uncertainties in the overall result requires special consideration. This is developed in the next section.

3. The complex ratio method has the same advantages as the net-benefit method. When the uncertainty is given by log-normal distributions, it is easy to express the uncertainty in simple terms.

Two other points should be noted. First, population dose and latent (cancer) fatalities are related and would be considered "double counting" if both attributes were considered in the same equation. Second, none of the numerical values obtained by the three methods should be used as the sole basis for regulatory decision making. These, along with other considerations such as uncertainty, unquantifiable attributes and other "engineering" and "societal" judgments should be used in arriving at a decision.

#### UNCERTAINTIES

As noted above, the presence of potentially large uncertainties in the various attributes must be taken into account by the decision maker. These uncertainties fall into three broad classes:

Class 1. Systematic errors, due to lack of agreement as to the most appropriate value for a specific parameter, e.g. the monetary value which should be placed on a latent cancer death averted.

Class 2. Systematic errors due to the difficulty in quantifying some of the values and or impacts (e.g. the time, mode and location of containment failure).

Class 3. Random errors, due to the statistical nature of the data, (e.g. failure rate data).

Class 1 uncertainties are best treated by a sensitivity analysis, while those of Class 3 can be handled statistically if there is sufficient data, or subjectively, to establish bounding values. Class 2 are the most difficult (defined as "unquantified residuals" in the Handbook), and can have a profound effect on any value-impact margin. It is these unquantified residuals which are considered further in this paper.

The impact or cost term has five major components, 1) capital expenditure, 2) replacement power during modification, 3) health costs incurred during modification, 4) changes in operating costs as a result of the modification and 5) changes in operating health costs as a result of the modification. Items 1-3 must be positive, but items 4 and 5 could be negative. Items 1,2 and 4 can be calculated directly in dollars, while for decision making, items 3) and 5) are usually given as \$1,000/ man-rem (occupational). As shown in Reference [3], the uncertainty in the impact term can be represented by an error factor of about 3 if the underlying distribution is regarded as log-normal, provided the costs are estimated on a plant specific basis.

The value or benefit term has several major components, depending upon the attribute considered. On-site costs averted are a function of initial and improved core-melt frequency, the present worth of the capital investment (which includes replacement power costs) and the accident clean-up costs. As shown in Reference [3], an error factor of about 6 would result if a log-normal distribution were assumed.

Off-site costs averted are a function of initial and improved core-melt frequency, containment failure, fission product behavior (pre-and post-containment failure), evacuation, interdiction and decontamination procedures, dose-response relationships, and dollar costs of medical treatment. Public health effects averted (population dose and/or early and latent deaths) are closely related to off-site costs because they depend on nearly the same

functions. There are however, several other important considerations. Most PRAs employ the CRAC computer code to determine both off-site economic and public health risks. In particular, the population dose and the latent cancer deaths are attributable to doses received from radioactive fall-out on the ground. Most calculations assume a 25 REM or less whole body dose over 30 years following interdiction; i.e. all land producing a dose greater than 25 REM will be interdicted. If this cutoff dose is lowered, interdiction costs go up and health effects go down; and conversely, if this dose is raised, interdiction costs go down and health effects increase. Hence the value of this interdiction dose can also have a profound effect on the value/impact margin. In a sense, interdiction (and for that matter decontamination) is a form of mitigation, and hence a "preemptive" decision has been made with respect to the value term.

For the illustrative purpose of this paper, it is assumed that the error factor is the same for off-site costs and health effects, and is assumed to have an error factor ranging between 30 and 100, using a lognormal distribution. To account for uncertainty, point or best estimate values can be used to determine the initial ratio or net benefit. Uncertainty is then included in the following way. Based on the discussion above, uncertainty in the "impact" or cost term is so small relative to that in the "value" term that it can be considered a point or best estimate value. The "value" on the other hand, is considered distributed. The risk at the C-th confidence level  $R_i^C$ , is defined by:

$$C \equiv \int_0^{R_i^C} p(R_i) dR_i = P_r(R_i < R_i^C) \quad (1)$$

In this definition,  $R_i$  is a random variable,  $p(R_i)$  is a density distribution function. The subscript  $i$  denotes the consequence of interest (e.g. early death, person-rem, etc.).  $C$  is then the probability that the expected risk is less than  $R_i^C$ .

The "value" or benefit can also be expressed in similar terms:

$$P_r(V < V^C) \equiv \int_0^{V^C} p(v) dv \quad (2)$$

where  $V$  is the total benefit in terms of  $\Delta R_i$ , and each change in risk is expressed in equivalent dollars (e.g. \$1000/person-rem, or \$1M/acute fatality averted, etc.).

If the total "impact" or cost is  $C_0$ , and  $L$  the "effective" remaining life of the plant (e.g. may or may not include discounting, present worth, etc.) then the probability there is a net benefit given by:

$$P_r(V > C_0/L) \equiv \int_{C_0/L}^{\infty} p(v) dv \quad (3)$$

Equation (3) is particularly useful when the point estimates  $V_0$  and  $C_0/L$  are close together. In practice, when  $V_0$  is small (because the initial best estimate risk  $R_0$  is small or  $\Delta R$  is small) and  $C_0/L$  is small,  $P_r$  tends to be large because the upper confidence level risk (say  $R_i^{95}$ ) is large (the tail

effect). Conversely, when  $V_0$  and  $C_0/L$  are large,  $P_r$  tends to be small because there tends to be an upper cut-off on risk and hence risk reduction. That is, according to Strip [4], on-site costs tend to dominate, are less uncertain, and are limited in dollar cost.

#### EXAMPLES

As an example of the methodology presented above, an analysis was performed for three different power plant configurations, on three population sites [5]. The first was a model of the 886 MWe Unit 3 Oconee Plant, with two steam generators and four generator loops. The Oconee plant is unique in that it has a three train AC dependent AFWs and a High Head Auxiliary Service System (HHASWS) with its own AC and DC power supplies, to remove residual heat from the steam generators following a plant trip. Other unique features of the Oconee No. 3 Unit include (a) emergency on-site AC hydro-power generators, and (b) feed-and-bleed capability. The system would remove decay heat by a process of direct injection of cool water (i.e. feed) into the reactor coolant system, and remove the hot water (i.e. bleed) from the reactor coolant system via pressurizer relief valves.

To perform a value assessment for a less reliable PWR, the Oconee model was first reconfigured to incorporate several Crystal River features while retaining the ability to feed and bleed. The three trains for auxiliary feedwater were reduced to two trains and the HHASWS was eliminated. The Oconee hydrogenerators were also replaced by two trains of diesel electrical power. This is the second plant configuration (i.e. Crystal River Simulation). The feed-and-bleed capability of the second configuration was then removed to provide the third PWR plant configuration.

In the examples, the Oconee model and two simulations of the Crystal River Power Plant (with or without feed-and-bleed capability) are provided with "perfect" (failure proof) AFW systems or HPI systems. A further analysis for Crystal River (without feed-and-bleed) using estimated unavailabilities [1,5] for both add-on systems are done as the fourth example. The data used in the examples is given by Lin [5], system costs and reductions in core melt frequencies are given by Berry and Sanders [1], and financial data by Strip [4].

Table I shows the ratio of system: cost to man-rem averted for the high and low population sites, which can be compared to the \$1000/man-rem averted criterion. Table II compares this ratio to the complex ratio: system cost/monetized benefit, which can be compared to unity. There is "net benefit" when Ratio 1 is less than \$1000/man-rem and Ratio 2 is less than 1.

Table I shows several interesting trends. For the cases where it can be demonstrated that the plants have feed-and-bleed capability, none of the improved decay heat removal fixes are cost effective using the \$1,000/man-rem criterion. Where feed-and-bleed cannot be demonstrated, both improved decay heat removal systems are cost effective at the high population site, but not on the low population site (when using the \$1,000/man-rem criterion).

Table II confirms the results above when examining the effect of feed-and-bleed capability, i.e. with this capability neither ratio gives a cost effective result. The results are different however, for the case without feed and bleed capability. At the low population site, Ratio 2 (system costs/monetized benefit) gives a cost effective result because it includes on-site costs averted.

Table III shows the probability that the value exceeds the impact for the Crystal River Simulation, with add-on AFW train, and with and without feed-and-bleed. The cases without feed-and-bleed capability, show a high confidence (above 75%) that value exceeds benefit, while those with feed-and-bleed capability show a low confidence (less than 5%). Hence the results shown in Table III



confirm those in Table II for Ratio 2. This is not necessarily the case for Ratio 1, because on-site costs are particularly dominant at low population sites.

#### CONCLUSIONS

Using an extension of the methodology presented in the Value/Impact Handbook [2], an assessment of alternative decay heat removal systems was presented. The results were presented by two ratios:

Ratio 1: System Cost (dollars)/population dose averted (man-rem).

Ratio 2: System Cost (dollars)/total risk averted (equivalent dollars).

and supplemented with  $P_r(V > I)$ , the probability that the value exceeds the impact, where value is treated as total risk averted (equivalent dollars).

It was found that Ratio 1 is sensitive to population density. Ratio 2 is somewhat independent of population because on-site costs are less sensitive to plant site. Note that system add-on costs include replacement power costs during an installation outage. Under the conditions of summary evacuation and man-rem averted in a 50 mile radius the following conclusions can be drawn:

(1) For those cases which have feed-and-bleed capability to begin with, neither of the cost/benefit criteria are satisfied.

(2) For those cases where there is no feed-and-bleed capability to begin with, both cost benefit ratios are satisfied.

Two considerations are important in drawing general conclusions from this work:

(a) These examples are given for the Crystal River Plant on three sites (high, medium and low population). The Crystal River Plant simulation has a high core melt frequency to begin with. Hence the benefit in terms of risk averted/year will be larger than for most plants.

(b) The work presented here is based on the WASH-1400 release categories and source terms. As term data becomes available, these measures will change in value.

Several important insights beyond those considered in the Value/Impact Handbook were gained in this study. Because of the controversy focused on the inclusion of on-site costs averted, they can be treated separately when using the complex ratio method. Secondly, there is an important need to recognize the inter-relationship between interdiction policy, population dose and off-site costs (interdiction and decontamination). The extensions presented in this paper include these considerations.

#### REFERENCES

1. D.L. Berry and G.A. Sanders, "Study of the Value and Impact of Alternative Decay Heat Removal Concepts for LWRs", SAND 82-1796, NUREG/CR 2883, 1982.
2. S.W. Heaberlin, et. al. "A Handbook for Value-Impact Assessment", PNL-4646, NUREG/CR 3568, 1983.
3. L. Cave and W.E. Kastenber, "Guidelines for the Conduct of Value/Impact Assessment for Task Action Plan A-45", UCLA Report to appear.

4. D. Strip, "Estimates of the Financial Risks of Nuclear Power Reactor Accidents", SAND 82-1110, NUREG/CR 2723, 1982.
5. K.Y. Lin, "Quantitative Value-Impact Measures Evaluating Improvements in Decay Heat Removal Systems", M.S. Thesis in Engineering, UCLA December, 1983.

TABLE I

Impact/Value Ratio Based on Dollars per Man-rem Averted out to 50 miles.

Item	Add-on Feed-and-Bleed with Small LOCA Makeup Capability		Add-on AFW Train With Small LOCA Makeup Capability	
	\$ 78.35 x 10 <sup>6</sup>		\$87.81 x 10 <sup>6</sup>	
Population	HIGH	LOW	HIGH	LOW
Oconee Model	\$ 2800/man-rem	\$ 140,000/man-rem	\$ 4000/man-rem	\$ 200,000/man-rem
Crystal River Simulation (w. Feed-&-Bleed)	\$ 1100/man-rem	\$ 53,000/man-rem	\$ 1300/man-rem	\$ 65,000/man-rem
Crystal River Simulation (w/o Feed-&-Bleed)	\$ 39/man-rem	\$ 2,000/man-rem	\$ 46/man-rem	\$ 2,300/man-rem
Crystal River Simulation (w/o F-&-B) real case	\$ 42/man-rem	\$ 2,100/man-rem	\$ 48/man-rem	\$ 2,400/man-rem

TABLE II

Impact/Value Ratios For Crystal River Simulation  
Add-on AFW Train with Small LOCA  
Makeup Capability

Population	with Feed and Bleed			without Feed and Bleed		
	HIGH	MED	LOW	HIGH	MEDIUM	LOW
Ratio 1	1,300	12,000	65,000	46	410	2,300
Ratio 2	6.3	15	15	0.22	0.51	0.53

Ratio 1 = system costs/man-rem averted in \$/man-rem averted

Ratio 2 = system costs/monitized benefit in \$/\$

monitized benefit = early death + latent death + onsite  
cost + offsite cost

TABLE III

Probability that Value Exceeds Impact  
Add-on AFW Train with Small  
LOCA Makeup Capability  
Crystal River Simulation

Population	with Feed and Bleed			without Feed and Bleed		
	HIGH	MED	LOW	HIGH	MED	LOW
$P_r(V > I)^*$	0.05	0.006	0.005	0.96	0.77	0.75

\* based on log-normal distribution

## COST BENEFIT ANALYSIS OF REACTOR SAFETY SYSTEMS

by H.A. Maurer

Commission of the European Communities, Brussels

## ABSTRACT

Cost/benefit analysis of reactor safety systems is a possibility appropriate to deal with reactor safety. The Commission of the European Communities supported a study on the cost-benefit or cost effectiveness of safety systems installed in modern PWR nuclear power plants. The following systems and their cooperation in emergency cases were in particular investigated in this study:

- the containment system (double containment)
- the leakage exhaust and control system
- the annulus release exhaust system and
- the containment spray system.

The benefit of a safety system is defined according to its contribution to the reduction of the radiological consequences for the environment after a loss-of-coolant accident.

The analysis is so far performed in two different steps:

- the emergency core cooling system is considered to function properly
- failure of the emergency core cooling system is assumed (with the possible consequence of core melt-down).

It is envisaged to investigate later the optimization of design and cooperation of reactor safety systems.

The results may demonstrate the evidence that striving for cost-effectiveness can produce a safer end result than the philosophy of safety at any cost.

## INTRODUCTION

To guarantee safe operation of nuclear power plants regardless of costs is a philosophy which was followed in the past at least in European countries by almost all safety organisations. But since the installation of reactor safety systems amounts to almost 10 % of the total construction costs of a nuclear power plant, it is evident that this money should be spent in the construction and improvement of those systems which are most effective in the reduction of radioactive releases during normal operation and in accident situations.

The philosophy of ALARA - as low as reasonably achievable - (as far as the radioactive releases are concerned) is another possibility appropriate to deal with reactor safety. If, consequently, we cannot longer follow the philosophy of safety at any cost, should ALARA dominate and what is reasonably achievable? The study tries to answer this question.

The safety systems of European nuclear power plants (and in particular of PWR plants) are of different design (e.g. single or double containment; with or without containment spray system; with or without concrete protection of primary system etc.) and the safety assessment of nuclear power plants is performed differently according to different national criteria.

In the course of this study it became obvious that different criteria based on different philosophies may have led to different designs.

In view of a possible harmonization of the already existing national criteria and in view of a possible optimization in the design of the different safety systems and their cooperation in emergency cases it was investigated under study contract by the Commission of the European Communities how the different safety systems contribute to the overall safety of the plant and at which costs.

The basis for the cost/benefit analysis of the safety systems of nuclear power plants is a PWR plant of 1300 MWe. Methodology and application of a cost-benefit analysis are demonstrated by a loss-of-coolant accident with the emergency core cooling functioning as an example. In order to compare the benefit of different safety systems, the dimension of the environmental pollutions was chosen to be the quantity of air necessary to dilute a released quantity of nuclides to concentrations permitted according to radiation protection regulations. The quantities of air necessary for several classes of a loss-of-coolant accident were calculated with the help of a computer programme. After determination of benefit and expenses for different systems of the containment a cost/benefit analysis is made. The results allow a judgement on the counterbalance of safety systems by comparing the remaining risks of different systems with the benefit of others. Thus the methodology given offers the possibility to develop bases to decide on the harmonization of safety requirements in the EC member countries.

#### BASIC CONSIDERATIONS

The following systems and their cooperation in emergency cases were investigated in the study:

- the containment system (double containment)
- the leakage exhaust and control system
- the annulus release exhaust system and
- the containment spray system.

In order to simplify the analysis and to avoid in a first step of the analysis the discussion on possible core melt-down, the emergency core cooling system was considered to function properly (an assumption which could possibly no longer be accepted after the Harrisburg experience and which was revised in the following steps of the analysis).

The basic data of design and costs were derived from a 1300 MWe PWR plant of German design. The benefit of a safety system is defined according to its contribution to the reduction of the radiological consequences for the environment after a loss-of-coolant accident. In the results the benefit is expressed in m<sup>3</sup> air necessary to reduce the radioactive releases below the allowable limits.

---

\* the study was performed by LAHMEYER International, Francfort in cooperation with Professor Röper, Technical University of Aachen.

The reliability data were first based on the report WASH 1400 (Rasmussen report) and in a later stage of the analysis the German Risk study was considered. Possibly it would have been simpler to express the benefit in reduction of Ci released but it was the intention to avoid extensive discussion on human effects.

In general, reactor safety systems are installed to reduce the risk of an accident and its consequences to an acceptable level. For a certain accident (x) the risk  $R_i(x)$  is described by the following equation under the condition that a safety system is available:

$$R_i(x) = (S_i(x) \cdot NV_i(x) + So_i(x) \cdot (1 - NV_i(x))) \cdot W(x)$$

when

- $S_i(x)$  = environmental pollution after an accident (x) when the safety system is out of operation  
 $So_i(x)$  = environmental pollution after an accident (x) when the safety system is operating  
 $NV_i(x)$  = non availability of the safety system i after an accident (x)  
 $W(x)$  = probability of the occurrence of an accident (x).

The benefit of a reactor safety system  $N_i$  is the sum of the differences in accident risks with or without safety systems installed (or operating) in the power plant.

$$\begin{aligned} N_i &= \sum^X (S_i^*(x) \cdot W(x) - R_i(x)) \quad \left[ \frac{m^3}{a} \right] \\ &= \sum^X (S_i(x) - So_i(x)) \underbrace{(1 - NV_i(x))}_{\approx 1} W(x) \end{aligned}$$

when

- $S_i^*$  = environmental pollution after accident (x) when a safety system is not available.

In a first approximation it can be considered that the availability of a safety system equals 1 that means  $(1 - NV_i(x)) \approx 1$ .

The benefit/cost relationship  $M_i = N_i / K_i \cdot \left[ \frac{m^3/a}{DM} \right]$

This means the quantity of air per year not required for delution by the effect of 1 DM invested in a safety system.

#### FIRST INVESTIGATION (ECCS FUNCTIONS PROPERLY)

On the basis of these general considerations the cost/benefit relationship of the four different safety systems were evaluated and the following results obtained:

TABLE I. COST BENEFIT OF REACTOR SAFETY SYSTEMS  
(ECCS FUNCTIONING)

System	Installation costs $K_i$ E6 DM	benefit $N_i$ $m^3/a$	cost benefit $M_i$ $\frac{m^3/a}{DM}$
containment system	35,0	1,24 E14	3,5 E6
leakage exhaust and control system	0,55	5,17 E8	9,4 E2
annulus release exhaust system	0,65	1,04 E9	1,6 E3
containment spray system	0,6	3,09 E7	5,2 E1

COST BENEFIT ANALYSIS, SECOND INVESTIGATION  
(ECCS FAILS TO OPERATE)

This second step of the investigation considers core melt-down. The two accidents of core melt-down examined are described by the following events.

Accident of core melt-down 1:

- important leakage in the main coolant pipe
- high pressure and low pressure injection systems are functioning
- switch to sump operation fails.

Accident of core melt-down 2:

- important leakage in the main coolant pipe
- high pressure injection functioning
- failure of low pressure injection.

By accident of core melt-down 1 all accident sequences with failing of prolonged heat removal and by accident of core melt-down 2 those with failing of active safety systems are covered.

It is assumed that with these events accidents of core melt-down will happen unavoidably.

After loss-of-coolant accidents the containment is the last tight barrier to the environment for the activity enclosed. Under the assumption of this study, this barrier will be, in any case, destroyed in accidents of core melt-down if it does not fail by itself. The two in principle possible failures are consequently:

1. Failure of the inclusive function when the containment is charged within design values.
2. Destruction of the containment by events for which it is not designed (failure by overpressure).

In the present study the malfunction of the containment with a leakage of 300 mm diameter was described as well as failure by overpressure with a leakage of 1 m<sup>2</sup> (e.g. steam explosion).



The diagram of event sequences (fig. 1) contains in the upper half the loss-of-coolant accident under control with containment failure. In the lower half the event sequences of core melt-down can be found the beginning of which is always failure of emergency core cooling.

In spite of the fact that in most cases failure of emergency core cooling has as a consequence failure of the containment, a branch is foreseen in the event sequence diagram which means malfunction of the containment.

After failure of the containment the inefficacy of other systems within the containment is assumed in a conservative way. The activity in the reactor core was calculated on the basis of an average highest burn-up of 33 500 MWd/t for 54 nuclides which are combined to seven groups in the beginning and to three groups considering deposition.

The accident sequences are essentially fixed by input data. In order to determine the benefit of the systems in the containment several sequences of each accident are investigated which are the result of combination of correct functioning of these systems.

A special position has to be assigned to the containment since already for the accident sequences a difference is made whether the containment fails by malfunction or by excessive demand.

Is there imperfection of the containment in the beginning of an accident, the difference of combinations of correct functioning can be dropped since the inefficacy of the other systems of the containment must be taken for granted.

Activities released during accident sequences will be diluted to the limit value for activity inhalation per year according to the Regulations for Radiation Protection and the quantity of air necessary represents, as it was defined, the damage caused by this nuclide. By summation of the quantity of air of all nuclides considered finally the damage of the sequence which is examined can be defined.

These influences are most evident for the example of the spray system. In the beginning phase of core melt-down activity in the containment is biggest so that a spray system is very efficient for the decreasing of activity. It has to be considered most effective for the accident sequence which is most frequent, failure by overpressure of the containment after about one day.

Conservative assumptions with regard to source terms of the activity may give the impression of a bigger benefit of the retaining systems since these systems, when functioning, keep away from the environment more activity.

Conservative assumptions as regards the sequence in time of accidents are essentially equivalent to an earlier failure of the containment by overpressure. They herewith curtail the benefit of the containment.

On the contrary the benefit of the spray system increases in a shorter period of time since the reduction of activity in the containment atmosphere by a spray system during the early failure of the containment is more effective than during a late failure.

In order to avoid erroneous estimation of the cost/benefit relationship of systems all conservative assumptions are to be replaced by "best-estimate" calculations.

RESULTS OF THE COST BENEFIT ANALYSIS  
(ECCS FAILS TO OPERATE)

The most important benefit is gained by the containment, followed by the leakage retention system. Evidently, the results would have been different for a single containment where especially the annulus release exhaust system is inexistent and the spray system therefore differently designed.

When the benefits are compared to the installation costs of the different safety systems a cost/benefit relationship can be deduced.

The study arrived at the following results indicating the benefit gained in relation to 1 DM of installation costs. (The benefit is expressed in m<sup>3</sup> of air volume to reduce the activity release to the allowable limit):

TABLE II. COST BENEFIT OF REACTOR SAFETY SYSTEMS  
(ECCS FAILING)

System	Installation costs * E6 DM	benefit in m <sup>3</sup> /a	cost/benefit m <sup>3</sup> /a DM
containment system	35,0	1,2 E14	3,4 E6
leakage exhaust and control system	0,55	6,2 E9	1,1 E4
annulus release exhaust system	0,65	3,4 E9	5,2 E3
containment spray system	0,60	2,4 E11	4,0 E5

\* on the basis of the costs in 1976.

Compared to the first analysis (emergency core cooling system functions properly) the most important difference concerns the benefit of the containment spray system. According to the calculation the cost/benefit relationship of this system was improved by several orders of magnitude. (M<sub>i</sub> = 5,1 E1 resp. 4,0 E5).

The methodology used allows to quantify

- the technological importance of a safety system judged according to the benefit for the environment
- the order of priority of necessary investments for different safety systems judged according to cost/benefit relationship.

The expenses to be made are less variable than the benefit, therefore, the benefit in most cases lays down the order of priority for the relation cost/benefit.

Another important information to make evident the relationship between a better benefit and the means used is given by the possibilities of still existing improvements to reduce the remaining risk by a certain system.

These remaining possibilities of benefit as to the retaining of radioactive material are twofold:

- the possibility of damage due to permeability of the containment
- the possibility of damage due to non-availability of safety systems in case of demand.

Technological safety can be considered in balance if the remaining risk of systems with high benefit is not bigger than the benefit of other systems.

The relationship cost/benefit of the considered systems depends always on the choice of accident and incident sequences. By considering accidents of core melt-down this relationship was displaced. The benefit per DM invested is several hundred times bigger for the containment than for the leakage exhaust system and the annulus exhaust system. The cost/benefit relationship of the spray system is one order of magnitude smaller than that of the containment.

#### ENVISAGED INVESTIGATIONS

The study is continued in order to supplement the static analysis - analysis of the different systems without any technical modification - by a dynamic analysis. This means comparison of modified safety systems in order to

1. investigate whether and to what extent the individual components of the safety systems can be modified to decrease the installation costs by increasing at the same time the system effectiveness, and
2. investigate whether and to what extent the safety systems can be substituted or are complementary to each other.

This leads to the application of marginal analysis which may finally answer the question whether it is possible to define the point at which the design of a safety device has attained a cost/benefit level at which any additional measure would only constitute a negligible additional benefit, or even, going above an optimum design, a negative benefit could be the result.

The total utility of safety devices and the increased benefit derived from an additional investment unit can therefore be examined. Conversely, it is also possible to determine the decrease in benefit resulting from a reduction of investment on safety by one unit.

An economist or theorist, however, could also ask whether variation of the different systems or their components would produce more favourable combinations. Assuming, for simplicity's sake, that only devices A and B exist, is it possible that an enlargement of device A and a reduction of device B would produce the same total utility at a lower cost?

In this context, total utility must be regarded as equivalent with the design, since no more than the permissible radioactivity must escape from the containment. Optimum plant design is attained when the relationship between marginal cost is equivalent in devices A and B.

The benefit derived from a safety device can also be regarded as the yield from the amount of money invested. This proposition can be clarified by assuming that there are only two safety devices.

The "quantities" of safety devices  $i_1$  and  $i_2$  are plotted on the axis of figure 2. The isoquants shown ( $R_1, R_2, R_3$ ) are the geometric location of the combinations which produce the same benefits or the same yield. Each isoquant corresponds to a certain benefit or yield level, in this case a certain residual risk exists, where  $R_3 < R_2$  and  $R_2 < R_1$ .

A reduction in radioactivity released during a malfunction could also be regarded as a yield.

A certain required safety level, to be attained at the lowest possible cost, is a given factor. The costs per "quantity unit" employed in the individual safety devices are designated  $k_1, k_2$ .

The following considerations are relevant to derivation of the minimum cost combination at a given safety level:

$$K_{tot.} = k_1 \times i_1 + k_2 \times i_2.$$

If, for example, all available resources are utilized for safety device 1,  $i_2 = 0$ , and  $i_1 = \frac{K_{tot.}}{k_1}$ . The ratio  $\frac{\Delta k_2}{\Delta k_1}$  determines the curve of the isocost

lines. Fig. 2 shows that a large number of parallel isocost lines are produced for alternative  $K_{tot.}$

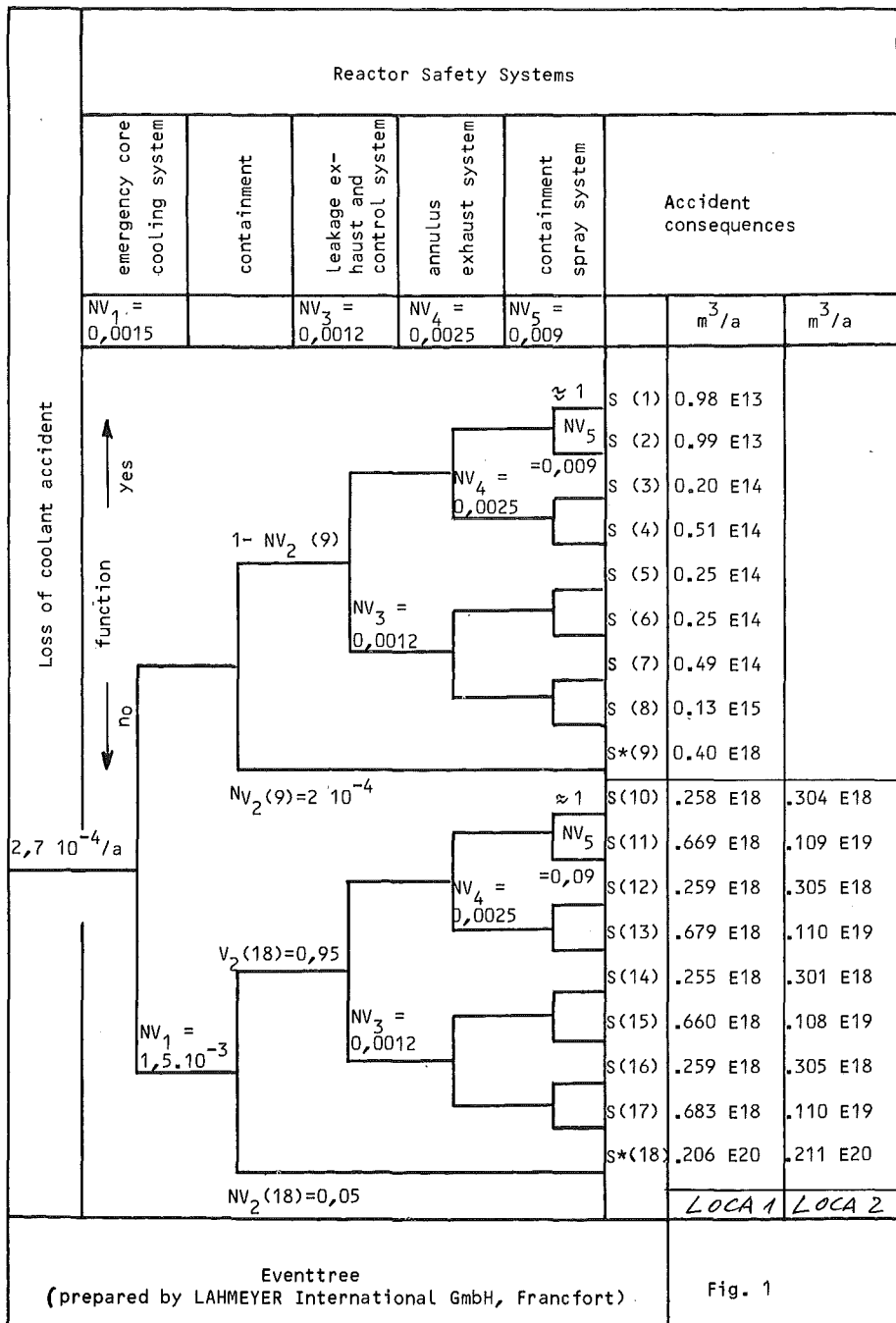
In the case of various total sums,  $K_{tot. 1}, K_{tot. 2}$  and  $K_{tot. 3}$ , the maximum possible yield is always obtained where the isocost line is tangential with an isoquant.

This tangential point can be interpreted in two ways:

1. At the tangential point a maximum degree of safety is obtained for a given budget, or
2. At the tangential point a target (predetermined) safety level is obtained at a minimum cost.

The second aspect is relevant to the present study since certain safety requirements, e.g. those laid down by law, must be met at the lowest possible cost.

The results of this envisaged investigation may demonstrate the evidence that striving for cost-effectiveness can lead to more efficiency of safety systems than the philosophy of safety at any cost.



Eventtree  
(prepared by LAHMEYER International GmbH, Francfort)

Fig. 1

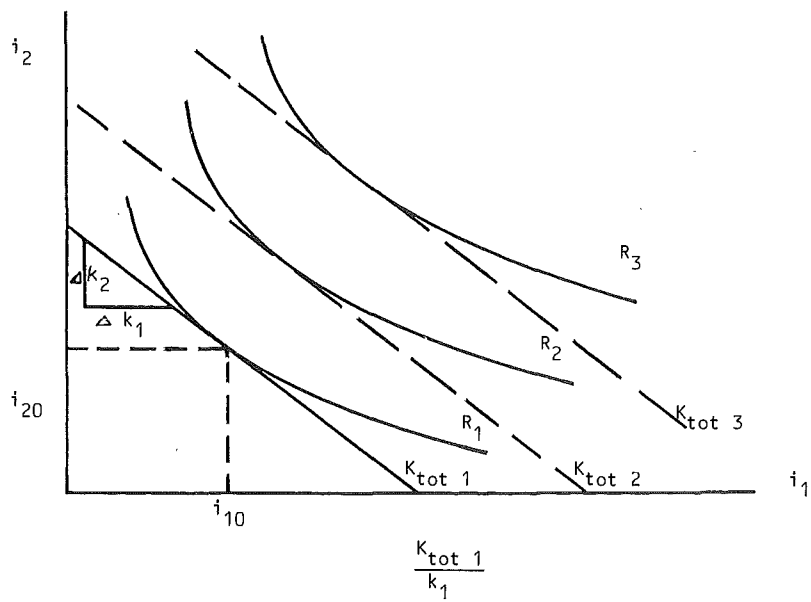


Fig. 2: Isoquants and isocost lines.

## SAFETY ASSESSMENT FROM STUDIES OF LWR'S BURNING PLUTONIUM FUEL

A. Renard\*, R. Holzer\*\*, J. Basselier\*, K. Hnilica\*\*, Cl. Vandenberg\*

\*BELGONUCLEAIRE (Brussels) - \*\*N.I.S. (Hanau)

## ABSTRACT

The introduction of mixed-oxide fuel assemblies was theoretically studied for seven light water reactors by several contributors. A synthesis of typical accident studies is presented including the comparative investigations of the reactor behaviour under the dynamic conditions for Rod Cluster Control Ejection and Steam Line Break in PWR and rod drop accident, main heat sink failure, mass flow transient and LOCA-heatup phase in BWR. The reactor fuelled only with Uranium is taken as the reference. The studies were performed under CEC contracts and connected with a steady-state physical parameter research.

Trends and general conclusions are deduced. The recycling of 30 % of mixed-oxide fuel in large LWR cores should not induce special safety problems nor system modifications when some cautions are taken in loading patterns.

## 1. INTRODUCTION

Theoretical studies were performed on the control and safety of LWR's burning Plutonium fuel by several contributors under contracts with the Commission of the European Communities (CEC) in the frame of a programme on "Pu recycle in LWR", and followed by a synthesis of the results. The comparative investigations for a selection of typical accidents refer to the reactors BIBLIS-B, BUGEY-2, TIHANGE-1, TRINO VERCELLESE, in five PWR studies (KWU, UKAEA, CEA/EdF, BELGONUCLEAIRE, CNEN/ENEL) and to the reactors KKI (ISAR), GARIGLIANO and CAORSO in BWR studies from two contributors (KWU, CNEN/ENEL). For each, the same reactor fuelled with Uranium assemblies only is taken as the standard reference. The dynamic analyses are connected with a steady-state analysis including research on reload strategy and physics characteristics, namely core power peaking, reactivity coefficients, control rod worth, reactivity balance, kinetic parameters [1]. In all cases, equilibrium (or near to equilibrium) cores have been defined for U and MOX fuel loading.

The accident analyses use various levels of sophistication for the whole plant and core modelling as well as in the computing methods. The philosophy of analysis is either a "best estimate" or a conservative approach, and sometimes a mixed one. A comparison and a synthesis of the detailed results are given in [1]; essential trends are deduced here.

## 2. PWR ACCIDENT SITUATIONS

The considered accidents are a rod cluster control ejection (RCCE) and a steam line break (SLB). Table 1 gives for each reference plant and both accidents, the name of the computer codes used and the conditions of the investigated cores. The fraction of core with mixed-oxide assemblies (MOX) is included between 30 % (P30) and 100 % (P100) and a range of critical initial conditions is adopted, so that general conclusions can be obtained from the set of results.

### 2.1. Rod Cluster Control Ejection

As the most reactive control rod to be ejected is not necessarily located at core centre, a fitting of the geometrical model and of the assumptions is generally needed to simulate the real situation with symmetry conditions reducing computer storage space or cost.

The large hot channel factors around the ejected rod and the important flux redistribution during the transient are obviously better simulated with 3D or 2D-space-dependent-kinetics models.

A wide spectrum of initial conditions is represented, being justified on the basis of pessimistic data or results for what concerns the power excursion severity, or the smaller delayed neutron fraction, or the maximum rod worth, or the maximum clad transient temperature, and its higher probability.

The time needed for a complete ejection of a fully inserted rod is assumed to be 0.1 second at constant velocity (as prescribed in the NRC Regulatory Guide 1.77) ; one "best estimate" case considers a total ejection in 0.23 s under constant pressure.

Fig. 1 gives the maximum relative power (P/P Nominal) reached during the transient as a function of the ejected rod worth (R) for 14 calculations. Due to different core-loading patterns, initial conditions and conservatism degrees, the ejected rod worths vary between 0.15 and 2.26 dollars (indeed, the rod efficiency is highly sensitive to the reloading strategy). The range of the five contributors is indicated by letters A to E ; a circle marks the U-core results. Hot-Full-Power and Hot-Zero-Power cases are distributed respectively along two straight lines on the semi-logarithmic graph.

For the "best estimate" analyses, the ejected rod worth is fairly less than 1 \$ and the power excursion induces a very modest temperature increase, without damage risk for fuel, owing to temperature feedbacks, even for one 100 % plutonium burner core option.

For the conservative evaluations with rod worth higher than 1 \$, the limit criteria for absence of catastrophic fuel pin failures are fulfilled (no fuel melting, maximum fuel average enthalpy at hot spot < 836 J/g, maximum clad temperature below the Zircaloy alpha-beta phase transition point), although the minimum DNB ratio margin (= 1.3) is exceeded in a limited core fraction.



Depending on specific assumptions, the MOX core behaviour is slightly worse or better than the Uranium core ; the higher cross-sections for fission and absorption of thermal neutrons in the core regions with Plutonium are mainly responsible of the better behaviour of a Plutonium core for rather severe power excursions.

## 2.2. Steam Line Break

Multiloop models of the primary and secondary coolant systems are needed to evaluate the thermal-hydraulic boundary conditions of the core, for which a detailed analysis is made separately.

The simulations differ essentially for the secondary side of heat exchangers and the connected secondary loop as well as for the safety system action, e.g. :

- . the most sophisticated models consider the intact steam-generator blow-down through the break until isolation valve closure ;
- . the reactivity history of the safety injection system is either introduced as input data using a constant boron reactivity worth at constant rate, or calculated by specialized modules.

Each primary system code represents the core by a point-kinetics module, but some associated core analyses are made by a space-dependent kinetics code.

All contributing studies use "End-of-Cycle" conditions, because the absence (or low concentration) of boron in the coolant gives the maximum absolute value of the moderator temperature coefficient, which is a crucial parameter. This reactivity coefficient is generally higher in absolute value for the cores including MOX assemblies ; for one contribution, a particular loading of MOX assemblies at core periphery is the origin of a reverse feature.

Hot-shutdown conditions are adopted by most with the most reactive control rod stuck out of the core, but with different time intervals between scram and steam-line-break occurrence ; this illustrates the influence of the accident sequence. This control rod aspect may induce high local power-peaking factors, depending also on fuel loading patterns.

Fig. 2 shows the maximum normalized power level  $P/P_N$  as a function of the moderator temperature reactivity coefficient  $M$  (varying between - 40 and - 75 pcm/°C) for 11 calculations. The results of each of the five contributors are located in separated parts of the graph. A circle marks the Uranium core cases.

Except for one "best estimate" case of an Uranium core, all the cores return to criticality during the transient. The recriticality durations are included between 6 and 80 seconds. The subsequent power excursion is always modest (the maximum normalized power level is less than 0.22) and the minimum DNB ratio is higher than 1.3. Some "best estimate" evaluations with the safety injection failure show that the situation can be mastered without higher failure risk, thanks to the dry-out of the steam generator

in the breached loop and the permanent operations of the main coolant pumps. For the conservative studies, the boron injection is the long-term decisive factor which guarantees that the risk of core damage is extremely small.

For the SLB, the behaviour of MOX cores is generally slightly worse than for U cores, but the differences of consequences are not very significant due to high margin to safety limits.

### 2.3. Conclusive Remarks

One remaining problem refers to the credible upper limit of the rod worths in any condition of the loading pattern with a not necessarily optimized strategy. The relevant uncertainty concerns the ejected rod worth in the RCCE as well as the stuck-rod worth at scram in the SLB.

Nevertheless, the consequences of plutonium recycling in 30 % of the MOX assemblies are not severe in those typical accidents and well-adapted methods of analysis are available. Each study has concluded that the introduction of MOX assemblies in a large PWR core does not lead to special problems.

## 3. BWR ACCIDENTAL SITUATIONS

The BWR MOX-fuelled cores have been designed similar to the Uranium reference cores (cycle length, power peaking). Island design has been used for the MOX fuel assemblies, so that the relative proportion of MOX fuel rods is 12 % for one-MOX reload cores in GARIGLIANO and CAORSO, and for full-MOX reloads, 35 % in KKI core and 51 % in GARIGLIANO core.

For CAORSO, only a core with one-MOX reload has been defined ; in the KKI case, only the full-MOX reload core was used in the comparative studies.

For the BWR studies, as shown in Table 2, the "best estimate" approach is represented by the GARIGLIANO/CAORSO studies, whereas the KKI studies use more conservative boundary conditions.

### 3.1. Main Heat Sink Failure (Turbine Trip)

As a result of a turbine trip, a pressure and mass flow transient occurs in the primary system of a reactor. The gradient of the pressure/mass flow ramp is determined by the global system design.

The integral power production evolution for the U and MOX cores has been studied for all three reactors and for various amounts of MOX reloads in the core.

A typical power history is shown in Fig. 3 for the KKI case. Two maxima in power occur during the transient. The first peak is caused by the reactivity ramp due to void reduction by the increasing pressure and is counteracted by the (prompt) void increase due to the power increase. The second peak is dominated by the delayed void and Doppler feedback effects initiated during the early phase of the transient.

At the end of the transient, as soon as pressure and mass flow have stabilized, the power stabilizes as well at a level determined by the static (void and Doppler) feedback coefficients.

As can be seen from Fig. 3 (KKI EOC case), MOX cores show a more pronounced power increase during the transient. This is a result of the more negative (approximately 20 %) void coefficient.

The following trends are deduced from that set of studies :

- for one-MOX reload core, only insignificant changes in power histories have been observed ;
- full-MOX recycling-cores show power transients up to 10 % higher than Uranium cores ;
- in all cases studied, the power transient, due to the turbine trip can be mastered by the existing core design features. No fuel damage (MCHFR limit) will be caused by the power transient.

In addition, it has been shown that such global transients as turbine trip or global mass flow transients (see next section) can be described by 1-D (axial) calculational models.

### 3.2. Trip of Recirculation Pumps (Mass Flow Transient)

The core power response to such a global mass flow transient initiated by a trip of the recirculation pumps has been studied for the KKI core. This transient is characterized by a mass flow reduction and therefore a void increase with a decrease in power. Again the power variation is slightly more pronounced in MOX loaded cores due to the enhanced void coefficient and the power response is slightly faster.

However, the difference between the U and MOX core behaviour is quite small (10 %).

### 3.3. Rod Drop Accident

In contrast to the global transients mentioned above the rod drop accident is a very local transient. Its dynamic behaviour can be described with sufficient accuracy only by 3D dynamic codes.

The driving force for the power excursion, especially at the beginning of the transient when Doppler feedback is still negligible, is the reactivity release of the dropping rod.

This reactivity release depends very sensitively on the following parameters :

- location of the dropping rod ;
- critical control rod insertion depth at the beginning of the transient (in this study : BOC, cold conditions) ;
- critical control rod pattern, which is a result of the control rod withdrawal sequence.

The following static dropping rod reactivities have been calculated :

	GARIGLIANO	CAORSO
Uranium core	680 pcm	324 pcm
One MOX Reload	480 pcm	343 pcm
All MOX Reload	250 pcm	---

Hence subsequent dynamic calculation for the GARIGLIANO Uranium reference case showed a prompt critical behaviour whereas the MOX core power excursion was much less severe. For the CAORSO case, the difference between U and one MOX reload core behaviour was negligible.

Especially for this accident, it can be concluded that the effects of the MOX island loading of the core are small compared to the normal range of uncertainties associated with core loading.

#### 3.4. Heat-Up Phase of a LOCA

Typical LOCA boundary conditions have been taken from the original reactor licensing reports of the CAORSO and the GARIGLIANO plants. They refer to :

- pressure vs time ;
- sequence of the accident (beginning of blowdown, beginning of the rewetting phase, etc) ;
- radial and axial core power peakings.

The design dependent fuel assembly characteristics affect the behaviour of the fuel rods under LOCA conditions, especially the differences in:

- material properties ;
- power production after shutdown due to delayed neutrons and fission product decay heat ;
- fuel-assembly pin power-density distribution (this is not necessarily a property specific to MOX fuel but strongly depends on fuel-assembly design).

The calculations show that the maximum cladding temperatures during LOCA, respectively for U and MOX cores, are 951 °C and 964 °C for GARIGLIANO as well as 1007 °C and 1010 °C for CAORSO.

These values are far below the 1200 °C limit which is the criterion for severe cladding damage. Moreover, the difference between the U and MOX fuel assemblies is practically zero.

This case too shows that fuel assembly design effects play a much more important role than the specific U/MOX difference.

#### 4. CONCLUSION

First, it should be mentioned that a normal U-fuelled LWR core at End-of-Cycle (32000 Mwd/t) generates more than 40 % of its power out of the fission of Plutonium isotopes. So it is to some extent a Pu-recycling system.

On the other hand, Pu-recycling on a greater scale has already been performed in several power reactors without serious problems for normal operation. Previous steady-state fuel management studies have shown that similar core parameters can be reached in MOX and Uranium assemblies owing to an appropriate fuel assembly and core design.

For accidental conditions, the situation was not so obvious, so that the interest was very large for an international comparative analysis of typical accidents in several power reactors assumed to burn Plutonium fuel in a large amount of the core.

Even if the various approaches are somewhat different, the general conclusions converge : the recycling of about 30 % of MOX fuel in large LWR cores should not induce safety problems, if some cautions are taken in core and fuel assembly design and if an adequate margin of uncertainty is kept for some important core parameters.

\* \* \*

#### REFERENCE

- [1] J. BASSELIER, A. RENARD, R. HOLZER, K. HNILICA,  
Analysis and Synthesis of the Theoretical Studies Performed on  
the Control and Safety of LWR's Burning Plutonium Fuel,  
Report EUR 8118 EN (1982).

\* \* \*

TABLE 1 : PWR Accidental Investigations

Reference Plant	Accident	Code Used	Core Initial Conditions	Core Investigated	Some Specific Features (h.w.r. = highest worth rod)
A/ BIBLIS-B	RCCE	IQSBOX (3D-2g)	EOC/HFP	P37 U P100	- h.w.r. at core centre, 1/8 symmetry core model
	SLB	BRUSEK + IQSBOX	EOC/HFP	U P100	- HFP with scram just after the SLB initiation
B/ BUGEY-2 (1)	RCCE	MEKIN (3D-2g)	BOC/HFP	U P100	- h.w.r. at edge, two symmetrical rods, 1/4 model of 1/2 real reactor core
	SLB	RELAP-UK + MEKIN	EOC/HZP	U P100	- starts at 12 seconds after scram from full power
C/ BUGEY-2 (2)	RCCE	CINTAX (1Dax-2g) + FLICA	BOC/HZP	U P30	- one average channel for whole core, same control rod worth for both cases
	SLB	FLICA-PREF	EOC/HZP	U P30	- steam-flow on steam generator secondary side imposed as a function of time, by input
D/ TIHANGE-1	RCCE	COSTANZA-RZ (2D-2g) + COBRA III-C	EOC/HZP	U P30	- 1/2 core macrocell centred around the h.w.r. located at periphery
	SLB	RETRAN	EOC/HZP	U P30 P70	- non equilibrium initial kinetic conditions (95 seconds after reactor trip)
E/ TRINO-VERCELLESE	RCCE	SYNTH-C (3D-3g)	EOC/HZP	U P32	- h.w.r. at periphery, whole core without symmetry
	SLB	RELAP4/MOD2 + LEUCIPPO	EOC/HZP	U P32	- colder core quadrant associated to the loop with SLB and including stuck control rod

TABLE 2 : BWR Accidental Investigations

Transient	Ref. Plant	Core Boundary Conditions	Operation State of eq.-core	Codes Used
Turbine trip (EOC) (dm/dt = 0)	KKI	Pressure ramp (25 %/s) Constant mass flow	EOC-full power	IQS-BWR for U COS-BWR for U and MOX
Turbine trip (EOC) (dm/dt < 0)	KKI	Pressure and mass flow ramps ; rate of change = 25 %/s pressure and ~ - 10 %/s mass flow	EOC-full power	IQS-BWR COS-BWR
Turbine trip (BOC) (dm/dt < 0)	KKI		BOC-full power	IQS-BWR COS-BWR
Trip of recirculation pumps	KKI	Constant pressure, mass flow varies	EOC-full power	COS-BWR IQS-BWR
Main heat sink failure (turbine trip)	GARIGLIANO	Mass flow and pressure curves given (pressure ramp : 3 %/s)	EOC-full power	DIREBO
	CAORSO	Mass flow and pressure curves given (respective ramps ~ 7%/s and 5 %/s)		
Rod drop accident	GARIGLIANO	Rod C8 drops	BOC-cold	SQUID SYNTH-C
	CAORSO		Zero-power	SYNTH-Trans
LOCA heat-up phase	GARIGLIANO	Pressure transient and core power density distribution given, burnup : 9000 MWd/t (MOX) 10000 MWd/t (U)	Full power	ARIEL
	CAORSO	Pressure transient and core power density distribution given, burnup : 12000 MWd/t (U and MOX)	Full power	ARIEL

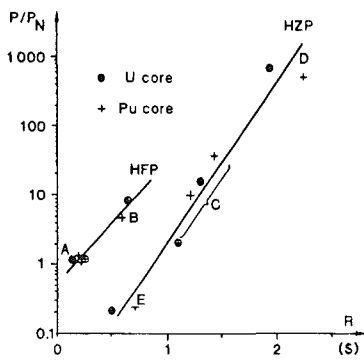


Fig. 1 - ROD EJECTION - PWR.  
NORMALIZED POWER VERSUS  
ROD WORTH.

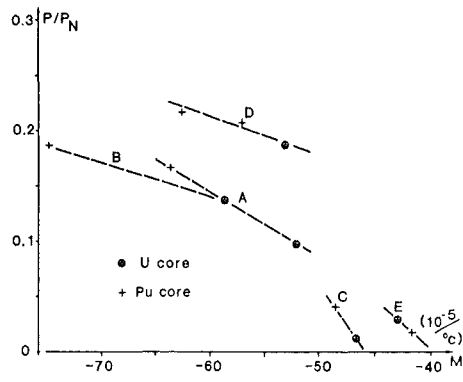


Fig. 2 - STEAM LINE BREAK - PWR.  
NORMALIZED POWER VERSUS  
MODERATOR TEMPERATURE  
REACTIVITY COEFFICIENT.

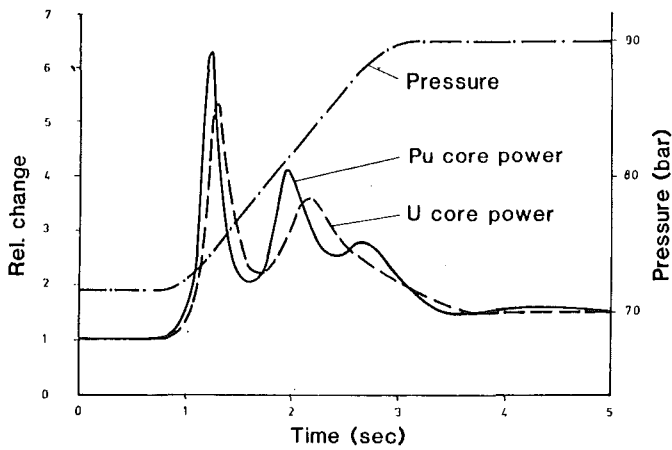


Fig. 3 - KKI TURBINE TRIPS NORMALIZED INTEGRAL POWER  
AND PRESSURE VERSUS TIME



PERIODIC (INSERVICE) INSPECTION OF NUCLEAR STATION PIPING WELDS,  
FOR THE MINIMUM OVERALL RADIATION RISK

J.L. Platten

Atomic Energy of Canada Limited  
Sheridan Park, Mississauga, Canada

ABSTRACT

Periodic (Inservice) Inspection of pressure-retaining components is a requirement in all nuclear stations.

A method is presented for determining the optimal number of piping welds to inspect which results in the minimum overall radiation risk. This risk has two parts, a) that incurred by inspection personnel, and b) the "expected" risk to the public due to piping system failure.

The probability of system failure may be quantified in terms of the number of welds inspected. Radiation exposures are evaluated by a method based on radiation detriment optimization measures advocated in the revised (1977) ALARA concept. Knowing the release to the public due to failure, it is possible to quantify the overall radiation risk in terms of the number of welds inspected. Optimization methods allow determination of the optimal number of welds to inspect, to minimize this overall radiation risk.

The method was applied to the example of a typical piping system in a CANDU station, with the apparent conclusion that no weld Periodic Inspection would be required for the purposes of safety. Further review of the specific assumptions involved would be necessary to confirm this result.

1.0

INTRODUCTION

All nuclear stations require Inservice Inspection of components in nuclear systems, to assure their safety and integrity. In CANDU stations this is termed Periodic Inspection.

Periodic Inspection in a CANDU station is the mandatory inspection of components whose failure could result in radioactive releases to the public, and is governed by National Standard of Canada CAN3-N285.4-M83, "Periodic Inspection of CANDU Nuclear Power Plant Components" [1], hereafter called "the Standard".

Among components to be inspected are the piping welds of heat transport circuits in which failure could result in radioactive releases. The number of welds to be inspected in a piping circuit, and the inspection intervals, are determined by rules in the Standard.

The intent of the Standard is protection of the public from radioactive releases. However, Periodic Inspection itself results in radiation exposure to the personnel carrying out inspections, due to the residual radioactive fields around nuclear station systems during shutdown.

This paper examines Periodic Inspection of piping welds from an optimization point of view with respect to radiation exposure. The paper quantifies the overall radiation risk, which has two parts a) that incurred by inspection personnel, and b) the "expected" risk to the public due to piping system failure. By minimizing this overall radiation risk, the optimal number of welds to inspect is determined.

## 2.0 OPTIMIZATION MODEL

### 2.1 MODEL FORMULATION

Consider a piping system with a total of  $N$  welds, where  $D$  welds are in a deteriorated state and  $I$  are Periodically Inspected. There are five inspection intervals during the assumed 40-year station life, and so each of the  $I$  welds is inspected five times. The same  $I$  welds are inspected in each interval, since a basic premise is that Periodic Inspection will detect deterioration by comparison of inspection results with those previously obtained for the same weld.

We assume that system deterioration is detected if the inspection sample  $I$  includes at least one of the  $D$  deteriorated welds. Hence the deterioration remains undetected if the sample  $I$  includes exactly zero of the  $D$  welds. The probability that the  $I$  welds inspected include exactly zero of the  $D$  welds is derived from the hypergeometric distribution [2];

$$P(0) = \frac{(N-D)! (N-I)!}{(N-D-I)! N!} \quad (1)$$

This is the probability of undetected system deterioration, given that deterioration does exist.

The emphasis of Periodic Inspection is on detection of "generic" deterioration due to unanticipated mechanisms, which could affect several or many of the system welds. Hence, generic deterioration is assumed to affect at least two and as many as all of the system welds. Then  $D$  is in the range;

$$2 \leq D \leq N \quad (2)$$

Of course, it is not certain that generic deterioration does exist in the system. Hence, we assume  $P(GD)$  to be the average value over the station life of the probability that generic deterioration does exist.

The crucial assumption is then made, that the system will definitely fail if generic deterioration exists and if this deterioration is not detected by inspection. Then the probability of system failure is:

$$P(F) = P(GD) \times P(O) \quad (3)$$

We now define CA as the radiation exposure "consequence" of piping system failure, and CI as the radiation exposure "consequence" of Periodic Inspection of one weld over the station life.

The risk due to Inspection over the station life is then;

$$I \times CI \quad (4)$$

The "expected" risk to the public due to possible failure of the piping system is;

$$CA \times P(F) = CA \times P(GD) \times P(O) \quad (5)$$

Then the overall radiation risk over the station life is the sum of contributions (4) and (5);

$$I \times CI + CA \times P(GD) \times \frac{(N-D)!(N-I)!}{(N-D-I)! N!} \quad (6)$$

Expression (6) is a minimum when the expression divided by CI is also a minimum. This results in an expression with the ratio  $\frac{CA}{CI} = CR$ , defined as the Consequence Ratio. Hence, the final expression to minimize is:

$$I + CR \times P(GD) \times \frac{(N-D)!(N-I)!}{(N-D-I)! N!} \quad (7)$$

For a given piping system, CR and N are fixed and P(GD) will equal an assumed value. Hence, expression (7) is a function of I and D.

Note that D is defined only as being within the range,  $2 \leq D \leq N$ . The approach taken during the minimization of expression (7) was to find the maximum value of I which results in this minimization, over all values of D in the range  $2 \leq D \leq N-I$ .

Several of the assumptions used for the model are simplifications of more rigorous descriptions; for example equation (3). These were chosen to give conservative (maximum) values of  $I_{opt}$ , the number of system welds to be inspected.

## 2.2

## MODEL RESULTS

Figure 1 shows the results of minimizing expression (7), in the form  $I_{opt}$  versus  $N$  with  $P(GD) \times CR$  as parameter, for  $N$  in the range 100 to 400. For each value of  $N$  and  $P(GD) \times CR$ , there was found to be a unique  $I_{opt}$  which gave the minimum.

An Atomic Energy of Canada Limited internal study was used to establish a realistic upper bound for  $P(GD)$ . The study reviewed U.S. nuclear station experience, and categorized piping system problems into "severances", "leaks" and "defects". It is assumed that "severances" is the relevant category. Under the assumption of a Poisson failure process, an upper limit failure rate  $\lambda = 1 \times 10^{-3}$  severances per station-year was recommended. For a station life of 40 years, the increase of  $(1 - e^{-\lambda t})$  which is the probability of at least one failure up to time  $t$ , is nearly linear with time. Hence we may think of this "probability of at least one failure" as increasing linearly with time to a value of  $\sim 0.04$  at 40 years. The average value over the station life is then  $\sim 0.02$ . Since the data used in the study covered all failure mechanisms, "generic" and "non-generic", and there is in fact no evidence of "generic" weld deterioration due to unanticipated mechanisms, it is assumed that 0.02 is a realistic upper bound on  $P(GD)$ .

## 3.0

## APPLICATION OF MODEL RESULTS

The results have been applied for  $N = 290$  welds, relevant to the Primary Heat Transport (PHT) piping system in a specific CANDU Station.

## 3.1 CONSIDERING RADIATION EXPOSURE CONSEQUENCES

Safety analyses for the specific CANDU station give information on the exposure consequences of piping failure. Failure of the PHT piping system is a "single-failure" accident in CANDU terminology.

Reference [3] provides a method of evaluating the "detriment" of radiation exposures under different conditions, to satisfy exposures being "AS LOW AS REASONABLY ACHIEVABLE, ECONOMIC AND SOCIAL FACTORS BEING TAKEN INTO ACCOUNT" known as the "Revised (1977) ALARA Concept". It accounts for the economic and social climate, administrative/legal exposure limits and the actual magnitude of risk. The upper bound on occupational detriment is obtained from the "cost of replacement manpower" which occurs at the limiting level of exposure. For the upper bound on detriment to the public, a similar relationship is used. The method incorporates a quadratic relationship for the dose-response curve for the response of humans to radiation.

## 3.1.1 OCCUPATIONAL RISK TO INSPECTION PERSONNEL

Using the terminology and equations of reference [3]; and relevant assumptions;

$-R_1$  = average exposure rate to Periodic Inspection Personnel  
 =  $1 \times 10^{-2}$  person-Sv/year-person (based on station operating experience)

$-E_{LIM}$  = occupational exposure limit to inspection personnel  
 =  $5 \times 10^{-2}$  person-Sv/year-person

$-L_c$  = annual labour cost = 60,000 \$/year-person

Then the "detriment value" of this exposure is;

$$\alpha_{occ} = \frac{L_c}{E_{LIM}} \left( \frac{R_1}{E_{LIM}} \right)^{0.5} = 537,000 \text{ \$/person-Sv} \quad (8)$$

The estimated radiation exposure to personnel, for piping Periodic Inspection in the station, is  $1.6 \times 10^{-2}$  person-Sv per PHT weld over the five inspections.

The value of CI, the radiation exposure consequence of Periodic Inspection of one weld, is the product of the exposure in person-Sv per weld and the detriment per person-Sv;

$$CI = 1.6 \times 10^{-2} \frac{\text{person-Sv}}{\text{weld}} \times \frac{537,000 \text{ \$}}{\text{person-Sv}} = 8590 \frac{\text{\$}}{\text{weld}}$$

### 3.1.2 PUBLIC RISK DUE TO AN ACCIDENT

From the station safety analyses, the single-failure exposure to an individual which results in the maximum detriment is  $1.6 \times 10^{-3}$  person-Sv. Using the terminology of reference [3] and making certain assumptions;

$-R_2$  = maximum exposure to a member of the public =  $1.6 \times 10^{-3}$  person-Sv

$-E_{LIM}^*$  = radiation limit to an individual member of the public for single-failure accident =  $5 \times 10^{-3}$  Person-Sv

$-L_c^*$  = per-capita income = 6000 \$/year-person

Then the detriment value of public radiation exposure is:

$$\alpha_{public} = \frac{L_c^*}{E_{LIM}^*} \left( \frac{R_2}{E_{LIM}^*} \right)^{0.5} = 679,000 \text{ \$/person-Sv} \quad (9)$$

From the safety analyses the maximum single-failure population exposure is 0.71 person-Sv. Finally, the value of CA is the product of this population exposure and the detriment value of the exposure;

$$CA = 0.71 \text{ person-Sv} \times \frac{679,000 \text{ \$}}{\text{person-Sv}} = \$482,000$$

### 3.1.3 OPTIMAL LEVEL OF PERIODIC INSPECTION

Since we had earlier established  $CI = 8590 \frac{\text{\$}}{\text{Weld}}$ , then

$$CR = \frac{CA}{CI} = \frac{\$482,000}{\$8,590} = 56.1 \sim 56. \text{ Using the assumption that } P(GD) = 0.02,$$

$$P(GD) \times CR = 0.02 \times 56 = 1.1.$$

Figure 1 shows that  $I_{opt}=0$  for  $P(GD) \times CR$  of 1.1 and  $N=290$ . The result that no Periodic Inspection of welds can be justified for safety purposes runs counter to accepted belief on this subject; a further review of the assumptions used is necessary in order to confirm these results.

We note that, for this specific PHT main circuit piping system with  $N = 290$  welds, the Standard requires Periodic Inspection of 43 welds, 15% of the total.

## 3.2 CONSIDERING ALL CONSEQUENCES INCLUDING ECONOMIC

Periodic Inspection as defined by the Standard is intended only for safety, and so the economic consequences of system failure are not within its scope. However, those consequences could be very large.

### 3.2.1 TOTAL CONSEQUENCE OF SYSTEM FAILURE

The economic consequences of system failure would include a) cost of replacement electrical power, b) costs of repair and cleanup, and c) indirect but likely significant costs due to the reaction of the public and regulatory authorities. It is difficult to put accurate costs on these effects. For the cost of replacement power, an estimate is 250,000\$ per day. If we assume the station to be shut down for 6 months following a failure, the total cost of lost power is  $\sim \$4.6 \times 10^7$ . The other costs identified would result in a total consequence of failure CA, including public radiation detriment, in the order of  $\$5.0 \times 10^7$ .

## 3.2.2 TOTAL CONSEQUENCE OF PIPING INSPECTION

The other costs incurred in piping inspection, due to equipment costs and straight labour costs, are believed to be about 20% of the radiation detriment. Hence the estimated total detriment per pipe weld inspection is:

$$CI = \$8590 \times 1.2 = 10,300 \text{ \$/Weld.}$$

## 3.2.3 OPTIMAL LEVEL OF INSPECTION

$$\text{In this case } CR = \frac{CA}{CI} = \frac{\$5.0 \times 10^7}{\$10,300} \sim 4900 \text{ and } P(GD) \times CR = 0.02 \times 4900 = 98.$$

Figure 1 shows that inspection of ~ 40 welds may be justified, in this case where all the consequences of system failure and of weld inspection have been considered. This compares with 43 welds, which the Standard requires for Periodic Inspection.

This suggests that the Standard may require excessive piping inspection in terms of protection of the public from the radiation consequences of system failure, subject to the further review as discussed in section 3.1.3. However, based on the assumptions used, the required level of inspection appears realistic when all the consequences of system failure and piping inspection are considered.

## REFERENCES

- [1] National Standard of Canada CAN3-N285.4-M83, "Periodic Inspection of CANDU Nuclear Power Plant Components", 1984.
- [2] Neter, J; Wasserman, W; Whitmore, G.A.; "Applied Statistics", Allyn and Bacon Inc., Boston, 1983.
- [3] Maan, M.A., "Cost Effective Radiation Risk Management in a Generic Nuclear Plant Design", AECL-7536, 1982 November, Atomic Energy of Canada Limited - CANDU Operations, Mississauga, Ontario.

## SYMBOLS

- CA = consequence of piping system failure
- CI = consequence of Periodic Inspection of one piping weld, over the station life
- CR = CA/CI, the Consequence Ratio
- D = number of system welds with deterioration

$E_{LIM}$	= occupational radiation exposure limit to inspection personnel (person-Sv/year)
$E^*_{LIM}$	= radiation limit to an individual member of the public, due to an accident (person-Sv)
$I$	= number of system welds which are Periodically Inspected
$I_{opt}$	= optimal number of welds to inspect, to minimize radiation risk
$J!$	= J factorial = $J(J-1)(J-2) \dots (2)(1)$ , where J is any integral number
$L_c$	= annual labour cost (\$ /year-person)
$L^*_C$	= per-capita income for public (\$ /year-person)
$N$	= total number of piping welds in system
$P()$	= probability of (an event)
$P(F)$	= probability of piping system failure
$P(GD)$	= average value over station life, of probability that piping system has generic deterioration
$P(o)$	= probability that deterioration is not detected by inspection, given that deterioration exists.
$R_1$	= average exposure rate to Periodic Inspection personnel (person-Sv/year-person)
$R_2$	= maximum radiation exposure to a member of the public due to an accident (person-Sv)
$t$	= station age (years)
$\alpha_{occ}$	= detriment value of occupational radiation exposure to inspection personnel (\$/person-Sv)
$\alpha_{public}$	= detriment value of public radiation exposure due to an accident (\$/person-Sv)
$\lambda$	= piping system failure rate (severances/station-year)
$\$$	= \$ (1982)



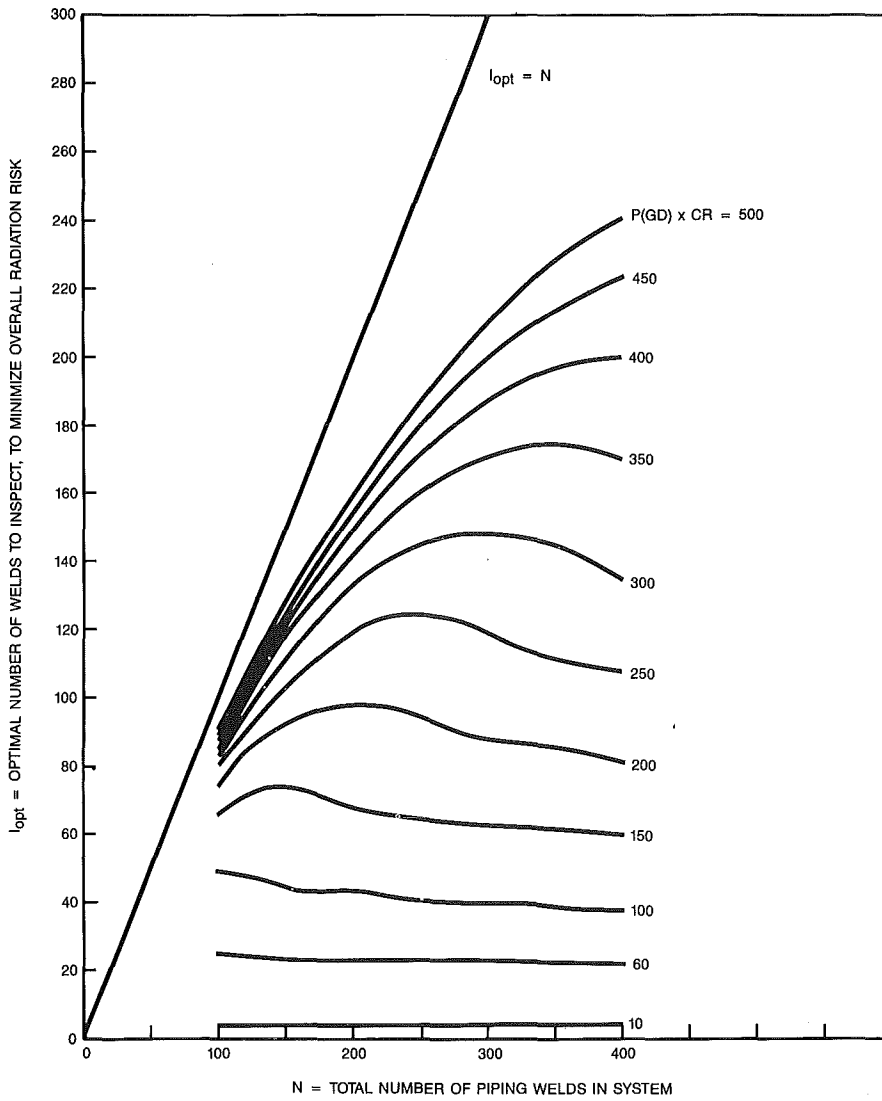


FIGURE 1 THE OPTIMAL NUMBER OF WELDS TO INSPECT ( $I_{opt}$ ) VERSUS THE TOTAL NUMBER OF WELDS IN SYSTEM ( $N$ ) TO MINIMIZE THE OVERALL RADIATION RISK (WITH  $P(GD) \times CR$  AS PARAMETER)

PARAMETRIC STUDIES ON THE REACTIVITY OF SPENT FUEL  
STORAGE POOLS

P. Grimm, J.M. Paratte, K. Foskolos, C. Maeder

Swiss Federal Institute for Reactor Research (EIR)  
CH-5303 Würenlingen, Switzerland

## ABSTRACT

The dependence of the multiplication factor of spent fuel storage pools without absorbing channels and with steel and Boral absorbers on assembly pitch, water density, and absorber thickness is investigated. The results show that the reactivity of the Boral pool is more sensitive to the assembly pitch than that of the other two pools. It is demonstrated that the  $k_{eff}$  of the pools without absorber and with steel channels has its maximum value at low water density. The multiplication factor of the Boral pool passes through a minimum as a function of absorber thickness if the assembly pitch is kept constant.

## INTRODUCTION

For a safe storage of nuclear fuel it is essential that the pools used for this purpose remain subcritical under all conceivable conditions. As the spent fuel assemblies discharged from a reactor usually have to be stored on site for several years a high storage density is desirable from an economic point of view. Careful and accurate criticality calculations are therefore required in order to guarantee the criticality safety of a storage pool as well as an economic construction.

In the present paper we want to show some important criticality characteristics of storage pools as well as the differences in sensitivity to various parameters for the three types of pools most commonly used, viz. pools without neutron absorbers and with steel or Boral absorbing channels. It is however not the intention of this paper to show the complete optimization of a storage pool.

## DESCRIPTION OF THE CALCULATED STORAGE POOLS

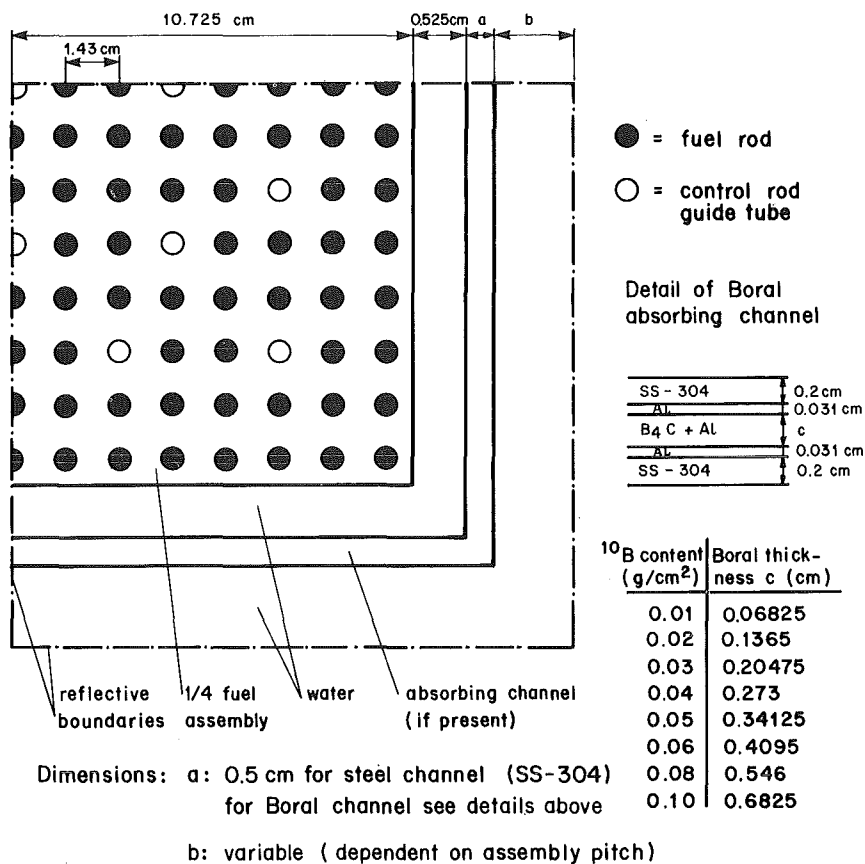
The calculations were performed for PWR spent fuel storage pools with a typical 15 x 15 rods fuel assembly. The characteristics of the fuel assembly are given in Table I. These data were taken from Ref. [1] as far as possible and realistic values were assumed for the remaining quantities.

Table I Dimensions and material densities  
of the fuel assembly

Number of fuel rods	204
Number of control rod guide tubes	21
Fuel UO <sub>2</sub>	
Density	10.4 g/cm <sup>3</sup>
Pellet diameter	0.911 cm
Clad Zircaloy	
Density	6.55 g/cm <sup>3</sup>
Outside diameter	1.07 cm
Thickness	0.072 cm
Rod pitch	1.43 cm
Guide tubes SS-304	
Density	7.91 g/cm <sup>3</sup>
Outside diameter	1.40 cm
Thickness	0.05 cm

The fuel was assumed to be fresh with a <sup>235</sup>U enrichment of 3.5 % by weight. The geometry of a lattice cell of the storage pool and the details of the absorbing channels are shown in Figure 1. The thickness of the Boral plate is variable; instead of Boral thickness we will usually give the boron content in grams of <sup>10</sup>B per cm<sup>2</sup> of plate surface. The relation between boron content and Boral thickness is also given in Figure 1, these data are taken from the manufacturer's publicity. The storage pools were assumed to be infinite in the x- and y-directions. The axial leakage was taken into account by means of an axial buckling of 0.8 m<sup>-2</sup> which corresponds to an extrapolated height of 3.5 m.

Figure 1 Geometry of fuel assembly and absorbing channel



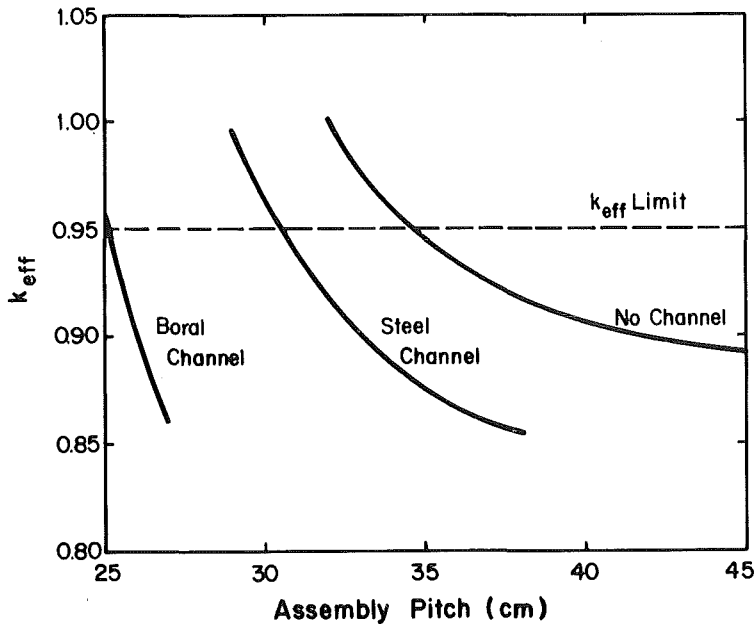
## CALCULATIONS AND RESULTS

All the calculations were performed by means of the two-dimensional LWR fuel assembly code BOXER [2,3]. This code was developed at EIR and successfully validated against critical experiments and benchmark problems which have similar characteristics to storage pools [3].

$k_{eff}$  as a Function of Assembly Pitch

The dependence of the multiplication factor on the assembly pitch is calculated for all three pools at normal water density (i.e.  $1.0 \text{ g/cm}^3$ ). A  $^{10}\text{B}$  content of the Boral channel of  $0.04 \text{ g/cm}^2$  is chosen for this investigation. The results are shown in Figure 2.

Figure 2  $k_{eff}$  of the three types of storage pools at a water density of  $1.0 \text{ g/cm}^3$  as a function of assembly pitch



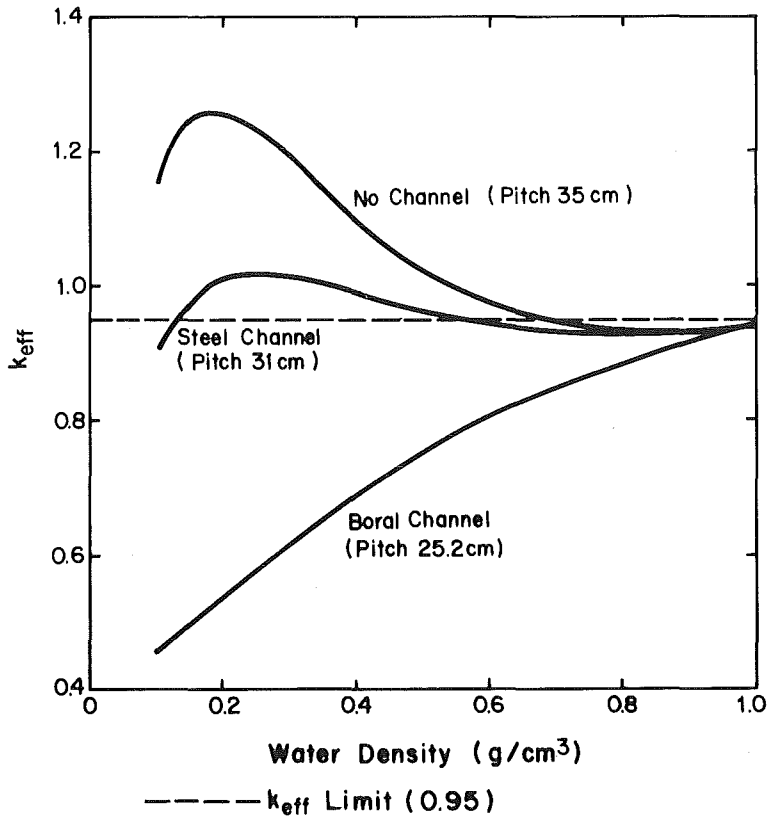
It can be seen that the  $k_{eff}$  of the pool without absorbing channel tends to an asymptotic value on the order of 0.85. The reactivity of the steel pool has a similar behaviour but with a smaller asymptotic  $k_{eff}$ . In most countries an upper limit of 0.95 for the  $k_{eff}$  at normal conditions is imposed by the authorities. Assembly pitches for which  $k_{eff}$  is around 0.9 to 0.95 are therefore of practical interest for actual pool designs. In this range the reactivity of the Boral pool is more sensitive to changes in assembly pitch than that of the other two pools: a 1 cm reduction of the assembly pitch increases the  $k_{eff}$  by 5 % for the Boral pool, by 2 % for

the steel pool, and by about 1 % for the pool without absorbing channel. From these results it follows that Boral pools require special care in criticality calculations and high precision in manufacturing.

#### $K_{eff}$ as a Function of Water Density

For the investigation of the dependence of the multiplication factor on the water density we choose a value of the assembly pitch for which  $k_{eff}$  at normal water density is just below 0.95 for each pool. These values are 25.2 cm for the Boral pool, 31 cm for the steel pool, and 35 cm

**Figure 3**  $K_{eff}$  of the three types of storage pools as a function of water density



for the pool without absorbing channel (see Figure 2). The calculated  $k_{eff}$ 's are shown in Figure 3. It can be seen that the dependence of  $k_{eff}$  on the water density is significantly different for the three pools: The  $k_{eff}$  of the Boral pool falls monotonously with decreasing water density, for the steel pool  $k_{eff}$  has a maximum value of approximately 1.02 at a water density of  $0.23 \text{ g/cm}^3$  whereas the  $k_{eff}$  of the pool without absorbing channel rises drastically at low water density and reaches a peak value of 1.26 at a density of  $0.18 \text{ g/cm}^3$ .

The maximum of  $k_{eff}$  at low water density can be explained as follows: The production to absorption ratio of the fuel assembly is almost constant for water densities greater than  $0.2$  to  $0.3 \text{ g/cm}^3$  and not equal to the  $k_{\infty}$  of the assembly (from a calculation of the assembly alone). This is due to the moderating effect of the large quantities of water in the gaps between the assemblies. On the other hand, as the water density decreases, a neutron leaving a fuel assembly has a greater probability to reach another assembly rather than being absorbed in the water, or in other words, the coupling between the assemblies improves. This is the reason for the increase of  $k_{eff}$ . At water densities below  $0.2 \text{ g/cm}^3$   $k_{eff}$  falls with decreasing water density because the production to absorption ratio of the fuel assembly decreases. The leakage, which is practically negligible at higher water densities, contributes also to the reduction of  $k_{eff}$  at low densities.

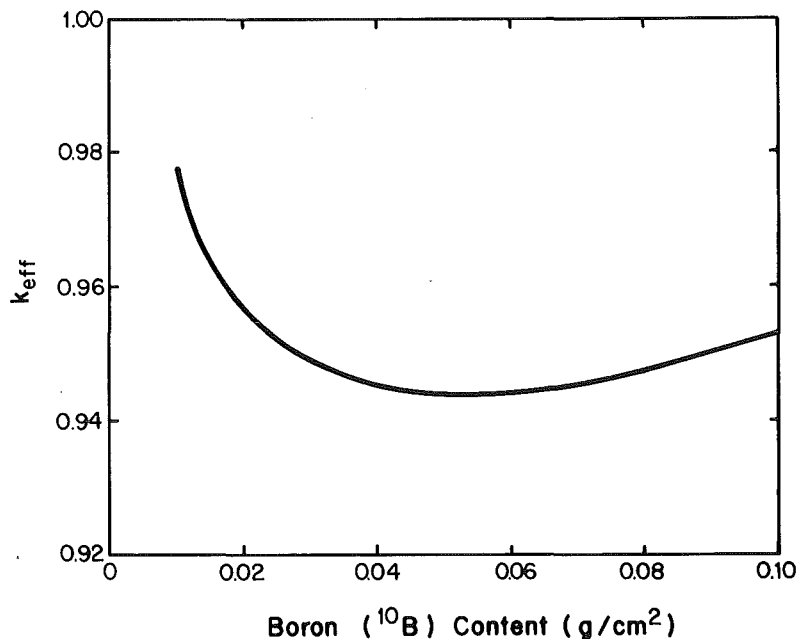
From these results it follows that for the design of a storage pool without absorbing channels or with steel channels it is not sufficient to compute  $k_{eff}$  at normal water density, but the maximum of  $k_{eff}$  has to be searched for. For the steel pool the increase in assembly pitch necessary to reduce  $k_{eff}$  to an acceptable value can be estimated as follows: Figure 2 shows that an increase of the assembly pitch by 1 cm reduces  $k_{eff}$  by approximately 2 %. If we assume that the curve of the multiplication factor versus assembly pitch at a water density of  $0.2 \text{ g/cm}^3$  has the same gradient as at  $1.0 \text{ g/cm}^3$  (in fact the curve at  $0.2 \text{ g/cm}^3$  can be expected to be steeper, see below) we can conclude that an increase of the assembly pitch by 2 cm to 33 cm reduces the maximum  $k_{eff}$  to 0.98 (the limit for  $k_{eff}$  at accidental conditions in the US regulations). For the pool without absorbing channels a greater increase of the assembly pitch would be necessary for an acceptable design. It must not be concluded however from Figure 2 that it is impossible to reduce the maximum  $k_{eff}$  of this pool below 1.0. Since the leakage at low water density increases strongly with the volume of the water zones and consequently with the assembly pitch the curve for the maximum  $k_{eff}$  versus assembly pitch would be steeper than the one in Figure 2.

#### $K_{eff}$ of the Boral Pool as a Function of Absorber Thickness

For this investigation we use again an assembly pitch of 25.2 cm. This dimension and the inside width of the absorbing channel are kept constant. An increase of the Boral thickness (or of the boron content, which means the same) is compensated by a reduction of the width of the water gap outside the absorbing channel. The calculated multiplication factors are shown in Figure 4.

It can be seen that the  $k_{eff}$  has a minimum value for a  $^{10}\text{B}$  content of  $0.05 \text{ g/cm}^2$  and increases slightly for higher absorber thicknesses. This may be surprising but it can easily be explained: As the width of the water gap between neighbouring channels is reduced the neutron spectrum at the outer edge of the Boral plate hardens and the absorption rate per unit volume of the Boral decreases rapidly. The absorption of the Boral plate (integrated over its volume) at a  $^{10}\text{B}$  content of  $0.06 \text{ g/cm}^2$  is only 20 % higher than at  $0.01 \text{ g/cm}^2$  and decreases for higher boron contents. The  $^{10}\text{B}$  content of  $0.04 \text{ g/cm}^2$  which was arbitrarily chosen for the previous sections was therefore not optimal from an economic point of view. For example a reduction of the  $^{10}\text{B}$  content to  $0.02 \text{ g/cm}^2$  would cause an increase of  $k_{eff}$  of 1.2 % (see Figure 4). From Figure 2 it can be seen that this reactivity increase can be compensated by a 0.2 cm increase of the assembly pitch. For a pool designed to contain several hundred assemblies this corresponds to an increase of the rack side length of a few cm which is small compared to the pool dimensions of several meters.

Figure 4  $k_{eff}$  of the Boral pool as a function of the boron content of the absorbing channel for a constant assembly pitch of 25.2 cm





## CONCLUSIONS

The present work, although it was not intended to show the complete optimization of a storage pool design, shows some characteristic problems which must be taken into account in criticality calculations for the different types of storage pools. The multiplication factor of a pool with Boral channels is more sensitive to the assembly pitch than that of the pools with steel channels or without neutron absorbers. For the latter two types of storage pools the maximum of  $k_{eff}$  does usually not occur at normal water density but it is normally reached at densities around  $0.2 \text{ g/cm}^3$  and must be searched for in the criticality calculations. The reactivity of the Boral pool has its maximum at a water density of  $1.0 \text{ g/cm}^3$ . This is a safety advantage of the use of Boral channels besides the economic benefit of the high storage density. On the other hand the  $k_{eff}$  cannot be reduced to arbitrarily low values by increasing the Boral thickness while keeping the assembly pitch constant.

## REFERENCES

- [ 1 ] Power Reactors 1983  
Nuclear Engineering International, 28, Supplement, August 1983
- [ 2 ] C. Maeder, J.M. Paratte  
Calculation of LWR Fuel Elements Containing Burnable Poison and Plutonium  
TANS - 20, p. 359, 1975
- [ 3 ] K. Foskolos, P. Grimm, C. Maeder, J.M. Paratte  
Qualification des méthodes LWR - EIR pour l'évaluation des bassins compacts  
EIR-Report Nr. 497, 1983

THE CEC SHARED COST ACTION RESEARCH PROGRAMME  
ON THE SAFETY OF THERMAL WATER REACTORS:  
RESULTS IN THE SUB-AREA  
"PROTECTION OF NUCLEAR POWER PLANTS AGAINST EXTERNAL  
GAS CLOUD EXPLOSIONS"

W. Geiger \*)

Battelle-Institut e.V.  
Frankfurt am Main, FRG

ABSTRACT

The structure and intentions of subject area B of the CEC cost sharing programme for LWR safety research are outlined. Area B is devoted to the study of external explosions of combustible heavy gas clouds due to accidental releases of hydrocarbons during transportation, and of their impact on nuclear power plant structures.

Research in area B deals with the three main stages of an unconfined gas cloud explosion scenario: cloud formation and spreading at ground level, explosion development after ignition, propagation in air and interaction with plant structures of the pressure wave generated in the explosion.

The scope of work in the 12 research projects of area B is presented. Work covers experiments as well as modelling and code development. A brief account of principal results and main conclusions is given.

INTRODUCTION

During 1979 the Commission of the European Communities (CEC) initiated a "Cost Sharing Programme" of research work in the area of LWR safety. Through this programme the CEC pays 20-50 % of the costs of a number of individual projects carried out in various national laboratories of the member countries of the European Community. The five years programme is intended to improve communication and to encourage collaboration between member countries and to avoid duplication of effort. Three subject areas are covered by the present programme:

- A. LOCA/ECCS
- B. Gas cloud explosion (external to containment)
- C. Fission product dispersion (to environment)

---

\*) acting on behalf of the Commission of the European Communities (CEC) and of the project leaders in the sub-area

The total CEC budget is 6.3 M.ECU's with about 5.5 M.ECU's for allocation to contracts, 50 % of which is devoted to LOCA/ECCS, the other 50 % being divided about equally between areas B and C. In each of the subject areas work progress in the research projects is monitored during project meetings of all contractors every six months, with the assistance of national experts groups. The programme was completed during the first half of 1984 when the bulk of the results became available.

A special meeting "The results of the Indirect Action Research Programme, Safety of Thermal Water Reactors (1979-1983)" will be organized by the Commission of the European Communities during the time October 1-3, 1984, in Brussels. At this meeting a detailed account will be given of the work performed and of the results achieved in each of the three subject areas.

In the following the scope of work in subject area B, i.e. gas cloud explosion, will be outlined, followed by a brief account of principal results and main conclusions.

#### SCOPE OF WORK IN SUBJECT AREA B

Subject area B is devoted to the study of external explosions of combustible heavy gas clouds, due to accidental releases of hydrocarbons during transportation, and of their impact on nuclear power plant structures. It deals more specifically with the three main sequential stages of an unconfined gas cloud explosion scenario which determine the load on the plant:

- 1) cloud formation and spreading at ground level
- 2) explosion development after ignition (flame propagation and pressure wave generation)
- 3) pressure wave propagation in air and interaction with plant structures

12 different research projects were allocated in area B, 4 projects respectively in each of the three fields. In Table I the titles of the projects and the laboratories in charge of the investigations are given.

#### Cloud formation and spreading

Clearly, the explosion history will depend significantly on the dimensions of the cloud and the concentration distribution at the time of ignition. Because the vapour formed by evaporation of accidentally released liquefied hydrocarbons is heavier than air the spreading of the vapour cloud and its dilution by entrainment of air is significantly influenced by gravitational forces. Investigations in the field of vapour cloud dispersion appeared to be indispensable because the available experimental data were scanty while the predictions of existing models differed widely.

Among the four projects in this field project 2B is by far the largest, in fact the largest of area B. In this project field tests were performed of the formation and spreading of heavy gas clouds at different meteorological conditions in order to generate reliable experimental data with which the various existing

**Table I: Projects in area B,  
Protection of nuclear power plants against external  
gas cloud explosions**

field	Title of research project	Project No.	Laboratory	Project leader
Cloud formation and spreading	Large-scale field trials on dense vapour dispersion: Phase I trials; Phase II trials	2 B	Health and Safety Executive, London (subcontractor: National Maritime Institute, Hythe)	J. Mc QUOID
	Computer processing of visual records from the Thorney Island large scale gas trials	14 B	Institut Von Karman de Dynamique des Fluides, Rhode St Genese	M. L. RIETHMULLER
	Aspects of the dispersion of heavier-than-air vapours that are of relevance to gas cloud explosion (study of mechanisms which cause dilution of the cloud to levels below the lower flammable limit)	3 B	United Kingdom Atomic Energy Authority, S.R.D. Culcheth	C. J. WHEATLEY
	Verification of various models for the expansion and dispersion of heavy gas clouds on the basis of large-scale experiments	9 B	Battelle-Institut, Frankfurt/Main	G. SCHNATZ
Explosion development	Characterization of the pressure field induced by the explosions in air of a hydro-carbon-air mixture, with slow deflagration or fast deflagration (pseudo-detonation)	10 B	Commissariat à l'Energie Atomique C.E.N. Fontenay-aux-Roses	J. L. GARNIER
	Validation of 1-dimensional codes for the computation of pressure waves caused by spherically symmetric unconfined vapour cloud explosions, evaluation of the use of 1-dimensional codes as an approximation for computation of pressure waves caused by non-spherical unconfined vapour cloud explosions and experimental determination of the behaviour of flames in the presence of obstacles	12 B	National Defense Research Organization TNO, Prins Maurits Laboratory	J. P. ZEEUWEN
	Transition from slow deflagration to detonation	6 B	Kraftwerk Union AG, Erlangen	W. DRENCKHANN
	Experimental investigation of the acceleration of deflagration in wake flow	8 B	Rheinisch-Westfälische Hochschule, Aachen	G. ADOMEIT
Pressure wave propagation, interaction with structures	Gas cloud explosions and their effect on nuclear power plants, phase I: Basic development of explosion codes	1 B	United Kingdom Atomic Energy Authority, S.R.D. Culcheth	S. F. HALL
	Gas explosion characterization, wave propagation	11 B	Risø National Laboratory	S. I. ANDERSEN
	Calculation of the wall pressure field generated on a group of buildings by an external explosion	7 B	Commissariat à l'Energie Atomique C.E.N. - Saclay	C. BERRIAUD
	Modelling and calculation of overpressure on the building of a plant due to the passage of a shock wave caused by an accidental explosion	15 B	Laboratoire National d'Hydraulique, Direction des Etudes et Recherches de l'Electricité de France	A. WARLUZEL

computer codes can be validated. The test site chosen was a former landing ground on Thorney Island at the south coast of England. In each of the tests 2000 m<sup>3</sup> of gas at ambient pressure and temperature were released instantaneously from a plastic bag 13 m high and 14 m in diameter. The gas used was a mixture of refrigerant-12 and nitrogen allowing to select initial densities relative to air up to 4.2. By releasing dense gas at ambient temperature instead of liquefied gas thermal effects are avoided which reduces the complexity of the dispersion process. The instrumentation of the field allowed to determine the development with time of the cloud dimensions and the concentration distribution in the cloud, as well as additional quantities relevant for model validation, in particular the turbulence structure within the cloud and in the ambient atmosphere. In the majority of the tests the cloud was released over uniform, unobstructed ground, but in several tests also the effect of simple types of obstructions (permeable fence, impermeable fence, cubical building) was investigated.

Within project 14B an advanced image processing method has been applied in order to refine the visual records of the Thorney Island tests.

Within project 3B the principal differences and restrictions of the various existing models were analysed with the intention to improve the understanding of the dispersion mechanisms and to reduce the uncertainties in prediction. In addition, a refined computer model was developed.

Within project 9B, after implementation of some 10 gas cloud dispersion models of different type and refinement on a computer, computations were performed with the boundary and initial conditions of the experimental tests to allow for validation of the models and for an assessment of their respective domains of application.

#### Explosion development

The pressure wave which is generated during explosion after ignition of the cloud can be evaluated by gasdynamic relations if the time history of the flame front propagating through the cloud is known. Accordingly, the main objective of the experimental work in the field of explosion development has been to obtain information about the acceleration mechanisms and the resulting flame speed in special configurations of unconfined and partially confined clouds. Certainly, only a limited number of configurations could be investigated within the scope of the program. The theoretical work was mainly directed to the development of explosion codes which enable to compute the generated pressure wave if the time history of the flame front (flame path) is known.

The aim of project 10B, the largest in the field of explosion development, was to determine experimentally the deflagration properties of unconfined hydrocarbon-air mixtures in spherical symmetry (balloon experiments). Main emphasis was placed on the question how much the flame is accelerated and the explosion pressure accordingly is enhanced in clouds with discontinuities in concentration. The arrangement used for studying this problem

consisted of two concentric balloons containing mixtures of different concentration. Furthermore, the influence of ignition energy on flame speed was investigated. This was done by reinforcing the electrical igniter by a variable mass of explosive up to a value inducing detonation.

Work within project 12B was partly theoretical, partly experimental. The theoretical work was concerned with the validation of one-dimensional codes for the computation of the generated pressure wave (based on measurements of flame path and pressure wave in the explosion experiments of project 10B) and with the evaluation of the suitability of one-dimensional methods to model multidimensional explosions, in particular flat cloud explosions. In the experimental part of work flame acceleration in special configurations with repeated obstacles was investigated.

In project 6B available experimental and theoretical results on fast deflagrations, in particular the results of the German PNP safety program, were analysed in order to find out the conditions for a transition from deflagration to detonation.

In project 8B deflagration in a special situation, the wake flow behind obstacles, was studied experimentally. For this situation large flame acceleration is expected due to the presence of large-scale turbulence.

#### Pressure wave propagation, interaction with structures

For evaluation of the structural response of a nuclear power plant to gas cloud explosion loading the pressure field resulting from interaction of the free-field pressure wave with the structures is needed as input. Accordingly, methods have to be provided which allow to evaluate possible modifications of the free-field pressure wave during its propagation from the gas cloud to the power plant and, in particular, the enhancement of peak pressure due to interaction of the free-field wave with the structures.

In project 1B existing one-dimensional computer models were used to conduct parametric studies of the factors which influence the pressure and velocity fields generated by gas cloud explosions. Herewith the range of possible overpressures produced by gas cloud explosions and the interaction of the pressure field with rigid boundaries was explored. In addition a two-dimensional code capable of modelling the pressure wave interaction with structures was developed.

In project 11B experimental investigations were carried out on the influence of uneven terrain and of inhomogeneous atmosphere on the propagation of the pressure wave.

Finally, in projects 7B and 13B methods were developed which allow to determine the loading pressure field resulting from the interaction of the free-field pressure wave with the power plant structures. In each of the two projects a three-dimensional computer code based on the acoustic approximation of the wave equation was developed. Moreover, an experimental method for two-dimensional simulation of the interaction, based on the analogy

between free surface hydraulic shock waves and shock waves in gases, was developed.

## PRINCIPAL RESULTS

### Cloud formation and spreading

In the Thorney Island large scale tests a large body of experimental data on the dispersion of heavy gas clouds at different meteorological conditions and different initial gas densities has been obtained. Altogether 26 tests have been performed (16 releases over uniform, unobstructed ground, 10 releases with obstructions present). The initial density of the heavy gas relative to air ranged from 1.4 up to 4.2, the wind speed from 1.4 m/s up to 9 m/s, and the atmospheric stability from category B to category F on the Pasquill scale. The acquired data comprise global data, such as the time-dependent dimensions of the flammable part of the cloud in downwind, upwind and transverse direction, as well as local data, such as the distribution of concentration, flow velocity and level of turbulence within the cloud.

Only a minor part of the Thorney Island data has been exploited so far. The validation of analytical models within project 9B using the experimental data has led to a classification of these models with respect to their performance in predicting dispersion. Satisfactory agreement between predictions and measured values over the whole range of meteorological conditions can obviously be attributed to only a few of the models.

The dispersion models that have been assessed within project 3B range from simpler analytical models ("box" models) by which only the overall behaviour of the dispersing cloud is predicted, to complex three-dimensional hydrodynamic models. The comparison of the models exhibits that the predictions of cloud dispersion for a given scenario differ widely. The reasons for the large differences in prediction have been identified, the main reason being the different treatment of turbulence and of its effect on dilution rate. Apparently, for the three-dimensional hydrodynamic codes the uncertainty of predictions is of the same order of magnitude as for the simple box models.

### Explosion development

The balloon experiments on the deflagration properties of unconfined hydrocarbon-air mixtures within project 10B have shown that discontinuities in gas concentration give rise to considerable flame acceleration. On the average an increase of flame speed by a factor of 1.5 and of explosion pressure by a factor between 2 and 3 was observed. Even small disturbances, like the turbulence generated in the mixture by the removal of the balloon envelopes, may lead to flame acceleration. The increase of ignition energy by means of an explosive charge up to a value at which detonation is induced has been shown to result in an increase of flame speed by a factor of about 2.5. The maximum values of flame speed and overpressure observed in the experiments of project 10B were 30 m/s and 20 mbar. Accordingly, although the relative increase of flame speed and overpressure appears to be quite

large the absolute values of flame speed and overpressure that may be attained through these effects in unconfined clouds remain far below those which could be hazardous to a nuclear power plant.

The same statement (large relative increase of flame speed and overpressure, but absolute values still rather low) holds also for the effects of repeated obstacles present in the cloud. This has been demonstrated by the experiments of project 12B where an increase of flame speed up to 50 m/s was observed, with a maximum overpressure of about 25 mbar. On the other hand, when a closed plate was placed over the array of obstacles the flame speed increased up to 420 m/s, with a peak overpressure of 750 mbar. It may be inferred from these findings that overpressures which would constitute a hazard to nuclear power plants, i.e. overpressures of the order of 0.1 bar or more, will be generated only if the cloud is partially confined.

Large-scale turbulence in the wake flow behind obstacles as investigated in project 8B also leads to significant flame acceleration. However, this requires large initial flow velocities in the unburned mixture, which is conceivable only for very special situations.

The assessment of experimental and theoretical results on fast deflagrations within project 6B has produced a set of criteria by which the susceptibility of gas cloud scenarios to a transition from deflagration to detonation can be estimated.

The validation of explosion codes in project 12B using the experimental data obtained in project 10B has demonstrated the suitability of the codes for modelling the explosion of spherical clouds and of flat clouds. It must be kept in mind, however, that computation of the generated pressure wave by these codes requires that the time history of the flame front is known.

#### Pressure wave generation, interaction with structures

By the parametric studies conducted in project 1B with available codes the influence of material properties (reaction energy, density and expansion ratio of the gas) and of flame speed on pressure generation has been elucidated. Certainly, the problem remains which figures are, in practical cases, to be assigned to the flame speed as this parameter depends strongly on the structure of turbulence in the particular configuration.

The investigations in project 11B have shown that the propagation of the pressure wave in air is, within the experimental error, not influenced by uneven terrain and by inhomogeneous atmosphere.

The loading pressure field at the reactor building due to interaction of the incident pressure wave with the assembly of plant buildings may be very complex. Considerable enhancement of peak overpressure may occur in corners, yards or lanes between buildings due to wave focusing and multiple reflections. The three-dimensional computer codes for the loading pressure field developed in projects 7B and 13B have been validated in the following way: by comparison with analytical solutions for



simple cases, by use of experimental data from tests in which models of the reactor building and the fuel building of a French nuclear reactor were impacted by the pressure wave generated by a high explosive charge (project 7B), and by use of data obtained with the method developed for experimental simulation of the interaction process (project 13B). The predictions of the codes are in fair agreement with the data used for validation. Because the codes are based on the linear wave equation, application is restricted to pressure levels of the incident wave up to about 0.2 bar. For complicated geometry the costs for running the codes may be considerable, hence the main field of application of the codes will be the evaluation of the pressure field for few selected cases. The experimental simulation method developed in project 13B is suitable in particular if the dependence of the pressure field on various parameters (e.g. shape of the incident wave, angle of incidence, arrangement of buildings) is to be explored.

#### MAIN CONCLUSIONS

Significant progress has been made in the overall problem of estimating the possible impact of gas cloud explosions on a nuclear power plant. The main conclusions may be summarized as follows:

- Heavy gas dispersion is distinctively different from passive dispersion, even for small density differences. The explosive cloud formed by a large release of hydrocarbons will be very flat and will accordingly have large horizontal dimensions. Existing models differ significantly, which means that the uncertainty of predictions for large-scale releases is still considerable. The effect of obstructions has scarcely been attached so far.
- In situations where the cloud is unconfined or only slightly confined the overpressure generated in the explosion will be small (below 0.1 bar). This statement holds for homogeneous clouds as well as for clouds with discontinuities in concentration.
- Fast deflagrations with flame speeds above 100 m/s and overpressures above 0.1 bar will result only if during explosion the cloud is in a highly turbulent state. This requires that either the initial turbulence is large (e.g. due to jet release from pressurized containers or due to jet ignition) or that the configuration is favourable for large production of turbulence during the explosion process itself. The latter will be the case in particular if repeated obstacles and, in addition, structures which provide partial confinement are present in the cloud. Of course, the sensitivity for the appearance of a fast deflagration will also depend on gas concentration in the cloud.
- Predictions of explosion development in configurations with obstacles and partial confinement are, at the time being, far more uncertain than predictions of gas cloud dispersion. This is due to principal difficulties in modelling the strong coupling between the gasdynamic flow field and the burning rate (turbulent flame velocity, flame area) in fast deflagrations.

Only a rough classification of hazardous configurations which may occur in practice can be given at present. There is a need for additional research in this field in order to improve the existing methods for explosion hazard evaluation.

- The loading pressure field which results from interaction of the incident pressure wave with the power plant structures can be predicted satisfactorily, at least up to overpressures of 0.2 bar, by use of the computer codes and the experimental simulation method developed. Considerable enhancement of peak overpressure may occur at specific locations of the nuclear power plant due to wave focusing and multiple reflections.

#### ACKNOWLEDGMENT

The author wishes to express his gratitude to the project leaders for providing summarized information on the scope of work and the most important results of the individual projects.

PHYSICAL INSIGHT IN THE EVALUATION OF JET FORCES  
IN LOSS OF COOLANT ACCIDENTS

G.P. Celata, M. Cumo, G.E. Farello, P.C. Incalcaterra

ENEA - Casaccia, Heat Transfer Laboratory  
Via Anguillarese, 301, Rome - Italy

R. Centi

Ansaldo Impianti, Genova, Italy

ABSTRACT

With reference to Loss of Coolant Accidents in LWR's, and particularly Small-Break LOCAs, a picture of the issuing two-phase jets is given.

Experimental data and evaluations concerning critical flows of subcooled and saturated liquid, together with saturated steam data are shown.

The analysis refers to the unbounded region of the discharge, considering:

- a) the jet external shape;
- b) the internal pressure and temperature distribution;
- c) the phases distribution.

Experimental data are obtained, employing two facilities of different scale, JF.1 and JF.2, by means of:

- a) photographic devices;
- b) a movable pressure and temperature gauge travelling inside the issuing jet;
- c) an X-rays device.

INTRODUCTION

The work described in the present paper deals with a research program developed in the frame of ENEA - A.I. Association Contract related to the problems of jet impingements following a high energy pipe break. Such a work is part of a wider research program still in progress at Heat Transfer Laboratory, ENEA, Casaccia, devoted to the improvement of the knowledge in the field of two-phase critical flows, particularly from the viewpoint of flow pattern and thermal-fluid-dynamic behaviour inside the discharge channel and in the unbounded jet /1, 6/.

The object of the present paper deals with the analysis of the issuing jet due to a pipe break in a pressurized system, mainly aimed to structures design of safety feature to be employed in Italian nuclear power plants. The full vessel blowdown has been examined:

- two-phase jets of initially subcooled water;
- two-phase jets of initially saturated water;
- single-phase jets of saturated steam.

The issuing unbounded jets have been investigated in their external shape by means of photographic devices, and inside them by measuring the pressure and temperature profiles both radially and axially by means of a movable pitot equipped with a thermocouple.

Besides the aim of the above mentioned investigations is also the formulation of a computer code, which turns out to be of general validity. The code, regarding to three well defined stages of

the research, should enable the prediction of the full evolution of the fluid, and exactly /8, 11/:

- a) modeling of two-phase critical flow discharge through tubes (prediction of critical mass flowrate, pressure and temperature profiles along the discharge channel);
- b) modeling of unbounded jet expansion region (prediction of jet external width, pressure and temperature profiles inside the jet, density and phase distribution);
- c) modeling of two-phase flow jet impingement forces against external objects.

#### THE EXPERIMENTAL APPARATUS

The experimental apparatus consists of two facilities each completely independent from the other, with different scale, geometry and philosophy: JF.1 and JF.2.

The JF.1 plant, in smaller scale, is schematically represented in fig. 1. The capacity of each of the two vessel is about 100 litres, and the heating power is 10 kW. The liquid containment is made up by the two vessels, one of which,  $S_1$ , is filled to capacity with degased water simulating the reactor pressure vessel.

The second one,  $S_2$ , is partially filled with cold water and connected, as a pressurizer, to  $S_1$  in order to allow subcooled discharges from the vessel  $S_1$ .

During the test, the heated water flows from the top of the vessel  $S_1$ , while the cold water of the pressurizer  $S_2$ , enters the bottom of  $S_1$ , through a turbine flow rate transducer. In the case of saturated liquid or steam discharge, the flow rate measurements are obtained by collecting the issuing fluid with an ice filled container, and by weighing the fluid discharged in a given time.

The employed test sections consist of straight tubes instrumented with pressure taps and thermocouples. Their geometry varies both in inner diameter ( $D = 1.63$  mm and  $4.61$  mm) and the ratio  $L/D$  (10, 100, 300).

The JF. 2 loop is represented in fig. 2. The capacity of the vessel is 160 litres and the heating power is 20 kW. The critical mass flowrate is measured, in the case of liquid discharge, by means of a special turbine flow-meter placed on the connection tube to the test section downstream the quick opening valve.

The employed test sections consist of straight tubes instrumented with pressure taps and thermocouples. Their geometry replies the previous ones concerning the  $L/D$  values, while the inner diameter is 12.5 mm.

#### EXPERIMENTAL RESULTS AND DATA ANALYSIS

##### Two-Phase Jets of Initially Subcooled Water

Photographic recording of the two-phase jets shape, as well as the detection of pressure and temperature distribution within the issuing jets, are considered in connection with the current stagnation condition. The analysis of the issuing two-phase jet shape has been particularly aimed at the study of the inlet subcooling and the discharging channel geometry influence on the jets characteristics.

In fig. 3 the non dimensional jet's width ( $\delta/D$ ) is plotted versus inlet subcooling for different diameters and ratio  $L/D$ . The diagrams show that, starting from the saturated condition and increasing the inlet subcooling, the jet first enlarges up to a maximum width, then becomes tighter and thigter, at values smaller than those corresponding to saturation conditions.

That behaviour is a general trend of all the experimental tests. An explanation may be attempted taking into account the ratio between the radial and the axial depressurization rate, and the consequent flashing of the issuing two-phase jet, essentially due to the tri-dimensional vaporization taking place in the unbounded region.

The emerging fluid particles have different exit velocities and enthalpies according to the subcooling conditions in the vessel, and undergo a strong acceleration both radially and axially. A rough estimation of the order of magnitude of radial and axial velocity components in the issuing jet is provided by the sketch in fig. 4, from which it appears that the radial velocity component may exceed the axial one. The evaluation of the outlet steam quality versus the inlet subcooling is shown in fig. 5. Decreasing the inlet subcooling, the thermal energy spent in the discharging channel owing to vaporization increases according to a more than a linear trend. The velocity of the mixture is higher for the saturated discharge as well as the critical pressure, but the mass flowrate is lower, and it increases with the inlet subcooling (fig. 6). The two opposite trends may be the responsible of the resulting jet shape and of the maximum jet width. Besides, for short test sections ( $L/D < 30$ ), in which, because of non-equilibrium effects, very little or no vaporization takes place, the trend of the jet external width versus inlet subcooling does not exhibit any maximum amplitude in the silhouette.

Referring to fig. 3, the channel length effect seems to be negligible while the channel inner diameter seems to show a more significant influence.

Typical pressure distribution profiles within the jets, detected at various distances from the outlet section are reported in fig. 7, together with the jet external width, as measured from jets' silhouette. Comparing the photographed jet diameter with that obtained with pressure transducers, it appears that only a fraction of the jet total area (close to one half) contributes practically to a jet force against external objects.

To allow an actual formulation of the jet expansion model, further information about the phases' distribution inside the jet are needed. To have a look inside the non-transparent cone of condensing steam, a series of pictures are taken employing an X-rays device. The research, in progress, will give densities distribution by means of X-rays attenuation measurements. In fig. 7a) it is possible to remark the big difference between the low density quick enlargement in comparison with the small shape of the central high density core.

In fig. 8 a comparison between JF.1 and JF.2 results is shown, as far as the pressure reliefs inside the jets, are concerned for  $L/D = 10$  and  $100$ , with  $D = 4.6$  mm (JF.1) and  $12.5$  mm (JF.2). The scale effect looks almost negligible.

### Two-Phase Jets of Initially Saturated Water

The two-phase jet of saturated water is analyzed in the figs. 9 through 11. In fig. 9 typical pictures of a saturated liquid jet are reported. The size of the jet width depends, of course, on the stagnation pressure.

In the following fig. 10 typical pressure and temperature profiles within the jet, detected at various distances from the outlet section, are represented. They show the pressure and temperature decay inside the jet against the distance from the exit section.

In fig. 11 it is plotted a comparison between JF.1 and JF.2 results, with regard to the pressure peaks within the jets, for  $L/D = 100$  and  $300$ , with  $D = 4.6$  mm and  $12.5$  mm. In this case too, the scale effect turns out to be completely negligible.

### Jets of Saturated Steam

The behaviour of the issuing jets of saturated steam is shown in the figs. 12 through 14. In fig. 12 typical pictures of saturated steam jet are reported. It is possible to notice that the saturated steam jet does not exhibit the strong enlargement typical of the two-phase jets. Such behaviour is essentially due to the quick vaporization taking place as soon as the two-phase mixture comes out from the break.

In fig. 13 typical temperature and pressure profiles within the jet, detected at various distances from the outlet section, are shown. Although the presence of two lateral peaks is not easily explaina-

ble, it can be said that such behaviour seems to be typical of gas jets. Experimental data with gas jets, carried out at the Aeronautical Research Associates of Princeton, NU, /7/, are very similar to those presented in this paper, also as far as the pressure peak decay along the jet axis is concerned (fig. 14).

#### CONCLUSIONS

With the aim of developing a computer code enabling the prediction of the unbounded jet expansion region in a two-phase critical flow discharge, an experimental investigation on two-phase critical discharges, with particular regard to the issuing jet, has been performed.

Some of the results, obtained with two loops of different scale are shown, while the computer code development is in progress.

#### ACKNOWLEDGEMENTS

The authors wish to thank Mr. G. Cipolla, Mr. G. Farina, Mr. A. Lattanzi and Mr. O. Levati, who performed all the experimental runs.

## REFERENCES

- / 1/ G. P. CELATA, M. CUMO, G. E. FARELLO, P. C. INCALCATERRA - Efflussi Critici di Vapore Saturo - XXXVI Congresso Nazionale ATI, Viareggio 5-9 Ottobre 1981.
- / 2/ G. P. CELATA, M. CUMO, G. E. FARELLO, P. C. INCALCATERRA - Thermodynamic Disequilibrium in the Critical Flow of Subcooled Liquids. Nuclear Technology. Vol. 60, pag. 137-142, 1983.
- / 3/ G. P. CELATA, M. CUMO, G. E. FARELLO, P. C. INCALCATERRA - Critical Flows and Jet Forces, ENEA, RT/ING (82) 18.
- / 4/ G. P. CELATA, M. CUMO, G. E. FARELLO, P. C. INCALCATERRA - Metastability Delays in Critical Flows. I Congresso Nazionale UIT, Trieste 24-25, Giugno 1983.
- / 5/ G. P. CELATA, M. CUMO, F. D'ANNIBALE, G. E. FARELLO, P. C. INCALCATERRA - Two-phase Boundary Layers in Critical Flows. Colloque Euromech 176, Grenoble, 21-23 September 1983.
- / 6/ G. P. CELATA, M. CUMO, G. E. FARELLO, P. C. INCALCATERRA, R. CENTI - Critical Flow Jets Investigations for Engineering Applications. 3rd Multiphase Flow and Heat Transfer Meeting, University of Miami, 18-20 April 1983.
- / 7/ C. P. DONALDSON, R. S. SNEDEKER - A Study of Free Jet Impingement Part. 1. Mean Properties of Free and Impinging Jets. J. Fluid Mech. (1971), vol. 45 pp. 281-319.
- / 8/ F. DOBRAN - Modeling of Critical Flow Discharge through Pipes and Jet Expansion. Research Proposal ME - 84 - 12, Stevens Institute of Technology, NJ, November, 1983.
- / 9/ F. DOBRAN - Modeling of Critical Flow Discharge through Tubes and Jet Expansion Region. Progress Report to ENEA, ME - RT - 84003, Stevens Institute of Technology, NJ, March, 1984 (Classified).
- /10/ F. DOBRAN - A Nonequilibrium Model for Two-phase Critical Flow Analysis in Variable Area Duct. Progress Report to ENEA, ME - RT - 84005, Stevens Institute of Technology, NJ, June 1984 (Classified).
- /11/ F. DOBRAN - Two-phase Flow Jet Impingement Forces. Research Proposal, Stevens Institute of Technology, NJ, October, 1984.

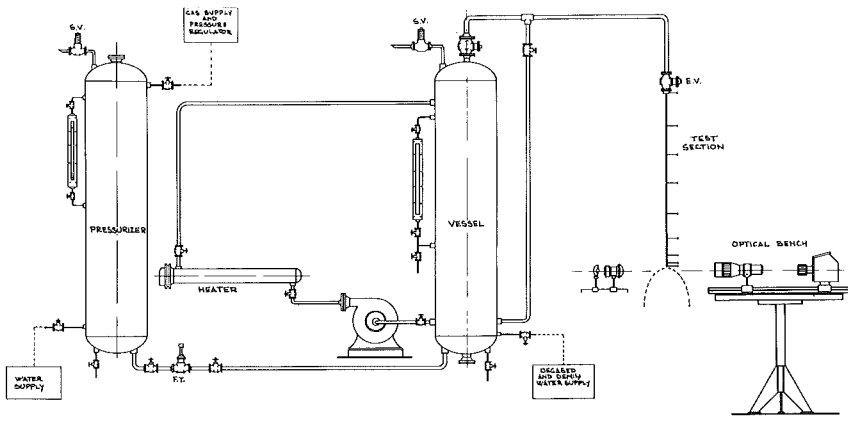


Fig. 1 - Sketch of JF.1 loop

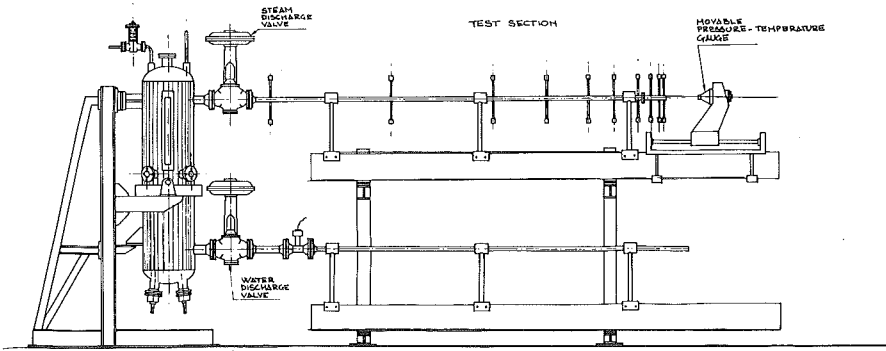


Fig. 2 - Sketch of JF.2 loop



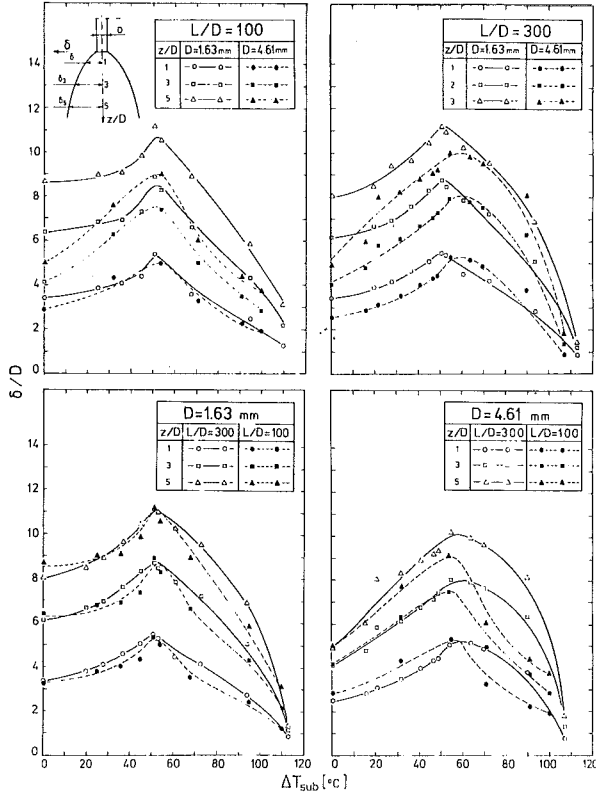


Fig. 3 – Jet external width versus inlet subcooling

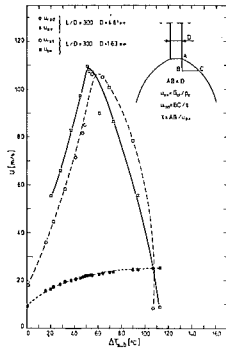


Fig. 4 – Order of magnitude of radial and axial velocity components of the emerging fluid particles at the periphery of the outlet section

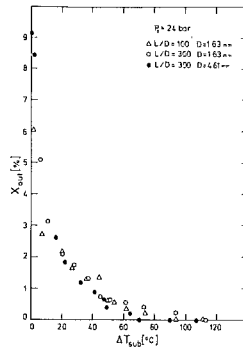


Fig. 5 – Outlet steam quality versus inlet subcooling for three test section geometries

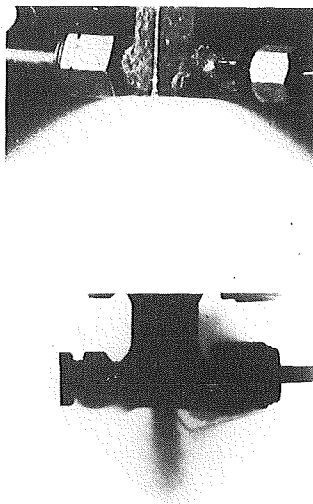
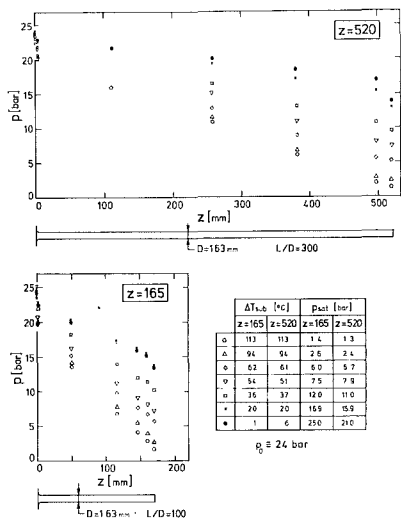


Fig. 6 – Typical pressure profiles along the discharge channels at different inlet subcoolings

Fig. 7a– Typical X-rays pictures of the jets

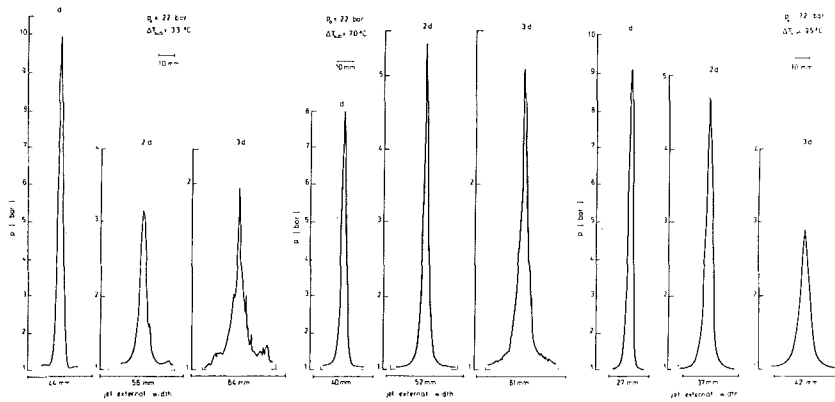


Fig. 7 – Typical pressure profiles within the jets for initially subcooled liquid

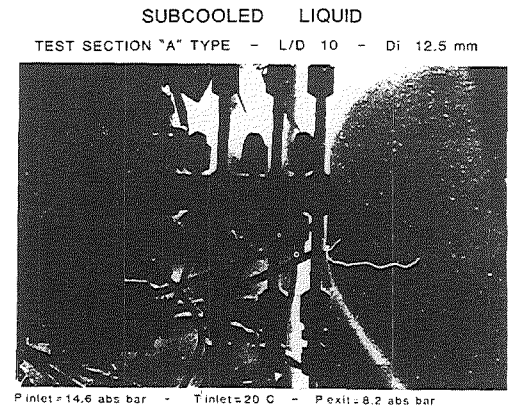
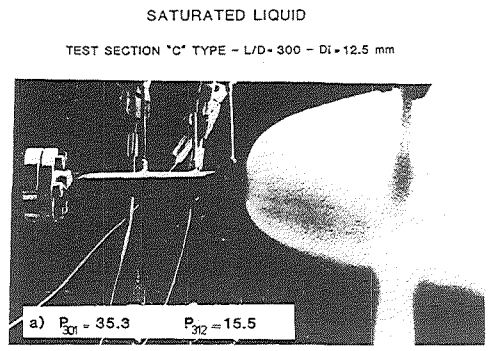
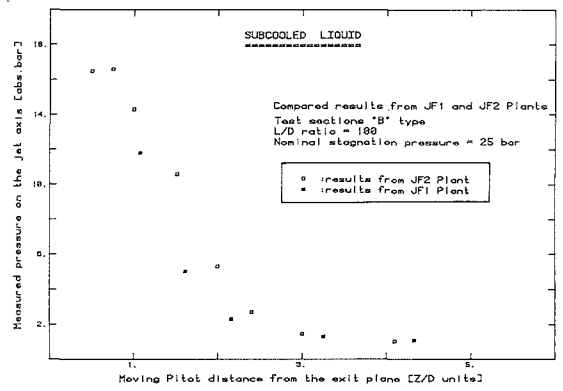
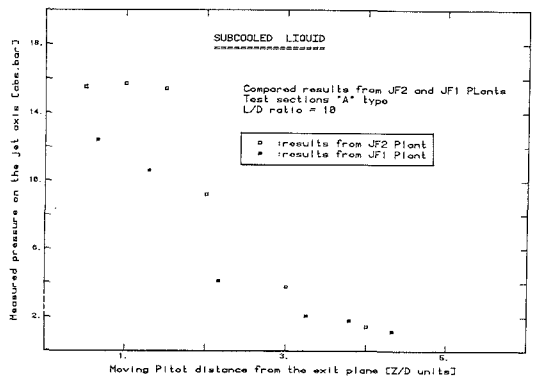


Fig. 8 - Compared results from JF.1 and JF.2 facilities: measured pressure peaks on the jets axis

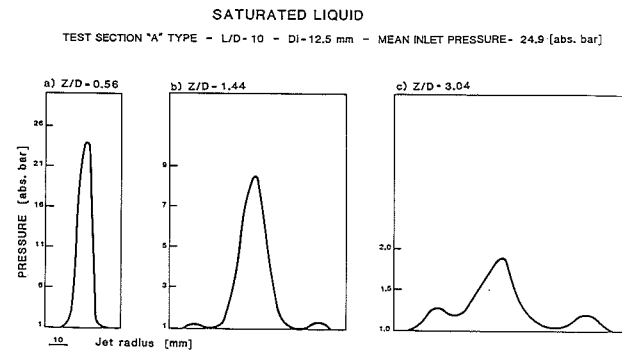
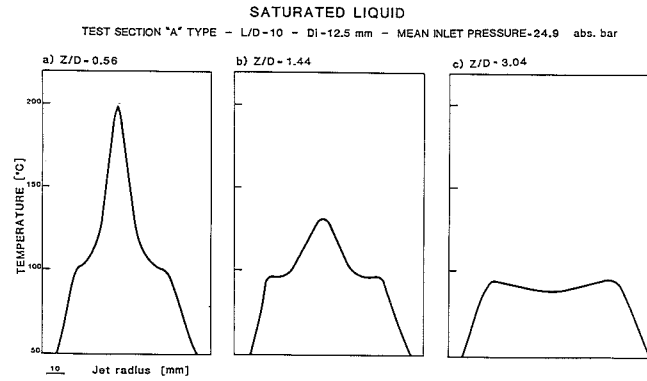


Fig. 10 – Typical temperature and pressure profiles within the jets for initially saturated liquid

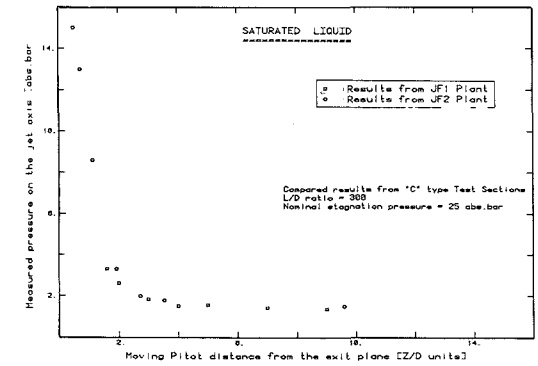
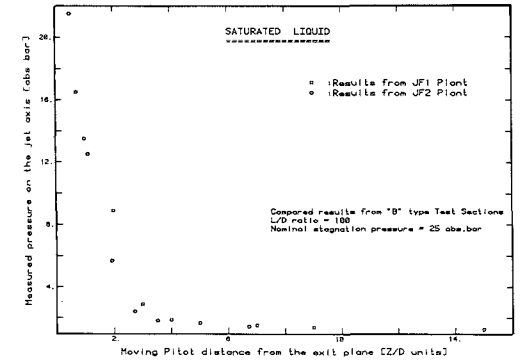
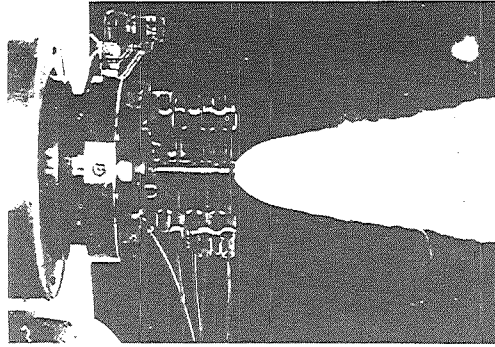
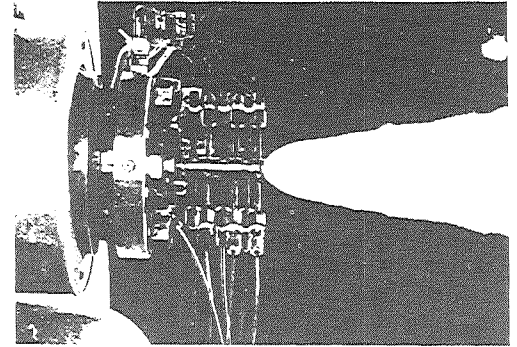


Fig. 11 – Compared results from JF.1 and JF.2 facilities: measured pressure peaks on the jet axis

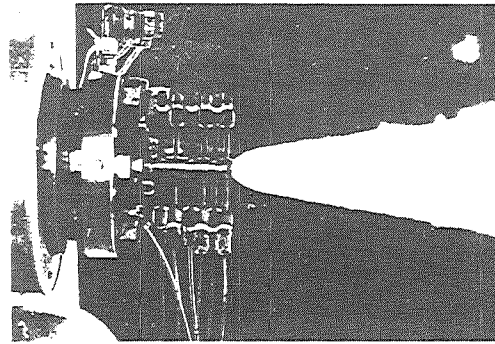
SATURATED STEAM  
TEST SECTION "A" TYPE - L/D=10 - Di=12.5 mm



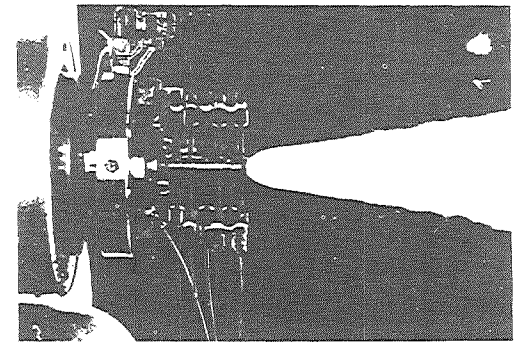
P inlet = 24.7 abs.bar  
P out = 10.0 abs.bar



P inlet = 18.7 abs.bar  
P out = 7.7 abs.bar



P inlet = 12.5 abs.bar  
P out = 5.3 abs.bar



P inlet = 10.5 abs.bar  
P out = 4.4 abs.bar

Fig. 12 - Photographic jet reliefs of saturated steam

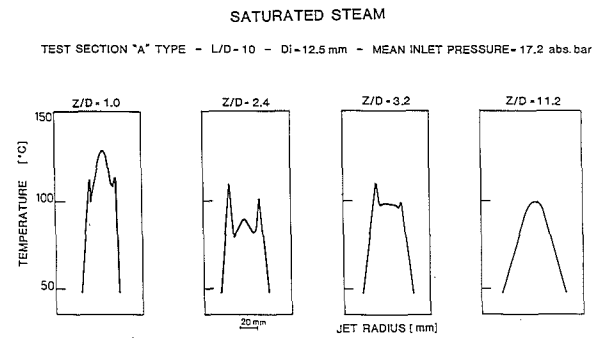
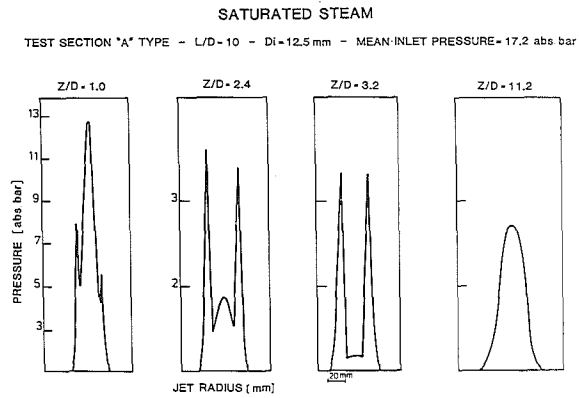


Fig. 13 - Typical pressure and temperature profiles within the jets for saturated steam

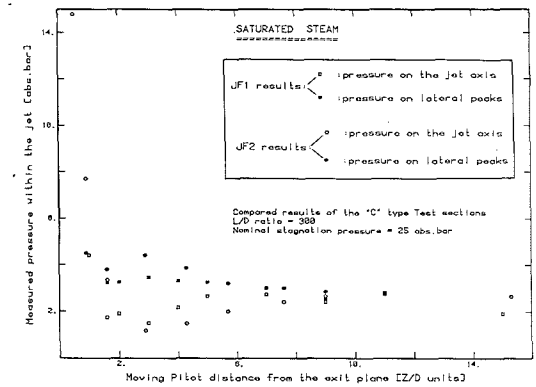
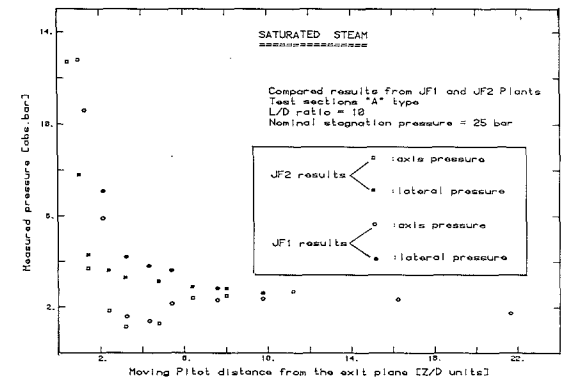


Fig. 14 - Compared results from JF.1 and JF.2 facilities: measured pressure peaks on the jet axis

## CRITICAL FLOW THRU SAFETY VALVES

A. Singh

Electric Power Research Institute, Palo Alto, California 94303, U.S.A.

D. Abdollahian

S. Levy Incorporated, Campbell, California 95008, U.S.A.

## ABSTRACT

Full scale data for critical mass flow thru safety valves have been correlated using simplified choked flow models. The test data covered a wide range of operating and accident conditions including single phase steam, water and two-phase flow. Flow data for five different valves of various types and sizes has been analyzed to determine flow discharge coefficients and appropriate critical flow models to predict valve discharge capacity. For the steam flow conditions, both the HEM and the Modified Napier's method, which includes a correction for the high pressures (>1500 psia) agrees reasonably well with the data. Comparisons against limited amount of applicable data available for subcooled water flow conditions indicates the importance of ability to predict the actual valve lift which directly affects the choke flow area and the resulting mass flow.

## INTRODUCTION

High pressure vessels in nuclear and other industries are protected against overpressure by spring-loaded safety valves and power operated relief valves. The safety valves are designed to open when the system pressure exceeds a specified value called the set pressure. Fluid discharge following the valve opening causes the system pressure to fall which subsequently reduces the upward forces acting on the valve disc to keep it open. The valve is expected to close when the pressure falls below a certain minimum value called the blowdown. The safety valves are designed for steam discharge, but under certain transient situations they may be exposed to liquid upstream conditions with a varying degree of subcooling.

The system depressurization following the valve opening is dictated by the discharge capacity of the valve. The flow through the valve will be choked or critical for a majority of the operating conditions involving single phase steam flow and generally this flow rate is determined from simple empirical relations along with a manufacturer provided discharge coefficient. However, during off normal conditions following an accident or plant transient, subcooled water or two phase conditions may exist upstream of the valve. In general, flow capacity of safety valves is not known under these off normal conditions. A series of full scale tests on a number of safety valves representing the valve population in PWR plants have been performed at the C.E./EPRI test facility [1].

The EPRI tests demonstrated that for most of the steam tests the valves popped open when the tank pressure was within  $\pm 3\%$  of the valve set pressure and operated under stable conditions. Only a few steam tests with long inlet configurations resulted in unstable valve operation. Most of the saturated water tests were stable and only under subcooled upstream conditions some chatter was observed. Since the measured inlet fluid conditions and the valve choking area cannot be accurately specified during the valve unstable behavior, only the tests which showed stable valve operation were used for correlating the discharge flow versus upstream conditions in the present study.

Six of the seven safety valve designs tested at the Combustion Engineering facility, were spring-loaded safety valves. Two of the safety valve designs were identical except for the material used for the internals (Crosby 3K6 valve with steam or loop seal internals). No measurement of flow was made for the Crosby 6N8 valve, hence it was not included in the present analysis. The Target Rock 69C is actually a pilot operated safety valve and the main disc stem position for this valve was not measured. The set pressure, stamped rated flow and lift, and the orifice area for these valves are listed in Table 1.

In the present study, the data from these tests were used to evaluate the common methods for determining the valve discharge capacity under a wide range of conditions and a discharge coefficient was established for every valve using the most appropriate calculational scheme.

Table 1  
SAFETY VALVE DESCRIPTION

Safety Valve	Orifice Area (in <sup>2</sup> )	Design Set Pressure (Psig)	Rated Flow (lb/hr)	Rated Lift (in)
Dresser 31739A	2.545	2500	297,845	0.45
Dresser 31709NA	4.340	2500	507,918	0.588
Crosby 3K6	1.841	2485	212,182	0.382
Crosby 6M6	3.644	2485	420,006	0.538
Target Rock 69C	3.513	2485	345,000	Not applicable

#### CRITICAL FLOW MODELS SELECTED FOR COMPARISON WITH THE VALVE DATA

##### a) Single-Phase Critical Flow Relations

Given the stagnation pressure and temperature,  $P_o$  and  $T_o$ , and assuming an isentropic flow between the stagnation and the choked plane, the critical mass flow is obtained from the application of acoustic velocity relation at the throat, i.e.,

$$G = \sqrt{\frac{K}{R} \left(\frac{2}{K+1}\right)^{\frac{K+1}{K-1}} \frac{P_o}{T_o}} \quad (1)$$

where  $K$  is the isentropic exponent and  $R$  is the universal gas constant. There are some approximate models for critical steam flow which are discussed below:

Napier's Formula, [2]: This is an approximate equation for critical discharge of saturated steam expressed as:



$$W = \frac{A_c P_o}{70} \quad \text{Napier's Formula} \quad (2)$$

where  $P_o$  is in psi,  $A_c$  is in square inches, and  $W$  is in Lbm/sec. This relation was originally intended as a rough check for critical flow of saturated steam through orifices but has been widely used for different conditions.

Grashof's and Rateau's Formulas [2]: These are also approximations for critical flow of saturated steam but are supposed to be applicable to well rounded convergent orifices:

$$W = 0.0165 A_c P_o^{0.97} \quad \text{Grashof's formula} \quad (3)$$

$$W = A_c P_o (16.367 - 0.96 \log P_o) / 1000 \quad \text{Rateau's formula} \quad (4)$$

Where  $P_o$  is in psia, the choking area,  $A_c$ , in square inch, and  $W$  in Lbm/hr.

The ASME Boiler and Pressure Vessel Code [3] uses Napier's equation in the following form for the capacity rating of the pressure relief valves:

$$\begin{aligned} W_T &= 51.5 A_c P \\ W &= 0.9 C_D W_T \\ A_c &= \text{Valve nozzle area (in}^2\text{)} \\ P &= (1.03 \times \text{set pressure}) + 14.7 \text{ (psia)} \end{aligned} \quad (5)$$

$C_D$  is the coefficient of discharge and  $W$  is in Lbm/hr in the above equation. The procedure for specifying the discharge coefficient,  $C_D$ , requires testing model valves with three different sizes and carrying at least three tests for every size. The resulting discharge coefficients are to be averaged to give  $C_D$  for the above equation. Note that the theoretical mass flow rate,  $W_T$ , is the same as Napier's equation (with the coefficient of 51.5 instead of 51.43) and the pressure is a specified function of the valve set pressure.

Among the above relations, Napier's equation is widely used in the industry and certain correction factors [4,5] have been developed recently which improve the predictive capability of Napier's relation. Thompson and Buxton's [4] correction factor for high pressure is included in the present ASME Boiler and Pressure Vessel Code and will be discussed later.

It should be noted that the single-phase models will be valid as long as the expansion from stagnation to throat results in single-phase condition at the throat. Otherwise, a two-phase critical flow model should be used for predicting the discharge flow rate through the valve.

#### b) Two-Phase Critical Flow Models

Previous studies of flow through power operated relief valves [6,7] have shown that for liquid upstream conditions the nonequilibrium models of Henry-Fauske [8] and Burnell [9] resulted in good agreement with data if used along with the single-phase liquid discharge coefficient. The Burnell model was

recommended since it has a closed form relation and does not require any iteration. For steam upstream conditions when expansion to exit resulted in two-phase flow, the homogeneous-equilibrium model [10] is used. These models are well known and will not be further discussed.

#### CRITICAL FLOW PREDICTIONS THROUGH SAFETY VALVES

##### a) Steam Upstream Conditions

As mentioned earlier, the safety valves are primarily designed for over-pressure protection under steam upstream conditions. Since, the safety valves are generally designed to open full under these conditions, the predictive capability of the critical flow models at full open position is of importance. Therefore the valve flow rate has been correlated for the full open period of the tests when choking occurs at the valve nozzle.

The single-phase equations apply as long as the isentropic expansion from the stagnation to choked plane does not result in steam condensation. During the expansion from stagnation to throat, the fluid conditions change and an accurate critical mass flux using equation (1) is obtained only if the variation of isentropic exponent is accounted for. If the expansion results in two-phase conditions at the throat, the single-phase equations are no longer valid and a two-phase critical flow model is required to accurately predict the flow rate.

There are some approximate models for the single-phase critical flow relation which have been proposed for the discharge of saturated steam. These are Napier's, Grashof's and Rateau's formulas, which were discussed in the previous section. Napier's equation is an empirical correlation for critical flow of dry saturated steam and was developed from a series of experiments on converging nozzles. Due to its simple formulation, it has been widely used in the industry and, as mentioned earlier, it is used for the capacity rating of the safety relief valves in the ASME Boiler and Pressure Vessel Code [3].

Thompson and Buxton [4] have compared the predictions from Napier's relation to the isentropic maximum flow results. It has been shown that the Napier's equation overpredicts the maximum isentropic flow between 100 and 1500 psia and underpredicts the same for upstream pressures over 1500 psia. In order to improve the predictions by the Napier's relation a pressure correction factor has been proposed as follows:

$$W = K_n \frac{A P_c}{70}, \text{ where} \quad (6)$$

$$K_n = \frac{0.1906 P_o - 1000}{0.2292 P_o - 1061} \quad 1500 < P_o < 3200 \text{ psia}$$

In the present study a calculational scheme (described later in this section) was used to predict the critical flow rate and to calculate the discharge coefficient by averaging the ratio of the measured to predicted flow rates during the valve full open period. The discharge coefficient accounts for the differences between the valve nozzle area and the actual choking area (Vena Contracta), and the frictional losses.

Theoretically, the pressure disturbances downstream of the choking plane should not travel upstream and affect the critical flow rate. However, the

experiments with nozzles of varying converging angles downstream of the throat have shown an effect of receiver pressure on the critical flow rates except for nozzles with specific shapes and angles. For the complex geometry of the valves, multiple flow separation points and multiple choking is possible. The critical flow is determined by the pressure at the first choking but since the valve geometries are far from the ideal nozzle situation, the back pressure may have some effect on the discharge flow rates. This phenomenon has been observed in the experiments on a model of the safety valve [11] where the critical pressure and flow rate were influenced, although only slightly, by the receiver pressure. The effect of downstream or back pressure on flow rate was observed to be insignificant during the full scale EPRI valve tests. The evaluated discharge coefficients for one of the safety valves tested in the EPRI program showed a variation with the upper guide ring position which demonstrates the effect of internal flow distribution and pressure drop on the critical flow rates.

The calculational scheme used in the present study is discussed in detail in Ref. [7]. It consists of using ideal gas equations when isentropic expansion to throat results in superheated vapor and flow maximization technique if the expansion results in two-phase conditions at the choking section. For the tests performed with saturated steam conditions, the stagnation pressure was input to the model used. The losses between the vessel and the valve were neglected and the vessel pressure was used as the stagnation pressure upstream of the valve. The effect of using the stagnation pressure calculated from the measured velocity and static pressure just upstream of the valve on the predicted flow rates was less than 5% when compared to the predicted flow rates based on the vessel pressure. The average discharge coefficients for the tested safety valves are listed below.

<u>Safety Valve</u>	<u>Average Discharge Coefficient</u>
Dresser 31709NA	1.0
Dresser 31739A	0.98
Crosby 3K6	0.85
Crosby 6M6	0.84
Target Rock 69C	0.86

The discharge coefficients calculated for the Crosby 3K6 valve showed a dependency to the valve ring position. This points to the possibility that the choking may not have occurred at the nozzle throat as the effective flow area at the rings may be slightly smaller than the throat area. Since only two discrete ring positions were included in the test matrix, an average discharge coefficient was used for the calculation of mass flow rates (average discharge coefficients calculated for the two guide ring positions of -55 and -115 notches were 0.95 and 0.76 respectively).

As mentioned earlier, the stem position for the Target Rock valve was not directly measured and the valve full open period had to be inferred from the measured pressure and flow rate histories. Of the four steam tests performed with the Target rock valve, one had multiple openings with sharp peaks and drops in pressure and flow, and the mass flow history of one other test was not representative of full open valve. Therefore only two steam tests which provided stable steam flow under fully open conditions were used for the specification of the discharge coefficient of the Target Rock valve.

Figures 1 to 5 show the rated flows at 3% overpressure and the flow rates calculated from the ASME equation (5) for the range of pressures observed in the

tests. Also shown are the predictions by the proposed calculational scheme and modified Napier's equation (6) using the calculated average discharge coefficients. The rated flows given in Table 1 were used to back out the manufacturer determined discharge coefficient which was used in conjunction with the ASME capacity rating method.

Figures 1 and 2 show that if the manufacturer recommended discharge coefficients and the ASME capacity rating method are used, the data for the tested Dresser valves is underpredicted by approximately 10%. This method is generally employed for the valve capacity specification at 3% accumulation over the set pressure and is used to give a conservative measure of the relieving capacity of the valve. The data for the Target Rock valve is also underpredicted by approximately 14% as shown in Figure 3.

The specified discharge coefficients for the Crosby valves did not always result in a conservative flow prediction as shown in Figures 4 and 5. The predicted flow rates fall between the data points and it is apparent that the manufacturer recommended discharge coefficients are larger than the calculated average values. As noted earlier, the position of the upper ring for the tested Crosby 3K6 valve affected the flow rates and, as shown in Figure 4. A different discharge coefficient may be calculated for each of the tested ring positions but an average value was used since only two settings were tested.

The pressure correction factor  $K_n$  for Napier's equation was evaluated in Ref. [4] by fitting the predictions to the results of HEM. Therefore, the flow rates obtained from the modified Napier's relation match closely with the HEM results. This relation, along with the average discharge coefficients, thus provides a simple method for calculating the critical flow rates through the tested or other valves with similar geometries.

#### b) Liquid Upstream Conditions

In the EPRI test program, the safety valves were tested under liquid upstream conditions with varying degrees of subcooling. Most of the tests with saturated or subcooled water with subcooling less than 50°F were stable. The tests with larger subcooling resulted in valve chatter and the data were not useful for the present analysis. During most of the water tests the valves did not open to a stable full lift and hence stable mass flow data could not be obtained. The reason for the smaller lift is the expansion past the valve nozzle. For steam upstream conditions, the fluid expands upon entering the huddle chamber which results in an upward force on the disc, causing the valve to pop open. For subcooled liquid upstream conditions, sufficient flashing into steam is needed so that the resulting compressible mixture can exert the necessary upward force on the disc when it expands in the huddle chamber. Apparently, for highly subcooled upstream conditions, the pressure drop is not enough to make sufficient steam for this process.

Among all the safety valves tested at the Combustion Engineering facility, only the Dresser 31709 and 31739 had a sufficient number of stable water tests to establish a discharge coefficient. The measured stagnation conditions and discharge flow rates were used to calculate discharge coefficients using homogeneous equilibrium and Burnell models. Study of the fluid flow path within the safety valves shows that the choking location will not be at the valve nozzle for all stem positions. For small lifts when the area downstream of the nozzle gets smaller than the throat area, the choking is expected to occur at some location along the valve seat. The seat inner radius location representing the smallest flow area was selected as the choking area under this condition. A logic was provided in the computer model to select the smaller of

the valve nozzle area and the flow area at the inner seat location as the choking area. For a major portion of the stable water tests, the valve lift was observed to be small enough that the choking occurred at the seat location.

The discharge coefficients using homogeneous equilibrium and Burnell models at different times during five water and/or transition tests for Dresser 31739 and four tests with Dresser 31709 were calculated. The average discharge coefficient for both valves using the HEM and Burnell model was found to be 1.

Figures 6 and 7 show the comparison between the predicted and measured mass flow rates for two tests. Predictions were obtained by using the Burnell model and the annular area between the seat and disc at the inner seat location as the choking area. Also shown are the predictions using the Burnell model with the nozzle area as the choking area. Obviously, the method of predicting the discharge rate with the annular area between valve disc and seat is preferable during valve closing period. Since sufficient data for valve full open period was not available, the reported discharge coefficient of 1.0 will only be valid for portions of the closing transient when nozzle area is larger than the annular area at the seat location.

#### REFERENCES

1. EPRI/PWR Safety and Relief Valve Test Program, Safety and Relief Valve Test Report, EPRI Report to Participating Utilities, April 1982.
2. T. Baumeister, E. A. Avallone, Mark's Standard Handbook for Mechanical Engineers, Eighth Edition, McGraw Hill, 1979.
3. ASME Boiler and Pressure Vessel Code, Section III, Division 1 - Subsection NB, Class 1 Components, ANSI/ASME BPV-III-1-NB, 1980 Edition.
4. L. Thompson, O. E. Buxton, "Maximum Isentropic Flow of Dry Saturated Steam Through Pressure Relief Valves," paper presented at the Third National Congress on Pressure Vessels and Piping, San Francisco, California, June 24-29, 1979.
5. J. W. Sale, "Safety Valve Mass Flow Rate Calculations and Correction Factors," paper presented at the Third National Congress on Pressure Vessels and Piping, San Francisco, California, June 24-29, 1979.
6. D. Abdollahian, A. Singh, "Prediction of Critical Flow Rates Through Power-Operated Relief Valves," Proceedings of the Second International Topical Meeting on Nuclear Reactors, Santa Barbara, California, January 1983.
7. D. Abdollahian, Critical Flow Predictions Through Safety and Relief Valves, EPRI Report NP-2878-LD.
8. R. E. Henry, H. F. Fauske, "The Two-Phase Critical Flow of One Component Mixture in Nozzles, Orifices, and Short Tubes," Journal of Heat Transfer, May 1971, pp. 179-187.
9. J. W. Burnell, "Flow of Boiling Water Through Nozzles, Orifices, and Pipes," Engineering, December 1947, pp. 572-576.
10. F. J. Moody, "Maximum Discharge Rate of Liquid-Vapor Mixtures from Vessels," ASME Symposium Vol. Non-Equilibrium Two-Phase Flows, 1975, pp. 27-36.
11. D. W. Sallet, W. Nasstoll, R. W. Knight, M. E. Palmer, and A. Singh, "An Experimental Investigation of the Internal Pressure and Flow Fields in a Safety Valve," ASME Paper No. 81-WA/NE-19, November 1981.

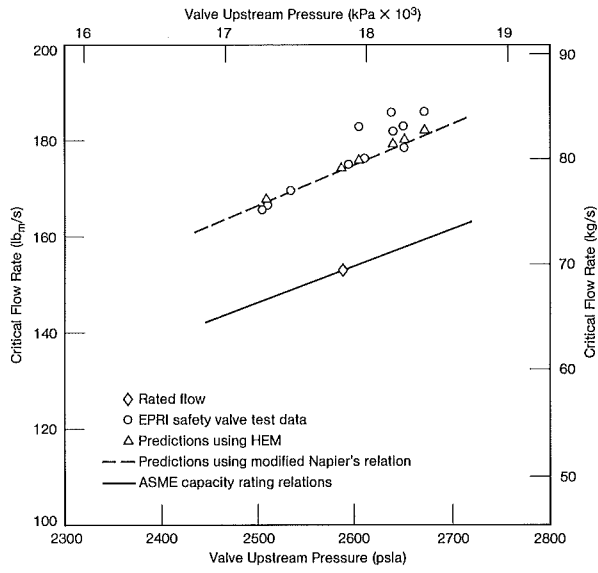


Figure 1 Critical flow rate predictions for Dresser 31709NA safety valve.

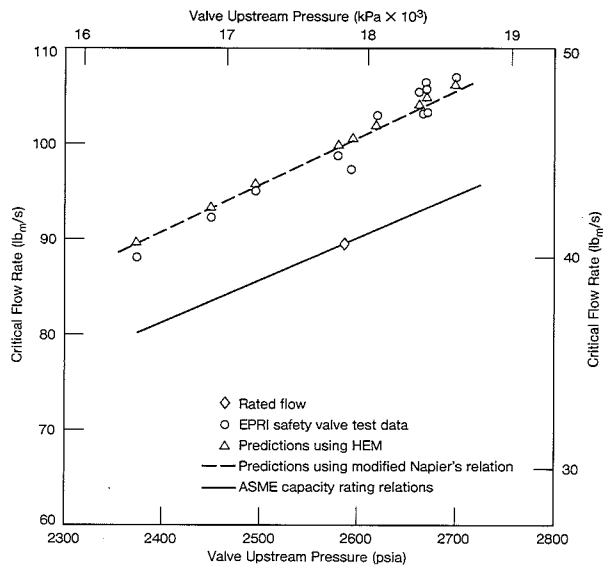


Figure 2 Critical flow rate predictions for Dresser 31739A safety valve.

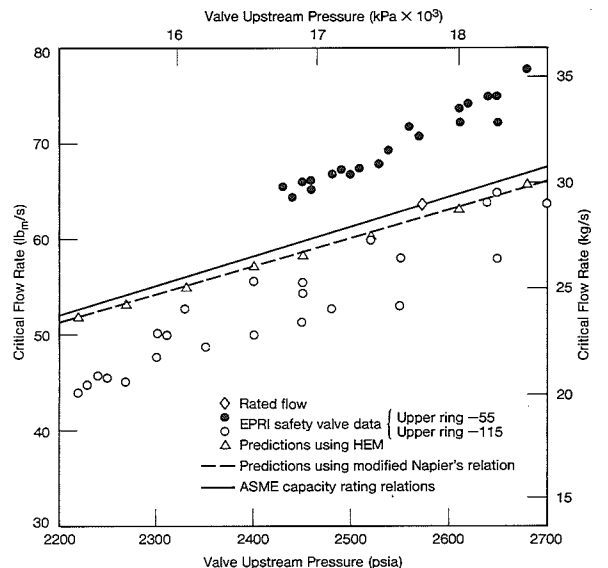


Figure 3 Critical flow rate predictions for Crosby 3K6 valve.

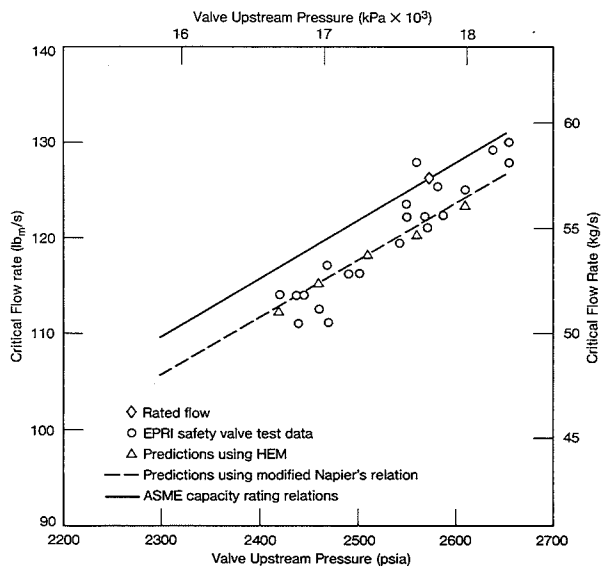


Figure 4 Critical flow rate predictions for Crosby 6M6 safety valve.

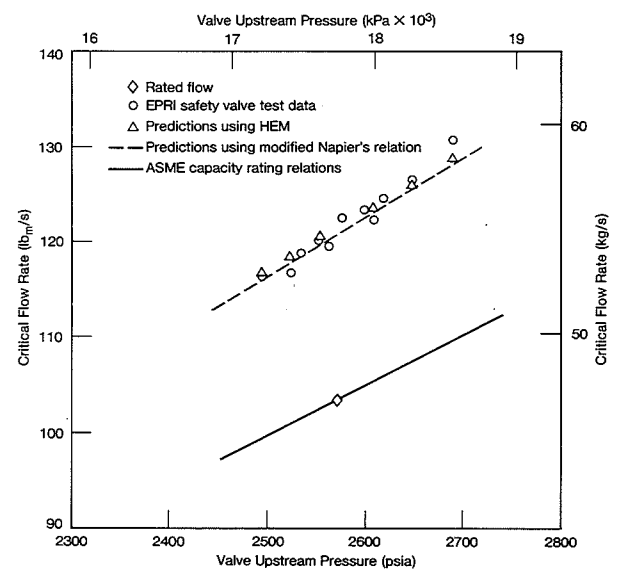


Figure 5 Critical flow rate predictions for target rock 69C safety valve.



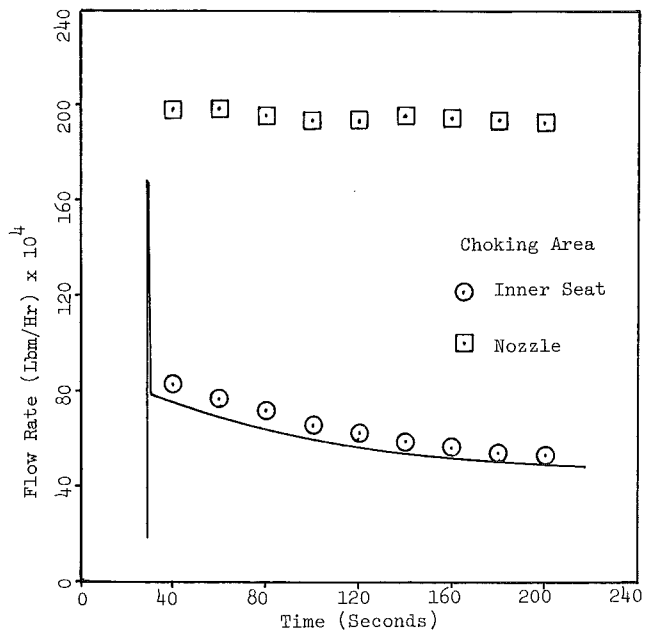


Figure 6. Predicted and Measured Flow Rates Using Burnell Model for Dresser 31709 Safety Valve

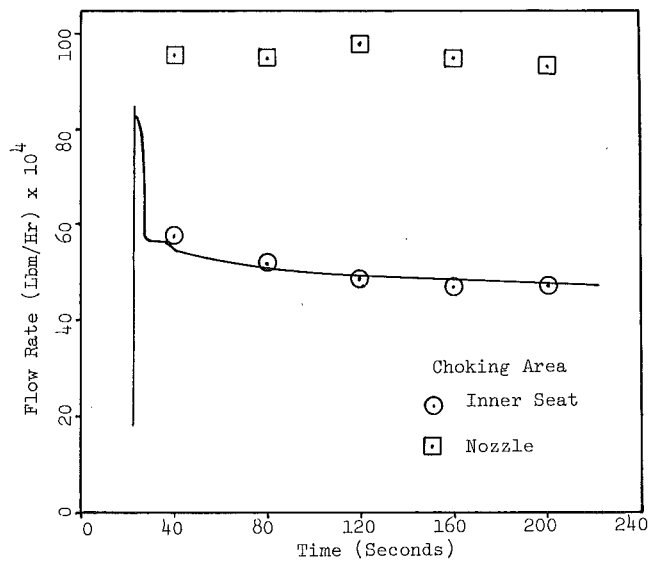


Figure 7. Measured and Predicted Flow Rates Using Burnell Model for Dresser 31739 Safety Valve

## CHUGGING-RELATED LOAD REDUCTION FOR PRESSURE SUPPRESSION SYSTEMS

E. Aust, H.-R. Niemann, H.D. Fürst, G.F. Schultheiss

GKSS-Forschungszentrum Geesthacht GmbH  
Institut für Anlagentechnik  
2054 Geesthacht, Federal Republic of Germany

## ABSTRACT

Experimental research of the loss-of-coolant-accident (LOCA)-behaviour of pressure suppression systems of BWR's has indicated at lower mass flow rate strong, cyclic pressure pulses resulting in dynamic loads. World-wide this phenomenon is called chugging.

Correlated evaluation of digital and visual data from our large scale test facility with e.g. original vent pipe diameter resulted in a substantial progress of understanding the essential physical mechanisms of this phenomenon. Based on these results, a successful chugging-related load reduction has been obtained by various simple geometrical changes at the vent pipe exit.

The paper contains a summarizing presentation of the developed mitigator constructions to completely avoid chugging and/or the induced dynamic loads.

## INTRODUCTION

GKSS has conducted an experimental research program focussed on the function of a pressure suppression system (PSS) during a postulated loss-of-coolant accident (LOCA). This research work was performed in a large scale three vent pipe test facility modelling main features of German and United States BWR-pressure containment design. Fig. 1 shows schematically the general arrangement of the PSS test facility.

About 40 experiments have been conducted, which gave quantified understanding of PSS-phenomena, research data for advanced code development and verification and led to the development of simple mitigators for dynamic load reduction in the case of low steam flow rates.

Fig. 2 shows, that in the PSS LOCA-behaviour can be separated into three distinct stages, which are called:

- vent clearing and air carry over,
- condensation oscillation (CO) with weak cyclic pressure oscillations,
- chugging with periodic, strong pressures pulses.

Because of the impulsive nature of chugging, the basic mechanism of this phenomenon and the mitigation of the produced dynamic loads were main research subjects in the GKSS experimental program.

## CHUGGING PHENOMENON

Time correlation of optical data, obtained from 1000 frames/s high speed camera-records and TV-movies, with pressure and temperature data evidences the basic mechanism of chugging (Fig. 3):

Chugging events occur late in the LOCA at a steam flow rate of about 10 kg/m<sup>2</sup>s and air content less than 5 % Vol. At the vent pipe exit a steam front intrudes into the pool about half a pipe diameter with cylindrical or conical shape (stage 1). This emerged steam volume condenses smoothly, sometimes by enveloping the vent pipe edge, producing a low frequency pressure oscillation near the acoustic frequency of the steam-filled vent pipe, which is in the GKSS facility 12 and 17 Hz with respect to the different vent pipe length. The high speed and TV-movies show, that outside-pipe-condensation is plume-like, a smooth steam condensation process without a true inpool steam "bubble". During outside-pipe-condensation (stage 2) pool water rapidly reenters the hollow core of the steam-filled vent pipe which acts with a sharp edge of its outlet as a BORDA-mouth (stage 3). High speed records indicate a steam annulus formation at the vent pipe wall within the stagnant space of the BORDA-constriction. This steam annulus remains stable for milliseconds and then suddenly condenses. The resulting rarefaction is followed by a strong positive pressure pulse which produces a ringdown frequency characteristic of the fundamental frequency of the pool-boundary system. After the collapse of the steam annulus, the submerged end of the vent pipe is entirely filled with water and the pressure in the drywell increases until it once again becomes sufficiently high for the steam to reenter the pool and to reinitiate the chugging process /1, 2/.

## CHUGGING-RELATED LOAD REDUCTION

The experimental result about the steam annulus formation inside the vent pipe exit led to two mitigator constructions, which are focused on a geometrical change of the vent pipe outlet. Main idea was to influence the thermal hydraulics of the condensation process at the pipe exit in order to smooth the dynamic chugging loads. The developed mitigators are described as followed.

## OUTLET COLLAR-MITIGATOR

The findings about the BORDA-constriction at the end of the outside chugging process led to the idea, to initiate attached back flow of the pool water into the vent pipe in order to avoid the steam annulus stage with its resulting sharp pressure pulse. The radius of the collar was roughly taken from the annulus radius, which could be clearly observed in the TV-movies. Fig. 4 shows a photo of the 3 vent pipes with outlet collars.

The construction was tested very successfully as shown in Fig. 6. This figure shows in comparison to the standard condition test M1-5 with the same mass and energy release into the dry well the obtained load reduction in the wetwell pressure history by the developed mitigators.

It is important to note, that by this design only the chugging produced pressure pulses have been avoided but not the chugging phenomenon itself. Water periodically reentered the vent pipe exit and initiated the well-known mixing effect of cold and hot water in the pool.

## 45 °-OUTLET CUT-MITIGATOR

A second geometrical mitigator construction was also tested very successfully. The basic idea of this construction was to provide a continuous steam flow path from the vent pipe to the pool to avoid the periodic steam release of a conventional pipe during chugging and to get a partial steam flow stabilisation. The pipe construction worked with a 45 °-exit cut. A photo of this mitigator is given in Fig. 5. The static pressure difference along the diagonal exit cut causes a cross flow of water and steam with a very intensive steam condensation and mixture of condensate and pool water. During the expected time of the chugging stage with relatively low mass flow rates this construction showed a very distinct self-regulating effect: less steam flow through the vent pipe, less steam flow area at the vent pipe exit. It should be noted, that in test M1-B.45 the cut was only arranged at one of the three vent pipes. So only the cutted vent pipe was loaded, while the other two pipes received no excitation from the process and remained unloaded and worked as tube condensers. In test M1-ABC.45 the three vent pipes were cutted to 45 ° at the exit. In the pool the dynamic pressure load reduction was clearly obtained, while in the drywell atmosphere some cyclic pressure drops of about 0.2 bar occurred at the beginning of chugging.

For all mitigation tests a complete replication of experimental results could be demonstrated.

Finally it should be mentioned, that dynamic load reduction by process engineering methods is possible. An increase in initial pool temperature or final pool back-pressure was found to reduce the dynamic loads. A distinct attenuation of pressure amplitudes during chugging was also obtained by injecting air into the vent pipe, in the range of 1 % of the steam mass flow /3, 4/.

## CONCLUSIONS

The insights into the basic physics of chugging led to the idea to develop a simple mitigator to reduce dynamic chugging loads. The first step was to avoid the sharp edge of the vent pipe outlet, in order to get attached back flow into the vent pipe without any constriction and a steam annulus stage. The successful tests with the collar mitigator indicated the correct interpretation of the physical character of chugging.

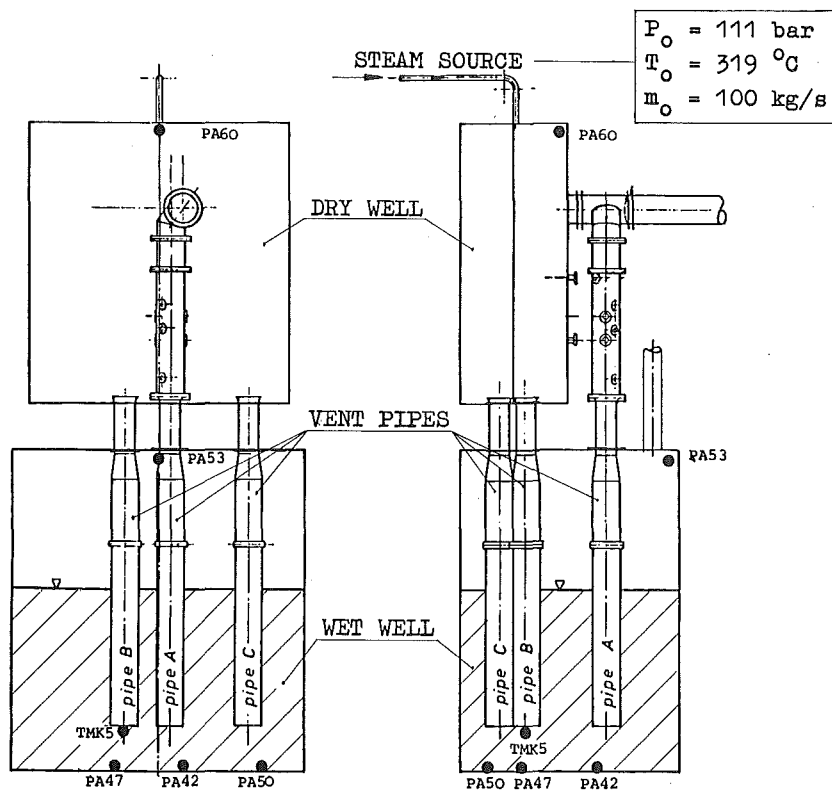
The second step was to smooth the steam flow in order to avoid the periodic steam flow with chugging events. The 45 °-cut led to the successful mitigator described above.

It can be concluded, that a mitigator construction with the collar or an outlet cut can be simple applied in present and future BWR-pressure suppression systems. Both constructions can help to enhance the safety margin of pressure suppression containments.

## REFERENCES

- /1/ Aust, E.; Sakkal, F.:  
"Review of GKSS 3-Vent Experimental Program and Results",  
Proc. Int. Spec. Meeting on BWR-Pressure Suppression Containment  
Technology, June 1-3, 1981, GKSS 81/E/27 pp. I-81 ff.

- /2/ Aust, E.; Seeliger, D.:  
"Pool Dynamic and Dynamic Loads in Pressure Suppression Containment Systems",  
Transactions of the 1982 annual meeting, Los Angeles, California,  
June 6-10, 1982, Vol. 41, ISSN 0003-018X, p. 696-699
- /3/ Schultheiss, G.F.; Niemann, H.-R.; Sakkal, F.:  
"Untersuchungen zur Verminderung der dynamischen Lasten bei  
SWR-Druckabbau-Vorgängen",  
Jahrestagung Kerntechnik '82, Tagungsbebericht ISSN 07209207, p.  
211-214
- /4/ Aust, E.; Schultheiss, G.F.; Seeliger, D.; McCauley, E.W.:  
"Experimental Results About Dynamic Load Mitigation for BWR-Pressure  
Suppression Containments Under LOCA-Conditions",  
Transactions of the 7th International Conference SMiRT, Chicago  
Illinois, USA, Aug. 22-26, 1983, Vol. J, pp. 43-50



● TRANSDUCERS USED IN

DIAGRAMS

TEMPERATURE - TM  
PRESSURE - PA

PLANT-LIKE KEY PARAMETERS

- 3 VENT PIPES
- 2,8 m SUBMERGENCE
- 0,6 m VENT DIAMETER
- 5,4 m<sup>2</sup> POOL AREA/VENT
- PRESSURE AND TEMPERATURE TRANSIENTS

**GKSS** <sup>A</sup>  
FORSCHUNGSZENTRUM GEESTHACHT GMBH

Fig. 1: SCHEME OF THE GKSS-MULTIVENT TEST FACILITY WITH FULL SCALE DESIGN FOR REAL PLANT LOCA-SIMULATION

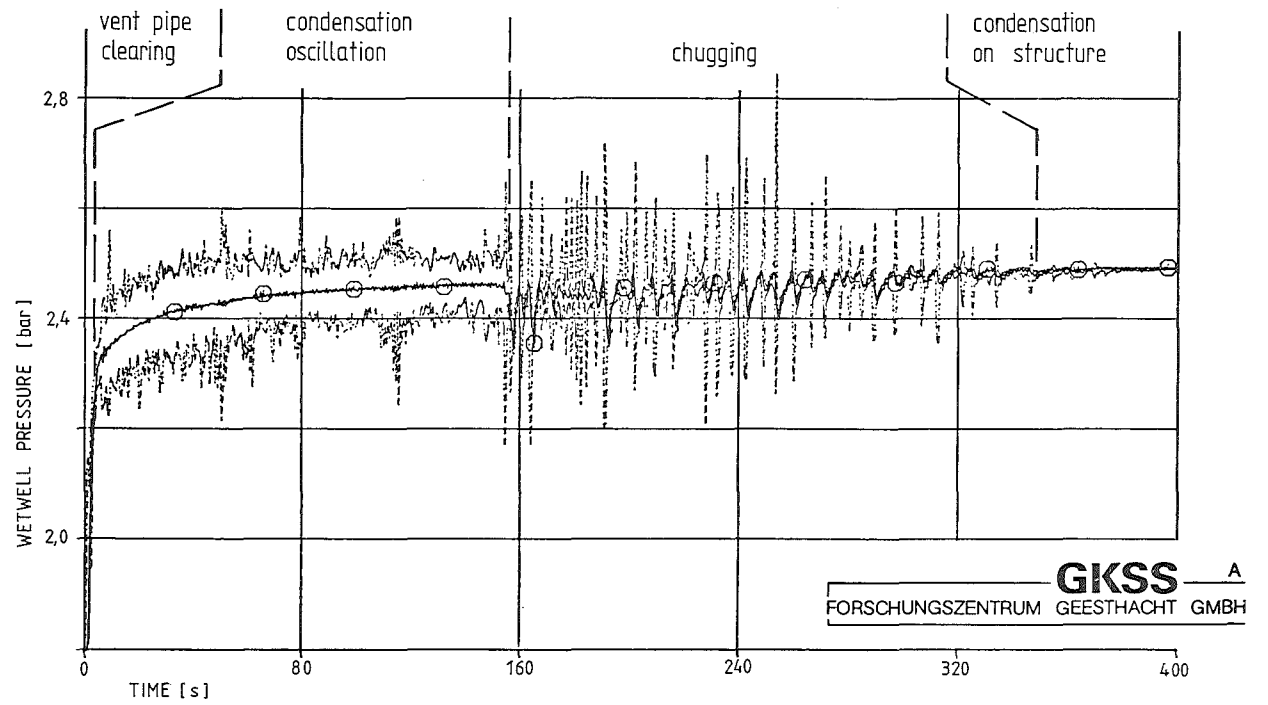


Fig. 2: WETWELL PRESSURE HISTORY WITH DYNAMIC PHENOMENA

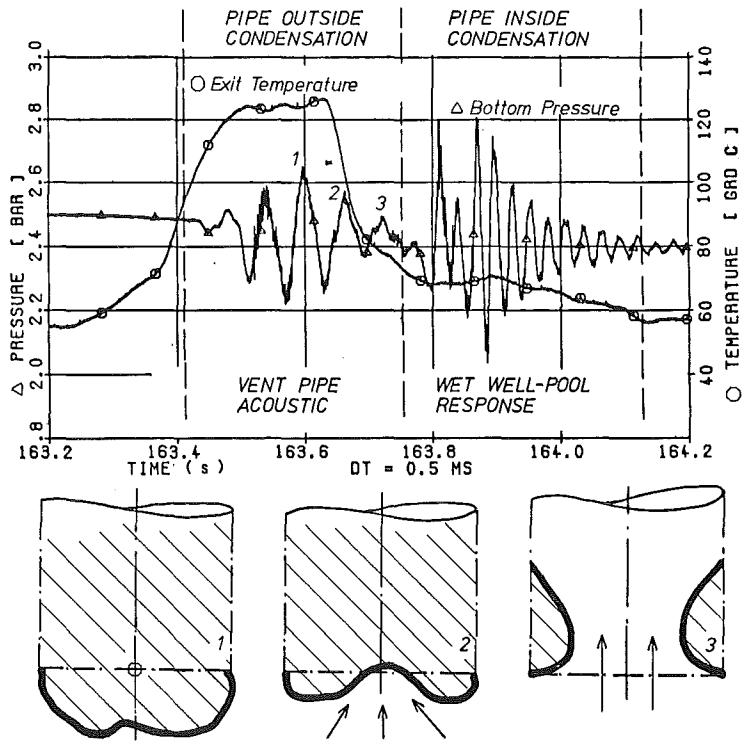


Fig. 3: CHARACTERISTIC FEATURES OF A SINGLE CHUGGING EVENT



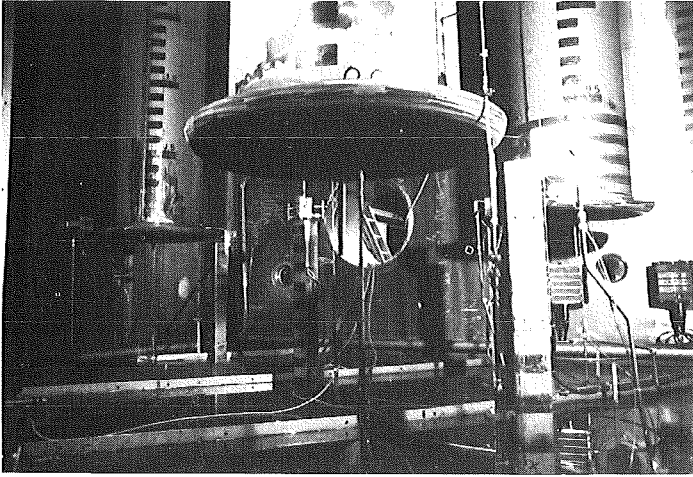


Fig. 4: PHOTO OF THE 3 VENT PIPES WITH  
OUTLET COLLAR-MITIGATORS

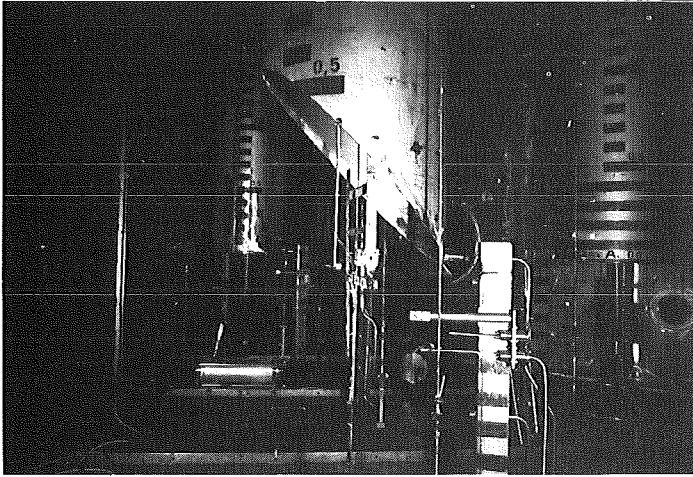
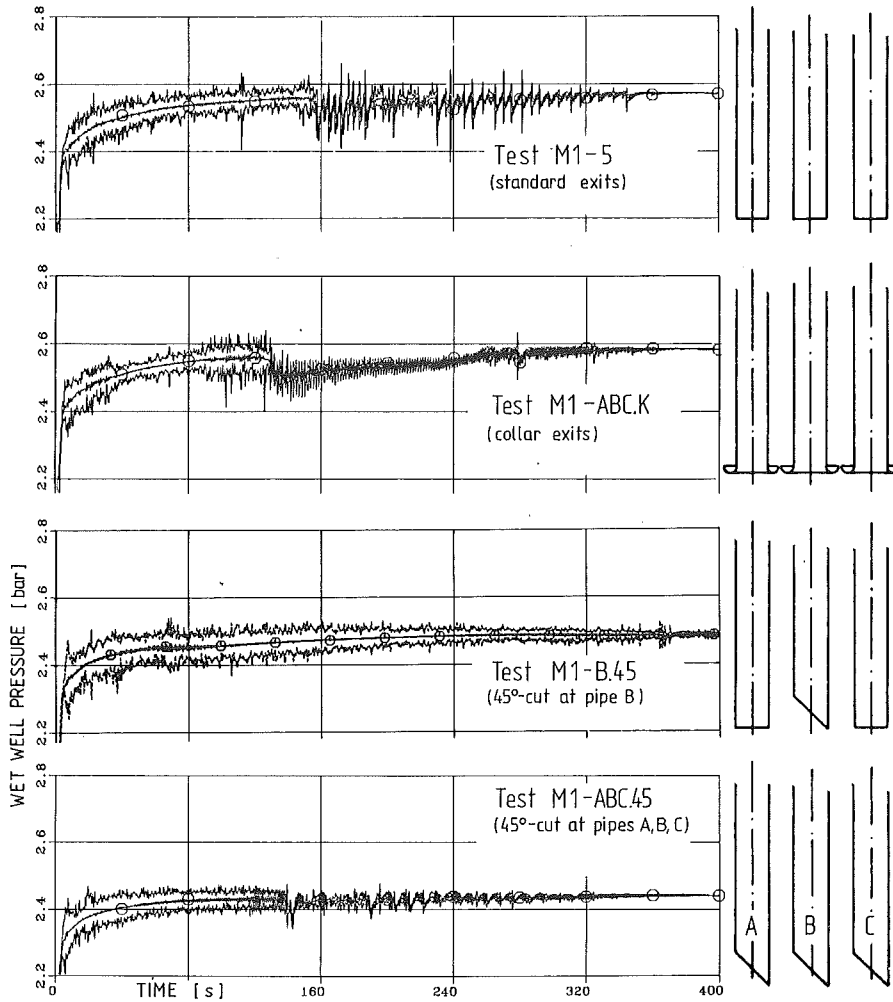


Fig. 5: PHOTO OF THE 3 VENT PIPES WITH A 45°-OUTLET CUT-  
MITIGATOR AT ONE PIPE



All tests under the same boundary conditions (especially mass flow rate and energy release into the dry well)

**GKSS** <sup>A</sup>  
FORSCHUNGSZENTRUM GEESTHACHT GMBH

Fig. 6: DYNAMIC LOAD REDUCTION BY GEOMETRICAL MITIGATORS

IMPROVED FUEL CYCLE FLEXIBILITY AND ECONOMY:  
VERIFICATION TESTS WITH BWR COOLANT FLOW RANGE EXTENSION

S A Andersson, S Helmersson and L-E Johansson

ASEA-ATOM  
Box 53, S-721 04 Västerås, SWEDEN

ABSTRACT

All Swedish and Finnish BWRs have been relicensed to permit operation at lower recirculation flow at rated power than the original design, which corresponded to a 10 % "flow window". This gives a number of advantages, among which lower fuel costs through spectral shift operation and increased core operation flexibility are the most important. The reduced coolant flow has been made possible by improvements in the core steady state operation leading to lower power peaking. Dynamic reactor characteristics are, however, of vital importance at low flow operation. A thorough theoretical analysis and experimental verification of reactor transients and stability thus form the basis for the applicability of the extended recirculation flow range concept.

INTRODUCTION

In order to minimize the costs for electricity generation and also to conserve the available uranium resources, the most efficient use of reactors is desirable. New fuel designs, for example designs with a more even moderator distribution in the BWR, like the SVEA water-cross fuel, make considerable savings possible as compared to traditional fuel designs.

Other means to improve the fuel economy are also available.<sup>1</sup> Among these, the so-called spectral shift operation strategy is an important contribution to optimize BWR fuel utilization. By running the reactor with high void contents in the core during the major part of the year, conversion of U-238 is improved. At the end of the operating season, the void contents are reduced to increase the reactivity. Compared to operation at constant void contents, fuel savings of the order of several percent may be obtained, the exact figure of course depending on the magnitude of variations in void contents that can be achieved.

The easiest way to achieve a variation in void contents in the BWR is by varying the recirculation flow. Net fuel savings of the order 1 % per 10 % flow variation is achieved in current practice. Possible flow variation at full power is bounded by operating limits referred to as the power/flow operating range. The minimum flow is determined, from those margins with respect to dryout or dynamic instability that are considered necessary. However, limits of this kind are usually constructed to be conservative under the licensing process of the plant. Considering recent achievements in power shaping and increased knowledge with respect to reactor instability limits, extension of the power/flow operating range has been found to be possible in all 9 BWRs now in operation in the Nordic countries: 7 reactors in Sweden and 2 in Finland. These include five different designs. Three designs have external recirculation pumps and two have internal pumps. The Asea-Atom fuel design with its low pressure drop spacer and excellent dryout performance also contributes to the margins that can be utilized for flow window extension.

The reactors were originally designed for a 10 % flow range at full power. By reducing the minimum permissible recirculation flow at full power and also taking advantage of pump overcapacity, the "flow window" has been considerably increased in all plants. As an example, the situation in the Oskarshamn 2 external pump plant is shown in fig 1.

Extension of the recirculation flow range may also be considered as a first step to power uprating, if there is overcapacity available in the plant's turbine and auxiliary systems. Such power increases have been put into effect in the Swedish Oskarshamn 2 reactor by 6 %, permanently from 1982, as shown in fig 1, and from 1984 also in the Finnish TVO reactors, by 8 %. Such upratings are also considered for other reactors.

#### THE BWR POWER/FLOW OPERATING RANGE

The power level and the reactivity of the BWR are controlled by basically two mechanisms:

- i) control rod movements
- ii) adjustment of recirculation pump flow

In Asea-Atom BWRs both mechanisms are available for either of these tasks: fine motion control rod drives make small power variations possible and, on the other hand, the large available range in recirculation pump speed enables fast and precise power adjustments by flow control.

In recent years, in addition, a third option takes care of most of the need for reactivity compensation due to burnup, i.e.

- iii) burnable absorber in the fuel

Usually, control rod manoeuvring is used for power control at start-up, in the power range up to 60 %, whereas above 60 % power changes are preferably carried out by means of recirculation flow control. This strategy minimizes the need for control rod movements at high power operation. Only when the available flow interval cannot accommodate reactivity changes due to burnup is control rod manoeuvring requested. Since use of burnable absorber has reached a high degree of maturity, only very few control rod manoeuvres are required at baseload operation and control rod sequences may be designed with very few rods inserted in the core. This is an important aspect for efficient fuel utilization and also means that the core can be operated with one single control rod sequence during one whole operating season, monosequence operation, MSO, thus eliminating the previous needs for time-consuming control rod shuffling in sequence changes.

Recirculation flow control is carried out by means of frequency converters that govern the speed of the recirculation pumps. In older Asea-Atom plants hydro-coupling converters were used, while in modern plants static (thyristor) converters are employed<sup>2</sup>. The latter permit very fast variation of pump speed, a feature which is used for very quick power reduction when called upon in order, for example, to avoid reactor scram due to disturbances or to reinforce the initial negative reactivity at scram with all control rods initially withdrawn.

At normal high power operation the frequency converters are controlled in parallel by a common plant power controller that regulates the plant output to agree with its set-point. The power controller also utilizes the reactor power as measured by the neutron flux monitoring system. The reactor power is used in an "inner control loop", which enables very fast and accurate changes in power level without violating stability requirements.

Plant power control by recirculation pump speed adjustment may be utilized in the power range from 20-100 % of rated power. In the range of approximately 60-100 % of rated power, flow control without additional control rod movements is used.

The allowable range of reactor power and flow (fig 1) is determined by several restrictions

- the low flow limit corresponds to minimum allowed speed of the recirculation pumps. Operation with stopped pumps, i.e. at natural circulation, is not included as a normal operating condition in Asea-Atom BWRs.
- the upper flow limit corresponds to the maximum permissible coolant flow with respect to channel creep deformation etc. Usually the recirculation pump drives are designed with some overcapacity so that, especially for stretch-out operation during a smaller part of the operating season, operation with escalated coolant flow is possible. This overcapacity is valuable in order to achieve the full merits of spectral shift operation.
- at low power, the upper flow limit may be lower in order to conserve the NPSH margin of the recirculation pumps when an uneven feedwater flow distribution may occur.
- the upper left limit of the diagram is in some BWRs simply a flow control line, i.e. the power versus flow line assuming Xenon concentration etc. to be constant. However, what actually limits the power at a given coolant flow is either the minimum allowed critical power ratio (margin to dryout) or criteria concerning the stability margin of the reactor. In recent Asea-Atom reactors the power/flow range has usually been designed with an upper-left power/flow-limit that corresponds approximately to constant critical power ratio. Stable operation at all points of this flow map has been demonstrated. This somewhat extended power range at low flow permits more flexible operation, allowing, for example, faster Xenon build-up at plant start-up.

#### IMPROVEMENTS IN FUEL ECONOMY BY MONOSEQUENCE AND SPECTRAL SHIFT OPERATION

The void content control capability at full power enables a neutron spectrum shift by operating at low core flow, i.e. with a high void content and a hard spectrum during most of the cycle, when excess reactivity is available. Use of monosequence operation, MSO, combined with burnable absorber in the fuel has made it possible to operate about 85-90 % of the cycle length at nearly constant recirculation flow in the left part of the flow range with high core void contents. The excess plutonium generated will provide extended cycle life time, when core flow is increased to its maximum and thus the average void content decreases at the end of the cycle. A decrease in average void content leads to an improved moderation, which utilizes the reactivity potential of the excess plutonium generated. The simultaneous upward tilting of the power distribution also contributes to the gain in cycle length.

In the long run net fuel savings of about 1 % per 10 % flow increase is achieved in consistent practice. Two-thirds of this can be attributed to the void effect on the neutron spectrum and the remainder to the resulting power tilt. The benefit of spectral shift in equilibrium cycles is rather independent of both cycle length and enrichment level of reload fuel.

The ASEA-ATOM MSO application is closely linked to advanced use of burnable absorber (gadolinia). In an advanced concept, axially distributed gadolinia is employed and in amounts that necessitate only a minor control rod inventory at full power. The concept with burnable absorber and MSO combined with a low core flow within the thermal limits provides good possibilities to establish a downward displaced axial power shape during the first part of the cycle. This leads to a downward displaced burnup distribution, which both amplifies the spectral shift effect (i.e. increases the contents of void and plutonium) and the tilting upwards of the power shape at the end of the cycle.

Monosequence operation (MSO) has been in routine use in Swedish and Finnish reactors since 1977. During 1984 the forty-third successful MSO cycle was completed. The MSO concept is thus very well proven in Nordic practice<sup>3</sup>.

The energy generation losses due to PCI-restrictions have been reduced from about 1 % to about 0,4 % thanks to the MSO-concept combined with a wide flow range at full power and an advanced burnable absorber design.

#### EXTENDED POWER/FLOW RANGE

Extension of the allowable recirculation flow range at full power would be beneficial since this would increase the fuel savings from "spectral shift" operation. Other advantages from an extended operating range, in particular one that permits a lower recirculation flow, are

- increased operational flexibility at load follow
- reduced number of control rod movements at high power, which mitigates PCI restrictions
- reduced long-term fuel channel pressure drop
- reduced recirculation pump power requirement

Extension of the recirculation flow range may be necessary, if power uprating is planned. The power increases by 6 and 8 %, respectively, in Oskarshamn 2 and TVO I and II were made possible - from a core operation point of view - by the extended flow range at the original full power level. In Oskarshamn 2 no hardware changes were needed to accomplish the increased power. In the TVO plants, some modifications in the high pressure turbine were made and one extra relief valve per plant was installed. The costs of these modifications are, however, very small as compared to the increased production capacity.

#### Introduction of extended power/flow range

Introduction of reduced recirculation flow at full power in Swedish and Finnish BWRs was started in 1976, when operation with reduced flow was demonstrated in Oskarshamn 1. This plant is the first plant designed by Asea-Atom and was put into full power operation for the first time in 1972. The original flow window at full power was as in all other Asea-Atom BWRs designed to be 10 % of rated flow with an additional 12 % overcapacity to be used at stretch-out operation. Extension of the minimum flow from 90 % to 65 % was shown possible, thereby increasing the allowable flow range at full power to 65-112 % of rated flow, i.e. permitting a variation in flow by almost a factor of 2.

In Ringhals 1, the second Asea-Atom plant, an extended flow range was introduced in 1980. In this plant the available flow range is 7000-11500 kg/s at full power, i.e. flow increase by more than a factor of 1.6 is available. In Oskarshamn 2 and Barsebäck 1 and 2 a similar flow range was introduced, starting in 1978, cf fig 1.

In later plant designs the design margins with respect to static and transient dryout margin limits are tighter and the possibilities for flow reduction thus somewhat smaller. However, in Forsmark 1 and 2 and in TVO I and II the permissible flow range has also been extended. In TVO I and II the original flow window of 90 to 105 % of rated flow was extended down to 79 %. This extended flow range made possible the 8 % increase in rated power, still maintaining a sufficient flow window at the new full power.

The basis for BWR operation at a reduced recirculation flow level is formed by several contributing achievements in core operation and design margins. The major contributions are

- a fuel design with a very efficient, low pressure drop spacer combined with thin corner rods in the 8x8 fuel bundles
- refined load patterns and extensive use of burnable absorber, which lead to reduced macroscopic power peaking
- detailed core tracking methods providing accurate on-line estimation of the thermal margins of the fuel
- improved fuel design with lower internal power peaking
- large inherent stability margins at high power and minimum flow
- select rods scram, i.e. hydraulic insertion of one scram group of control rods, comprising 6-10 control rods, being used in conjunction with flow reduction to amplify the power reduction capability for transients like turbine trip or load rejection, when full reactor scram should be avoided.

#### Evaluation of thermal margins of the fuel

The power distribution in the BWR is controlled on one hand by the balanced distribution of enrichment levels and contents of burnable absorber in the fresh fuel, and on the other hand by proper choice of the control rod withdrawal sequence. Among all possible power distributions only those that satisfy the core thermal limits are allowed. These limits relate to evaluated values at steady state operation for

- 1) minimum dryout margin, i.e. minimum critical heat flux ratio, in the fuel bundles
- 2) maximum surface heat flux on the fuel cladding
- 3) maximum linear heat generation rate due to the maximum calculated fuel cladding temperature at LOCA (limiting only in external pump reactors)

In Asea-Atom BWRs, the thermal margins of the core are continuously supervised by the use of a 3D on-line core simulator, POLCA<sup>4</sup>, coupled to an interpolating scheme correcting for deviations between actual and calculated power distribution as observed in detector readings.

At reduced recirculation flow the dryout margin limit is bounding for the power distribution. It poses a maximum limit on the radial power peaking, i.e. limits the maximum bundle power. This can very well be controlled by proper reload fuel design. To some extent, however, the economic benefits of recirculation flow reduction are counteracted by the need for a somewhat flatter power distribution. The optimum fuel economy is thus obtained as a rather delicate balance of different parameters within the restrictions posed by the thermal limits.

## Stability margins

At low flow conditions the power of the BWR is known to be limited by restrictions due to either dryout or inherent instability. By proper design and adequate choice of limits on power and flow, sufficient stability margins can, however, be acquired. In the "upper left" corner of the power/flow-map, in particular, proper stability margins must be assured.

In Asea-Atom BWRs, measurements of reactor stability at low flow conditions have been performed for all plant designs, with an emphasis on later designs, which utilize a larger power level at minimum flow<sup>5</sup>. Starting with Barsebäck 2 in 1977, all the latest BWRs to be commissioned have been demonstrated to have large stability margins at all points in the permissible power/flow range. One plant, Ringhals 1, has been tested with larger burnup.

In order to investigate reactor stability also under very low flow conditions, tests with natural circulation have also been performed, starting with Barsebäck 2 in 1977. Natural circulation conditions are not considered to be an expected plant condition, so these tests are set up merely as an experimental procedure to reach the most unstable conditions for BWR operation<sup>6</sup>. The tests performed have shown repeatedly that a controlled power increase up to and even above the threshold of instability can be achieved and that, in spite of large power oscillations, safe operation of the plant is still possible. One other important finding is that the power and flow level, at which instability occurs, is not possible to reach from the normal power/flow range without additional reactivity, since the core and bypass voids are effective means for limiting the power. This fact can also be expressed as an increasing slope of the power/flow control line at very low flow conditions.

## ANALYSES AND VERIFICATION TESTS WITH EXTENDED FLOW RANGES

The introduction of extended power/flow ranges in the BWRs in Sweden and Finland was carried out in a set of analyses and tests that was repeated for each reactor design. The analyses form amendments to the Safety Analysis Reports of the plants. They cover static and transient conditions and show the calculated influence of the new proposed power/flow conditions. After approval by the national nuclear inspectorates, the proposed new flow ranges were demonstrated in a test series. The tests included verification of the static and dynamic reactor performance.

### Analyses of impact on transients and accidents

Transient and accident analyses for the Safety Analysis Report are carried out with computer programs that have been developed by Asea-Atom. The main tools are BISON for transient analyses and GOBLIN for LOCA analyses<sup>4</sup>.

BISON has a 1D thermal-hydraulic model for the coolant loop in the reactor vessel coupled to a 1D (axial) neutron kinetics model and a 1D (radial) model for heat transfer in the fuel rods. The central reactor model is complemented with models for other parts of the plant, e.g. steam lines, turbine, feedwater-and condensate systems, control systems, safety systems, etc. Altogether, the code is able to simulate a large variety of transients, ranging from detailed analyses of reactivity and heat transfer in the core under safety-related, postulated transients to realistic analyses of plant characteristics.

For analyses of accident conditions, where a 1D core model is unsatisfactory, a 3D transient core simulator, ANDYCAP, is also available. ANDYCAP has been used for control rod drop analyses in safety reports.



The GOBLIN code can be used for thermal hydraulic analyses of almost any flow system, but is primarily devoted to analysis of loss of coolant accidents in BWRs. The code uses a 1D thermal-hydraulic four-equation thermal equilibrium model to simulate the various flow paths in the BWR. This model is complemented with a 1D heat conduction model for the fuel rods as well as models for pumps, safety systems etc needed to perform a complete LOCA analysis.

The analyses performed for the different plant designs have shown that the impact of an extended power/flow range for most transients and at LOCA conditions is small. Design basis transients like large LOCAs in external pump reactors or pressurization transients at postulated loss of heat sink are hardly affected at all by the relatively small change in initial conditions. This is also true for the transient that produces the largest reduction in dryout margin in an internal pump reactor, i.e. pump trip caused by an auxiliary power disturbance, provided that the operational limit to the static dryout margin is unchanged at the new minimum permissible core flow.

#### Verification tests

The verification tests with extended flow range have included verification of

- core thermal margins
- core stability margins
- power control system characteristics

as well as an overall verification of the plant performance with the modified operating conditions.

The tests comprised reduction of the recirculation flow at full power and power reduction along the flow control line in the new part of the operating map. Both at full power and at maximum permissible power at minimum flow the reactor stability was evaluated by sinusoidal pressure perturbations. The thermal margins of the fuel were continuously evaluated by routine procedures. The capability and stability of the power control system were demonstrated by introducing fast ramps in the power set-point.

The test results show that the behaviour of the plants is well in line with pre-test analyses:

- the thermal margins of the fuel are kept well below the thermal limits and can be predicted in a consistent way
- the stability margins at full power are only very slightly affected by the flow reduction. At minimum flow, the least stable conditions of normal operation are fully acceptable
- the capability of fast and precise power control by means of pump speed adjustment is unaffected by the reduced core flow

In summary, the extended flow range has a very small impact on the stationary operation, providing that relevant incore fuel management is maintained. Also under transient conditions the impact is small, as shown by the analyses performed, and by the continued, very satisfactory operating records of the Asea-Atom reactors.

## REFERENCES

1. Ö Bernander, E Tenerz, Trends in the Flexibility of BWR Core Operation, *Trans. Am. Nucl. Soc.*, 33, 801 (1979)
2. Operation Flexibility of the Asea-Atom BWR 75. Information brochure, Asea-Atom
3. S Olsson, Operation With Monosequences in Asea-Atom BWR - A Way of Reducing the Impact of PCI, IAEA Specialists' Meeting on Pellet-Cladding Interaction in Water Reactors, Risø, Denmark, 1980
4. Computer programs for LWR design. Information brochure, Asea-Atom
5. J H Blomstrand, S-Å Andersson, BWR Core Response to Fluctuations in Coolant Flow and Pressure, with Implications on Noise Diagnosis and Stability Monitoring, ANS Topical Meeting on Advances in Reactor Physics and Core Thermal Hydraulics, Kiamesha Lake, New York, 1982
6. Y Waaranperä, S Andersson, BWR Stability Testing: Reaching the Limit-Cycle Threshold at Natural Circulation, *Trans. Am. Nucl. Soc.*, 39, 868 (1981)

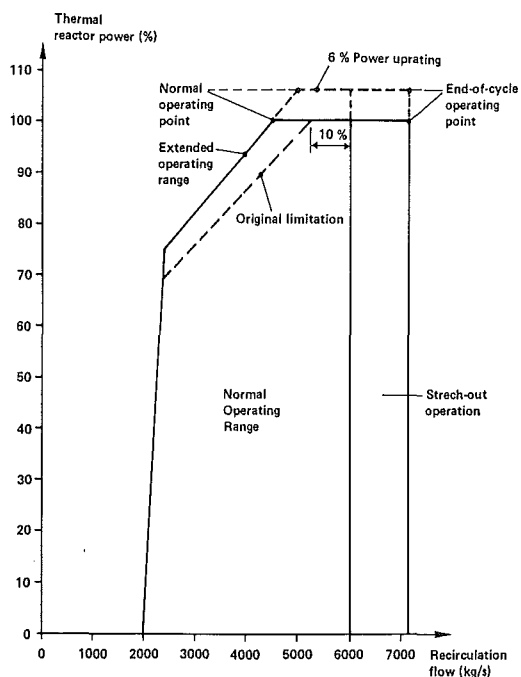


Figure 1. Oskarshamn 2. Extended recirculation flow range/power uprating

INVESTIGATION OF THE ECC-EFFICIENCY IN THE CASE OF SMALL LEAKS  
IN A 1300 MW<sub>e1</sub> BOILING WATER REACTOR

M. Bielmeier, M. Schindler, H. Unger

Institut für Kernenergetik und Energiesysteme (IKE)  
University of Stuttgart, Pfaffenwaldring 31, 7000 Stuttgart 80, FRG

H. Gasteiger, H. Stepan

TÜV Bayerh e.V., Eichstätter Str.5, 8000 München 21, FRG

H. Körber

Beratungsbüro für angewandte Physik, Meisenweg 6, Gechingen, FRG

ABSTRACT

Presented are two blowdown calculations for an 80 cm<sup>2</sup> reactor vessel leak and an 1/40 area (i.e. 17.68 cm<sup>2</sup>) emergency core cooling pipe break in a boiling water reactor of the modern German 1300 MW<sub>e1</sub> series. The calculations were performed using the RLEAP4/MOD6 reactor analysis code in order to analyze the effect of the emergency core cooling. For the investigation the plant is presumed working at 106 % power level and there is only one of three emergency core cooling injection systems available. The results presented are on system behavior, reactor safety system actions and pressure, mixture level and cladding temperature development. The results prove, that even under conservative assumptions, the safety system holds the plant in a safe state and no severe core damages are to be expected.

INTRODUCTION

Nuclear reactors have a much higher risk potential than conventional power plants. In the case of a loss of coolant accident (LOCA), special care has to be taken that no long term core uncovering and in consequence severe core heatup takes place. To avoid such forbidden conditions, boiling water reactors (BWR) of the modern 1300 MW<sub>e1</sub> series have among others three redundant emergency core cooling systems (ECCS). They have to provide enough water to hold the core covered and to ensure the removal of the radioactive decay heat. In the work presented here, it is investigated, if the emergency system of a BWR is able to hold the reactor in a secure state in the cases of medium and small leaks, such as 80 cm<sup>2</sup> reactor vessel leak and 1/40 area emergency core cooling pipe break, using conservative assumptions and methods. The calculations were performed with the RELAP4/MOD6 reactor analysis code.

## DESCRIPTION OF THE PLANT

Table 1 shows some characteristic data of a BWR of the 1300 MW<sub>e1</sub> series. For this analysis the interesting part of the plant consists of the reactor pressure vessel (RPV) including its installations, four steam pipes and four feedwater pipes. From the RPV installations, especially the reactor core with its container, the steam separators and the steam dryers have to be mentioned. Eight axial pumps provide for the internal circulation of the coolant.

The core consists of 784 fuel assemblies, each of them containing 8 x 8 fuel rods. The active core length is 3.71 m and its diameter is about 5 m. The cross shaped control rods are inserted from the bottom into the core.

The most important parts of the reactor safety system are the reactor shutdown system, system isolation, and emergency core cooling system (ECCS). The ECCS consists of three parts: The pressure limiter valves, three redundant high (HP) and low pressure (LP) emergency cooling injection systems and in addition one system for slow (SAD) and one for fast (FAD) automatic depressurization.

For reactor shut down, 193 control rods are available, providing a shut down reactivity of about -40 \$. The pressure limiter system consists of three groups of relief valves, which are activated at different pressures and they are closed with a hysteresis of 5 bar. The automatic depressurization system consists of two groups of valves, one group for slow (SAD) and the other one for fast depressurization (FAD), which are opened depending on the course of the accident (see Table 2).

## PLANT MODELING FOR RELAP4/MOD6

For the analysis the system was modeled by 14 control volumes and 25 junctions as shown in Fig. 1. The parts of the RPV are represented by control volumes as follows:

Volume 1:	Water steam mixture space
Volume 2:	Steam separators
Volume 3:	Steam dome
Volume 4:	Steam outlet volume
Volume 5:	Upper part of the downcomer
Volume 6:	Lower part of the downcomer (annulus)
Volume 7:	Pump plenum
Volume 8:	Lower plenum
Volume 9:	Core bypass
Volume 10,11,12:	Reactor core
Volume 13:	Stagnation volume (space within the control rod tubes)
Volume 14:	Volume to simulate boundary conditions (depressurization chamber).

The junctions connecting the adjacent volumes can be seen in Fig. 1, too. The feedwater and steam lines are simulated by time dependent fills until the pressure limitation and depressurization system is modeled by leak or normal junctions which are to be opened or closed by valves. Pressure dependent fill junctions connected to Volume 6 provide for the high and the low pressure ECC injection.

The power generation during the transient is calculated by a reactor point kinetics model using 6 groups of delayed neutrons. For the radioactive decay heat the ANS Standard 1.5 is used with 20 % error additioning. The energy generated in the core is added to the coolant by three core heatslabs and the heat stored in RPV components is taken into consideration by 5 additional heatslabs.

Out of the program options, available in RELAP4/MOD6, the following ones are applied:

The Wilson phase separation model in all volumes except those, representing pumps, lower plenum and space inside the control rod tubes. The vertical slip model is used in the lower part of the RPV, which is usually filled with water or water steam mixture. Within the reactor core volumes, the water steam mixture room and the steam separator volume the single mixture level calculation model is applied.

The homogeneous equilibrium critical flow model (HEM) is used to calculate the leakage mass flow.

#### BOUNDARY CONDITIONS

At the start of the accident the thermal power of the reactor is 4070 MW. For the reactor safety system, the most important signal is the pressure in the depressurization chamber ( $p > 1.25$  bar). This criterion is met after about 0,5 s. In the presented analysis it is used for scram, system isolation and to activate ECC injection.

For the reactor scram it is presumed, that the control rods are inserted within 3 s and the shut down reactivity of  $-40 \text{ \$}$  is on effect linear with time. Out of three ECC injection systems only one should be available, this means, that in the case of the ECCS leak only the low pressure injection can work, for in a conservative manner the high pressure system is assumed to feed into the broken line. Concerning the automatic depressurization system, the assumption is taken, that out of 6 valves 2 will fail, this means, that for SAD only one and for FAD only 3 valves are available.

The criterion for activating the valves is pressure in the depressurization chamber higher than 1.25 bar. The FAD valve is opened then with a delay time of 60 s and the SAD is initiated when the system pressure falls below 30 bar.

#### RESULTS

##### System Depressurization

Comparing the results (Figs. 2 and 3) it turns out, that the courses of the accidents are very similar. However, an important difference is, that the 80 cm<sup>2</sup> RPV leak runs about 1.4 times faster than the 1/40-F-ECCS pipe break.

The first few seconds after leak opening, there is almost no effect on the system pressure because of the relative low leakage mass flow and of the low energy of the escaping flow. Just when the system isolation has closed, fast changes take place in the system after 3 s. There is no more energy removed by the steam lines but the reactor still works at 20 % of its nominal power level. Therefore a fast pressure rise in the RPV is the consequence and the pressure relief valves of Group 1 and Group 2 open. By this, the

pressure rise is limited to 78.5 bars. Now the pressure decreases within a few seconds below 72 bars and the relief valves of Group 2 close again. From now on, besides the leakage mass flow, one valve of Group 1 is the only energy sink, therefore causing the pressure to rise again until 30 s when the power generation is low enough to allow continuous depressurization.

After about 60 s, the valves of the SAD open. But because of the closing of the Group 1 relief valve 10 s later, there is only a short period of increased pressure drop. There is no accelerated pressure drop until the system pressure decreases below 30 bars (1050 s, see Figs. 2 and 3) when the valves of the PAD open. After nearly 790 s in the case of the RPV leak (1150 s for the ECCS leak), the pressure falls below 15 bars and the low pressure injection starts to deliver coolant into the RPV.

#### Mixture Level Evaluation

In the case of the RPV leak (Fig. 4), immediately after starting, the mixture level in the annulus begins to drop continuously. Inside the core container it begins to fall not before 140 s and the top of the core is reached after approx. 590 s. Then the mixture level drops into the upper core region, shortly thereafter. When the SAD causes flashing, it rises above the top of the core so that the core is covered again. On long term, the mixture level is rising in the whole RPV when the low pressure injection is achieved ( $p < 15$  bars).

For the ECCS leak the mixture level develops similar to the RPV leak (Figs. 5 and 6). Caused by the different location of the leak and by the slower transient, the mixture level drop begins later, the core uncovering lasts considerably longer and a greater part of the core becomes uncovered.

#### Fuel Rod Temperatures

As shown by Figs. 7 and 8, the cladding temperatures strictly follow the temperature of the saturated coolant, which itself is determined by the system pressure. In the case of the RPV leak, the short term uncovering of the upper core region has no effect on the cladding temperatures. Because of the longer lasting core uncovering in the case of the ECCS leak, the fuel rods are heated up temporarily in the upper core region. But even in this case the temperature rise is limited and the temperatures stay below the degree of normal operating.

#### CONCLUSION

The investigation shows in both cases, that the emergency system of the 1300 MW<sub>el</sub> boiling water reactor is able to control the LOCA and to protect the core from severe damage. This remains true even under such conservative restrictions like availability of only one of three ECC systems.

## REFERENCES

- /1/ M. Bielmeier, H. Körber: "Untersuchung des 1/40-F Kernflutleitungsbruch beim Kraftwerk KRB II mit RELAP4/MOD6", IKE 2TF-48, Dezember 1982
- /2/ M. Bielmeier: "Analyse des 80 cm<sup>2</sup> RDB-Bodenlecks für das Kernkraftwerk KRB II B Gundremmingen mit RELAP4/MOD6", IKE, 2TF-50, Januar 1983
- /3/ Fischer, Nelson, et al.: "RELAP4/MOD6 - A Computer Program for Thermal-Hydraulic Analysis of Nuclear Reactors and Related Systems", EG&G Idaho, Januar 1978
- /4/ Proposed ANS Standard Decay Energy Release Rates Following Shutdown of Uranium-Fueled Thermal Reactors, ANS-5-1, October 1971

Table 1: Data of the Analysed 1300 ME<sub>e1</sub> Boiling Water Reactor

Nominal thermal power	3840 MW
Number of loops	4
Normal operating pressure	70 BAR
Steam generation rate	2078 kg/s
Saturated steam temperature	286 °C
Feed water temperature	215 °C
Core mass flow	12580 kg/s
Recirculation number	6.5
Number of recirculation pumps	8
Number of fuel assemblies	784
Number of fuel rods	50176
Number of control rods	193
Shut down reactivity	-40 $\beta$
Number of ECC injection systems	3 HP 3 LP
RPV inner height	22.35 m
RPV inner diameter	6.62 m
Heated core length	3.71 m
Diameter of Core	5 m
Fuel rod diameter	11 mm

Table 2: Data of the Automatic Depressurization System and Pressure Limiter Valves

Automatic Depressurization System		SAD	FAD	
Number of Valves		2	4	
Flow Area		158.3 cm		
Opening Time		.3 s		
Delay Time		.0 s		
Initiation Criterion		$P_{DC} > 1.25 \text{ bar}$ and $P_{SYS} < 30 \text{ bar}$ or $ML < 11 \text{ m}$		
Relief Valves		Group 1	Group 2	Group 3
Number of Valves		1	6	4
Opening pressure (bar)		75	77	79
Closing Pressure (bar)		70	72	74
Flow Area			1.58	
Opening Time			.3 s	
Closing Time			.7 s	
Delay for Opening			.438 s	
Delay for Closing			.7 s	

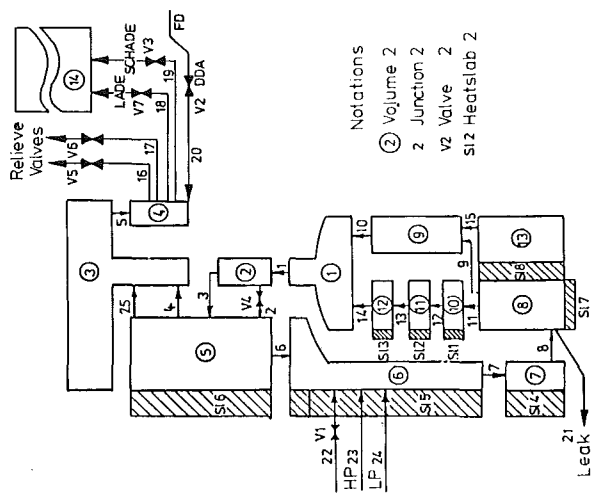


Fig. 1: Boiling water reactor nodalization scheme



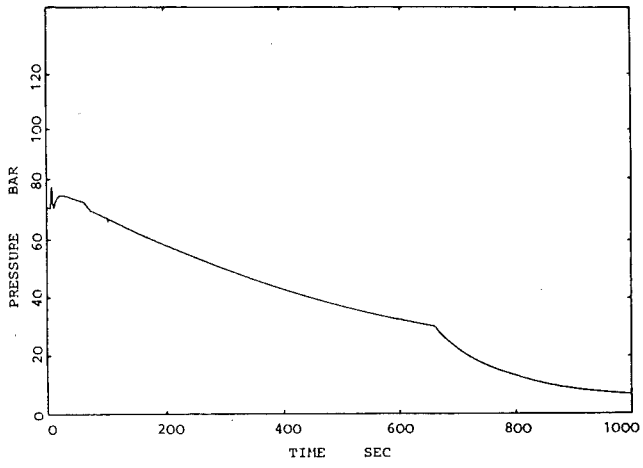


Fig. 2: BWR 80 cm<sup>2</sup> RPV leak.  
Pressure versus time in the RPV

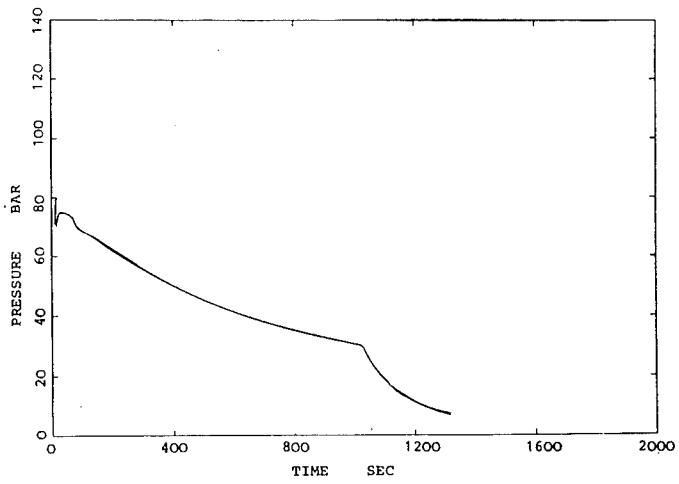


Fig. 3: BWR 1/40 area ECCS pipe break.  
Pressure versus time in the RPV

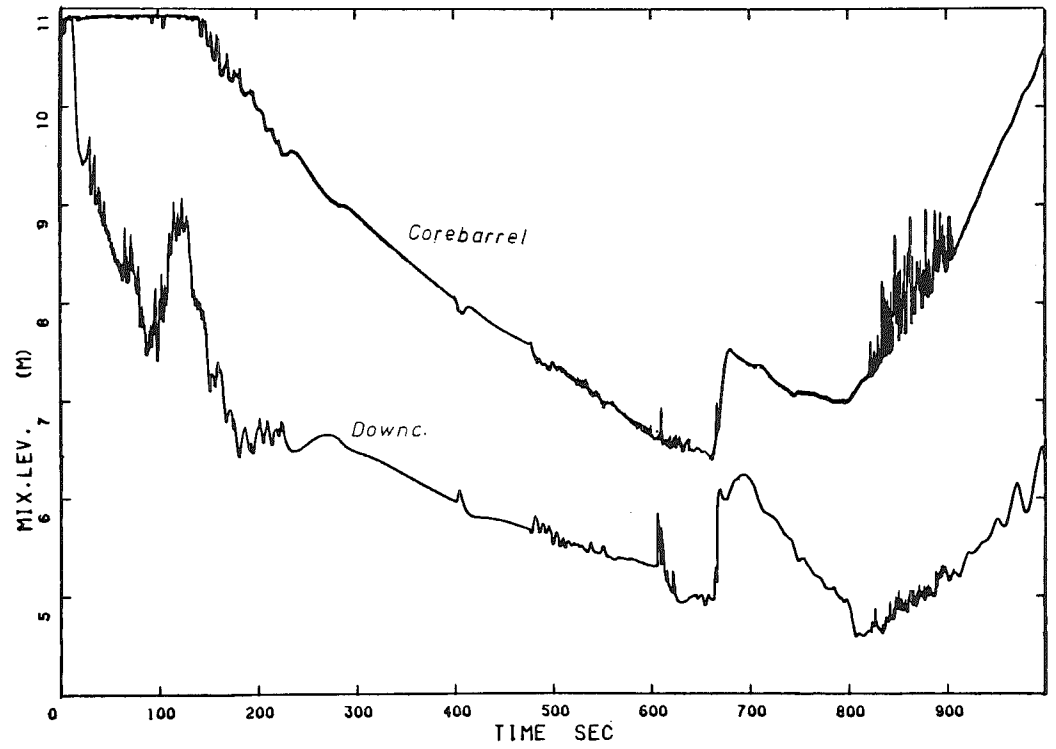


Fig. 4: BWR 80 cm<sup>2</sup> RPV leak.  
Mixture level above downcomer bottom

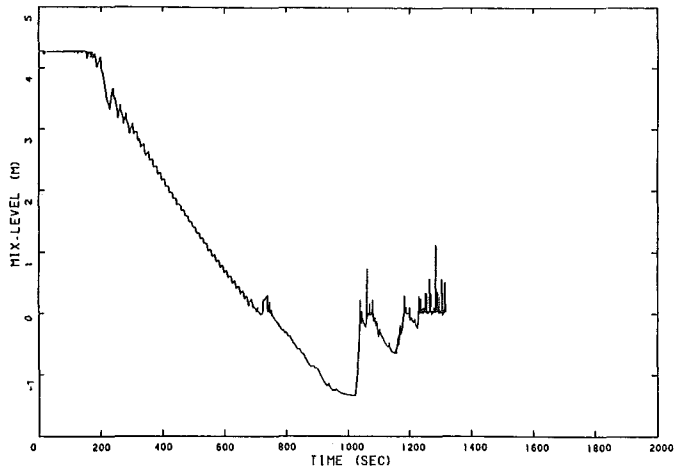


Fig. 5: BWR 1/40 area ECCS break.  
Core container mixture level above core top

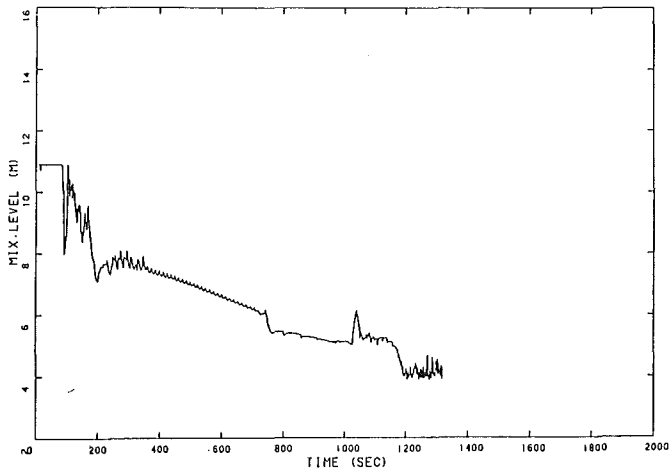


Fig. 6: BWR 1/40 area ECCS pipe leak.  
Downcomer mixture level

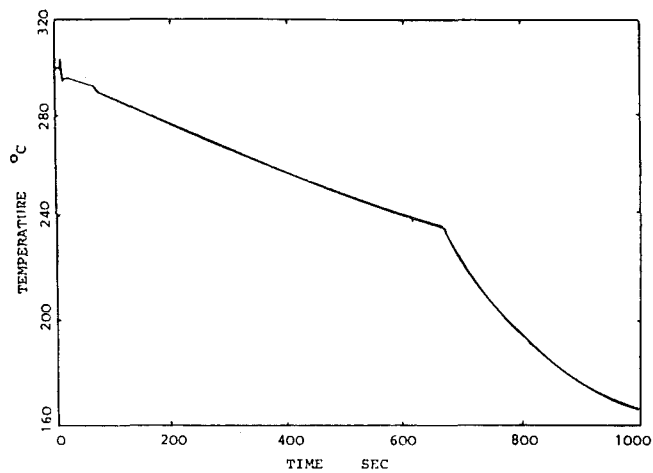


Fig. 7: BWR 80 cm<sup>2</sup> RPV leak.  
Cladding temperature in the upper core region

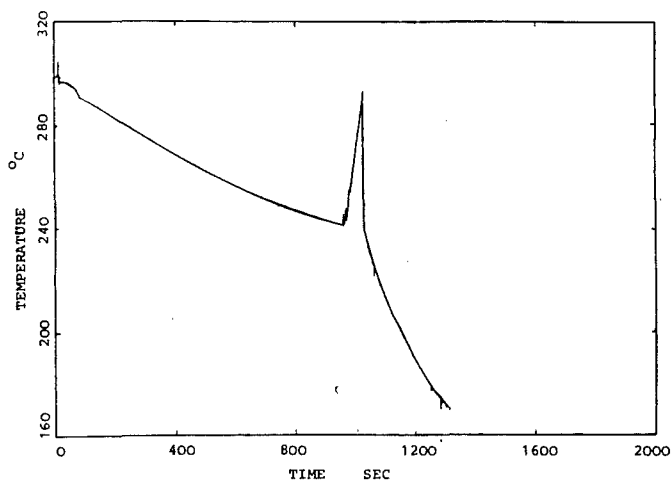


Fig. 8: BWR 1/40 are ECCS pipe break.  
Cladding temperature in the upper core region

SAFETY CONCEPT AND EVALUATION OF THE  
745 MW KWU-PRESSURIZED HEAVY WATER REACTOR (PHWR)

H. Fabian, K. Frischengruber

Kraftwerk Union AG  
Hammerbacherstr. 12+14, 8520 Erlangen, FRG

ABSTRACT

In parallel to the light water reactors KWU follows the line of heavy water reactors of the pressure vessel type. A 745 MWe-PHWR is actually under construction in Atucha, Argentina.

Part I

The safety concept of the PHWR is principally based on the same safety features as the light water PWR, e.g. reactor building consisting of a spherical steel containment and an outer concrete building with vented annulus inbetween. However, there are some specialities adherent to the heavy water reactor. Safety related systems are designed to be both, diverse and redundant. The moderator cooling system can be used as a high pressure heat removal system and thus is an addition to the heat removal via the steam generators. For reactor shut-down a control rod system and a boron injection system exist independently.

Part II

A safety evaluation has been performed via a probabilistic risk analysis (PRA). The assessed core damage frequency shows the same safety level as for light water reactors. The contribution of the different accidents proves the balance of the safety concept. The environmental dose resulting from accidents is beyond a given dose frequency criterion.

INTRODUCTION

The design of the recent KWU heavy water ( $D_2O$ ) moderated and led pressurized water reactor (PHWR) bases on the 57 MWe-ti-purpose research reactor (MZFR) at the nuclear research center, Karlsruhe, which went into operation in 1966 and on the first merical PHWR of KWU design, Atucha I (Argentina), which was ded over in 1974. The concept of this 340 MWe-PHWR (1977 in-ased to 367 MWe) was confirmed by the excellent availability 80% since start of operation. At the moment the advanced 745 MWe-R Atucha II is under construction. The design of this plant ves here as reference. Part I of this paper describes the safety cept of this plant. Part II deals with the results of the pro-ilistic safety evaluation.

PART I: SAFETY CONCEPT OF THE 745 MWe PHWR ATUCHA II

The KWU PHWRs are pressure vessel type reactors and thus there exist many common design features between this PHWR and the pressurized light water reactor (PWR). See Fig. 1.



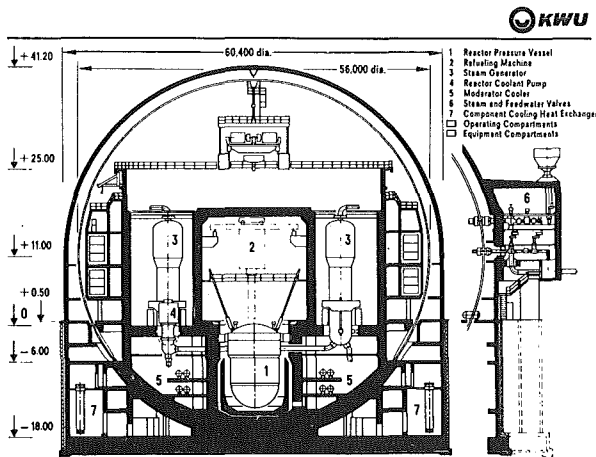
**Main Similarities to KWU-PWR**

- Reactor Pressure Vessel
- Main Coolant Loops
- Pressurizer System
- Spherical Steel Containment
- Secondary Concrete Shielding
- Annulus
- Active Engineered Safeguards
- J&C Concept

Moreover, the 150 years operating experience with KWU's LWRs can be used. The components of the reactor coolant system are fully comparable with a PWR in their design and their arrangement inside the reactor building, also similar to the PWR is the layout of the reactor building with the leak-tight spherical steel containment, the concrete shield building including the valve compartment for external impact protection and the vented annulus in-between for the arrangement of safety related systems and components. See Fig. 2.

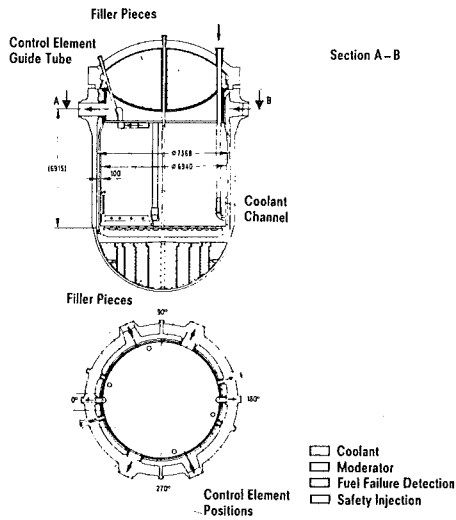
ATUCHA II PHWR 745 MW

Fig. 1



Nuclear Power Plant with Heavy Water Reactor (750 MW Class) Reactor Building

Fig. 2

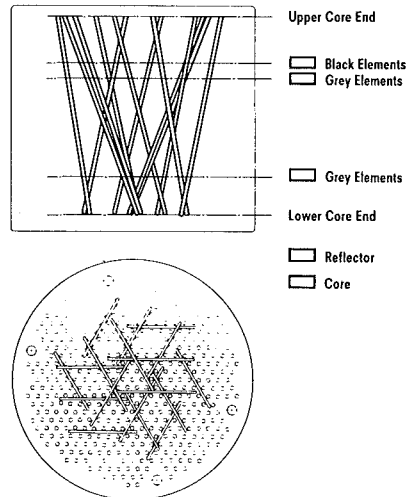


The reactor pressure vessel (RPV) is somewhat larger than that of a PWR at equal thermal output. All connections are arranged above the area of the active core. The nozzles for the cooling channels and control rods are arranged around the periphery of the cover in order to allow room for the on-load refueling machine. The control rods are inserted into the reactor core at angles of about  $20^\circ$  (see Figs. 3 and 4).

Nuclear Power Plant with Heavy Water Reactor  
Reactor Pressure Vessel with Internals

Fig. 3

Due to the considerably longer moderation length of  $D_2O$ , the fuel elements can be arranged in discrete cooling channels with a grid pitch of 272 mm. In total, the core contains 451 channels, each with one fuel element (37 rod bundles).



Nuclear Power Plant with Heavy Water Reactor  
Arrangement of Control Rods

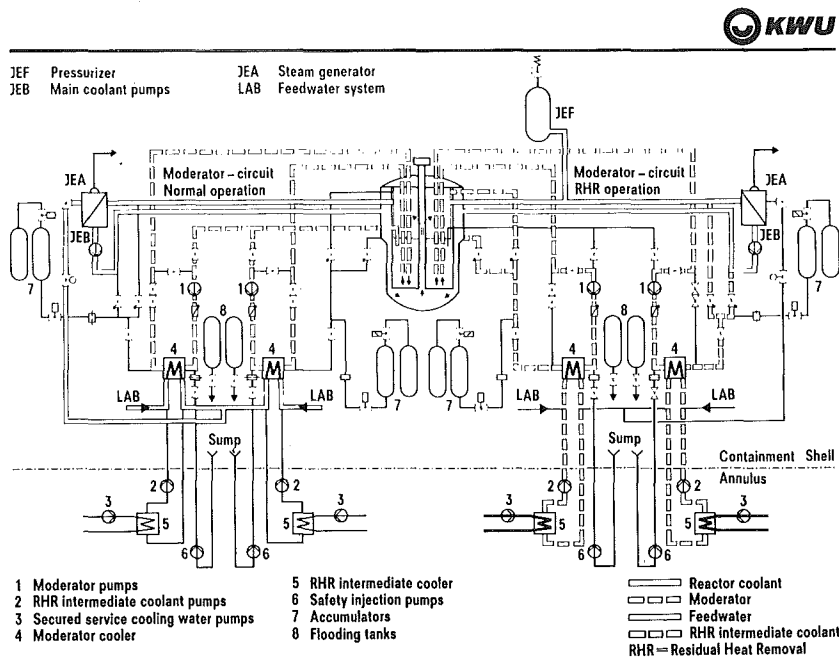
Fig. 4

The coolant channels pass through the moderator tank inside the reactor pressure vessel (RPV). The moderator tank is connected to separate moderator loops.

The pressure between the D<sub>2</sub>O coolant and the D<sub>2</sub>O moderator is equalized through pressure equalization openings in the moderator tank head, so that there are no significant pressure differentials acting on the internals of the RPV.

The moderator temperature can be varied within certain limits and serves besides the control rods and the normal operation borating system for reactivity control. For safety purposes there is also a fast boron injection system as a second independent and diverse shut-down system.

The reactor coolant system of the PHWR is built up analogous to that of the PWR and consists of two identical loops, each with steam generator and reactor coolant pump, and a common pressurizer, see Fig. 5.



**Nuclear Power Plant with Heavy Water Reactor**  
**KWU - PHWR Reactor Coolant and Moderator System, Safety Related Systems**

Fig. 5

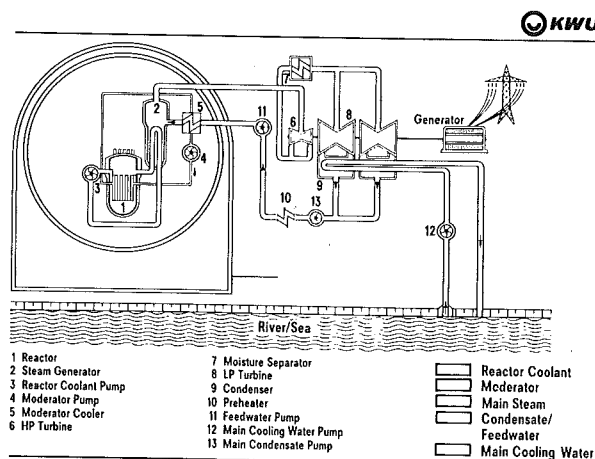


The moderator system consists of 4 identical loops, each with a moderator cooler, a moderator pump, and the associated connecting systems. This system has to perform a number of functions. During normal operation it has to keep the moderator temperature lower than that of the coolant (Fig. 5 left). In order to increase plant efficiency, the heat extracted from the moderator in the moderator cooler is used to pre-heat the feedwater. In the residual heat removal mode (RHR), the system is re-configured by changeover of some valves so that the residual heat is removed via 4 independent residual heat removal chains, see Fig. 5 (right). In the emergency cooling mode the system serves as a high-pressure injection system. In addition to the residual heat removal mode, the core can be flooded and cooled in this mode by water injection from the sump via the safety injection system.

In its function as a primary-side high pressure residual heat removal system, the moderator system represents one of the characteristic features of KWU's PHWR.

In parallel to primary-side RHR, heat can also be removed via the secondary side in the same way as in the PWR, either with the aid of the main heat sink (main condenser) or by dumping main steam to the atmosphere via the main steam relief station, which is designed to withstand external impacts. The steam generators are supplied with feedwater by the main feedwater system or, depending on the plant operating mode, by the start-up and shut-down system, which is connected to the emergency power supply. Due to the primary side and therefore secured high-pressure cooling system, there is no need for a separate emergency feedwater system. Thus, KWU's PHWR plant is equipped with two independent and redundant high-pressure heat sinks.

The connection between primary and secondary systems is shown principally in the simplified flow diagram, Fig. 6.



Nuclear Power Plant with Heavy Water Reactor  
Simplified Flow Diagram

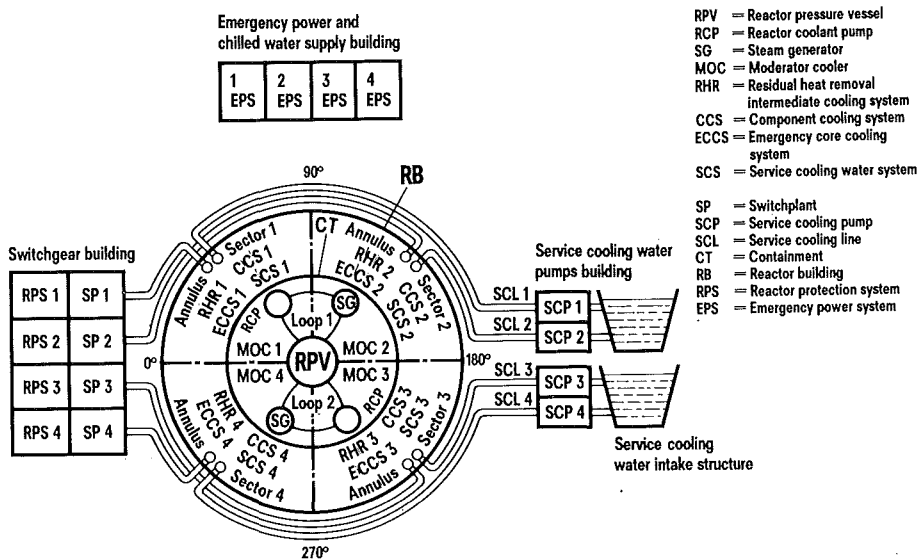
Fig. 6

The design of the engineered safety features is based on the same safety philosophy as applied to the PWR, especially since the responsible licensing authority requires that applicable German codes and standards have to be met. Design lays primary emphasis on preventive measures to mitigate accidents, in particular quality-assurance measures, on the conservative design of the components and high reliability of active safety features. For instance, the instrumentation and control systems are built up in accordance with the same hierarchical principle that has proved effective in the PWR, and with the same quality standards:

- process-related instrumentation and control
- limitation systems
- reactor protection system

The active engineered safeguard features are required to function within the short term ( $\leq 30$  min) following a malfunction. They are automatically initiated and controlled by the reactor protection system. These systems are of four train redundancy ( $n+2$ ) to cope with single failure and simultaneous repair case. The redundant trains are physically separated to prevent consequential failure, see Fig. 7.

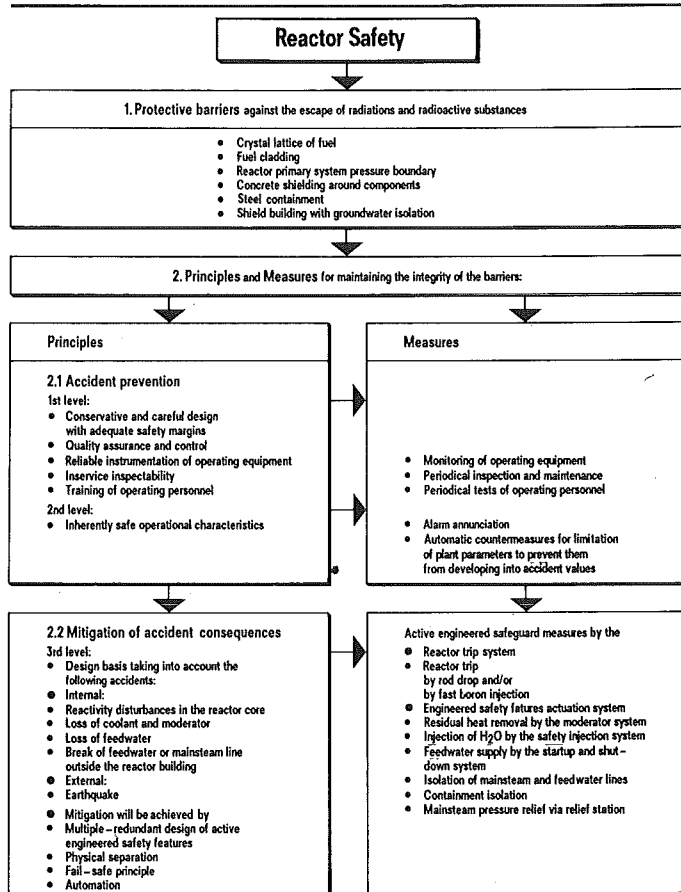
Apart from these active engineered safeguard features the PHWR also incorporates the passive measures against release of radioactive materials according to the barrier principle as applied in the PWR.



**Nuclear Power Plant with Heavy Water Reactor  
Layout of Active Engineered Safeguard Systems**

Fig. 7

The principles and measures involved in reactor safety are summarized in Fig. 8



**Principles and Measures involved in Reactor Safety**

Fig. 8



**Special Safety Related Features**

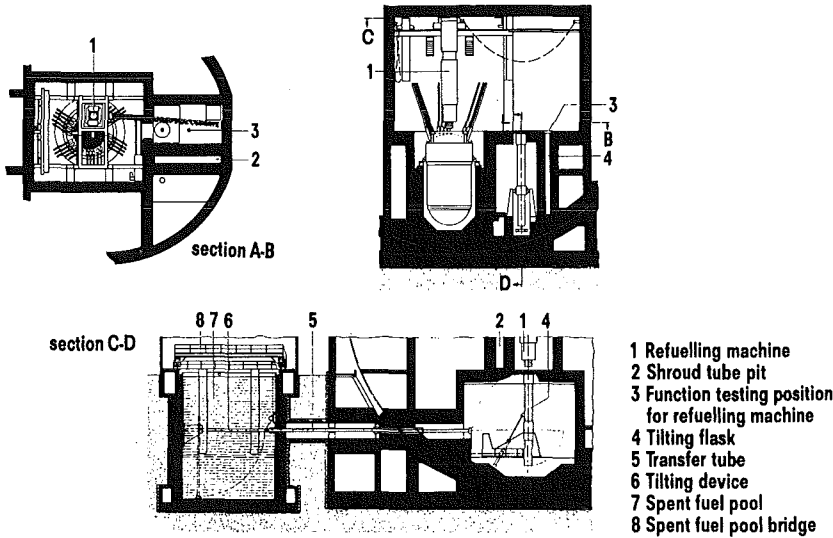
- **Shutdown Systems**
  - Controls Rods
  - Fast Boron Injection
  - Boron Acid Dosification
- **Heat Removal Systems**
  - Steam Generator Feed and Bleed
  - Closed High Pressure Residual Heat Removal
- **(n + 2) - Concept for Design of Safety Systems**
- **Activity Confinement**
  - Full Pressure Steel Containment
  - Concrete Shield Building
- **Hierarchical I & C Concept**
  - Process Related I & C
  - Condition Limitation System
  - Reactor Protection System

Fig. 9 gives a brief overlook over the most important special safety related features of the Atucha PHWR 745 MW.

This brief description would be incomplete without mentioning the on-load refueling, which is a special feature of heavy water reactors. The PHWR refueling system is shown in Fig. 10.

Atucha II PHWR 745 MW

Fig. 9

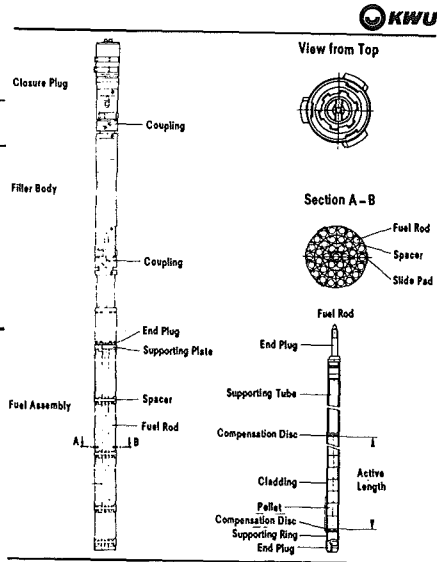


**Heavy Water Reactor Refuelling System (Example Atucha I)**

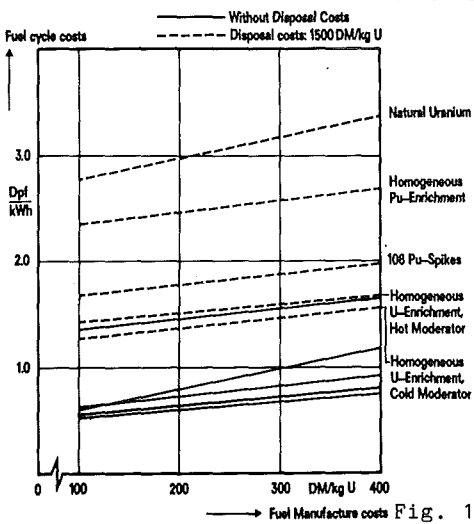
Fig. 10

Refueling of the PHWR is carried out during normal operation of the reactor by one refueling machine. The refueling machine with-draws a fuel bundle column with a spent fuel assembly from the cool-ant channel and transports it to a reclinable container, called tilter, where the exchange of the cooling medium from  $D_2O$  to  $H_2O$  is performed. The fuel bundle column (see Fig. 11) is tilted from the vertical to the horizontal position and transported to the trans-fer tube, which leads through the steel containment by way of locks to the fuel pool building. The refueling procedures are per-formed fully automatically. They are monitored from the control room.

On-load refueling is a rou-tine operation in KWU-PHWRs since 1966. It has been demonstrated that this relatively complicated process can be performed safely and without major perturbancies, thus increasing the plant availa-bility.



Heavy Water Reactor Nuclear Power Plant Fuel Bundle Column Fig. 11



Fuel Cycle Costs of the 750 MW PHWR for Different Fuel Strategies Fig. 12

The PHWR is designed for natural uranium fuel. However, several dif-ferent fuel cycles are possible without major modifications on the plant. Those alternatives increase the fuel burnup, increase the uranium ex-ploitation and finally result in lower fuel cycle costs, as shown in Fig. 12.

Table I shows a comparison of the main technical data of the nuclear power plants Atucha 1 (CNA 1) and Atucha 2 (CNA 2)



	Dimension	CNA 1	CNA 2
<b>Overall Plant</b>			
Reactor Type		Heavy Water Moderated and Cooled Pressurized Reactor with natural Uranium	
Gross Generator Output	MW	367	744,7
Thermal Reactor Output	MW	1179	2160
<b>Reactor Core</b>			
Type of Fuel		Sintered Pelletized natural Uranium Dioxide, 37 Rod Cluster Elements	
Refueling		on Load	
Number of Fuel Elements	-	253	451
Active Length	mm	5300	5300
Burnup	MWD/Mg	6000	7500
Mean Fuel-Rod Power	W/cm	232	232
Number of Control Rods	-	29	18
<b>Main Circuits</b>			
Number/Main Coolant Loops	-	2	2
Number/Moderator Cool. Circ.	-	2	4
Flow Rate per Coolant Loop	kg/s	3080	5150
Moderator Flow Rate	kg/s	445	889
Operating Pressure	bar	113	115
Coolant Temperature	°C	262/296	277,9/312,3
Average Moderator Temperature	°C	140-210	170-220
<b>Reactor Pressure Vessel</b>			
Internal Diameter	mm	5360	7368
Weight of Bottom Portion	Mg	320	670

Main Data of Nuclear Power Plants Atucha

Table I

PART II: SAFETY EVALUATION OF THE 745 MWe PHWR ATUCHA II

The PHWR plant Atucha II had to be evaluated via a probabilistic risk assessment (PRA) by KWU. This part of the paper describes the objective, the performance and the results of the analysis as well as the evaluation of the safety concept of the 745 MWe PHWR of KWU.

Objective

The responsible licensing authority in Argentina requires for the PHWR-plant Atucha II, supplementary to the deterministic safety analysis which had to be performed in accordance with the international practice, as additional information a probabilistic risk assessment for the evaluation of the plant and safety concept. Before construction of the plant was permitted a preliminary PRA had to be presented and was handed over in December 1980, the final analysis must be prepared for the operation permit.

The PRA has been performed to verify the following main objectives:

- The risk resulting from accidents in the Atucha II plant fulfills the risk criterion valid in Argentina. The associated dose-frequency correlation is shown in figure 18.
- The plant and systems design is adequately selected and the safety concept is balanced in itself.
- The risk level of the PHWR plant Atucha II is in agreement with the state of the art in the country by which the plant is supplied.

Performance

The analysis was to be performed with respect to the methodology, data and modelling in analogy to the German Risk Study, Phase A (GRS) /2/ which represents the state of the art in the PRA technique. The results of the GRS have also to serve as reference PWR-values for the comparative evaluation of the PHWR safety concept. The PHWR study is performed in three steps:

- accident sequence analysis to determine the frequency of the core damage, which means in reality, due to the efficiency conditions used, the frequency of design limits being exceeded
- valuation of the radioactivity release into the containment and containment behaviour conservatively starting from a core meltdown
- determination of the consequences of that release to the environment with respect to the dose and corresponding frequency for a given critical group.

## Results

### Accident Sequence Analysis

All potential accidents to be considered in the safety analysis report are identified with respect to the risk relevance and grouped to the following four event classes:

- LOCA
- Transients
- Fuel Handling Accidents
- External Impacts

As representative LOCA events the large, medium and small breaks in the primary circuit are analysed in detail. Emergency Power Mode, Loss of Main Feedwater and Main Steam Line Break are valuated from the category of Transients. The site relevant External Impacts are also valuated and possible failures in Fuel Handling are estimated.

Due to the lack of specifically risk oriented accident sequence calculations using best-estimate boundary conditions, the valuation of the systems engineering was based on conservative boundary conditions and postulates as specified for the deterministic licensing procedure, such as for instance 2-out-of-4 efficiency conditions for safety systems in accordance with the (n+2)-redundancy concept.

Thus the preliminary analysis results for the PHWR Atucha II on basis of conservative assumptions in an integral core damage frequency of  $f \sim 2 \times 10^{-7}/a$ , as summarized in table II. In accordance with the GRS the thus valuated plant state is conservatively defined as core meltdown and used for further calculations.



Event Sequence	Frequency of Core Meltdown [1/a]
LOCA <sub>Large</sub>	$< 0,1 \times 10^{-6}$
LOCA <sub>Medium</sub>	$0,2 \times 10^{-6}$
LOCA <sub>Small</sub>	$0,6 \times 10^{-6}$
Emergency Power Mode	$10 \times 10^{-6}$
Other Transients	$\sim 10 \times 10^{-6}$
Fuel Handling Accidents External Events	- } No Relevant - } Contribution to - } Risk Expected
$\Sigma$	$\sim 20 \times 10^{-6}$
German Risk Study	$40 \times 10^{-6}$
US-Reactor Safety Study	$60 \times 10^{-6}$

Summary of Results of Accident Sequence Analysis for PHWR Atucha II (Median Values)

Table II



The integral core damage frequency of the PHWR is lower than that obtained for PWR plants in the GRS or US-Reactor Safety Study /3/ as shown in table II, but within the same order of magnitude with respect to the uncertainties.

LOCA events do not make any dominant contribution to the integral frequency of core damage. The valuation of the large LOCA is based on a multi-stage analysis concerning the pipe break behaviour of a primary coolant line. A fracture mechanics analysis shows that, with respect to the clearly ductile material selected, the pipe design, the catalogue of loads and the high level of non-destructive examination, a spontaneous failure of a coolant line can be precluded, which is in accordance with the German PWR technique and stated in the guidelines of the reactor safety commission. Figure 13 shows that for the PHWR primary coolant line there exists a considerable safety margin between the allowable crack after acceptance test and the critical through-wall crack length even taking into account the crack propagation.

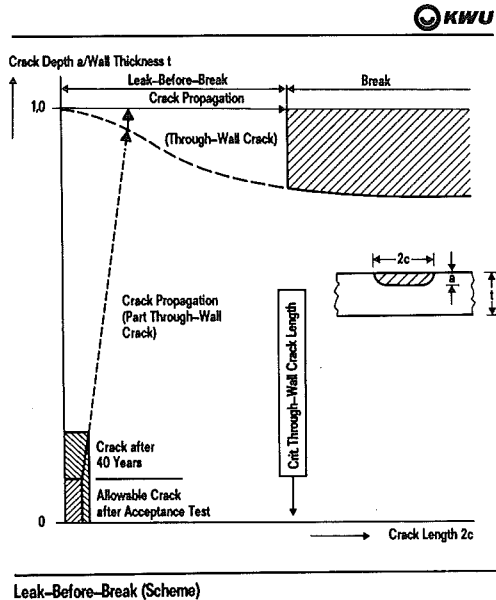
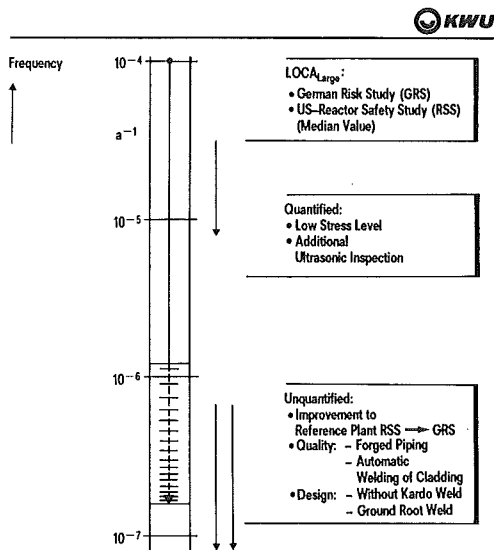


Figure 13

With the help of the highly sensitive and reliable leak detection equipment at the Atucha plant even the smallest possible leak will be immediately measured and indicated.

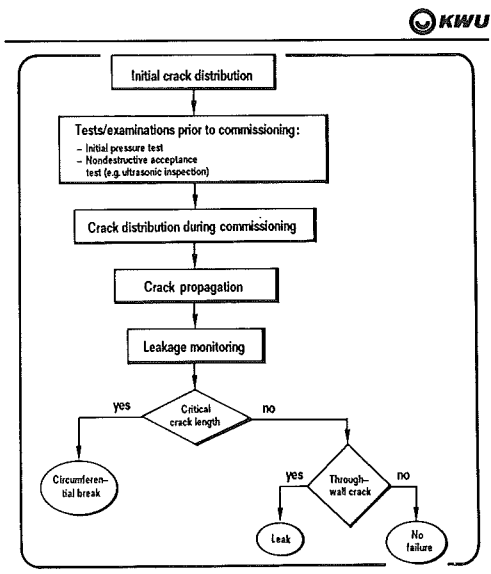
The occurrence frequency of a large LOCA is calculated both relative to the value used in the GRS (and RSS) only by quantifying the influence of the low stress level and an additional ultrasonic inspection - compare figure 14.- and by an absolute valuation in analogy to an investigation ordered by the US-NRC /4/ for a primary coolant loop of a PWR plant (the calculation scheme is shown in figure 15).

Both analyses result in an extremely low occurrence frequency. Thus it can be concluded that the large LOCA is less frequent than  $10^{-7}/a$ , which is underlined by the results of the deterministic approach.



Frequency of LOCA-Large  
Relative Comparison to German Risk Study

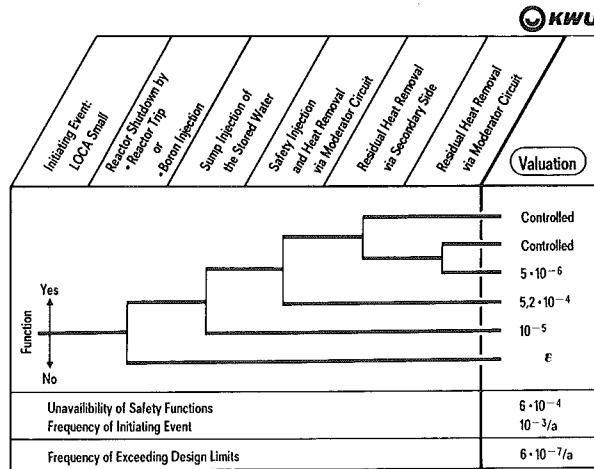
Figure 14



Frequency of LOCA-Large  
Calculation by Probabilistic Fracture Mechanics

Figure 15

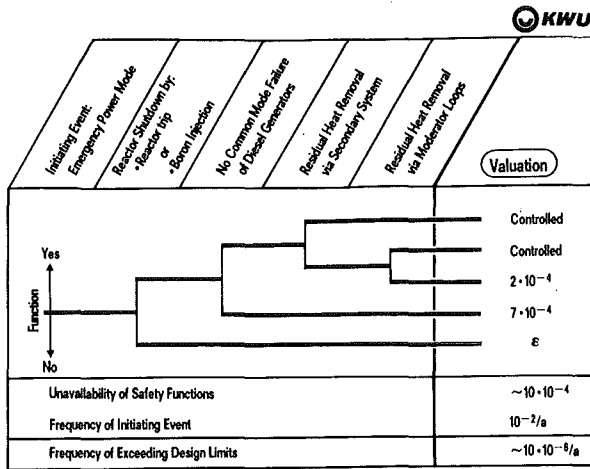
Medium and small LOCA have been valuated just as the transients via an event tree/fault tree analysis. The small LOCA in the KWU PHWR is less dominant than in the PWR because the PHWR is designed with two diverse high-pressure heat removal systems. The event tree for small LOCA in figure 16 shows the residual heat removal performed via secondary side systems or via the moderator circuit. The short term safety injection and heat removal is highly reliable because the moderator system is used which is already in operation and only some valves have to be switched and operated. The reactor shutdown function is ensured in diverse modes, by the trip system or the fast boron injection system, both highly redundant, so that the unavailability of this function is low.



Valuation of "LOCA-Small" for PHWR Atucha II

Figure 16

The main contribution is accounted for by the transients. The 'Emergency Power Mode' was analysed in detail, because this event makes severe demands on the systems engineering both by its relatively high frequency of occurrence compared to the LOCA events and because of the restrictions in power supply; the corresponding event tree is shown in figure 17. Applying the restrictive approach of common mode failure used in the GRS reference study for the quantification of the emergency power diesel system this fault makes a contribution of about 70 % to the system's unavailability. The necessary safety functions shutdown and heat removal are performed by above mentioned diverse systems, so that their unavailability is low



Valuation of "Emergency Power Mode" for PHWR Atucha II

Figure 17

The further transients are taken into account with respect to the core damage frequency as 'Other Transients' by a contribution to be of the same order of magnitude as the 'Emergency Power Mode', see table II. The explicitly valuated events 'Loss of Main Feed-water' and 'Main Steam Line Break' underline the conservativeness of this estimation by being slightly more than  $10^{-6}/a$  each.

'Fuel Handling Accidents' do not contribute significantly to the risk due to the activity inventory, the handling procedure and the equipment design.

Because of the low occurrence frequency and the plant design, no relevant contribution to the risk is estimated also from 'External Events'.

#### Radioactivity Release

A complete core meltdown analysis has been performed for a representative meltdown accident using, due to the similarity in systems and plant design between the PHWR and PWR of KWU and with respect to the comparability of both the frequency and the amounts of the radioactivity release into the containment and from there into the environment, the same approach and the same modelling as in the reference GRS taking into account the PHWR specific, e.g. the core and reactor pressure vessel structure. Thus the release categories (RC) used are the same as those selected in the GRS, see table III.

The frequency of the different release categories has been estimated by an analysis of the containment response basing on a pressure - time history calculation and a reliability assessment for the containment isolation.



RC	Description	Frequency of Release (1/a)
1	Core Meltdown, Steam Explosion	$2 \times 10^{-7}$
2	Core Meltdown, Large Containment Leak ( $\varnothing$ 300 mm)	$2,3 \times 10^{-7}$
3	Core Meltdown, Medium Containment Leak ( $\varnothing$ 80 mm)	$< 2,3 \times 10^{-7}$
4	Core Meltdown, Small Containment Leak ( $\varnothing$ 25 mm) Late Overpressure Failure	$< 2,3 \times 10^{-7}$
5	Core Meltdown, Late Containment Overpressure Failure, Failure of Filtersystems	$4,5 \times 10^{-6}$
6	Core Meltdown, Late Containment Overpressure Failure	$1,5 \times 10^{-5}$

Release Categories (RC) for Core Meltdown Accidents and Occurrence Frequency for PHWR Atucha II (RC acc. to German Risk Study)

Table III

The most significant failure of the containment due to overpressure (RC 5 and 6) is to be expected not earlier than 7 days after the onset of an accident, because of the favorable relationship between the volume of the containment (same as 1300 MWe PWR) and the reactor power. In this case, most of the radioactivity is released in the conservatively quantified leakage outflow.

The distribution of aerosols including iodine in the containment atmosphere has been calculated with the NAUA-code /5/.

The PHWR analysis does not yet include the recent findings of reactor safety research concerning in the valuation of the accident consequences, e.g. the sedimentation of radioactivity especially in the annulus and the binding and retention of iodine in the liquid phase or the reduction of the probability of steam explosion /6/. Thus the accident consequences will be reduced considerably.

#### Consequences of Radioactivity Release

The valuation of the consequences of the release of radioactivity to the environment refers to a given critical group of persons in the realistic position relative to the Atucha plant, which nearly corresponds with the point of the maximum dose. The amount and frequency of the dose is influenced by the weather conditions at the time of release. The radiation dose is determined with respect to the German recommendations for dose calculation taking into account dose factors acc. to ICRP 30.

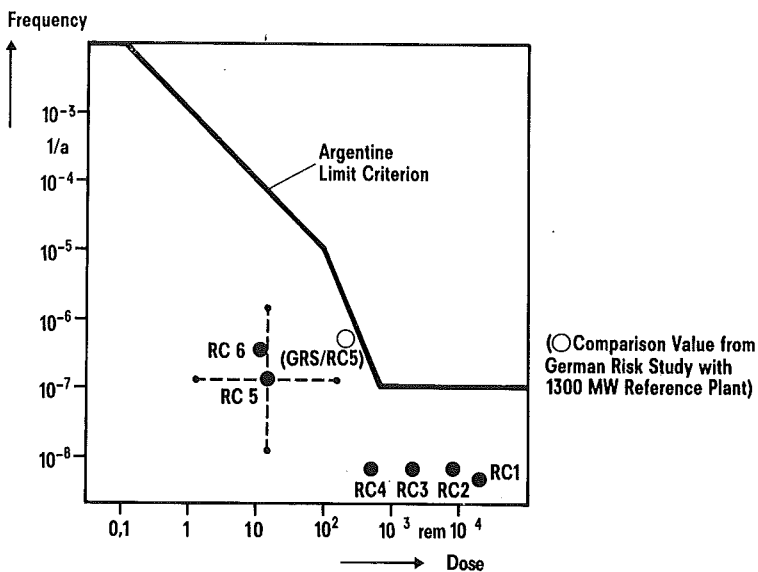
The results of the analysis are summarized in figure 18 where the calculated dose and corresponding frequency for each release category are shown.

### Evaluation

The comparison of the dose-frequency values for the various release categories (RC) for the PHWR plant Atucha II with the applicable Argentine limit criterion appropriate to figure 18 shows that the risk resulting from accidents is well below the given limit. Even if uncertainty bands of one order of magnitude in each direction are conservatively assumed as demonstrated for RC 5, the limit line is not reached. Thus the valid risk criterion is fulfilled by the 745 MWe PHWR Atucha II.

The analysis confirms that the plant and systems design of the PHWR Atucha II have been adequately selected. The safety concept is well balanced, there is no dominant contributor from accident sequences or safety functions to the core damage frequency. The accident consequences are considerably mitigated by the containment function.

A comparison of results achieved for the PHWR with the corresponding results calculated for the reference PWR (1300 MWe) in the GRS with respect to the core damage frequency and a release category that is equally representative of both types of plant permits the conclusion to be drawn that the risk level of the KWU 745 MWe PHWR is comparable with that of a KWU PWR. Thus from the probabilistic point of view the KWU 745 MWe PHWR would be licensable in the country of the supplier.



**Dose/Frequency-Values for various Release Categories (RC) for the PHWR Atucha II in Comparison with the Argentine Limit Criterion**

Figure 18

Literature

- /1/ Building a 745 MWe pressure-vessel PHWR in Argentine  
Nuclear Engineering International  
Vol. 27, No. 332, Sept. 1982
- /2/ Gesellschaft für Reaktorsicherheit  
"Deutsche Risikostudie Kernkraftwerke"  
Verlag TÜV-Rheinland, Köln 1979
- /3/ Rasmussen N.C.  
US-Reactor Safety Study  
US-NRC, Wash 1400 (NUREG-75/014), Oct. 1975
- /4/ Probability of Pipe Fracture in the Primary Coolant Loop  
of a PWR Plant  
NUREG/CR-2189, Vol. 1-9  
Lawrence Livermore Laboratory, Sept. 1981
- /5/ A. Bunz, W. Schock  
Aerosol Behaviour in the Condensing Steam Atmosphere of a  
Postaccident LWR-Containment  
ENS/ANS - Int. Topical Meeting on NPP safety,  
Brüssel, 1978
- /6/ K. Haßmann, J.P. Hosemann  
Consequences of degraded core accidents  
SMIRT 83, Chicago

SURVEY OF KWU'S SAFETY RELATED CONTAINMENT  
WORK FOR AMERICAN BOILING WATER REACTORS

P. Antony-Spies, D. Göbel and M. Becker

Kraftwerk Union Aktiengesellschaft  
Berliner Straße 295 - 303, D-6050 Offenbach/M.  
Federal Republic of Germany

ABSTRACT

KWU's experimental and analytical work on the safety relief system and on the pressure suppression system performed for American BWR's during the last few years is presented. For the safety relief system, loads were measured during the Karlstein Quencher Verification Tests and applied to Mark II containments. The loads due to air clearing were corrected analytically for amplitude and frequency according to the different plant conditions. For the pressure suppression system, LOCA-loads were measured in a test facility at the Großkraftwerk Mannheim. The application to the plants for design verification was performed using hydrodynamic point sources combined with probabilistic amplitude factors accounting for multi-vent effects.

1 INTRODUCTION

In 1976 KWU's first boiling water (BWR) reactor of product line 69 started for operation. During the licensing period before much experimental and analytical work had to be done to meet the German safety requirements. An important part of this work was the solution of containment problems concerning the loads in the pressure suppression system due to safety relief valve (SRV) actuations and loss of coolant accidents (LOCA) as well /1/. After 1976, KWU performed safety related containment work also for American boiling water reactors with Mark II containments (Fig. 1). The methods were improved taking advantage of the experience of the work already done for the KWU type plants. Of course also some adjustments had to be made according to the acceptance criteria in US licensing procedures.



## 2 SAFETY RELIEF SYSTEM

The safety relief system consists of the safety relief valve, the discharge pipe and a quencher device. The quencher is situated at the end of the discharge pipe and is submerged in the wetwell water pool (Fig. 2).

One purpose of the quencher is to reduce the loads in the wetwell pool due to air bubble pulsations following air clearing and the loads due to steam condensation. Another one is to condense the steam up to the boiling temperature in the pool.

### 2.1 QUENCHER DESIGN AND VERIFICATION TESTS

KWU has designed a two-leg type quencher 2 for ten Mark II plants in the USA including the corresponding load definitions. The design had to be tested in an extensive test program (Karlstein Quencher Verification Tests) because of significant differences with respect to the German devices (mass flux, valve opening time, pipe length, etc.).

In the test facility a single quencher was installed in a tank. The tank geometry was designed such that its walls simulate the neighbouring quenchers in one of the Mark II plants in case of all valve actuation.

The loads measured were forces, moments and temperatures acting on the quencher, the discharge pipe and the supports, loads on other submerged structures in the pool and pool pressures.

### 2.2 CONTAINMENT APPLICATION

Most of measured loads could be immediately applied to the plants without major corrections. For the pool pressures due to air clearing this was possible only for the particular plant geometry and operating conditions simulated. In cases with a smaller number of quenchers actuated, different operating conditions or cases of other plants the loads must be modified.

For that purpose an analytical model was used which accounts for the hydrodynamic interaction between the pulsating quencher air bubble and the pool boundaries quantitatively 3 .

An increase of the pool size for example causes an increase of the pulsation frequency and the strength of the equivalent hydrodynamic source accompanied by a decrease of the pool boundary pressure. A decrease of the bubble pulsation frequency is caused by an increase of the bubble volume. Fig. 2

shows an example of the frequency dependence together with experimental verification.

All such effects were quantitatively taken into account for various load cases and for different power plants by multiplying the measured pressure traces with corresponding amplitude and frequency factors.

Furthermore pool mixing with respect to water temperature was considered. The analyses yielded relatively good temperature mixing for the present two-leg quenchers designed for Mark II containments.

### 3 LOSS OF COOLANT ACCIDENT

The containment work with respect to LOCA-loads consists of a new test series in the modified GKM test facility /1/ and the corresponding evaluations for the plants using further developed analytical methods.

#### 3.1 TESTS

The test facility represented a single cell of the pressure suppression system of a Mark II plant (Fig. 3). The LOCA's simulated were main steam line and recirculation line breaks under various conditions (break size, pool temperature, back pressure etc.) which cover the plant operation fields.

The instrumentation allowed for comprehensive measurements of pool pressures, lateral loads on the vent pipe and loads on submerged structures and the measurement of the various physical quantities and conditions during the blow-downs (Temperature, steam flux, air content, phase boundaries etc.).

The measurements revealed the characteristic phenomena like pool acoustics, vent acoustics and their excitation mechanism. The resulting pool boundary loads could be categorized as pressure-time histories (Fig. 4) being quasi-harmonic pressure oscillations ("condensation oscillations", CO) or being pressure events with oscillatory ringout behaviour ("chugging"). During the tests thousands of pressure events were registered having large stochastic amplitude variations.

#### 3.2 CONTAINMENT APPLICATION

Extensive analytical work has been done to convert the various test results into loads for the plants. The most

interesting loads were those which affect the dynamic response of relevant components within the reactor building. For the corresponding load definitions the existing analytical tools had to be improved, and new one had to be developed.

The containment load definition lead to a symmetric and an asymmetric pressure distribution at the wetwell pool boundaries. Its generation methodology contained a probabilistic and a deterministic part.

A number of representative events was selected such that they cover the governing frequencies with their mean amplitudes during the various blowdowns. The selection criteria based on band pass filtered pressure traces of overlapping frequency ranges and power spectral densities as well.

The mean events were corrected by certain multipliers according to adequate exceedance criteria.

The computation of the multipliers was subject to probabilistic methods. To each of the different vents in the pressure suppression system stochastic pool pressure amplitudes were assigned having a probability density distribution derived from the tests. The analysis then yielded amplitude multipliers for symmetric and asymmetric loads as functions of an exceedance probability. The numerical values for the load definition were taken according to a permissible exceedance of  $10^{-5}$  per LOCA.

The deterministic part was the conversion of the measured pressure time histories into pressure time histories at plant's pool boundaries. Two methods were investigated, the direct application of measured pressure traces to the pool boundaries, and the application of hydrodynamic point sources /4/ at the vent exits followed by analytical calculation of the pressure (Fig. 5). Both methods gave similar results with respect to the dynamic containment response (Fig. 6). The second one was used in the case being because it is less conservative.

As observed in several multi-vent tests the events at different downcomers are synchronized only within a time window of at least 50 ms. This has been accounted for by introducing adequate desynchronization of the source functions. The load definition was verified by application to the JAERI-multivent tests /5/.

For the lateral loads on the downcomers a similar probabilistic load definition was performed.

## REFERENCES

- /1/ Hupe, H. R. and K. D. Werner  
Kondensationsversuch zur Bestätigung der Lastannahme für  
die KWU-Druckabbausysteme der Baulinie 69  
Reaktortagung 1977, Mannheim, W-Germany
- /2/ Göbel, D. and M. Becker  
Die Zweiarm-Lochrohrdüse als Ausströmgeometrie für das  
Druckentlastungssystem eines Siedewasserreaktors  
Jahrestagung Kerntechnik, 1981, Düsseldorf, W-Germany
- /3/ Antony-Spies, P.  
Dynamics of safety relief valve and LOCA-loading sources  
in the pool of BWR pressure suppression systems  
SMIRT6-Post-Conference Seminar, 1982, Ispra, Italy
- /4/ Class, G.  
Multi-Vent-Problems  
Proc. Int. Spec. Meeting on BWR-Pressure Suppression  
Containment Technology, 1981, Geesthacht, W-Germany
- /5/ Kukita, Y. et al  
State for JAERI full-scale Mark II CRT-program  
Proc. Int. Spec. Meeting on BWR-Pressure Suppression  
Containment Technology, 1981, Geesthacht, W-Germany

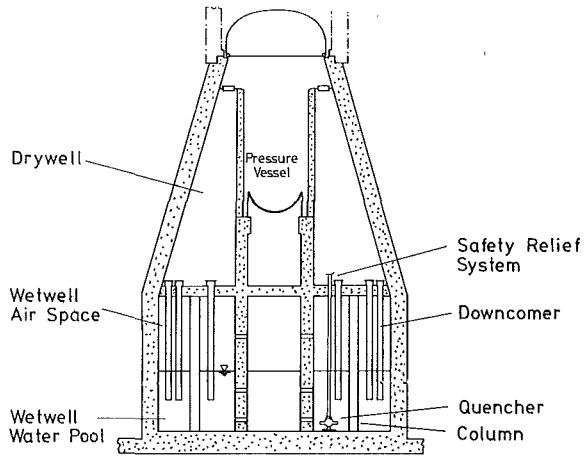


Fig.1: Pressure Suppression System of MarkII Type

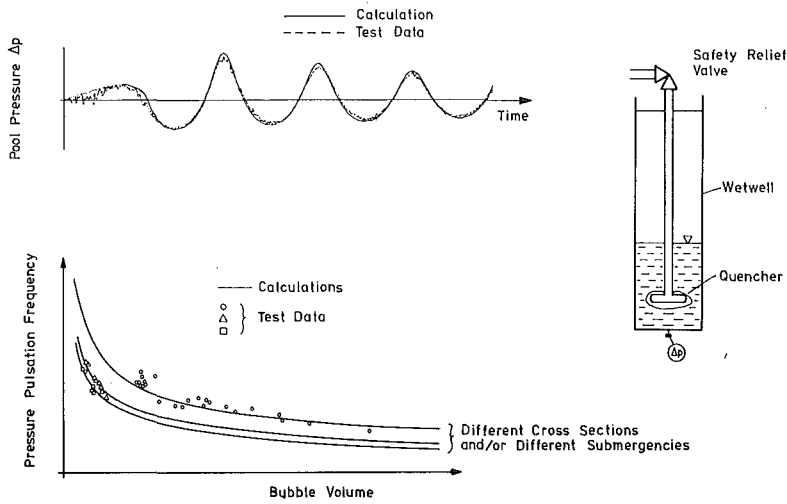


Fig.2: Safety Relief System with Quencher  
Pool Boundary Loads Following Air Clearing (Example)

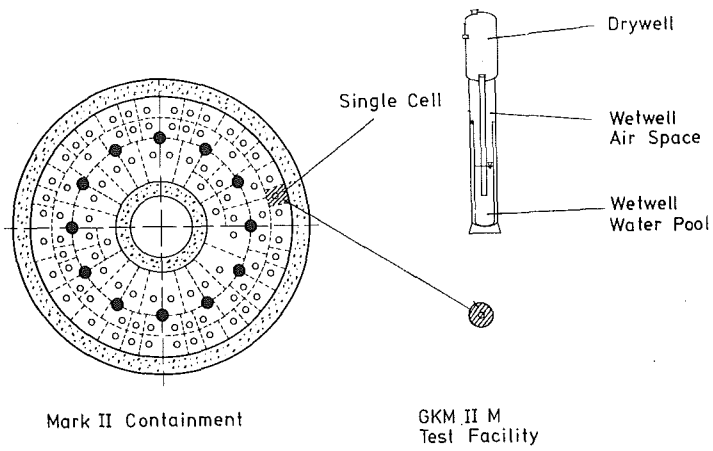


Fig.3: Simulation of MarkII Type Pressure Suppression System by GKM II M Test Facility

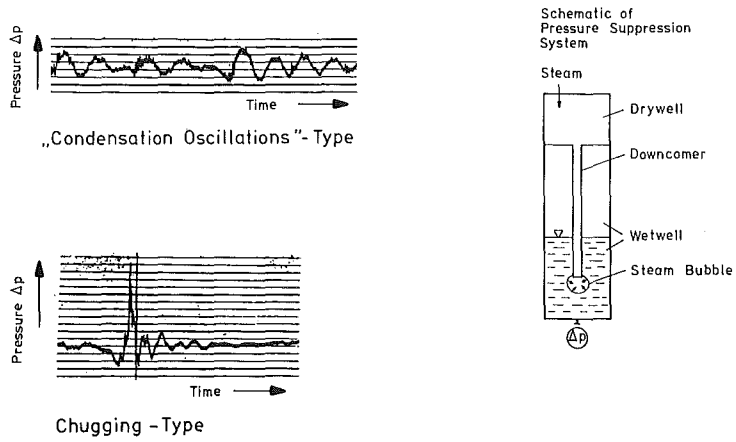


Fig.4: Containment Loads During LOCA (Condensation Phase) Typical Pool Pressure Time Histories Measured in Tests

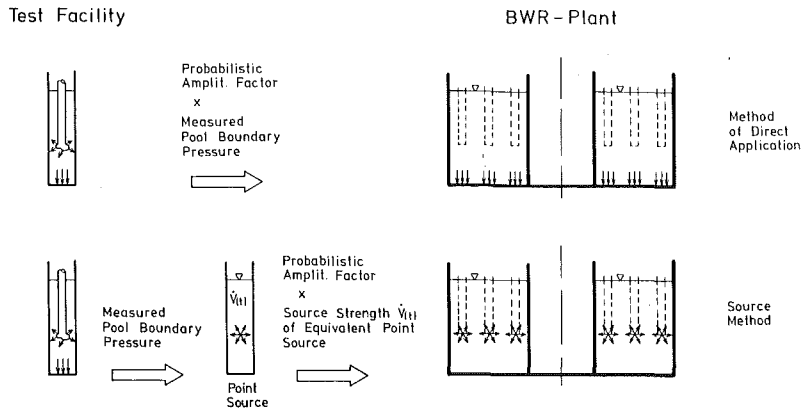


Fig.5: Definition of Wetwell Pool Boundary Loads due to LOCA Condensation Phase

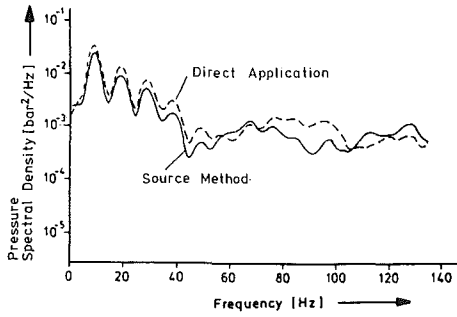


Fig.6: Spectral Density of Wetwell Pool Boundary Pressures due to LOCA Condensation Phase (Example)